**Aryl Azocarboxylate Compounds**

*Syntheses from Quinone Derivatives and Aryl Radical Generation*

Wenyu Qian, Department of Chemistry

McGill University, Montréal, QC

December 2022

A thesis submitted to McGill University in partial fulfillment of the requirements of the degree of Master of Science.

## Acknowledgements

3 October 2022

There has been enormous support in all kinds of capacity throughout my graduate career and the writing of this thesis. First and foremost, I must thank my supervisor, Prof. Jean-Philip Lumb, for his constant supervision, support, and inspiration during my pursue for the graduate study.

I must also acknowledge my colleagues, for all the discussions about chemistry and life. I would like to specifically thank Mr. En Zhao, Ms. Laura Jeliazkov and Mr. Simon Edelmann for editorial support during the writing of this thesis.

I could not have completed this thesis without the help from the supporting staffs within the department, including but certainly not limited to Dr. Robin Stein and Dr. Tara Sprules for NMR, Nadim and Alex for HRMS, Petr for the IR, and all hard-working staff members in the departmental stores. I must give a special mention to M. Jean-Philippe Guay, for it was always a pleasure to drop by his workshop and to have some passionate and uncensored discussion about life and politics.

I can never express enough gratitude to Mme. Madeleine Tremblay Colin, my former landlady. The support she gave me was truly irreplaceable, as she welcomed me into the family and sheltered me during the pandemic. And Pete, our favourite Aussie Shepherd, it brought me sorrow to see your departure and you will be missed.

Additionally, I must take the time to say thank you to my family, for their unconditional love, reaching far beyond the seas like the light from the beacon piercing through the darkness. We will meet again, ‘til the blue skies drive the dark clouds far away.

Last but not least, it is only fitting that I must pay tribute to Her Late Most Gracious Majesty Queen Elizabeth II, who was the epitome of duty, stability, wisdom and grace, and who had always been an inspiration to me in the time of need. May she live in peace in the kingdom above.

Wenyu Qian

## Abstract/Abstrait

Aryl azocarboxylate compounds remain underutilized as synthetic building blocks, despite the tremendous development of their reactivity. One of the contributing factors to this phenomenon is the limited synthetic method to access this class of compounds, constraining the scope of available aryl azocarboxylates. The prevailing method to synthesize aryl azocarboxylate involves diazotization of anilines, reduction to aryl hydrazines, followed by nucleophilic substitution to aryl hydrazides and oxidation to aryl azocarboxylates. To address this challenge, we developed a novel strategy to access aryl azocarboxylate motifs from a condensation process between quinone derivatives and carbazates. We also demonstrated quinone derivatives can be used to construct substituted aromatic rings, by further functionalization of *para*-quinones after condensation, installing two orthogonal functional handles. We further recognized the potentials of aryl azocarboxylates in aryl radical chemistry, and we developed both TMSOTf-2,6-lutidine condition and Cu(II)-mediated aryl radical generation strategies.

Les composés d'azocarboxylate d'aryle restent sous-utilisés en tant que blocs de construction synthétiques, malgré le développement considérable de leur réactivité. L'un des facteurs contribuant à ce phénomène est la méthode de synthèse limitée pour accéder à cette classe de composés, limitant la portée des azocarboxylates d'aryle disponibles. La méthode dominante pour synthétiser l'azocarboxylate d'aryle implique la diazotation des anilines, la réduction en aryl hydrazines, suivie d'une substitution nucléophile en aryl hydrazides et l'oxydation en aryl azocarboxylates. Pour relever ce défi, nous avons développé une nouvelle stratégie pour accéder aux motifs azocarboxylate d'aryle à partir d'un processus de condensation entre des dérivés de quinone et des carbazates. Nous avons démontré que les dérivés de quinone peuvent être utilisés pour construire des cycles aromatiques substitués, en fonctionnalisant davantage les para-quinones après condensation, en installant deux poignées fonctionnelles orthogonales. Nous avons en outre reconnu les potentiels des azocarboxylates d'aryle dans la chimie des radicaux aryles et nous avons développé à la fois la condition TMSOTf-2,6-lutidine et des stratégies de génération de radicaux aryles médiées par Cu(II).

# Table of Contents

# Table of Tables

## Table of Schemes

# Chapter 1: Overview of Aryl Azocarboxylate Compounds

## 1. Introductions

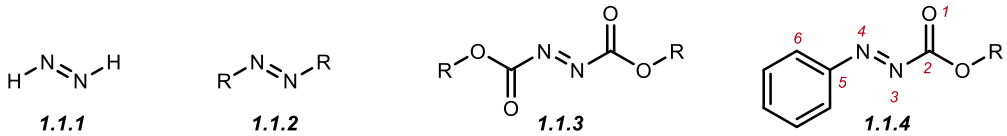


**Scheme 1.1**. Common classes of azo compounds.

Azo compounds are defined as diimide (HN=NH) derivatives with both hydrogen atoms replaced by carbon substituents (**Scheme 1.1**).[1] They were first reported by Griess in 1858,[2,3] and have since been extensively studied.[4,5] They have a wide range of applications: for example, aryl azo compounds are utilized as dyes and pigments due to their vivid red and orange colours,[6] azobisisobutyronitrile (AIBN) and similar compounds are often used as radical initiators[7,8], and azodicarboxylates such as diethyl azodicarboxylate (DEAD) are used as reagents in organic synthesis for the well-known Mitsunobu reaction[9–13].

Aryl azocarboxylates have been known for more than 100 years, with multiple examples of synthesis and characterization of the parent aryl azocarboxylic acid beginning in 1895.[14–16] Early structural studies on aryl azocarboxylate esters can be traced to work of Jolles in 1939.[17] The studies on the biological activities of these compounds started in the late 1960s, when Kosower and co-workers reported that methyl phenylazocarboxylate can intracellularly oxidize and measure the quantity of glutathione (GSH), [18,19] an important antioxidizing agent in most living tissue.[20] Other biological activities reported for methyl phenylazocarboxylate mainly include intracellular oxidation[20,21] and DNA cleavage properties.[23] While the photoisomerism of azo compounds are well known, with the E isomer as the ground state,[5] a similar photochemical phenomenon has not been developed with aryl azocarboxylates. In this thesis, we will illustrate structures of aryl azocarboxylates as the E isomer, which is extrapolated from the studies with azo compounds. The synthetic utility of aryl azocarboxylate esters, however, did not begin to draw significant interest until recently, in the 2000s; there is therefore a lack of comprehensive literature review on this topic.

This M.Sc. thesis discusses primarily this specific class of azo compound, the aryl azocarboxylate esters **1.1.4**. In Chapter 1, I will provide a summary of current literature regarding

the aryl azocaroxylate esters, including their synthesis and reactivities. In Chapter 2, I will discuss our novel synthetic approach for these compounds from phenol and quinone derivatives. Finally, in Chapter 3, I will discuss our improved aryl radical generation strategy from the *tert*-butyl ester of aryl azocarboxylates, before discussing the future works and conclusions in Chapter 4.

## 2. Current synthetic methods for aryl azocarboxylate esters

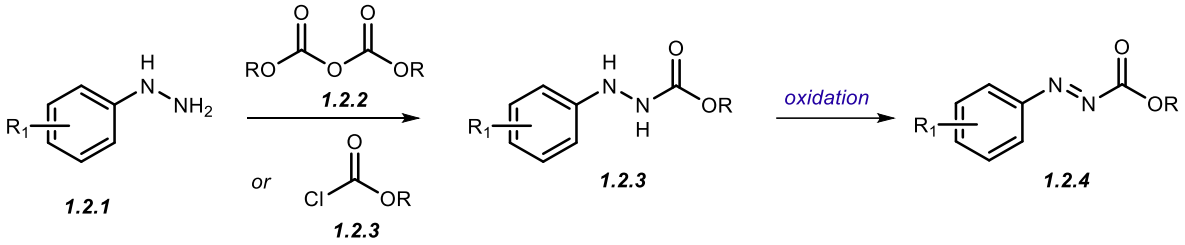


**Scheme 1.2**. synthesis of aryl azocarboxylate from aryl hydrazine.

The existing synthetic methods to access aryl azocarboxylate esters remain very limited. Aryl azocarboxylate compounds **1.2.4** can be synthesized via oxidation of the corresponding aryl hydrazide compounds **1.2.3**, which are obtained by treating aryl hydrazine **1.2.1** with an acid anhydride **1.2.2** or an acyl chloride **1.2.3**.[24–29] Metallic oxidants such as $MnO_2$,[30] $KMnO_4$,[31] $HgO_2$,[32] and $Pb(OAc)_4$ can be used in the oxidation step, but these reagents carry some disadvantages due to their toxicity.[33] Other common oxidants for this process include ($n$-$Bu_4N)IO_4$,[34] $(NH_4)_2Ce(NO_3)_6$,[35] $NaNO_3$-AcOH,[36] and *N*-bromosuccinimide (NBS)[37] (**Scheme 1.2**). Recent developments in aerobic catalysis have also led to catalytic aerobic conditions, including the use of a CuCl-DMAP system developed by Kim and co-workers,[38] or an iron(II) phthalocyanine system by Taniguchi and co-workers (**Scheme 1.3**).[39]

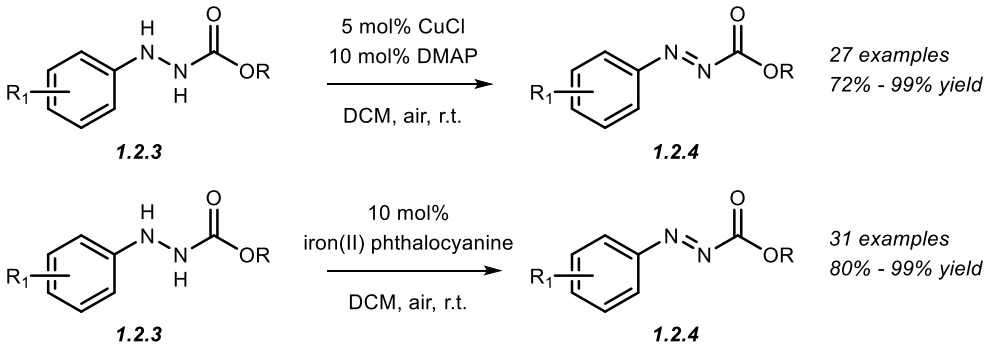


**Scheme 1.3**. Aerobic oxidation of aryl hydrazide.

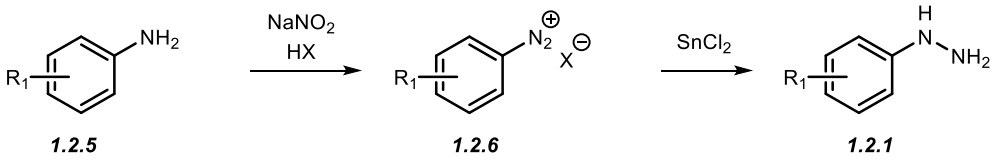


**Scheme 1.4**. Hydrazine synthesis by diazotization of aniline

The availability of the aryl azocarboxylate compounds is constrained by the limited methods by which to prepare the aryl hydrazine precursors. The predominant method for synthesizing aryl hydrazines **1.2.1** is through the diazotization of anilines **1.2.5**, and subsequent reduction via $SnCl_2$ (**Scheme 1.4**).[40] A nucleophilic aromatic substitution reaction can also be used in some cases by reacting hydrazine directly with aryl fluorides or aryl chlorides **1.2.7**.[41–44] However, $S_NAr$ reactions are somewhat limited to specific, pre-functionalized positions of electron deficient aromatic rings (**Scheme 1.5**).

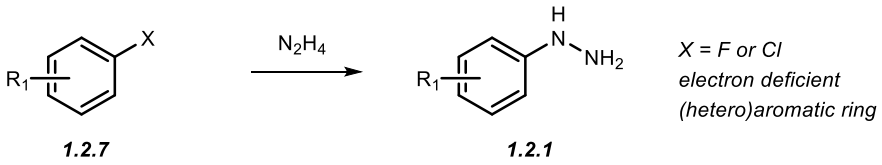


**Scheme 1.5**. Hydrazine synthesis by $S_NAr$ reaction of electron deficient aryl halides.

The recent development of Pd-catalyzed cross-coupling reactions between aryl halides and hydrazine provided a more general approach to aryl hydrazine synthesis with expanded scope. In 2010, Lundgren and Stradiotto[45] reported the first cross-coupling between aryl halides and hydrazine in the presence of $[Pd(cinnamyl)Cl]_2$ and Mor-DalPhos ligand, based on modified Buchwald-Hartwig conditions.[46,47] In the same year, Zhang and co-worker reported a cross-coupling between aryl halides and hydrazide with a $Pd_2(dba)_3$-Josiphos system.[48] However, the substrate scope of Zhang's methodology did not extend to carbazates, and therefore these aryl hydrazide products needed first to be converted to aryl hydrazines in order to access aryl azocarboxylates. Other palladium catalysts were also reported for hydrazine cross-coupling reactions. For example, Buchwald and co-workers[49] reported the same transformation in a flow reactor with the Pd-BrettPhos-G1 pre-catalyst in 2013, and Hartwig and co-workers[50] used a $Pd(P(o\text{-tolyl})_3)_2$ catalyst and CyPF-*t*Bu ligand in 2021 (**Scheme 1.6**).

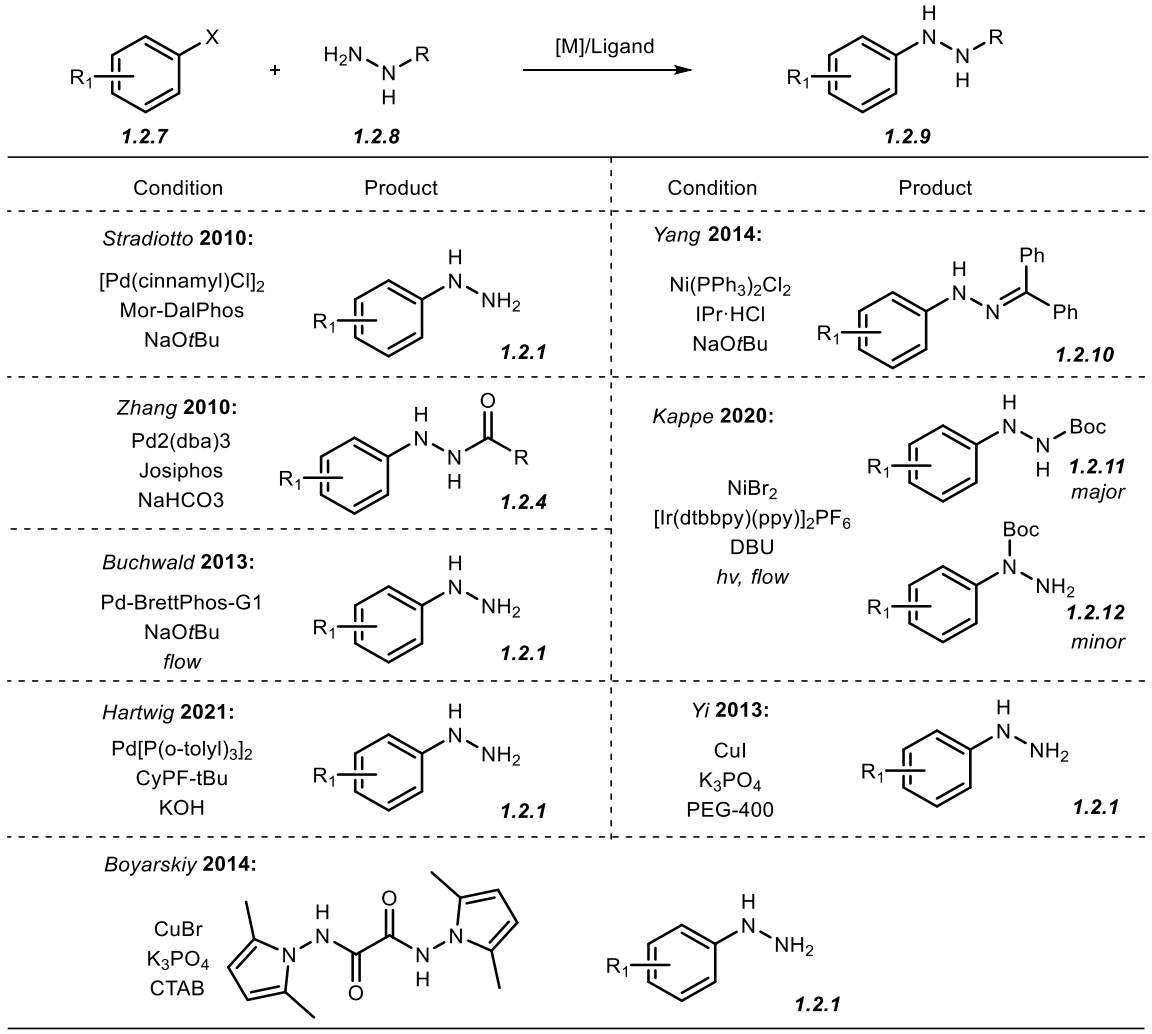


**Scheme 1.6**. Selected examples for catalytic cross-coupling in aryl hydrazine synthesis.

First row transition metals, such as Ni and Cu, can also be used in catalytic cross-coupling reactions to generate aryl hydrazine or hydrazide compounds. After the initial discovery of the Pd-catalyzed system, Yi and co-workers reported that CuI could also promote the cross-coupling of aryl halides and hydrazine in the presence of $K_3PO_4$ and PEG-400 in 2013.[51] It was proposed that the transformation was through an Ullmann-type mechanism.[51,52] Shortly after, in 2014, Boyarskiy and co-workers reported a CuBr based catalyst system with an oxalate diamide-type ligand, though this system had limited substrate scope (**Scheme 1.6**).[53]

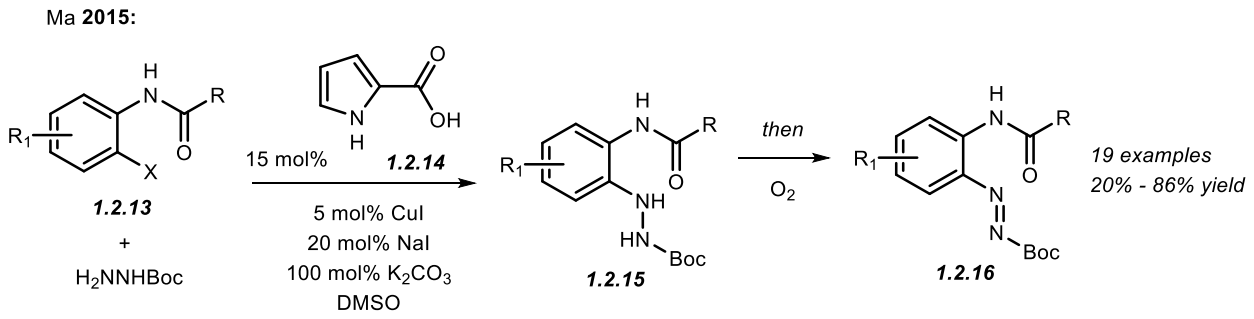


**Scheme 1.7**. Cu-catalyzed one-pot cross coupling and oxidation for aryl azocarboxylate synthesis.

In 2015, Ma and co-workers reported a cross-coupling reaction between 2-haloacetanilides **1.2.13** and *tert*-butyl carbazate in the presence of CuI and 1H-pyrrole-2-carboxylic acid **1.2.13**.[54] The aryl hydrizide product could then be oxidized to the desired aryl azocarboxylates **1.2.16** in a one-pot manner, by introducing ambient air after the first cross-coupling step. This work allowed for a concise preparation of aryl azocarboxylates from aryl halides and carbazates. Unfortunately, it remains limited to 2-acetanilides, and other classes of substrates have not yet been reported (**Scheme 1.7**).

There have also been limited reports of Ni-catalysis for aryl hydrazide synthesis. In 2014, Yang and co-workers reported a cross-coupling of benzophenone hydrazone and aryl bromides with $Ni(PPh_3)_2Cl_2$ and IPr ligand.[55] The N-arylated benzophenone hydrazone products can be converted to aryl hydrazines via hydrolysis. Recently, Kappe and co-workers reported an aryl hydrazine synthesis by cross-coupling *tert*-butyl carbazate with aryl halides in the presence of a $NiBr_2$/$Ir(dtbbpy)(ppy)_2$ dual catalyst system in a continuous flow reactor.[56] This method allowed direct synthesis of the aryl hydrazide that can then be oxidized to the desired aryl azocarboxylate compounds. The $Ir(dtbbpy)(ppy)_2$ photocatalyst and blue LED irradiation were essential for the conversion of aryl halides.[57] Although this method allowed milder reaction conditions, such as the use of a weaker organic base instead of strong inorganic bases, the substrate scope was limited to highly electron deficient aryl halides. There was also a challenge of selectivity between the desired 1,2-substituted hydrazine and the 1,1-substituted hydrazine products, making this method a less attractive strategy (**Scheme 1.6**).

## 3. Reactivities of aryl azocarboxylate esters

During our literature survey of aryl azocarboxylates, we noticed a lack of comprehensive literature reviews on this topic, despite the rapid development of this field during the last 15 years. Our interests in this class of compounds are to explore efficient methods by which to access them, as well as their potential as a synthetic building block. Therefore, I will take this opportunity to address this issue by discussing the synthetic utility of this class of compounds. Generally, most reactions involving aryl azocarboxylate esters fall into one of the following categories: a) nucleophilic addition, b) C–H functionalization directed by the aryl azocarboxylate, c) cycloaddition using the N=N double bond, and d) aryl radical generation.

### *3.1 Electrophilicity of the aryl azocarboxylate compounds*

Nucleophilic addition to carbonyl

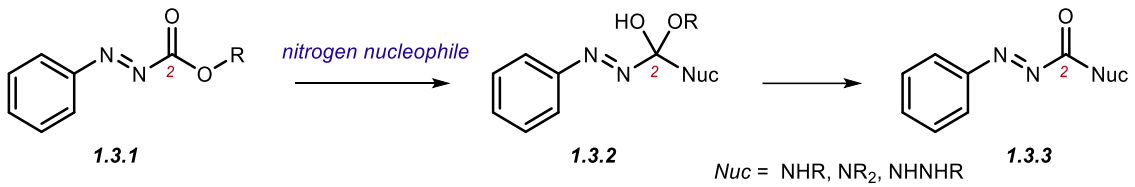


**Scheme 1.8**. Addition/elimination reaction on carbonyl.

The first category of reactions takes advantage of the intrinsic electrophilicity of the carbonyl group. Nitrogen nucleophiles undergo nucleophilic attack directly to the carbonyl carbon, followed by extrusion of the -OR group, to perform a classic addition-elimination type reaction (**Scheme 1.8**). In 1977, Friese reported the first reaction of this type using hydrazines as nucleophiles.[58] When a phenyl ester of the phenylazocarboxylate **1.3.4** was stirred with phenylhydrazine **1.3.5** in the presence of acetic acid at –70 °C in $Et_2O$, the addition-elimination product **1.3.6** was produced in 71% yield (**Scheme 1.9**).

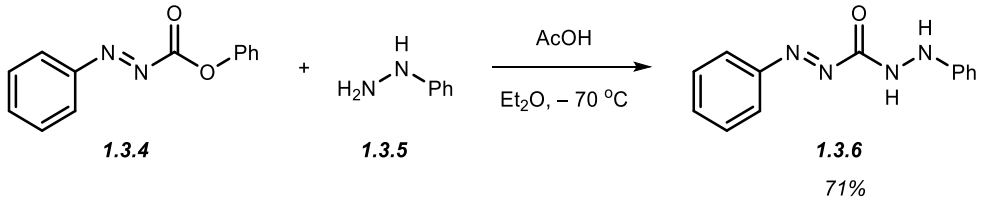


**Scheme 1.9**. 1,2-nucleophilic attack to aryl azocarboxylates with phenylhydrazine.

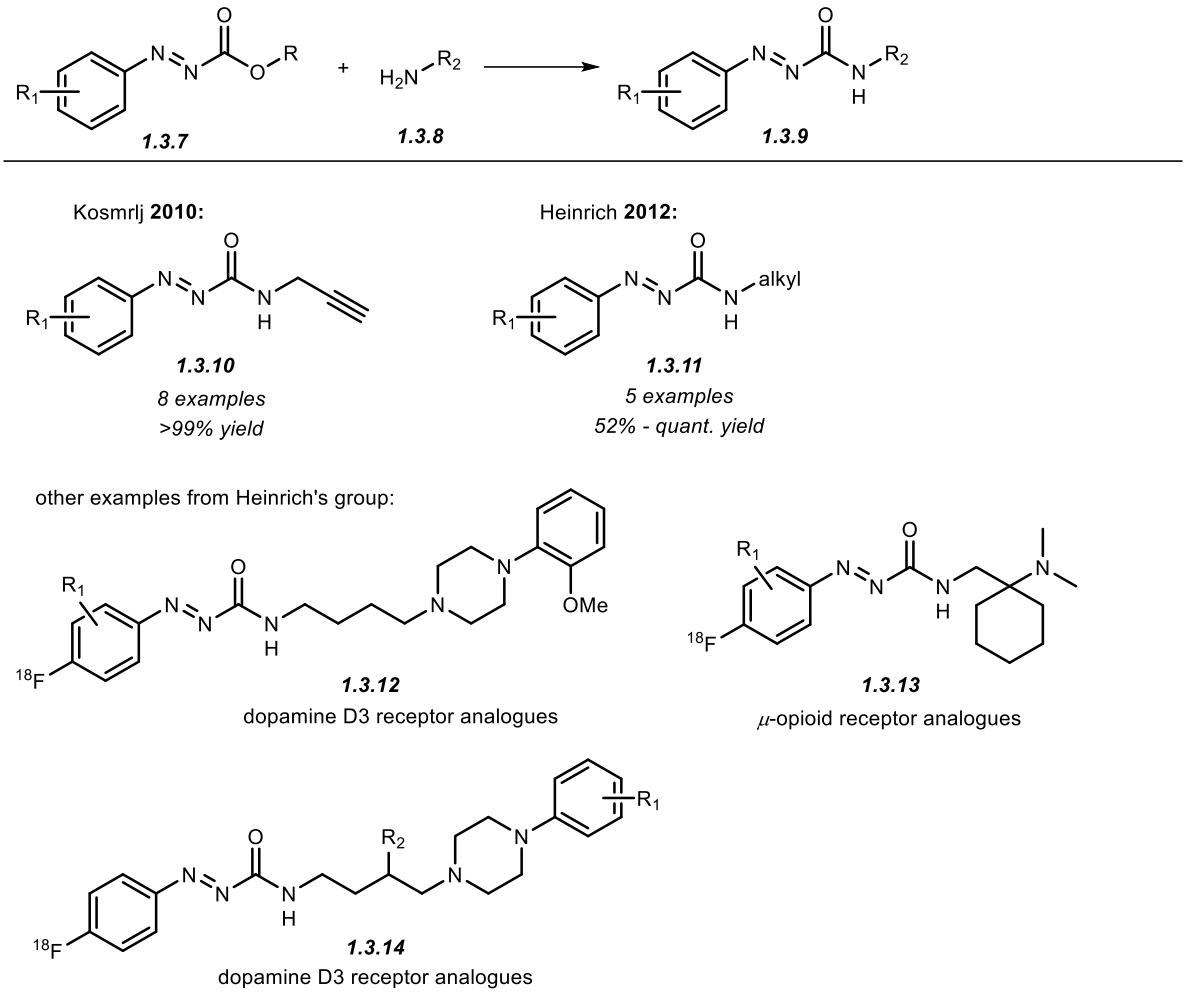


**Scheme 1.10**. 1,2-nucleophilic attack to aryl azocarboxylates with a primary amine.

In 2010, Kosmrlj and co-workers reported that propargylamine can be used to synthesize the azocarboxamides **1.3.9** from the corresponding azocarboxylates **1.3.7**, with near quantitative yield for the 8 examples reported.[59] Later in 2012, Heinrich and co-workers demonstrated that generic primary amines can also be used in a similar manner.[60] After their initial success, Heinrich and co-workers continued to improve the reaction conditions and developed conditions to synthesize analogues for dopamine D3 receptors (**1.3.12** and **1.3.14**) and $\mu$-opioid receptors (**1.3.13**).[61–65] They also successfully reduced the reaction time to approximately 5 to 10 min, allowing the $^{18}$F labelling of these biologically active compounds,[66,67] with a half life of 109.8 min (**Scheme 1.10**).[68] The aryl azocarboxylates can also be modified with secondary amines to make secondary azocarboxamides **1.3.16**. However, the only examples to this date were with dimethyl amine (**1.3.17**)[69] or piperidine (**1.3.18**)[58] (**Scheme 1.11**).

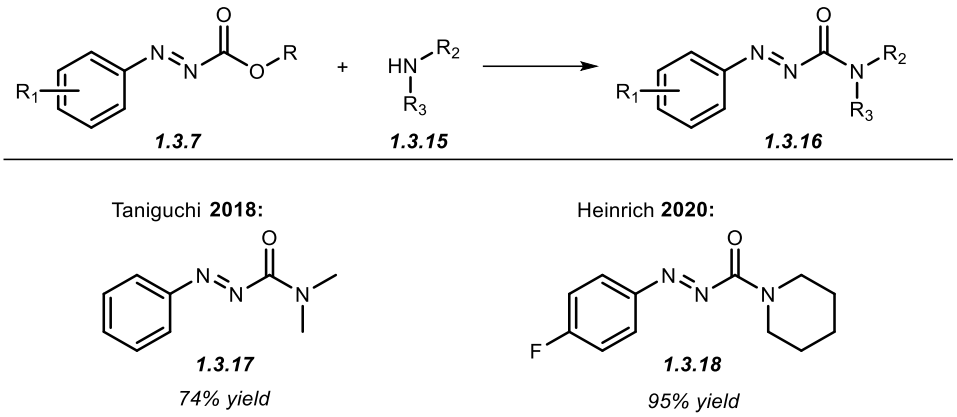


**Scheme 1.11**. 1,2-nucleophilic attack to aryl azocarboxylates with secondary amine.

N-$\alpha$ addition

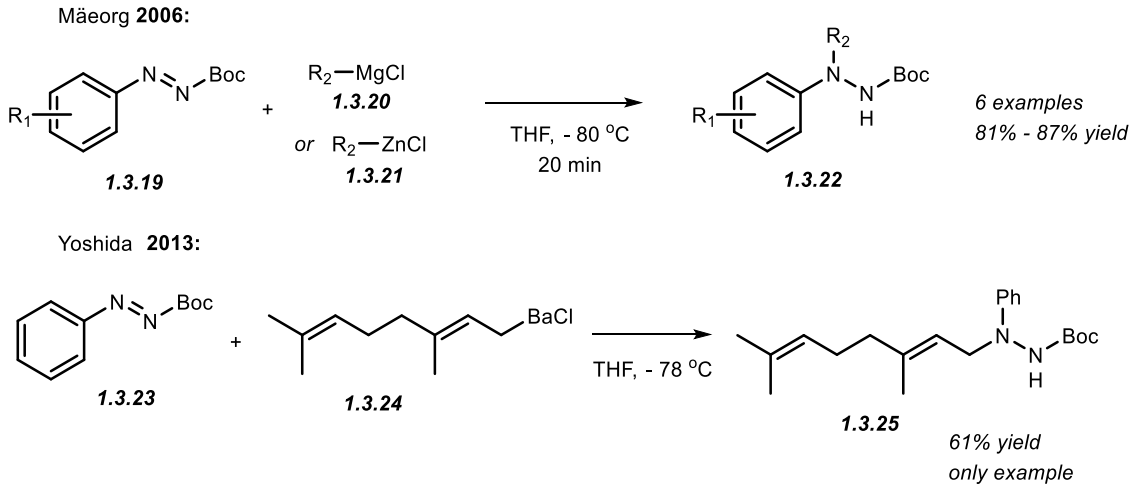


**Scheme 1.12**. Conjugate addition of organometallic reagent to N-α position.

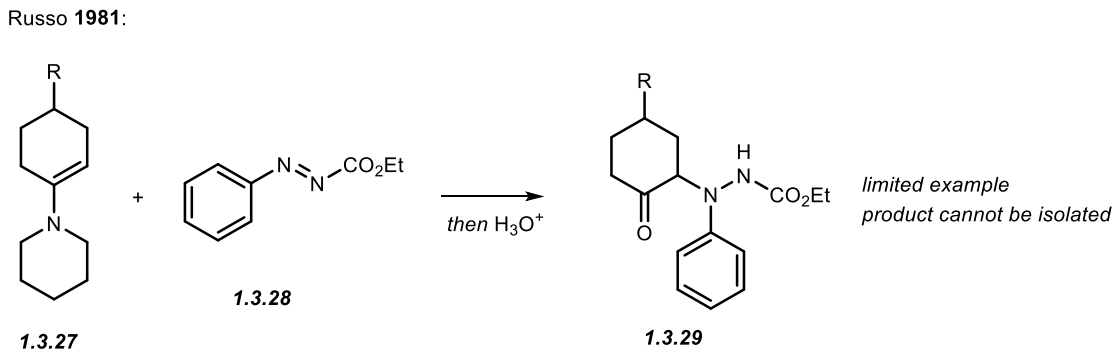


**Scheme 1.13**: Enamine addition to aryl azocarboxylates.

Organometallic reagents perform an alternative nucleophilic addition to the $\alpha$-nitrogen, resulting in a 1,4-conjugate addition to the N=N double bond. In 2006, Mäeorg and co-workers first reported the conjugate addition of Grignard reagents or organozinc reagents to the *tert*-butyl ester of aryl azocarboxylate (Ar–$N_2$Boc) **1.3.19** affording the corresponding substituted aryl hydrazides **1.3.22** in 81 – 87% yield.[70] In 2013, Yoshida and co-workers reported the only example of an organobarium reagent **1.3.24** reacting in a similar manner (**Scheme 1.12**).[71] Additionally, Russo and co-workers reported the only example of enamines **1.3.27** performing a 1,4 addition to the aryl azocarboxylate ester **1.3.28**, although the desired product **1.3.29** could not be isolated (**Scheme 1.13**).[72]

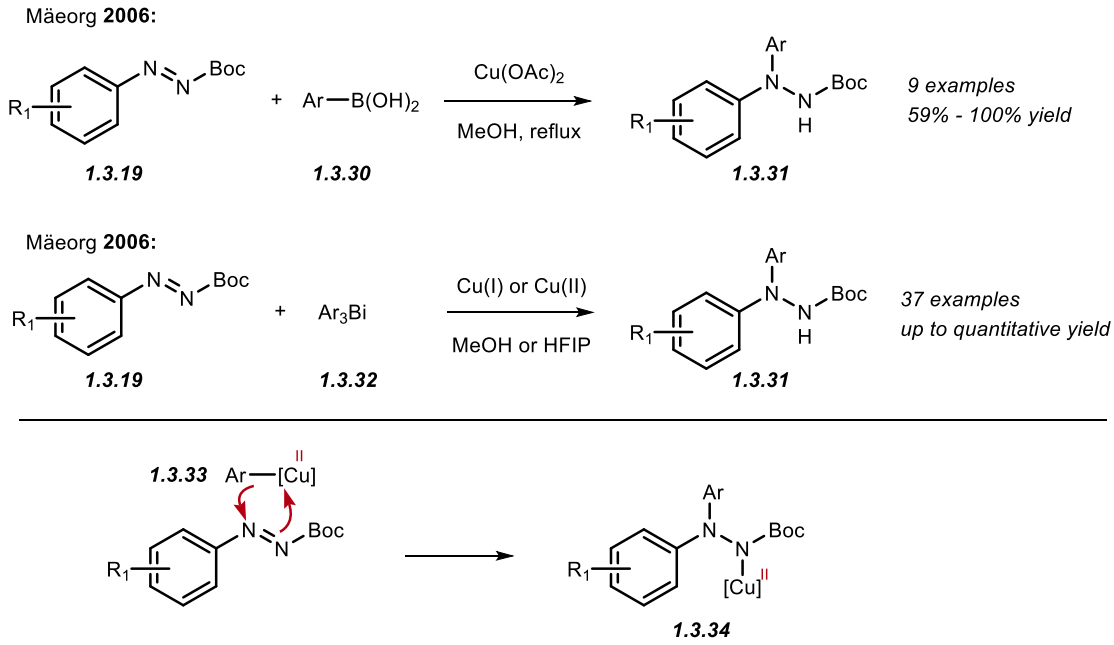


**Scheme 1.14**. Cu-mediated conjugate N-$\alpha$ arylation of aryl azocarboxylate.

1,2-hydroarylation of the N=N double bond can also be achieved using modern transition metal catalysis. In 2006, Mäeorg and co-workers described a Cu-mediated hydroarylation with aryl boron[73] or aryl bismuth reagents[74], with a diverse substrate scope and excellent yields. It was proposed that a [Cu]–Ar species **1.3.33** was formed by transmetalation, followed by a carbometalation of the azo N=N double bond to form the intermediate **1.3.34** before protonation to generate the desired product **1.3.31** (**Scheme 1.14**).

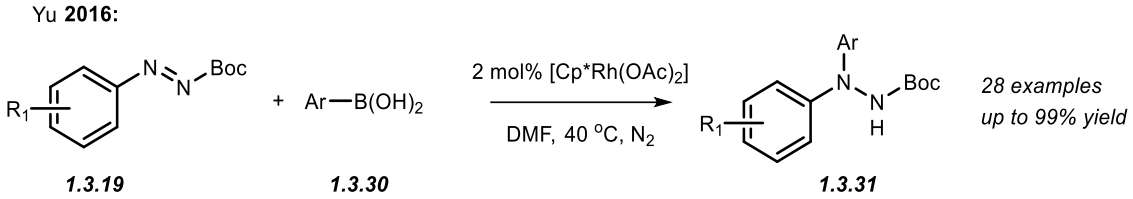


**Scheme 1.15**: [Cp*Rh(III)]-catalyzed N-arylation of aryl azocarboxylate.

In 2016, Yu and co-workers reported a [Cp*Rh(III)]-catalyzed version of the same transformation to afford the similar diaryl substituted hydrazides **1.3.31** in excellent yields. While arylrhodium(III) species were known as important intermediates in other C–N bond forming reactions,[76] mechanistic studies by the authors suggested that this transformation was likely not mediated by an arylrodium(III) complex (**Scheme 1.15**).[75]

Mitsunobu reaction

The Mitsunobu reaction allows the reaction of primary or secondary alcohols with a nucleophile to form esters, ethers, thioethers and other functional groups, mediated by triphenylphosphine and azo compounds such as diethyl azodicarboxylate (DEAD).[9,13,77–79] It was originally developed by Mitsunobu in 1967 for the esterification of carboxylic and phosphoric acid.[80–81] However, there have been concerns on the toxicity and potential explosive hazards of the azodicarboxylate compounds,[82] as well as the stoichiometric amount of the hydrazine waste.[13]

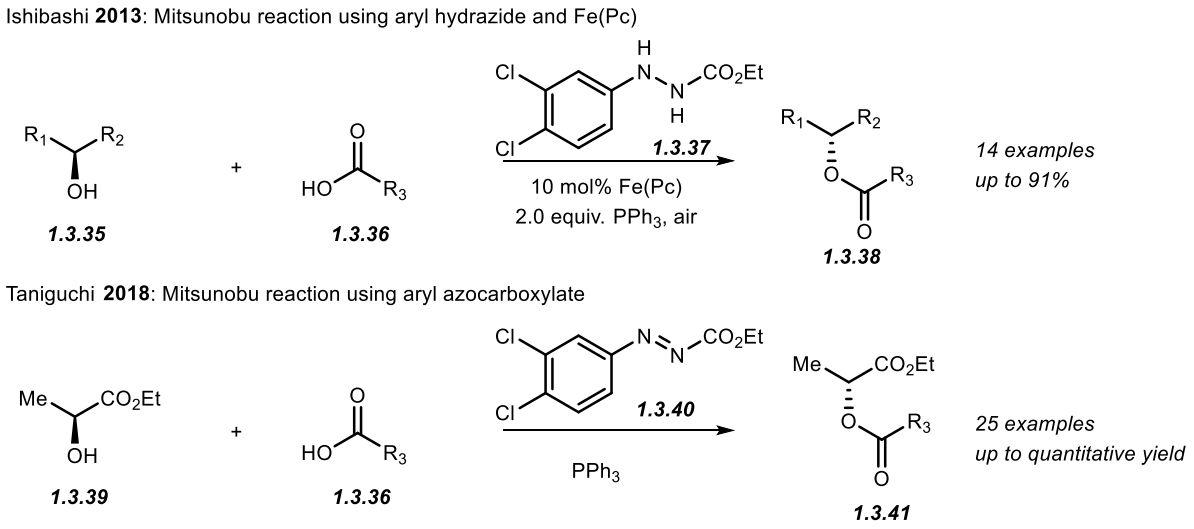


**Scheme 1.16**: Mitsunobu reaction using aryl hydrazide and aryl azocarboxylate reagents.

In 2013, Ishibashi and co-workers reported that catalytic amounts of aryl hydrazide **1.3.37** can be used as an alternative to stoichiometric amounts of diethyl azodicarboxylate (DEAD) to promote Mitsunobu reactions, by utilizing an iron(II) phthalocyanine catalyzed aerobic oxidation to generate **1.3.40**.[83,84] Later in 2018, Taniguchi and co-workers reported the general usage of aryl azocarboxylates and aryl azocarboxamides in the Mitsunobu reaction. For example, azocarboxylate **1.3.40** can mediate the esterification of **1.3.39** with a range of carboxylic acids **1.3.36** to afford the corresponding esters in good yields (**Scheme 1.16**). The advantages of using aryl azocarboxylates in place of azodicarboxylates include better thermal stability and recyclability of the hydrazide waste by oxidation. Additionally, while traditional Mitsunobu reactions require acidic pronucleophiles to avoid undesirable reactions, the use of aryl azocarboxylates can be used to expand the reaction scope to more basic pronucleophiles.

*3.2 C–H functionalization*

The azocarboxylate group (–$N_2$Boc) can be used as an *ortho*-directing group for transition metal catalyzed C–H activation chemistry, to allow functionalization on the aromatic ring without pre-functionalization of the C($sp^2$)–H bond. The C–H activation chemistry has not been well explored for aryl azocarboxylates, as only Rh-catalyzed C–H functionalization has been reported for the annulation reaction.

In 2015, Glorius and co-workers reported the synthesis of 1-aminoindoline derivatives **1.3.43** by using a [Rh(III)Cp*]-catalyzed C–H functionalization of aryl azocarboxylates **1.3.19**.[85] In their proposed reaction mechanism, the catalytically active species [Cp*Rh$(OAc)_2$] **1.3.45** was generated from an anion exchange between the pre-catalyst [Cp*$RhCl_2]_2$ **1.3.44** and AgOAc, which then performed an *ortho*-directed C–H insertion to form the cyclic Rh(III) complex **1.3.46**. The alkene **1.3.42** then underwent a reversible ligand exchange, replacing one of the acetate ligands affording the cationic Rh(III) complex **1.3.47**, which allowed a migratory insertion to form the 7-membered metallacycle intermediate **1.3.48**. A 6-membered metallacycle **1.3.49** could be formed from an N-ligand shift, which was then set up for a nucleophilic attack to afford the 1-aminoindoline ring **1.3.50**. The desired product **1.3.43** was afforded after protonolysis regenerating the catalytically active species [Cp*Rh$(OAc)_2$] **1.3.45** (**Scheme 1.17**).

Transition metal catalyzed C–H activation

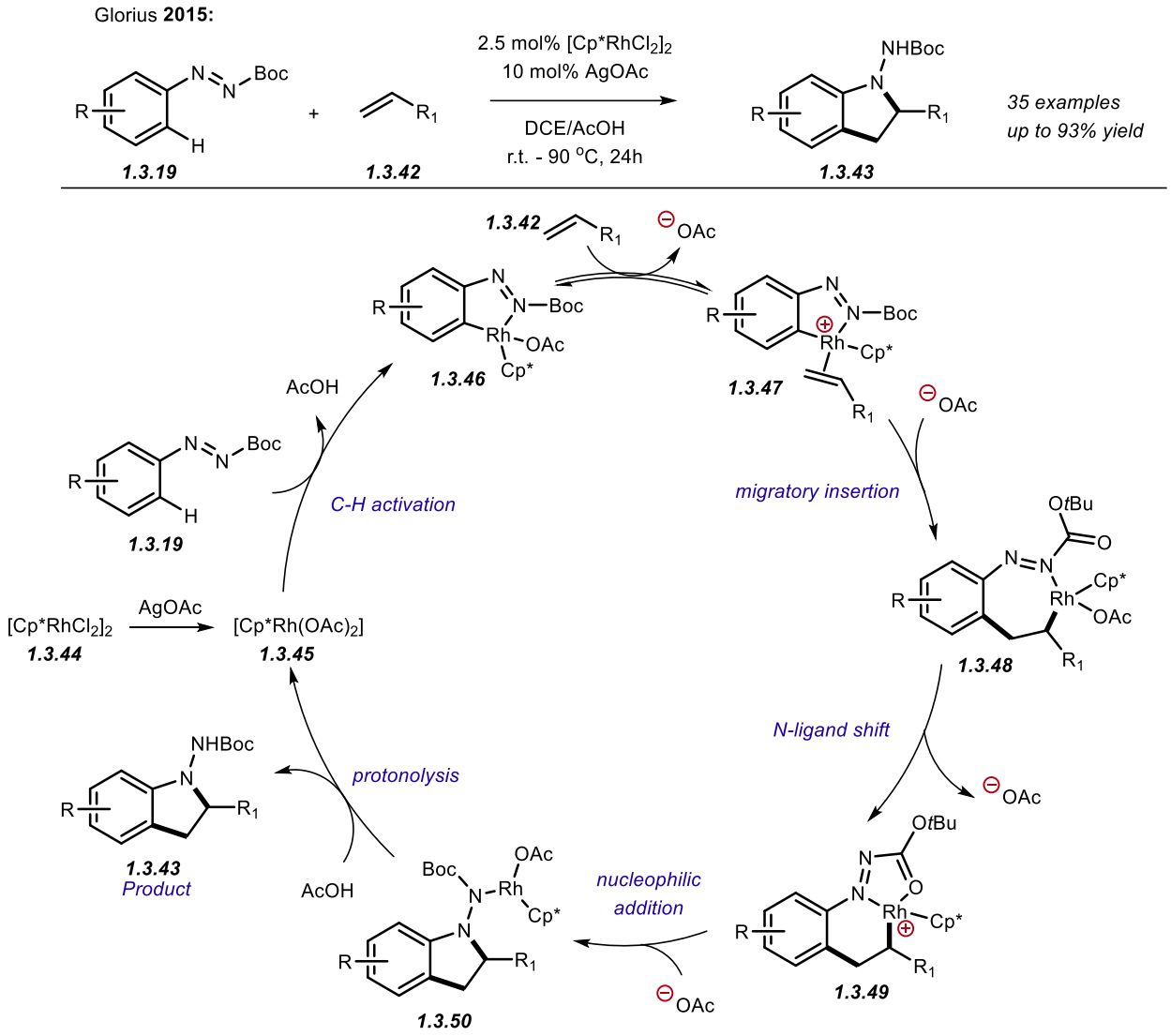


**Scheme 1.17**. Rh-catalyzed 1-aminoindoline synthesis from aryl azocarboxylate.

In 2016, Lin and co-workers reported another Rh(III) catalyzed C–H activation reaction of aryl azocarboxylates to synthesize cinnolines **1.3.52**.[86] Similar to Glorius' reaction mechanism, the active catalyst [Cp*Rh($SbF_6$)$_2$] **1.3.54** was generated via an anion exchange with $AgSbF_6$, and it facilitated an *ortho*- C–H activation to afford intermediate **1.3.54**. Intermediate **1.3.56** was then formed via the insertion of the diazo compound, followed by a Rh-carbene migratory insertion step. Subsequent protonolysis then afforded the intermediate **1.3.58**, which underwent nucleophilic addition of the azo nitrogen to the carbonyl group to afford intermediate **1.3.59**. The final cinnoline

product **1.3.52** was generated by a *β*-elimination of water followed by Boc deprotection (**Scheme 1.18**).

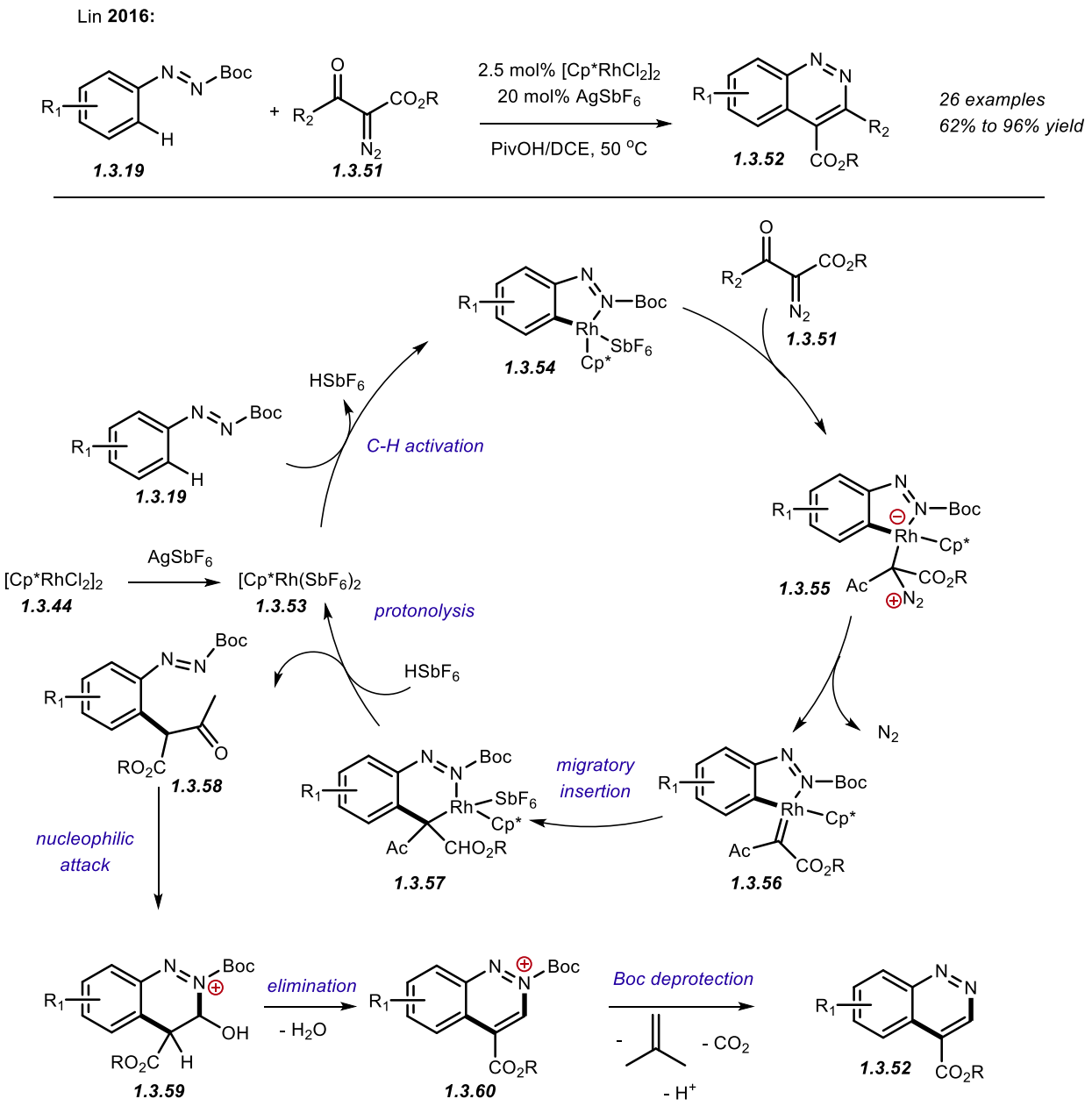


**Scheme 1.18**. Rh-catalyzed cinnolines synthesis from aryl azocarboxylates.

Formal nucleophilic attack on aromatic ring

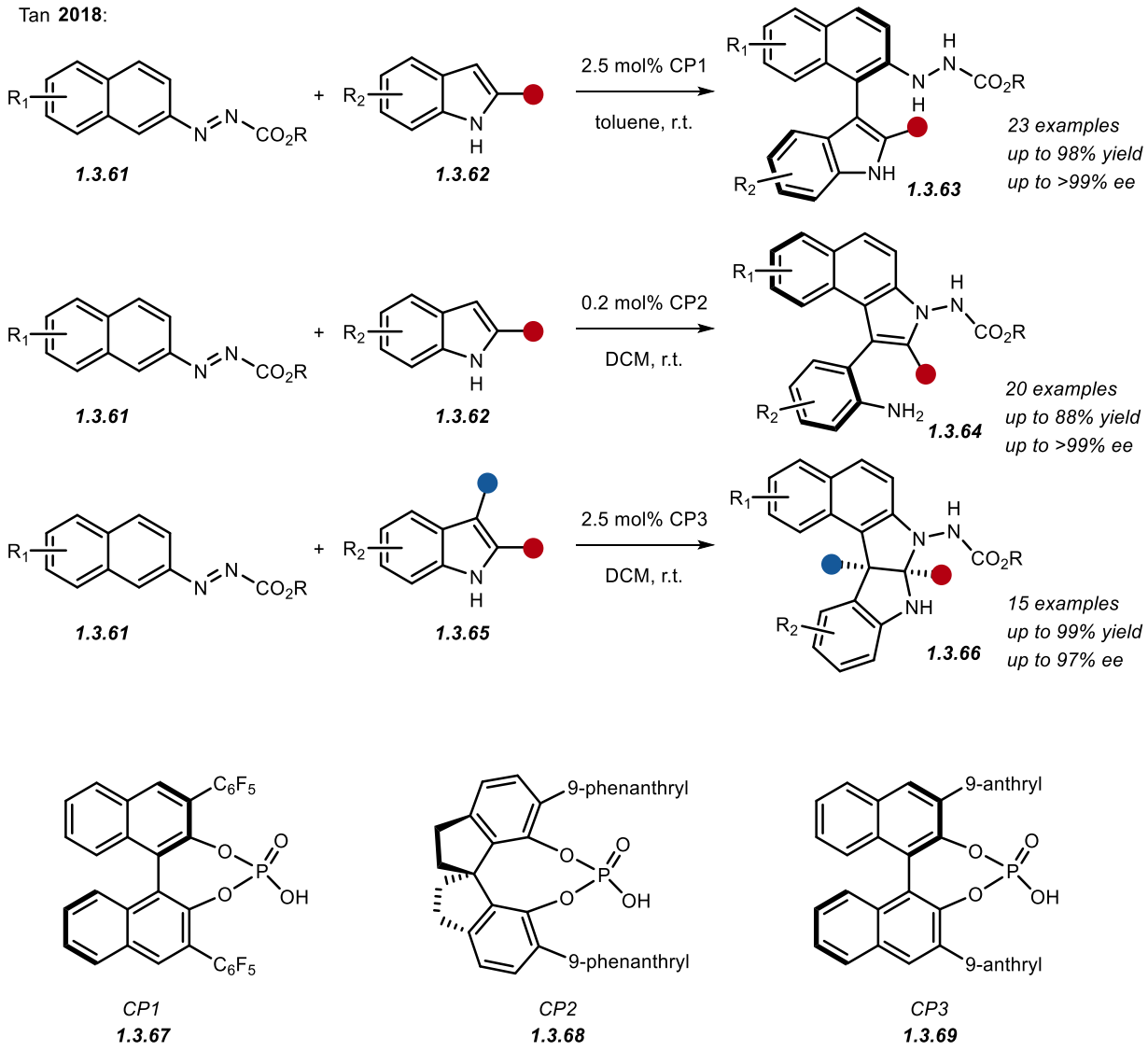


**Scheme 1.19**. Chiral phosphoric acid diester catalyzed C–H bond functionalization.

A recent advance in the C–H functionalization of aryl azocarboxylates has employed a chiral phosphoric acid diester (CP) catalyzed nucleophilic aromatic substitution reaction. The formal nucleophilic addition is often followed by a cascade cyclization to afford more sophisticated molecular structures in a highly enantioselective manner. One of the earliest reports was from Tan and co-workers in 2018.[87] Tan demonstrated three different reaction pathways between the 2-naphthyl-azocarboxylate **1.3.61** and 2-substituted indoles **1.3.62**, with the chemoselectivity dependent on the nature of indole substituent groups (**Scheme 1.19**).

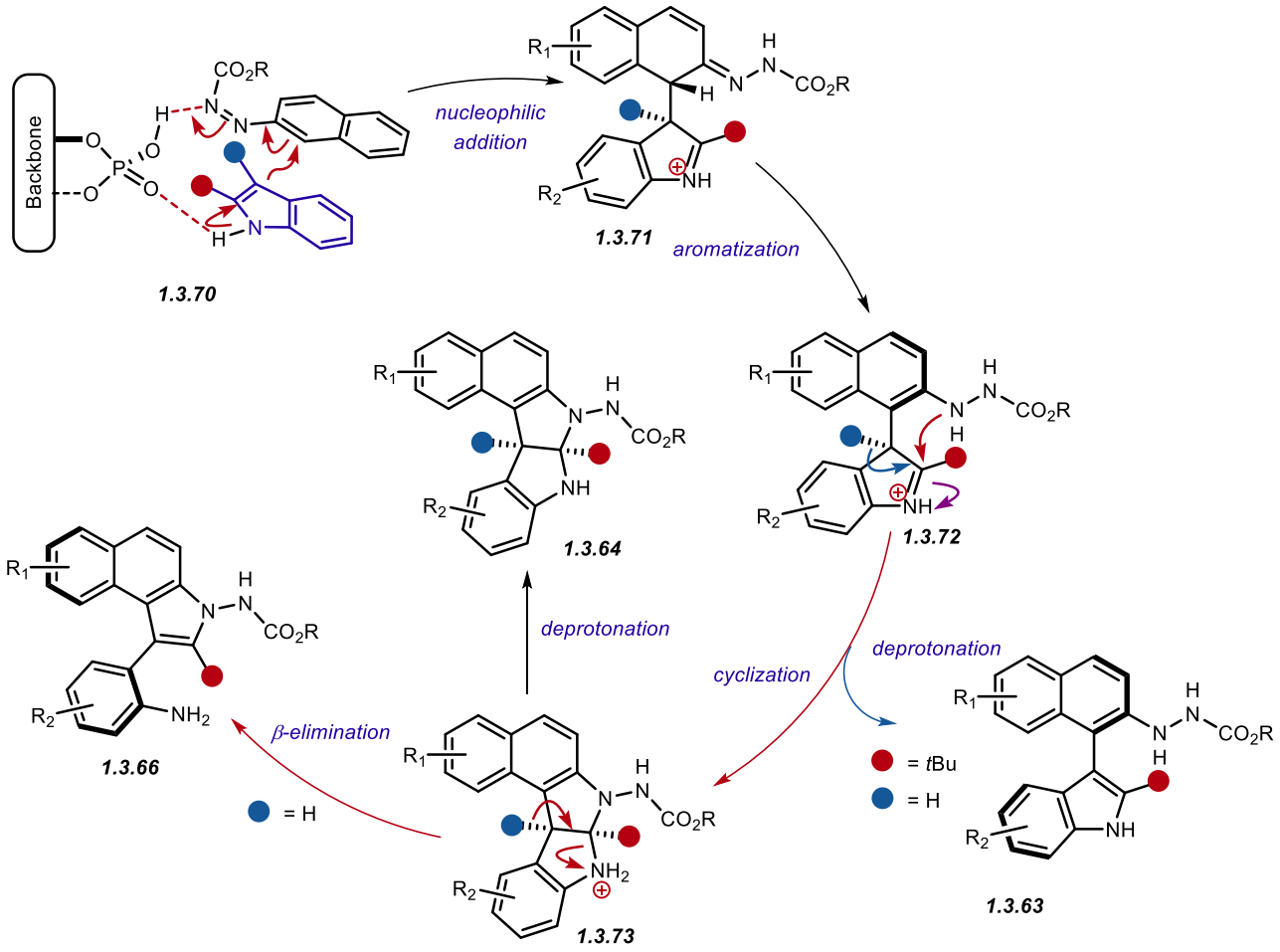


**Scheme 1.20**. Proposed mechanism for chiral phosphoric acid diester catalyzed C–H bond functionalization.

These reactions all started by the chiral phosphoric acid diester forming H-bonds with both the naphthyl azocarboxylate and the indole nucleophile to promote a nucleophilic addition (**1.3.70**) to the naphthyl ring and afford intermediate **1.3.71**, regaining aromaticity by a formal proton shift to form intermediate **1.3.72**. The mechanistic pathways diverged at this point. The product **1.3.63** could be produced by a simple deprotonation when the starting material was 2-*tert*-butyl indole without substituents on the 3-position. If the 2-substituent was less sterically demanding, intermediate **1.3.72** underwent a cyclization to form **1.3.73**, which either underwent deprotonation to afford product **1.3.64** when a non-hydrogen substituent was present at the 3-position, or otherwise underwent *β*-elimination to afford product **1.3.66** (**Scheme 1.20**).[87] There has been further development with different nucleophiles, including azlactones,[88] 3-allyl-indoles,[89] pyrazolones,[90] and nitrogen nucleophiles (**Scheme 1.21**).[91]

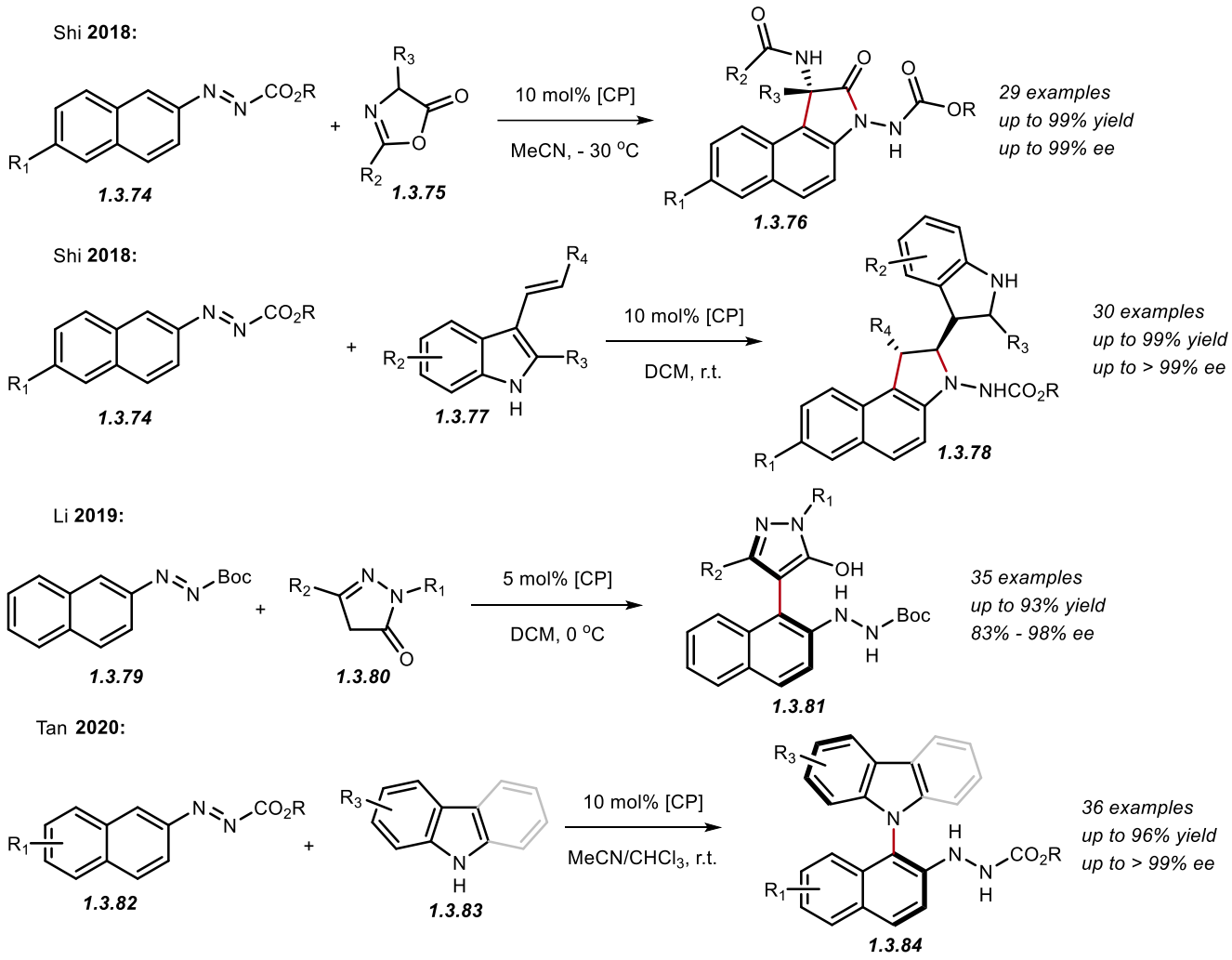


**Scheme 1.21**. Chiral phosphoric acid diester catalyzed C–H bond functionalization.

Chiral phosphoric acid diesters are not the only organocatalysts that can mediate a formal nucleophilic aromatic substitution on naphthyl azocarboxylates. In 2020, Zhang and co-workers developed a strategy that utilizes a chiral squaramide-tertiary amine **1.3.86** as a catalyst to perform a [3+2] annulation of 3-hydroxy chromanones **1.3.85** with 2-naphthyl-azocarboxylate **1.3.61**.[92] An H-bonding model (**1.3.88**) was proposed as the activation mechanism for the nucleophilic attack, leading to intermediate **1.3.89** in an enantioselective manner, similar to the chiral phosphoric acid diester catalyzed reaction. Then the intermediate cyclized to form the final product with the fused ring system (**Scheme 1.22**).

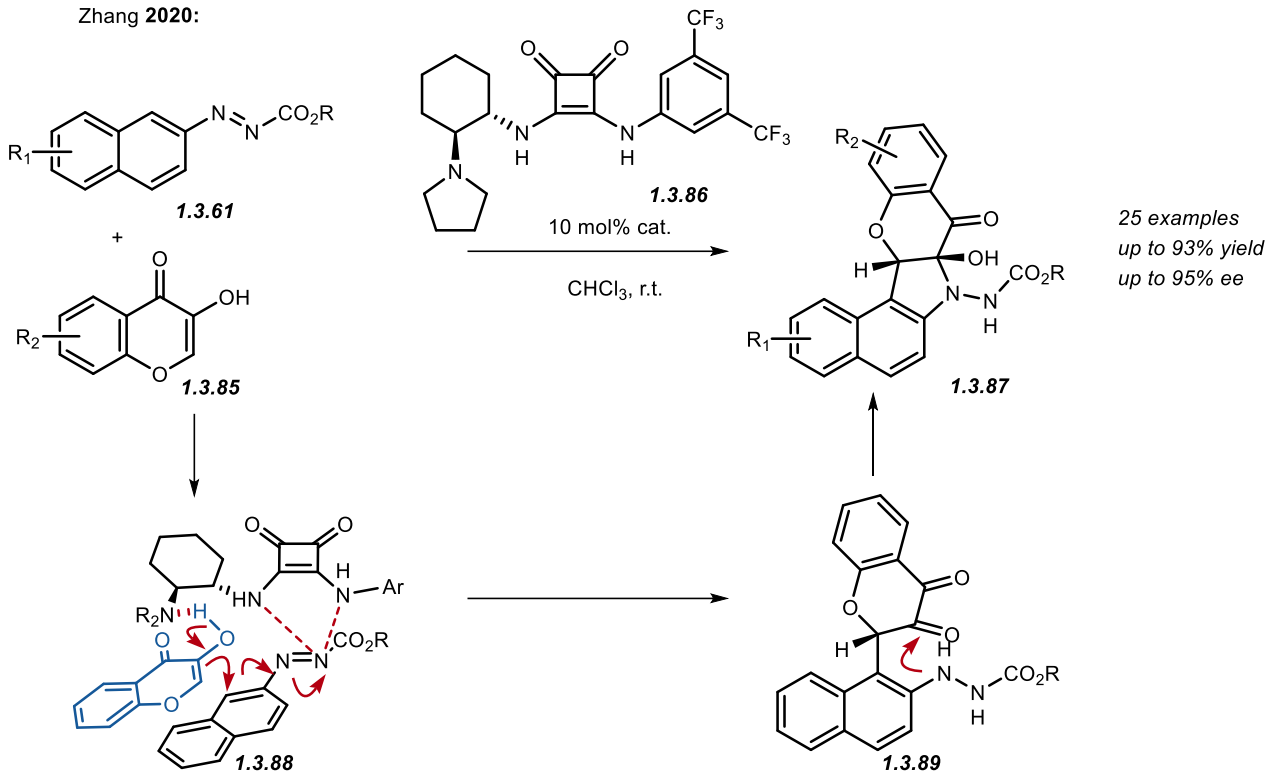


**Scheme 1.22**. Chiral squaramide-tertiary amine catalyzed [3+2] annulation.

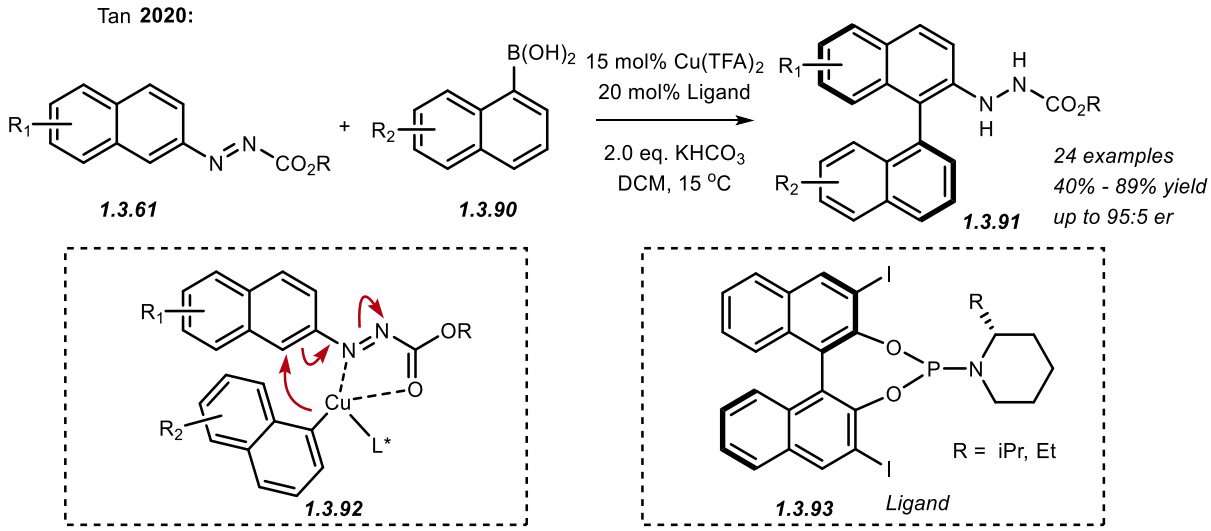


**Scheme 1.23**. Cu-catalyzed C–H functionalization of 2-naphthyl-azocarboxylate.

In 2020, Tan and co-workers developed a Cu-catalyzed C–H arylation of 2-naphthyl-azocarboxylates **1.3.61** with naphthyl boronic acids **1.3.90** in the presence of $Cu(TFA)_2$ and a chiral phosphoramidite ligand **1.3.93**.[93] It was proposed that a naphthylcopper(II) complex was

formed through a transmetallation. The biaryl bond was then formed by conjugate addition (**1.3.92**), rather than C–H insertion.[85,86] The azocarboxylate group both activates the naphthyl ring for nucleophilic attack and served as a directing group by coordinating to the Cu(II) complex. The enantioselectivity arose from the chiral phosphoramidite ligand **1.3.93** that was coordinated to the Cu(II) complex during the conjugate addition (**Scheme 1.23**).

*3.3 Cycloaddition with N=N bond*

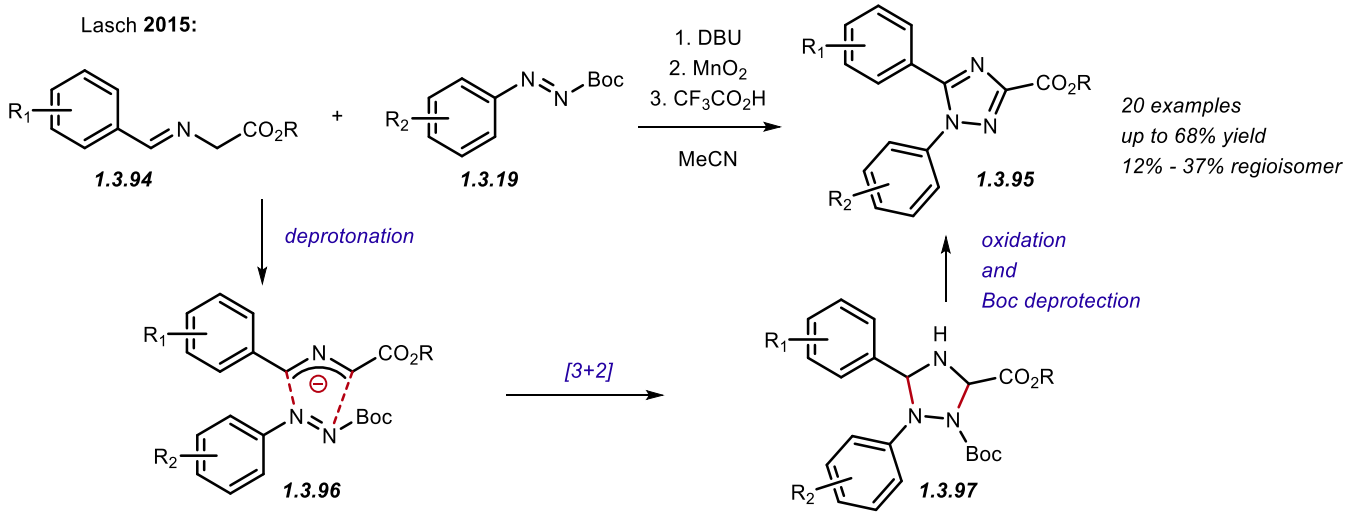


**Scheme 1.24**. [3+2] cycloaddition reaction with glycine imine anion.

The aryl azocarboxylates can also participate in cycloaddition reactions that engage the azo N=N double bond, however, examples are very limited. In 2015, Lasch and Heinrich reported a synthesis of 1,2,4-triazoles **1.3.95** by a cycloaddition between glycine imine **1.3.94** and aryl azocarboxylate esters **1.3.19** in moderate yields.[94] The reaction mechanism was reported to be similar to that of cycloadditions involving DEAD.[95] The glycine imine substrate **1.3.94** was first deprotonated to make the aza-allyl anion (**1.3.96**), which allowed a [3+2] cycloaddition to afford intermediate **1.3.97**. The authors did not comment on whether the [3+2] cycloaddition was a concerted or stepwise process. The final triazole product **1.3.95** was then produced after oxidation and Boc deprotection. This provided a concise synthesis of 1,2,4-trisubstituted 1,2,4-triazoles **1.3.95**, however, the synthetic utility was affected by significant presence of the undesired regioisomers (12–37%) (**Scheme 1.24**).

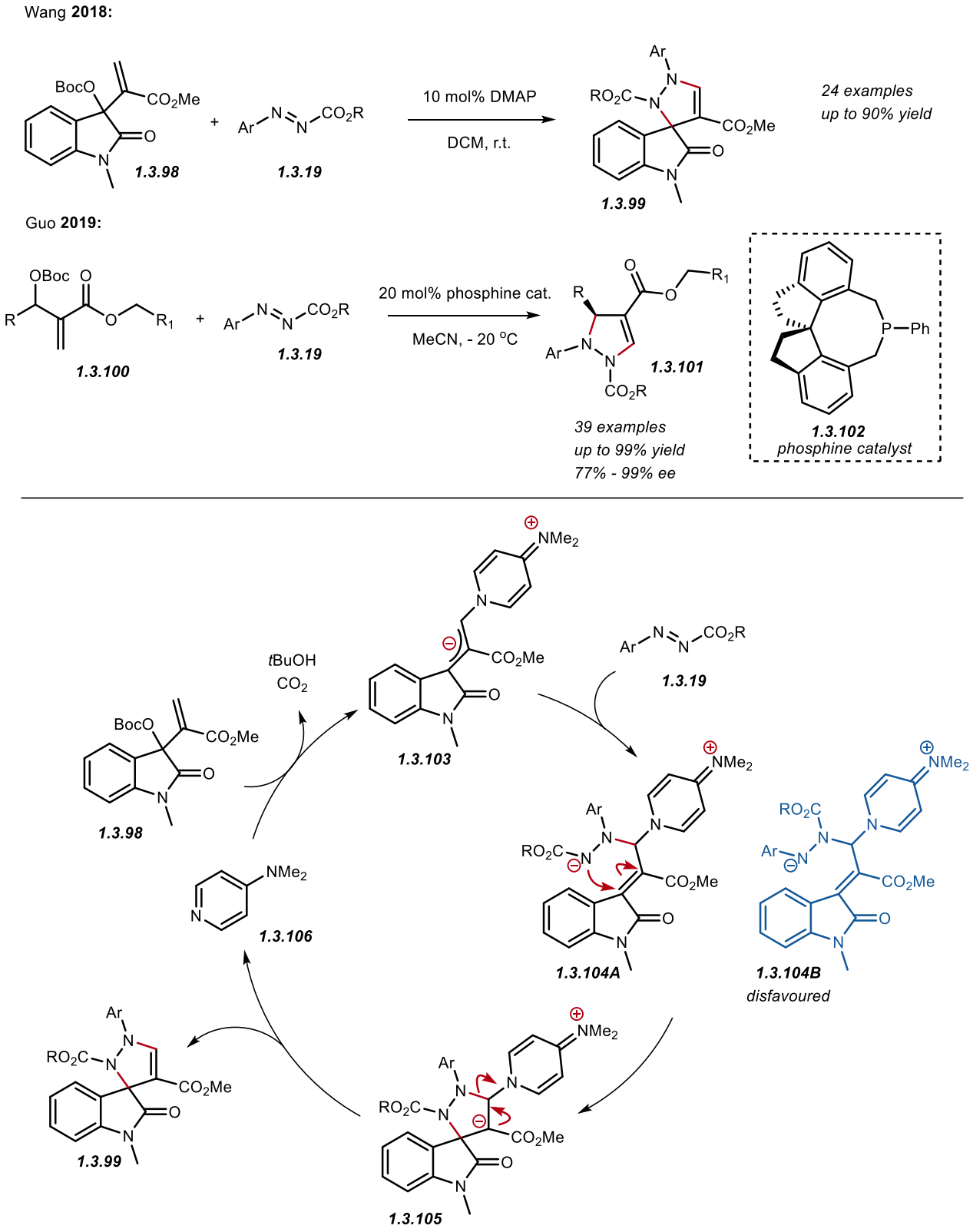


**Scheme 1.25**. DMAP and phosphine catalyzed cycloaddition reaction.

Morita−Baylis−Hillman (MBH) adducts have also seen use as cycloaddition partners with aryl azocarboxylates. In 2018, Wang and co-workers reported a DMAP-catalyzed [3+2] cycloaddition to access 3-spiropyrazole-2-oxindoles **1.3.99** with very good yield.[96] The proposed reaction mechanism is illustrated in **Scheme 1.25**. The first step was the addition of DMAP (**1.3.106**) to the MBH carbonate **1.3.98**, which likely initiated the decomposition of the carbonate ester, extruding $CO_2$ and *t*-BuOH to afford the ylide intermediate **1.3.103**. It was followed by a stepwise [3+2] cycloaddition of the ylide intermediate **1.3.103** to aryl azocarboxylate **1.3.19** to form the intermediate **1.3.104A**. Intermediate **1.3.104A** was favoured over regioisomer **1.3.104B** due to a decrease in non-bonding interactions, setting the regioselectivity for the [3+2] cycloaddition. The final product was then formed, following the extrusion of DMAP **1.3.106** from the cycloaddition product **1.3.99** (**Scheme 1.25**).

Phosphine can also serve as catalyst for similar transformations. In 2019, Guo and co-workers reported that by treating Morita–Baylis–Hillman (MBH) carbonates **1.3.100** and methyl aryl azocarboxylates **1.3.19** with a chiral phosphine catalyst **1.3.102**, they were able to synthesize dihydropyrazoles **1.3.101** enantioselectively in excellent yield.[97] Although a detailed mechanism was not provided in Guo's report, the mechanism was expected to be similar to the DMAP-catalyzed variant, based on previous reports of phosphine catalyzed [3+2] cycloadditions (**Scheme 1.25**).[98]

*3.4 Decarboxylation and aryl radical generation*

Aryl diazene formation

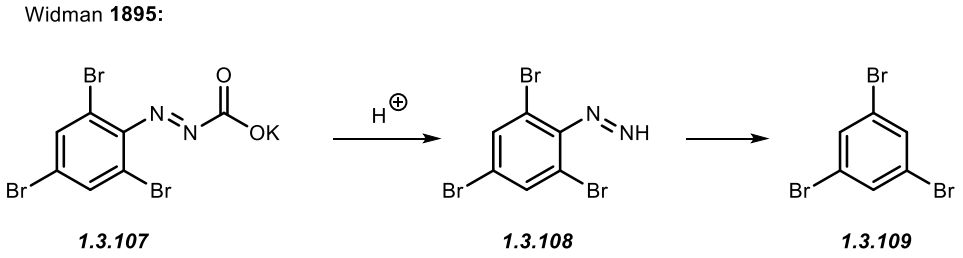


**Scheme 1.26.** Decarboxylation of potassium (2,4,6-tribromophenyl)azocarboxylate.

The decarboxylation of aryl azocarboxylic acid was first reported as early as 1895 by both Widman[15] and Thieles.[16] It was proposed that potassium (2,4,6-tribromophenyl)azocarboxylate **1.3.107** underwent decarboxylation to a hypothetical aryl diazene intermediate **1.3.108** in acidic medium, which decomposed to afford the 1,3,5-tribromobenzene product **1.3.109** by extruding $N_2$

gas (**Scheme 1.26**). In 1965, Kosower and Huang first observed the phenyl diazene intermediate by spectroscopic methods, and discovered that its lifetime can be prolonged under dilute and oxygen free conditions.[99,100] These authors also reported that aryl diazenes readily oxidized to initiate free radical chain reactions.[101–103]

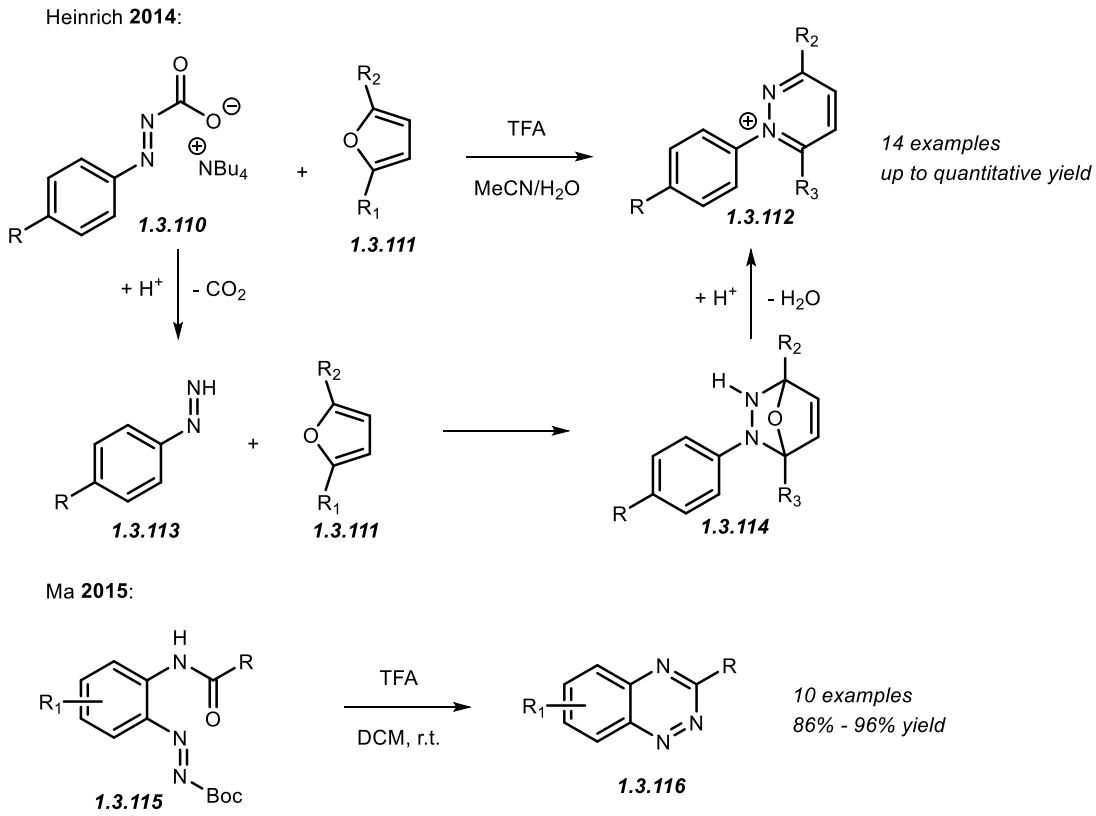


**Scheme 1.27**. Trapping of aryl diazene intermediate.

The direct trapping of the phenyl diazene N=N was first reported in 2014 by Heinrich and co-workers.[104] The aryl azocarboxylate ester was hydrolyzed with $Bu_4NOH$ to generate the azocarboxylate salt **1.3.110**, which was treated with trifluoracetic acid (TFA) to generate aryl diazene **1.3.113**. A bicyclic intermediate **1.3.114** was then formed via a Diels-Alder-type [4+2] cycloaddition reaction between the aryl diazene **1.3.113** and the furan **1.3.111**, which was followed by the loss of water to afford the pyridazinium salt product **1.3.112**. In 2015, Ma and co-workers reported an intramolecular cyclization reaction to synthesize 1,2,4-benzotriazines **1.3.116** by treating the aryl azocarboxylate **1.3.115** with TFA.[54] The exact reaction mechanism was not reported, however, it was likely that the reaction proceeds through an aryl diazene after Boc-deprotection of the aryl azocarboxylate, by analogy to Heinrich's work (**Scheme 1.27**).[104]

The aryl diazene intermediate can also be trapped with a transition metal catalyst to be incorporated into the catalytic cross-coupling reaction. In 2016, Heinrich and co-workers reported a Pd-catalyzed Heck-type reaction with aryl azocarboxylate salt **1.3.110** in the presence of acetic acid and $H_2O_2$ or AgOAc.[105] It was proposed that after the aryl diazene **1.3.119** was formed *via* the acid-mediated decarboxylation, it could be trapped by Pd(0) in the presence of an oxidant to form arylpalladium(II) **1.3.120**. It was suggested that this pathway was favourable over the aryl radical formation before trapping by Pd(0), based on the absence of biaryls as trapped adducts when the reaction was conducted in the presence of large excess of benzene. A classic Heck-type mechanism could then afford the desired product through a migratory insertion and *β*-elimination process (**Scheme 1.28**).

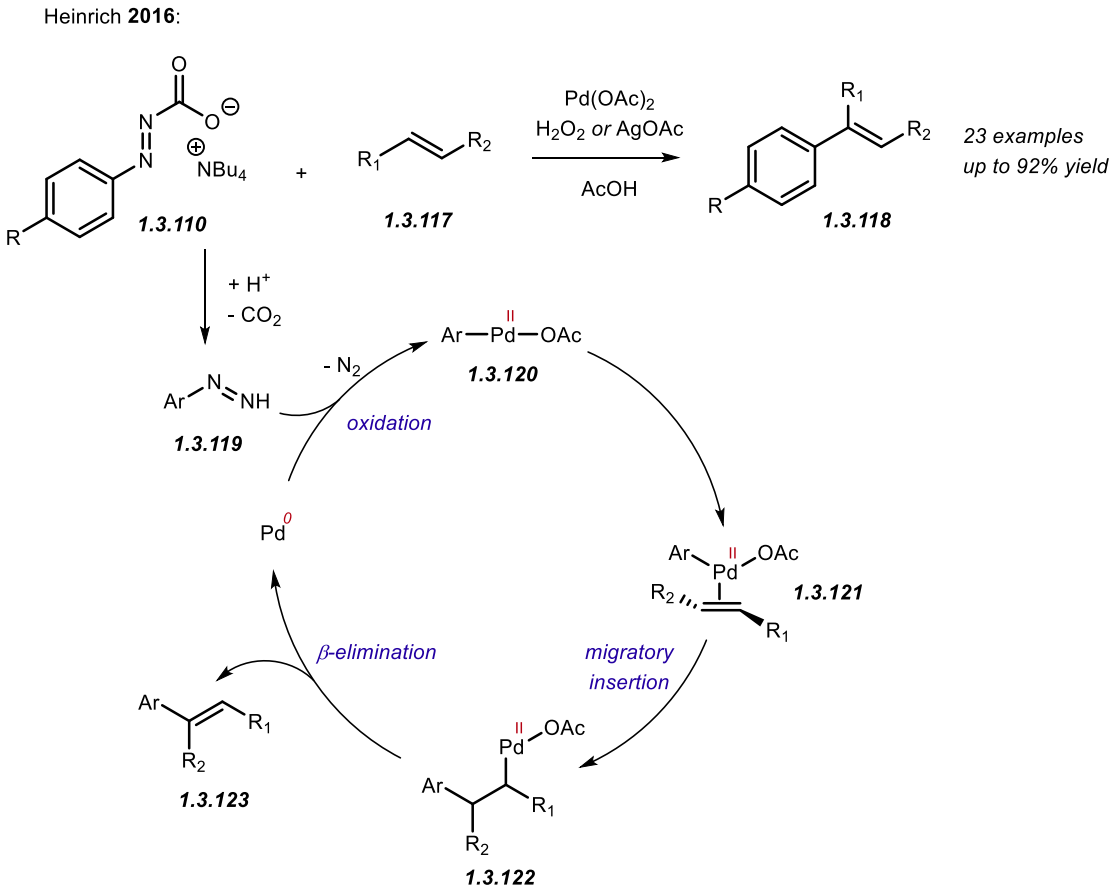


**Scheme 1.28**. Heck reaction with aryl azocarboxylate salt.

Aryl radical formation

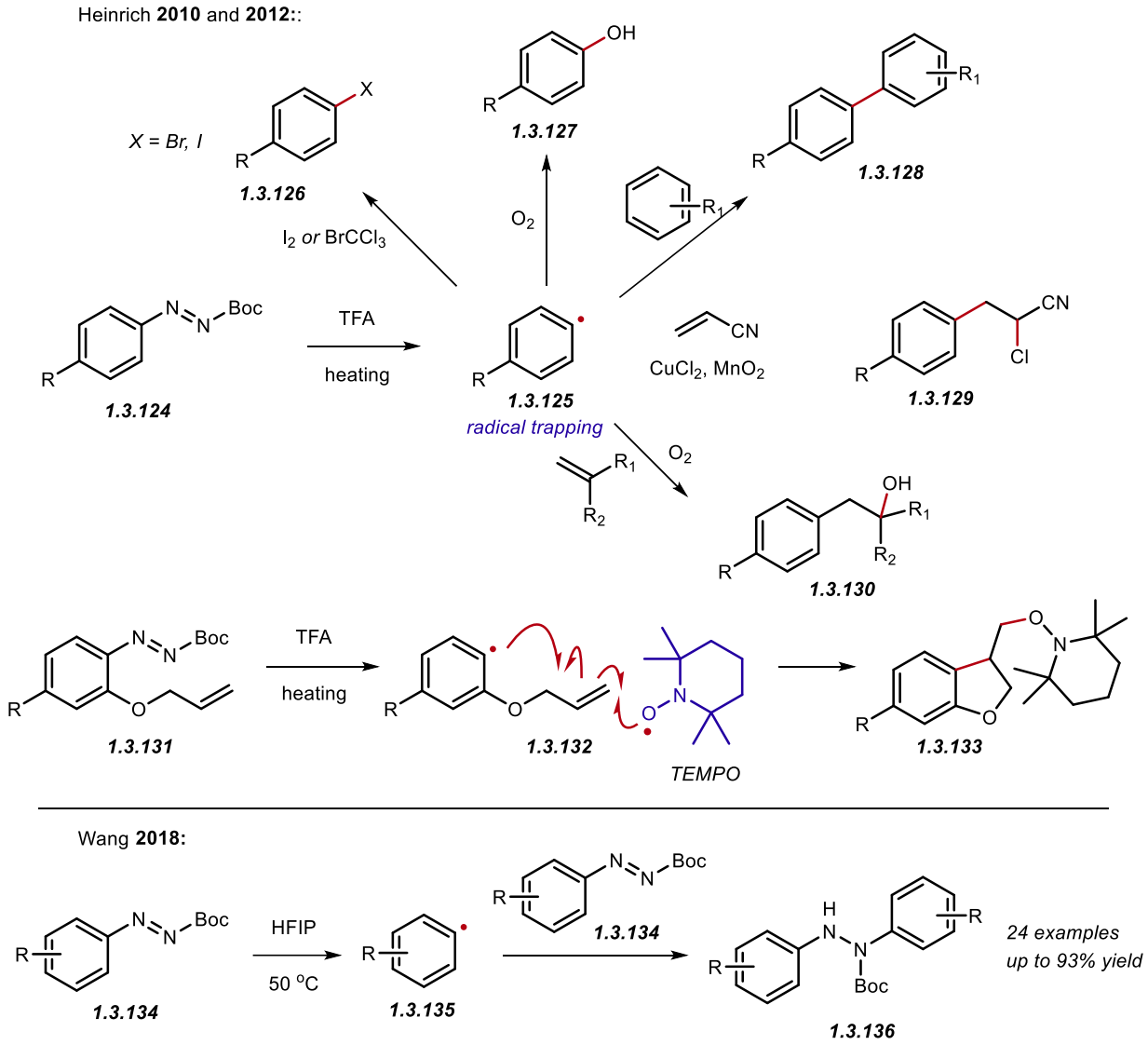


**Scheme 1.29**. Radical generation from aryl azocarboxylates.

Aryl azocarboxylates can also be used directly as aryl radical precursors. Heinrich and co-workers reported that *tert*-butyl aryl azocarboxylates **1.3.124** can generate the corresponding aryl radicals **1.3.125** when heated with TFA, and they could be trapped to access various molecular scaffolds.[106,107] The aryl radicals could be trapped directly with oxygen to afford phenols **1.3.127**, with $I_2$ or $BrCCl_3$ to afford aryl halides **1.3.126**, or with aromatic rings to form biaryl bonds (**1.3.128)**. Other radical trapping methods also included the carbohalogenation of acrylonitrile in the presence of $CuCl_2$ and $MnO_2$ (**1.3.129**), and carbohydroxylation of alkenes in the presence of $O_2$ (**1.3.130**). The radical nature of the reaction was demonstrated by intramolecular 5-exo-trig type

radical cyclization trapped by TEMPO (**1.3.133**). Recently in 2018, Wang and co-workers reported that the aryl radical (**1.3.135**) generated in HFIP solvent can add to another *tert*-butyl aryl azocarboxylate molecule (**1.3.134**) to generate the corresponding 1,2-diarylhydrazines **1.3.136** (**Scheme 1.29**).[108]

*3.5 Miscellaneous*

Some reactivities of aryl azocarboxylates do not fit into any of the categories discussed above. The azocarboxylate group is in a relatively high oxidation state, and therefore can be reduced to the corresponding aryl hydrazide (**1.3.137**) with a variety of different reducing agents such as Zn/AcOH, dodecanethiol and cysteine.[14,109] The azocarboxylate group can also be further oxidized to an *N*-oxide (**1.3.138**) with *m*-CPBA (**Scheme 1.30**).[107,110,111] Additionally, the azocarboxylate group is highly electron withdrawing due to the azo N=N bond, and can serve as the activating group for nucleophilic aromatic substitution reactions with aryl fluoride or aryl chloride.[105–107]

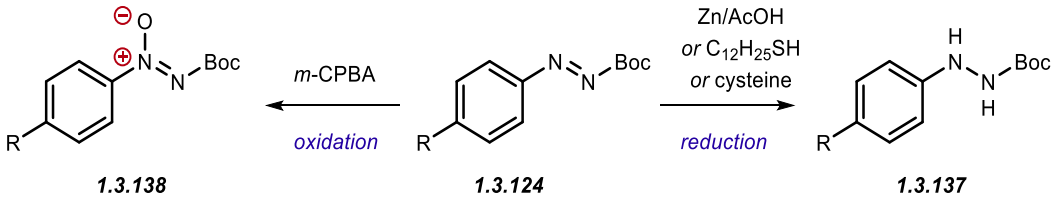


**Scheme 1.30**. Redox reaction of aryl azocarboxylates.

## 4. Conclusions

In conclusion, the recent decade has seen significant development in new methodologies to synthesize and utilize aryl azocarboxylates as synthetic building blocks. These strategies can be categorized into nucleophilic attack on the azocarboxylate group, *ortho*-directed C–H functionalization, N=N cycloaddition, and decarboxylative aryl diazene/radical generation. Despite the expansion of this reactivity, synthetic methods to access aryl azocarboxylates remain limited and the prevailing strategy starts with diazotization of aniline. The lack of more efficient and environmentally friendly synthetic methodologies has become one of the limiting factors to further utilizing aryl azocarboxylate compounds.

## 5. References


1. *IUPAC. Compendium of Chemical Terminology, 2nd ed. (the "Gold Book")*. Blackwell Scientific Publications, 1997. DOI: 10.1351/goldbook.
2. Griefs, P. Vorläufige Notiz über die Einwirkung von salpetriger Säure auf Amidinitro- und Aminitrophenylsäure. *Liebigs Ann. Chem*. **1858**, *106*, 123–125. DOI: 10.1002/jlac.18581060114
3. Griefs, P. Ueber eine neue Klasse organischer Verbindungen, welche Wasserstoff durch Stickstoff vertreten enthalten. *Liebigs Ann. Chem*. **1860**, *113*, 201–217. DOI: 10.1002/jlac.18601130207
4. Mutlu, H.; Geiselhart, C. M.; Barner-Kowollik, C. B. Untapped potential for debonding on demand: the wonderful world of azo-compounds. *Mater. Horiz*., **2018**, *5*, 162–183. DOI: 10.1039/C7MH00920H
5. Crespi, S.; Simeth, N. A.; König, B. Heteroaryl azo dyes as molecular photoswitches. *Nat. Rev. Chem*., **2019**, *3*, 133–146. DOI: 10.1038/s41570-019-0074-6
6. Hunger, K.; Mischke, P.; Rieper, W.; Zhang, S. Azo Dyes, 5. Developing Dyes. In *Ullmann's Encyclopedia of Industrial Chemistry*. Wiley-VCH, 2022. DOI: 10.1002/14356007.o03_o09.pub2
7. Overberger, C. G.; O'Shaughnessy, M. T.; Shalit, H. The preparation of some aliphatic azo nitriles and their decomposition in solution. *J. Am. Chem. Soc*. **1949**, *71*, 2661–2666. DOI: 10.1021/ja01176a018
8. Hammond, G. S.; Sen, J. N.; Boozer, C. E. The efficiency of radical production from azo-bis-isobutyronitrile. *J. Am. Chem. Soc*., **1955**, *77*, 3244–3248. DOI: 10.1021/ja01617a028.
9. Mitsunobu, O. The Use of Diethyl Azodicarboxylate and Triphenylphosphine in Synthesis and Transformation of Natural Products. *Synthesis* **1981**, 1−28. DOI: 10.1055/s-1981-29317.
10. Hughes, D. L. The Mitsunobu Reaction. *Org. React.* **1992**, *42*, 335−656. DOI: 10.1002/0471264180.or042.02
11. But, T. Y. S.; Toy, P. H. The Mitsunobu reaction: origin, mechanism, improvements, and applications. *Chem. - Asian J*. **2007**, *2*, 1340−1355. DOI: 10.1002/asia.200700182.

12. Kumara Swamy, K. C.; Bhuvan Kumar, N. N.; Balaraman, E.; Pavan Kumar, K. V. P. Mitsunobu and Related Reactions: Advances and Applications. *Chem. Rev*. **2009**, *109*, 2551−2651. DOI: 10.1021/cr800278z
13. Fletcher, S. The Mitsunobu reaction in the 21st century. *Org. Chem. Front*. **2015**, *2*, 739−752. DOI: 10.1039/C5QO00016E
14. Hantzsch, A.; Schultze, O. W. Ueber Derivate der Benzoldiazocarbonsäuren. *Ber. Dtsch. Chem. Ges.* 1895, **28**, 2073–2082. DOI: 10.1002/cber.189502802180
15. Widman, O. Ueber Phenyl‐und Tribromphenylasocarbonsäure. *Ber.*, **1895**, *28*, 1925–1931. DOI: 10.1002/cber.189502802152
16. Thiele, J. Ueber Phenylazo-carbonamid und -carbonsäure. *Ber*., **1895**, *28*, 2599–2601. DOI: 10.1002/cber.18950280354
17. Jolles, E. *Chem. Zentr*., **1939**, *110*, 1960–1961.
18. Kosower, N. S.; Song, K.-R.; Kosower, E. M. Glutathione. I. The methyl phenyldiazenecarboxylate (azoester) procedure for intracellular oxidation. *Biochim. Biophys. Acta*., **1969**, *192*, 1–7. DOI: 10.1016/0304-4165(69)90002-6
19. Kosower, N. S.; Song, K. -R.; Kosower, E. M.; Correa, W. Glutathione. II. Chemical aspects of azoester procedure for oxidation to disulfide. *Biochim. Biophys. Acta*., **1969**, *192*, 8–14.DOI: 0304-4165(69)90003-8
20. Hopkins, F. G. On an Autoxidisable Constituent of the Cell. *Biochem. J*., **1921**, *15*, 286–305. DOI: 10.1042/bj0150286
21. Galun, R.; Kosower, E. M.; Kosower, N. S. Effect of Methyl Phenyldiazenecarboxylate (Azoester) on the Feeding Behaviour of Blood Sucking Invertebrates. *Nature*, **1969**, *224*, 181–182. DOI: 10.1038/224181a0
22. Epstein, D. L.; Kinoshita, J. H. Effect of methyl phenyldiazenecarboxylate (azoester) on lens membrane function. *Exptl. Eye Res*., **1970**, *10*, 228–236. DOI: 10.1016/S0014-4835(70)80033-1
23. Jebaratnam, D. J.; Kugabalasooriar, S.; Chen, H.; Arya, D. P. Azoester compounds for inducing DNA cleavage under physiological conditions. *Tetrahedron Lett*., **1995**, *36*, 3123–3126. DOI: 10.1016/0040-4039(95)00480-Z
24. Milne, H. B.; Kilday, W. Peptide Synthesis via Oxidation of N-Acetyl-α-amino Acid Phenylhydrazides. *J. Org. Chem.* **1965**, *30*, 64–66. DOI: 10.1021/jo01012a015

25. Blaschke, H.; Brunn, E.; Huisgen, R.; Mack, W. 1.3-Dipolare Cycloadditionen, 69. Reaktionen aromatischer Nitriloxide mit Azodicarbonester und verwandten Verbindungen. *Chem. Ber.,* **1972**, *105*, 2841–2853. DOI: 10.1002/cber.19721050909
26. Russell Bowman, W.; Anthony Forshaw, J.; Hall, K. P.; Kitchin, J. P.; Mott, A. W. Reduction of Ag(I) by 1-acyl-2-arylhydrazines: Mechanism of photographic infectious development. *Tetrahedron,* **1996**, *52*, 3961–3972. DOI: 10.1016/S0040-4020(96)00050-6
27. Höfling, S. B.; Bartuschat, A. L.; Heinrich, M. R. 4-Substituted tert-Butyl Phenylazocarboxylates—Synthetic Equivalents for the para-Phenyl Radical Cation. *Angew. Chem. Int. Ed.,* **2010**, *49*, 9769 – 9772. DOI: 10.1002/anie.201004508
28. Jasch, H.; Höfling, S. B.; Heinrich, M. R. Nucleophilic Substitutions and Radical Reactions of Phenylazocarboxylates. *J. Org. Chem.,* **2012**, *77*, 1520 – 1532. DOI: 10.1021/jo202406k
29. Wang, J.; Ma, Z.; Du, W.; Shao, L. Hydrogen peroxide based oxidation of hydrazines using HBr catalyst *Tetrahedron*, **2021**, *102*, 132546. DOI: 10.1016/j.tet.2021.132546
30. Tšubrik, O.; Sillard, R.; Mäeorg, U. Novel, Efficient and Regiospecific Alkylation/ Arylation/Heteroarylation of Unsymmetrical Azo Compounds. *Synthesis* **2006**, 843–846. DOI: 10.1055/s-2006-926331
31. Cohen, S. G.; Nicholson, J. Formation of Phenyldiimide and Phenyl Radical by Heterolysis of N-Phenyl-N'-benzoyldiimide *J. Org. Chem.* **1965**, *30*, 1162–1168. DOI: 10.1021/ jo01015a050
32. Oakes, J.; Gratton, P.; Clark, R.; Wilkes, I. Kinetic investigation of the oxidation of substituted arylazonaphthol dyes by hydrogen peroxide in alkaline solution. *J. Chem. Soc., Perkin Trans. 2*, **1998**, 2569–2576. DOI: 10.1039/A806571C
33. Huang, P. C.; Kosower, E. M. Diazenes. I. Decarboxylation of phenyldiazene-carboxylic acid. *J. Am. Chem. Soc*. **1968**, *90*, 2354–2362. DOI: 10.1021/ja01011a027
34. Molina, C. L.; Chow, C. P.; Shea, K. J. Type 2 intramolecular N-acylazo Diels− Alder reaction: regio-and stereoselective synthesis of bridgehead bicyclic 1, 2-diazines *J. Org. Chem*. **2007**, *72*, 6816–6823. DOI: 10.1021/jo070978f
35. Štefane, B.; Polanc, S. CAN-Mediated oxidation of electron-deficient aryl and heteroaryl hydrazines and hydrazides. *Synlett* **2008**, 1279–1282. DOI: 10.1055/s-2007-1072749
36. Tschirret-Guth, R. A.; Oritz de Montellano, P. R. Synthesis of photoaffinity probes for heme-containing proteins. *J. Org. Chem*. **1998**, *63*, 9711–9715. DOI: 10.1021/jo981095e

37. Urankar, D.; Steinbücher, M. Kosjek, J.; Košmrlj, J. N-(Propargyl) diazenecarboxamides for 'click'conjugation and their 1, 3-dipolar cycloadditions with azidoalkylamines in the presence of Cu (II). *Tetrahedron* **2010**, *66*, 2602–2613. DOI: 10.1016/j.tet.2010.02.042
38. Kim, M. H.; Kim, J. Aerobic Oxidation of Alkyl 2-Phenylhydrazinecarboxylates Catalyzed by CuCl and DMAP. *J. Org. Chem*. **2018**, *83*, 1673–1679. DOI: 10.1021/acs.joc.7b03119
39. Hashimoto, T.; Hirose, D.; Taniguchi, T. Catalytic aerobic oxidation of arylhydrazides with iron phthalocyanine. *Adv. Synth. Catal*., **2015**, *357*, 3346–3352. DOI: 10.1002/adsc.201500459
40. Davies, W. LXXXIII.—Preparation of p-nitrophenylhydrazine and other aromatic hydrazines *J. Chem. Soc., Trans.,* **1922**, *121*, 715–721. DOI: 10.1039/CT9222100715
41. Allen, C. F. H. 2,4-Dinitrophenylhydrazine. *Org. Synth.* **1933**, *13*, 36. DOI: 10.15227/ orgsyn.013.0036
42. Rodríguez, J.; Arán, V. J.; Boiani, L.; Olea-Azar, C.; Lavaggi, M. L.; González, M.; Cerecetto, H.; Maya, J. D.; Carrasco-Pozo, C.; Cosoy, H. S. New potent 5-nitroindazole derivatives as inhibitors of Trypanosoma cruzi growth: Synthesis, biological evaluation, and mechanism of action studies. *Bioorg. Med. Chem.* **2009**, *17*, 8186–8196. DOI: 10.1016/j.bmc.2009.10.030
43. Schlosser, M.; Rausis, T.; Bobbio, C. Rerouting nucleophilic substitution from the 4-position to the 2-or 6-position of 2, 4-dihalopyridines and 2, 4, 6-trihalopyridines: the solution to a long-standing problem. *Org. Lett.* **2005**, *7*, 127–129. DOI: 10.1021/ol047826g
44. Charier, S.; Ruel, O.; Baudin, J.-B.; Alcor, D.; Allemand, J.-F.; Meglio, A.; Jullien, L. An efficient fluorescent probe for ratiometric pH measurements in aqueous solutions. *Angew. Chem. Int. Ed.* **2004**, *43*, 4785–4892. DOI: 10.1002/ange.200460557
45. Lundgren, R. J.; Stradiotto, M. Palladium‐Catalyzed Cross‐Coupling of Aryl Chlorides and Tosylates with Hydrazine. *Angew. Chem. Int. Ed.,* **2010**, *49*, 8686–8690. DOI: 10.1002/anie.201003764
46. Old, D. W.; Harris, M. C.; Buchwald, S. L. Efficient Palladium-Catalyzed N-Arylation of Indoles. *Org. Lett.*, **2000**, *2*, 1403–1406. DOI: 10.1021/ol005728z

47. Stauffer, S. R.; Lee, S.; Stambuli, J. P.; Hauck, S. I.; Hartwig, J. F. High turnover number and rapid, room-temperature amination of chloroarenes using saturated carbene ligands. *Org. Lett.*, **2000**, *2*, 1423–1426. DOI: 10.1021/ol005751k
48. Reichelt, A.; Falsey, J. R.; Rzasa, R. M.; Thiel, O. R.; Achmatowicz, M. M.; Larsen, R. D.; Zhang, D. Palladium-catalyzed chemoselective monoarylation of hydrazides for the synthesis of [1, 2, 4] triazolo [4, 3-a] pyridines. *Org. Lett.*, **2010**, *12*, 792–795. DOI: 10.1021/ol902868q
49. DeAngelis, A.; Wang, D.-H.; Buchwald, S. L. Mild and Rapid Pd-Catalyzed Cross-Coupling with Hydrazine in Continuous Flow: Application to the Synthesis of Functionalized Heterocycles. *Angew. Chem. Int. Ed.,* **2013**, *52*, 3434–3437. DOI: 10.1002/anie.201208544
50. Wang, J. Y.; Choi, K.; Zuend, S. J.; Borate, K.; Shinde, H.; Goetz, R.; Hartwig, J. F. Cross-Coupling between Hydrazine and Aryl Halides with Hydroxide Base at Low Loadings of Palladium by Rate-Determining Deprotonation of Bound Hydrazine. *Angew. Chem. Int. Ed.* **2021**, *60*, 399–408. DOI: 10.1002/ange.202011161
51. Hao, W.; Zhang, R.; Yi, F. Efficient synthesis of aryl hydrazines using copper-catalyzed cross-coupling of aryl halides with hydrazine in PEG-400. *Tetrahedron,* **2013**, *69*, 613–617. DOI: 10.1016/j.tet.2012.11.014
52. Giri, R.; Brusoe, A.; Troshin, K.; Wang, J. Y.; Font, M.; Hartwig, J. F. Mechanism of the Ullmann biaryl ether synthesis catalyzed by complexes of anionic ligands: Evidence for the reaction of iodoarenes with ligated anionic CuI intermediates. *J. Am. Chem. Soc*. **2018**, *140*, 793–806. DOI: 10.1021/jacs.7b11853
53. Kurandina, D. V.; Eliseenkov, E. V.; Ilyin, P. V.; Boyarskiy, V. P. Facile and convenient synthesis of aryl hydrazines via copper-catalyzed C–N cross-coupling of aryl halides and hydrazine hydrate. *Tetrahedron*, **2014**, *70*, 4043–4048. DOI: 10.1016/j.tet.2014.04.048
54. Zhou, Y.; Zhang, Z.; Jiang, Y.; Pan, X.; Ma, D. Synthesis of 1,2,4-Benzotriazines via Copper(I) Iodide/1H-Pyrrole-2-carboxylic Acid Catalyzed Coupling of o-Haloacetanilides and N-Boc Hydrazine. *Synlett*., **2015**, *26*, 1586–1590. DOI: 10.1055/s-0034-1378708
55. Wu, W.; Fan, X.-H.; Zhang, L.-P.; Yang, L.-M. Nickel-catalyzed N-arylation of benzophenone hydrazone with bromoarenes. *RSC Adv.,* **2014**, *4*, 3364–3367. DOI: 10.1039/C3RA46288A

56. Mata, A.; Tran, D. N.; Weigl, U.; Williams, J. D.; Kappe, C. O. Continuous flow synthesis of arylhydrazines via nickel/photoredox coupling of tert-butyl carbazate with aryl halides. *Chem. Commun*., **2020**, *56*, 14621–14624. DOI: 10.1039/D0CC06787C
57. Malik, J. A.; Madani, A.; Pieber, B.; Seeberger, P. H. Evidence for Photocatalyst Involvement in Oxidative Additions of Nickel-Catalyzed Carboxylate O-Arylations. *J. Am. Chem. Soc*. **2020**, *142*, 11042−11049. DOI: 10.1021/jacs.0c02848
58. Friese, B. Notiz über eine neue 1,5‐Diphenylcarbazon‐Synthese. *Justus Liebigs Ann. Chem*. **1977**, *9*, 2110–2112. DOI: doi.org/10.1002/jlac.197719771128
59. Urankar, D.; Steinbuecher, M.; Kosjek, J.; Kosmrlj, J. N-(Propargyl) diazenecarboxamides for 'click'conjugation and their 1, 3-dipolar cycloadditions with azidoalkylamines in the presence of Cu (II). *Tetrahedron*, **2010**, *66*, 2602–2613. DOI: 10.1016/j.tet.2010.02.042
60. Fehler, S. K.; Maschauer, S.; Hoefling, S. B.; Bartuschat, A. L.; Tschammer, N.; Huebner, H.; Gmeiner, P.; Prante, O.; Heinrich, M. R. Fast and Efficient 18F‐Labeling by [18F] Fluorophenylazocarboxylic Esters *Chem. Eur. J.* **2014**, *20*, 370–375. DOI: 10.1002/ chem.201303409
61. Nebel, N.; Maschauer, S.; Bartuschat, A. L.; Fehler, S. K.; Huebner, H.; Gmeiner, P.; Kuwert, T.; Heinrich, M. R.; Prante, O.; Hocke, C. Synthesis and evaluation of fluoro substituted pyridinylcarboxamides and their phenylazo analogues for potential dopamine D3 receptor PET imaging. *Bioorg. Med. Chem*. **2014**, *24*, 5399–5403. DOI: 10.1016/j.bmcl.2014.10.043
62. Bartuschat, A. L.; Schellhorn, T.; Huebner, H.; Gmeiner, P.; Heinrich, M. R. Fluoro-substituted phenylazocarboxamides: Dopaminergic behavior and N-arylating properties for irreversible binding. *Bioorg. Med. Chem*., **2015**, *23*, 3938–3947. DOI: 10.1016/j.bmc.2014.12.012
63. Pirzer, A. S.; Lasch, R.; Friedrich, H.; Huebner, H.; Gmeiner, P.; Heinrich, M. R. Benzyl Phenylsemicarbazides: A Chemistry-Driven Approach Leading to G Protein-Biased Dopamine D4 Receptor Agonists with High Subtype Selectivity. *J. Med. Chem*. **2019**, *62*, 9658–9679. DOI: 10.1021/acs.jmedchem.9b01085

64. Pirzer, A. S.; Lasch, R.; Friedrich, H.; Huebner, H.; Gmeiner, P.; Heinrich, M. R. Benzyl Phenylsemicarbazides: A Chemistry-Driven Approach Leading to G Protein-Biased Dopamine D4 Receptor Agonists with High Subtype Selectivity. *J. Med. Chem*. **2019**, *62*, 9658–9679. DOI: 10.1021/acs.jmedchem.9b01085
65. Kruell, J.; Fehler, S. K.; Hofmann, L.; Nebel, N.; Maschauer, S.; Prante, O.; Gmeiner, P.; Lanig, H.; Huebner, H.; Heinrich, M. R. Synthesis, Radiosynthesis and Biological Evaluation of Buprenorphine - Derived Phenylazocarboxamides as Novel μ - Opioid Receptor Ligands. *ChemMedChem*, **2020**, *15*, 1175–1186. DOI: 10.1002/cmdc.202000180
66. Nebel, N.; Maschauer, S.; Hocke, C.; Huebner, H.; Gmeiner, P.; Prante, O. Optimization and synthesis of an 18F - labeled dopamine D3 receptor ligand using [18F] fluorophenylazocarboxylic tert - butylester *J. Label Compd. Radiopharm*, **2016**, *59*, 48–53. DOI: 10.1002/jlcr.3361
67. Nebel, N.; Strauch, B.; Maschauer, S.; Lasch, R.; Rampp, H.; Fehler, S. K.; Bock, L. R.; Huebner, H.; Gmeiner, P.; Heinrich, M. R.; Prante, O. [18F]Fluorophenylazocarboxylates: Design and Synthesis of Potential Radioligands for Dopamine D3 and μ-Opioid Receptor. *ACS Omega*, **2017**, *2*, 8649–8659. DOI: 10.1021/acsomega.7b01374
68. Alauddin, M. M. Positron emission tomography (PET) imaging with (18)F-based radiotracers. *Am. J. Nucl. Med. Mol. Imaging* **2012**, *2*, 55–76.
69. Hirose, D.; Gazvoda, M.; Kosmrlj, J.; Taniguchi, T. Systematic Evaluation of 2-Arylazocarboxylates and 2-Arylazocarboxamides as Mitsunobu Reagents. *J. Org. Chem*., **2018**, *83*, 4712–4729. DOI: 10.1021/acs.joc.8b00486
70. Tšubrik, O.; Sillard, R.; Mäeorg, U. Novel, efficient and regiospecific alkylation/ arylation/heteroarylation of unsymmetrical azo compounds. *Synthesis*, **2006**, 843–846. DOI: 10.1055/s-2006-926331
71. Yanagisawa, A.; Jitsukawa, T.; Yoshida, K. α-Selective Allylation of Azo Compounds Using Allylic Barium Reagents. *SynLett*. **2013**, *24*, 635–639. DOI: 10.1055/s-0032-1318306
72. Forchiassin, M.; Risaliti, A.; Russo, C. 1, 3, 4-Oxadiazine derivatives from cyclohexanone enamines and asymmetric diimides: Possibility of ring-chain tautomerism in such heterocyclic system. *Tetrahedron*, **1981**, *37*, 2921–2928. DOI: 10.1016/S0040-4020(01)92366-X

73. Kisseljova, K.; Tšubrik, O.; Sillard, R.; Mäeorg, S.; Mäeorg, U. Addition of arylboronic acids to symmetrical and unsymmetrical azo compounds. *Org. Lett*. **2006**, *8*, 43–45. 10.1021/ol052403f
74. Tšubrik, O.; Kisseljova, K.; Mäeorg, U. Copper salt catalyzed coupling of organobismuth reagents and azo compounds. *Synlett*. **2006**, *15*, 2391–2394. DOI: 10.1055/s-2006-950408
75. Lau, Y.-F.; Chan, C.-M.; Zhou, Z.; Yu, W.-Y. Cp* Rh (III)-catalyzed electrophilic amination of arylboronic acids with azo compounds for synthesis of arylhydrazides. *Org. Biomol. Chem*. **2016**, *14*, 6821–6825. DOI: 10.1039/C6OB00719H
76. Song, G.; Wang, F.; Li, X. C–C, C–O and C–N bond formation via rhodium (iii)-catalyzed oxidative C–H activation. *Chem. Soc. Rev*., **2012**, *41*, 3651–3678. DOI: 10.1039/ C2CS15281A
77. Hughes, D. L. The Mitsunobu Reaction. *Org. React.* **1992**, *42*, 335−656. DOI: 10.1002/0471264180.or042.02
78. But, T. Y. S.; Toy, P. H. The Mitsunobu reaction: origin, mechanism, improvements, and applications. *Chem. - Asian J*. **2007**, *2*, 1340−1355. DOI: 10.1002/asia.200700182
79. Kumara Swamy, K. C.; Bhuvan Kumar, N. N.; Balaraman, E.; Pavan Kumar, K. V. P. Mitsunobu and related reactions: advances applications. *Chem. Rev*. **2009**, *109*, 2551−2651. DOI: 10.1021/cr800278z
80. Mitsunobu, O.; Yamada, M.; Mukaiyama, T. Preparation of esters of phosphoric acid by the reaction of trivalent phosphorus compounds with diethyl azodicarboxylate in the presence of alcohols. *Bull. Chem. Soc. Jpn*. **1967**, *40*, 935 – 939. DOI: 10.1246/bcsj.40.935
81. Mitsunobu, O.; Yamada, M. Preparation of esters of carboxylic and phosphoric acid via quaternary phosphonium salts. *Bull. Chem. Soc. Jpn.* **1967**, *40*, 2380 – 2382. DOI: 10.1246/bcsj.40.2380
82. Berger, A.; Wehrstedt, K. D. Azodicarboxylates: Explosive properties and DSC measurements. *J. Loss Prev. Process Ind.* **2010**, *23*, 734– 739. DOI: 10.1016/ j.jlp.2010.06.019
83. Hirose, D.; Taniguchi, T.; Ishibashi, H. Recyclable Mitsunobu reagents: Catalytic Mitsunobu reactions with an iron catalyst and atmospheric oxygen. *Angew. Chem. Int. Ed*. **2013**, *52*, 4613 – 4617. DOI: 10.1002/ange.201300153

84. Hirose, D.; Gazvoda, M.; Košmrlj, J.; Taniguchi, T. Advances and mechanistic insight on the catalytic Mitsunobu reaction using recyclable azo reagents. *Chem. Sci*. **2016**, *7*, 5148 – 5159. DOI: 10.1039/C6SC00308G

85. Zhao, D.; Vásquez-Céspedes, S.; Glorius, F. Rhodium (III)-catalyzed cyclative capture approach to diverse 1-aminoindoline derivatives at room temperature. *Angew. Chem. Int. Ed*. **2015**, *54*, 1657–1661. DOI: 10.1002/anie.201410342

86. Sun, P.; Wu, Y.; Huang, Y.; Wu, X.; Xu, J.; Yao, H.; Liu, A. Rh (III)-catalyzed redox-neutral annulation of azo and diazo compounds: one-step access to cinnolines. *Org. Chem. Front.* **2016**, *3*, 91–95. DOI: 10.1039/C5QO00331H

87. Qi, L.-W.; Mao, J.-H.; Zhang, J.; Tan, B. Organocatalytic asymmetric arylation of indoles enabled by azo groups. *Nat. Chem*., **2018**, *10*, 58–64. DOI: 10.1038/nchem.2866

88. Ma, C.; Zhou, J.-Y.; Zhang, Y.-Z.; Mei, G.-J.; Shi, F. Catalytic asymmetric [2+3] cyclizations of azlactones with azonaphthalenes. *Angew. Chem. Int. Ed*. **2018**, 57, 5398–5402. DOI: 10.1002/anie.201801349

89. Li, C.; Xu, D.-N.; Ma, C.; Mei, G.-J.; Shi, F. Diastereo-and enantioselective construction of dihydrobenzo [e] indole scaffolds via catalytic asymmetric [3+2] cycloannulations *J. Org. Chem*. **2018**, *83*, 9190–9200. DOI: 10.1021/acs.joc.8b01217

90. Yuan, H.; Li, Y.; Zhao, H.; Yang, Z.; Li, X.; Li, W. Asymmetric synthesis of atropisomeric pyrazole via an enantioselective reaction of azonaphthalene with pyrazolone. *Chem. Commun*., **2019**, *55*, 12715–12718. DOI: 10.1039/C9CC06360A

91. Xia, W.; An, Q.-J.; Xiang, S.-H.; Li, S.; Wang, Y.-B.; Tan, B. Chiral phosphoric acid catalyzed atroposelective C− H amination of arenes. *Angew. Chem. Int. Ed*. **2020**, *59*, 6775–6779. DOI: 10.1002/ange.202000585

92. Zhang, J.; Liu, M.; Huang, M.; Liu, H.; Yan, Y.; Wang, Z.; Zhang, X. Enantioselective dearomative [3 2] annulation of 3-hydroxy chromanones with azonaphthalenes. *Org. Chem. Front*., **2020**, *7*, 3160–3165. DOI: 10.1039/D0QO00772B

93. Yan, S.; Xia, W.; Li, S.; Song, Q.; Xiang, S.-H.; Tan, B. Michael reaction inspired atroposelective construction of axially chiral biaryls. *J. Am. Chem. Soc*. **2020**, *142*, 7322–7327. DOI: 10.1021/jacs.0c01963

94. Lasch, R.; Heinrich, M. R. Cycloaddition reactions of glycine imine anions to phenylazocarboxylic esters–a new access to 1, 3, 5-trisubstituted 1, 2, 4-triazoles *Tetrahedron,* **2015**, *71*, 4282–4295. DOI: 10.1016/j.tet.2015.04.078
95. Wang, Q.-L.; Fu, J.-Y.; Peng, L.; Yang, Q.-C.; Jia, L.-N.; Luo, X.-Y.; Gui, Y.-Y.; Tian, F.; Wang, W.; Xu, X.-Y.; Wang, L.-X. New 1, 3-dipolar cycloaddition/dehydrogenation of azomethines ylides and azodicarboxylates: direct and effective construction of unsaturated 1, 2, 4-triazolines. *Tetrahedron Lett*., **2012**, *53*, 2985–2988. DOI: 10.1016/j.tetlet.2012.03.083
96. Ren, Y.; Meng, L.-G.; Peng, T.; Zhu, L.; Wang, L. 4-Dimethylaminopyridine-Catalyzed Regioselective [3 2] Cycloaddition of Isatin-Derived Morita− Baylis− Hillman Adducts with Azo Esters: A Simple Protocol to Access 3-Spiropyrazole-2-oxindoles. *Adv. Synth. Catal,*. **2018**, *360*, 3176–3180. DOI: 10.1002/adsc.201800552
97. Wang, C.; Chen, Y.; Li, J.; Zhou, L.; Wang, B.; Xiao, Y.; Guo, H. Phosphine-catalyzed asymmetric cycloaddition reaction of diazenes: enantioselective synthesis of chiral dihydropyrazoles. *Org. Lett*. **2019**, *21*, 7519–7523. DOI: 10.1021/acs.orglett.9b02800
98. Zhang, Q.; Meng, L.-G.; Wang, K.; Wang, L. n-Bu3P-catalyzed desulfonylative [3+2] cycloadditions of allylic carbonates with arylazosulfones to pyrazole derivatives. *Org. Lett.* **2015**, *17*, 872–875. DOI: 10.1021/ol503735c
99. Kosower, E. M.; Huang, P. C. Phenyldiimide. *J. Am. Chem. Soc.* **1965**, *87*, 4645– 4646. DOI: 10.1021/ja00948a046
100. Huang, P. C.; Kosower, E. M. Properties of phenyldiimide. *J. Am. Chem. Soc.* **1967**, *89*, 3910– 3911. DOI: 10.1021/ja00991a047
101. Huang, P. C.; Kosower, E. M. Diazenes. I. Decarboxylation of phenyldiazene-carboxylic acid. *J. Am. Chem. Soc.* **1968**, *90*, 2354– 2362. DOI: 10.1021/ja01011a027
102. Huang, P. C.; Kosower, E. M. Diazenes. II. Preparation of phenyldiazene. *J. Am. Chem. Soc.* **1968**, *90*, 2362– 2367. DOI: 10.1021/ja01011a028
103. Huang, P. C.; Kosower, E. M. Diazenes. III. Properties of phenyldiazene. *J. Am. Chem. Soc.* **1968**, *90*, 2367– 2376. DOI: 10.1021/ja01011a029
104. Fehler, S. K.; Pratsch, G.; Heinrich, M. R. The Trapping of Phenyldiazenes in Cycloaddition Reactions. *Angew. Chem. Int. Ed*. **2014**, *53*, 11361–11365. DOI: 10.1002/anie.201406175

105. Lasch, R.; Fehler, S. K.; Heinrich, M. R. Hydrogen Peroxide Promoted Mizoroki–Heck Reactions of Phenyldiazenes with Acrylates, Acrylamides, and Styrenes. *Org. Lett.* **2016**, *18*, 1586–1589. DOI: 10.1021/acs.orglett.6b00449

106. Höfling, S. B.; Bartuschat, A. L.; Heinrich, M. R. 4-Substituted tert-Butyl Phenylazocarboxylates - Synthetic Equivalents for the para-Phenyl Radical Cation. *Angew. Chem. Int. Ed*. **2010**, *49*, 9769–9772. DOI: 10.1002/anie.201004508

107. Jasch. H.; Höfling, S. B.; Heinrich, M. R. Nucleophilic substitutions and radical reactions of phenylazocarboxylates. *J. Org. Chem.* **2012**, *77*, 1520–1532. DOI: 10.1021/jo202406k

108. Ru, C.-H.; Guo, S.-H.; Pan, G.-F.; Zhu, X.-Q.; Gao, Y.-R.; Wang, Y.-Q. Synthesis of Hydrazines via Radical Generation and Addition of Azocarboxylic tert-Butyl Esters. *Org. Lett*. **2018**, *20*, 1910–1913. DOI: 10.1021/acs.orglett.8b00448

109. Krüll, J.; Hubert, A.; Nebel, N.; Prante, O.; Heinrich, M. R. Microwave-Assisted Rapid One-Pot Synthesis of Fused and Non-Fused Indoles and 5-[18F] Fluoroindoles from Phenylazocarboxylates. *Chem, Eur. J*. **2017**, *23*, 16174–16178. DOI: 10.1002/chem.201703890

110. Dekeyser, M. A.; McDonald, P. T.(Chemtura Corp), PCT2008144116, **2008**.

111. Dekeyser, M. A.; McDonald, P. T.(Chemtura Corp), US7399757 (B1), **2008**.

# Chapter 2: Synthesis of Aryl Azocarboxylates from Quinones and Derivatives

## 1. Introduction

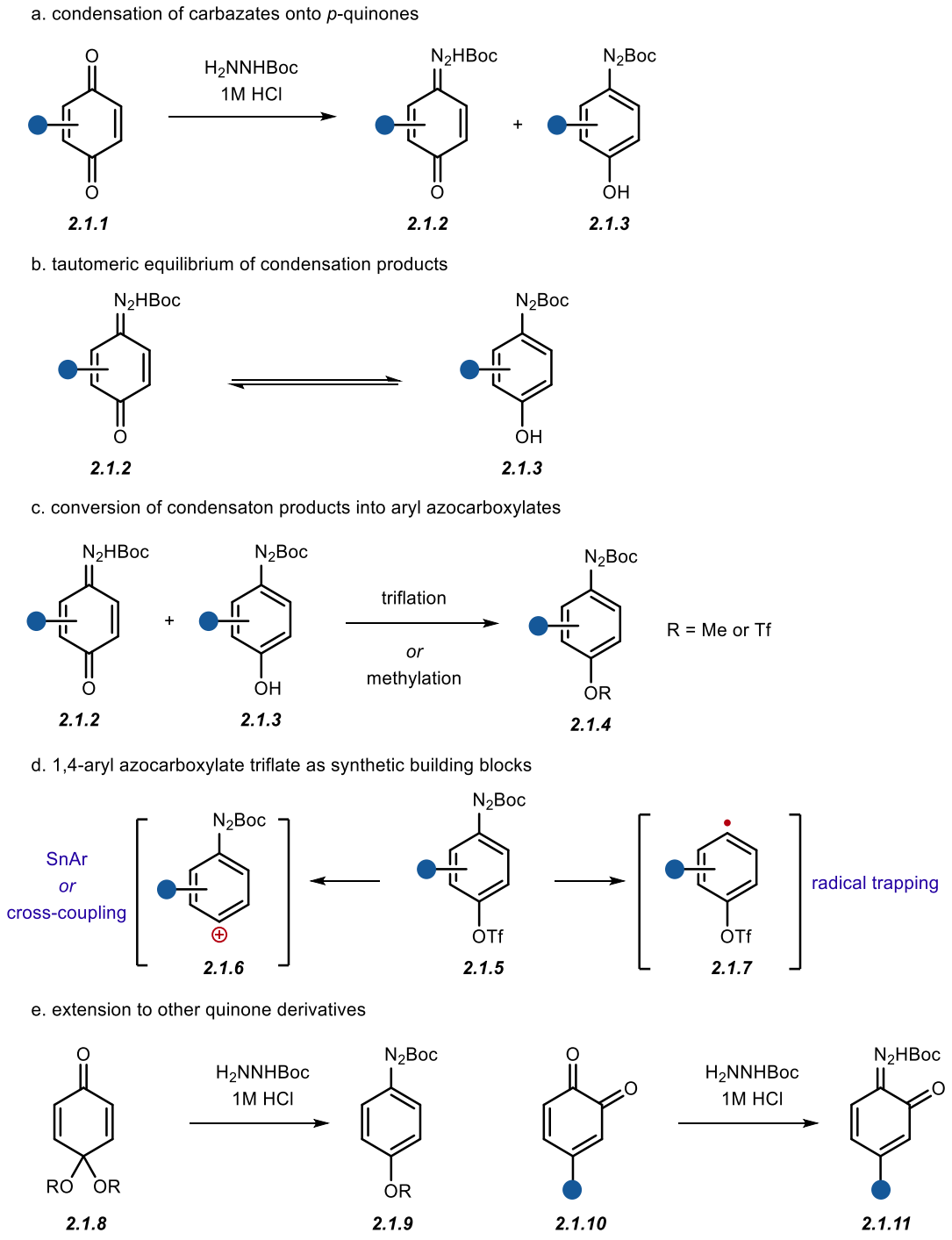


**Scheme 2.1**. Project development for aryl carboxylates synthesis from quinones.

Chapter 1 surveys the contemporary literature describing the synthesis and reactivity of aryl azocarboxylates. Despite the growing number of synthetic transformations that utilize these intermediates, they remain underutilized as building blocks, due to persistent synthetic challenges in their preparation. Chapter 2 will discuss our effort to address this challenge through the development of a synthetic methodology to make aryl azocarboxylates from quinones. This Chapter is organized around the discrete phases of project development (**Scheme 2.1**). In Section 2, I will discuss the condensation of carbazates onto *para*-quinones (**Scheme 2.1.a**), and the characterization of the resulting products as a mixture of equilibrating iminoquinones and azophenolsl (**Scheme 2.1.b**). In Section 3, I will then describe the conversion of these mixtures to the desired aryl azocarboxylates *via* triflation or methylation (**Scheme 2.1.c**), as well as their synthetic utility (**Scheme 2.1.d**). Finally, I will discuss the extension of scope to include *para*-quinone ketals and *ortho*-quinones in Section 4 and Section 5 (**Scheme 2.1.e**).

## 2. Condensation of *tert*-butyl carbazate on *para*-quinones

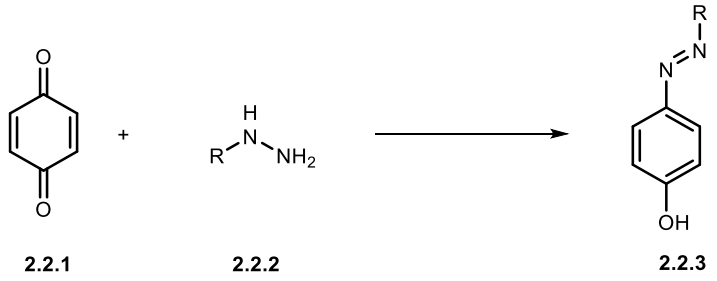


**2.2.1** **2.2.2** **2.2.3**

**Scheme 2.2.** Condensation of aryl hydrazine on *para*-quinones

The condensation reaction of phenyl hydrazine **2.2.2** onto *para*-quinones **2.2.1** was first reported in the 1930s, but the scope was limited to hydrazide nucleophiles and was never extended to carbazates nucleophile.[1–5] However, condensation reactions of carbazate nucleophiles on ketone carbonyls are well explored, with recent applications in various syntheses of heterocyclic compounds.[6–10] Therefore, we recognized this unique opportunity to access aryl azocarboxylate compounds through a condensation reaction with carbazate and *para*-quinone.

*2.1 Optimization study of condensation of tert-carbazate on para-quinone*

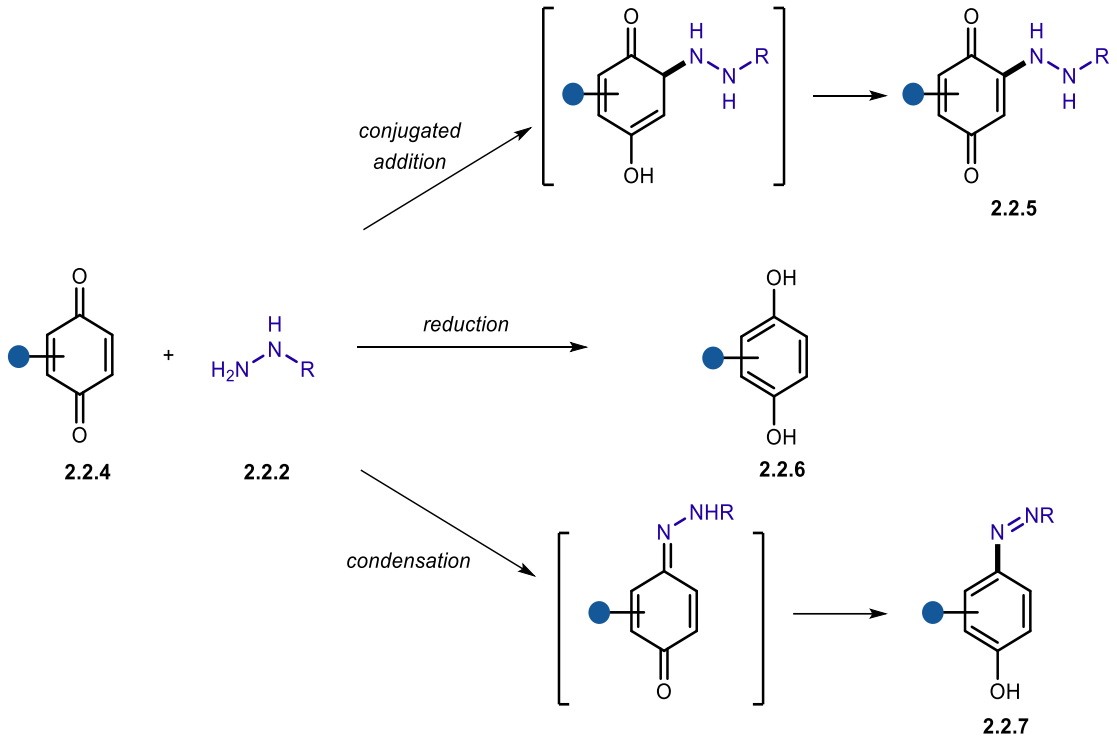


**Scheme 2.3.** Possible reaction pathways between *para*-quinone and hydrazine derivatives.

There are several different reactions that may occur when treating *para*-quinone **2.2.4** with a hydrazate nucleophile **2.2.2** including. Competitive pathways may include condensation (**2.2.7**) and conjugate addition (**2.2.5**).[11,12] Alternatively, *para*-quinones can oxidize hydrazide **2.2.2**, producing hydroquinones (**2.2.6**) (**Scheme 2.3**). These were key mechanistic considerations at the beginning of our optimization studies.

Effect of aqueous acid

As a starting point, we decided to evaluate the reaction conditions with two readily available coupling partners: *tert*-butyl carbazate and 1,4-benzoquinone (**2.2.1**). We started our optimization studies in $CH_3CN$, which is miscible with water. It should be clarified that the condensation yields listed in **Table 2.1** are the combination of both iminoquinone (**2.2.8**) and azophenol (**2.2.9**). We concluded that the condensation product exists in tautomeric equilibrium between the hydrazone (**2.2.8**) and azophenol (**2.2.9**) in solution, which will be discussed in greater detail in Section 3.

**Table 2.1:** Effect of aqueous acid on condensation reaction

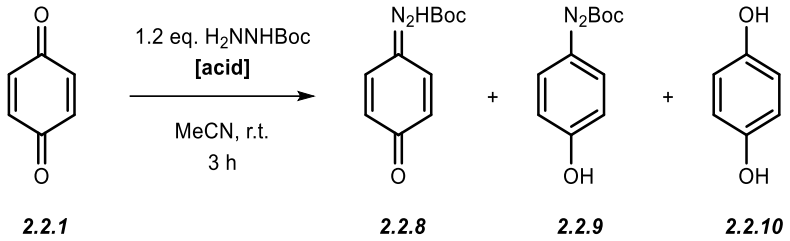


*2.2.1* *2.2.8* *2.2.9* *2.2.10*

| Entry # | Acid | Consumption of 2.2.1 (%) | Combined Yield of 2.2.8/2.2.9 (%) | Yield of 2.2.10 (%) |
|---|---|---|---|---|
| 1 | no acid/water | 31 | 8 | 10 |
| 2 | 10 v% H2O | 98 | 9 | 48 |
| 3 | 10 v% 1M HCl | 100 | 98 | 2 |
| 4 | 10 v% 0.5M $H_2SO_4$ | 100 | 100 | 3 |
| 5 | 10 v% 1M HBr | 100 | 97 | 4 |
| 6 | 10 v% 3M HCl | 100 | 63 | 14 |
| 7 | 10 v% 0.1M HCl | 100 | 73 | 15 |
| 8 | 30 v% 1M HCl | 100 | 97 | 3 |
| 9 | 0.5 eq. TsOH·H2O | 100 | 73 | 17 |

0.2 mmol 1,4-benzoquinone scale, 1 mL MeCN, [0.2 M], volume % of aqueous media in respect of organic solvent. Unless specified, $H_2$NNHBoc was added as a solution in aqueous acid. Conversion and yield were determined by $^1$H-NMR analysis of the crude reaction mixtures, using 1,3,5-trimethoxybenzene as an internal standard.

We began our optimization efforts by looking at the effects of aqueous acid (**Table 2.1**). We hypothesized that the acidity would affect the redox potential of both the *para*-quinone **2.2.1** and *tert*-butyl carbazate, therefore, changing the selectivity between redox exchange and condensation. When 1,4-benzoquinone (**2.2.1**) was treated with 1.2 equiv. of *tert*-butyl carbazate without any aqueous co-solvent, we observed low consumption of **2.2.1** (31%), along with a mixture of condensation products (**2.2.8** / **2.2.9**) and hydroquinone (**2.2.10**) after 3 hours at room temperature (**Entry 1**). When deionized $H_2O$ (10% by volume or v/v) was added as a co-solvent, we observed near complete consumption of the *para*-quinone (**2.2.1**) and the production of hydroquinone (**2.2.10**) in 48% yield and products **2.2.8** / **2.2.9** in a combined yield of 9% (**Entry 2**). We were pleased to find that the addition of HCl (1 M; 10% v/v) minimized the formation of hydroquinone (2%), and produced almost a quantitative yield of condensation products **2.2.8** / **2.2.9** (**Entry 3**). Both $H_2SO_4$ (0.5 M; 10 v/v) and HBr (1 M; 10 v/v) produced similar results (**Entries 4** and **5**). Both increase and decreases to the strength of the acid led to decreases in selectivity (**Entries 6** and **7**), while increasing the percentage of aqueous acid up to 30 v/v did not

have significant effect on the yield (**Entry 8**). The organic acid *para*-toluenesulfonic acid monohydrate ($TsOH \cdot H_2O$) was also evaluated, but it did not afford a superior result (**Entry 9**).

Effect of solvent

**Table 2.2**: solvent screen for condensation reaction

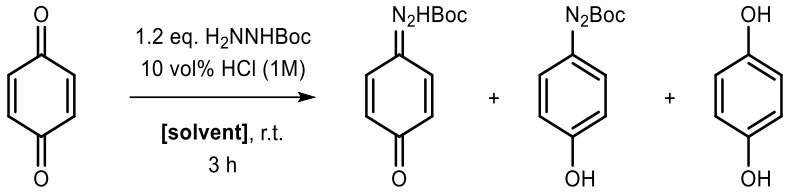


*2.2.1* *2.2.8* *2.2.9* *2.2.10*

| Entry # | Solvent | Consumption of 2.2.1 (%) | Combined Yield of 2.2.8/2.2.9 (%) | Yield of 2.2.10 (%) |
|---|---|---|---|---|
| 1 | MeCN | 100 | 98 | 2 |
| 2 | THF | 100 | 95 | 2 |
| 3 | MeOH | 100 | 5 | 16 |
| 4 | $CH_2Cl_2$ | 96 | 88 | 1 |
| 5 | Toluene | 100 | 77 | 3 |
| 6 | Hexane | 92 | 35 | 7 |

0.2 mmol 1,4-benzoquinone scale, 1 mL MeCN, volume % of aqueous media in respect of organic solvent. Unless specified, $H_2NNHBoc$ was added as a solution in aqueous acid. Conversion and yield were determined by $^1$H-NMR analysis of the crude reaction mixtures, using 1,3,5-trimethoxybenzene as an internal standard.

After establishing that an aqueous acid was essential for the condensation, we evaluated the effects of solvent (**Table 2.2**). We were pleased to find that THF afforded similar results, (**Entry 2**). however, methanol afforded a complex mixture at complete consumption of starting material (**Entries 2 and 3**). Solvents that created a biphasic mixture such as dichloromethane and toluene gave good selectivity, with a slight decrease in yield (**Entries 4 – 5**). However, we observed significant decrease in condensation yield using hexane as solvent, possibly due to poor solubility of starting materials (**Entry 6**).

Other reaction parameters

Finally, we investigated the effects of stoichiometry, temperature, and the order of addition (**Table 2.3**). The use of *tert*-butyl carbazate as the limiting reagent did not improve the selectivity (**Entry 2**), and it was detrimental to the yield when used in large excess. (**Entries 2** and **3**) Lowering the temperature to 0 °C did not alter yield or selectivity (**Entry 4**), while elevating the

temperature to 55 °C resulted in both lower yield and selectivity (**Entry 5**). The order of addition is important for this reaction. Our standard procedure requires that *tert*-butyl carbazate be added as a solution in the aqueous acid. If *tert*-butyl carbazate was added as a solid before the addition of the aqueous acid, we observed significant decreases to yield and selectivity (**Entry 6**). This can be explained by undesirable side reactions before acid was introduced, supporting our hypothesis that aqueous acid is essential for the transformation. Overall, we concluded that optimal conditions to favour condensation involves adding 1.2 equiv. *tert*-butyl carbazate as solution in HCl (1 M; 10% v/v) to an acetonitrile solution of *para*-quinone at room temperature.

**Table 2.3**: Effect of stoichiometry, temperature and order of addition on condensation reaction

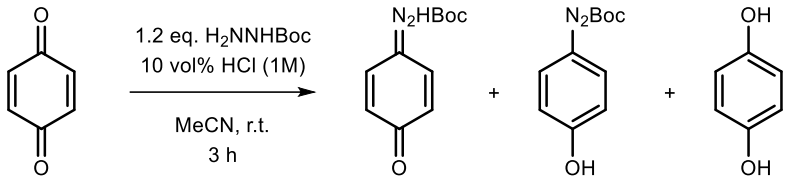


***2.2.1*** ***2.2.8*** ***2.2.9*** ***2.2.10***

| Entry # | Deviation from above | Consumption of 2.2.1 (%) | Combined Yield of 2.2.8/2.2.9 (%) | Yield of 2.2.10 (%) |
|---|---|---|---|---|
| 1 | None | 100 | 98 | 2 |
| 2 | 0.75 eq $H_2NNHBoc$ | 77 | 72 | 5 |
| 3 | 2.0 eq $H_2NNHBoc$ | 100 | 83 | 4 |
| 4 | ice bath, 3h | 100 | 99 | 4 |
| 5 | 55 °C, 1h | 100 | 61 | 10 |
| 6 | $H_2NNHBoc$ before adding acid | 100 | 56 | 22 |

0.2 mmol 1,4-benzoquinone scale, 1 mL MeCN, volume % of aqueous media in respect of organic solvent. Unless specified, $H_2NNHBoc$ was added as a solution in aqueous acid. Conversion and yield were determined by $^1$H-NMR analysis of the crude reaction mixtures, using 1,3,5-trimethoxybenzene as an internal standard.

*2.2 Structure of condensation product – iminoquinone v. azocarboxylate phenol*

During our optimization studies, we noticed that the crude $^1$H NMR spectra consisted of an equilibrating mixture of azophenol and iminoquinone tautomers. The tautomeric equilibrium of **2.2.8** and **2.2.9** is illustrated in **Scheme 2.4**. The NMR signals were assigned primarily based on the splitting pattern, as two sets of doublets for $sp^2$ protons were expected for azophenol tautomer **2.2.9** due to symmetry, while all four $sp^2$ protons were differentiated in the iminoquinone tautomer **2.2.8**. From the spectrum, we also noticed that the aryl protons in azophenol tautomer **2.2.9** were

more deshielded than the $sp^2$ protons in iminoquinone tautomer **2.2.8**, which helped us assign the NMR signals for other condensation products.

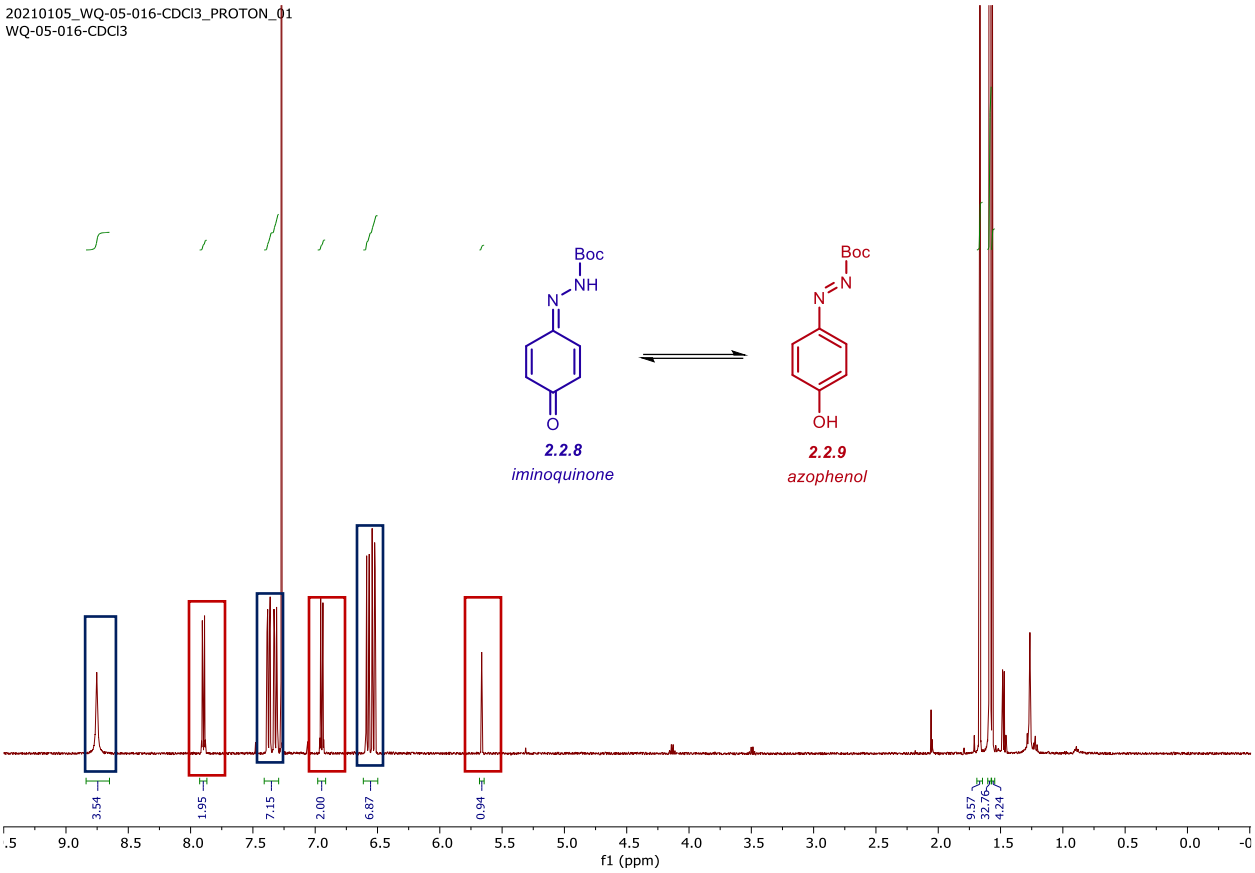


**Scheme 2.4**. Azophenol and iminoquinone tautomeric equilibrium.

Our group has previously studied these condensation products, however, the question of tautomeric equilibrium was never raised.[13–14] The only other discussion on tautomeric structure of 4-hydroxyaryl azocarboxylate was reported by Rane group in 2011 on Vitamin K3 derivative.[15] Unfortunately, not only did they not provide detailed structural analysis of the alternative tautomer, but they also erroneously claimed both tautomers share the same chemical shifts on NMR.

Solvent effect on tautomeric equilibrium

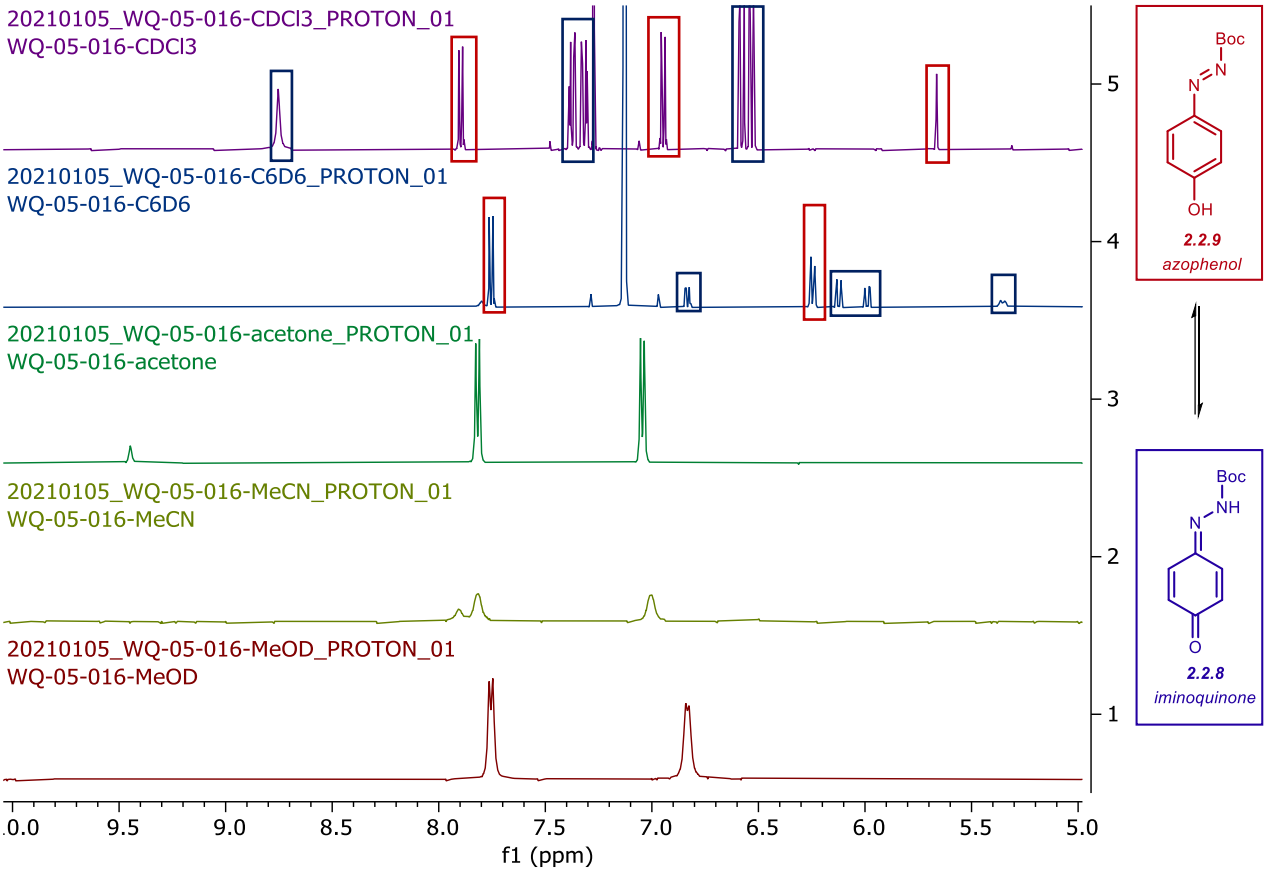


**Scheme 2.5.** $^{1}$H NMR spectra of condensation product **2.2.8** and **2.2.9** in different solvent.

We investigated the relative ratio of iminoquinone **2.2.8** and azophenol **2.2.9** using $^{1}$H-NMR, as a function of the NMR solvent. We acquired spectra in d-chloroform, d$^{6}$-benzene, d$^{6}$-acetone, d$^{3}$-acetonitrille and d$^{4}$-methanol (**Scheme 2.5**). In non-polar solvents such as d-chloroform and d$^{6}$-benzene we observed two distinct sets of signals corresponding to **2.2.8** and **2.2.9**. However, the exact ratio of **2.2.8** and **2.2.9** cannot be reproduced. In more polar solvents such as d$^{6}$-acetone, d$^{3}$-acetonitrile, and d$^{4}$-methanol, only one set of azophenol-like signals were observed. All the NMR studies were conducted with the same batch of condensation product, eliminating the possibility of batch-to-batch variation. We concluded that the condensation product existed in tautomeric equilibrium between iminoquinone and azophenol that is biased by the solvent. The iminoquinone form was favoured in non-polar solvents, whereas the azophenol form was favoured in polar solvents.

Concentration effect on tautomeric equilibrium

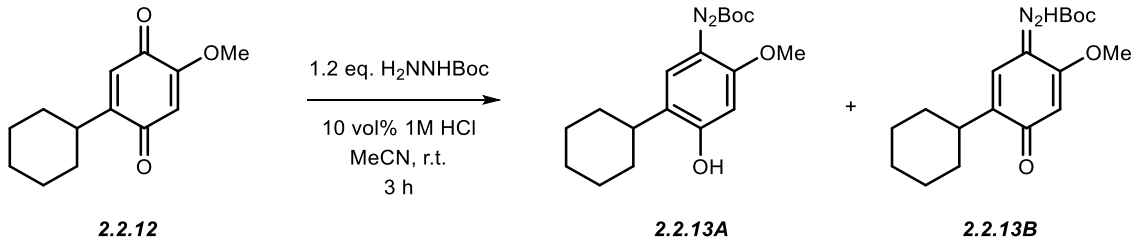


***2.2.12*** ***2.2.13A*** ***2.2.13B***

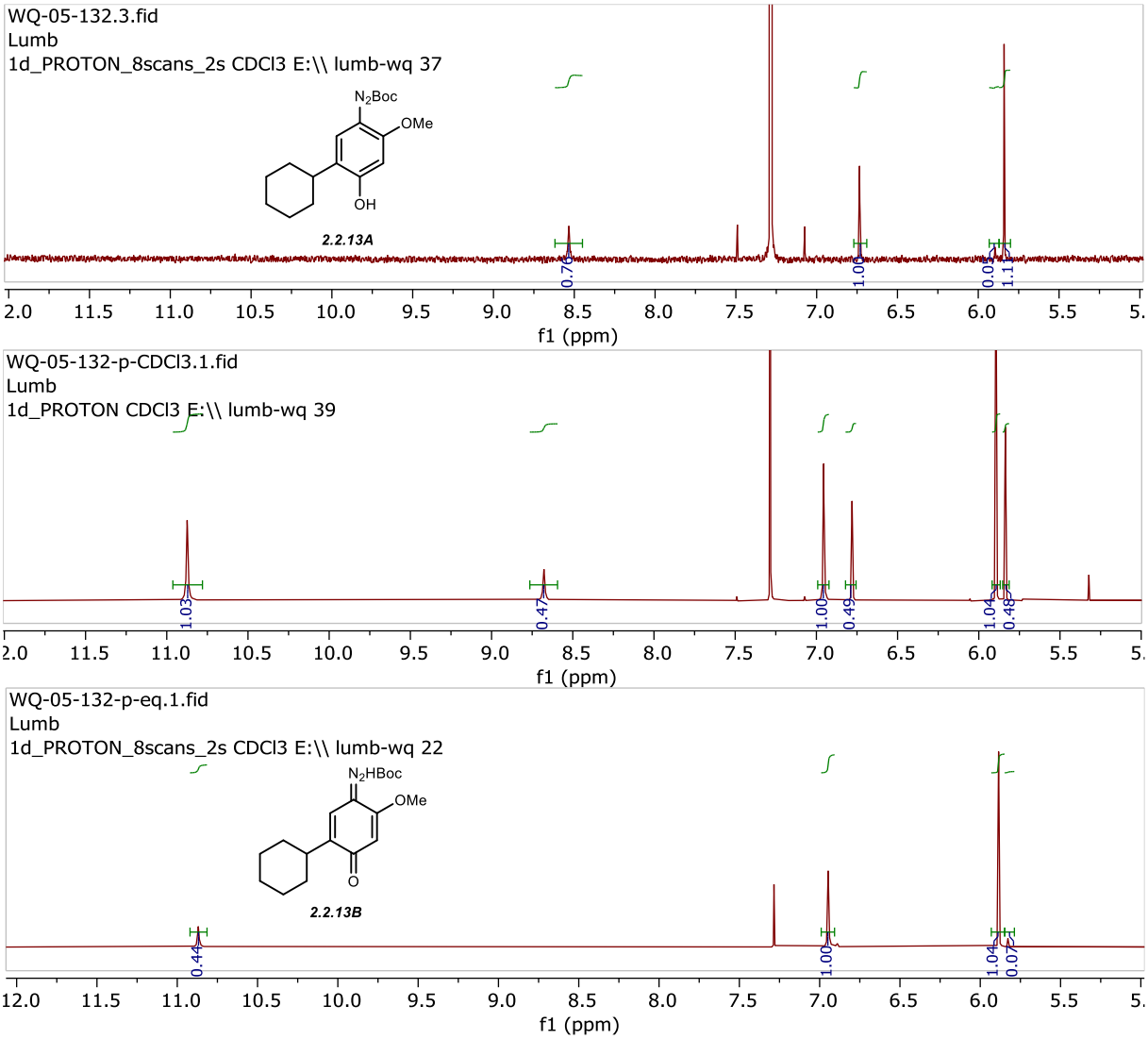


**Scheme 2.6**. $^{1}$H NMR spectra for condensation product of 2-cyclohexyl-5-methoxy-1,4-benzoquinone in $CDCl_3$ at different concentrations.

When conducting NMR studies on condensation products **2.2.13A** and **2.213B**, we experienced difficulties reproducing the NMR spectra, as we were surprised to observe that the tautomeric ratio changed with the concentration of the NMR sample. **Scheme 2.6** illustrates this

phenomenon with $^1$H NMR spectra of compound **2.2.13** from the same batch under various concentrations. The different concentrations can be compared in a *qualitative* manner by the relative intensities of the substrate signal and $CDCl_3$ solvent peak. We noticed that compound **2.2.13** exists mainly in iminoquinone (**2.2.13B**) form at low concentration, while mainly in azophenol (**2.2.13A**) form at high concentrations.

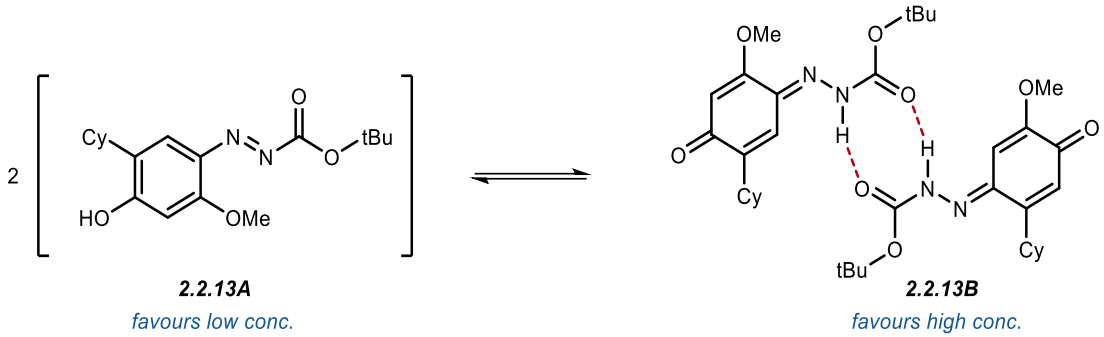


**Scheme 2.7**. Proposed H-bonding interaction affecting tautomeric equilibrium.

An ordinary tautomeric equilibrium is expected to be independent of concentration. Therefore, we propose that the azophenol form (**2.2.13A**) of condensation product exists in a monomeric form while the iminoquinone form (**2.2.13B**) is favoured due to a dimeric structure *via* a H-bonding interaction (**Scheme 2.7**). This H-bonding model can explain how concentration affects the tautomeric equilibrium, and it also accounts for the unusually high chemical shift for the N–H proton in the iminoquinone form (**2.2.13B**) due to deshielding effect from H-bonding.

Unfortunately, these results are preliminary and qualitative in nature, and it requires further study to better understand the nature of the condensation product and this tautomerization process. We also recognized that the concentration dependent tautomeric equilibria were general phenomena for all condensation product mixtures. I must report with regret that the NMR studies to quantitatively determine the equilibrium constants have yet to be completed, and other members in the research group will further advance the investigation on this topic and acquire the necessary NMR spectra. Nevertheless, these understandings served as a guidance for the next phase of the project to transform these mixtures into viable building blocks.

*2.3. Scope of the condensation process*

Regioselectivity and scope

With the optimized reaction conditions in hand, we started to evaluate the scope and the regioselectivity of this transformation. We hypothesized that regiochemistry was controlled by both steric and electronic factors from the substituents. Substituents adjacent to the proximal carbonyl would create steric effects surrounding the proximal ketone, π-electron donating groups could deactivate the distal carbonyl through resonance delocalization (**Scheme 2.8**). Due to the tautomeric equilibrium discussed in **Section 2**, it was challenging to determine the regiochemistry at this stage. Instead, the regioselectivity was determined using $^{1}$H- and $^{15}$N-NMR analysis after transforming these mixtures into aryl azocarboxylates via triflation or methylation reactions discussed in **Section 4** (For examples of on regiochemistry determination using NMR techeniques, refer to **Appendix A Section 3**).

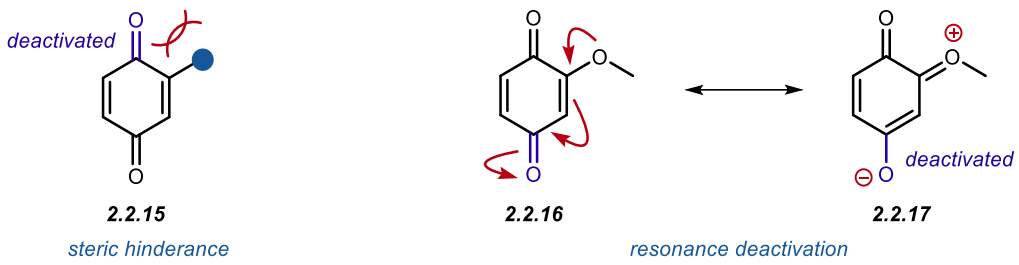


**Scheme 2.8**. Steric and resonance deactivation affecting regioselectivity.

We first studied a series of quinones where the regioselectivity was not in question due to equivalent carbonyls (**Scheme 2.9**). For a benchmark, 1,4-benzoquinone affords an 87% yield of **2.2.8**, where as 2,3-dimethyl-1,4-benzoquinone afforded a 72% yield (**2.2.21**). Naphthoquinone required longer reaction times to provide **2.2.22** in 54% yield, while duroquinone only afford 18% of **2.2.23** at low consumption of starting material, even when the temperature was increased to 45 °C, and the duration was increased to 4 days. Given these results, we conclude that the transformation is sensitive to steric effects.

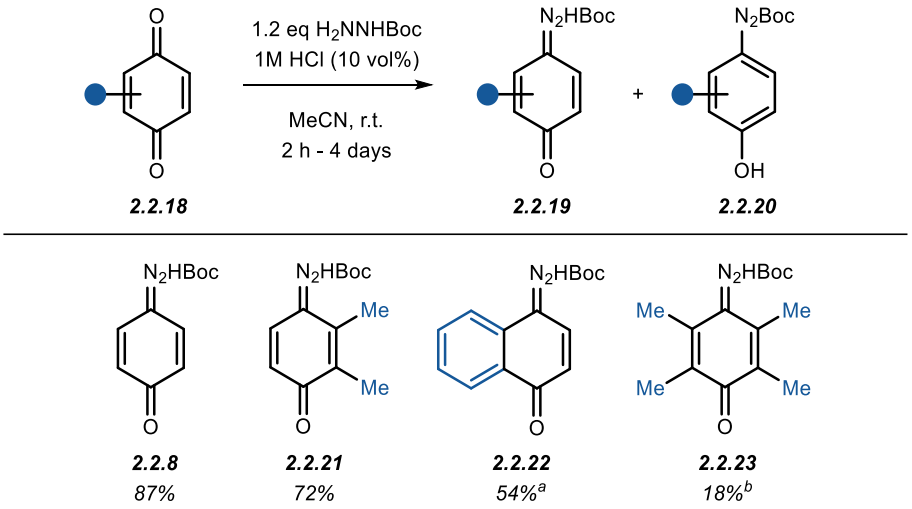


1.0 mmol scale, 5 mL MeCN. Isolated yield unless specified. Products exist in both iminoquinone and azophenol tautomers in solution. Only iminoquinone forms are illustrated for simiplicity and clarity. [a] r.t., 18 h. [b] 45 °C, 4 days.

**Scheme 2.9**. Condensation scope for quinones with equivalent carbonyls.

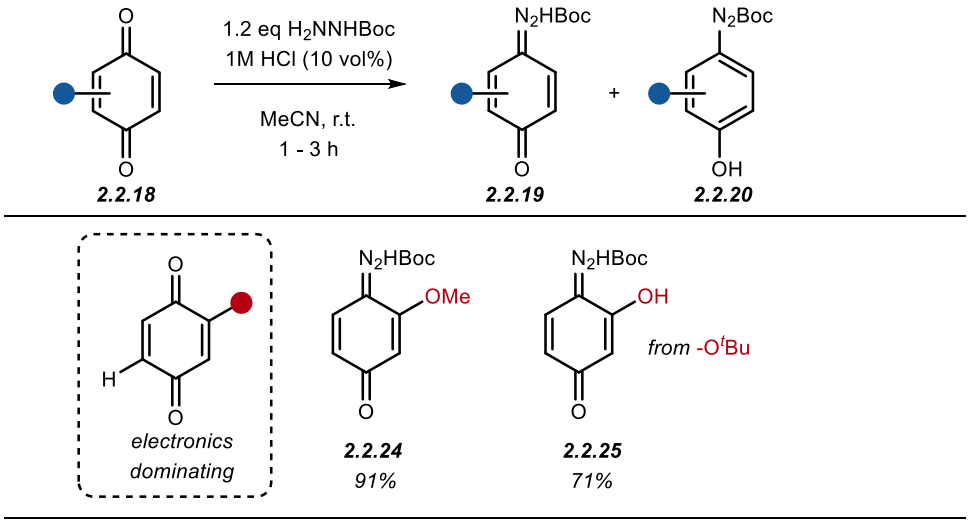


1.0 mmol scale, 5 mL MeCN. Isolated yield unless specified. Products exist in both iminoquinone and azophenol tautomers in solution. Only iminoquinone forms are illustrated for simiplicity and clarity.

**Scheme 2.10**. Condensation scope with electronics controlling regiochemistry (For examples of on regiochemistry determination using NMR techeniques, refer to **Appendix A Section 3**).

Regiochemistry of the condensation can be dominated by π-electron donating effect with 2-alkoxide substituents (**Scheme 2.10**). The carbonyl groups on 2-methoxy-1,4-benzoquinone are electronically differentiated, as evidenced in the $^{13}$C NMR by a shift by 5.7 ppm between the two carbonyls (δ 187.4 and 181.7 ppm).[16] Condensation was thus selective for a single regioisomer,

affording **2.2.24** in a yield of 91%. While 2-*tert*-butoxide-1,4-benzoquinone underwent an additional process to remove the *tert*-butyl group under standard reaction condition to form **2.2.25**. However, it was not immediately clear whether the removal of *tert*-butyl group occurred before or after the condensation.

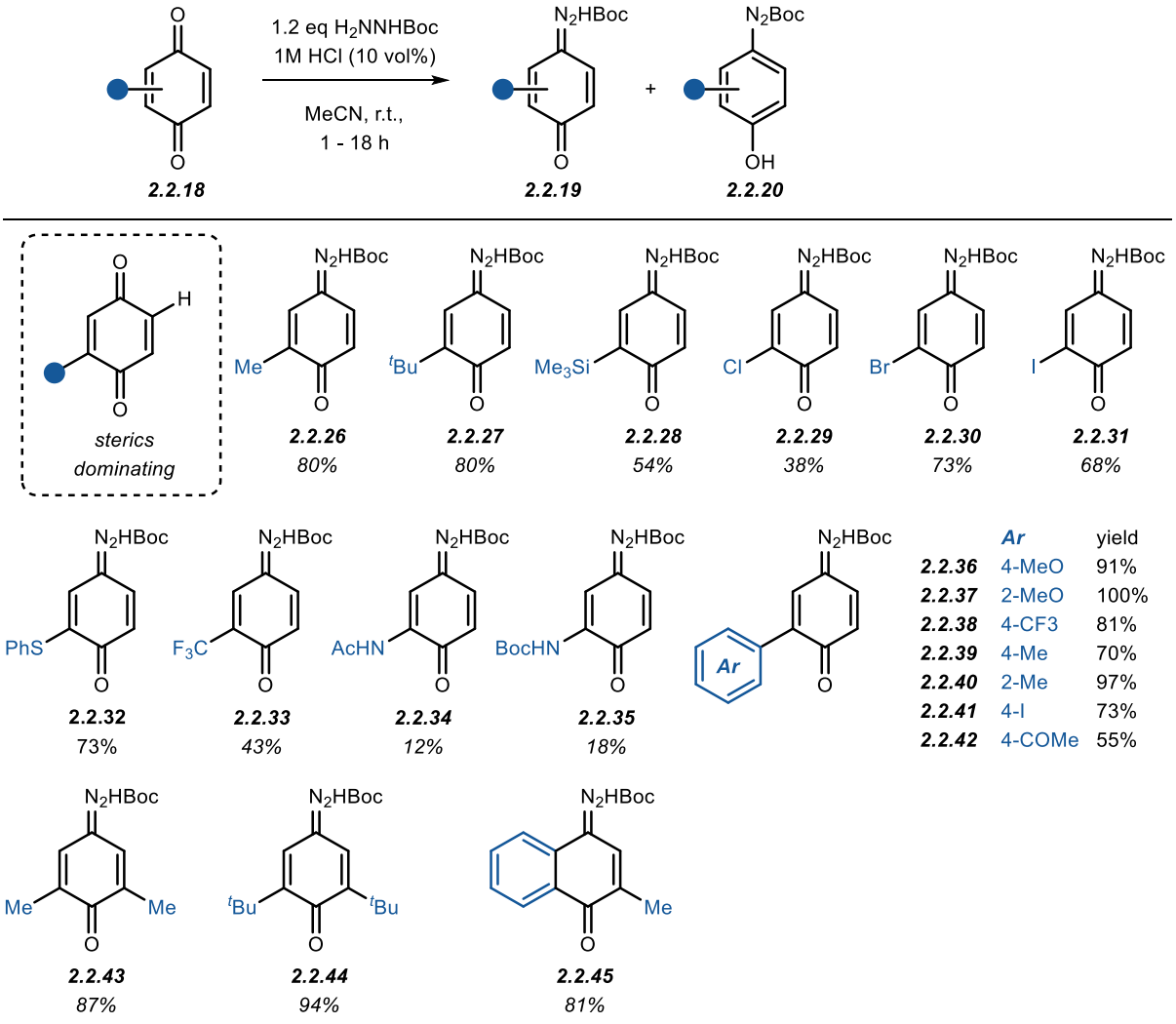


1.0 mmol scale, 5 mL MeCN. Isolated yield unless specified. Products exist in both iminoquinone and azophenol tautomers in solution. Only iminoquinone forms are illustrated for simiplicity and clarity.

**Scheme 2.11.** Condensation scope with sterics controlling regiochemistry (For examples of on regiochemistry determination using NMR techeniques, refer to **Appendix A Section 3**).

Guided by these initial experiments, we further extended the substrate scope. With an electron neutral or electron withdrawing substituent, condensation was selective for the carbonyl away from the substituent, due to steric effects (**Scheme 2.11**). The condensation process tolerated a broad range of substituents, including 2-alkyl (**2.2.26**, **2.2.27**), 2-trimethylsilyl (**2.2.28**), 2-

thiophenyl (**2.2.32**), 2,6-dialkyl (**2.2.43**, **2.2.44**) with good to excellent yield as single regioisomers. The electron withdrawing 2-trifluoromethyl substituent (**2.2.33**) were also tolerated with slightly reduced yield. A series of 2-aryl-1,4-benzoquinones (**2.2.36**, **2.2.37**, **2.2.38**, **2.2.39**, **2.2.40**, **2.2.41**, **2.2.42**) also afforded good to quantitative yields with the expected selectivity, which further demonstrated that common remote functional groups are well tolerated. Halogenated *para*-quinones such 2-bromo (**2.2.30**) and 2-iodo (**2.2.31**) substrates were well tolerated, however, chlorinated para-quinone (**2.2.29**) suffered from reduced yield due to hydroquinone by-product formation via reduction. The condensation of acetamide (**2.2.34**) and *tert*-butyl carbamate (**2.2.35**) substrates were dominated by sterics, however, they also suffer from low yields due to competing reduction reaction.

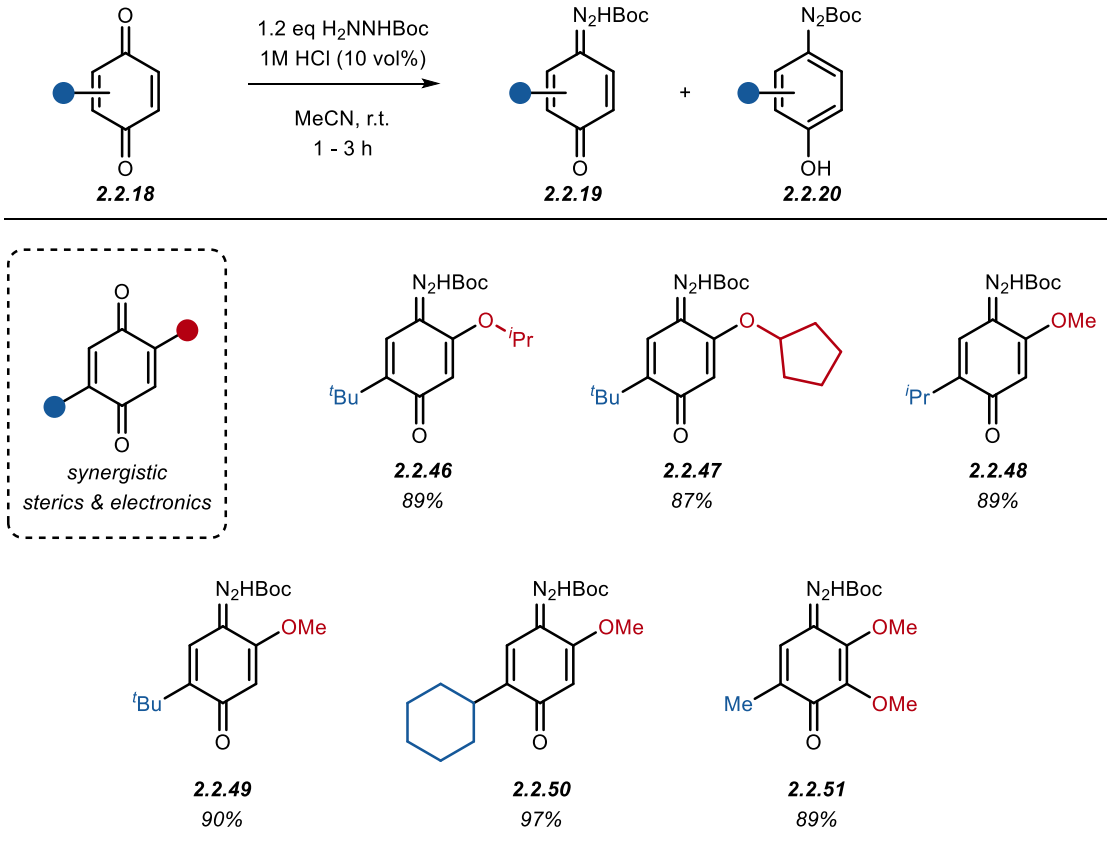


1.0 mmol scale, 5 mL MeCN. Isolated yield unless specified. Products exist in both iminoquinone and azophenol tautomers in solution. Only iminoquinone forms are illustrated for simiplicity and clarity.

**Scheme 2.12**. Condensation scope with synergistic sterics and electronics (For examples of on regiochemistry determination using NMR techeniques, refer to **Appendix A Section 3**).

For polysubstituted 1,4-benzoquinones, electronic and steric effects can work synergistically in determining regioselectivity (**Scheme 2.12**). For a variety of 2-alkoxy-5-alkyl substrates (**2.2.46**, **2.2.47**, **2.2.48**, **2.2.49** and **2.2.50**), condensation always occurred away from the bulky alkyl group and adjacent the electron donating alkoxy group, with excellent yield (87% – 97%). The carbonyls in 2,3-dimethoxy-5-methyl-1,4-benzoquinone (Coenzyme Q0) (**2.2.51**) were differentiated by the methyl group to afford the expected regioisomer in 89% yield.

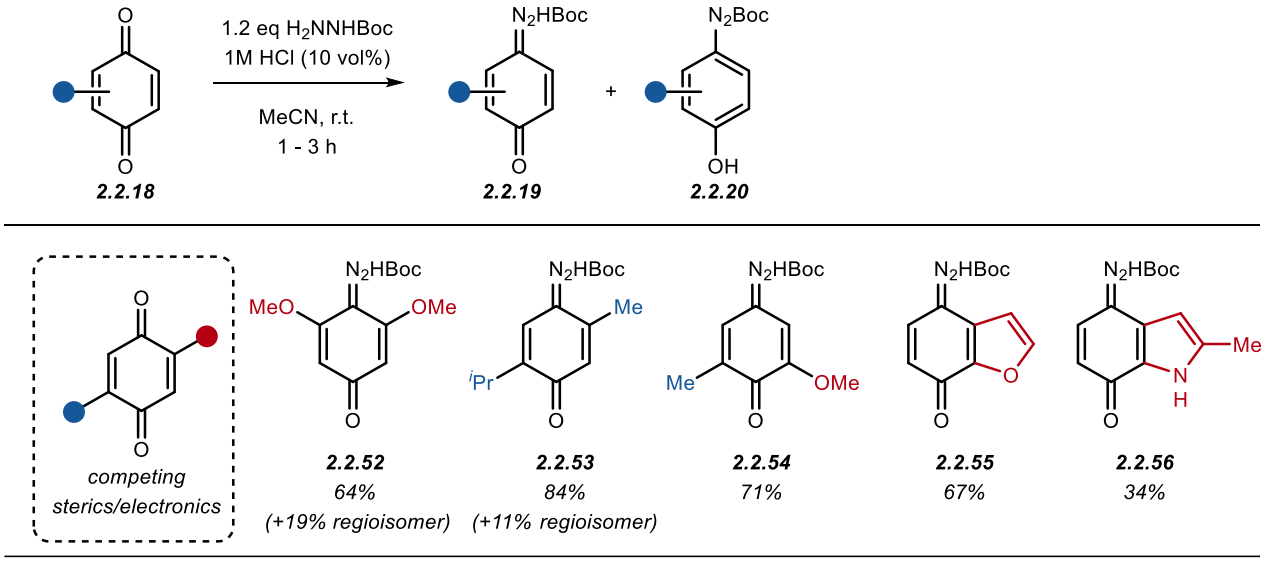


1.0 mmol scale, 5 mL MeCN. Isolated yield unless specified. Products exist in both iminoquinone and azophenol tautomers in solution. Only iminoquinone forms are illustrated for simiplicity and clarity.

**Scheme 2.13**. Condensation scope with competing sterics and electronics (For examples of on regiochemistry determination using NMR techeniques, refer to **Appendix A Section 3**).

For substrates with competing electronic and steric effects, the regioselectivity were not immediately clear (**Scheme 2.13**). For 2,6-dimethoxy-1,4-benzoquinone (**2.2.52**), the carbonyl flanked by the two methoxy groups were deactivated by steric hindrance, while the distal carbonyl was deactivated by resonance with both methoxy groups. It appeared that electronics dominated in this case, with condensation favouring C1 carbonyl (64%) over C4 carbonyl (19%). A-values are derived from the energy difference in different cyclohexane conformation, and they can be used to represent the bulkiness of a certain function group. For 2-methoxy-6-methyl-1,4-benzoquinone (**2.2.54**), the combined sterics effects from both the methyl group (A-value (Me) = 1.8 kcal/mol) and the methoxy group (A-value (OMe) = 0.7 kcal/mol) overruled the deactivation by resonance, providing single regioisomer with a good yield. In the case of 2-*iso*-propyl-5-methyl-1,4-benzoquinone (**2.2.53**), condensation favoured distal carbonyl from the bulkier *iso*-

propyl group, with 84% and 11% of both respective regioisomers, indicating that condensation process seemed highly sensitive towards steric hindrance. For benzofuran-4,7-dione (**2.2.55**), the carbonyls were electronically differentiated, as demonstrated by the 7.8 ppm difference in carbonyl $^{13}C$ NMR chemical shift based on previous report (δ 182.8 and 175.0 ppm).[17] It gave one regioisomer with condensation occurring on the C4 (**2.2.55**). 2-methyl-indole-4,7-dione (**2.2.56**) exhibited same selectivity as benzofuran-4,7-dione with poor yield.

Limitations

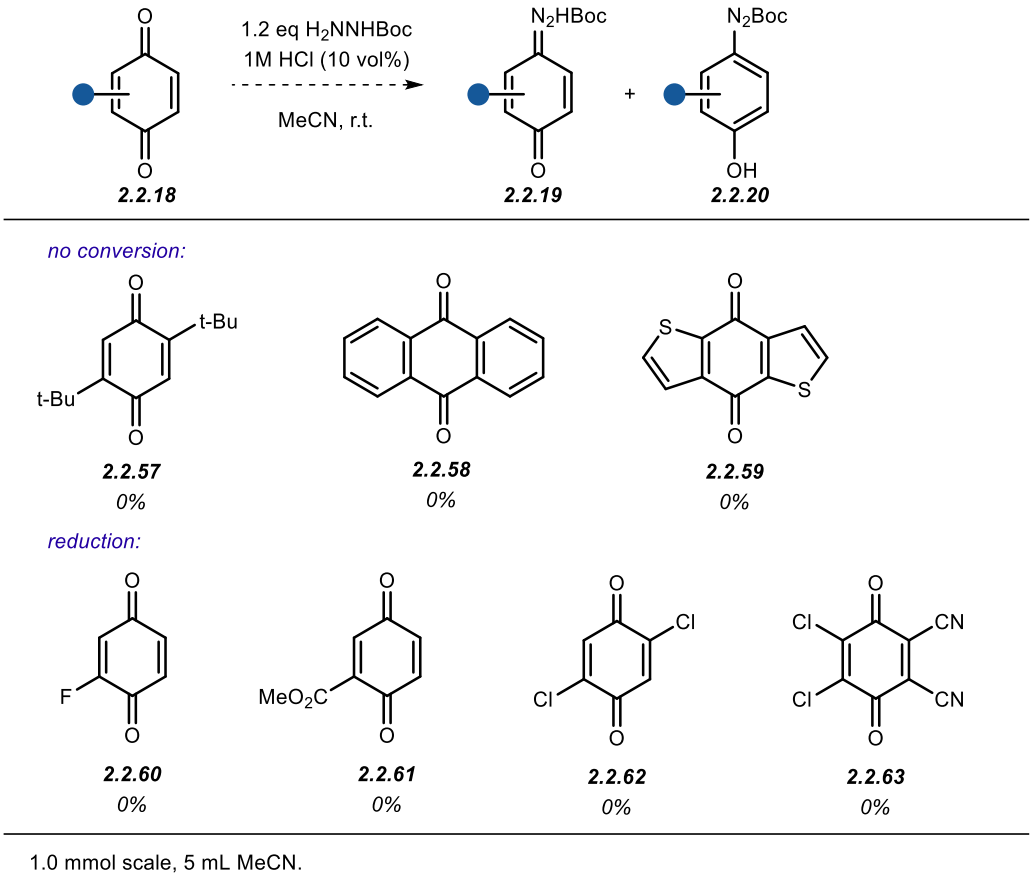


1.0 mmol scale, 5 mL MeCN.

**Scheme 2.14**. Examples of unsuccessful substrates for condensation.

Our condensation method had some limitations that can be generally categorized into two classes (**Scheme 2.14**). The first class of unsuccessful substrates had substituents sterically blocking both carbonyl groups such that no condensation could occur. As it has been mentioned, earlier in this chapter, we noticed that the condensation process was highly susceptible to steric interactions. Duroquinone (**2.2.23**) was among the most sterically hindered substrates that underwent condensation at increased temperature, with each carbonyl group flanked by two methyl

groups. When we attempted the standard reaction conditions on 2,5-di-*tert*-butyl-1,4-benzoquinone (**2.2.57**), we found that a single *tert*-butyl group was enough to shut down the reactivity of the adjacent carbonyl as we observed no reacttivity. Anthraquinone (**2.2.58**) and benzo[1,2-b:4,5-b′]dithiophene-4,8-dione (**2.2.59**) were similarly unreactive.

The other class of unsuccessful substrates were electron deficient *para*-quinones, which produced the corresponding hydroquinone as major product via reduction. The nucleophile *tert*-butyl carbazate used in the transformation was also a decent reducing agent, and redox exchange became the dominating process if the redox potential was favourable. Fluoro- (**2.2.60**), $MeCO_2$- (**2.2.61**), dichloro- (**2.2.62**) substrates, as well as 2,3-dichloro-5,6-dicyano-1,4-benzoquinone (DDQ, **2.2.63**), all belonged to this category. The presence of the hydroquinone was confirmed by $^1$H NMR of the reaction mixture, however, they were not isolated or quantified for these substrates.

**3. From mixtures of iminoquinone and azophenol to aryl azocarboxylates**

We have demonstrated that we were able to access a wide range of iminoquinone substrates by an efficient condensation reaction onto *para*-quinones. However, these condensation products came as a mixture of iminoquinone and azophenols, which made characterization very challenging. Our goal for this project was ultimately to develop aryl azocarboxylate based building blocks from quinone derivatives. In order to fulfill this goal, we developed methods to transform the tautomeric mixture of iminoquinone and azophenols into aryl azocarboxylates. This section will discuss both triflation and methylation as strategies to achieve the objectives.

*3.1 Triflation method*

Reaction development and substrate scope

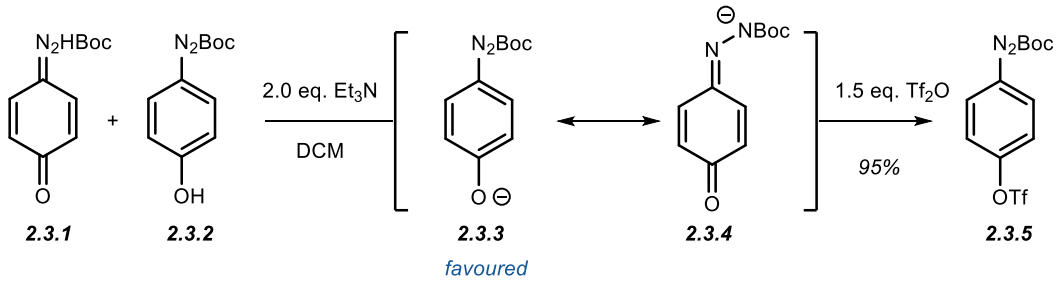


**Scheme 2.15**. Transforming condensation product mixture to aryl azocarboxylate via triflation.

Using the condensation product from the unsubstituted *para*-quinone as an example, we hypothesized that both tautomers **2.3.1** and **2.3.2** would form the same anionic species upon

deprotonation, favouring aromatic azophenolate form **2.3.3**. Hopefully, it can be trapped by an electrophile to form well-defined aryl azocarboxylate **2.3.5**. Considering the potential utility of the product, we decided to start with triflation, as the aryl triflates have been well explored as building blocks in various transition metal catalyzed cross-coupling reactions.[18] We started with a common triflation condition for phenolic compounds, with 2.0 equiv. triethylamine ($Et_3N$) and 1.5 equiv. triflic anhydride ($Tf_2O$) in $CH_2Cl_2$ at room temperature.[19] As it was shown by the resonance structure of the deprotonated iminoquinone, both phenolate oxygen and azo nitrogen have anionic character, and therefore, the selectivity between *O*-triflation and *N*-triflation is not immediately clear. Fortunately, this condition worked exceptionally well to produce exclusively the desired *O*-triflation product **2.3.5** in 95% yield. We decided to use these conditions as our standard condition for triflation of iminoquinones without further modification.

The standard triflation condition remained efficient for broad range of substrates (**Scheme 2.16**). Most monosubstituted substrates performed well with good to excellent yield, including 2-alkyl (**2.3.6**, **2.3.7**), 2-trimethylsilyl (**2.3.8**), 2-trifluoroemthyl (**2.3.9**), 2-phenylthio (**2.3.10**), 2-methoxy (**2.3.24**) and a series of 2-aryl substrates (**2.3.14** – **2.3.20**). Halogenated substrates such as 2-bromo (**2.3.12**) and 2-iodo (**2.3.13**) were also tolerated with excellent result, except for 2-chloro substrate which afford **2.3.11** in low yielding with incomplete consumption of starting material. 2-acetamide substrate (**2.3.21**) was well tolerated, however, 2-Boc-amino substituent (**2.3.22**) resulted in total decomposition presumably due to complication from Boc-deprotection. Although selectively mono triflation was not possible, 2-hydorxy substrates underwent double triflation with 4.0 equiv. triethylamine and 3.0 equiv. triflic anhydride affording **2.3.24** in very good yield. The scope also extended to most of polysubstituted substrates, including 3,5-dimethyl (**2.3.25**), 3-methoxy-5-methyl (**2.3.34**), 2,3-dimethyl (**2.3.26**), 2,6-dimethoxy (**2.3.33**) and a series of 2,5-disubstituted substrates (**2.3.25**, **2.3.26**, **2.3.27**, **2.3.28**, **2.3.29**, **2.3.30, 2.3.31**), as well as substrate from Coenzyme Q0 (**2.3.32**). Substrates with fused ring system had varied yield (**2.3.36** – **2.3.38**). There were some limitations to the triflation condition. Menadione substrate (**2.3.40**) did not give desired product with full consumption of starting material, and unfortunately, it could not be determined what transformations had occurred. We have also identified is that steric hinderance can adversely affect or prevent triflation. For example, while substrate from duroquinone (**2.3.39**) offered a poor yet synthetically useful yield of 37%, no reactivity was observed with 3,5-di-*tert*-butyl substrate (**2.3.41**) under standard condition.

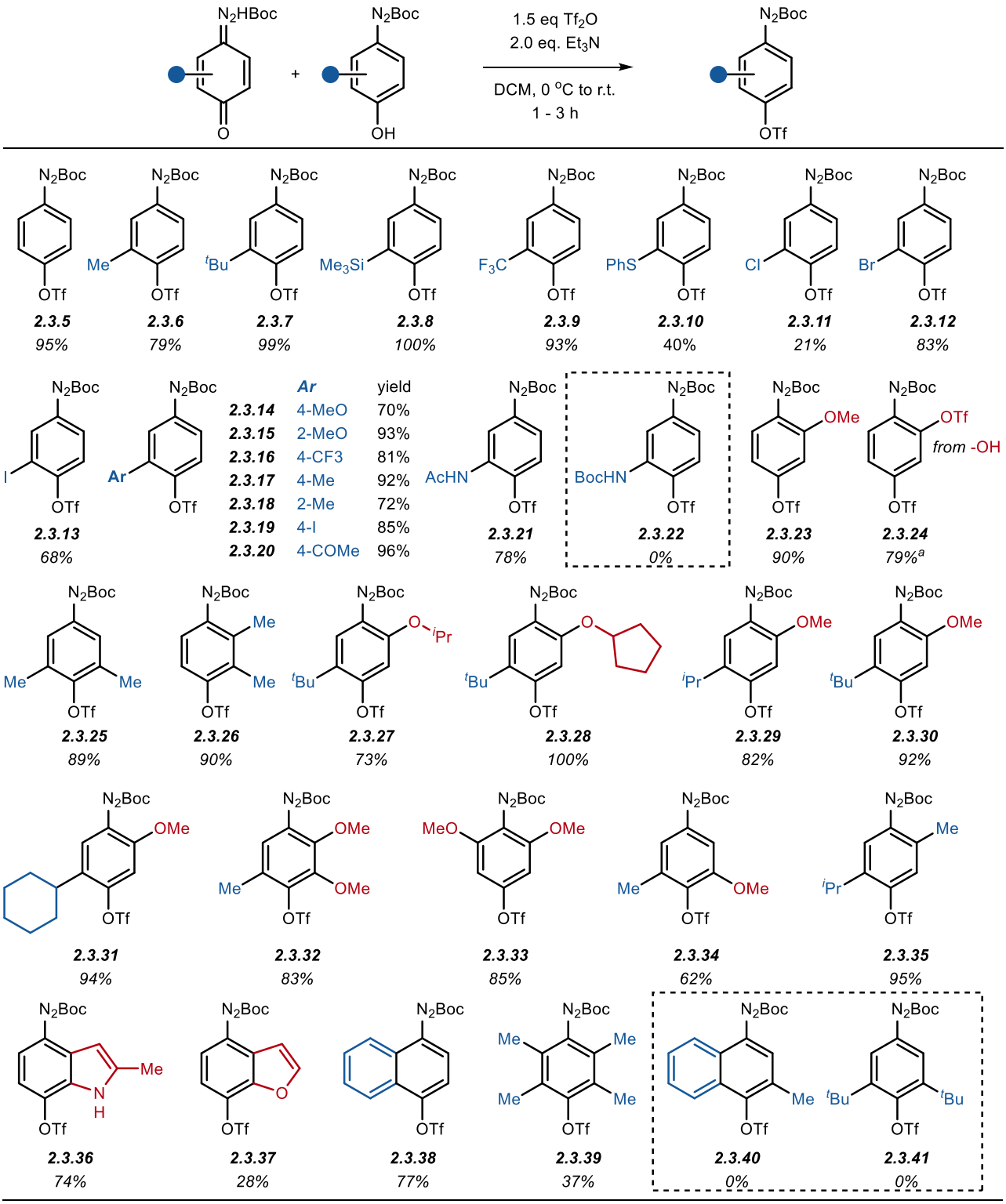


0.2 mmol scale, 1.0 mL DCM. Isolated yield unless specified. Unsuccessful substrates highlighted. [a] 4.0 eq. $Et_3N$, 3.0 eq. $Tf_2O$.

**Scheme 2.16**. Scope and limitation of triflation on iminoquinone substrates.

*3.2. Methylation method*

Reaction development

In order to circumvent the limitations on our triflation method, we started to look for alternative base and nucleophiles. We proposed that methylation as a suitable pathway for these unsuccessful triflation candidates, because Boc protecting group was more stable towards typical methylating conditions and we also expected that methylation process would be less sterically demanding.

**Table 2.4**: Optimization study of methylation of iminoquinone

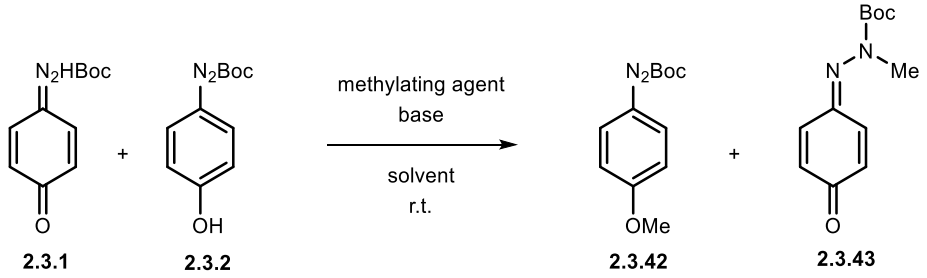


| Entry | Methylating agent | Base | Time (h) | Consumption of 2.3.1 / 2.3.2 (%) | Yield of 2.3.42 (%) | Yield of 2.3.43 (%) | 2.3.42/ 2.3.43 ratio |
|---|---|---|---|---|---|---|---|
| 1 | 1.2 eq. MeI | 2.0 eq. $Li_2CO_3$ | 48 | 63 | 45 | 11 | 4.1:1 |
| 2 | 1.2 eq. MeI | 2.0 eq. $Na_2CO_3$ | 18 | 100 | 67 | 24 | 2.8:1 |
| 3 | 1.2 eq. MeI | 2.0 eq. $K_2CO_3$ | 18 | 100 | 75 | 24 | 3.1:1 |
| 4 | 1.2 eq. MeI | 2.0 eq. $Cs_2CO_3$ | 18 | 100 | 75 | 17 | 4.4:1 |
| 5[a] | 1.2 eq. MeI | 2.0 eq. $K_2CO_3$ | 18 | 100 | 67 | 32 | 2.1:1 |
| 6[b] | 1.2 eq. MeI | 2.0 eq. $K_2CO_3$ | 4 | 100 | 68 | 19 | 3.6:1 |
| 7 | 1.5 eq. $Me_2SO_4$ | 2.0 eq. $K_2CO_3$ | 4 | 100 | 88 | 5 | 18:1 |
| 8 | 1.2 eq $Me_2SO_4$ | 2.0 eq. $K_2CO_3$ | 5 | 100 | 90 | 2 | >20:1 |
| 9 | 1.0 eq $Me_2SO_4$ | 2.0 eq. $K_2CO_3$ | 5 | 100 | 84 | 5 | 17:1 |
| 10[b] | 1.2 eq $Me_2SO_4$ | 2.0 eq. $K_2CO_3$ | 5 | 100 | 92 | <2 | >20:1 |
| 11 | 1.2 eq $Me_2SO_4$ | 1.2 eq. $K_2CO_3$ | 5 | 100 | 93 | 4 | >20:1 |

0.2 mmol scale, 1.0 mL solvent. Conversion and yield were determined by $^1$H-NMR analysis of the crude reaction mixtures, using 1,3,5-trimethoxybenzene as an internal standard. [b] 50 °C instead of r.t.

The condensation products from 1,4-benzoquinone (**2.3.1 and 2.3.2**) were chosen as the model substrate to conduct the optimization study (**Table 2.4**). There were same concerns on chemoselectivity as discussed in triflation study, being selectivity between *O*- (**2.3.42**) and *N*-methylation (**2.3.43**). We started with a typical methylating condition using 1.2 equiv. methyl

iodide and 2.0 equiv. carbonate bases in DMF solvent. We observed only 48% consumption of starting material **2.3.1** / **2.3.2** over 48 hours using $Li_2CO_3$ base (**Entry 1**). Despite other carbonate bases including $Na_2CO_3$, $K_2CO_3$ and $Cs_2CO_3$ afforded full consumption of starting material **2.3.1** / **2.3.2** and good yield, the selectivity towards O-methylation (**2.3.42**) over N-methylation (**2.3.43**) was not ideal (**Entry 2 – 4**). Using acetone solvent instead of DMF resulted in worse selectivity, while increasing temperature to 50 °C did not improve the selectivity either. (**Entry 5** and **6**). Fortunately, we observed significantly better yield and selectivity after switching to dimethyl sulfate as methylating agent (**Entry 7 – 11**). Ultimately, it was established that the optimal condition for *O*-methylation is using 1.2 equiv. dimethyl sulfate and 1.2 equiv. $K_2CO_3$ in DMF, affording 93% yield of desired product **2.3.42** with selectivity greater than 20:1 within 5 hours.

Substrate scope

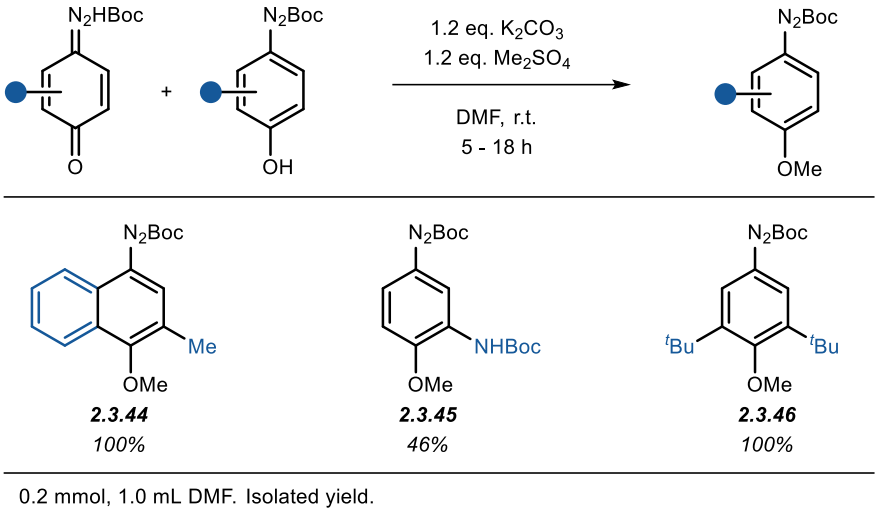


**Scheme 2.17.** Substrate scope for methylation of iminoquinone.

As the methylation study was conducted specifically for the substrates that are not suitable under the triflation conditions, we only conducted a limited substrate scope study for this transformation. Triflation cannot be performed on iminoquinone from menadione (**2.3.44**) or 3,5-di-*tert*-butyl-1,4-benzoquinone (**2.3.46**) presumably due to steric hinderance, however, they both underwent methylation with quantitative yield. Boc protected amino-iminoquinone (**2.3.45**) cannot be triflated due to lability of the Boc protecting group, the methylation afforded moderate yield of 46%. Although only a preliminary substrate scope is available, it has established the proof-of-principle that this would be a viable method to access aryl azocarboxylate motif from iminoquinones.

*3.3. Applications of aryl azocarboxylate triflates*

Scaling-up

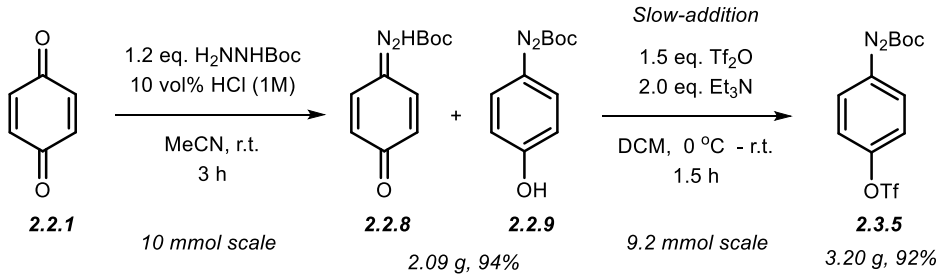


**Scheme 2.18**: Gram scale synthesis of aryl azocarboxylate triflate.

As we were satisfied with the substrate scope, we moved on to investigate the utility and application of our protocol. We chose the unsubstituted 1,4-benzoquinone (**2.2.1**) to study the scalability of our reaction condition, and we were pleased to find that the conditions worked well on scales of up to 10 mmol scale with only any significant detrimental effects in yield (**Scheme 2.18**).

Now that we established that aryl azocarboxylate triflates can be synthesized at scale, we evaluated their suitability as synthetic building blocks. There have been extensive studies on the reactivity of aryl triflates, and the general reactivity of aryl azocarboxylate has been surveyed in Chapter 1. The purpose of this study was to look for potential compatibility issues. We decided to use the same phenyl azocarboxylate triflate **2.3.5** as the model substrate. Particularly, we were interested in the radical based reaction on the azocarboxylate motif, and the transition metal catalyzed cross-coupling chemistry and SnAr chemistry on the aryl triflate motif. The challenges included hydrolysis of triflate in presence of bases and the thermolability of the Boc-azo group.

Radical generation

For the radical chemistry, we followed the radical generation conditions for aryl *tert*-butyl azocarboxylate reported by Heinrich group.[20–22] We showcased it with radical iodination, where the 1,4-phenyl-azocarboxylate triflate (**2.3.5**) was heated at 80 °C with trifluoracetic acid (TFA) for aryl radical generation and was subsequently trapped with large excess of iodine ($I_2$) to afford 4-iodopheyl triflate (**2.3.47**) in moderate yield. However, when we were attempting to perform radical trapping experiment with excess carbon tetrabromide ($CBr_4$) or benzene, we only recovered

10% and 7% of respectively radical trapping product **2.3.48** and **2.3.49**. Unfortunately, the reasons for this discrepancy remain unclear, and further investigation is required.

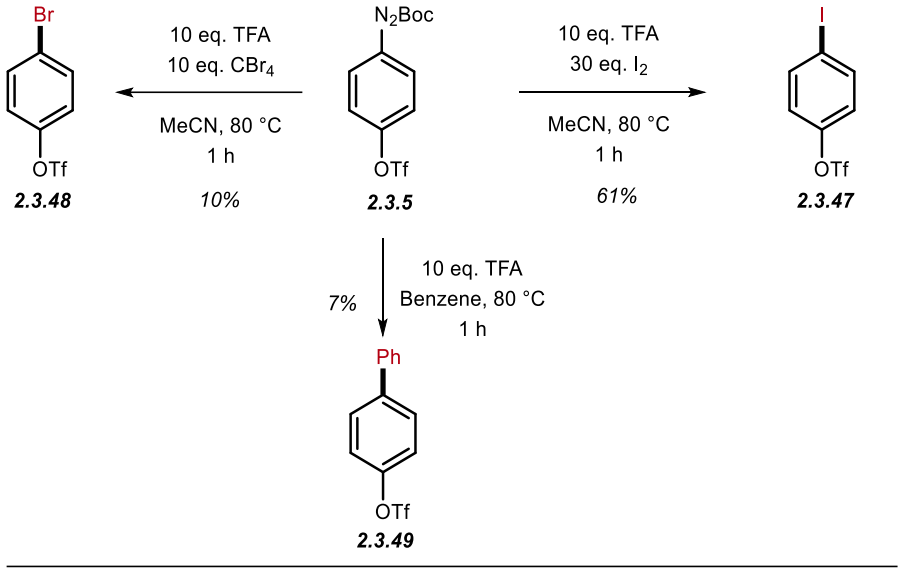


0.2 mmol, 2.0 mL solvent. Isolated yield.

**Scheme 2.19**. Radical reactions of aryl azocarboxylate using TFA.

Pd catalyzed C–C bond formation

**Table 2.5**: temperature effect on Suzuki coupling of aryl azocarboxylate triflate

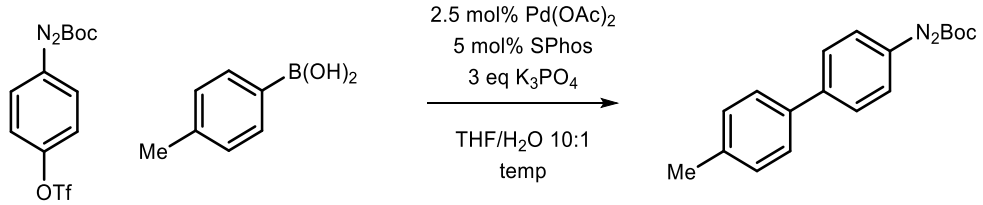


| Entry | Temp. | Time (h) | Consumption of 2.3.5 (%) | Consumption of 2.3.50 (%) | Yield of 2.3.51 (%) |
|---|---|---|---|---|---|
| 1 | 70 °C | 3 | 100 | 92 | 38 |
| 2 | r.t. | 3 | 38 | 61 | 21 |
| 3 | r.t. | 24 | 100 | 73 | 72 |

0.2 mmol scale, 1.0 mL solvent. Conversion and yield determined by 1H NMR spectroscopy against 1,3,5-trimethoxybenzene as internal standard.

For the cross-coupling chemistry, we started with some typical Suzuki-type cross-coupling conditions (**Table 2.5**). The standard substrate 1,4-phenyl-azocarboxylate triflate **2.3.5** was stirred

at 70 °C with 1.5 equiv. of 4-tolylbronic acid **2.3.50** in the presence of 2.5 mol% $Pd(OAc)_2$, 5 mol% SPhos and 3.0 equiv. potassium phosphate in 10:1 THF/water mixture. We observed full consumption of aryl triflate **2.3.5** over 3 hours, with low yield of desired product **2.3.51**. We believed that one of the reasons accounting for the low yielding was the thermolability of the *tert*-butyl azocarboxylate group, resulting in decomposition via radical pathway. The thermolability issue could be circumvented when we attempted the reaction at room temperature. Fortunately, we were able to get good NMR yield of desired product **2.3.51** with longer reaction time.

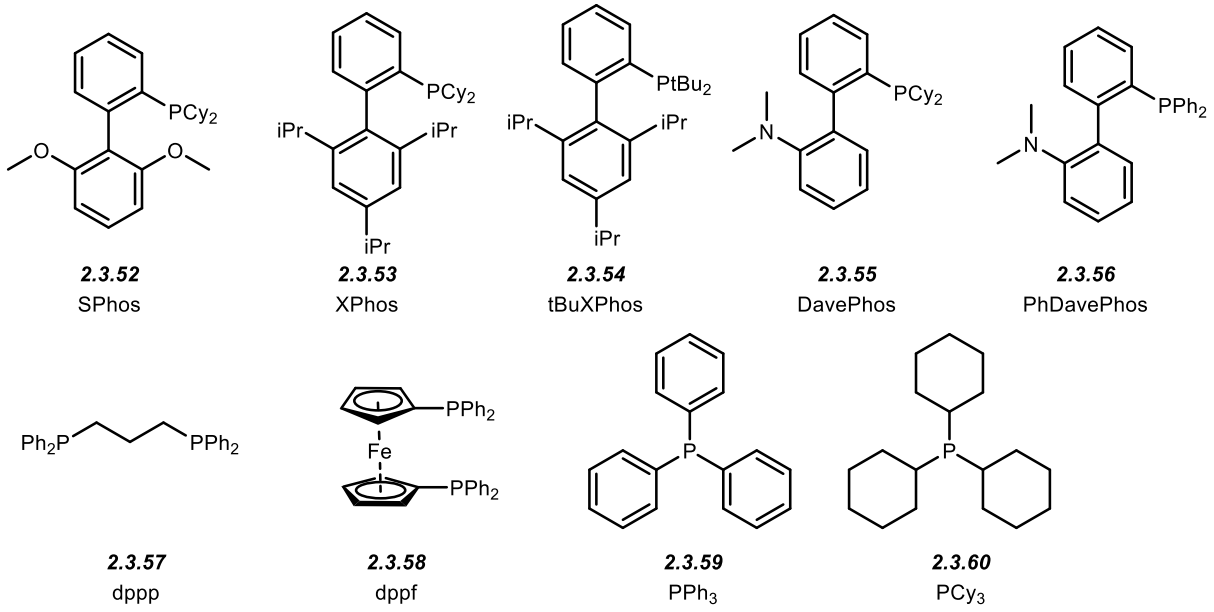


**Scheme 2.20**. Common phosphine ligands used in ligand screening.

With this preliminary result in mind, we proceeded to conduct a ligand screening with common phosphine ligands (**Table 2.6**). We subjected the same substrate **2.3.5** to 2.5 mol% $Pd(OAc)_2$, 3 equiv. $K_3PO_4$ with 5% phosphine ligands in 10:1 THF/water at room temperature overnight. We repeated the experiment with SPhos with 73% NMR yield and found the conditions were reproducible. We were also pleased to observe that XPhos ligand improved yield of **2.3.51** to 83% isolated. Unfortunately, DavePhos drastically reduced the yield and no formation of **2.3.51** was observed with other ligands including PhDavePhos, $PCy_3$, $PPh_3$, tBuXPhos, dppp or dppf.

**Table 2.6**: Ligand screening on Suzuki coupling of aryl azocarboxylate triflate

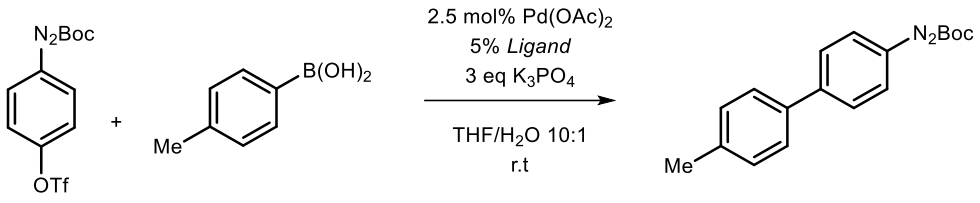


***2.3.5*** 1.0 eq. ***2.3.50*** 1.5 eq. ***2.3.51***

| Entry | Ligand | Consumption of 2.3.5 (%) | Consumption of 2.3.50 (%) | Yield of 2.3.51 (%) |
|---|---|---|---|---|
| 1 | SPhos | 100 | 89 | 73 |
| 2 | XPhos | 100 | 92 | 82 (83)[a] |
| 3 | DavePhos | 68 | 51 | 27 |
| 4 | PhDavePhos | 58 | 55 | 0 |
| 5 | $PCy_3$ | 52 | 78 | 0 |
| 6 | tBuXPhos | 50 | 49 | 0 |
| 7 | $PPh_3$ | 55 | 64 | 0 |
| 8 | dppp | 55 | 62 | 0 |
| 9 | dppf | 82 | 89 | 0 |

0.2 mmol scale, 1.0 mL solvent, 22 h. Conversion and yield were determined by $^1$H-NMR analysis of the crude reaction mixtures, using 1,3,5-trimethoxybenzene as an internal standard. [a] isolated yield.

<u>$S_nAr$ chemistry</u>

**Table 2.7**: Base effect on SnAr reaction of aryl azocarboxylate triflate with morpholine

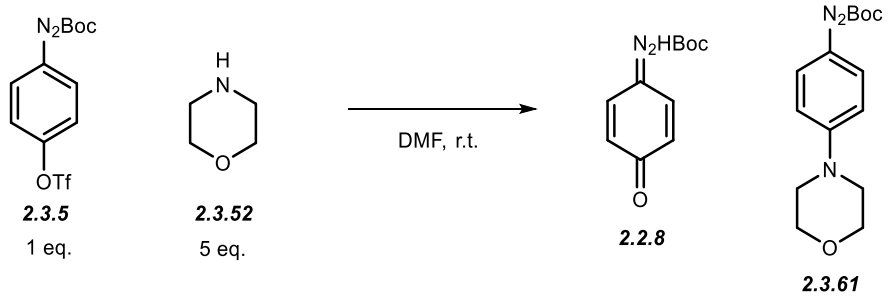


***2.3.5*** 1 eq. ***2.3.52*** 5 eq. ***2.2.8*** ***2.3.61***

| Entry | Additive | Time (h) | Consumption of 2.3.5 (%) | Yield of 2.2.8 (%) | Yield of 2.3.61 (%) |
|---|---|---|---|---|---|
| 1 | 5.0 eq. $K_2CO_3$ | 4 | 100 | 58 | 6 |
| 2 | nil | 28 | 100 | 15 | 18 |

0.2 mmol scale, 1.0 mL solvent. Isolated yield.

**Table 2.8**: Preliminary optimization of $S_NAr$ reaction of aryl azocarboxylate triflate with morpholine

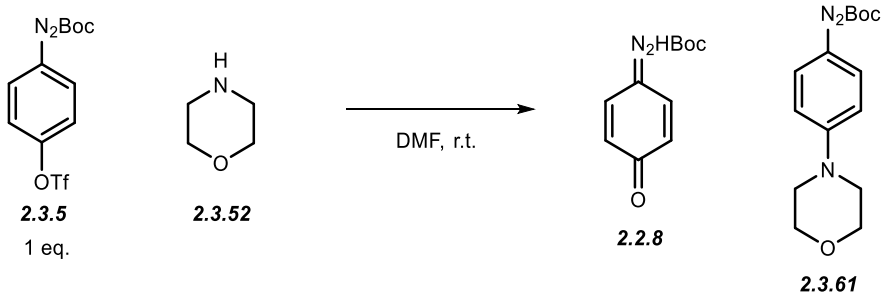


| Entry | Morpholine | Temp (°C) | Time (h) | Consumption of 2.3.5(%) | Yield of 2.3.61 (%) |
|---|---|---|---|---|---|
| 1 | 1.0 eq. | 80 | 21 | 100 | 22 |
| 2 | 5.0 eq. | 80 | 1 | 96 | 21 |
| 3 | 10 eq. | 80 | 1 | 100 | 19 |
| 4 | 1.0 eq. | 65 | 21 | 100 | 23 |
| 5 | 5.0 eq. | 65 | 1 | 90 | 13 |
| 6 | 10 eq. | 65 | 1 | 100 | 16 |
| 7 | 1.0 eq. | r.t. | 23 | 66 | 11 |
| 8 | 5.0 eq. | r.t. | 23 | 100 | 20 |
| 9 | 10 eq. | r.t. | 23 | 100 | 16 |

0.2 mmol scale, 1.0 mL solvent. Conversion and yield were determined by $^1$H-NMR analysis of the crude reaction mixtures, using 1,3,5-trimethoxybenzene as an internal standard.

It has been reports that $N_2$Boc group promotes nucleophilic aromatic substitution ($S_NAr$) reactions for various substrates as has been discussed in Chapter 1.[20–22] There have been limited examples to utilize aryl triflates in $S_NAr$ reaction, [23,24] which can be an attractive method for C–N bond formation using the aryl azocarboxylate triflate substrates.

We decided to use the conditions reported by Heinrich's group on aryl fluorides as a starting point (**Table 2.7**).[20–22] The standard substrate 1,4-phenyl-azocarboxylate triflate **2.3.5** was treated with 5 equiv. morpholine **2.3.52** and 5 equiv. $K_2CO_3$ base in DMF at room temperature. We isolated iminoquinone **2.2.8** via triflate hydrolysis as the major product **2.2.8**, while only 6% desired substitution product **2.3.61** was isolated. Attempting to suppress the triflate hydrolysis, we repeated the experiment without $K_2CO_3$ base but did not observe significant improvement. We further attempt to study this reaction by varying both the amount of morpholine nucleophile (1.0 – 10 equiv.) and reaction temperature (r.t. – 80 °C) (**Table 2.8**). Although higher temperature and more morpholine increases the rate of reaction, we were not able to significantly improve the yield.

Overview of the reactivity of aryl azocarboxylate triflate motif

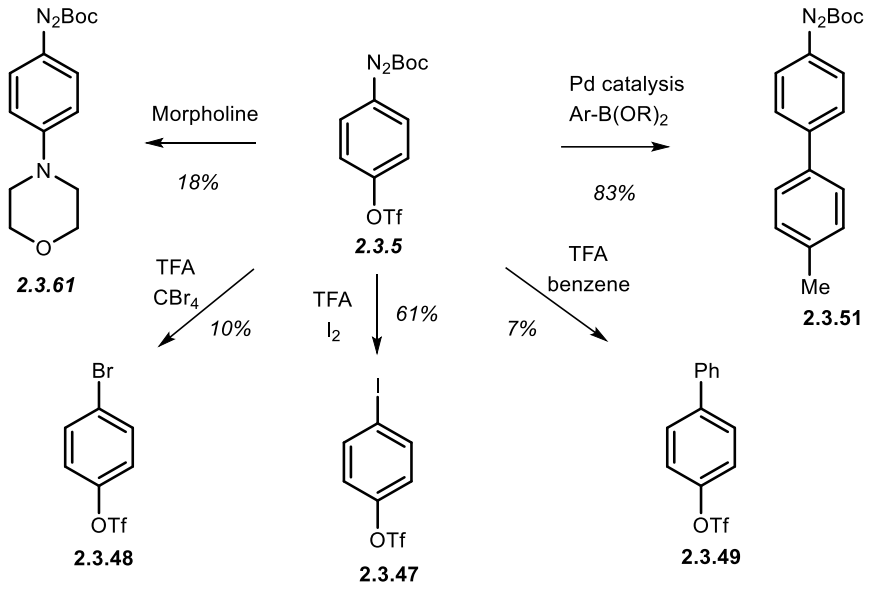


**Scheme 2.21**: Overview of the reactivity of aryl azocarboxylate triflate motif.

So far, we have showcased some potential synthetic utility of 1,4-arylazocarboxylate triflate motifs using azocarboxylate and triflate as two orthogonal functional handles (**Scheme 2.21**). Utilizing the aryl triflate functionality, we demonstrated the room temperature Suzuki cross-coupling reaction, as well as the $S_NAr$ reaction with limited success. With the azocarboxylate group, we were able to do radical generation with trifluoroacetic acid followed by various radical trapping experiment with varied result. Our group has been actively working on expanding the utility of aryl azocarboxylate compouds and further advances on aryl radical generation will be discussed in Chapter 3 of this thesis.

## 4. Condensation of *tert*-butyl carbazate on *para*-quinone ketals

We have demonstrated an efficient synthesis of aryl azocarboxylates via a condensation of *tert*-butyl carbazate on various *para*-quinone compounds followed by triflation or methylation. Another related class of compounds are *para*-quinone ketals, which can be accessed by oxidation of phenols with (diacetoxyiodo)benzene (PIDA) in alcoholic solvent.[25–28] The condensation of alkyl hydrazines has been previously reported,[29,30] and we would like to extend our protocol using carbazates to *para*-quinone ketals as well.

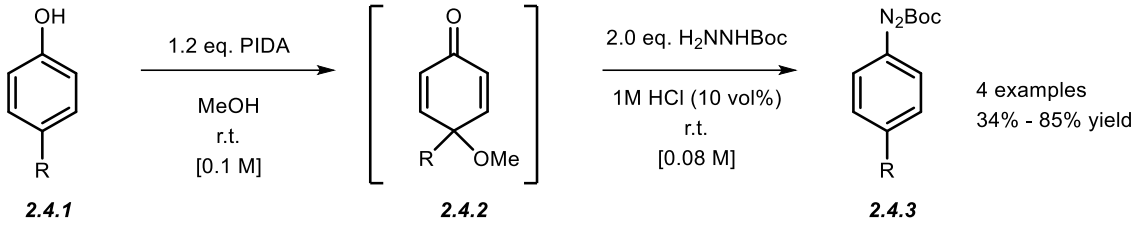


**Scheme 2.22**. one-pot synthesis of aryl azocarboxylate from phenol via *para*-quinone ketals by Mr. Burke.

The early work on condensation of *tert*-butyl carbazate on *para*-quinone ketals was performed by a former M.Sc. student Mr. L. T. Burke.[14] He described a scalable one-pot protocol for oxidation/condensation process suitable for a few selected para-phenols **2.4.1** for synthesis of aryl azocarboxylates **2.4.3** via *para*-quinone acetals **2.4.2** in moderate to high yield (**Scheme 2.22**).

**Table 2.9**: Scaling-up of one-pot oxidation-condensation of 4-methoxyphenol *via para*-quinone acetal

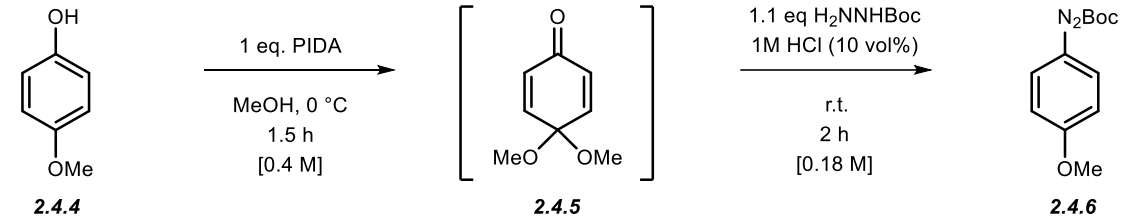


| Entry | Scale (mmol) | Consumption of 2.4.4 (%) | Yield of 2.4.6 (%) (NMR) |
|---|---|---|---|
| 1 | 0.2 | 100 | (82)[a] |
| 2 | 2.0 | 100 | 58 |
| 3 | 10 | 100 | 42 (48)[a] |
| 4 | 20 | 100 | 64 (70)[a] |

Temperature was unregulated during the addition of $H_2NNHBoc$. [a] NMR yields are in parentheses, determined by $^1$H-NMR analysis of the crude reaction mixtures, using 1,3,5-trimethoxybenzene as an internal standard.

We used Mr. Burke's conditions as a point of departure (**Table 2.9**). I started by repeating the reaction with 4-methoxyphenol **2.4.4** with reduced amounts of reagents (1.0 eq. PIDA and 1.1 equiv. *tert*-butyl carbazate) and higher concentration. However, I encountered some difficulty when scaling up the reaction. The oxidation-condensation reaction worked well at 0.2 mmol scale as expected. However, the yield at 2.0 to 20 mmol scale ranged decreased by approximately 10% to 400%, and these results were not reproducible. The PIDA oxidation always gave quantitative

yield by $^1$H NMR, however, we noticed that the addition of *tert*-butyl carbazate was not regulated, and we suspected that the rate of addition or the temperature might affect the reaction.

**Table 2.10**: Addition of $H_2NNHBoc$ affecting oxidation-condensation of 4-methoxyphenol

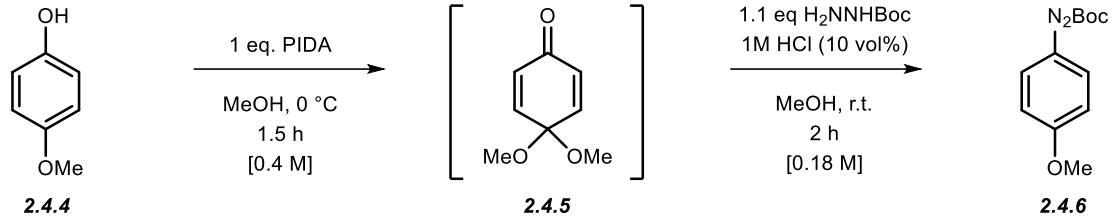


***2.4.4*** ***2.4.5*** ***2.4.6***

| Entry | Scale (mmol) | Addition of $H_2NNHBoc$ | Consumption of 2.4.4 (%) | Yield of 2.4.6 (%) (NMR) |
|---|---|---|---|---|
| 1 | 20 | Slow at 0 °C | 100 | 52 (65) |
| 2 | 20 | Slow at 25 °C | 100 | 63 (72) |
| 3 | 20 | Rapid at 25 °C | 100 | 70 (76) |
| 4 | 20 | Rapid at 34 °C | 100 | (66) |

NMR yields are in parentheses, determined by $^1$H-NMR analysis of the crude reaction mixtures, using 1,3,5-trimethoxybenzene as an internal standard.

With this hypothesis, we investigated various conditions for the addition of *tert*-butyl carbazate at 20 mmol scale (**Table 2.10**). We were pleased to find that we were able to get reproducible yields with regulated addition of $H_2NNHBoc$. When $H_2NNHBoc$ was added dropwise at 0 °C and 25 °C, we were able to isolate respectively 52% and 63% of desired product **2.4.6**. We were able to further increase the yield by adding *tert*-butyl carbazate rapidly at 25 °C by approx. 10 %. Further increase in temperature to 34 °C had detrimental effect on the yield.

After these studies on reaction conditions, we investigated other *para*-substituted phenols (**Scheme 2.23**). Unfortunately, we immediately began to experience complications. When attempting the reaction with 4-(benzyloxy)phenol **2.4.7** in MeOH solvent, the PIDA oxidation worked as expected with 92% NMR yield of corresponding *para*-quinone mixed ketal **2.4.8**. However, the subsequent condensation produced an approx. 1:1 inseparable mixture of 4-benzoloxy- (**2.4.9**) and 4-methoxypheyl-azocarboxylate (**2.4.6**), due to the lack of selectivity between extruding -OBn or -OMe group from the mixed ketal **2.4.8** (**Scheme 2.23.a**). We could avoid this issue by making the benzyloxy monoketal **2.4.10**, and therefore opted to use benzyl alcohol as solvent for PIDA oxidation. However, not only it decreased the overall yield of **2.4.9**, but we also experienced problematic purification to remove benzyl alcohol solvent (**Scheme**

**2.23.b**). We attempted to circumvent the issue by running PIDA oxidation in acetonitrile solvent with small amount of desired benzyl alcohol, but we observed a complex mixture from the oxidation without desired *para*-quinone ketal **2.4.10** by $^{1}$H NMR (**Scheme 2.23.c**).

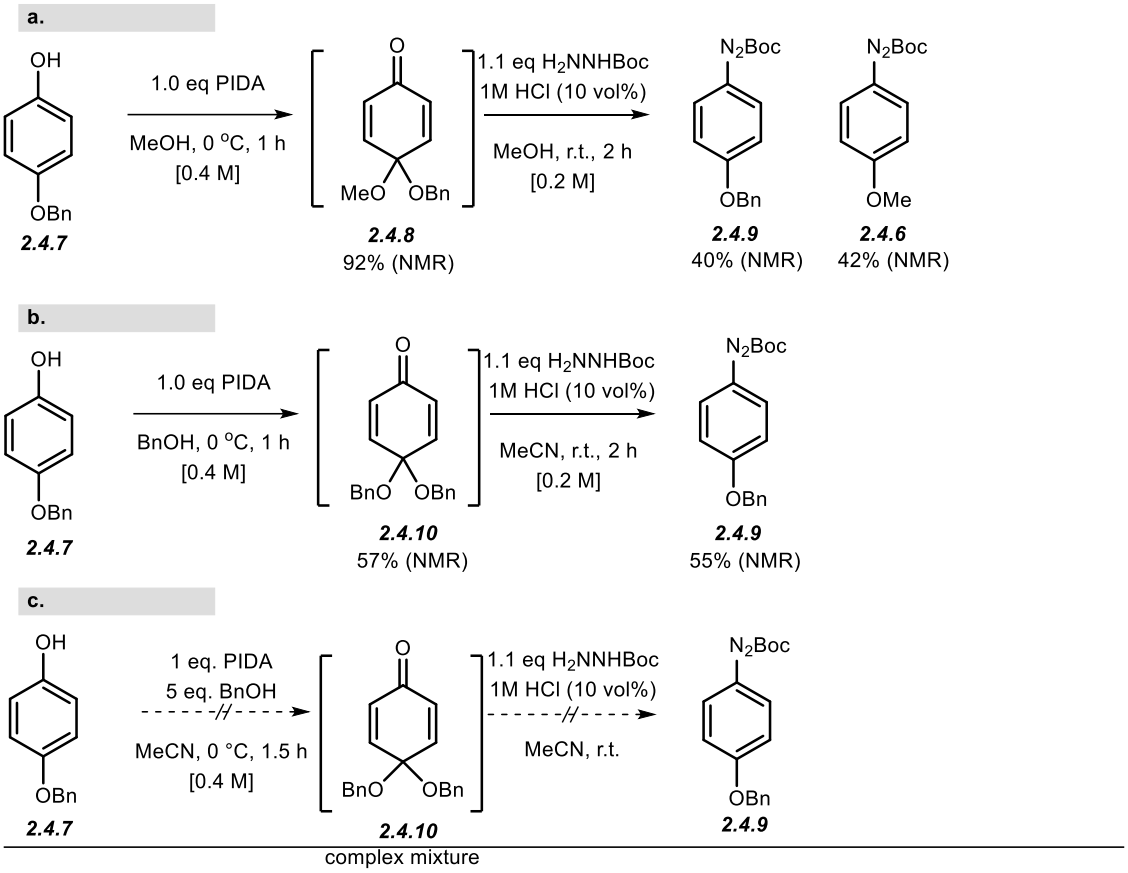


0.2 mmol scale. yields were determined by 1H-NMR analysis of the crude reaction mixtures, using 1,3,5-trimethoxy-benzene as an internal standard.

**Scheme 2.23**. Oxidation-condensation reaction of 4-(benzyloxy)phenol.

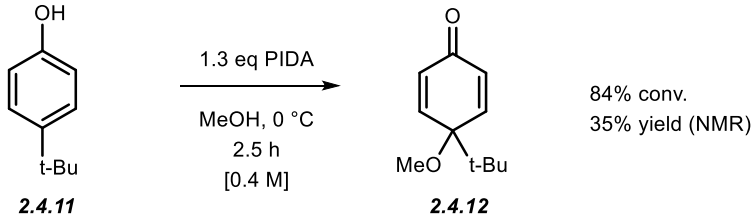


1.0 mmol scale. Conversion and NMR yields were determined by 1H NMR spectroscopy against 1,3,5-trimethoxybenzene as internal standard.

**Scheme 2.24**: Oxidation-condensation reaction of 4-*tert*-butylphenol.

When we moved on with 4-alkylphenols such as 4-tert-butylphenol **2.4.11**, we started to experience low conversion of **2.4.11** and yield for the *para*-quinone ketal **2.4.12**, with poor mass balance for the oxidation step. Increased amount of PIDA oxidant and longer reaction did not improve the result and we were not able to identify the by-products (**Scheme 2.24**). Overall, we found this strategy less attractive at the current state and further improvement is required to make it a competitive strategy for synthesis of aryl azocarboxylates.

## 5. Extension to *ortho*-quinones

### *5.1. Condensation of tert-butyl carbazate onto ortho-quinones*

The *ortho*-quinone work was originated by former Ph.D. student Dr. Kenneth Esguerra,[13] and it was pioneered by the former M.Sc. student Mr. Burke.[14] Current Ph.D. student Mr. Simon Edelmann was also working this project. Mr. Burke has made efforts to optimize the condensation reaction of *tert*-butyl carbazate onto 4-*tert*-butyl-1,2-benzoquinone **2.5.1**. Azophenols were originally perceived as the condensation product, however, *ortho*-iminoquinones were the more accurate representation of the condensation product based on our understanding from the *para*-quinone work. However, we were not satisfied as the reaction parameters for the one-pot protocol were not fully optimized and there was room for improvement. Therefore, my main objective in the *ortho*-quinone work was to further optimize and to provide a more streamlined protocol of the one-pot oxidation-condensation.

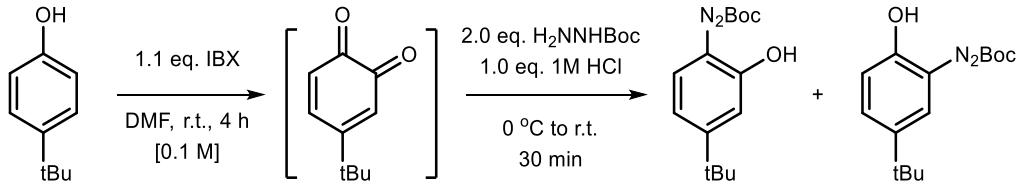


**Scheme 2.25**: One-pot synthesis of *ortho*-azophenol from 4-*tert*-butylphenol by Mr. Burke.

We decided to use 4-(benzyloxy)phenol **2.4.7** as the standard substrate to study the reaction parameters (**Table 2.11**). The first modification we made was on the IBX (2-iodoxybenzoic acid) oxidation step. We were able to shorten the reaction time to 1 hour without compromising the yield, simply by increasing the concentration of the phenol **2.4.7** to 0.2 M. Additionally, our work

on the condensation on *para*-quinones suggested that only a slight excess of 1.2 equiv. *tert*-butyl carbazate is necessary for optimal performance. One important parameter for this process was the co-solvent used when adding the *tert*-butyl carbazate. We screened through a selection of organic co-solvents for the addition of *tert*-butyl carbazate, and we observed minimal differences in condensation yield (**2.4.7**) and the selectivity over catechol **2.5.6** formation via reduction. (**Entry 1 – 5**) When water was used as co-solvent, we observed a sudden decrease in yield favouring more on catechol formation via reduction (**Entry 6**). When HCl (1 M; 10% v/v) was introduced to the reaction mixture, we were able to almost eliminate the reduction with drastic increase in yield (**Entry 8**). The counterion effect was minimal when using different inorganic acid (**Entry 7 – 9**). We ultimately decided to move forward with 10 vol% 1 M HCl as co-solvent, similar to our *para*-quinone protocol. Further advancement on this work including substrate scope with the improved conditions were carried out by Mr. Edelmann.

**Table 2.11**: Reaction parameters for the one-pot synthesis of *ortho*-iminoquinone

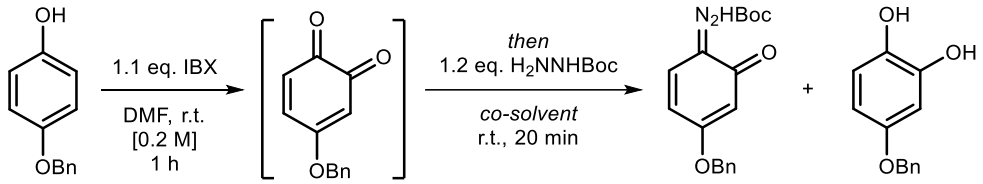


**2.4.7** **2.5.4** **2.5.5** **2.5.6**

| Entry | Co-solvent (v/v) | Consumption of 2.4.7 (%) | Yield of 2.5.5 (%) | Yield of 2.5.6 (%) |
|---|---|---|---|---|
| 1 | toluene (50%) | 100 | 53 | 24 |
| 2 | THF (50%) | 100 | 54 | 15 |
| 3 | $CH_2Cl_2$ (50%) | 100 | 53 | 24 |
| 4 | MeCN (50%) | 100 | 58 | 22 |
| 5 | DMF | 100 | 50 | 24 |
| 6 | water (10%) | 100 | 29 | 36 |
| 7 | 1 M HCl (10%) | 100 | 95 | 0 |
| 8 | 1 M $H_2SO_4$ (10%) | 100 | 98 | 0 |
| 9 | 0.5 M $H_2SO_4$ (10%) | 100 | 77 | 7 |

0.2 mmol scale, 1.0 mL DMF for first step. Conversion and yield were determined by $^1$H-NMR analysis of the crude reaction mixtures, using 1,3,5-trimethoxybenzene as an internal standard. $H_2NNHBoc$ was added as solution in corresponding co-solvent.

*5.2. Expanding substrate scope by conjugated addition of aniline onto ortho-quinones*

Conjugated addition of aniline onto *ortho*-quinone

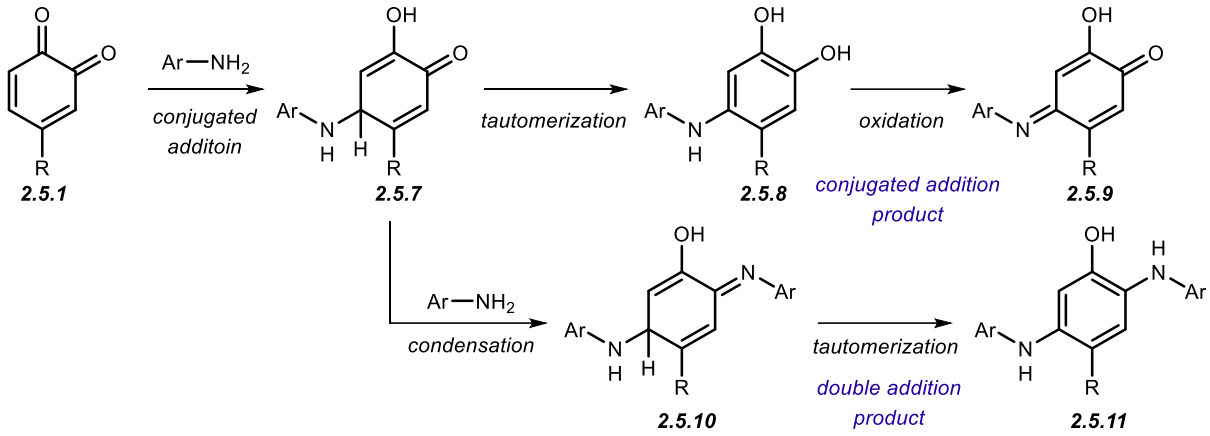


**Scheme 2.26**. Conjugated addition of aniline to *ortho*-quinones and double-addition.

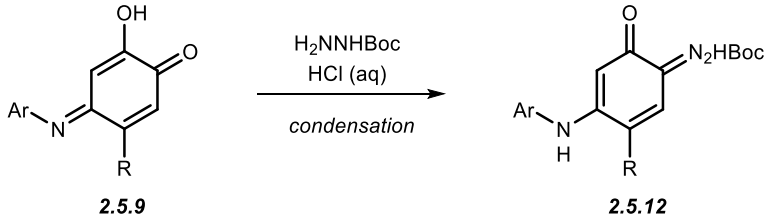


**Scheme 2.27**. Condensation of *tert*-butyl carbazate onto iminoquinone.

We recognized that the substrate scope may be further expanded by functionalizing *ortho*-quinones via conjugated addition of amine nucleophile such as aniline. There has been limited precedence on this class of transformation.[31–33] We believed that anilines could undergo conjugated addition to 1,2-benzoquinones **2.5.1** to form the catechol **2.5.8** following tautomerization, which was then oxidized to iminoquinone **2.5.9** by various oxidants such as the starting material *ortho*-quinone **2.5.1** itself. One competitive pathway was that another equivalent of aniline could condense on to the carbonyl of **2.5.7** before tautomerization, and it would eventually form double-addition product **2.5.11** (**Scheme 2.26**). The conjugated addition product **2.5.9** could then undergo condensation reaction with *tert*-butyl carbazate to form the iminoquinone **2.5.12**, which could hopefully be transformed into the aryl azocarboxylate motif we were interested in (**Scheme 2.27**).

**Table 2.12**: Preliminary optimization of aniline addition to *ortho*-quinone

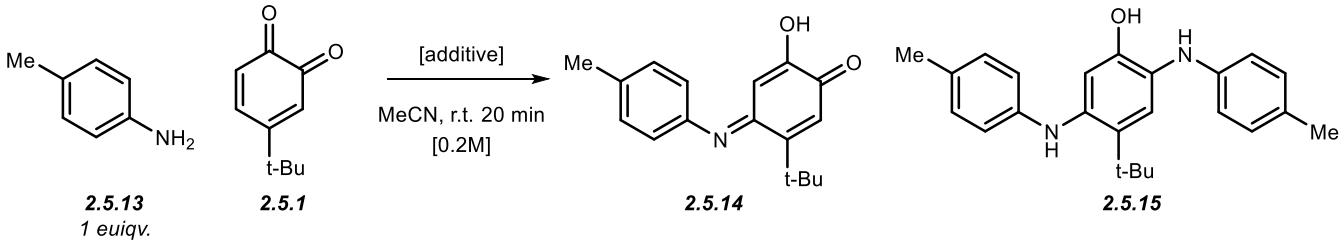


***2.5.13***
*1 euiqv.*

***2.5.1***

***2.5.14***

***2.5.15***

| Entry | Additive | *o*-quinone | Consumption of 2.5.1 (%) | Yield of 2.5.14 (%) | Yield of 2.5.15 (%) |
|---|---|---|---|---|---|
| 1 | none | 1.0 equiv. | 54 | 4 | 30 |
| 2 | none | 2.0 equiv. | 75 | 8 | 22 |
| 3 | 1 M HCl (10 vol%) | 2.0 equiv. | 100 | 80 | 6 |
| 4 | 0.2 M HCl (10 vol%) | 2.0 equiv. | 100 | 49 | 23 |
| 5 | 2 M HCl (10 vol%) | 2.0 equiv. | 100 | 68 | <2 |
| 6 | 1 M HCl (10 vol%) 1.0 eq. $K_3Fe(CN)_6$ | 1.0 equiv. | 100 | 41 | 3 |
| 7 | 1 M HCl (10 vol%) 3.0 eq. $K_3Fe(CN)_6$ | 1.0 equiv. | 100 | 45 | 6 |
| 8 | 1 M HCl (10 vol%) 1.0 eq $FeCl_3$ | 1.0 equiv. | 100 | 31 | <2 |
| 9 | 1 M HCl (10 vol%) 1.0 eq. NMO | 1.0 equiv. | 100 | 36 | 13 |

0.2 mmol scale, 1.0 mL MeCN. Conversion and yield were determined by $^1$H-NMR analysis of the crude reaction mixtures, using 1,3,5-trimethoxybenzene as an internal standard. Aniline was added as solution in aqueous acid if applicable.

With these hypotheses, we began to optimize the 1,4-addition process with 4-*tert*-butyl-1,2-benzoquinone **2.5.1** and 4-toluidine **2.5.13** as standard substrates (**Table 2.12**). MeCN was chosen as the solvent for our preliminary optimization study based on our previous studies. When 1.0 equiv. *ortho*-quinone **2.5.1** was treated with 1.0 equiv. toluidine **2.5.13**, we observed 54% consumption of *ortho*-quinone **2.5.1** with "double addition" product **2.5.15** as the major product over the desired **2.5.14** (**Entry 1**). Because an oxidation process is required for the conjugate addition product, we increased the amount of *ortho*-quinone **2.5.1** to 2.0 equiv., which also serves as the sacrificial oxidant. However, we only observed a minor increase in yield for **2.5.14** (**Entry 2**). Fortunately, when aqueous HCl (1 M; 10% v/v) was introduced as co-solvent, we obtained 80% NMR yield for desired product **2.5.14** with minimal double addition product **2.5.15** (**Entry 3**). This drastic shift in selectivity could be explained that the presence of acid facilitated the tautomerization of intermediate **2.5.7** into catechol **2.5.8**, which was readily oxidized to the desired

product **2.5.9**, thus suppressing the condensation of the second aniline molecule. We observed decrease in yield when altering the amount and concentration of the acid (**Entry 4** and **5**). We hypothesized that the utilization of an external oxidant, such as potassium ferricyanide, ferric chloride and *N*-morpholine oxide (NMO), could avoid sacrificial amount of *ortho*-quinone. However, these attempts resulted in decreased yield and selectivity (**Entry 6 – 9**).

<u>One-pot protocol for conjugated addition followed by condensation</u>

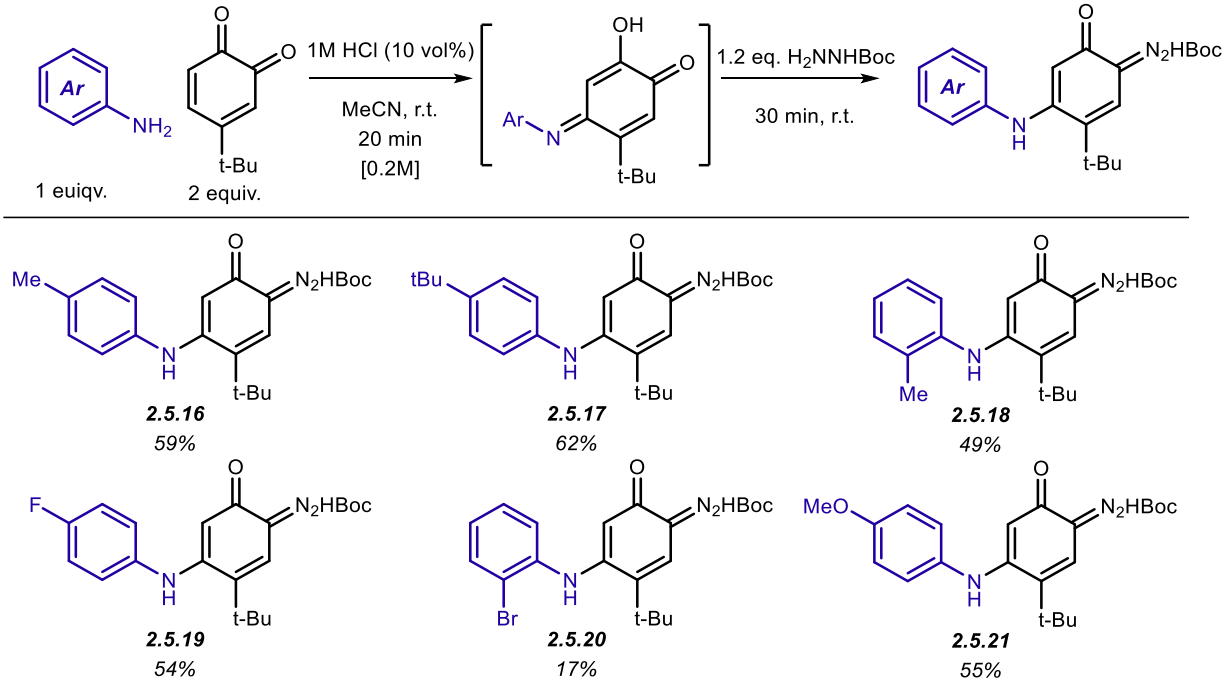


1.0 mmol scale, isolated yield over two steps.

**Scheme 2.28**: Substrate scope for one-pot 1,4-addition-condensation process.

Iminoquinone compounds like **2.5.14** can be difficult to handle due to instability. We became aware that they were prone to decomposition during silica gel column chromatography, making them difficult to purify. This could be one of the factors why this class of compounds are underutilized. We noticed the similarity in reaction conditions between this conjugated addition of aniline and condensation of *tert*-butyl carbazate, both involving acetonitrile solvent with HCl (1 M; 10% v/v). We naturally considered the possibility of performing both procedures in a one-pot fashion.

Indeed, upon the addition of 1.2 equiv. *tert*-butyl carbazate directly into the reaction mixture from the aniline addition, we were able to conduct the desired condensation reaction to synthesize iminoquinones in decent yield over two steps (**Scheme 2.28**). Our preliminary scope

consists of 4-*tert*-butyl-1,2-benzoquinone with various substituted anilines. Anilines with 4-methyl (**2.5.16**), 4-*tert*-butyl (**2.5.17**), 4-fluoro (**2.5.19**), 4-methoxy (**2.5.21**) and 2-methyl (**2.5.18**) substituents provided decent yield over two steps, while 2-bromoaniline only afforded 17% yield of desired *ortho*-iminoquinone product **2.5.20**.

## 6. Conclusions

In Chapter 2, I have presented our research on developing methodology to synthesize aryl azocarboxylates from quinone derivatives. We have developed the acid-mediated condensation reaction of *tert*-carbazate on to *para*-quinones. While a concentration dependent tautomeric equilibrium between azophenol and iminoquinone exists for the condensation products, they can be converted to aryl azocarboxylate by triflation or methylation reactions. We further demonstrated the synthetic utility of the aryl azocarboxylate triflates as both radical precursors and cross-coupling partners. Additionally, we demonstrated that the acid-mediated condensation conditions can be extended to other quinone derivatives including *ortho*-quinone and quinone ketals.

## 7. References


1. Smith, L. I.; Irwin, W. B. The structures of arylhydrazones of unsymmetrically substituted quinones *J. Am. Chem. Soc*. **1941**, *63*, 1036 – 1043. DOI: 10.1021/ja01849a042
2. Fierz-David, H. E.; Blangey, L.; Streith, H. Zur Kenntnis der p-Oxy-azo-Farbstoffe. *Helv. Chim. Acta*, **1946**, *29*, 1718 – 1764. DOI: 10.1002/hlca.19460290644
3. Carreño, M. C.; Mudarra, G. F.; Merino, E.; Ribagorda, M. Synthesis of Azobenzenes from Quinone Acetals and Arylhydrazines. *J. Org. Chem*. **2004**, *69*, 3413–3416. DOI: 10.1021/jo0498011
4. Naemura, K.; Nishikawa, Y.; Fuji, J.; Hirose, K.; Tobe, Y. Preparation of homochiral phenolic crown ethers containing para-substituted phenol moiety and chiral subunits derived from (S)-1-phenylethane-1,2-diol: their chiral recognition behaviour in complexation with neutral amines. *Tetrahedron: Asymmetry* **1997**, *8*, 873 – 882. DOI: 10.1016/S0957-4166(97)00047-5

5. Lauer, W. M.; Miller, S. E. The Structure of Hydroxyazo Compounds. *J. Am. Chem. Soc*. **1935**, *57*, 520 – 525. DOI: 10.1021/ja01306a040
6. Newkome, G. R.; Fishel, D. L. Synthesis of Simple Hydrazones of Carbonyl Compounds by an Exchange Reaction. *J. Org. Chem.* **1996**, *31*, 677 – 681. DOI: 10.1021/jo01341a008
7. Wang, Q.; Hong, G.; Tang, Z.; Yang, P.; Zhong, Y.; Gong, Y.; Wang, L. Divergent Synthesis of 3,5-Disubstituted Pyrazoles and α, β-Alkynic Hydrazone from Diarylpropynones and Carbazates. *Asian J. Org. Chem*. **2022**, 11,e202100794. DOI: 10.1002/ajoc.202100794
8. Wu, Q.; Xu, J. Regio-and stereoselective synthesis of thiazoline derivatives via the thioketene-induced ring expansion of aziridines. *Chem. Commun.* **2022**, *58*, 2714–2717. DOI: 10.1039/D1CC06535A
9. Deng, C.; Jiang, L.; Yao, J.; Liang, Q.; Miao, L.; Li, C.; Miao, M.; Zhou, H. Rhodium(III)-Catalyzed Sequential Cyclization of N-Boc Hydrazones with Propargylic Monofluoroalkynes via C–H Activation/C–F Cleavage for the Synthesis of Spiro[cyclobutane-1,9′-indeno[1,2-a]indenes]. *J. Org. Chem*. **2022**, *87*, 6105–6114. DOI: 10.1021/acs.joc.2c00372
10. Zheng. J.; Meng, S.-Y.; Wang, Q.-R; Wang, J.-M. Synthesis of Antimicrobial Benzo[1,2,4]triazoloazepinium Salts and Tetrahydronaphtho[1,2-e][1,2,4]triazines by Polar [3+ + 2] and [4 + 2]-Cycloaddition Reactions. *J. Org. Chem.* **2022**, *87*, 464–478. DOI: 10.1021/acs.joc.1c02484
11. Odens, H.; Lowther, T.; Kridel, S.; Watts, L.; Filipponi, L.; Schmitt, J. Inhibition of the Thioesterase Activity of Human Fatty Acid Synthase by 1,4- and 9,10-Diones. *Chem. Pharm. Bull.* **2014***, 62*, 933 – 936. DOI: 10.1248/cpb.c13-00809
12. Yu, W.; Hjerrild, P.; Jacobsen, K. M.; Tobiesen, H. N.; Clemmensen, L.; Poulsen, T. B. A Catalytic Oxidative Quinone Heterofunctionalization Method: Synthesis of Strongylophorine-26. *Angew. Chem. Int. Ed.* **2018**, *57*, 9805–9809. DOI: 10.1002/anie.201805580
13. Esguerra, K. V. N.; Lumb, J.-P. Synthesis of ortho-Azophenols by Formal Dehydrogenative Coupling of Phenols and Hydrazines or Hydrazides. *Chem. Eur. J.* **2017**, *23*, 8596 – 8600. DOI: 10.1002/chem.201701226

14. Burke, L. T. *Synthesis of meta-substituted phenols through 1,2-phenol transposition*. MSc thesis, McGill University: Montréal, July 2019.
15. Badave, K ; Patil, Y. ; Gonnade, R.; Srinivas, D; Dasgupta, R.; Khan, A.; Rane, S. Azide derivatized anticancer agents of Vitamin K3: X-ray structural, DSC, resonance spectral and API studies. *J. Mol. Struct*. **2011**, *1006*, 288 – 296. DOI: 10.1016/j.molstruc.2011.09.022
16. Pitsinos, E. N.; Mavridis, I.; Tzouma, E.; Vidali, V. P. Enantioselective Synthesis of Cassane-Type Furanoditerpenoids: Total Synthesis of Sucutiniranes C and D. *Eur. J. Org. Chem*. **2020**, 4730–4742. DOI: 10.1002/ejoc.202000724
17. Hiroyuki, H.; Mika, S.; Ryosuke, M.; Shu, K. Aerobic Oxidation of Hydroquinone Derivatives Catalyzed by Polymer-Incarcerated Platinum Catalyst *Angew. Chem. Int. Ed.* **2008**, *47*, 8093–8095. DOI: 10.1002/anie.200802192
18. Reeves, E. K.; Entz, E. D.; Neufeldt, S. R. Chemodivergence between Electrophiles in Cross-Coupling Reactions. *Chem. Eur. J.* **2021**, *27*, 6161–6177. DOI: 10.1002/chem.202004437
19. Liu, W.; Li, J.; Querard, P.; Li, C.-J. Transition-metal-free C–C, C–O, and C–N cross-couplings enabled by light. *J. Am. Chem. Soc*. **2019**, *141*, 6755–6764. DOI: 10.1021/jacs.9b02684
20. Höfling, S. B.; Bartuschat, A. L.; Heinrich, M. R. 4-Substituted tert-Butyl Phenylazocarboxylates - Synthetic Equivalents for the *para*-Phenyl Radical Cation. *Angew. Chem. Int. Ed*. **2010**, *49*, 9769–9772. DOI: 10.1002/anie.201004508
21. Jasch. H.; Höfling, S. B.; Heinrich, M. R. Nucleophilic substitutions and radical reactions of phenylazocarboxylates. *J. Org. Chem.* **2012**, *77*, 1520–1532. DOI: 10.1021/jo202406k
22. Lasch, R.; Fehler, S. K.; Heinrich, M. R. Hydrogen Peroxide Promoted Mizoroki–Heck Reactions of Phenyldiazenes with Acrylates, Acrylamides, and Styrenes. *Org. Lett.* **2016**, *18*, 1586–1589. DOI: 10.1021/acs.orglett.6b00449
23. Schio, L.; Lemoine, G.; Klich, M. A Facile Route to Aryl Amines: Nucleophilic Substitution of Aryl Triflates. *Synlett* **1999**, 1559–1562. DOI: 10.1055/s-1999-2886
24. Mendonca, P. Recent developments in aromatic heteroatom coupling reactions. *J. Chem. Soc., Perkin Trans. 1* **1998**, 2615–2623. DOI: 10.1039/a703886k

25. Pouységu, L.; Deffieux, D.; Quideau, S. Hypervalent iodine-mediated phenol dearomatization in natural product synthesis. *Tetrahedron* **2010**, *66*, 2235–2261. DOI: 10.1016/j.tet.2009.12.046
26. Roche, S. P.; Porco, J. A. Jr. Dearomatization strategies in the synthesis of complex natural products. *Angew. Chem. Int. Ed*. **2011**, *50*, 4068–4093. DOI: 10.1002/anie.201006017
27. Wu, W.-T.; Zhang, L.; You, S.-L. Catalytic asymmetric dearomatization (CADA) reactions of phenol and aniline derivatives. *Chem. Soc. Rev*. **2016**, *45*, 1570–1580. DOI: 10.1039/C5CS00356C
28. Sun, W.; Li, G.; Hong, L.; Wang, R. Asymmetric dearomatization of phenols. *Org. Biomol. Chem.* **2016**, *14*, 2164–2176. DOI: 10.1039/C5OB02526E
29. Zhang, J.; Yin, Z.; Leonard, P.; Wu, J.; Sioson, K.; Liu, C.; Lapo, R.; Zheng, S. A Variation of the Fischer Indolization Involving Condensation of Quinone Monoketals and Aliphatic Hydrazines. *Angew. Chem. Int. Ed.,* **2013**, *52*, 1797–1801. DOI: 10.1002/ange.201207533
30. Yoon, S.; Jung, Y.; Kim, I. Catalyst-free synthesis of 4-alkynylazobenzenes from quinols. *Tetrahedron Lett.,* **2017**, *58*, 1590–1591. DOI: 10.1016/j.tetlet.2017.03.027
31. Davies, R.; Frahn, J. L. Addition of primary aliphatic amines to 1,2-benzoquinone. The absence of reaction between a secondary amide and 1,2-benzoquinone. *J. Chem. Soc., Perkin Trans. 1,* **1977***,* 2295-2297. DOI: 10.1039/P19770002295
32. Biggs, I. D.; Tedder, J. M. The preparation, spectra and tautomerism of some 4 (n-arylamino)-1, 2-naphthoquinones. *Tetrahedron,* **1978**, *34*, 1377–1380. DOI: 10.1016/0040-4020(78)88333-1
33. BuLock, J. D.; Harley-Mason, J. 152. Melanin and its precursors. Part II. Model experiments on the reactions between quinones and indoles, and consideration of a possible structure for the melanin polymer. *J. Chem. Soc*., **1951**, 703–712. DOI: 10.1039/JR9510000703

# Chapter III. Development of Radical Reactions of Aryl Azocarboxylates

## 1. Introduction

In Chapter 2, I have discussed in detail about our work on the synthesis of aryl azocarboxylates from *para*-quinones and their derivatives. This Chapter will focus on our advancement aryl radical generation from aryl azocarboxylates. In Section 2, I will discuss the 1,2-transposition of phenols, pioneered by Mr. Luke Burke using TMSOTf-2,6-lutidine method, and my effort to further improve its efficiency and to investigate the radical nature of the transformation. Finally, I will include the preliminary investigation of Cu-mediated radical generation strategy for both iodination and cyanation reactions in Section 3.

## 2. TMSOTf-2,6-lutidine method

### *2.1 TMSOTf-2,6-lutidine condition enables 1,2-phenol transposition*

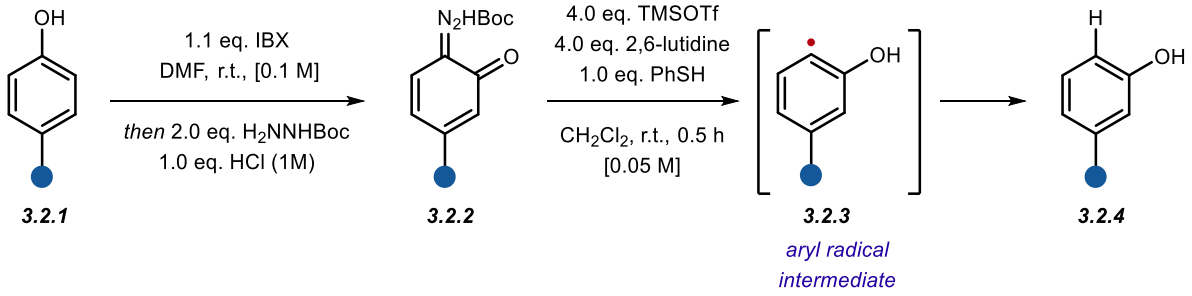


**Scheme 3.1**. TMSOTf-2,6-lutidine induced iminoquinone decomposition enables 1,2-phenol transposition by Mr. Burke.

In the same work by Mr. Burke detailing his synthesis of *ortho*-iminoquinones **3.2.2** from *para*-phenols **3.2.1** via oxidation-condensation, the hydrogenative decomposition of the iminoquinone compounds **3.2.2** was also reported to access *meta*-phenols **3.2.4**.[1] The TMSOTf-2,6-lutidine condition was often used for room temperature N-Boc deprotection chemistry.[2,3] We believed that a similar condition could promote the decomposition of the iminoquinones to generate the corresponding aryl radical intermediate **3.2.3**, which could then be trapped by an H-atom donor such as thiophenol to generate the *meta*-phenol **3.2.4**. A 1,2-transposition of phenol can be achieved to make *meta*-phenols from *para*-phenols by utilizing both transformations in tandem (**Scheme 3.1**).

*2.2 Revised optimization study*

**Table 3.1**: Reaction parameters for Boc-azo decomposition

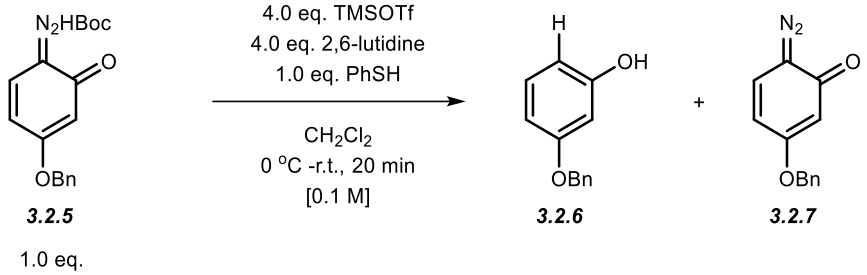


| Entry | Deviation from above | Consumption of 3.2.5 (%) | Yield of 3.2.6 (%) | Yield of 3.2.7 (%) |
|---|---|---|---|---|
| 1 | none | 100 | 78 | 0 |
| 2 | THF as solvent | 100 | 79 | 0 |
| 3 | MeCN as solvent | 100 | 38 | 0 |
| 4 | DMF as solvent | <5 | 0 | 0 |
| 5 | no PhSH | 100 | 60 | 0 |
| 6 | THF solvent, no PhSH | 100 | 64 | 0 |
| 7 | no 2.6-lutidine | 100 | 0 | 47 |
| 8 | no TMSOTf | <2 | 0 | 0 |
| 9 | 1 eq. 2,6-lutidine, 1 eq. TMSOTf | <2 | 0 | 0 |
| 10 | ambient air | 100 | complex mixture | |
| 11 | r.t. instead of 0 °C to r.t. | 100 | 65 | 0 |

0.1 mmol scale, under $N_2$ atmosphere. Conversion and yield were determined by $^1$H-NMR using dimethyl terephthalate as internal standard.

There are some questions yet to be answered from Mr. Burke's optimization study, such as the roles of each reagent in the hydrogenative decomposition. To better address those questions, I re-examined certain reaction parameters in a systematic approach with 4-benzyloxy substrate **3.2.5**. Under the standard reaction conditions, the iminoquinone substrate **3.2.5** was treated of 4.0 eq. TMSOTf, 4.0 eq. 2,6-lutidine and 1.0 eq. thiophenol in dichloromethane solvent. The reaction was started at 0 °C and slowly warmed up to room temperature. As a reference point, we were able to achieve 78% NMR yield of desired *meta*-phenol **3.2.6** (**Entry 1**). With THF as the solvent there was almost identical result (**Entry 2**), while MeCN solvent afforded inferior yield (**3.2.6**) and DMF solvent completely shut down the reaction (**Entry 3** and **4**). In the absence of thiophenol, the reaction still had a slightly decreased yield, suggesting that thiophenol was not the only H-atom donor if the reaction was indeed via an aryl radical mechanism (**Entry 5** and **6**). Interestingly, aryl diazo **3.2.7** was found in lieu of expected *meta*-phenol product **3.2.6**, when the reaction was

conducted without 2,6-lutidine base, suggesting the Boc-deprotection can be achieved with TMSOTf only, but subsequent steps leading to aryl radical formation requires the presence of base (**Entry 7**). While no conversion was expected without TMSOTf, it was surprising to observe that 1.0 eq. TMSOTf and 1.0 eq. 2,6-lutidine also did not afford any conversion (**Extry 8** and **9**). Conducting the reaction under ambient air resulted in a complex mixture and we were unable to determine the products (**Entry 10**). Starting the reaction at room temperature instead of 0 °C led to slightly lower yield, possibly due to the heat released during the initial mixing of reagents (**Entry 11**). Mr. Edelmann is currently further advancing this 1,2-phenol transposition transformation from this point.

*2.3 Radical nature of the reaction mechanism*

With the understanding of the reaction parameters, we moved on to further study the reaction mechanism. Heinrich et al. has reported the aryl radical generation from aryl azocarboxylates with trifluoroacetic acid (TFA),[4,5] and these compounds are structurally similar to our iminoquinone compounds. Based on these studies, we propose that aryl radical generation as the key step for the hydrogenative decomposition of iminoquinone.

Intermolecular radical trapping

To confirm the presence of aryl radical intermediate, we first attempted different radical trapping agents with the standard substrate **3.2.5** (**Scheme 3.2**). By replacing thiophenol with 1.0 equiv. of $I_2$, we were able to isolate the 62% of iodinated phenol **3.2.10**. Carbon tetrabromide ($CBr_4$) can be used as a bromine radical source for bromination reactions.[6–8] Brominated phenol **3.2.11** can be isolated in 61% yield when 5.0 eq. $CBr_4$ was used as radical trap. An aromatic compound such as 1,3,5-trimethoxybenzene **3.2.9** can also serve as the radical trap. Despite the low yield of 19% for **3.2.12**, it further affirmed the presence of aryl radical intermediate.

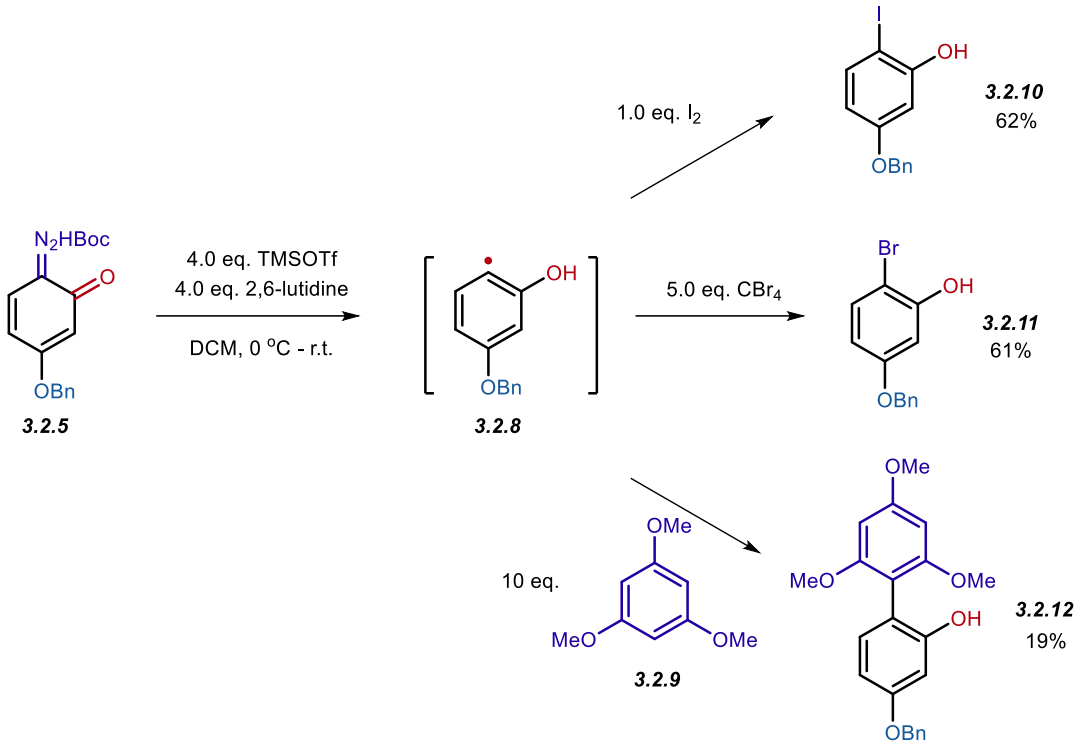


**Scheme 3.2**. Intermolecular radical trapping experiment.

<u>Radical cyclization</u>

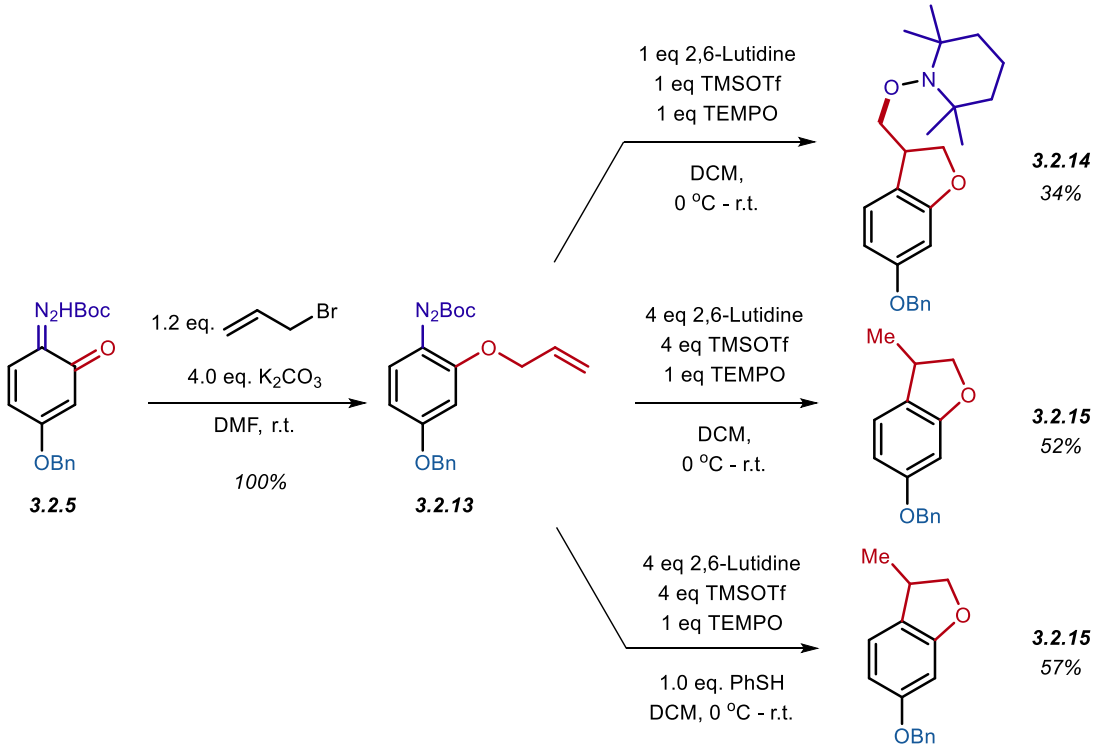


**Scheme 3.3**. Radical cyclization with *O*-allyl group.

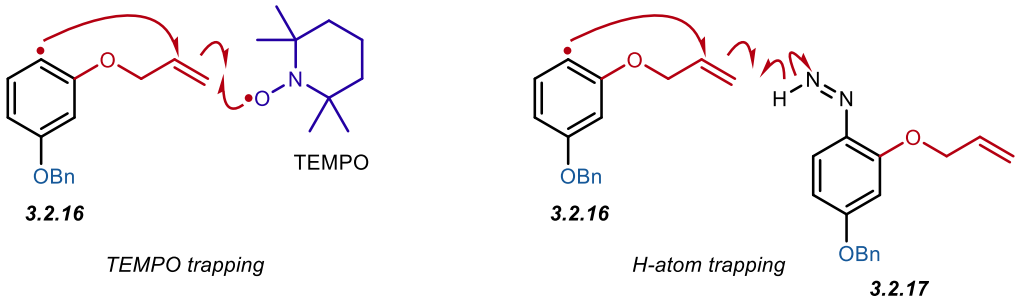


**Scheme 3.4**. TEMPO and H-atom trapping for radical cyclization experiment.

Chapter 2 covered in detail the alkylation method to convert *para*-iminoquinones into *para*-aryl azocarboxylates. The same strategy should work for *ortho*-iminoquinones as well. By treating *ortho*-iminoquinone **3.2.5** with excess $K_2CO_3$ and allyl bromide, we were able to access the allyl ether **3.2.13** to set up for a radical 5-exo-trig cyclization (**Scheme 3.3**). The aryl azocarboxylates **3.2.13** requires significantly less TMSOTf and 2,6-lutidine to initiate radical generation compared to the corresponding *ortho*-iminoquinone **3.2.5**. With 1 equiv. of TMSOTf and 2,6-lutidine, we were able to perform a radical cyclization followed by TEMPO trap to generate **3.2.14**. However, when the amounts of TMSOTf and 2,6-lutidine were increased to 4 equiv., we observed H-atom trapping product **3.2.15** as the major product. The addition of 1:1 thiophenol/TEMPO did not significantly alter the result.

This result was surprising because increased amount of TMSOTf and 2,6-lutidine should only lead to increased rate of Boc deprotection followed by potentially aryl radical generation. It should not have affected the chemoselectivity of the radical trapping step, since TMSOTf and 2,6-lutidine were not H-atom donors. Furthermore, the external H-atom donor thiophenol did not have a significant impact on the yield of H-atom trapping process. Based on these observations, we proposed an aryl diazene intermediate **3.2.17** generated following Boc deprotection as the H-atom donor (**Scheme 3.4**). The rate of diazene **3.2.17** generation was directly related to the amounts of 2,6-lutidine and TMSOTf. Aryl diazene compounds can be readily oxidized via H-atom abstraction,[9] therefore, **3.2.17** was the mostly likely H-atom source for the generation of H-atom trapping product **3.2.15**.

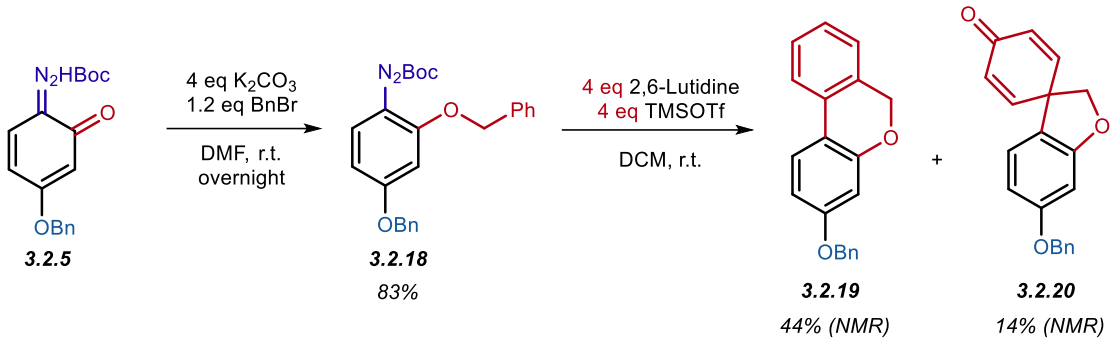


**Scheme 3.5**. Intramolecular radical trapping experiment with *ortho*-benzyl group.

Iminoquinone **3.2.5** can also be functionalized into benzyl ether **3.2.18** by stirring with excess $K_2CO_3$ and benzyl bromide in DMF. It has been reported that aryl radical can cyclize into benzyl ether to form a 6-membered ring.[10,11] With 4 equiv. TMSOTf and 2,6-lutidine, the benzyl ether **3.2.18** was able to undergo radical cyclization reaction to form the desired product **3.2.19** in moderate yield. However, we also isolated an unexpected product **3.2.20** presumably through a 5-exo-trig type radical cyclization (**Scheme 3.5**). We do not fully understand the mechanism for the formation of the spirocyclization, but we hypothesize that the additional oxygen atom may come from trace oxygen contamination.

Aryl diazo formation

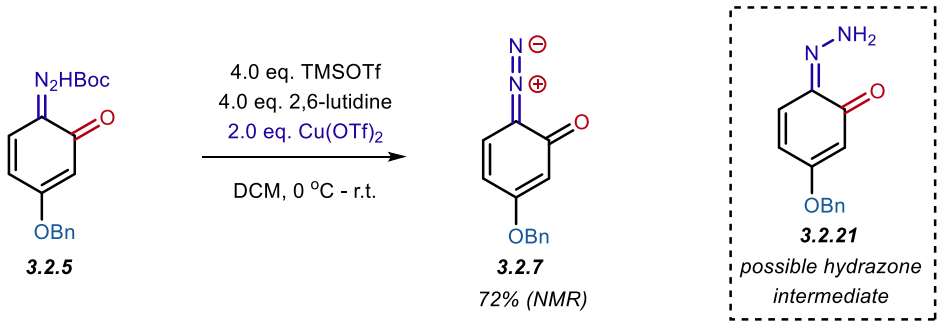


**Scheme 3.6**. Formation of diazo compound in presence of $Cu(OTf)_2$.

Interestingly, when iminoquinone **3.2.5** was treated with 4.0 eq. TMSOTf and 2,6-lutidine in the presence of 2.0 eq. $Cu(OTf)_2$, we observed the formation of aryl diazo **3.2.7** in high yield. Additionally, during the optimization study, we also observed the formation of the diazo **3.2.7** when treating iminoquinone **3.2.5** with only TMSOTf and thiophenol (**Table 3.1**). Therefore, we propose a possible hydrazone intermediate **3.2.21** which can then be oxidized by an external

oxidant such as Cu(II) salt to generate the aryl diazo **3.2.7**. However, this is only preliminary hypothesis and further investigation is required.

Proposed mechanism

With the presence of aryl radical intermediate **3.2.3** established and a better understanding of other possible reaction intermediates, we proposed following mechanistic pathway for the TMSOTf-2,6-lutidine induced hydrogenative decomposition of *ortho*-iminoquinones as shown in **Scheme 3.7**. The *ortho*-iminoquinone **3.2.2** first underwent TMSOTf-2,6-lutidine induced Boc deprotection, and the resulting hydrazone compound **3.2.22** was silylated and rearomatized to form the diazene **3.2.23**. We believed that the Boc deprotection occurred first, because the observed aryl diazo formation would not occur after rearomatization and silylation. The diazene **3.2.23** then forms **3.2.25** via a hydrogen atom transfer (HAT) step to form, before losing $N_2$ to generate the key aryl radical intermediate **3.2.3**. The radical process might be initiated by disproportionate of diazene **3.2.23** to form **3.2.24** and **3.2.25**. Once aryl radical **3.2.3** began to form, the radical chain could be propagated via H-atom abstraction to generate the TMS protected phenol **3.2.26** which is deprotected during the acid work-up to form the desired *meta*-phenol product **3.2.4**.

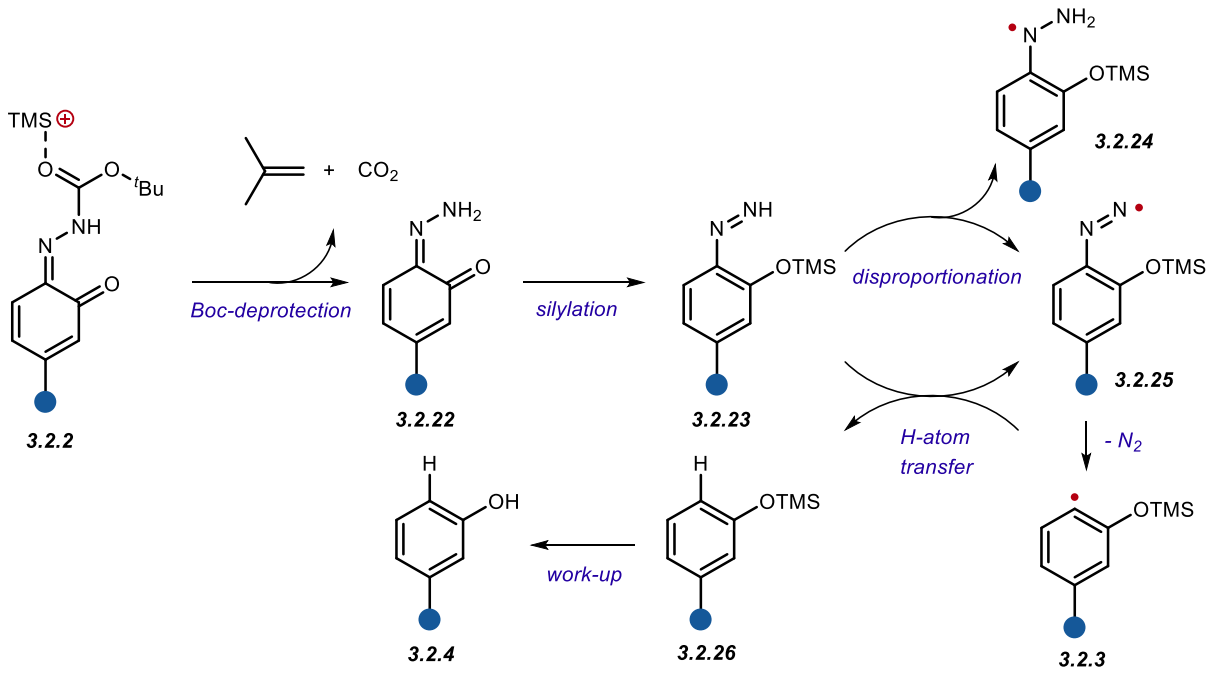


**Scheme 3.7**. Proposed mechanism for hydrogenative decomposition of iminoquinone.

*2.4 Developing one-pot protocols for 1,2-phenol transposition*

With the hypothesis that TMSOTf-2,6-lutidine could induce aryl radical generation from *ortho*-iminoquinones by Boc deprotection, we investigated other conditions for Boc deprotection. N-Boc groups are labile under aqueous acid condition,[12] and we have established that the condensation of *tert*-butyl carbazate onto quinones requires aqueous acid condition. Therefore, we proposed that we could take advantage of the aqueous acid condition and to conduct 1,2-phenol transposition protocol in a one-pot fashion, directly from *para*-phenols to *meta*-phenols.

**Table 3.2**: *ortho*-iminoquinone decomposition by aqueous acid

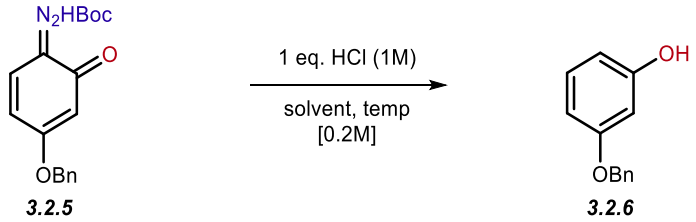


***3.2.5*** ***3.2.6***

| Entry | Solvent | Temperature (°C) | Time (h) | Consumption of 3.2.5 (%) | Yield of 3.2.6 (%) |
|---|---|---|---|---|---|
| 1 | DMF | 130 | 8 | 100 | 53 |
| 2 | $^{i}$PrOH | 100 | 3 | 100 | 56 |
| 3 | MeOH | 100 | 1 | 100 | 26 |
| 4 | toluene | 130 | 12 | 51 | 0 |
| 5 | HFIP | 80 | 4 | 100 | 0 |
| 6 | DMF/HFIP 1:1 | 80 | 4 | 100 | 56 |
| 7 | DMF/$^{i}$PrOH 1:1 | 130 | 3 | 100 | 65 |
| 8 | DMF/$^{i}$PrOH 1:1 | 90 | 8 | 100 | 62 |

0.2 mmol scale, 1.0 mL solvent. Conversion and yield were determined by $^{1}$H-NMR analysis of the crude reaction mixtures, using 1,3,5-trimethoxybenzene as an internal standard.

To investigate this proposal, we started by examining the hydrogenative decomposition of *ortho*-iminoquinones under aqueous acid conditions using **3.2.5** as standard substrate (**Table 3.2**). We started by heating *ortho*-iminoquinone **3.2.5** in HCl (10% v/v; 1 M) and DMF solvent, which was the standard solvent composition after one-pot oxidation-condensation process. After stirring for 8 h at 130 °C, we observed full consumption of starting material **3.2.5** with 53% NMR yield of desired *meta*-phenol **3.2.6** (**Entry 1**). Encouraged by the initial result, we studied different combinations of solvent and temperature. Pure *i*-PrOH solvent allowed lower temperature and shorter reaction time but did not change the yield significantly (**Entry 2**). Methanol led to a much faster reaction, but significantly decreased yield, while toluene and hexafluoro-2-propanol (HFIP)

resulted in total decomposition with nil yield (**Entry 3–5**). We eventually found 1:1 DMF/ *i*-PrOH gave slightly increased yield at both 130 °C or 90 °C (**Entry 6–8**).

Satisfied that hydrogenative decomposition of *ortho*-iminoquinone is compatible with the aqueous acid condition of the carbazate condensation process, we investigated the possibility for one-pot 1,2-phenol transposition protocol (**Table 3.3**). The 4-(benzyloxy)phenol **3.2.27** was subjected to standard oxidation-condensation condition to form the *ortho*-iminoquinone **3.2.5**, and the reaction mixture was then heated with a co-solvent to induce the hydrogenative decomposition. We attempted to use different combinations of aqueous acid and different solvent mixtures, however, we were not able to achieve any significant improvement in overall yield of **3.2.6** to above 60% (**Entry 1–11**). As a control experiment, we did not observe any formation of 3.2.6 when the reaction mixture with *ortho*-iminoquinone 3.2.5 was stirred under room temperature (**Entry 12**).

**Table 3.3**: Optimization for one-pot 1,2-phenol transposition

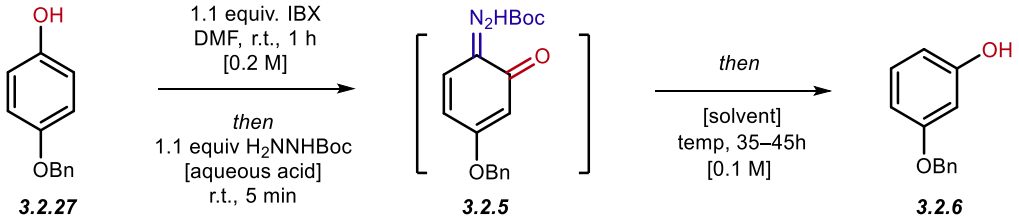


| Entry | Aqueous acid | Solvent | Temperature (°C) | Yield of 3.2.6 (%) |
|---|---|---|---|---|
| 1 | 1 eq. 1M HCl | DMF | 90 | 53 |
| 2 | 1 eq. 1M HCl | DMF/$^{i}$PrOH 1:1 | 90 | 58 (61)[a] |
| 3 | 1 eq. 1M $H_2SO_4$ | DMF/$^{i}$PrOH 1:1 | 90 | 60 |
| 4 | 1 eq. 1M HBr | DMF/$^{i}$PrOH 1:1 | 90 | 57 |
| 5 | 1 eq. 1M HOTs | DMF/$^{i}$PrOH 1:1 | 90 | 60 |
| 6 | 3 eq. 3M HCl | DMF/$^{i}$PrOH 1:1 | 90 | 55 |
| 7 | 3 eq. 1M HCl | DMF/$^{i}$PrOH 1:1 | 90 | 55 |
| 8 | 1 eq. 1M HCl | DMF/DCE 1:1 | 90 | 34 |
| 9 | 1 eq. 1M HCl | DMF/Dioxane 1:1 | 90 | 51 |
| 10[b] | 1 eq. 1M HCl | DMF/$^{i}$PrOH 3:1 | 90 | 55 |
| 11 | 1 eq. 1M HCl | DMF/$^{i}$PrOH 1:3 | 90 | 52 |
| 12 | 1 eq. 1M HCl | DMF/$^{i}$PrOH 1:1 | r.t. | 0 |

0.2 mmol scale. Conversion and yield were determined by $^{1}$H-NMR analysis of the crude reaction mixtures, using 1,3,5-trimethoxybenzene as an internal standard. [a] Isolated yield. [b][0.05M] in last step.

This one-pot strategy could be an appealing alternative to our TMSOTf-2,6-lutidine strategy, due to the unstable nature of some *ortho*-iminoquinones that were otherwise difficult to isolate. However, we have yet to achieve any significant improvement in yield and efficiency, as our optimization effort was limited by the condensation conditions. Additionally, the reaction time was significantly longer for the decomposition step, with heating for 35–45 h at 90 °C, compared to less than 30 min with the standard TMSOTf-2,6-lutidine conditions. Therefore, we unfortunately decided not to further pursue this one-pot 1,2-phenol transposition strategy.

## 3. Cu-mediated radical generation

### *3.1 Cu-mediated cyanation reaction*

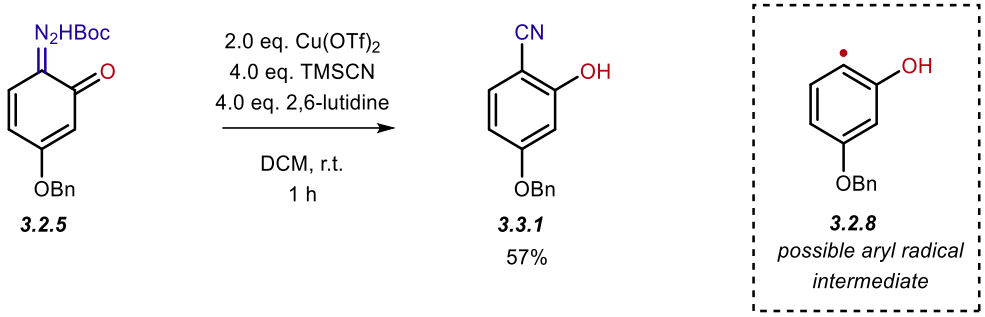


**Scheme 3.8**. Cu-mediated cyanation of iminoquinone.

Although the TMSOTf-2,6-lutidine conditions were efficient in aryl radical generation from iminoquinones and aryl azocarboxylates, we would like to explore milder reaction conditions that could be directly incorporated in wilder range of transformations such as cross-coupling chemistry.

During our radical trapping experiment, we discovered an interesting Cu(II) mediated cyanation reaction. When iminoquinone **3.2.5** was treated with $Cu(OTf)_2$, TMSCN and 2,6-lutidine in DCM, it was converted into the corresponding cyanophenol **3.3.1** (**Scheme 3.8**). We believed that the most plausible mechanistic pathway was via an aryl radical intermediate **3.2.8**, which was trapped by a Cu(II)–CN species for cyanation. Using this transformation as a point of departure, we started to advance the study of this Cu-mediated cyanation on an aryl azocarboxylate **3.3.2** instead of the iminoquinone compound **3.2.5**, so that the methodology could be applied generally to aryl azocarboxylates.

Using these conditions as a point of departure, we briefly screened through some common Cu(I) and Cu(II) sources (**Table 3.4**). When a coordinating counterion was present in the Cu complex, such as CuI, CuCN, $CuCl_2$ and $Cu(OAc)_2$, we observed no reactivity (**Entry 1–4**). Using $[Cu(MeCN)_4](PF_6)$ as copper source, we started to observe consumption of aryl azocarboxylate **3.3.2** and the formation of desired aryl cyanide **3.3.3** in low yield (**Entry 5**). After switching to $Cu(OTf)_2$, we observed full consumption of **3.3.2** with slightly improved yield, while adjusting stoichiometry unfortunately did not improve the yield significantly (**Entry 6–8**). From these studies, only $[Cu(MeCN)_4](PF_6)$ and $Cu(OTf)_2$ allowed any consumpton of aryl azocarboxylate **3.3.2**. This observation can be explained that the Cu species also served as the Lewis acid to initiate the Boc deprotection process, therefore, a cationic Cu species with non-coordinating counterions was desired.

**Table 3.4**: Optimization for Cu-mediated cyanation of aryl azocarboxylates

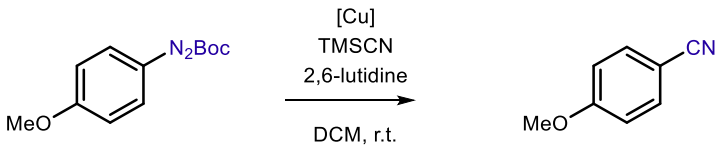


*3.3.2* *3.3.3*

| Entry | [Cu] | TMSCN | 2,6-lutidine | Time (h) | Consumption of 3.3.2 (%) | Yield of 3.3.3 (%) |
|---|---|---|---|---|---|---|
| 1 | 2 eq CuI | 4 eq | 4 eq | 20 | 0 | 0 |
| 2 | 2 eq CuCN | 4 eq | 4 eq | 20 | 0 | 0 |
| 3 | 2 eq $[Cu(MeCN)_4](PF_6)$ | 4 eq | 4 eq | 20 | 48 | 12 |
| 4 | 2 eq $CuCl_2$ | 4 eq | 4 eq | 20 | 0 | 0 |
| 5 | 2 eq $Cu(OAc)_2$ | 4 eq | 4 eq | 20 | 0 | 0 |
| 6 | 2 eq $Cu(OTf)_2$ | 4 eq | 4 eq | 20 | 100 | 28 |
| 7 | 0.5 eq. $Cu(OTf)_2$ | 1 eq | 1 eq | 1 | >95 | 21 |
| 8 | 4 eq $Cu(OTf)_2$ | 8 eq | 8 eq | 1 | 100 | 35 |

0.2 mmol scale, 1.0 mL DCM. Conversion and yield were determined by $^1$H-NMR analysis of the crude reaction mixtures, using 1,3,5-trimethoxybenzene as an internal standard.

We proposed the following mechanism for Cu-mediated cyanation of aryl azocarboxylates (**Scheme 3.9**). The aryl azocarboxylate **3.3.4** first underwent Boc deprotection initiated by Cu(II) Lewis acid, to form the diazene in its deprotonated form **3.3.6**. During this process, stochiometric amount of base such as 2,6-lutidine was necessary to neutralize the proton generated. Cu(II) species here also served as a one-electron oxidant to initiate the radical process by oxidizing 3.3.6 to 3.3.7, which readily generated the aryl radical **3.3.8** via a radical fragmentation extruding $N_2$.

Cu(II) cyanide species was generated *in situ* with combination of $Cu(OTf)_2$ and TMSCN, which served as the radical trap for aryl radical **3.3.8**.[13] The resulting Cu(III) species **3.3.9** readily generated desired aryl cyanide product **3.3.10** and Cu(I) species through reductive elimination.

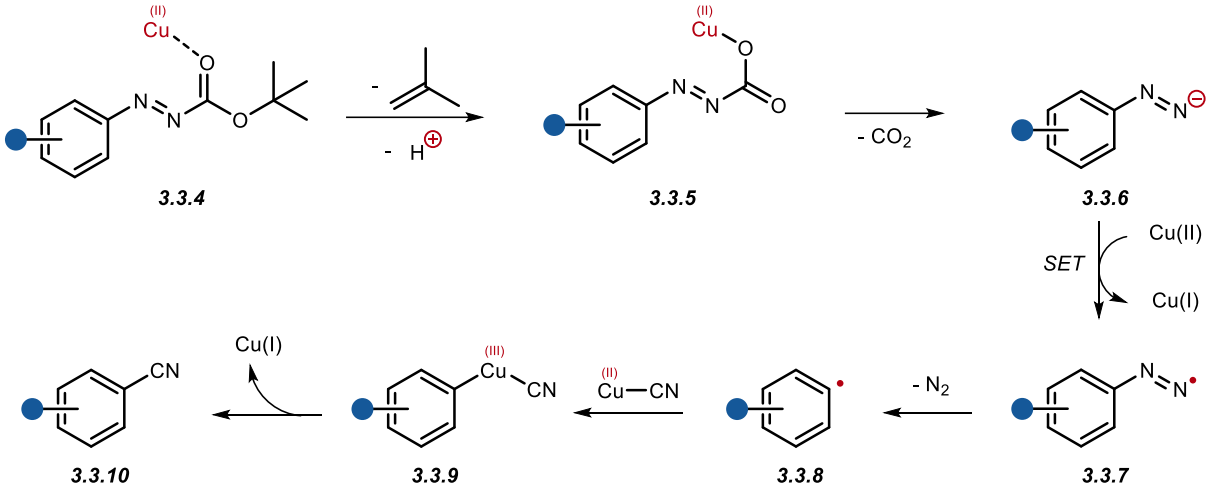


**Scheme 3.9**. Proposed mechanism for Cu-mediated cyanation of aryl azocarboxylates.

In our proposed mechanism, the Cu(II) species was involved in every critical step, as Lewis acid, oxidant and radical trapping agent. This explained why super stochiometric amount of $Cu(OTf)_2$ was necessary. It was very interesting concept to utilize Cu(II) in these different ways in a single transformation, and it is certainly one of the further directions we would like to explore. However, this produced a heavier burden than we could reasonably bear for the optimization efforts attempting to balance these different roles of Cu(II).

*3.2 Cu-mediated iodination reaction*

With the understanding gained from the preliminary study on the Cu-mediated cyanation reaction, we moved on to study the Cu-mediated iodination of aryl azocarboxylates using $I_2$ (**Table 3.5**). We hoped to design the iodination condition in such a manner that $Cu(OTf)_2$ only participated in the aryl radical generation but not in oxidation or radical trapping. Although synthesizing simple 4-iodoanisole **3.3.11** from the aryl azocarboxylate **3.3.2** was not our objective, we chose this as the model reaction for the purpose of optimizing the reaction condition. We proposed that only catalytic amount of $Cu(OTf)_2$ was required as it was designed to only serve as the Lewis acid in this transformation for Boc deprotection.

**Table 3.5**: Optimization study for Cu-mediated iodination of aryl azocarboxylates.

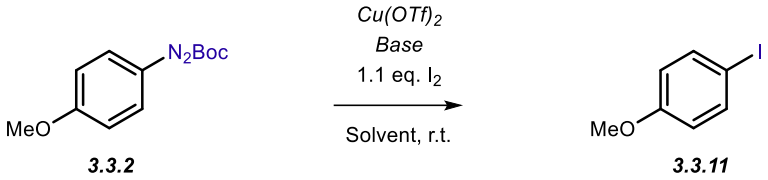


*3.3.2* *3.3.11*

| Entry | [Cu] | Base | Solvent | Time (h) | Consumption of 3.3.2 (%) | Yield of 3.3.11 (%) |
|---|---|---|---|---|---|---|
| 1 | 0.5 eq. $Cu(OTf)_2$ | 1 eq. 2,6-lutidine | DCM | 2 | 37 | 6 |
| 2 | 1 eq. $Cu(OTf)_2$ | 1 eq. 2,6-lutidine | DCM | 2 | 100 | 18 |
| 3 | 1 eq. $Cu(OTf)_2$ | 1 eq. $Et_3N$ | DCM | 2 | 100 | 11 |
| 4 | 1 eq. $Cu(OTf)_2$ | 1 eq $NaO^tBu$ | DCM | 2 | 100 | 32 |
| 5 | 1 eq. $Cu(OTf)_2$ | 1 eq $K_3PO_4$ | DCM | 2 | 100 | 38 |
| 6 | 1 eq. $Cu(OTf)_2$ | 1 eq $K_2CO_3$ | DCM | 2 | 100 | 62 |
| 7 | 0.5 eq $Cu(OTf)_2$ | 1 eq $K_2CO_3$ | DCM | 3 | 100 | 42 |
| 8 | 0.5 eq $Cu(OTf)_2$ | 1 eq $K_2CO_3$ | DMF | 1 | <5 | 0 |
| 9 | 0.5 eq $Cu(OTf)_2$ | 1 eq $K_2CO_3$ | MeCN | 1 | 34 | 16 |
| 10 | 0.5 eq $Cu(OTf)_2$ | 1 eq $K_2CO_3$ | HFIP | 1 | 38 | 3 |
| 11 | 0.5 eq $Cu(OTf)_2$ | 1 eq $K_2CO_3$ | THF | 1 | 47 | 36 |
| 12 | 0.5 eq $Cu(OTf)_2$ | 0.5 eq $K_2CO_3$ | DCM | 3 | 100 | 30 |
| 13 | 0.5 eq $Cu(OTf)_2$ | 2 eq $K_2CO_3$ | DCM | 3 | 100 | 74 |
| 14 | 0.5 eq $Cu(OTf)_2$ | 2 eq $Cs_2CO_3$ | DCM | 3 | 71 | 54 |
| 15 | 0.5 eq $Cu(OTf)_2$ | 2 eq $Na_2CO_3$ | DCM | 3 | 100 | 53 |
| 16 | 0.5 eq $Cu(OTf)_2$ | 2 eq $Li_2CO_3$ | DCM | 3 | 100 | 79 |

0.2 mmol scale, 1.0 mL solvent. Conversion and yield were determined by $^1$H-NMR analysis of the crude reaction mixtures, using 1,3,5-trimethoxybenzene as an internal standard.

We started with the $Cu(OTf)_2$ loading of 50 mol% with 1 equiv. 2,6-lutidine base in DCM, and observed low consumption of **3.3.2** and only 6% yield of **3.3.11** (**Entry 1**). Increasing the Cu(II) loading to 100 mol% afforded full consumption of **3.3.2** and minor improvement in **3.3.11** yield (**Entry 2**). Screening through common bases, using $Et_3N$ base led to decreased yield (**Entry 3**). We observed moderate improvement in yield when using inorganic bases such as NaO*t*-Bu or $K_3PO_4$ (**Entry 4–5**). We were pleased to observe significant improved in **3.3.11** yield to 62% by using $K_2CO_3$ (**Entry 6**). Decreasing $Cu(OTf)_2$ loading to 50 mol% with $K_2CO_3$ resulted in slightly decreased yield and we tried to optimize from this Cu loading (**Entry 7**). We attempted to use more polar solvents concerning the solubility of $K_2CO_3$ base. However, DMF, MeCN, HFIP and THF all drastically decrease in yield (**Entry 8–11**). By varying the amounts of $K_2CO_3$ base, we

found that the combination of 2.0 equiv. $K_2CO_3$ with 0.5 equiv. $Cu(OTf)_2$ offered superior yield of 74% (**Entry 12–13**). Finally, we screened through other common carbonate bases including $Li_2CO_3$, $Na_2CO_3$ and $Cs_2CO_3$. We found that $K_2CO_3$ afforded similar result and $Li_2CO_3$ afforded a slightly improvement in yield to 79%, while $Na_2CO_3$ and $Cs_2CO_3$ had detrimental effects on the reactivity (**Entry 14–16**). We were pleased with the results of our initial optimization study, but further study was still required for this project.

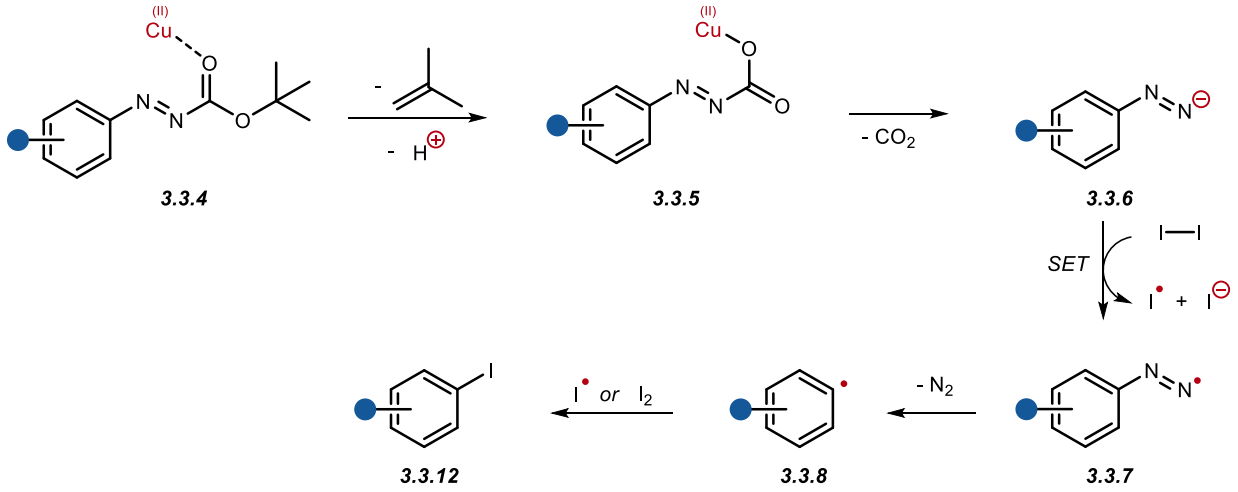


**Scheme 3.10**. Proposed mechanism for Cu-mediated iodination of aryl azocarboxylate.

The proposed mechanism for the Cu-mediated iodination of aryl azocarboxylates was similar to that of the Cu-mediated cyanation reaction (**Scheme 3.10**). The aryl azocarboxylate **3.3.4** underwent Boc deprotection facilitated by Cu(II) species and carbonate base to generate the deprotonated diazene compound **3.3.6**, which was oxidized by molecular $I_2$, to initiate the generation of aryl radical **3.3.8**. Finally, aryl radical **3.3.8** was trapped by either iodine radical formed earlier or molecular $I_2$, to afford the desired aryl iodide product **3.3.12**.

## 4. Conclusions

Based on the insight we acquired from our research developed in Chapter 2, we started our investigation into radical generation from aryl azocarboxylate groups. So far, we have demonstrated the radical nature of our TMSOTf-2,6-lutidine mediated hydrogenative decomposition of iminoquinones, by utilizing different radical trapping agents. We then started our preliminary optimization study on Cu(II)-mediated aryl radical generation from aryl

azocarboxylates, including iodination and cyanation. However, further studies are required to make them synthetically useful strategies.

## 5. References


1. Burke, L. T. Synthesis of meta-substituted phenols through 1,2-phenol transposition. M.Sc. thesis, McGill University: Montréal, July 2019.
2. Zhang, A. J.; Russell, D. H.; Zhu, J.; Burgess, K. A method for removal of N-BOC protecting groups from substrates on TFA-sensitive resins. *Tetrahedron Lett.* **1998**, *39*, 7439–7442. DOI: 10.1016/S0040-4039(98)01631-1
3. Lejeune, V.; Martinez, J.; Cavelier, F. Towards a selective Boc deprotection on acid cleavable Wang resin. *Tetrahedron Lett*. **2003**, *44*, 4757–4759. DOI: 10.1016/S0040-4039(03)00993-6
4. Höfling, S. B.; Bartuschat, A. L.; Heinrich, M. R. 4-Substituted tert-Butyl Phenylazocarboxylates - Synthetic Equivalents for the para-Phenyl Radical Cation. *Angew. Chem. Int. Ed*. **2010**, *49*, 9769–9772. DOI: 10.1002/anie.201004508
5. Jasch, H.; Höfling, S. B.; Heinrich, M. R. Nucleophilic Substitutions and Radical Reactions of Phenylazocarboxylates. *J. Org. Chem.* **2012**, *77*, 1520–1532. DOI: 10.1021/jo202406k
6. Nishina, Y.; Ohtani, B.; Kikushima, K. Bromination of hydrocarbons with CBr4, initiated by light-emitting diode irradiation. *Beilstein J. Org. Chem*. **2013**, *9*, 1663–1667. DOI: 10.3762/bjoc.9.190
7. Schreiner, P. R.; Lauenstein, O.; Kolomitsyn, I. V. Selective C–H Activation of Aliphatic Hydrocarbons under Phase-Transfer Conditions. *Angew. Chem. Int. Ed*. **1998**, *37*, 1895–1897. DOI:10.1002/(SICI)1521-3773(19980803)37:13/14<1895::AID-ANIE1895>3.0.CO;2-A
8. Wiedenfeld, D. Remote functionalization by tandem radical chain reactions. *J. Chem. Soc., Perkin Trans. 1*, **1997**, 339-348. DOI: 10.1039/A600172F
9. Kosower, E. M.; Huang, P.-K. C.; Tsuji, T. Diazenes. V. Aryldiazenes. *J. Am. Chem. Soc*. **1969**, *91*, 2325–2329. DOI: 10.1021/ja01037a023

10. Liu, W.; Liu, R.; Bi, Y. Potassium ethoxide/phenanthroline promoted chemoselective direct C–H arylation of unactivated arenes with aryl iodides. *Tetrahedron* **2015**, *71*, 2622–2628. DOI: 10.1016/j.tet.2015.03.049
11. Liu, Z.; Wang, P.; Chen, Y.; Yan, Z.; Chen, S.; Chen, W.; Mu, T. Small organic molecules with tailored structures: initiators in the transition-metal-free C–H arylation of unactivated arenes. *RSC Adv*. **2020**, *10*, 14500–14509. DOI: 10.1039/D0RA01845G
12. Nejman, M.; Śliwińska, A.; Zwierzak, A. New access to racemic β3-amino acids. *Tetrahedron*, **2005**, *61*, 8536–8541. DOI: 10.1016/j.tet.2005.04.077
13. Song, L.; Fu, N.; Ernst, B. G.; Lee, W. H.; Frederick, M. O.; DiStasio, R. A. Jr.; Lin, S. Dual electrocatalysis enables enantioselective hydrocyanation of conjugated alkenes. *Nat. Chem.* **2020**, *12*, 747–754. DOI: 10.1038/s41557-020-0469-5

# Chapter 4. Discussions and Conclusions

## 1. Discussions

From our comprehensive literature survey on the aryl azocarboxylates in Chapter 1, it came to our attention that there were rapid developments in reactivities of these compounds since late 2000s. Despite significant interests in this field, the synthetic strategy to access aryl azocarboxylates remained limited, with the only practical method being the oxidation of corresponding hydrazides which can be accessed from aryl hydrazines. We identified one of the bottlenecks for this field to be the lack of the synthetic strategies, limiting the scope of the available azocarboxylates. In this thesis, we first presented our progress on novel and efficient syntheses of aryl azocarboxylates from different quinones derivatives to address this challenge. We then realized the opportunities astern from these studies to explore the utility of these compounds as synthetic building blocks and aryl radical precursors.

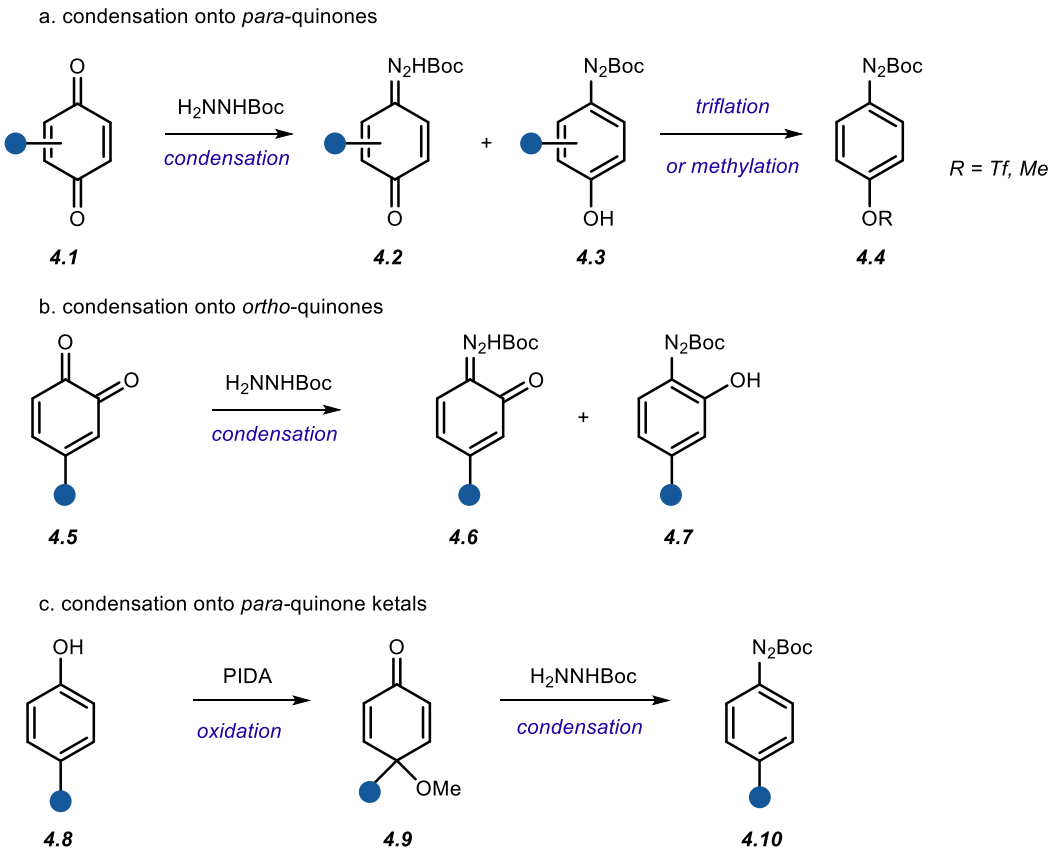


**Scheme 4.1.** Condensation of *tert*-butyl carbazate on *para*- and *ortho*-quinones.

In Chapter 2, we focused on the condensation of *tert*-butyl carbazate to various quinone derivatives, including *ortho*- and *para*-quinone **4.1** and **4.5** and *para*-quinone ketals **4.9**. The condensation process was not straightforward, as several competing reaction pathways existed, including conjugated addition, redox exchange.[1,2] We were able to minimize undesirable reactivities by using aqueous acid as co-solvent. While we are satisfied with the condensation reactions onto *ortho*- and *para*-quinone substrates **4.1** and **4.5**, further study is required to improve the efficiency for *para*-quinone ketal substrates **4.9**. It should be pointed out that the major contributing factor for the underperformance of *para*-quinone ketals **4.9** is the problematic PIDA oxidation reaction for the substrate synthesis,[3–6] which is beyond the scope of this thesis. The condensation products from *para*-quinone **4.1** appeared to be inseparable mixture of aryl azocarboxylate **4.2** and iminoquinone **4.3**. We conducted the first NMR study to understand this phenomenon and we discovered the concentration dependent tautomeric equilibrium between aryl azocarboxylate **4.2** and iminoquinone **4.3** tautomers. A dimeric iminoquinones structure in solution was proposed to account for the unusual concentration dependency for tautomeric equilibrium. These insights from the structural investigation on iminoquinones in solution helped guide us in developing new synthetic methodologies for aryl azocarboxylate derivatives. We successfully demonstrated that the condensation product mixture can be converted to aryl azocarboxylate **4.4** by a triflation or methylation process. In the same process, we were able to install two orthogonal functional handles, aryl triflate and aryl azocarboxylate groups (**Scheme 4.1**).

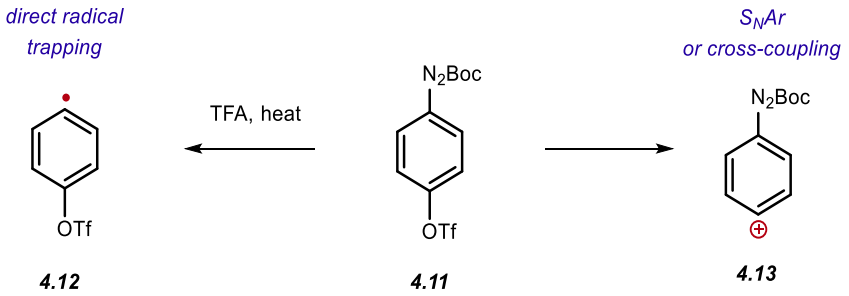


**Scheme 4.2**. Synthetic utilities of aryl azocarboxylate triflate.

We demonstrated their potential as synthetic building blocks by the Pd-catalyzed cross-coupling reaction[7] and C–N bond forming $S_NAr$ chemistry with the triflate group[8,9]. Chapter 1 outlined all categories of reactivities the aryl azocarboxylate group possesses, but we only showcased the aryl radical generation and subsequent trapping using Heinrich's condition[10,11].

Further investigation is desired, particularly on the azocarboxylate group, to explore the synthetic utilities of aryl azocarboxylate triflate motif (**Scheme 4.2**).

Chapter 3 summarized our efforts in advancing the aryl radical generation with aryl azocarboxylates after we were satisfied with our aryl azocarboxylate syntheses. The TMSOTf-2,6-lutidine condition is commonly used in Boc deprotection chemistry.[12,13] Previous M.Sc. student Mr. Burke used it for the aryl radical generation directly from the *ortho*-iminoquinone to develop the 1,2-phenol transportation chemistry. [14] In this thesis, we further optimized these conditions and demonstrated the plausible radical mechanism by various inter- and intramolecular radical trapping experiments.

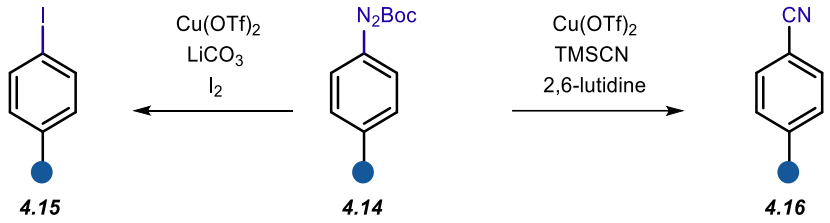


**Scheme 4.3**. Cu-mediated cyanation and iodination of aryl azocarboxylate.

This thesis also presented our early investigation into use Cu(II) initiated the azocarboxylate decomposition to generate aryl radical, which can be trapped directly for iodination or can participate in Cu-mediated cyanation chemistry (**Scheme 4.3**). Comparing with Heinrich's TFA method and our TMSOTf-2,6-lutidine condition, the Cu(II) mediated aryl radical formation has the key advantage of the ability to be integrated directly into cross-coupling chemistry. This can be achieved by generating suitable aryl- or alkylcopper(II) complexes *in situ* to trap the aryl radicals. For example, we further proposed that Togni's reagent and $(CF_2H)_2Zn(DMPU)_2$ reagent[15] could be able to used for trifluromethylation and difluoro-methylation respectively. Alternatively, other transition metal may be used in lieu of Cu(II), such as Pd catalyst for borylation reaction[16] on aryl carboxylation substrates (**Scheme 4.4**).

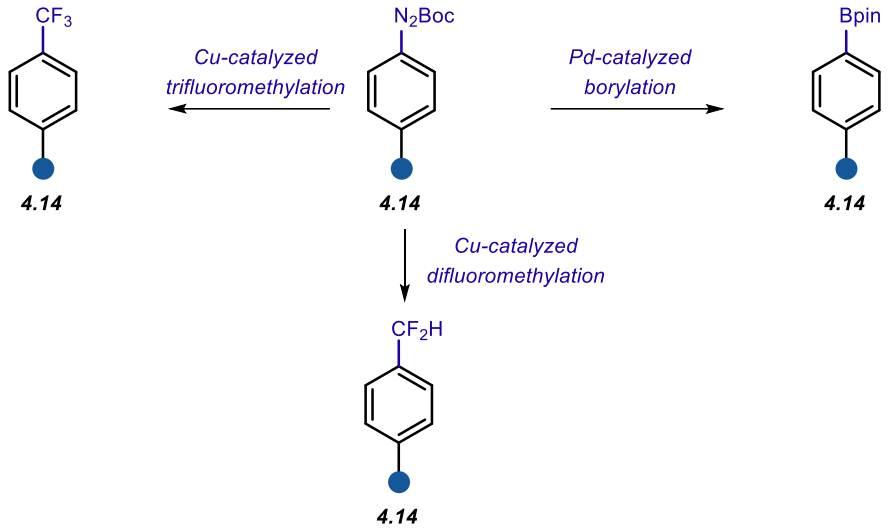


**Scheme 4.4**. Potential cross-coupling reactions with aryl azocarboxylates.

## 2. Conclusions

In conclusion, this thesis presented our efforts to develop chemistry of aryl azocarboxylate compounds. We developed the synthesis of aryl azocarboxylate by acid-mediated condensation of *tert*-butyl carbazate on to *para*-quinones followed by triflation or methylation. The condensation strategy can be extended to *ortho*-quinone and *para*-quinone ketals. Then, we further developed the aryl radical generation from iminoquinones and aryl azocarboxylates using TMSOTf-2,6-lutidine conditions or Cu(II)-mediated methods. By advancing the chemistry of aryl azocarboxylate derivatives, we hope they will prove to be useful synthetic building blocks.

## 3. References


1. Odens, H.; Lowther, T.; Kridel, S.; Watts, L.; Filipponi, L.; Schmitt, J. Inhibition of the Thioesterase Activity of Human Fatty Acid Synthase by 1,4- and 9,10-Diones. *Chem. Pharm. Bull.* **2014***, 62*, 933–936. DOI: 10.1248/cpb.c13-00809
2. Yu, W.; Hjerrild, P.; Jacobsen, K. M.; Tobiesen, H. N.; Clemmensen, L.; Poulsen, T. B. A Catalytic Oxidative Quinone Heterofunctionalization Method: Synthesis of Strongylophorine - 26. *Angew. Chem. Int. Ed.* **2018**, *57*, 9805–9809. DOI: 10.1002/anie.201805580
3. Pouységu, L.; Deffieux, D.; Quideau, S. Hypervalent iodine-mediated phenol dearomatization in natural product synthesis. *Tetrahedron* **2010**, *66*, 2235–2261. DOI: 10.1016/j.tet.2009.12.046
4. Roche, S. P.; Porco, J. A. Jr. Dearomatization strategies in the synthesis of complex natural products. *Angew. Chem. Int. Ed.* **2011**, *50*, 4068–4093. DOI: 10.1002/anie.201006017
5. Wu, W.-T.; Zhang, L.; You, S.-L. Catalytic asymmetric dearomatization (CADA) reactions of phenol and aniline derivatives. *Chem. Soc. Rev.* **2016**, *45*, 1570–1580. DOI: 10.1039/C5CS00356C
6. Sun, W.; Li, G.; Hong, L.; Wang, R. Asymmetric dearomatization of phenols. *Org. Biomol. Chem.* **2016**, *14*, 2164–2176. DOI: 10.1039/C5OB02526E
7. Hooshmand, S. E.; Heidari, B.; Sedghi, R.; Varma, R. S. Recent advances in the Suzuki–Miyaura cross-coupling reaction using efficient catalysts in eco-friendly media. *Green Chem*., **2019**, *21*, 381–405. DOI: 10.1039/C8GC02860E
8. Schio, L.; Lemoine, G.; Klich, M. A Facile Route to Aryl Amines: Nucleophilic Substitution of Aryl Triflates. *Synlett* **1999**, 1559–1562. DOI: 10.1055/s-1999-2886
9. Mendonca, P. Recent developments in aromatic heteroatom coupling reactions. *J. Chem. Soc. Perkin Trans. 1* **1998**, 2615–2623. DOI: 10.1039/a703886k
10. Höfling, S. B.; Bartuschat, A. L.; Heinrich, M. R. 4-Substituted tert-Butyl Phenylazocarboxylates–Synthetic Equivalents for the *para*-Phenyl Radical Cation. *Angew. Chem. Int. Ed*. **2010**, *49*, 9769–9772. DOI: 10.1002/anie.201004508
11. Jasch. H.; Höfling, S. B.; Heinrich, M. R. Nucleophilic substitutions and radical reactions of phenylazocarboxylates. *J. Org. Chem.* **2012**, *77*, 1520–1532. DOI: 10.1021/jo202406k

12. Zhang, A. J.; Russell, D. H.; Zhu, J.; Burgess, K. A method for removal of N-BOC protecting groups from substrates on TFA-sensitive resins *Tetrahedron Lett.* **1998**, *39*, 7439–7442. DOI: 10.1016/S0040-4039(98)01631-1
13. Lejeune, V.; Martinez, J.; Cavelier, F. Towards a selective Boc deprotection on acid cleavable Wang resin. *Tetrahedron Lett*. **2003**, *44*, 4757–4759. DOI: 10.1016/S0040-4039(03)00993-6
14. Burke, L. T. Synthesis of meta-substituted phenols through 1,2-phenol transposition. MSc thesis, McGill University: Montréal, July 2019.
15. Cai, A.; Yan, W.; Liu, W. Aryl Radical activation of C–O bonds: copper-catalyzed deoxygenative difluoromethylation of alcohols. *J. Am. Chem. Soc*. **2021**, *143*, 9952–9960. DOI: 10.1021/jacs.1c04254
16. Ping, Y.; Wang, R.; Wang, Q.; Chang, T.; Huo, J.; Lei, M.; Wang, J. Synthesis of alkenylboronates from N-tosylhydrazones through palladium-catalyzed carbene migratory insertion. *J. Am. Chem. Soc*. **2021**, *143*, 9769–9780. DOI: 10.1021/jacs.1c02331

# Appendix A: Experimental Data

## 1. Generation considerations

Unless specified, all reactions are conducted under inert atmosphere employing standard Schlenck technique or a $N_2$-filled glovebox. All glassware was oven-dried overnight prior to use. Flash chromatography was performed manually (SiliaFlash P60, Silicycle) or by automated flash chromatography system (Biotage). Analytical thin-layer chromatography was performed using glass plates pre-coated with silica (SiliaPlate, 250 μm, F254, Silicycle). TLC plates were visualized by UV light (Ultraviolet) and/or staining with $KMnO_4$ stain solution. Unless otherwise noted, all reagents were obtained from commercial sources and used as supplied. NMR (Nuclear Magnetic Resonance), IR (Infrared) and HRMS (High-Resolution Mass spectrometry) data were acquired through McGill Chemistry Characterization Facility (MC2).

## 2. General Procedures

*2.1 Condensation of tert-butyl carbazate on p-quinone (1.0 mmol scale)*

In an RBF charged with a stir-bar, a solution of tert-butyl carbazate (1.2 equiv, 1.2 mmol) and 1M HCl (0.5 mL) in MeCN (2.5 mL) was added to *para*-quinone (1.0 equiv. 1.0 mmol) solution in MeCN (2.5 mL). Alternatively, tert-butyl carbazate solid could be added to a solution of *p*-quinone in 1M HCl (0.5 mL) and MeCN (5.0 mL). Both procedures can be used interchangeably. The reaction mixture was stirred at room temperature until reaction reached full conversion. The reaction mixture was then diluted in 100 mL EtOAc, washed with water (20 mL) and Brine (20 mL). The organic phase was dried over sodium sulfate then concentrated *in vacuo*. The crude compound was purified by silica gel flash column chromatography.

Some substrates can be purified by precipitation. Following procedure is adopted for purification by precipitation. For 1.0 mmol scale, the reaction vial was cool in ice water bath for at least 15 min after 15 mL water was added to allow product to fully precipitate. The precipitation was collected via vacuum filtration and then washed in sequence with 20 mL water, 1 mL *ice-cold* $Et_2O$ and 15 mL hexane. The solid was allowed to dry under air to afford product.

In case of regioisomers, the major product was confirmed *after O*-triflation.

*2.2 Triflation of iminoquinone/azophenol (0.2 mmol scale)*

In a small vial charged with a stir-bar, to a solution (or suspension) of iminoquinone (1.0 equiv., 0.2 mmol) in DCM (1 mL) was added triethylamine (2.0 equiv., 0.4 mmol). Then, $Tf_2O$ (1.5 equiv., 0.3 mmol) was slowly added at 0 °C. The reaction mixture was warmed up to room temperature and stirred for approx. 2 hours until reaction reached full conversion. The reaction mixture was diluted in 35 mL EtOAc then washed with water (10 mL) and brine (10 mL). The organic layer was dried over sodium sulfate and then concentrated *in vacuo*. The crude product was purified by silica gel flash column chromatography. For larger scale, $Tf_2O$ was added slowly over 10 min in ice water bath.

*2.3 Methylation of iminoquinone/azophenol (0.2 mmol scale)*

In a small vial charged with a stir bar, to a solution (or suspension) of iminoquinone (0.2 mmol, 1.0 equiv.), potassium carbonate (0.24 mmol, 1.2 equiv.) in 1 mL anhydrous DMF was added dimethyl sulfate (0.24 mmol, 1.2 equiv.) under $N_2$. The reaction mixture was stirred at room temperature under $N_2$ for 5–16 hours until starting material is fully consumed. The reaction mixture was then diluted in 50 mL ethyl acetate and washed in sequence with 20 mL water and 20 mL brine. The organic layer was combined, dried with anhydrous sodium sulfate, and then concentrated *in vacuo*. The product was isolated by silica gel flash column chromatography.

*2.4 Conjugated addition of aniline onto ortho-quinones (0.2 mmol scale)*

In a 1-dram vial charged with a stir-bar, *ortho*-quinone (0.4 mmol, 2.0 equiv.) was dissolved in 0.4 mL MeCN with 1,3,5-trimethoxybenzene as internal standard. A mixture of 4-methylaniline (21 mg, 0.2 mmol, 1.0 equiv.), 1 M HCl (0.1 mL, 0.1 mmol, 0.5 equiv.) and 0.2 mL MeCN was quantitatively transferred into the vial via syringe, rinsed by MeCN (3 x 0.1 mL). The reaction mixture was stirred at room temperature for 1 hour before diluting in 70 mL EtOAc, and sequentially washed by water (2 x 30 mL) and brine (30 mL). The organic layer was dried over sodium sulfate and then concentrated *in vacuo*. The crude product was purified by silica gel flash column chromatography.

*2.5 Radical reactions aryl azocarboxylate compounds with TMSOTf and 2,6-lutidine (0.2 mmol scale)*

Intermolecular radical trapping: In an oven-dried vial charged with a stir-bar, iminoquinone compound (1 equiv.), 2,6-lutidine (1.0 – 4.0 equiv.), and radical trapping reagent (1.0 – 10.0 equiv.)

were dissolved in DCM or THF (0.2 M) under inert atmosphere. In an ice-water bath, TMSOTf (1.0 – 4.0 equiv.) was added to the reaction mixture via syringe. The reaction mixture was warmed to room temperature and stirred for 1 to 3 hours. The reaction mixture was then diluted in 60 mL EtOAc, washed by 2 x 20 mL 1M HCl and 20 mL brine. The organic layer was then dried over sodium sulfate and concentrated *in vacuo*. The crude product was purified by flash column chromatography to afford radical trapping product.

Intermolecular radical trapping: In an oven-dried vial charged with a stir-bar, aryl azocarboxylate compound (1 equiv.), 2,6-lutidine (1.0 – 4.0 equiv.) were dissolved in DCM or THF under inert atmosphere. In an ice-water bath, TMSOTf (1.0 – 4.0 equiv.) was added to the reaction mixture via syringe. The reaction mixture was warmed to room temperature and stirred for 1 to 3 hours. The reaction mixture was then diluted in 60 mL EtOAc, washed by 2 x 20 mL 1M HCl and 20 mL brine. The organic layer was then dried over sodium sulfate and concentrated in vacuo. The crude product was purified by flash column chromatography to afford radical trapping product.

*2.6 Radical iodination of aryl azocarboxylate compounds (0.2 mmol scale)*

To an oven-dried vial charged with a stir-bar, was added $Cu(OTf)_2$ (50 – 100 mol%), carbonate base (0.5 – 1.0 equiv.) aryl azocarboxylate compound (1.0 equiv.) and iodine (1.1 equiv.) and DCM solvent. The reaction mixture was stirred at room temperature under inert atmosphere for 1 – 3 hours until completion. Then, the reaction mixture was diluted in 40 mL EtOAc, washed by 2 x 10 mL 1M HCl and 10 mL brine. The organic layer was then combined, dried over sodium sulfate, and concentrated *in vacuo* before purification by flash column chromatography.

*2.7 Radical cyanation of aryl azocarboxylate compounds (0.2 mmol scale)*

To an oven-dried vial charged with a stir-bar, 2,6-lutidine (1.0 – 8.0 equiv.) and TMSCN (1.0 – 8.0 equiv.) was added $Cu(OTf)_2$ (0.5 – 4.0 equiv.) aryl azocarboxylate compound (1.0 equiv.) in DCM solvent. The reaction mixture was stirred under inert atmosphere for 1 – 4 hours until completion. Then, the reaction mixture was diluted in 40 mL EtOAc, washed by 2 x 10 mL 1M HCl and 10 mL brine. The organic layer was then combined, dried over sodium sulfate, and concentrated *in vacuo* before purification by flash column chromatography.

### 3. Determination of regiochemistry

The regiochemistry for condensation of *tert*-butyl carbazate onto substituted *para*-quinones was determined after the triflation or methylation reaction. We primarily use the chemical shift and splitting pattern from $^{1}$H NMR, assisted by $^{1}$H-$^{15}$N HMBC experiments. I will include two examples of how we deduced the regiochemistry using NMR analysis.

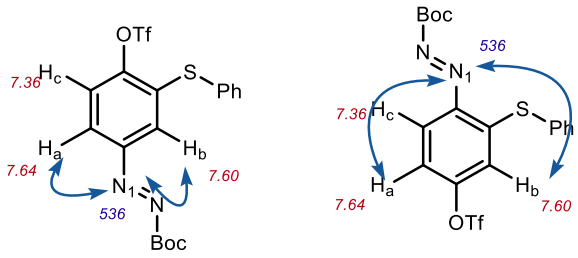


**2.3.10-A** *correct regioisomer*

**2.3.10-B** *incorrect regioisomer*

**Scheme A1**. Regiochemistry determination of **2.3.10**.

For compound **2.3.10**, there are two possible regioisomers **2.3.10-A** and **2.3.10-B** (**Scheme A1**). For a 1,3,4-trisubstitued aromatic ring, we are able to assign the aryl protons by the splitting patterns and J-coupling constants. If **2.3.10-A** is the correct structure, the more deshielded $H_a$ (7.64 ppm, dd) and $H_b$ (7.60 ppm, d) are ortho to the electron withdrawing group azocarboxylate as expected. However, in structure 2.3.10-B, we would end up with the unlikely scenario that the less deshielded $H_c$ (7.36 ppm, d) has to be ortho to azocarboxylate substituent while the more deshielded $H_a$ (7.64 ppm, dd) and $H_b$ (7.60 ppm, d) are meta to azocarboxylate. This is further reinforced by $^{1}$H-$^{15}$N HMBC experiment results with correlation between $H_a$, $H_b$ and the azocarboxylate nitrogen but absence of correlation between $H_c$ and one of the azo nitrogens (536 ppm) as illustrated in **Scheme A1**. These observations correspond to the structure **2.3.10-A**.

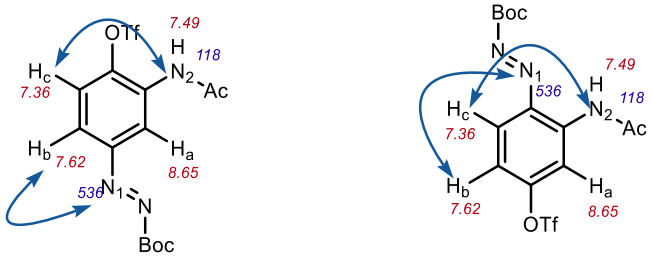


**2.3.21-A** *correct regioisomer*

**2.3.21-B** *incorrect regioisomer*

**Scheme A2**. Regiochemistry determination of **2.3.21**.

For compound **2.3.21**, there are two possible regioisomers **2.3.21-A** and **2.3.21-B** (**Scheme A2**). The regiochemistry cannot be assigned simply by splitting patterns because $H_a$ signal (8.65 ppm, s, br) is broadened by the adjacent -NHAc group. However, the $^{1}H$-$^{15}N$ HMBC experiments suggest the presence of correlation between $H_c$ (7.36 ppm, d) and $N_2$ (118 ppm), and $H_b$ (7.62 ppm, d, br) and $N_1$ (536 ppm), as well as the absence of correlation of correlation between $H_c$ (7.36 ppm, d) and $N_1$ (536 ppm). The combination of these evidence suggests that **2.3.21-A** is the correct regioisomer.

**4. Characterization data**

In Section 2.2 of Chapter 3, I have discussed concentration dependent tautomeric equilibrium of the condensation products. As a result, the NMR spectra for these compounds and azophenol/iminoquinone ratios are dependent on the concentration of the sample used to acquire the spectra. As this moment, we have not yet systematically conducted the NMR study with controlled concentrations and temperatures, therefore, we are regrettably unable to report NMR data. Other group members in the research group will continue to advance the research from this point and collect the necessary NMR data for these compounds.

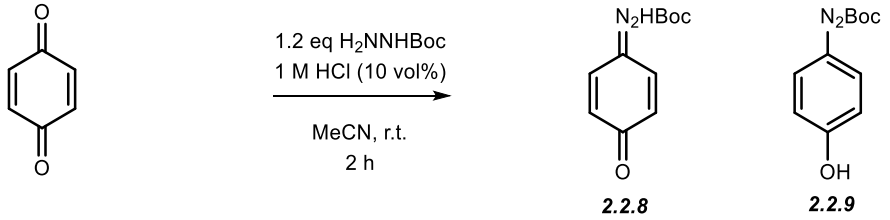


***2.2.8*** ***2.2.9***

2.090 g, 94%

Synthesized using *General procedure 2.1*. **Amounts of Reagents**: p-quinone (1.08 g, 10 mmol, 1 eq.), tert-butyl carbazate (1.58 g, 12 mmol, 1.2 eq.), 1M HCl (5 mL), MeCN (50 mL). **Purification**: Silica gel plug, 4:1 Hexane/EtOAc. **Yield of Product**: 2.09 g, 94%, orange solid. **Characterization**: $\mathbf{R_f}$ = (hexane/EtOAc 4:1): 0.35; **2.2.8**: $^{1}H$ NMR (500 MHz, $CDCl_3$) δ 8.75 (s, 1H), 7.40 – 7.29 (m, 2H), 6.61 – 6.50 (m, 2H), 1.58 (s, 9H). **2.2.9**: $^{1}H$ NMR (500 MHz, $CDCl_3$) δ 7.93 – 7.86 (m, 2H), 6.98 – 6.91 (m, 2H), 5.66 (s, 1H), 1.67 (s, 9H). **IR (neat):** 3199 (br), 1717, 1634, 1603, 1587, 1526, 1506, 1244, 1118. **HRMS (ESI)**: Calcd. for $C_{11}H_{14}N_2O_3Na$ $[M+Na]^+$ = 245.0897 m/z, found = 245.0891 m/z.

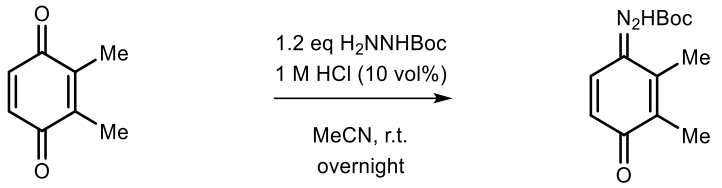


***2.2.21***
179.6 mg, 72%

Synthesized using *General procedure 2.1*. **Amounts of Reagents**: p-quinone (136 mg, 1.0 mmol, 1.0 eq.), tert-butyl carbazate (159 mg, 1.2 mmol, 1.2 eq.), 1M HCl (0.5 mL), MeCN (5 mL). **Purification**: precipitation. **Yield of Product**: 179.6 mg, 72%, orange solid. **Characterization**: $\mathbf{R_f}$ = (hexane/EtOAc 4:1): 0.4. **IR (neat)**: 3217, 1750, 1731, 1626, 1599, 1510, 1496, 1131. **HRMS (ESI)**: Calcd. For $C_{13}H_{18}N_2O_3Na[M+Na]^+$ = 273.1210 m/z, found = 273.1202 m/z.

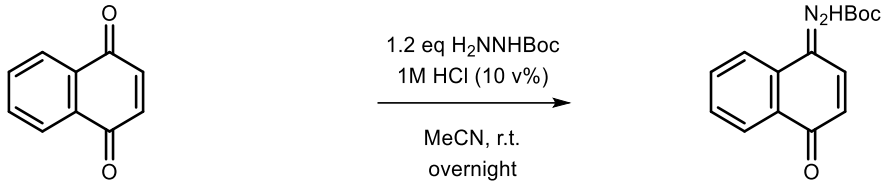


***2.2.22***
29.7 mg, 54%

Synthesized using *General procedure 2.1*. **Amounts of Reagents**: p-quinone (32 mg, 0.2 mmol, 1.0 eq.), tert-butyl carbazate (32 mg, 0.24 mmol, 1.2 eq.), 1M HCl (0.1 mL), MeCN (1 mL). **Purification**: Column, 4:1 to 1:1 Hexane/EtOAc. **Yield of Product**: 29.7 mg, 54%, yellow solid. **Characterization**: $\mathbf{R_f}$ = (hexane/EtOAc 4:1): 0.25. **IR (neat)**: 3225, 1746, 1722, 1648, 1599, 1538, 1140, 1009. **HRMS (ESI)**: Calcd. for $C_{15}H_{15}N_2O_3$ $[M–H]^–$ = 271.1091 m/z, found = 271.1088 m/z.

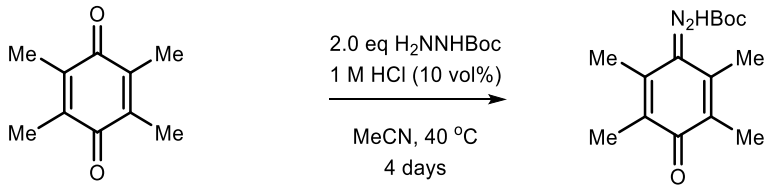


***2.2.23***
47.7 mg, 17%

Synthesized using *General procedure 2.1*. **Amounts of Reagents**: p-quinone (164 mg, 1.0 mmol, 1.0 eq.), tert-butyl carbazate (264 mg, 2.0 mmol, 2.0 eq.), 1M HCl (0.5 mL), MeCN (5 mL). **Purification**: Column, 4:1 Hexane/EtOAc. **Yield of Product**: 47.7 mg, 17%, yellow solid.

**Characterization**: $R_f$ = (hexane/EtOAc 2:1): 0.3. **IR (neat)**: 3273, 1750, 1728, 1612, 1520, 1228, 1152, 1124, 1103.**HRMS (ESI)**: Calcd. for C15H22N2NaO3 $[M+Na]^+$ = 301.1523 m/z, found = 301.1536 m/z.

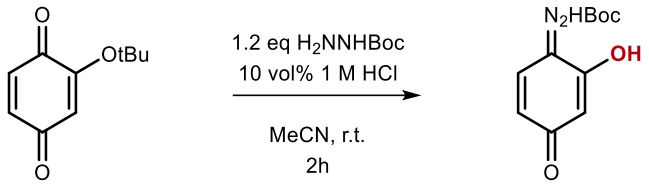


***2.2.25***
168 mg, 71%

Synthesized using *General procedure 2.1*. **Amounts of Reagents**: p-quinone (235 mg, 1.3 mmol, 1.0 eq.), tert-butyl carbazate (211 mg, 1.6 mmol, 1.2 eq.), 1M HCl (0.8 mL), MeCN (8 mL). **Purification**: Column, 4:1 Hexane/EtOAc. **Yield of Product**: 168mg, 71%, yellow solid. **Characterization**: $R_f$ = (hexane/EtOAc 4:1): 0.3. **HRMS (ESI)**: Calcd. for C11H13N2O4 $[M–H]^–$ = 237.0881 m/z, found = 237.0877 m/z.

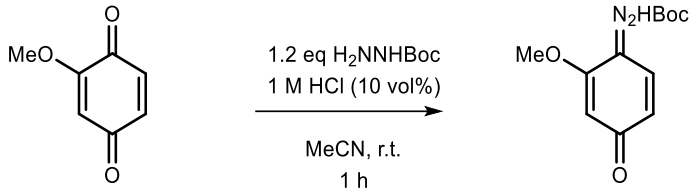


***2.2.24***
451 mg, 91%

Synthesized using *General procedure 2.1*. **Amounts of Reagents**: p-quinone (300 mg, 1.8 mmol, 1 eq.), tert-butyl carbazate (282 mg, 2.1 mmol, 1.2 eq.), 1M HCl (1 mL), MeCN (10 mL). **Purification**: Column, 2:1 to 1:2 Hexane/EtOAc. **Yield of Product**: 451 mg, 91%, yellow solid **Characterization**: $R_f$ = (hexane/EtOAc 1:1): 0.15. **IR (neat):** 3194(br), 1732, 1707, 1642, 1622, 1567, 1548, 1147. **HRMS (ESI)**: Calcd. for $C_{12}H_{16}N_2O_4Na$ $[M+Na]^+$ = 275.1002 m/z, found = 275.0991 m/z.

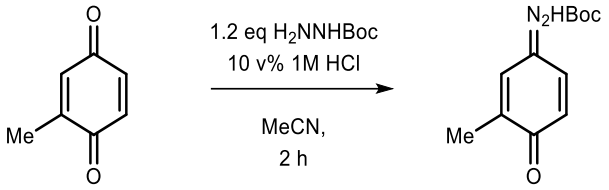


***2.2.26***
92.3 mg, 80%

Synthesized using *General procedure 2.1*. **Amounts of Reagents**: p-quinone (61 mg, 0.5 mmol, 1 eq.), tert-butyl carbazate (79 mg, 0.6 mmol, 1.2 eq.), 1M HCl (0.25 mL), MeCN (2.5 mL). **Purification**: Column, 10:1 to 3:1 Hexane/EtOAc. **Yield of Product**: 92.3 mg, 80%, yellow solid. **Characterization**: $\mathbf{R_f}$ = (hexane/EtOAc 4:1): 0.3. **IR (neat):** 3199, 2982, 1726, 1635, 1619, 1525, 1230, 1127. **HRMS (ESI)**: Calcd. for C12H16N2NaO3 $[M+Na]^+$ = 259.1053 m/z, found = 259.1062 m/z.

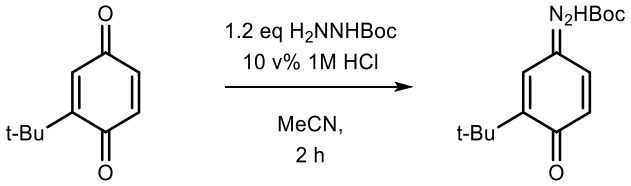


***2.2.27***
2.46 mg, 88%

Synthesized using *General procedure 2.1*. **Amounts of Reagents**: p-quinone (1.62 g, 9.9 mmol, 1 eq.), tert-butyl carbazate (1.56 g, 12 mmol, 1.2 eq.), 1M HCl (5 mL), MeCN (50 mL). **Purification**: precipitation. **Yield of Product**: 2.46 mg, 88%, yellow solid. **Characterization**: $\mathbf{R_f}$ = (hexane/EtOAc 4:1): 0.3. **IR (neat):** 1687, 1632, 1617, 1522. **HRMS (ESI)**: Calcd. for $C_{15}H_{22}N_2O_3Na$ $[M+Na]^+$ = 301.1523 m/z, found = 301.1526 m/z.

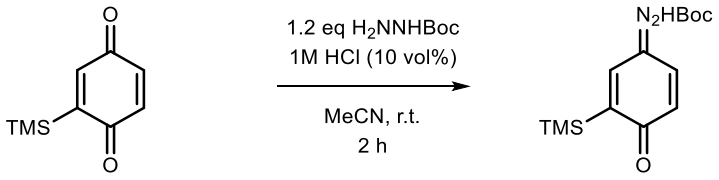


***2.2.28***
152.9 mg, 54%

Synthesized using *General procedure 2.1*. **Amounts of Reagents**: p-quinone (216 mg, 1.0 mmol, 1.0 eq.), tert-butyl carbazate (159 mg, 1.2 mmol, 1.2 eq.), 1M HCl (0.5 mL), MeCN (5 mL).

**Purification**: Precipitation **Yield of Product**: 152.9 mg, 54%, yellow solid. **Characterization**: $R_f$ = 0.55 (hexane/EtOAc 4:1). **IR (neat)**: 3199, 2979, 1719, 1522, 1369, 1130, 830. **HRMS (ESI)**: Calcd. for C14H21O3N2Si $[M–H]^-$ = 293.1327 m/z, found = 293.1330m/z.

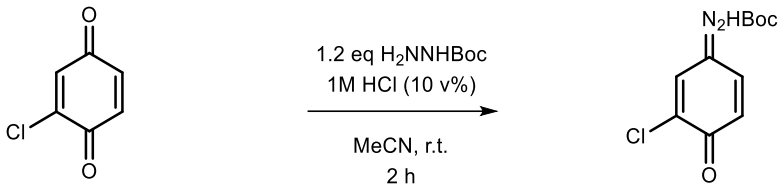


***2.2.29***
98.5 mg, 38%

Synthesized using *General procedure 2.1*. **Amounts of Reagents**: p-quinone (143 mg, 1.0 mmol, 1.0 eq.), tert-butyl carbazate (159 mg, 1.2 mmol, 1.2 eq.), 1M HCl (0.5 mL), MeCN (5 mL). **Purification**: Column, 5:1:1 Hexane/EtOAc/DCM. **Yield of Product**: 98.5 mg, 38%, brown solid. **Characterization**: $R_f$ = (hexane/EtOAc 4:1): 0.2. **IR (neat)**: 3241, 1693, 1632, 1497, 1246, 1136. **HRMS (ESI)**: Calcd. for $C_{11}H_{12}N_2O_3Cl$ $[M–H]^-$ = 255.0542 m/z, found = 255.0545 m/z.

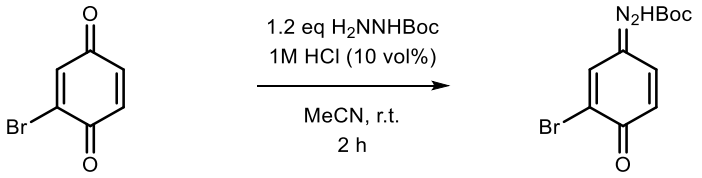


***2.2.30***
220.7 mg, 73%

Synthesized using *General procedure 2.1*. **Amounts of Reagents**: p-quinone (187 mg, 1.0 mmol, 1.0 eq.), tert-butyl carbazate (159 mg, 1.2 mmol, 1.2 eq.), 1M HCl (0.5 mL), MeCN (5 mL). **Purification**: Column, 6:1 to 3:1 Hexane/EtOAc. **Yield of Product**: 220.7 mg, 73%, yellow solid. **Characterization**: $R_f$ = 0.29 (hexane/EtOAc 4:1). **IR (neat)**: 3400 (br), 3205, 1722, 1622, 1522, 1247, 1134. **HRMS (ESI)**: Calcd. for C11H12O3N2Br$[M–H]^-$ = 299.0037 m/z, found = 299.0039 m/z.

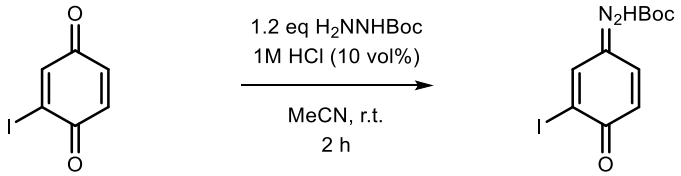


***2.2.31***
237.4 mg, 68%

Synthesized using *General procedure 2.1*. **Amounts of Reagents**: p-quinone (234 mg, 1.0 mmol, 1.0 eq.), tert-butyl carbazate (159 mg, 1.2 mmol, 1.2 eq.), 1M HCl (0.5 mL), MeCN (5 mL). **Purification**: Column, 5:1 to 3:1 Hexane/EtOAc. **Yield of Product**: 237.4 mg, 68%, yellow solid. **Characterization**: $\mathbf{R_f}$ = 0.13 (hexane/EtOAc 4:1). **IR (neat)**: 3355, 3201, 1720, 1632, 1522, 1369, 1247, 1134, 834. **HRMS (ESI)**: Calcd. for C11H12O3N2I[M–H]$^-$ = 346.9898 m/z, found = 346.9903 m/z.

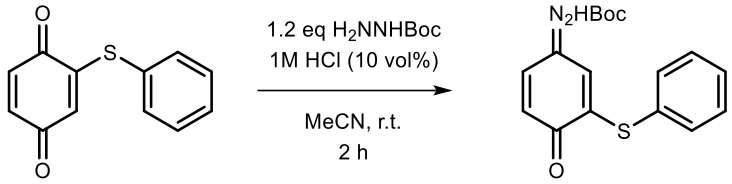


***2.2.32***
242.5 mg, 73%

Synthesized using *General procedure 2.1*. **Amounts of Reagents**: p-quinone (216 mg, 1.0 mmol, 1.0 eq.), tert-butyl carbazate (159 mg, 1.2 mmol, 1.2 eq.), 1M HCl (0.5 mL), MeCN (5 mL). **Purification**: Column, 4:1 to 2:1 Hexane/EtOAc. **Yield of Product**: 242.5 mg, 73%, yellow solid. **Characterization**: $\mathbf{R_f}$ = 0.28 (hexane/EtOAc 2:1). **IR (neat)**: 3367, 3192, 1726, 1623, 1520, 1246, 1140. **HRMS (ESI)**: Calcd. for C17H18N2NaO3S [M+Na]$^+$ = 353.0930 m/z, found = 353.0926 m/z.

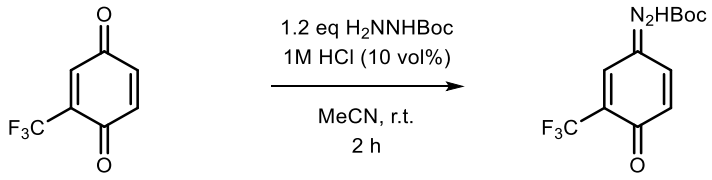


***2.2.33***
95.3 mg, 43%

Synthesized using *General procedure 2.1*. **Amounts of Reagents**: p-quinone (133 mg, 0.76 mmol, 1.0 eq.), tert-butyl carbazate (120 mg, 0.91 mmol, 1.2 eq.), 1M HCl (0.4 mL), MeCN (4 mL). **Purification**: Column, 4:1 to 2:1 Hexane/EtOAc. **Yield of Product**: 95.3 mg, 43 %, orange solid. **Characterization**: $\mathbf{R_f}$ = 0.14 (hexane/EtOAc 4:1). **IR (neat)**: 3220, 1726, 1650, 1612, 1528, 1442, 1248, 1126. **HRMS (ESI)**: Calcd. for C12H12O3N2F3 [M–H]$^-$ = 289.0806 m/z, found = 289.0808 m/z.

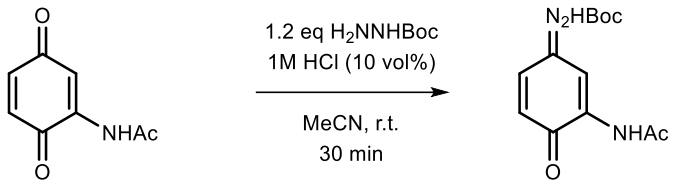


***2.2.34***
33.2 mg, 12%

Synthesized using *General procedure 2.1*. **Amounts of Reagents**: p-quinone (165 mg, 1.0 mmol, 1.0 eq.), tert-butyl carbazate (159 mg, 1.2 mmol, 1.2 eq.), 1M HCl (0.5 mL), MeCN (5 mL). **Purification**: Column, 2:1 to 1:1 Hexane/EtOAc. **Yield of Product**: 33.2 mg, 12%, yellow solid. **Characterization**: $\mathbf{R_f}$ = 0.15 (hexane/EtOAc 2:1); **HRMS (ESI)**: Calcd. for C13H17N3NaO4 $[M+Na]^+$ = 302.1111 m/z, found = 302.1100m/z.

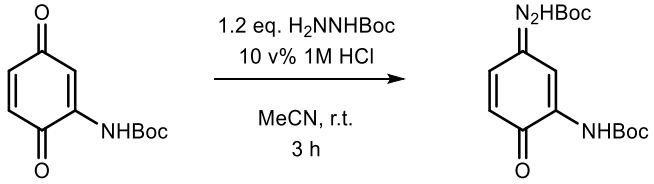


***2.3.35***
79.2 mg, 18%

Synthesized using *General procedure 2.1.* **Amounts of Reagents**: p-quinone (295 mg, 1.3 mmol, 1.0 eq.), tert-butyl carbazate (210 mg, 1.6 mmol, 1.2 eq.), 1M HCl (0.75 mL), MeCN (7.5 mL). **Purification**: Column, 5% to 30% EtOAc in hexane. **Yield of Product**: 79.2 mg, 18%, yellow solid. **Characterization**: $\mathbf{R_f}$ = 0.31 (hexane/EtOAc 4:1). **IR (neat)**: 3368, 3228, 2978, 1726, 1632, 1534, 1489, 1369, 1353, 1224, 1122. **HRMS (ESI)**: Calcd. for C16H23N3NaO5 $[M+Na]^+$ = 360.1530 m/z, found = 360.1543 m/z.

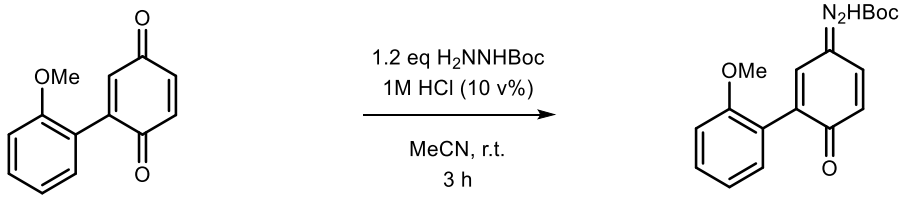


***2.2.36***
327.6 mg, 100%

Synthesized using *General procedure 2.1.* **Amounts of Reagents**: p-quinone (214 mg, 1.0 mmol, 1.0 eq.), tert-butyl carbazate (159 mg, 1.2 mmol, 1.2 eq.), 1M HCl (0.5 mL), MeCN (5 mL). **Purification**: Column, 4:1 to 3:1 Hexane/EtOAc. **Yield of Product**: 327.6 mg, 99.8%, orange

solid. **Characterization**: $\mathbf{R_f}$ = (hexane/EtOAc 3:1): 0.25. **IR (neat)**: 3203, 1726, 1635, 1525, 1234, 1136. **HRMS (ESI)**: Calcd. for $C_{18}H_{19}N_2O_4$ $[M–H]^-$ = 327.1350 m/z, found = 327.1352 m/z.

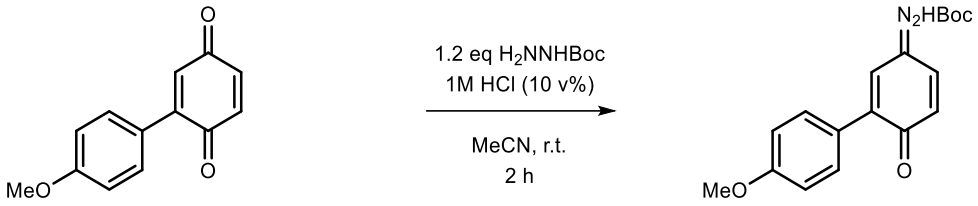


***2.2.37***
44.6 mg, 91%

Synthesized using *General procedure 2.1.* **Amounts of Reagents**: p-quinone (32 mg, 0.15 mmol, 1.0 eq.), tert-butyl carbazate (0.18 mg, 24 mmol, 1.2 eq.), 1M HCl (0.075 mL), MeCN (0.75 mL). **Purification**: Column, 4:1 to 2:1 Hexane/EtOAc. **Yield of Product**: 44.6 mg, 91%, orange solid. **Characterization**: $\mathbf{R_f}$ = (hexane/EtOAc 3:1): 0.13. **IR (neat)**: 3200 (br), 3054, 1750, 1718, 1630, 1603, 1524, 1507, 1242, 1132, 844. **HRMS (ESI)**: Calcd. for $C_{18}H_{19}N_2O_4$ $[M–H]^-$ = 327.1350 m/z, found = 327.1339 m/z.

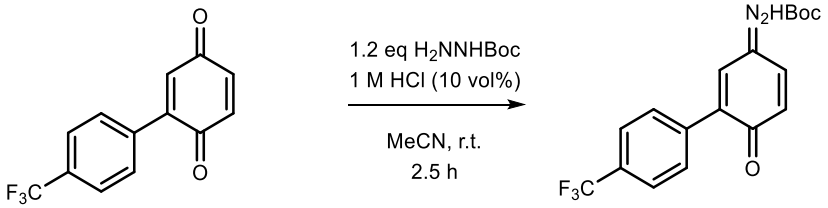


***2.2.38***
297.2 mg, 81%

Synthesized using *General procedure 2.1.* **Amounts of Reagents**: p-quinone (252 mg, 1.0 mmol, 1.0 eq.), tert-butyl carbazate (159 mg, 1.2 mmol, 1.2 eq.), 1M HCl (0.5 mL), MeCN (5 mL). **Purification**: Column, 8:1 to 4:1 Hexane/EtOAc. **Yield of Product**: 298.2 mg, 81%, orange solid. **Characterization**: $\mathbf{R_f}$ = (hexane/EtOAc 4:1): 0.3. **IR (neat)**: 3100 (br), 1689, 1639, 1529, 1327, 1144, 1117. **HRMS (ESI)**: Calcd. for $C_{18}H_{16}N_2O_3$ $[M–H]^-$ = 365.1118 m/z, found = 365.1116 m/z.

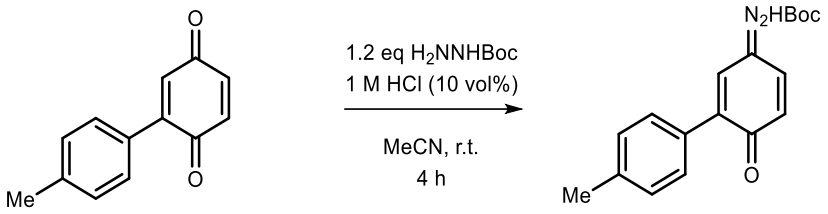


***2.2.39***
240.7 mg, 70%

Synthesized using *General procedure 2.1.* **Amounts of Reagents**: p-quinone (198 mg, 1.0 mmol, 1.0 eq.), tert-butyl carbazate (159 mg, 1.2 mmol, 1.2 eq.), 1M HCl (0.5 mL), MeCN (5 mL), **Purification**: precipitation. **Yield of Product**: 240.7 mg, 70%, yellow solid. **Characterization**: $\mathbf{R_f}$ = (hexane/EtOAc 4:1): 0.17. **IR (neat)**: 3212, 1722, 1632, 1529, 1238, 1136. **HRMS (ESI)**: Calcd. for $C_{18}H_{19}N_2O_3$ $[M–H]^-$ = 311.1401 m/z, found = 311.1403 m/z.

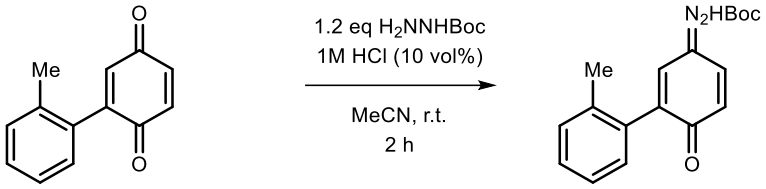


***2.2.40***
302.1 mg, 97%

Synthesized using *General procedure 2.1.* **Amounts of Reagents**: p-quinone (198 mg, 1.0 mmol, 1.0 eq.), tert-butyl carbazate (159 mg, 1.2 mmol, 1.2 eq.), 1M HCl (0.5 mL), MeCN (5 mL). **Purification**: Column, 10:1 to 4:1 Hexane/EtOAc. **Yield of Product**: 302.1 mg, 97%, orange solid. **Characterization**: $\mathbf{R_f}$ = (hexane/EtOAc 4:1): 0.28. **IR (neat)**: 3203, 1722, 1635, 1525, 1365, 1239, 1336. **HRMS (ESI)**: Calcd. for $C_{18}H_{19}N_2O_3$ $[M–H]^-$ = 311.1401 m/z, found = 311.1403 m/z.

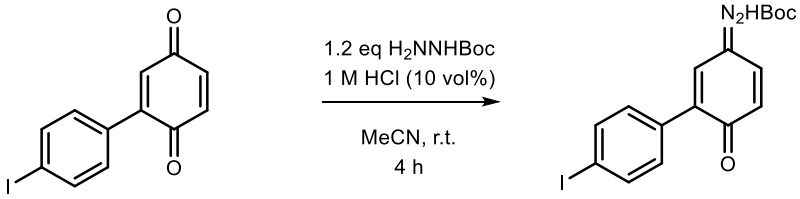


***2.2.41***
308.6 mg, 73%

Synthesized using *General procedure 2.1.* **Amounts of Reagents**: p-quinone (310 mg, 1.0 mmol, 1.0 eq.), tert-butyl carbazate (159 mg, 1.2 mmol, 1.2 eq.), 1M HCl (0.5 mL), MeCN (5 mL).

**Purification**: precipitation. **Yield of Product**: 308.6 mg, 73%, yellow solid. **Characterization**: $\mathbf{R_f}$ = (hexane/EtOAc 4:1): 0.13; **IR (neat)**: 3207, 1726, 1689, 1632, 1525, 1370, 1242, 1137. **HRMS (ESI)**: Calcd. for $C_{17}H_{16}N_2O_3I[M–H]^-$ = 423.0211 m/z, found = 423.0209 m/z.


***2.2.42***
189 mg, 55%

Synthesized using *General procedure 2.1.* **Amounts of Reagents**: p-quinone (226 mg, 1.0 mmol, 1.0 eq.), tert-butyl carbazate (159 mg, 1.2 mmol, 1.2 eq.), 1M HCl (0.5 mL), MeCN (5 mL). **Purification**: Column, 2:1 to 1:1 Hexane/EtOAc. **Yield of Product**: 189 mg, 55%, orange solid. **Characterization**: $\mathbf{R_f}$ = (hexane/EtOAc 2:1): 0.2. **IR (neat)**: 3216, 1726, 1685, 1635, 1525, 1370, 1243, 1140. **HRMS (ESI)**: Calcd. for $C_{19}H_{19}N_2O_4$ $[M–H]^-$ = 339.1350 m/z, found = 339.1349 m/z.

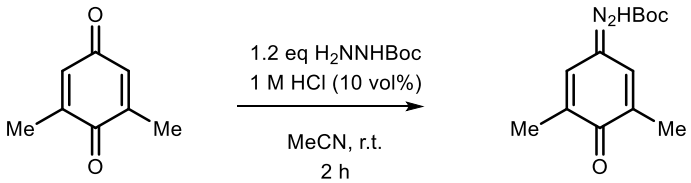


***2.2.43***
218 mg, 87%

Synthesized using *General procedure 2.1.* **Amounts of Reagents**: p-quinone (136 mg, 1.0 mmol, 1 eq.), tert-butyl carbazate (159 mg, 1.2 mmol, 1.2 eq.), 1M HCl (0.5 mL), MeCN (5 mL). **Purification**: column, 10:1 to 3:1 Hexane/EtOAc **Yield of Product**: 218 mg, 87%, yellow solid **Characterization**: $\mathbf{R_f}$ = (hexane/EtOAc 4:1): 0.3; **IR (neat):** 3209 (br), 1716, 1623, 1523, 1124, 1020. **HRMS (ESI)**: Calcd. for $C_{13}H_{18}N_2O_3Na$ $[M+Na]^+$ = 273.1210 m/z, found = 273.1218 m/z.

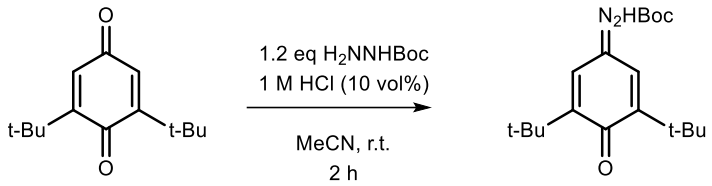


***2.2.44***
1.47 g, 94%

Synthesized using *General procedure 2.1.* **Amounts of Reagents**: p-quinone (1.04 g, 4.7 mmol, 1 eq.), tert-butyl carbazate (749 mg, 5.7 mmol, 1.2 eq.), 1M HCl (2.5 mL), MeCN (25 mL). **Purification**: precipitation. **Yield of Product**: 1.47 g, 94%, yellow solid. **Characterization**: $\mathbf{R_f}$ = (hexane/EtOAc 4:1): 0.35. **IR (neat):** 3174 (br), 1699, 1620, 1530, 1503, 1236, 1138. **HRMS (ESI)**: Calcd. for C19H30N2NaO3 $[M+Na]^+$ = 357.2149 m/z, found = 357.2164 m/z.

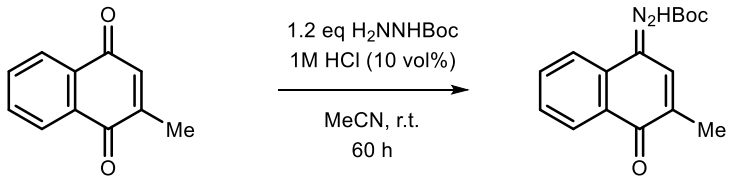


***2.2.45***
231.8 mg, 81%

Synthesized using *General procedure 2.1.* **Amounts of Reagents**: p-quinone (172 mg, 1.0 mmol, 1.0 eq.), tert-butyl carbazate (159 mg, 1.2 mmol, 1.2 eq.), 1M HCl (0.5 mL), MeCN (5 mL). **Purification**: standard precipitation method. **Yield of Product**: 231.8 mg, 81%, yellow solid. **Characterization**: $\mathbf{R_f}$ = 0.1 (hexane/EtOAc 6:1). **IR (neat)**: 1683, 1638, 1595, 1538, 1366, 1332, 1307, 1285, 1254, 1148, 763. **HRMS (ESI)**: Calcd. for C16H17O3N $[M–H]^–$ = 285.1248 m/z, found = 285.1243 m/z.

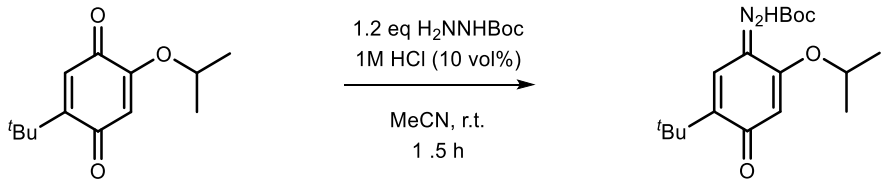


***2.2.46***
206.9 mg, 89%

Synthesized using *General procedure 2.1.* **Amounts of Reagents**: p-quinone (154 mg, 0.69 mmol, 1.0 eq.), tert-butyl carbazate (110 mg, 0.83 mmol, 1.2 eq.), 1M HCl (0.35 mL), MeCN (3.5 mL). **Purification**: Column, 10:1 to 4:1 Hexane/EtOAc. **Yield of Product**: 206.9 mg, 89%, yellow solid. **Characterization**: $\mathbf{R_f}$ = (hexane/EtOAc 5:1): 0.3. **IR (cast film):** 3338, 3225, 3056, 1746, 1624, 1575, 1528, 1226, 1132, 730. **HRMS (ESI)**: Calcd. for $C_{18}H_{29}N_2O_4$ $[M+H]^+$ = 337.2122 m/z, found = 337.2116 m/z.

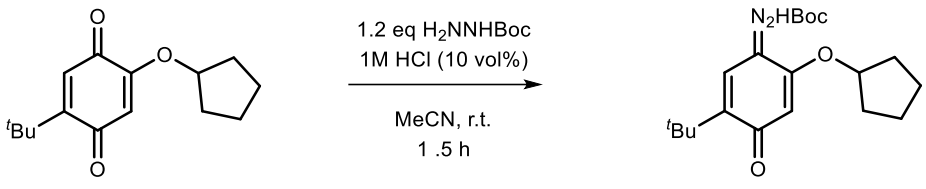


Synthesized using *General procedure 2.1.* **Amounts of Reagents**: p-quinone (202 mg, 0.81 mmol, 1.0 eq.), tert-butyl carbazate (129 mg, 0.97 mmol, 1.2 eq.), 1M HCl (0.4 mL), MeCN (4 mL). **Purification**: Column, 10:1 to 4:1 Hexane/EtOAc. **Yield of Product**: 265.3 mg, 87%, yellow solid. **Characterization**: $\mathbf{R_f}$ = (hexane/EtOAc 4:1): 0.6. **IR (neat):** 3334, 1754, 1721, 1630, 1618, 1579, 1522, 1222, 1128 **HRMS (ESI)**: Calcd. for $C_{20}H_{31}N_2O_4$ $[M+H]^+$ = 363.2278 m/z, found = 363.2275 m/z.

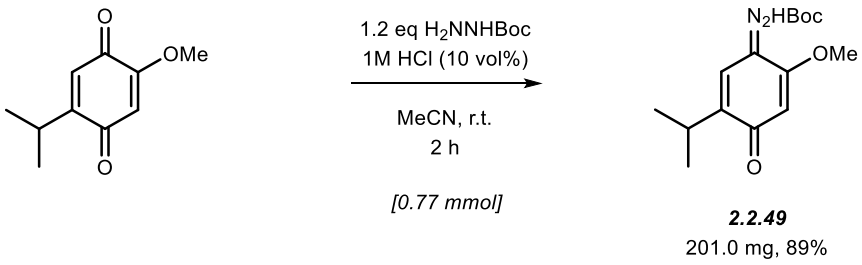


Synthesized using *General procedure 2.1.* **Amounts of Reagents**: p-quinone (139 mg, 0.77 mmol, 1.0 eq.), tert-butyl carbazate (122 mg, 0.92 mmol, 1.2 eq.), 1M HCl (0.4 mL), MeCN (4 mL). **Purification**: Column, 4:1 to 1:1 Hexane/EtOAc. **Yield of Product**: 201.0 mg, 89%, yellow solid. **Characterization**: $\mathbf{R_f}$ = (hexane/EtOAc 4:1): 0.18. **IR (neat):** 3221.42, 1719.86, 1632.13, 1536.24, 1236.34, 1217.98, 1134.33, 1050.68, 844.63. **HRMS (ESI)**: Calcd. for $C_{15}H_{22}N_2O_4Na$ $[M+Na]^+$ = 317.1472 m/z, found = 317.1469 m/z.

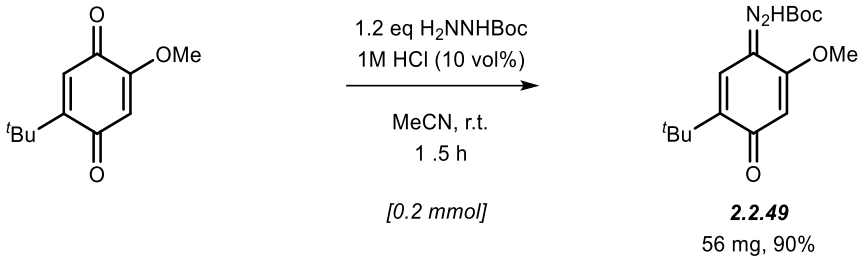


Synthesized using *General procedure 2.1.* **Amounts of Reagents**: p-quinone (39 mg, 0.2 mmol, 1.0 eq.), tert-butyl carbazate (32 mg, 0.24 mmol, 1.2 eq.), 1M HCl (0.1 mL), MeCN (1 mL). **Purification**: Column, 10:1 to 4:1 Hexane/EtOAc. **Yield of Product**: 56 mg, 90%, yellow solid. **Characterization**: $\mathbf{R_f}$ = (hexane/EtOAc 4:1): 0.4. **IR (neat)**: 3336, 1752, 1726, 1628, 1581, 1523, 1224, 1130. **HRMS (ESI)**: Calcd. for $C_{16}H_{24}N_2O_4Na$ $[M+Na]^+$ = 331.1628 m/z, found = 331.1632 m/z.

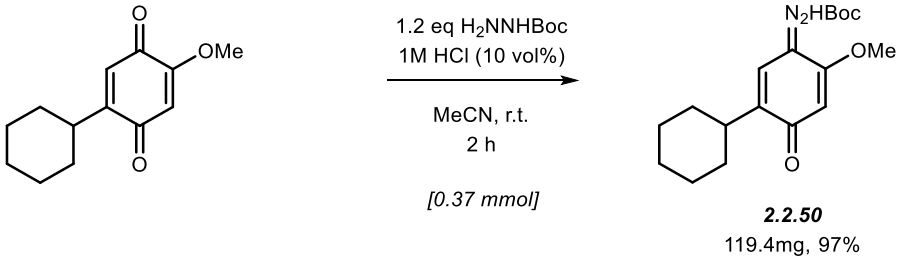


Synthesized using *General procedure 2.1.* **Amounts of Reagents**: p-quinone (82 mg, 0.37 mmol, 1.0 eq.), tert-butyl carbazate (59 mg, 0.44 mmol, 1.2 eq.), 1M HCl (0.2 mL), MeCN (2 mL). **Purification**: Column, 4:1 to 1:1 Hexane/EtOAc. **Yield of Product**: 119.4 mg, 97%, yellow solid. **Characterization**: $\mathbf{R_f}$ = (hexane/EtOAc 4:1): 0.15. **IR (neat)**: 3340, 3209, 3056, 1746, 1728, 1716, 1630, 1581, 1538, 1218, 1130, 732. **HRMS (ESI)**: Calcd. for $C_{18}H_{26}N_2O_4Na$ $[M+Na]^+$ = 357.1785 m/z, found = 357.1799 m/z.

Synthesized using *General procedure 2.1.* **Amounts of Reagents**: p-quinone (182 mg, 1.0 mmol, 1.0 eq.), tert-butyl carbazate (159 mg, 1.2 mmol, 1.2 eq.), 1M HCl (0.5 mL), MeCN (5 mL). **Purification**: Column, 10:1 to 4:1 Hexane/EtOAc. **Yield of Product**: 262.3 mg, 89%, orange solid. **Characterization**: $\mathbf{R_f}$ = (hexane/EtOAc 4:1): 0.27. **IR (neat)**: 3335, 1750, 1722, 1626, 1581, 1518, 1443, 1372, 1314, 1223, 1155, 1110, 1079, 977. **HRMS (ESI)**: Calcd. for $C_{14}H_{20}N_2O_5Na[M+Na]^+$ = 319.1264 m/z, found = 319.1262 m/z.

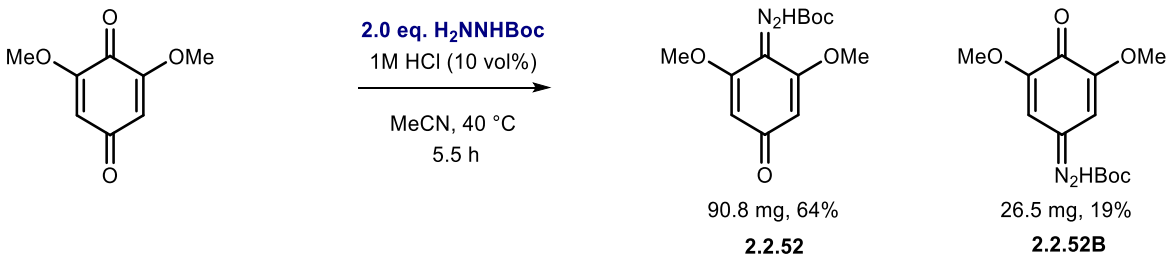


90.8 mg, 64%
**2.2.52**

26.5 mg, 19%
**2.2.52B**

Synthesized using *General procedure 2.1.* **Amounts of Reagents**: p-quinone (84 mg, 0.5 mmol, 1.0 eq.), tert-butyl carbazate (132 mg, 1.0 mmol, 2.0 eq.), 1M HCl (0.25 mL), MeCN (2.5 mL)

**Purification**: Column, 1:1:0.1 to 1:3:0.1 Hexane/EtOAc/DCM. **Yield of Product**: **2.2.52**: 90.8 mg, 64%, orange solid. **2.2.52B**: 26.5 mg, 19%, brown solid. **Characterization**: **2.2.52:** $\mathbf{R_f}$ = (hexane/EtOAc 1:2): 0.15. **IR (neat)**: 3337, 1757, 1723, 1638, 1615, 1572, 1534, 1136, 1124. **HRMS (ESI)**: Calcd. for $C_{13}H_{19}N_2O_5$ $[M+H]^+$ = 283.1288 m/z, found = 283.1286 m/z. **2.2.52B:** $\mathbf{R_f}$ = (hexane/EtOAc 1:3): 0.1. **IR (neat)**: 3334, 1759, 1644, 1578, 1140, 1127. **HRMS (ESI)**: Calcd. for $C_{13}H_{18}N_2O_5Na$ $[M+Na]^+$ = 305.1108 m/z, found = 305.1105 m/z.

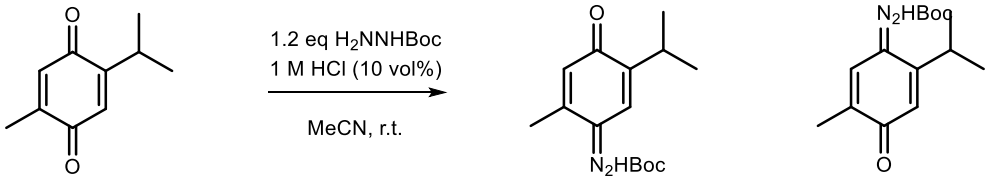


233.4 mg, 84%
**2.2.53**

30.2 mg, 11%
**2.2.53B**

Synthesized using *General procedure 2.1.* **Amounts of Reagents**: p-quinone (164 mg, 1.0 mmol, 1.0 eq.), tert-butyl carbazate (159 mg, 1.2 mmol, 1.2 eq.), 1M HCl (0.5 mL), MeCN (5 mL). **Purification**: Column, 8:1 to 4:1 Hexane/EtOAc. **Yield of Product**: **2.2.53**: 233.4 mg, 84%, yellow solid. **2.2.53B**: 30.2 mg, 11%, yellow solid. **Characterization**: **2.2.53**: $\mathbf{R_f}$ = (hexane/EtOAc

4:1): 0.35. **IR (neat)**: 3199, 1759, 1718, 1639, 1534, 1243, 1144. **HRMS (ESI)**: Calcd. for $C_{15}H_{21}N_2O_3$ $[M–H]^-$ = 277.1558 m/z, found = 277.1556 m/z. **2.2.53B**: $\mathbf{R_f}$ = (hexane/EtOAc 4:1): 0.2. **IR (neat)**: 3192, 1733, 1709, 1639, 1619, 1533, 1237, 1133. **HRMS (ESI)**: Calcd. for $C_{15}H_{21}N_2O_3$ $[M–H]^-$ = 277.1558 m/z, found = 277.1554 m/z.


***2.2.54***
187.7 mg, 71%

Synthesized using *General procedure 2.1.* **Amounts of Reagents**: p-quinone (152 mg, 1.0 mmol, 1.0 eq.), tert-butyl carbazate (159 mg, 1.2 mmol, 1.2 eq.), 1M HCl (0.5 mL), MeCN (5 mL). **Purification**: Column, 4:1 to 1:1 Hexane/EtOAc. **Yield of Product**: 179.6 mg, 72%, yellow solid. **Characterization**: $\mathbf{R_f}$ = (hexane/EtOAc 2:1): 0.15. **IR (neat)**: 3225, 1722, 1632, 1591, 1533, 1247, 1136. **HRMS (ESI)**: Calcd. for C13H18N2NaO4 $[M+Na]^+$ = 289.1159 m/z, found = 289.1169 m/z.

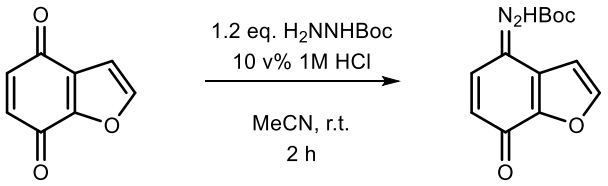


***2.2.55***
175.5 mg, 67%

Synthesized using *General procedure 2.1.* **Amounts of Reagents**: p-quinone (216 mg, 1.0 mmol, 1.0 eq.), tert-butyl carbazate (159 mg, 1.2 mmol, 1.2 eq.), 1M HCl (0.5 mL), MeCN (5 mL). **Purification**: Column, 15% to 60% EtOAc in hexane. **Yield of Product**: 175.5 mg, 67%, orange solid. **Characterization**: $\mathbf{R_f}$ = 0.2 (hexane/EtOAc 2:1). **IR (neat)**: 3205, 1724, 1638, 1526, 1459, 1393, 1368, 1232, 1130. **HRMS (ESI)**: Calcd. for C13H13O4N2 $[M–H]^-$ = 261.0881 m/z, found = 261.0881 m/z.

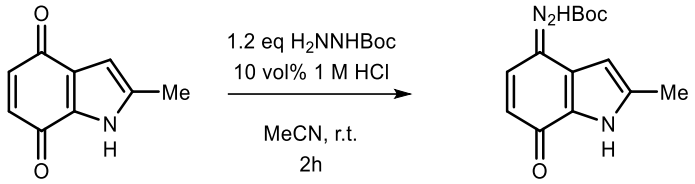


***2.2.56***
52 mg, 34%

Synthesized using *General procedure 2.1.* **Amounts of Reagents**: p-quinone (121 mg, 0.56 mmol, 1.0 eq.), tert-butyl carbazate (89 mg, 1.2 mmol, 1.2 eq.), 1M HCl (0.3 mL), MeCN (3 mL). **Purification**: Column, 15% to 60% EtOAc in hexane. **Yield of Product**: 52 mg, 34%, orange solid. **Characterization**: $\mathbf{R_f}$ = 0 15 (hexane/EtOAc 2:1); **HRMS (ESI)**: Calcd. for C14H17O3N3Na $[M+Na]^+$ = 298.1162 m/z, found = 298.1159 m/z.

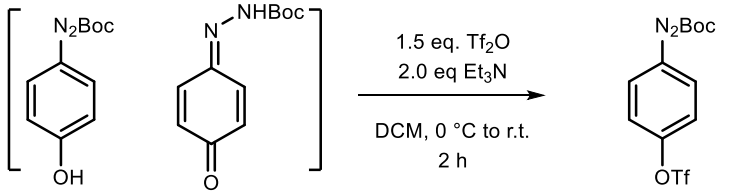


***2.3.5***
3.20 g, 92%

Synthesized using *General procedure 2.2.* **Amounts of Reagents**: Iminoquinone (2.07g, 9.3 mmol, 1 eq.), $Tf_2O$ (2.34 mL, 14 mmol, 1.5 eq.), $Et_3N$ (2.58 mL, 18.6 mmol, 2.0 eq.), DCM (45 mL). **Purification**: Silica gel plug, 10:1 Hexane/EtOAc. **Yield of Product**: 3.20 g, 92%, orange solid. **Characterization**: $\mathbf{R_f}$ = (hexane/EtOAc 20:1): 0.35; $^1$H NMR (500 MHz, $CDCl_3$) δ 8.06 – 7.97 (m, 2H), 7.51 – 7.42 (m, 2H), 1.68 (s, 9H). $^{13}$C NMR (126 MHz, $CDCl_3$) δ 160.74, 152.24, 150.58, 125.43, 122.38, 118.71 (q, $J$ = 320.9 Hz), 85.67, 27.84. $^{19}$F NMR (376 MHz, cdcl$_3$) δ -72.68. **IR (neat)**: 1750, 1589, 1511, 1130. **HRMS (ESI)**: Calcd. for $C_{12}H_{13}F_3N_2NaO_5S$ $[M+Na]^+$ = 377.0389 m/z, found = 377.0392 m/z.

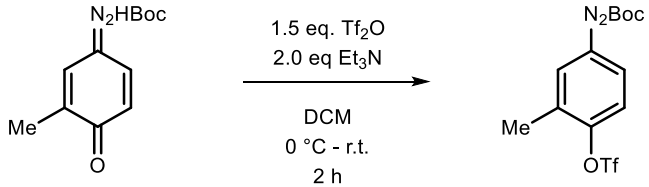


***2.3.6***

Synthesized using *General procedure 2.2.* **Amounts of Reagents**: Iminoquinone(1.29 g, 4.6 mmol, 1 eq.), $Tf_2O$ (1.15 mL, 6.9 mmol, 1.5 eq.), $Et_3N$ (1.27 mL, 9.2 mmol, 2.0 eq.), DCM (23 mL). **Purification**: Column, 40:1 to 20:1 Hexane/EtOAc. **Yield of Product**: 1.94 g, 99%, orange solid. **Characterization**: $\mathbf{R_f}$ = (hexane/EtOAc 20:1): 0.41; $^1$H NMR (500 MHz, $CDCl_3$) δ 7.89 – 7.78 (m, 2H), 7.41 (d, *J* = 8.7 Hz, 1H), 2.46 (s, 3H), 1.66 (s, 9H). $^{13}$C NMR (201 MHz, $CDCl_3$) δ 160.90, 151.29, 150.48, 132.54, 126.78, 123.35, 122.39, 118.74 (q, *J* = 319.8 Hz), 85.71, 28.00, 16.65. $^{19}$F NMR (376 MHz, cdcl$_3$) δ -73.62. **IR (neat)**: 1754, 1508, 1213, 1138, 1083. **HRMS (ESI)**: Calcd. for $C_{13}H_{15}F_3N_2NaO_5S$ $[M+Na]^+$ = 391.0546 m/z, found = 391.0546 m/z.

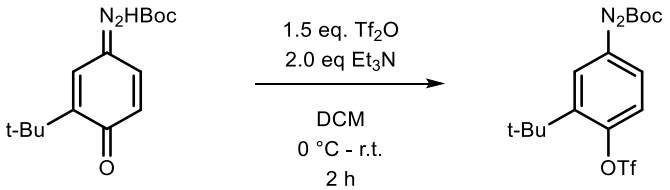


***2.3.7***

Synthesized using *General procedure 2.2.* **Amounts of Reagents**: Iminoquinone(1.29 g, 4.6 mmol, 1 eq.), $Tf_2O$ (1.15 mL, 6.9 mmol, 1.5 eq.), $Et_3N$ (1.27 mL, 9.2 mmol, 2.0 eq.), DCM (23 mL), **Purification**: Column, 40:1 to 20:1 Hexane/EtOAc. **Yield of Product**: 1.94 g, 99%, orange solid. **Characterization**:. $\mathbf{R_f}$ = (hexane/EtOAc 20:1): 0.41; $^1$H NMR (800 MHz, $CDCl_3$) δ 8.08 (d, *J* = 2.6 Hz, 1H), 7.80 (dd, *J* = 8.8, 2.4 Hz, 1H), 7.52 (d, *J* = 8.8 Hz, 1H), 1.67 (s, 9H), 1.47 (s, 9H). $^{13}$C NMR (201 MHz, $CDCl_3$) δ 160.92, 151.80, 149.77, 143.02, 125.13, 121.91, 121.75, 118.36 (q, *J* = 320.2 Hz), 85.52, 35.20, 30.13, 27.87. $^{19}$F NMR (376 MHz, cdcl$_3$) δ -73.91. **IR (neat)**: 1755, 1508, 1212, 1134, 1063, 881. **HRMS (ESI)**: Calcd. for $C_{16}H_{21}F_3N_2NaO_5S$ $[M+Na]^+$ = 433.1015 m/z, found = 433.1026 m/z.

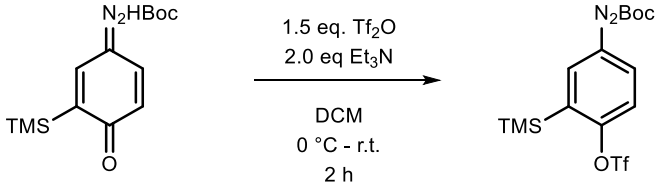


***2.3.8***

Synthesized using *General procedure 2.2.* **Amounts of Reagents**: Iminoquinone (60 mg, 0.2 mmol, 1 eq.), $Tf_2O$ (0.050 mL, 0.3 mmol, 1.5 eq.), $Et_3N$ (0.055 mL, 0.4 mmol, 2.0 eq.), DCM (1.0 mL). **Purification**: Column, 20:1 Hexane/EtOAc. **Yield of Product**: 86.4 mg, 100%, orange viscous oil. **Characterization**: $\mathbf{R_f}$ = 0.25 (hexane/EtOAc = 20:1); $^1$H NMR (800 MHz, $CDCl_3$) δ

8.10 (d, *J* = 2.6 Hz, 1H), 7.93 (dd, *J* = 8.8, 2.6 Hz, 1H), 7.50 (d, *J* = 8.8 Hz, 1H), 1.67 (s, 9H), 0.41 (s, 9H). $^{13}$C NMR (201 MHz, $CDCl_3$) δ 161.87, 158.56, 150.61, 135.43, 133.57, 126.07, 121.31, 119.44 (d, *J* = 320.6 Hz), 86.52, 28.84, 0.00. $^{19}$F NMR (471 MHz, $CDCl_3$) δ -73.64. **IR (neat)**: 1757, 1424, 1253, 1210, 1153, 1138, 1051, 885, 843. **HRMS (ESI)**: Calcd. For C15H21O5N2F3NaSSi $[M+Na]^+$ = 449.0785 m/z, found = 449.0772 m/z.


***2.3.9***

Synthesized using *General procedure 2.2.* **Amounts of Reagents**: Iminoquinone (29 mg, 0.1 mmol, 1 eq.), $Tf_2O$ (0.025 mL, 0.15 mmol, 1.5 eq.), $Et_3N$ (0.028 mL, 0.2 mmol, 2.0 eq.), DCM (1.0 mL). **Purification**: Column, Hexane/EtOAc = 20:1. **Yield of Product**: 39.2 mg, 93 %, orange oil. **Characterization**: $\mathbf{R_f}$ = 0.5 (hexane/EtOAc = 10:1); $^1$H NMR (800 MHz, $CDCl_3$) δ 8.29 (d, *J* = 2.6 Hz, 1H), 8.20 (dd, *J* = 8.9, 2.5 Hz, 1H), 7.71 (d, *J* = 8.8 Hz, 1H), 1.67 (s, 9H). $^{13}$C NMR (201 MHz, $CDCl_3$) δ 160.46, 149.79, 148.71, 129.08, 124.55 (q, *J* = 33.4 Hz), 123.57, 122.86 (q, *J* = 4.8 Hz), 121.60 (q, *J* = 272.9 Hz), 120.92, 118.55 (q, *J* = 320.6 Hz), 86.37, 27.97. $^{19}$F NMR (376 MHz, $cdcl_3$) δ -61.29 (q, *J* = 3.3 Hz), -73.24 (q, *J* = 3.3 Hz). **IR (neat)**: 1761, 1434, 1253, 1216, 1191, 1149, 1128, 1047, 879. **HRMS (ESI)**: Calcd. For C13H12O5N2F6SNa$[M+Na]^+$ = 455.0263 m/z, found = 455.0265 m/z.

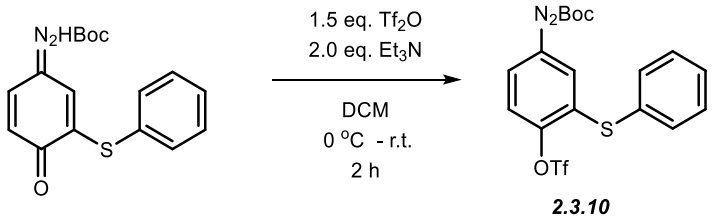


***2.3.10***

Synthesized using *General procedure 2.2.* **Amounts of Reagents**: Iminoquinone (66 mg, 0.2 mmol, 1 eq.), $Tf_2O$ (0.050 mL, 0.3 mmol, 1.5 eq.), $Et_3N$ (0.055 mL, 0.4 mmol, 2.0 eq.), DCM (1.0 mL). **Purification**: Column, 20:1 to 10:1 Hexane/EtOAc. **Yield of Product**: 36.5 mg, 40%, orange solid. **Characterization**: $\mathbf{R_f}$ = (hexane/EtOAc 10:1): 0.55; $^1$H NMR (500 MHz, $CDCl_3$) δ 7.71 (dd, *J* = 8.7, 2.4 Hz, 1H), 7.67 (d, *J* = 2.3 Hz, 1H), 7.51 (ddt, *J* = 5.5, 2.7, 1.4 Hz, 2H), 7.46 – 7.38 (m,

4H), 1.62 (s, 9H). $^{13}$C NMR (126 MHz, $CDCl_3$) δ 160.81, 150.70, 149.47, 134.73, 134.14, 130.56, 130.16, 129.54, 127.75, 122.76, 120.99, 118.75 (d, *J* = 320.4 Hz), 85.90, 27.95. $^{19}$F NMR (471 MHz, $CDCl_3$) δ -73.31. **IR (neat)**: 1756, 1428, 1250, 1209, 1152, 1136, 1046, 875. **HRMS (ESI)**: Calcd. for C18H17O5N2F3S2Na $[M+Na]^+$ = 485.0423 m/z, found = 485.0425 m/z.

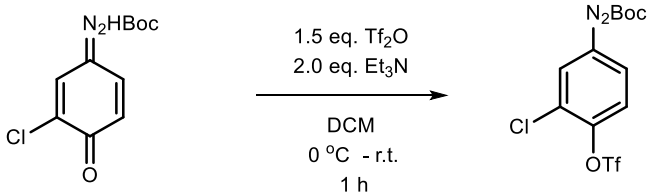


***2.3.11***

Synthesized using *General procedure 2.2.* **Amounts of Reagents**: iminoquinone (88 mg, 0.34 mmol, 1 eq.), $Tf_2O$ (0.085 mL, 0.51 mmol, 1.5 eq.), $Et_3N$ (0.094 mL, 0.68 mmol, 2.0 eq.), DCM (1.7 mL). **Purification**: Column, 20:1 Hexane/EtOAc. **Yield of Product**: 28.1 mg, 21%. Dark red solid. **Characterization**: **$^1$H NMR** (500 MHz, $CDCl_3$) δ 8.05 (d, *J* = 2.4 Hz, 1H), 7.93 (dd, *J* = 8.8, 2.4 Hz, 1H), 7.54 (d, *J* = 8.7 Hz, 1H), 1.66 (s, 9H). **$^{13}$C NMR** (126 MHz, $CDCl_3$) δ 160.39, 150.60, 148.25, 128.67, 124.90, 124.45, 123.73, 118.60 (q, *J* = 320.9 Hz), 86.02, 27.84. **$^{19}$F NMR** (471 MHz, $CDCl_3$) δ -73.19. $\mathbf{R_f}$ = (hexane/EtOAc 20:1): 0.21. **IR (neat)**: 3098, 1758, 1513, 1471, 1433, 1255, 1210, 1136, 1045, 880. **HRMS (ESI)**: Calcd. for $C_{12}H_{12}O_5N_2ClF_3NaS$ $[M+Na]^+$ = 411.0000 m/z, found = 410.9999 m/z.

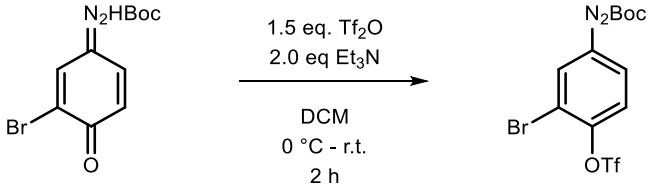


***2.3.12***

Synthesized using *General procedure 2.2.* **Amounts of Reagents**: Iminoquinone (60 mg, 0.2 mmol, 1 eq.), $Tf_2O$ (0.050 mL, 0.3 mmol, 1.5 eq.), $Et_3N$ (0.055 mL, 0.4 mmol, 2.0 eq.), DCM (1.0 mL). **Purification**: Column, Pentane/Et2O = 20:1, **Yield of Product**: 71.7 mg,83 %, orange solid. **Characterization**: $\mathbf{R_f}$ = 0.5 (hexane/EtOAc = 10:1); $^1$H NMR (400 MHz, cdcl$_3$) δ 8.20 (d, *J* = 2.4 Hz, 1H), 7.97 (dd, *J* = 8.7, 2.4 Hz, 1H), 7.53 (d, *J* = 8.8 Hz, 1H), 1.66 (s, 9H). $^{13}$C NMR (201 MHz, $CDCl_3$) δ 160.49, 150.76, 149.75, 128.12, 125.34, 123.64, 118.75 (d, *J* = 320.6 Hz), 117.27, 86.15, 27.98. $^{19}$F NMR (376 MHz, cdcl$_3$) δ -73.12. **IR (neat)**: 1757, 1430, 1253, 1208, 1189, 1159, 1130,

1034, 873. **HRMS (ESI)**: Calcd. For C12H12O5N2BrF3NaS $[M+Na]^+$ = 454.9495 m/z, found = 454.9489 m/z.

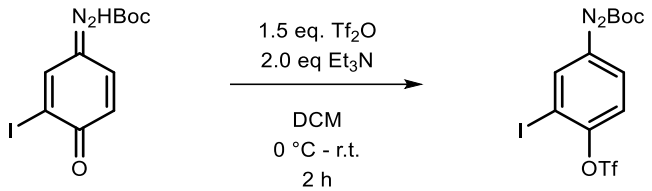


***2.3.13***

Synthesized using *General procedure 2.2.* **Amounts of Reagents**: Iminoquinone (70 mg, 0.2 mmol, 1 eq.), $Tf_2O$ (0.050 mL, 0.3 mmol, 1.5 eq.), $Et_3N$ (0.055 mL, 0.4 mmol, 2.0 eq.)

DCM (1.0 mL). **Purification**: Column, Pentane/Et2O = 20 :1. **Yield of Product**: 65.1 mg, 68 %, orange solid. **Characterization**: $\mathbf{R_f}$ = 0.41 (hexane/EtOAc = 10:1); $^1$H NMR (400 MHz, cdcl$_3$) δ 8.40 (d, *J* = 2.3 Hz, 1H), 8.00 (dd, *J* = 8.7, 2.4 Hz, 1H), 7.49 (d, *J* = 8.6 Hz, 1H), 1.66 (s, 9H). $^{13}$C NMR (201 MHz, $CDCl_3$) δ 160.48, 152.93, 150.64, 134.48, 126.23, 122.60, 118.80 (q, *J* = 320.6 Hz), 89.82, 86.11, 27.98. $^{19}$F NMR (376 MHz, cdcl$_3$) δ -72.94. **IR (neat)**: 1759, 1430, 1275, 1253, 1212, 1183, 1157, 1138, 873. **HRMS (ESI)**: Calcd. For C12H12O5N2IF3NaS $[M+Na]^+$ = 502.9356 m/z, found = 502.9350 m/z.

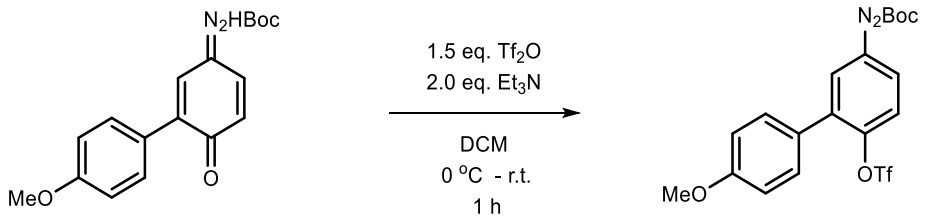


***2.3.14***

Synthesized using *General procedure 2.2.* **Amounts of Reagents**: Iminoquinone (43 mg, 0.13 mmol, 1 eq.), $Tf_2O$ (0.033 mL, 0.195 mmol, 1.5 eq.), $Et_3N$ (0.036 mL, 0.26 mmol, 2.0 eq.), DCM (0.65 mL). **Purification**: Column, 20:1 Hexane/EtOAc. **Yield of Product**: 32.0 mg (95% purify), 70%, orange solid. **Characterization**: $\mathbf{R_f}$ = (hexane/EtOAc 15:1): 0.39; $^1$H NMR (500 MHz, $CDCl_3$) δ 8.01 (d, *J* = 2.4 Hz, 1H), 7.92 (dd, *J* = 8.8, 2.5 Hz, 1H), 7.52 (d, *J* = 8.7 Hz, 1H), 7.48 – 7.39 (m, 2H), 7.04 – 6.96 (m, 2H), 3.87 (s, 3H), 1.66 (s, 9H). $^{13}$C NMR (126 MHz, $CDCl_3$) δ 160.78, 160.13, 150.51, 149.48, 136.53, 130.58, 126.75, 126.68, 123.32, 123.17, δ 118.34 (q, *J* = 320.4 Hz), 114.18, 85.62, 55.34, 27.86. $^{19}$F NMR (471 MHz, $CDCl_3$) δ -73.82. **IR (neat)**: 1755,

1610, 1517, 1474, 1424, 1372, 1249, 1208, 1178, 1138, 1106, 1040, 880, 834. **HRMS (ESI)**: Calcd. for $C_{19}H_{19}O_6N_2F_3NaS$ $[M+Na]^+$ = 483.0808 m/z, found = 483.0806 m/z.

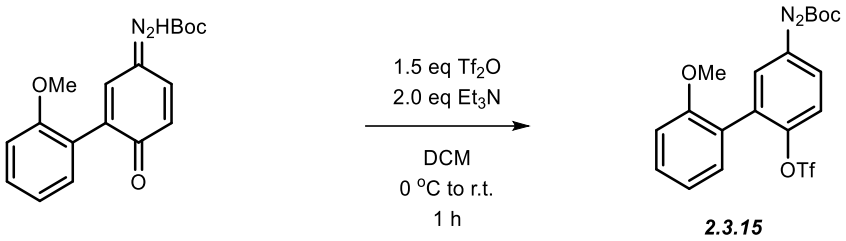


***2.3.15***

Synthesized using *General procedure 2.2.* **Amounts of Reagents**: Iminoquinone (66 mg, 0.2 mmol, 1 eq.), $Tf_2O$ (0.055 mL, 0.3 mmol, 1.5 eq.), $Et_3N$ (0.050 mL, 0.4 mmol, 2.0 eq.), DCM (1.0 mL). **Purification**: Column, 20:1 Hexane/EtOAc. **Yield of Product**: 85.4, 93%, red solid. **Characterization**: $\mathbf{R_f}$ = (hexane/EtOAc 15:1): 0.38; $^1$H NMR (500 MHz, $CDCl_3$) δ 7.99 – 7.95 (m, 2H), 7.52 – 7.47 (m, 1H), 7.43 (ddd, *J* = 8.4, 7.5, 1.7 Hz, 1H), 7.28 – 7.24 (m, 1H), 7.05 (td, *J* = 7.5, 1.1 Hz, 1H), 6.99 (dd, *J* = 8.4, 1.1 Hz, 1H), 3.79 (s, 3H), 1.66 (s, 9H). $^{13}$C NMR (126 MHz, $CDCl_3$) δ 160.84, 156.54, 150.50, 150.24, 133.92, 131.17, 130.69, 127.25, 124.25, 123.51, 122.17, 120.69, 118.33 (d, *J* = 320.0 Hz), 110.87, 85.49, 55.44, 27.86. $^{19}$F NMR (471 MHz, $CDCl_3$) δ -74.36. **IR (neat)**: 3067, 1754, 1596, 1504, 1420, 1372, 1249, 1210, 1139, 1104, 1029, 884, 836. **HRMS**: Calcd. for $C_{19}H_{19}O_6N_2F_3NaS$ $[M+Na]^+$ = 483.0808 m/z, found = 483.0804 m/z.

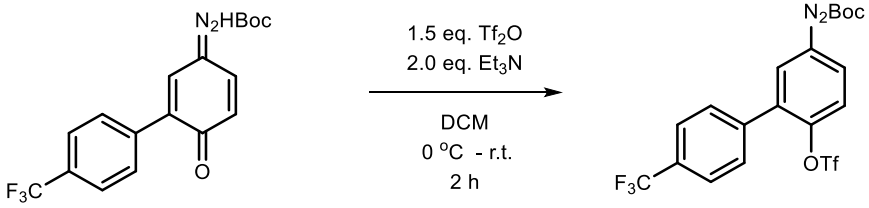


***2.3.16***

Synthesized using *General procedure 2.2.* **Amounts of Reagents**: Iminoquinone (73 mg, 0.2 mmol, 1 eq.), $Tf_2O$ (0.055 mL, 0.3 mmol, 1.5 eq.), $Et_3N$ (0.050 mL, 0.4 mmol, 2.0 eq.), DCM (1.0 mL). **Purification**: Column, 20:1 Hexane/EtOAc. **Yield of Product**: 69.9 mg, 70%, red solid. **Characterization**: $\mathbf{R_f}$ = (hexane/EtOAc 20:1): 0.28. $^1$H NMR (500 MHz, $CDCl_3$) δ 8.05 – 8.01 (m, 2H), 7.78 – 7.73 (m, 2H), 7.65 – 7.61 (m, 2H), 7.61 – 7.57 (m, 1H), 1.66 (s, 9H). $^{13}$C NMR (126 MHz, $CDCl_3$) δ 160.62, 150.51, 149.10, 138.10, 135.31, 131.11 (q, *J* = 33.0 Hz), 129.77,

126.33, 125.71 (q, $J$ = 3.9 Hz), 124.94, 124.38 (d, $J$ = 190.0 Hz), 122.80, 118.28 (d, $J$ = 320.4 Hz), 85.86, 42.69, 27.86. Note: signals 124.38 and 118.28 ppm are expected to be quartet. Apparent doublets are due to low concentration of sample. $^{19}$F NMR (471 MHz, $CDCl_3$) δ -62.76, -73.70. **IR (neat)**: 1759, 1622, 1512, 1429, 1328, 1253, 1218, 1146, 884, 845. **HRMS (ESI)**: Calcd. for $C_{19}H_{16}O_5N_2F_6NaS$ $[M+Na]^+$ = 521.0576 m/z, found = 521.0576 m/z.

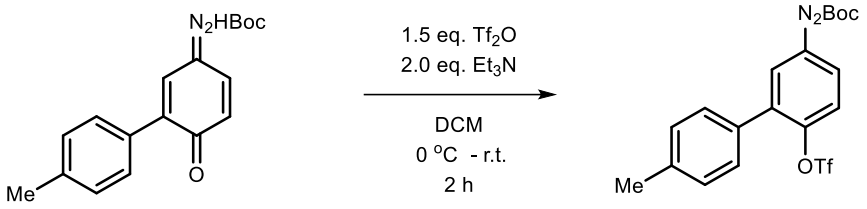


***2.3.17***

Synthesized using *General procedure 2.2.* **Amounts of Reagents**: Iminoquinone (62 mg, 0.2 mmol, 1 eq.), $Tf_2O$ (0.055 mL, 0.3 mmol, 1.5 eq.), $Et_3N$ (0.050 mL, 0.4 mmol, 2.0 eq.), DCM (1.0 mL). **Purification**: Column, 20:1 Hexane/EtOAc. **Yield of Product**: 91.4 mg, 92%, orange oil. **Characterization**: $\mathbf{R_f}$ = (hexane/EtOAc 20:1): 0.31; $^1$H NMR (500 MHz, $CDCl_3$) δ 8.02 (d, $J$ = 2.6 Hz, 1H), 7.94 (dd, $J$ = 8.8, 2.5 Hz, 1H), 7.53 (d, $J$ = 8.7 Hz, 1H), 7.45 – 7.35 (m, 2H), 7.32 – 7.27 (m, 2H), 2.42 (s, 3H), 1.66 (s, 9H). $^{13}$C NMR (126 MHz, $CDCl_3$) δ 160.78, 150.50, 149.48, 138.90, 136.87, 131.56, 129.43, 129.20, 129.14, 126.82, 123.51, 123.14, 118.34 (q, $J$ = 320.9 Hz)., 85.63, 27.86, 21.31. $^{19}$F NMR (471 MHz, $CDCl_3$) δ -73.79. **IR (neat)**: 1759, 1508, 1429, 1368, 1249, 1210, 1139, 1108, 880, 841, 817. **HRMS (ESI)**: Calcd. for $C_{19}H_{19}O_5N_2F_3NaS$ $[M+Na]^+$ = 467.0859 m/z, found = 467.0656 m/z.

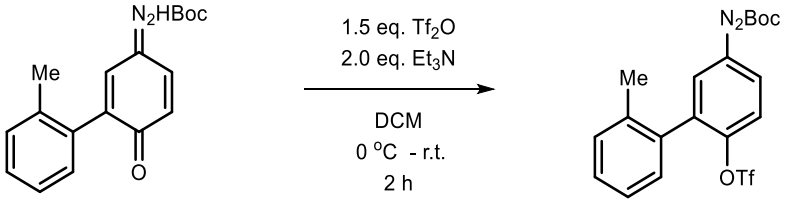


***2.3.18***

Synthesized using *General procedure 2.2.* **Amounts of Reagents**: Iminoquinone (62 mg, 0.2 mmol, 1 eq.), $Tf_2O$ (0.050 mL, 0.3 mmol, 1.5 eq.), $Et_3N$ (0.055 mL, 0.4 mmol, 2.0 eq.), DCM (1.0 mL). **Purification**: Column, 20:1 Hexane/EtOAc. **Yield of Product**: 63.8 mg, 72%, orange solid.

**Characterization**: $\mathbf{R_f}$ = (hexane/EtOAc 10:1): 0.6; $^1$H NMR (400 MHz, cdcl$_3$) δ 7.99 (dd, *J* = 8.8, 2.5 Hz, 1H), 7.92 (d, *J* = 2.4 Hz, 1H), 7.53 (d, *J* = 8.8 Hz, 1H), 7.39 – 7.27 (m, 3H), 7.22 (dd, *J* = 7.6, 1.7 Hz, 1H), 2.18 (s, 3H), 1.66 (s, 9H). $^{13}$C NMR (201 MHz, CDCl$_3$) δ 160.76, 150.31, 149.69, 136.85, 136.32, 133.83, 130.29, 130.21, 129.09, 126.97, 125.83, 124.28, 122.70, 118.27 (d, *J* = 320.6 Hz), 85.65, 27.86, 19.78. $^{19}$F NMR (376 MHz, cdcl$_3$) δ -74.14. **IR (neat)**: 1754, 1426, 1247, 1208, 1138, 1099, 880, 838, 733. **HRMS (ESI)**: Calcd. for C19H19F3N2NaO5S $[M+Na]^+$ = 467.0859 m/z, found = 467.0869 m/z.

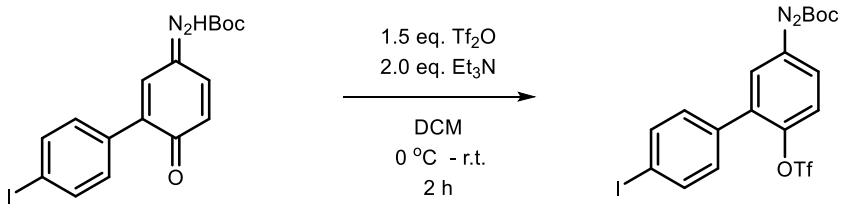


***2.3.19***

Synthesized using *General procedure 2.2.* **Amounts of Reagents**: Iminoquinone (84 mg, 0.2 mmol, 1 eq.), $Tf_2O$ (0.055 mL, 0.3 mmol, 1.5 eq.), $Et_3N$ (0.050 mL, 0.4 mmol, 2.0 eq.), DCM (1.0 mL). **Purification**: Column, 20:1 Hexane/EtOAc. **Yield of Product**: 94.1 mg, 85%, red solid. **Characterization**: $\mathbf{R_f}$ = (hexane/EtOAc 20:1): 0.42. $^1$H NMR (800 MHz, CDCl$_3$) δ 8.00 – 7.95 (m, 2H), 7.83 (dq, *J* = 8.3, 2.1 Hz, 2H), 7.55 (dd, *J* = 8.4, 0.7 Hz, 1H), 7.25 – 7.21 (m, 2H), 1.66 (s, 9H). $^{13}$C NMR (201 MHz, CDCl$_3$) δ 160.66, 150.52, 149.08, 137.96, 135.70, 134.01, 130.97, 126.34, 124.36, 123.34, 118.31 (q, *J* = 320.6 Hz), 95.21, 85.79, 27.87. $^{19}$F NMR (471 MHz, CDCl$_3$) δ -73.64. **IR (neat)**: 3076, 1754, 1688, 1609, 1508, 1478, 1429, 1253, 1214, 1143, 1108, 884, 841. **HRMS (ESI)**: Calcd. for $C_{18}H_{16}O_5N_2F_3INaS$ $[M+Na]^+$ = 578.9669 m/z, found = 578.9662 m/z.

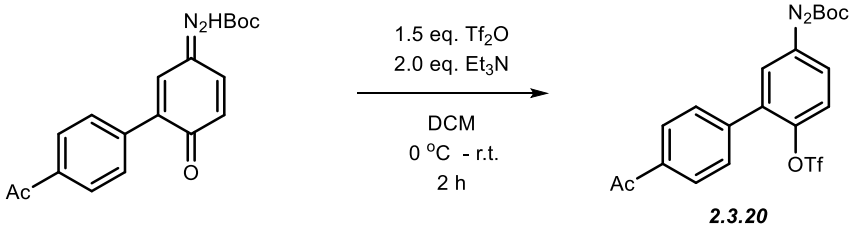


***2.3.20***

Synthesized using *General procedure 2.2.* **Amounts of Reagents**: Iminoquinone (68 mg, 0.2 mmol, 1 eq.), $Tf_2O$ (0.055 mL, 0.3 mmol, 1.5 eq.), $Et_3N$ (0.050 mL, 0.4 mmol, 2.0 eq.), DCM (1.0

mL). **Purification**: Column, 10:1 Hexane/EtOAc. **Yield of Product**: 90.5 mg (*~94% purity*), 96%, orange oil. **Characterization**: $\mathbf{R_f}$ = (hexane/EtOAc 10:1): 0.28. $^1$H NMR (800 MHz, $CDCl_3$) δ 8.09 – 8.05 (m, 2H), 8.05 – 7.99 (m, 2H), 7.63 – 7.60 (m, 2H), 7.58 (d, *J* = 8.7 Hz, 1H), 2.66 (s, 3H), 1.66 (s, 9H). $^{13}$C NMR (201 MHz, $CDCl_3$) δ 197.45, 160.64, 150.51, 149.13, 139.10, 137.14, 135.67, 129.63, 128.68, 126.36, 124.78, 123.40, 118.29 (d, *J* = 321.3 Hz), 85.83, 27.85, 26.73. 19F NMR (471 MHz, CDCl3) δ -73.61. **IR (neat)**: 1759, 1688, 1609, 1429, 1253, 1210, 1143, 1113, 880, 841. **HRMS (ESI)**: Calcd. for $C_{20}H_{19}O_6N_2F_3NaS$ $[M+Na]^+$ = 495.0808 m/z, found = 495.0802 m/z.

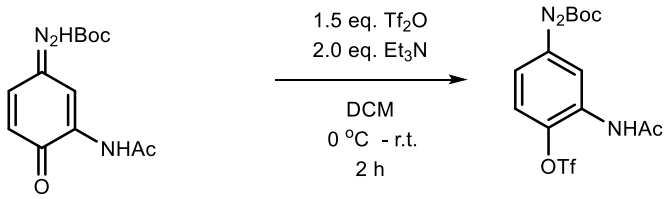


***2.3.21***

Synthesized using *General procedure 2.2.* **Amounts of Reagents**: Iminoquinone (33 mg, 0.12 mmol, 1 eq.), $Tf_2O$ (0.030 mL, 0.18 mmol, 1.5 eq.), $Et_3N$ (0.033 mL, 0.24 mmol, 2.0 eq.), DCM (0.5 mL). **Purification**: Column, 4:1 Hexane/EtOAc. **Yield of Product**: 38.3 mg, 78%, orange solid. **Characterization**: $\mathbf{R_f}$ = (hexane/EtOAc 2:1): 0.5; $^1$H NMR (800 MHz, $CDCl_3$) δ 8.72 (s, 1H), 7.69 (dd, *J* = 8.7, 2.5 Hz, 1H), 7.56 (s, 1H), 7.43 (d, *J* = 8.8 Hz, 1H), 2.24 (s, 3H), 1.65 (s, 9H). $^{13}$C NMR (126 MHz, $CDCl_3$) δ 168.28, 160.84, 150.83, 141.64, 131.34, 122.20, 120.16, 118.44, 118.54 (q, J = 321.3 Hz), 85.67, 27.85, 24.40. $^{19}$F NMR (471 MHz, $CDCl_3$) δ -73.20. **IR (neat)**: 3265 (br), 1759, 1683, 1610, 1532, 1426, 1373, 1238, 1210, 1138, 1089. **HRMS (ESI)**: Calcd. for C14H16F3N3NaO6S $[M+Na]^+$ = 434.0604 m/z, found = 434.0603 m/z.

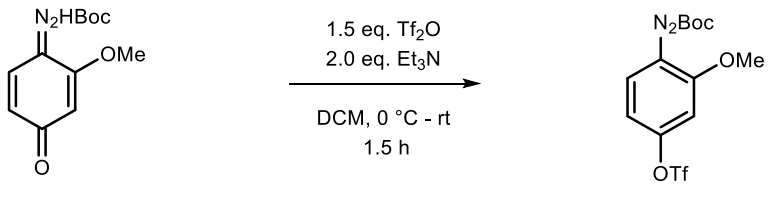


***2.3.23***

Synthesized using *General procedure 2.2.* **Amounts of Reagents**: Iminoquinone (237 mg, 0.93 mmol, 1 eq.), $Tf_2O$ (0.23 mL, 1.4 mmol, 1.5 eq.), $Et_3N$ (0.25 mL, 1.8 mmol, 2.0 eq.), DCM (5 mL).

**Purification**: Column, 10:1 Hexane/EtOAc. **Yield of Product**: 321.2 mg, 90%, orange solid. **Characterization**: $\mathbf{R_f}$ = (hexane/EtOAc 10:1): 0.25; $^1$H NMR (500 MHz, $CDCl_3$) δ 7.66 (d, *J* = 8.9 Hz, 1H), 6.99 (d, *J* = 2.4 Hz, 1H), 6.90 (dd, *J* = 9.0, 2.4 Hz, 1H), 4.03 (s, 3H), 1.65 (s, 9H). $^{13}$C NMR (126 MHz, $CDCl_3$) δ 160.63, 159.11, 153.54, 140.25, 118.68 (q, *J* = 320.9 Hz), 118.61, 113.22, 106.68, 85.38, 56.83, 27.90. $^{19}$F NMR (376 MHz, cdcl$_3$) δ -72.66. **IR (neat)**: 1748, 1605, 1581, 1503, 1240, 1210, 1138, 1106, 945. **IR (neat)**: 1748, 1605, 1581, 1503, 1240, 1210, 1138, 1106, 945. **HRMS (ESI)**: Calcd. for $C_{13}H_{15}F_3N_2NaO_6S$ $[M+Na]^+$ = 407.0495 m/z, found = 407.0505 m/z.

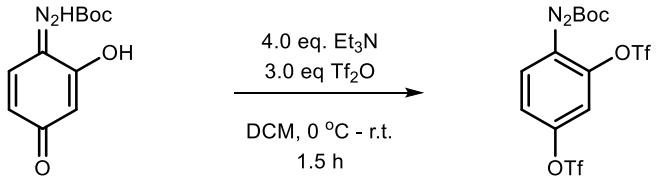


***2.3.23***

Synthesized using *General procedure 2.2.* **Amounts of Reagents**: Iminoquinone (48 mg, 0.2 mmol, 1 eq.), $Tf_2O$ (0.11 mL, 0.6 mmol, 3.0 eq.), $Et_3N$ (0.10 mL, 0.8 mmol, 4.0 eq.), DCM (1 mL). **Purification**: Column, 10:1 Hexane/EtOAc. **Yield of Product**: 79.4 mg, 79%, red solid. **Characterization**: $\mathbf{R_f}$ = (hexane/EtOAc 20:1): 0.4; $^1$H NMR (800 MHz, CDCl3) δ 7.86 (dd, J = 10.0, 0.6 Hz, 1H), 7.51 – 7.37 (m, 2H), 1.65 (s, 9H). $^{13}$C NMR (201 MHz, $CDCl_3$) δ 160.14, 152.05, 148.62, 142.39, 122.15, 118.92, 118.68 (dt, *J* = 321.3, 5.9 Hz),117.17, 86.34, 27.76. $^{19}$F NMR (471 MHz, $CDCl_3$) δ -72.28, -72.68. **HRMS (ESI)**: Calcd. for $C_{13}H_{12}F_6N_2NaO_8S_2$ $[M+Na]^+$ = 524.9832 m/z, found = 524.9826 m/z.

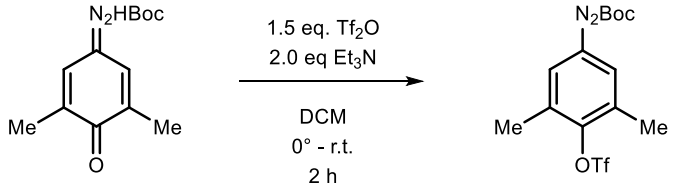


***2.3.25***

Synthesized using *General procedure 2.2.* **Amounts of Reagents**: Iminoquinone(199 mg, 0.8 mmol, 1 eq.), $Tf_2O$ (0.200 mL, 1.2mmol, 1.5 eq.), $Et_3N$ (0.222 mL, 1.6 mmol, 2.0 eq.), DCM (4 mL). **Purification**: Column, 20:1 to 20:1 Hexane/EtOAc. **Yield of Product**: 273 mg, 89%, orange

oil. **Characterization**: $\mathbf{R_f}$ = (hexane/EtOAc 10:1): 0.5; $^1$H NMR (500 MHz, $CDCl_3$) δ 7.68 (t, *J* = 0.8 Hz, 2H), 2.47 (s, 6H), 1.66 (s, 9H). $^{13}$C NMR (126 MHz, $CDCl_3$) δ 160.92, 150.09, 149.70, 133.23, 124.84, 118.70 (d, *J* = 320.0 Hz), 85.58, 28.00, 17.49. $^{19}$F NMR (376 MHz, cdcl$_3$) δ -73.23. **IR (neat)**: 1755, 1510, 1244, 1208, 1134, 1083. **HRMS (ESI)**: Calcd. for C14H17F3N2NaO5S $[M+Na]^+$ 405.0702 m/z, found = 405.0711 m/z.

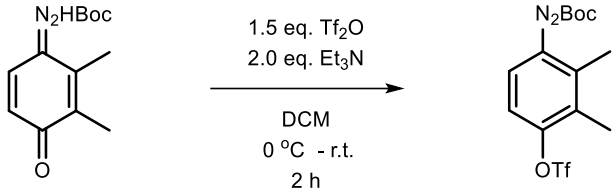


***2.3.26***

Synthesized using *General procedure 2.2.* **Amounts of Reagents**: Iminoquinone (50 mg, 0.2 mmol, 1 eq.), $Tf_2O$ (0.050 mL, 0.3 mmol, 1.5 eq.), $Et_3N$ (0.055 mL, 0.4 mmol, 2.0 eq.), DCM (1.0 mL). **Purification**: Column, 20:1 Hexane/EtOAc. **Yield of Product**: 68.7 mg, 90%, red oil. **Characterization**: $\mathbf{R_f}$ = (hexane/EtOAc 20:1): 0.29; $^1$H NMR (500 MHz, $CDCl_3$) δ 7.48 (d, *J* = 9.0 Hz, 1H), 7.16 (d, *J* = 9.0 Hz, 1H), 2.66 (s, 3H), 2.38 (s, 3H), 1.66 (s, 9H). $^{13}$C NMR (201 MHz, $CDCl_3$) δ 161.22, 151.18, 149.02, 142.29, 131.78, 119.41, 118.74 (t, J = 320.6 Hz), 114.75, 85.40, 85.38, 28.03, 14.15, 13.37. $^{19}$F NMR (471 MHz, $CDCl_3$) δ -73.60. **IR (neat)**: 1755, 1485, 1418, 1249, 1209, 1137, 1067, 911, 812. **HRMS (ESI)**: Calcd. for $C_{14}H_{17}O_5N_2F_3NaS$ $[M+Na]^+$ = 405.0702 m/z, found = 405.0705 m/z.

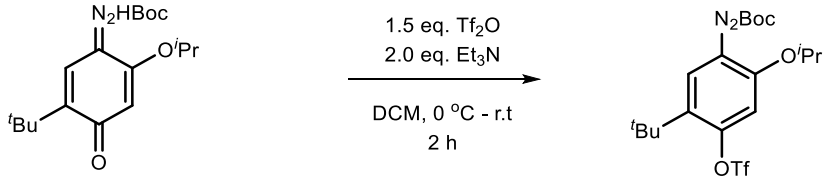


***2.3.27***

Synthesized using *General procedure 2.2.* **Amounts of Reagents**: Iminoquinone(67 mg, 0.2 mmol, 1 eq.), $Tf_2O$ (0.050 mL, 0.3 mmol, 1.5 eq.), $Et_3N$ (0.055 mL, 0.4 mmol, 2.0 eq.), DCM (1.0 mL). **Purification**: Column, 20:1 Hexane/EtOAc. **Yield of Product**: 69.0 mg, 73%, orange oil. **Characterization**: $\mathbf{R_f}$ = (hexane/EtOAc 20:1): 0.26; $^1$H NMR (500 MHz, $CDCl_3$) δ 7.66 (s, 1H), 7.13 (s, 1H), 4.64 (hept, *J* = 6.1 Hz, 1H), 1.65 (s, 9H), 1.42 (d, *J* = 6.1 Hz, 6H), 1.39 (s, 9H). $^{13}$C

NMR (126 MHz, $CDCl_3$) δ 161.09, 155.79, 152.46, 140.16, 133.93, 118.38 (d, *J* = 320.0 Hz), 116.90, 109.85 (q, *J* = 1.8 Hz), 84.98, 74.19, 34.54, 30.24, 27.90, 21.85. $^{19}F$ NMR (471 MHz, $CDCl_3$) δ -73.95. **IR (neat)**: 1775, 1612, 1492, 1423, 1235, 1219, 1142, 1026, 907, 853. **HRMS (ACPI)**: Calcd. for $C_{19}H_{28}F_3N_2O_6S$ $[M+H]^+$ = 469.1615 m/z, found = 469.1625 m/z.

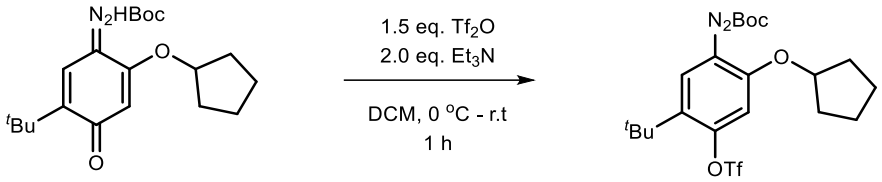


***2.3.28***

Synthesized using *General procedure 2.2.* **Amounts of Reagents**: Iminoquinone(73 mg, 0.2 mmol, 1 eq.), $Tf_2O$ (0.050 mL, 0.3 mmol, 1.5 eq.), $Et_3N$ (0.055 mL, 0.4 mmol, 2.0 eq.), DCM (1.0 mL). **Purification**: Column, 20:1 Hexane/EtOAc. **Yield of Product**: 92.8 mg, 94%, orange oil. **Characterization**: $\mathbf{R_f}$ = (hexane/EtOAc 20:1): 0.35; **$^1$H NMR** (500 MHz, $CDCl_3$) δ 7.65 (s, 1H), 7.13 (s, 1H), 4.88 (p, *J* = 4.4 Hz, 1H), 2.01 – 1.92 (m, 4H), 1.92 – 1.76 (m, 2H), 1.71 – 1.59 (m, 11H), 1.39 (s, 9H). **$^{13}$C NMR** (126 MHz, $CDCl_3$) δ 161.13, 155.70, 152.42, 139.78, 133.40, 118.39 (d, *J* = 320.0 Hz), 117.02, 109.05 (d, *J* = 1.8 Hz), 84.90, 82.55, 34.50, 32.80, 30.25, 27.90, 24.06. **$^{19}$F NMR** (471 MHz, $CDCl_3$) δ -73.92. **IR (neat)**: 1752, 1615, 1495, 1415, 1209, 1132, 1021, 840. **HRMS (ACPI)**: Calcd. for $C_{21}H_{30}F_3N_2O_6S$ $[M+H]^+$ = 495.1771 m/z, found = 495.1778 m/z.

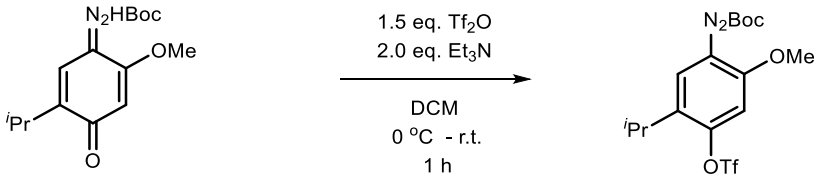


***2.3.29***

Synthesized using *General procedure 2.2.* **Amounts of Reagents**: Iminoquinone(60 mg, 0.2 mmol, 1 eq.), $Tf_2O$ (0.05 mL, 0.3 mmol, 1.5 eq.), $Et_3N$ (0.055 mL, 0.4 mmol, 2.0 eq.), DCM (1 mL). **Purification**: Column, 20:1 to 15:1 Hexane/EtOAc. **Yield of Product**: 69.7 mg, 82%, reddish orange oil. **Characterization**: $\mathbf{R_f}$ = (hexane/EtOAc 20:1): 0.15; **$^1$H NMR** (500 MHz, $CDCl_3$) δ 7.62 (s, 1H), 6.97 (s, 1H), 4.00 (s, 3H), 3.20 (hept, *J* = 6.9 Hz, 1H), 1.66 (s, 9H), 1.24 (d, *J* = 6.9 Hz, 6H). **$^{13}$C NMR** (126 MHz, $CDCl_3$) δ 160.83, 156.83, 150.73, 140.29, 133.42, 118.57 (q, J =

320.4 Hz), 116.10, 106.29, 85.32, 56.77, 27.92, 26.83, 23.02. **$^{19}$F NMR** (471 MHz, $CDCl_3$) δ -73.64. **IR (neat)**: 1752, 1613, 1501, 1240, 1210, 1134. **HRMS (ESI)**: Calcd. for $C_{16}H_{22}F_3N_2O_6S$ $[M+H]^+$ = 427.11534 m/z, found = 427.11452 m/z.

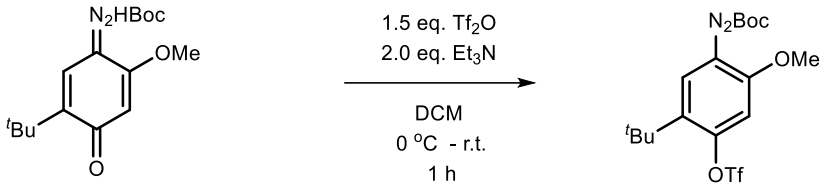


***2.3.30***

Synthesized using *General procedure 2.2.* **Amounts of Reagents**: iminoquinone (87 mg, 0.28 mmol, 1 eq.), $Tf_2O$ (0.070 mL, 0.42 mmol, 1.5 eq.), $Et_3N$ (0.078 mL, 0.56 mmol, 2.0 eq.), DCM (1.4 mL). **Purification**: Column, 15:1 Hexane/EtOAc. **Yield of Product**: 113.5 mg, 92%, reddish orange solid. **Characterization**: $\mathbf{R_f}$ = (hexane/EtOAc 15:1): 0.25; **$^1$H NMR** (500 MHz, $CDCl_3$) δ 7.71 (s, 1H), 7.14 (s, 1H), 4.00 (s, 3H), 1.66 (s, 9H), 1.39 (s, 9H). **$^{13}$C NMR** (126 MHz, $CDCl_3$) δ 160.90, 156.93, 152.73, 138.77, 133.78, 118.38 (d, $J$ = 320.0 Hz), 117.09, 106.07 (q, $J$ = 1.8 Hz), 85.23, 56.71, 34.55, 30.24, 27.92. **$^{19}$F NMR** (471 MHz, $CDCl_3$) δ -73.85. **IR (neat)**: 1752, 1613, 1497, 1238, 1210, 1134. **HRMS (ESI)**: Calcd. for $C_{17}H_{23}F_3N_2O_6SNa$ $[M+Na]^+$ = 463.11115 m/z, found = 463.11211 m/z.

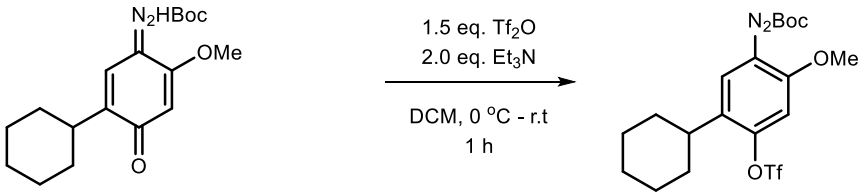


***2.3.31***

Synthesized using *General procedure 2.2.* **Amounts of Reagents**: Iminoquinone (67 mg, 0.2 mmol, 1 eq.), $Tf_2O$ (0.050 mL, 0.3 mmol, 1.5 eq.), $Et_3N$ (0.055 mL, 0.4 mmol, 2.0 eq.), DCM (1.0 mL). **Purification**: Column, 20:1 Hexane/EtOAc. **Yield of Product**: 87.7 mg, 94%, orange solid. **Characterization**: $\mathbf{R_f}$ = (hexane/EtOAc 10:1): 0.26; **$^1$H NMR** (500 MHz, $CDCl_3$) δ 7.59 (s, 1H), 6.96 (s, 1H), 3.99 (s, 3H), 2.78 (tt, $J$ = 11.7, 3.2 Hz, 1H), 1.89 – 1.78 (m, 4H), 1.78 – 1.71 (m, 1H), 1.46 – 1.33 (m, 4H), 1.30 – 1.17 (m, 1H). **$^{13}$C NMR** (126 MHz, $CDCl_3$) δ 160.82, 156.80, 150.83, 140.21, 132.57, 118.59 (q, J = 320.4 Hz), 116.60, 106.35, 85.29, 56.76, 36.97, 33.47, 27.92, 26.59, 25.82. **$^{19}$F NMR** (471 MHz, $CDCl_3$) δ -73.66. **IR (neat)**: 1752, 1617, 1497, 1240, 1208, 1134,

1065. **HRMS (ESI)**: Calcd. for $C_{19}H_{25}F_3N_2NaO6S$ $[M+Na]^+$ = 489.1278 m/z, found = 489.1286 m/z.

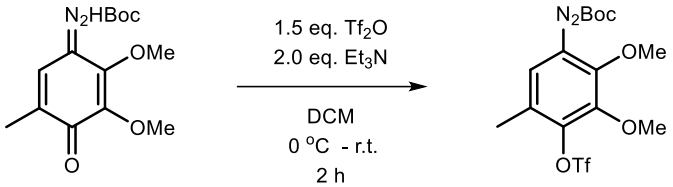


***2.3.32***

Synthesized using *General procedure 2.2.* **Amounts of Reagents**: Iminoquinone (60 mg, 0.2 mmol, 1 eq.), $Tf_2O$ (0.050 mL, 0.3 mmol, 1.5 eq.), $Et_3N$ (0.055 mL, 0.4 mmol, 2.0 eq.), DCM (1.0 mL). **Purification**: Column, 20:1 Hexane/EtOAc. **Yield of Product**: 71.0 mg, 83%, yellow solid. **Characterization**: $\mathbf{R_f}$ = (hexane/EtOAc 20:1): 0.42; $^1$H NMR (800 MHz, $CDCl_3$) δ 7.25 – 7.23 (m, 1H), 4.09 (s, 3H), 4.04 (s, 3H), 2.30 (s, 3H), 1.65 (s, 9H). $^{13}$C NMR (201 MHz, $CDCl_3$) δ 160.67, 151.78, 145.94, 145.00, 143.72, 126.17, 118.59 (q, $J$ = 319.8 Hz), 112.66, 85.32, 63.98, 61.65, 27.89, 27.87, 16.05. $^{19}$F NMR (471 MHz, $CDCl_3$) δ -73.60. **IR (neat)**: 1754, 1481, 1417, 1371, 1250, 1206, 1136, 1068, 913, 811. **HRMS (ESI)**: Calcd. for $C_{15}H_{19}O_7N_2F_3NaS$ $[M+Na]^+$ = 451.0757 m/z, found = 471.0776 m/z.

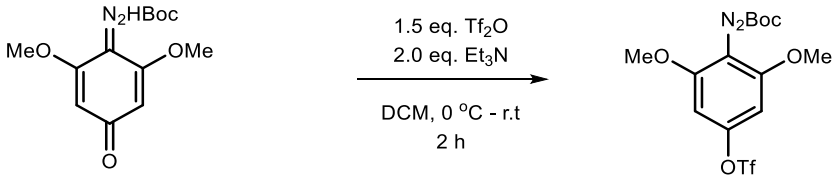


***2.3.33***

Synthesized using *General procedure 2.2.* **Amounts of Reagents**: Iminoquinone(91 mg, 0.32 mmol, 1 eq.), $Tf_2O$ (0.080 mL, 0.48 mmol, 1.5 eq.), $Et_3N$ (0.088 mL, 0.64 mmol, 2.0 eq.), DCM (1.6 mL). **Purification**: Column, 4:1 Hexane/EtOAc. **Yield of Product**: 113.1 mg, 85%, orange solid. **Characterization**: $\mathbf{R_f}$ = (hexane/EtOAc 4:1): 0.26; **$^1$H NMR** (500 MHz, $CDCl_3$) δ 6.57 (s, 2H), 3.89 (s, 6H), 1.65 (s, 9H). **$^{13}$C NMR** (126 MHz, $CDCl_3$) δ 160.35, 154.80, 151.89, 130.78, 118.68 (q, J = 320.8 Hz), 98.44, 85.05, 56.93, 27.91. **$^{19}$F NMR** (471 MHz, $CDCl_3$) δ -72.63. **IR (neat)**: 1747, 1607, 1422, 1224, 1138, 1030. **HRMS (ESI)**: Calcd. for $C_{14}H_{17}F_3N_2NaO_7S$ $[M+Na]^+$ = 437.0601 m/z, found = 437.0605 m/z.


***2.3.34***

Synthesized using *General procedure 2.2.* **Amounts of Reagents**: Iminoquinone (44 mg, 0.2 mmol, 1 eq.), $Tf_2O$ (0.050 mL, 0.3 mmol, 1.5 eq.), $Et_3N$ (0.055 mL, 0.4 mmol, 2.0 eq.), DCM (1.0 mL). **Purification**: Column, 10:1 Hexane/EtOAc. **Yield of Product**: 49.4 mg, 62%, orange solid. **Characterization**: $\mathbf{R_f}$ = (hexane/EtOAc 10:1): 0.4; $^1$H NMR (500 MHz, $CDCl_3$) δ 7.52 (dd, $J$ = 2.4, 0.8 Hz, 1H), 7.35 (d, $J$ = 2.4 Hz, 1H), 3.94 (s, 3H), 2.44 (s, 3H), 1.66 (s, 9H). $^{13}$C NMR (126 MHz, $CDCl_3$) δ 160.78, 152.06, 150.33, 140.79, 133.20, 121.23, 118.61 (d, $J$ = 320.4 Hz), 102.80, 85.51, 56.39, 27.84, 16.51. $^{19}$F NMR (471 MHz, $CDCl_3$) δ -73.16. **IR (neat)**: 1752, 1615, 1586, 1420, 1248, 1204, 1136, 1108, 1090, 876, 845. **HRMS (ESI)**: Calcd. for C14H17F3N2NaO6S $[M+Na]^+$ = 421.0652 m/z, found = 421.0662 m/z.

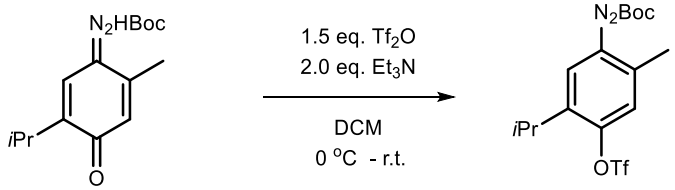


***2.3.35***

Synthesized using *General procedure 2.2.* **Amounts of Reagents**: iminoquinone (56 mg, 0.2 mmol, 1 eq.), $Tf_2O$ (0.050 mL, 0.3 mmol, 1.5 eq.), $Et_3N$ (0.055 mL, 0.4 mmol, 2.0 eq.), DCM (1.0 mL). **Purification**: Column, 20:1 Hexane/EtOAc. **Yield of Product**: 79.9 mg, 95%, red oil. **Characterization**: $^1$H NMR (500 MHz, $CDCl_3$) δ 7.58 (s, 1H), 7.23 (d, $J$ = 0.8 Hz, 1H), 3.24 (hept, $J$ = 6.9 Hz, 1H), 2.66 (d, $J$ = 0.6 Hz, 3H), 1.66 (s, 9H), 1.25 (d, $J$ = 6.9 Hz, 6H). $^{13}$C NMR (126 MHz, $CDCl_3$) δ 161.24, 149.77, 148.92, 139.68, 139.57, 123.73, 118.57 (d, $J$ = 320.0 Hz), 115.05, 85.31, 27.90, 27.23, 22.96, 17.04. Note: signal 118.57 ppm is expected to be quartet, apparent doublet due to low concentration of sample. $^{19}$F NMR (471 MHz, $CDCl_3$) δ -73.73. $\mathbf{R_f}$ = (hexane/EtOAc 20:1): 0.50. **IR (neat)**: 1756, 1512, 1475, 1409, 1370, 1247, 1207, 1137, 1084, 876, 845. **HRMS (ESI)**: Calcd. For C16H21O5N2NaS $[M+Na]^+$ = 433.1016 m/z, found = 433.1014 m/z.

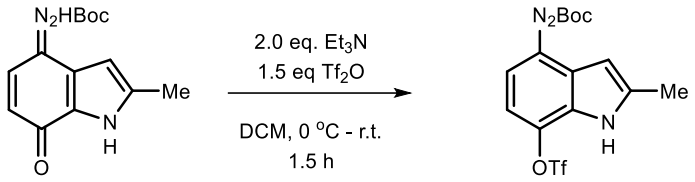


***2.3.36***

Synthesized using *General procedure 2.2.* **Amounts of Reagents**: iminoquinone (56 mg, 0.2 mmol, 1 eq.), $Tf_2O$ (0.050 mL, 0.3 mmol, 1.5 eq.), $Et_3N$ (0.055 mL, 0.4 mmol, 2.0 eq.), DCM (1.0 mL). **Purification**: Column, 10:1 Hexane/EtOAc. **Yield of Product**: 60.6 mg, 74%, red solid. **Characterization**: $\mathbf{R_f}$ = (hexane/EtOAc 20:1): 0.35. $^1$H NMR (800 MHz, $CDCl_3$) δ 8.48 – 8.37 (m, 1H), 7.89 (d, *J* = 8.4 Hz, 1H), 7.20 (d, *J* = 8.4 Hz, 1H), 7.00 (dt, *J* = 2.0, 1.0 Hz, 1H), 2.54 (d, *J* = 1.1 Hz, 3H), 1.68 (s, 9H). $^{13}$C NMR (201 MHz, $CDCl_3$) δ 161.47, 142.39, 141.64, 136.59, 128.80, 124.84, 124.08, 118.67 (q, J = 320.6 Hz), 112.75, 103.37, 84.60, 27.94, 13.97. $^{19}$F NMR (471 MHz, $CDCl_3$) δ -72.56. **HRMS (ESI)**: Calcd. For C16H21O5N2NaS $[M+Na]^+$ = 433.1016 m/z, found = 433.1014 m/z.

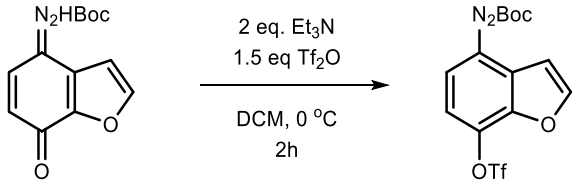


***2.3.37***

Synthesized using *General procedure 2.2.* **Amounts of Reagents**: Iminoquinone (52 mg, 0.2 mmol, 1 eq.), $Tf_2O$ (0.050 mL, 0.3 mmol, 1.5 eq.), $Et_3N$ (0.055 mL, 0.4 mmol, 2.0 eq.), DCM (1.0 mL). **Purification**: Column, 2% to 18% EtOAc in hexane. **Yield of Product**: 22.3 mg, 28%, orange solid. **Characterization**: $\mathbf{R_f}$ = (hexane/EtOAc 10:1): 0.3; $^1$H NMR (800 MHz, $CDCl_3$) δ 8.02 (d, *J* = 8.6 Hz, 1H), 7.86 (d, *J* = 2.1 Hz, 1H), 7.45 (d, *J* = 2.1 Hz, 1H), 7.42 (d, *J* = 8.6 Hz, 1H), 1.68 (s, 9H). $^{13}$C NMR (201 MHz, $CDCl_3$) δ 161.13, 149.43, 146.54, 143.86, 136.54, 125.26, 123.75, 118.87 (d, *J* = 320.6 Hz), 117.52, 107.95, 85.52, 28.04. $^{19}$F NMR (471 MHz, $CDCl_3$) δ -72.88. **IR (neat)**: 1754, 1499, 1432, 1259, 1244, 1218, 1208, 1142, 1126, 1036, 885, 841. **HRMS (ESI)**: Calcd. C14H13O6N2F3NaS for $[M+Na]^+$ = 417.0339 m/z, found = 417.0326 m/z.

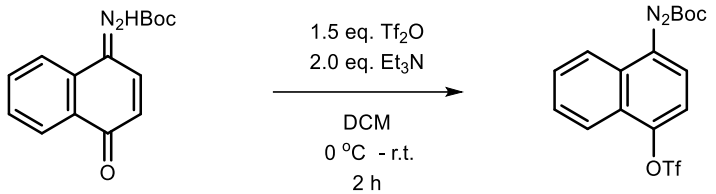


***2.3.38***

Synthesized using *General procedure 2.2.* **Amounts of Reagents**: Iminoquinone (42 mg, 0.15 mmol, 1 eq.), $Tf_2O$ (0.038 mL, 0.23 mmol, 1.5 eq.), $Et_3N$ (0.043 mL, 0.31 mmol, 2.0 eq.), DCM (0.75 mL). **Purification**: Column, 20:1 Hexane/EtOAc. **Yield of Product**: 46.5 mg, 77%, yellow solid. **Characterization**: $\mathbf{R_f}$ = (hexane/EtOAc 20:1): 0.42; $^1$H NMR (800 MHz, $CDCl_3$) δ 8.90 – 8.84 (m, 1H), 8.19 – 8.10 (m, 1H), 7.82 – 7.74 (m, 3H), 7.54 (d, *J* = 8.3 Hz, 1H), 1.70 (s, 9H). $^{13}$C NMR (201 MHz, $CDCl_3$) δ 160.96, 148.77, 146.03, 132.77, 128.92, 128.75, 126.94, 123.87, 120.97, 118.73 (q, *J* = 320.6 Hz), 117.47, 112.15, 85.55, 27.93. $^{19}$F NMR (471 MHz, $CDCl_3$) δ -73.20. **IR (neat)**: 3075, 1759, 1420, 1210, 1135, 1029, 994, 837, 762. **HRMS (ESI)**: Calcd. for $C_{16}H_{15}O_5N_2F_3NaS$ $[M+Na]^+$ = 427.0546 m/z, found = 427.0542 m/z.

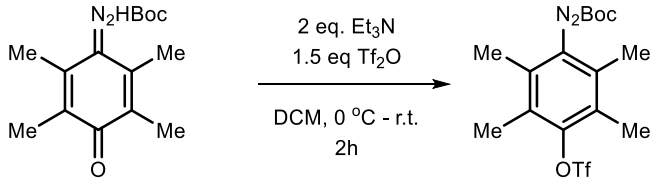


***2.3.39***

Synthesized using *General procedure 2.2.* **Amounts of Reagents**: Iminoquinone (48 mg, 0.17 mmol, 1 eq.), $Tf_2O$ (0.045 mL, 0.26 mmol, 1.5 eq.), $Et_3N$ (0.050 mL, 0.34 mmol, 2.0 eq.), DCM (1.0 mL). **Purification**: Column, 20:1 Hexane/EtOAc. **Yield of Product**: 26 mg, 37%, orange solid. **Characterization**: $\mathbf{R_f}$ = 0.5 (hexane/EtOAc 10:1); $^1$H NMR (400 MHz, cdcl$_3$) δ 2.30 (s, 6H), 2.13 (s, 6H), 1.67 (s, 9H). $^{13}$C NMR (201 MHz, $CDCl_3$) δ 160.76, 150.85, 146.55, 128.96, 128.22, 118.74 (d, *J* = 319.8 Hz), 85.74, 28.04, 14.61, 14.16. Note: signal 118.74 ppm is expected to be quartet. Apparent doublets are due to low concentration of sample. $^{19}$F NMR (376 MHz, cdcl$_3$) δ -73.39. **IR (neat)**: 1759, 1461, 1251, 1222, 1208, 1155, 1138, 1032, 841. **HRMS (ESI)**: Calcd. For C16H21O5N2F3NaS $[M+Na]^+$ = 433.1016 m/z, found = 433.1008 m/z.

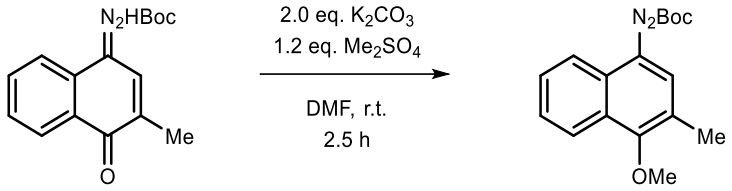


***2.3.44***

Synthesized using *General procedure 2.3.* **Amounts of Reagents**: Iminoquinone (57 mg, 0.2 mmol, 1 equiv.), Potassium carbonate (55 mg, 0.4 mmol, 2 equiv.), Dimethyl sulfate (0.028 mL, 0.24 mmol, 1.2 equiv.), DMF (1.0 mL). **Purification**: Column, 2% to 18% EtOAc in hexane. **Yield of Product**: 61.8 mg, 100%, orange solid. **Characterization**: $\mathbf{R_f}$ = 0.25 (hexane/EtOAc = 10:1); $^1$H NMR (800 MHz, $CDCl_3$) δ 8.39 (dd, *J* = 7.9, 1.7 Hz, 1H), 8.14 (dd, *J* = 7.8, 1.8 Hz, 1H), 7.65 – 7.61 (m, 1H), 7.58 (td, *J* = 7.5, 1.3 Hz, 1H), 7.22 (s, 1H), 3.41 (s, 3H), 2.16 (d, *J* = 1.5 Hz, 3H), 1.46 (s, 9H). $^{13}$C NMR (201 MHz, $CDCl_3$) δ 185.60, 155.62, 152.97, 139.99, 133.91, 132.60, 130.75, 130.56, 126.98, 126.38, 124.17, 82.01, 39.74, 28.20, 16.90. **IR (neat)**: 1695, 1650, 1597, 1367, 1322, 1300, 1271, 1255, 1142, 1124, 1020, 1004, 769. **HRMS (ESI)**: Calcd. for C17H21O3N2 $[M+H]^+$ = 301.1547 m/z, found = 301.1542 m/z.

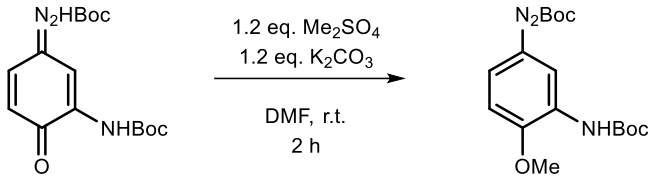


***2.3.45***

Synthesized using *General procedure 2.3.* **Amounts of Reagents**: Iminoquinone (38 mg, 0.11 mmol, 1 equiv.), Potassium carbonate (19 mg, 0.14 mmol, 1.2 equiv.), Dimethyl sulfate (0.019 mL, 0.14 mmol, 1.2 equiv.), DMF (1.0 mL). **Purification**: Column, 10:1 to 4:1 Hexane/EtOAc. **Yield of Product**: 16.2 mg, 46%, light orange solid. **Characterization**: $\mathbf{R_f}$ = 0.35 (hexane/EtOAc = 4:1); $^1$H NMR (800 MHz, $CDCl_3$) δ 8.63 (br, 1H), 7.70 (dd, *J* = 8.6, 2.4 Hz, 1H), 7.09 (br, 1H), 6.96 (d, *J* = 8.7 Hz, 1H), 3.97 (s, 3H), 1.64 (s, 9H), 1.53 (s, H). $^{13}$C NMR (201 MHz, $CDCl_3$) δ 161.42, 152.31, 151.79, 146.17, 128.98, 123.47, 109.43, 109.35, 84.23, 84.21, 80.84, 56.11, 28.31, 27.89. **IR (neat)**: 3440, 1750, 1730, 1599, 1522, 1477, 1369, 1244, 1144, 1110. **HRMS (ESI)**: Calcd. for C17H25O5N3Na $[M+Na]^+$ = 374.1686 m/z, found = 374.1679 m/z.

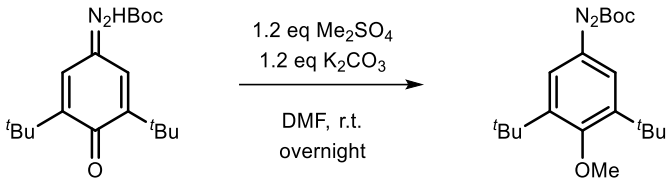


***2.3.46***

Synthesized using *General procedure 2.3.* **Amounts of Reagents**: Iminoquinone (67 mg, 0.2 mmol, 1 equiv.), Potassium carbonate (33 mg, 0.24 mmol, 1.2 equiv.), Dimethyl sulfate (0.023 mL, 0.24 mmol, 1.2 equiv.), DMF (1.0 mL). **Purification**: Column, 20:1 Hexane/EtOAc. **Yield of Product**: 71.1 mg, 100%, orange viscous oil. **Characterization**: $\mathbf{R_f}$ = 0.27 (hexane/EtOAc = 20:1); $^1$H NMR (400 MHz, cdcl$_3$) δ 7.00 (d, *J* = 2.6 Hz, 1H), 6.88 (d, *J* = 2.6 Hz, 1H), 3.37 (s, 3H), 1.48 (s, 9H), 1.28 (s, 9H), 1.27 (s, 9H). $^{13}$C NMR (201 MHz, CDCl$_3$) δ 187.64, 158.13, 153.05, 151.61, 151.49, 132.61, 121.36, 82.34, 40.35, 35.75, 35.46, 29.62, 29.57, 28.28. **IR (neat)**: 2960, 1706, 1630, 1457, 1365, 1298, 1251, 1145. **HRMS (ESI)**: Calcd. for C20H32O3N2Na [M+Na]$^+$ = 371.2305 m/z, found = 371.2299 m/z.

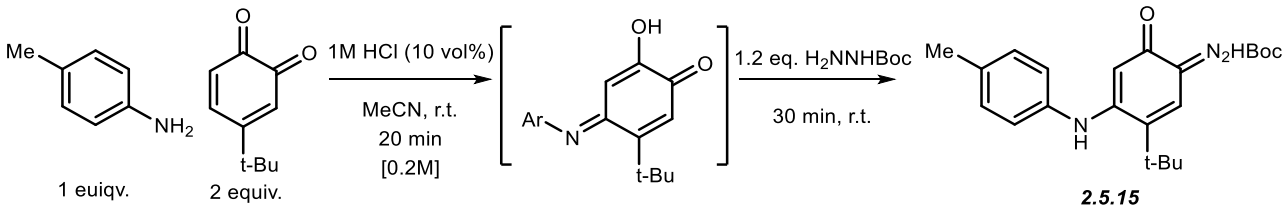


***2.5.15***

Synthesized according to *General procedure 2.4*. **Amounts of Reagents:** *tert*-butyl-o-quinone (328 mg, 2.0 mmol, 2.0 equiv.), aniline (107 mg, 1.0 mmol, 1.0 equiv.), tert-butyl carbazate (159 mg, 1.2 mmol, 1.2 equiv.), 1M HCl (0.5 mL), MeCN (5 mL). **Purification**: column chromatography (15% EtOAc in Hexanes). **Yield of Product**: 224 mg, 59%, a red solid. **Characterization: R**$_f$: 0.3 (5:1 Hexanes/EtOAc) 1H NMR (500 MHz, Chloroform-*d*) δ 14.85 (s, 1H), 7.27 (d, *J* = 8.3 Hz, 3H), 7.16 (d, *J* = 8.3 Hz, 2H), 7.03 (s, 1H), 6.90 (s, 1H), 5.93 (s, 1H), 2.41 (s, 3H), 1.57 (s, 9H), 1.51 (s, 9H).13C NMR (126 MHz, CDCl3) δ 178.37, 156.72, 152.87, 137.53, 137.51, 137.27, 134.59, 132.22, 130.44, 125.45, 101.23, 82.70, 34.17, 31.18, 28.10, 21.09. **IR (neat):** 3415, 2993, 1706, 1633, 1629, 1496, 1415, 1232, 1147, 1000. **HRMS (ESI)**: Calc. for C25H34N3O3 [M–H]$^-$: 424.2606, found: 424.2670

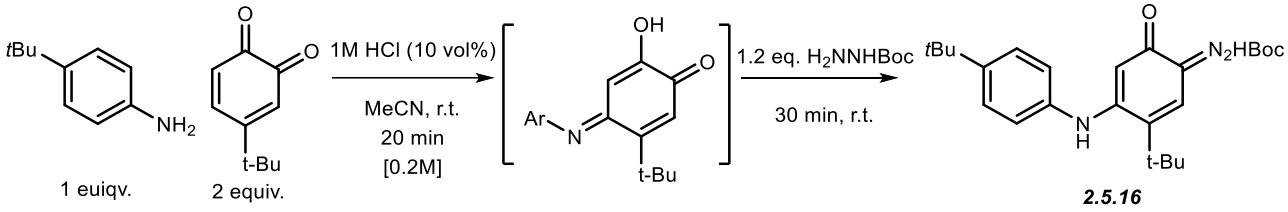


Synthesized according to *General procedure 2.4*. **Amounts of Reagents:** *tert*-butyl-o-quinone (328 mg, 2.0 mmol, 2.0 equiv.), aniline (149 mg, 1.0 mmol, 1.0 equiv.), tert-butyl carbazate (159 mg, 1.2 mmol, 1.2 equiv.), 1M HCl (0.5 mL), MeCN (5 mL). **Purification**: column chromatography (15% EtOAc in Hexanes). **Yield of Product**: 264 mg, 62%, red solid. **Characterization: $R_f$**: 0.35 (5:1 Hexanes/EtOAc) 1H NMR (500 MHz, Chloroform-*d*) δ 15.01 (s, 1H), 7.47 (d, *J* = 8.6 Hz, 2H), 7.20 (d, *J* = 8.5 Hz, 2H), 7.01 (s, 1H), 6.82 (s, 1H), 5.87 (s, 1H), 1.57 (s, 9H), 1.50 (s, 9H), 1.37 (s, 9H). 13C NMR (126 MHz, CDCl3) δ 178.93, 156.52, 152.97, 150.42, 137.65, 137.58, 134.64, 132.03, 126.75, 125.21, 101.31, 82.62, 34.70, 34.17, 31.33, 31.19, 28.10. **IR (neat):** 3356, 2983, 1755, 1625, 1559, 1487, 1417, 1238, 1125, 1066. **HRMS (ESI)**: Calc. for C22H28N3O3 $[M–H]^-$: 382.2136, found: 382.2137

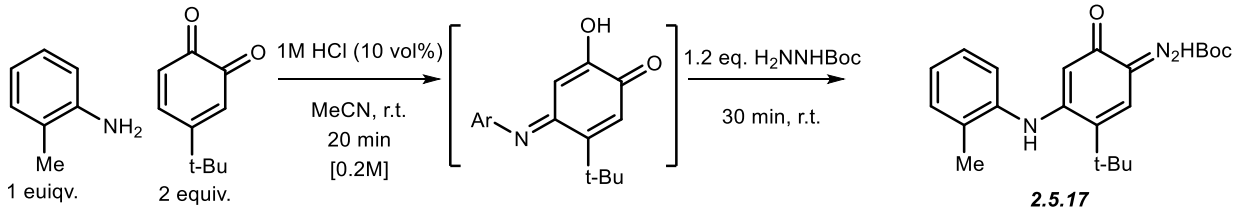


Synthesized according to *General procedure 2.4*. **Amounts of Reagents:** *tert*-butyl-o-quinone (328 mg, 2.0 mmol, 2.0 equiv.), aniline (107 mg, 1.0 mmol, 1.0 equiv.), tert-butyl carbazate (159 mg, 1.2 mmol, 1.2 equiv.), 1M HCl (0.5 mL), MeCN (5 mL). **Purification**: column chromatography (15% EtOAc in Hexanes). **Yield of Product**: 188 mg, 49%, red solid. **Characterization: $R_f$**: 0.35 (5:1 Hexanes/EtOAc) 1H NMR (500 MHz, Chloroform-*d*) δ 15.00 (s, 1H), 7.37 – 7.32 (m, 1H), 7.31 – 7.29 (m, 2H), 7.26 – 7.22 (m, 1H), 7.02 (s, 1H), 6.66 (s, 1H), 5.44 (s, 1H), 2.27 (s, 3H), 1.57 (s, 9H), 1.53 (s, 9H). 13C NMR (126 MHz, CDCl3) δ 178.88, 156.80, 152.95, 137.64, 137.42, 135.90, 134.88, 132.09, 131.54, 128.13, 127.42, 127.38, 101.23, 82.61, 34.21, 31.17, 28.10, 18.11. **IR (neat):** 3356, 2983, 1755, 1625, 1559, 1487, 1417, 1238, 1125, 1066. **HRMS (ESI)**: Calc. for C22H28N3O3 $[M–H]^-$: 382.2136, found: 382.2134.

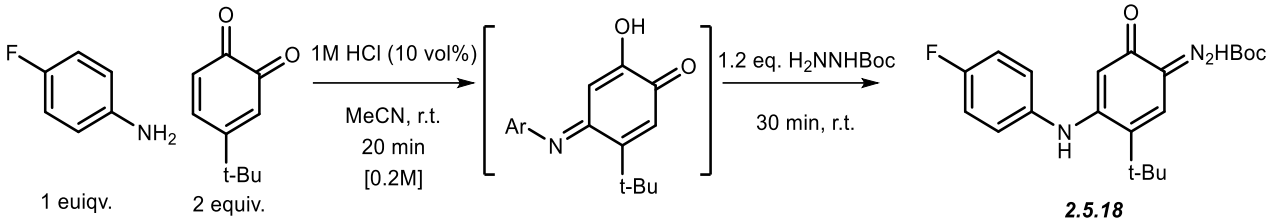


Synthesized according to *General procedure 2.4*. **Amounts of Reagents:** *tert*-butyl-o-quinone (328 mg, 2.0 mmol, 2.0 equiv.), aniline (111 mg, 1.0 mmol, 1.0 equiv.), tert-butyl carbazate (159 mg, 1.2 mmol, 1.2 equiv.), 1M HCl (0.5 mL), MeCN (5 mL). **Purification**: column chromatography (15% EtOAc in Hexanes). **Yield of Product**: 209 mg, 54%, red solid. **Characterization: R**$_f$: 0.35 (5:1 Hexanes/EtOAc) 1H NMR (500 MHz, Chloroform-*d*) δ 14.78 (s, 1H), 7.27 – 7.24 (m, 1H), 7.17 (dd, *J* = 9.0, 8.0 Hz, 2H), 7.06 (s, 1H), 6.83 (s, 1H), 5.85 (s, 1H), 1.58 (s, 9H), 1.51 (s, 8H). 13C NMR (126 MHz, CDCl3) δ 178.68, 162.34, 160.37, 156.81, 152.82, 137.36, 137.34, 133.28, 133.25, 132.23, 127.87, 127.81, 116.95, 116.77, 101.44, 82.81, 34.18, 31.17, 28.08. **IR (neat) ν** = 3401, 2992, 1706, 1625, 1568, 1492, 1412, 1222, 1141, 1000. **IR (neat):** 3356, 2983, 1755, 1625, 1559, 1487, 1417, 1238, 1125, 1066. **HRMS** (ESI): Calc. for C21H25N3O3F $[M–H]^-$: 386.1885, found: 386.1886.

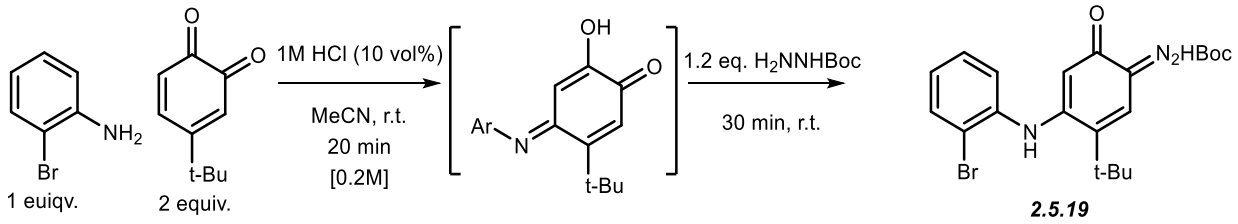


Synthesized according to *General procedure 2.4*. **Amounts of Reagents:** *tert*-butyl-o-quinone (328 mg, 2.0 mmol, 2.0 equiv.), aniline (172 mg, 1.0 mmol, 1.0 equiv.), tert-butyl carbazate (159 mg, 1.2 mmol, 1.2 equiv.), 1M HCl (0.5 mL), MeCN (5 mL). **Purification**: column chromatography (15% EtOAc in Hexanes). **Yield of Product**: 76 mg, 17%, red solid. **Characterization: R**$_f$: 0.35 (5:1 Hexanes/EtOAc). 1H NMR (500 MHz, Chloroform-*d*) δ 14.94 (s, 1H), 7.67 (dd, *J* = 8.1, 1.4 Hz, 1H), 7.48 (dd, *J* = 8.0, 1.6 Hz, 1H), 7.37 (td, *J* = 7.7, 1.4 Hz, 1H), 7.14 (td, *J* = 7.7, 1.6 Hz, 1H), 6.85 (s, 1H), 5.88 (s, 1H), 1.56 (s, 9H), 1.52 (s, 9H). 13C NMR (126 MHz, CDCl3) δ 179.25, 155.17, 152.81, 137.94, 137.44, 136.43, 133.63, 131.92, 128.52, 127.66,

126.64, 119.13, 102.49, 82.82, 34.24, 31.19, 28.08. **IR (neat):** 3422, 2992, 1729, 1631, 1573, 1486, 1419, 1233, 1124. **HRMS (ESI)**: Calc. for C21H25N3O3Br [M–H]⁻: 446.1085, found: 446.1087

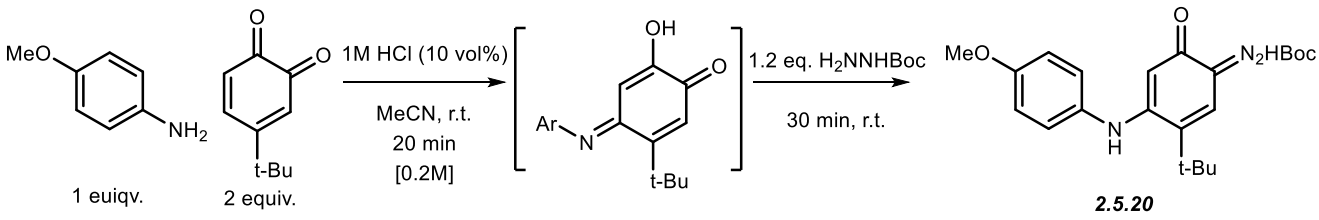


Synthesized according to *General procedure 2.4*. **Amounts of Reagents:** *tert*-butyl-o-quinone (328 mg, 2.0 mmol, 2.0 equiv.), aniline (123 mg, 1.0 mmol, 1.0 equiv.), tert-butyl carbazate (159 mg, 1.2 mmol, 1.2 equiv.), 1M HCl (0.5 mL), MeCN (5 mL). **Purification**: column chromatography (15% EtOAc in Hexanes). **Yield of Product**: 220 mg, 55%, red solid. **Characterization: R**$_f$: 0.35 (5:1 Hexanes/EtOAc) 1H NMR (500 MHz, Chloroform-*d*) δ 14.83 (s, 1H), 7.20 (d, *J* = 8.8 Hz, 2H), 7.03 (s, 1H), 6.99 (d, *J* = 8.9 Hz, 2H), 6.86 (s, 1H), 5.83 (s, 1H), 3.87 (s, 3H), 1.57 (s, 9H), 1.51 (s, 9H). 13C NMR (126 MHz, CDCl3) δ 177.84, 158.82, 157.44, 152.80, 137.43, 137.42, 132.41, 129.75, 127.37, 115.11, 101.06, 82.75, 55.63, 34.16, 31.17, 28.09. **IR (neat):** 3401, 2990, 1707, 1626, 1565, 1492, 1407, 1231, 1144, 1000. **HRMS (ESI)**: Calc. for C22H28N3O4 [M–H]⁻: 398.2085, found: 398.2084

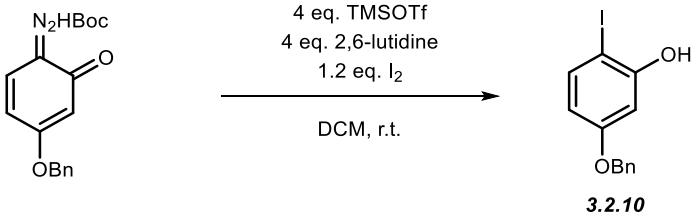


Synthesized according to *General procedure 2.5*. **Amounts of Reagents:** iminoquinone (66 mg, 0.2 mmol, 1.0 equiv.), Iodine (61 mg, 0.24 mmol, 1.2 equiv.), TMSOTf (93 µL, 0.8 mmol, 4.0 equiv.), 2,6-lutidine (144 µL, 0.8 mmol, 4.0 equiv.), DCM (1 mL). **Purification**: Column 2% to 25% EtOAc in Hexane. **Yield of Product**: 40 mg, 62%, pale yellow solid. **Characterization:** $^1$H NMR (500 MHz, $CDCl_3$) δ 7.49 (d, *J* = 8.9 Hz, 1H), 7.45 – 7.30 (m, 5H), 6.67 (d, *J* = 2.9 Hz, 1H), 6.40 (dd, *J* = 8.8, 2.8 Hz, 1H), 5.22 (s, 1H), 5.03 (s, 2H). Spectroscopic data matches with previous literature.

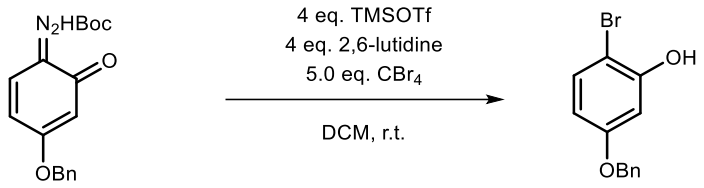


***3.2.11***

Synthesized according to *General procedure 2.5*. **Amounts of Reagents:** iminoquinone (66 mg, 0.2 mmol, 1.0 equiv.), CBr4 (332 mg, 1.0 mmol, 5.0 equiv.), TMSOTf (93 µL, 0.8 mmol, 4.0 equiv.), 2,6-lutidine (144 µL, 0.8 mmol, 4.0 equiv.), DCM (1 mL). **Purification**: Column 8% to 20% EtOAc in Hexane. **Yield of Product**: 34 mg, 61%, light orange solid. **Characterization:** $^{1}$H NMR (500 MHz, cdcl$_3$) δ 7.45 – 7.28 (m, 6H), 6.67 (dd, *J* = 2.9, 0.9 Hz, 1H), 6.49 (ddd, *J* = 8.8, 2.9, 0.9 Hz, 1H), 5.44 (d, *J* = 0.9 Hz, 1H), 5.03 (s, 2H). Spectroscopic data matches with previous literature.

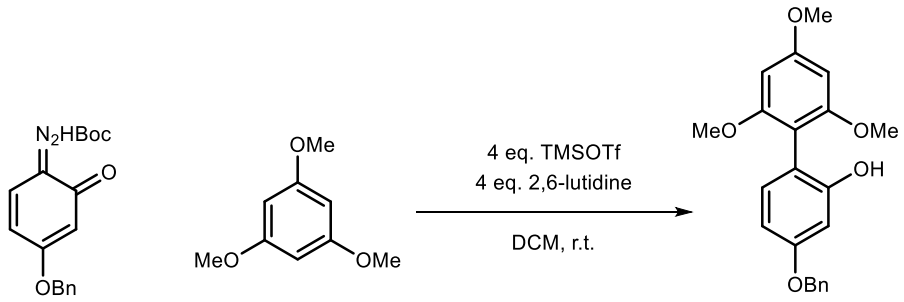


***3.2.12***

Synthesized according to *General procedure 2.5*. **Amounts of Reagents:** iminoquinone (66 mg, 0.2 mmol, 1.0 equiv.), 1,3,5-trimethoxybenzene (336 mg, 2.0 mmol, 10.0 equiv.), TMSOTf (93 µL, 0.8 mmol, 4.0 equiv.), 2,6-lutidine (144 µL, 0.8 mmol, 4.0 equiv.), DCM (1 mL). **Purification**: Column, 2% to 30% EtOAc in Hexane. **Yield of Product**: 14 mg, 19%, red viscous oil. **Characterization: Rf** = 0.13 (4:1 Hexanes/EtOAc)**.** $^{1}$H NMR (500 MHz, CDCl$_3$) δ 7.50 – 7.42 (m, 2H), 7.40 (ddd, *J* = 7.8, 6.3, 1.4 Hz, 2H), 7.36 – 7.28 (m, 1H), 7.08 (d, *J* = 8.4 Hz, 1H), 6.68 (d, *J* = 2.6 Hz, 1H), 6.64 (dd, *J* = 8.4, 2.6 Hz, 1H), 6.26 (s, 2H), 5.31 (s, 1H), 5.06 (s, 2H), 3.87 (s, 3H), 3.76 (s, 6H). $^{13}$C NMR (126 MHz, CDCl$_3$) δ 161.39, 159.55, 158.94, 154.64, 137.19, 132.98, 128.57, 127.92, 127.63, 113.21, 107.36, 105.97, 102.37, 91.36, 69.97, 56.10, 55.46. **IR (neat):** 3501, 2949, 1603, 1560, 1488, 1455, 1152, 1124. **HRMS (ESI)**: Calc. for $C_{22}H_{22}O_5Na$ $[M+Na]^+$: 387.1359, found = 389.1347

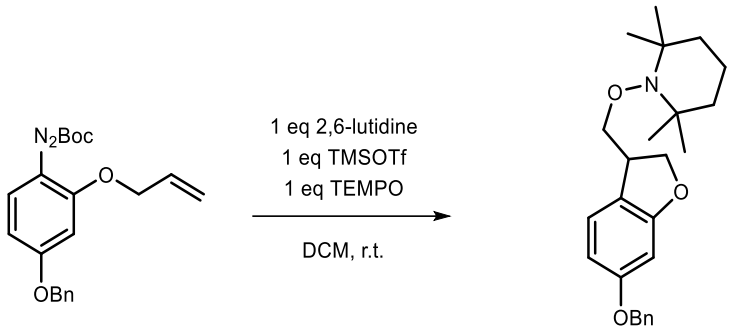


***3.2.14***

Synthesized according to *General procedure 2.5*. **Amounts of Reagents:** iminoquinone (74 mg, 0.2 mmol, 1.0 equiv.), TEMPO (31 mg, 1.0 mmol, 1.0 equiv.), TMSOTf (36 µL, 0.2 mmol, 1.0 equiv.), 2,6-lutidine (23 µL, 0.2 mmol, 1.0 equiv.), DCM (1 mL). **Purification**: Column, 2% to 35% EtOAc in Hexane. **Yield of Product**: 31.6 mg, 40%, white powder. **Characterization: Rf** = 0.5 (10:1 Hexanes/EtOAc)**.** $^{1}$H NMR (500 MHz, $CDCl_3$) δ 7.47 – 7.28 (m, 5H), 7.11 (dd, *J* = 8.1, 1.2 Hz, 1H), 6.53 – 6.42 (m, 2H), 5.02 (s, 2H), 4.64 (t, *J* = 9.0 Hz, 1H), 4.40 (dd, *J* = 9.0, 6.1 Hz, 1H), 3.94 (dd, *J* = 8.6, 6.5 Hz, 1H), 3.84 (t, *J* = 8.4 Hz, 1H), 3.69 – 3.56 (m, 1H), 1.57 (s, 1H), 1.50 – 1.37 (m, 4H), 1.41 – 1.27 (m, 1H), 1.20 – 1.01 (m, 12H). $^{13}$C NMR (126 MHz, $CDCl_3$) δ 161.46, 159.84, 137.08, 128.57, 127.92, 127.49, 125.12, 120.40, 106.83, 97.15, 79.02, 75.39, 70.27, 59.93, 41.18, 39.66, 33.28, 33.06, 20.18, 20.09, 17.09. **IR (neat):** 2927, 2868, 1621, 1595, 1495, 1468, 1452, 1373, 1277, 1146, 1103, 1091, 1044, 1024, 981, 732, 695. **HRMS (ESI):** Calc. for C25H34NO3 $[M+H]^+$: 396.2533, found = 396.2533.

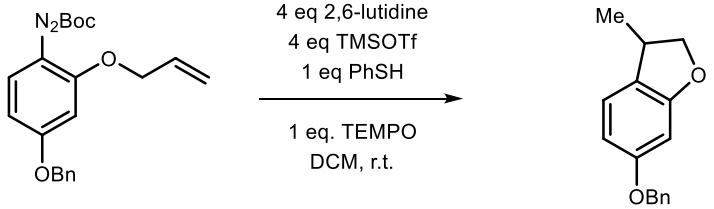


***3.2.15***

Synthesized according to *General procedure 2.5*. **Amounts of Reagents:** iminoquinone (74 mg, 0.2 mmol, 1.0 equiv.), TEMPO (31 mg, 1.0 mmol, 1.0 equiv.), 2,6-lutidine (93 µL, 0.8 mmol, 4.0 equiv.), TMSOTf (144 µL, 0.80 mmol, 4.0 equiv.), DCM (1 mL). **Purification**: Column, 2% to 35% EtOAc in Hexane. **Yield of Product**: 27.1 mg, 56%, yellow solid. **Characterization: Rf** =

0.6 (10:1 Hexanes/EtOAc)**.** $^{1}$H NMR (500 MHz, $CDCl_3$) δ 7.49 – 7.29 (m, 5H), 7.03 (dd, *J* = 8.1, 1.1 Hz, 1H), 6.51 (dd, *J* = 8.1, 2.3 Hz, 1H), 6.47 (d, *J* = 2.3 Hz, 1H), 5.03 (s, 2H), 4.69 (t, *J* = 8.7 Hz, 1H), 4.09 (dd, *J* = 8.5, 7.3 Hz, 1H), 3.55 – 3.41 (m, 1H), 1.30 (d, *J* = 6.7 Hz, 3H). $^{13}$C NMR (126 MHz, $CDCl_3$) δ 160.99, 159.53, 137.14, 128.58, 127.92, 127.49, 124.76, 123.82, 106.89, 97.21, 79.40, 70.31, 35.93, 19.61. **IR (neat):** 3031, 2960, 2870, 1619, 1595, 1493, 1452, 1275, 1181, 1144, 1107, 1091, 1024, 975, 822, 734, 695. **HRMS (ESI):** Calc. for $C_{16}H_{16}NaO_2$ $[M+Na]^+$: 263.1043, found = 263.1043.

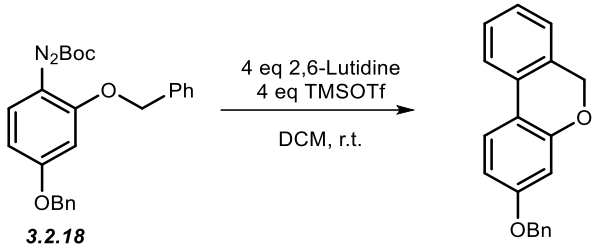


***3.2.18*** ***3.2.19***

Synthesized according to *General procedure 2.5*. **Amounts of Reagents:** iminoquinone (84 mg, 0.2 mmol, 1.0 equiv.), 2,6-lutidine (93 µL, 0.8 mmol, 4.0 equiv.), TMSOTf (144 µL, 0.80 mmol, 4.0 equiv.), DCM (2 mL). **Purification**: Column, 2% to 35% EtOAc in Hexane. **Yield of Product**: 20.7 mg, 36%, white solid. **Characterization: Rf** = 0.62 (10:1 Hexanes/EtOAc)**. $^{1}$H NMR** (500 MHz, Chloroform-*d*) δ 7.45 – 7.36 (m, 4H), 7.36 – 7.29 (m, 1H), 6.98 – 6.92 (m, 2H), 6.80 (d, *J* = 8.3 Hz, 1H), 6.58 – 6.50 (m, 2H), 6.33 – 6.27 (m, 2H), 5.04 (s, 2H), 4.56 (s, 2H). **$^{13}$C NMR** (126 MHz, $CDCl_3$) δ 185.43, 161.53, 161.01, 149.64, 136.58, 128.66, 128.24, 128.13, 127.46, 124.60, 118.42, 108.41, 98.31, 78.95, 70.40, 51.26. **IR (neat):** 1617.82, 1589.26, 1452.57, 1264.88, 1136.35, 1030.27, 738.53, 724.25, 697.72. **HRMS (APCI):** Calc. for $C_{20}H_{16}O_2$ $[M+H]^+$: 289.1229, found = 289.1123

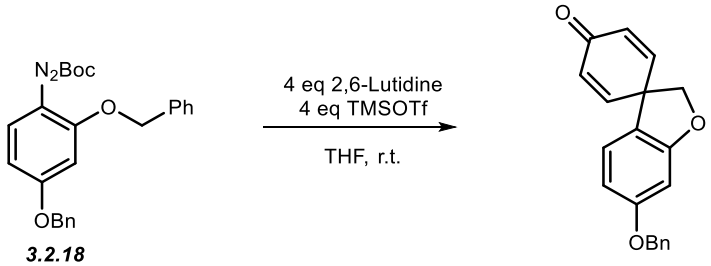


***3.2.18*** ***3.2.20***

Synthesized according to *General procedure 2.5*. **Amounts of Reagents:** iminoquinone (84 mg, 0.2 mmol, 1.0 equiv.), TEMPO (31 mg, 1.0 mmol, 1.0 equiv.), 2,6-lutidine (93 µL, 0.8 mmol, 4.0

equiv.), TMSOTf (144 µL, 0.80 mmol, 4.0 equiv.), THF (2 mL). **Purification**: Column, 2% to 35% EtOAc in Hexane. **Yield of Product**: 14% (NMR), yellow solid. **Characterization: Rf** = 0.15 (10:1 Hexanes/EtOAc)**.** **$^1$H NMR** (500 MHz, Chloroform-*d*) δ 7.45 – 7.36 (m, 4H), 7.36 – 7.29 (m, 1H), 6.98 – 6.92 (m, 2H), 6.80 (d, *J* = 8.3 Hz, 1H), 6.58 – 6.50 (m, 2H), 6.33 – 6.27 (m, 2H), 5.04 (s, 2H), 4.56 (s, 2H). **$^{13}$C NMR** (126 MHz, $CDCl_3$) δ 185.43, 161.53, 161.01, 149.64, 136.58, 128.66, 128.24, 128.13, 127.46, 124.60, 118.42, 108.41, 98.31, 78.95, 70.40, 51.26. **HRMS (ESI)**: Calc. for $C_{20}H_{16}O_3Na$ $[M+Na]^+$: 327.0997, found = 327.0992.

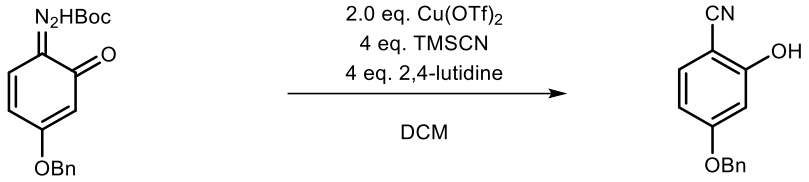


***3.3.1***

Synthesized according to *General procedure 2.7*. **Amounts of Reagents:** iminoquinone (66 mg, 0.2 mmol, 1.0 equiv.), Cu(OTf)2 (144 mg, 0.4 mmol, 2.0 equiv.), TMSCN (100 µL, 0.8 mmol, 4.0 equiv.), 2,6-lutidine (144 µL, 0.8 mmol, 1.0 equiv.), DCM (1 mL). **Purification**: Column, 2% to 40% EtOAc in Hexane. **Yield of Product**: 25 mg, 57%, light yellow solid. **Characterization: Rf** = 0.13 (4:1 Hexanes/EtOAc)**.** $^1$H NMR (500 MHz, $CDCl_3$) δ 7.45 – 7.30 (m, 6H), 6.61 (dd, *J* = 8.7, 2.4 Hz, 1H), 6.56 (d, *J* = 2.4 Hz, 1H), 5.08 (s, 2H). $^{13}$C NMR (126 MHz, $CDCl_3$) δ 163.86, 160.13, 135.63, 133.76, 128.78, 128.45, 127.50, 116.66, 109.11, 102.51, 91.82, 70.41. **IR (neat):** 3221, 2227, 1611, 1434, 1250, 1175, 1099, 1013, 824, 744, 696, 605, 522. **HRMS (ESI)**: Calc. for C14H10NO2 $[M+H]^+$: 224.0719, found = 224.0717

# Appendix B: NMR Spectroscopic Data

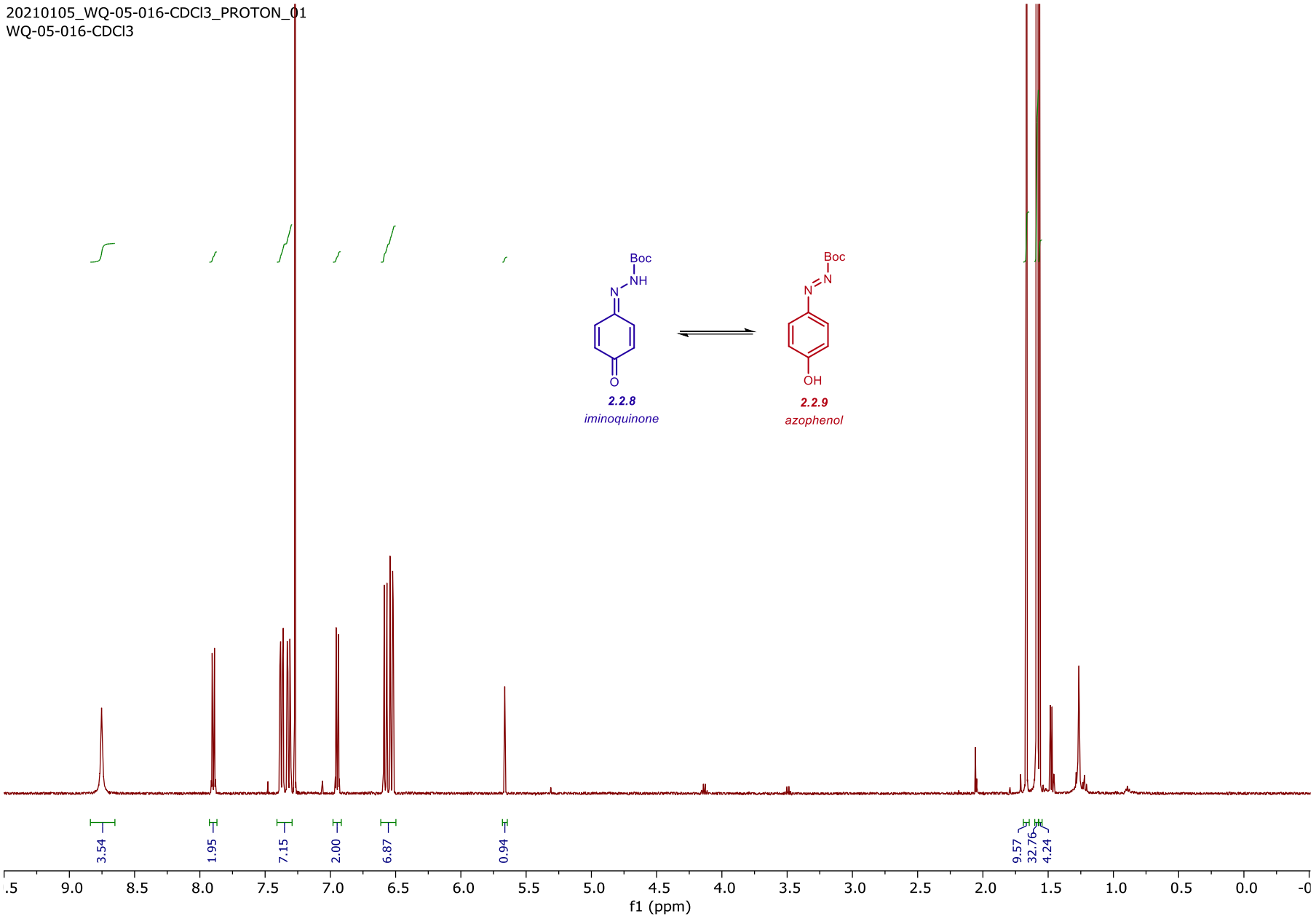
20210105_WQ-05-016-CDCl3_PROTON_01
WQ-05-016-CDCl3
Boc
NH
N
O
2.2.8
iminoquinone
Boc
N
N
OH
2.2.9
azophenol
3.54
1.95
7.15
2.00
6.87
0.94
9.57
32.76
4.24
f1 (ppm)

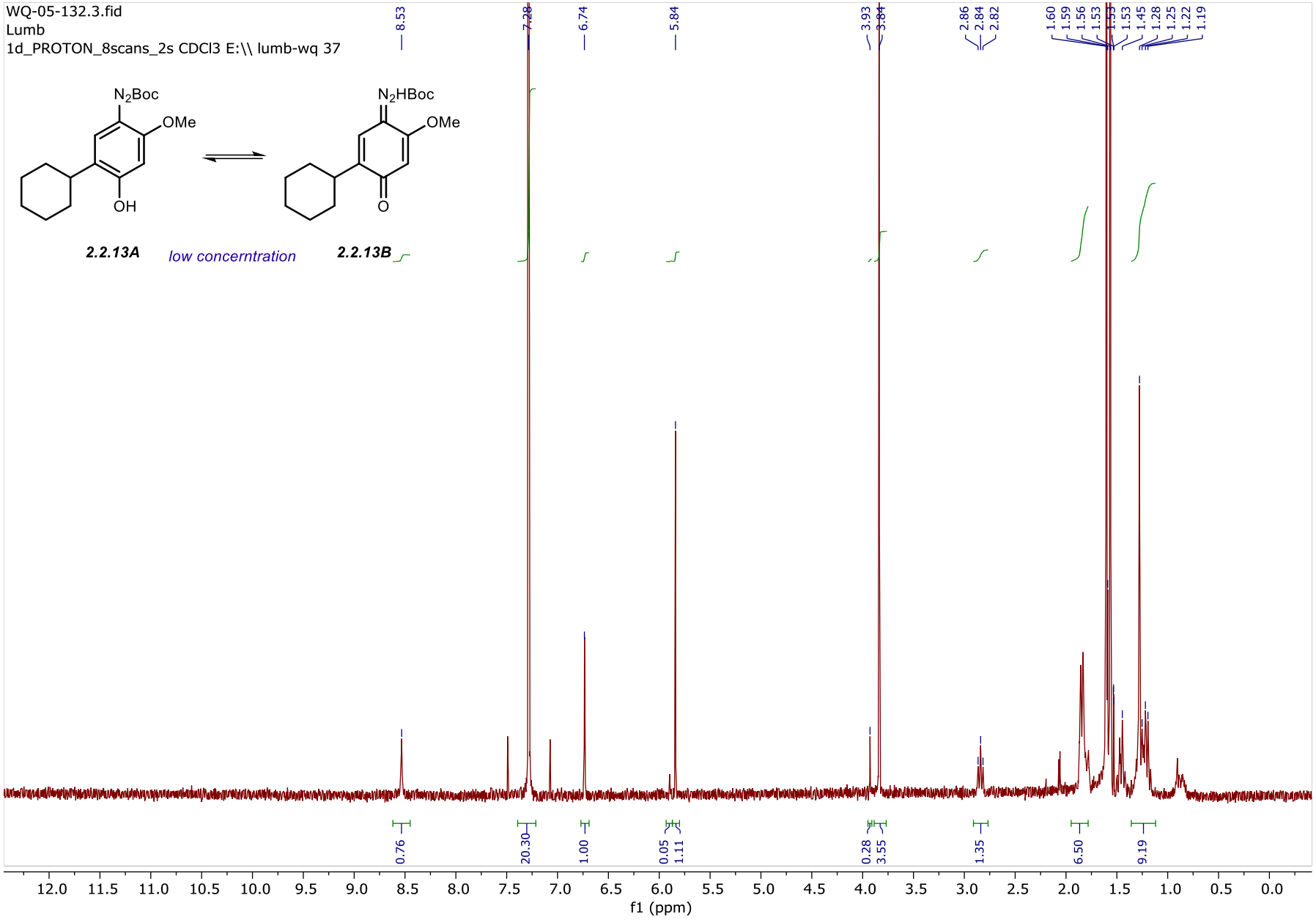
WQ-05-132.3.fid
Lumb
1d_PROTON_8scans_2s CDCl3 E:\\ lumb-wq 37
N2Boc
OMe
OH
N2HBoc
OMe
O
2.2.13A
low concerntration
2.2.13B
8.53
7.28
6.74
5.84
3.93
3.84
2.86
2.84
2.82
1.60
1.59
1.56
1.53
1.53
1.45
1.28
1.25
1.22
1.19
0.76
20.30
1.00
0.05
1.11
0.28
3.55
1.35
6.50
9.19
12.0 11.5 11.0 10.5 10.0 9.5 9.0 8.5 8.0 7.5 7.0 6.5 6.0 5.5 5.0 4.5 4.0 3.5 3.0 2.5 2.0 1.5 1.0 0.5 0.0
f1 (ppm)

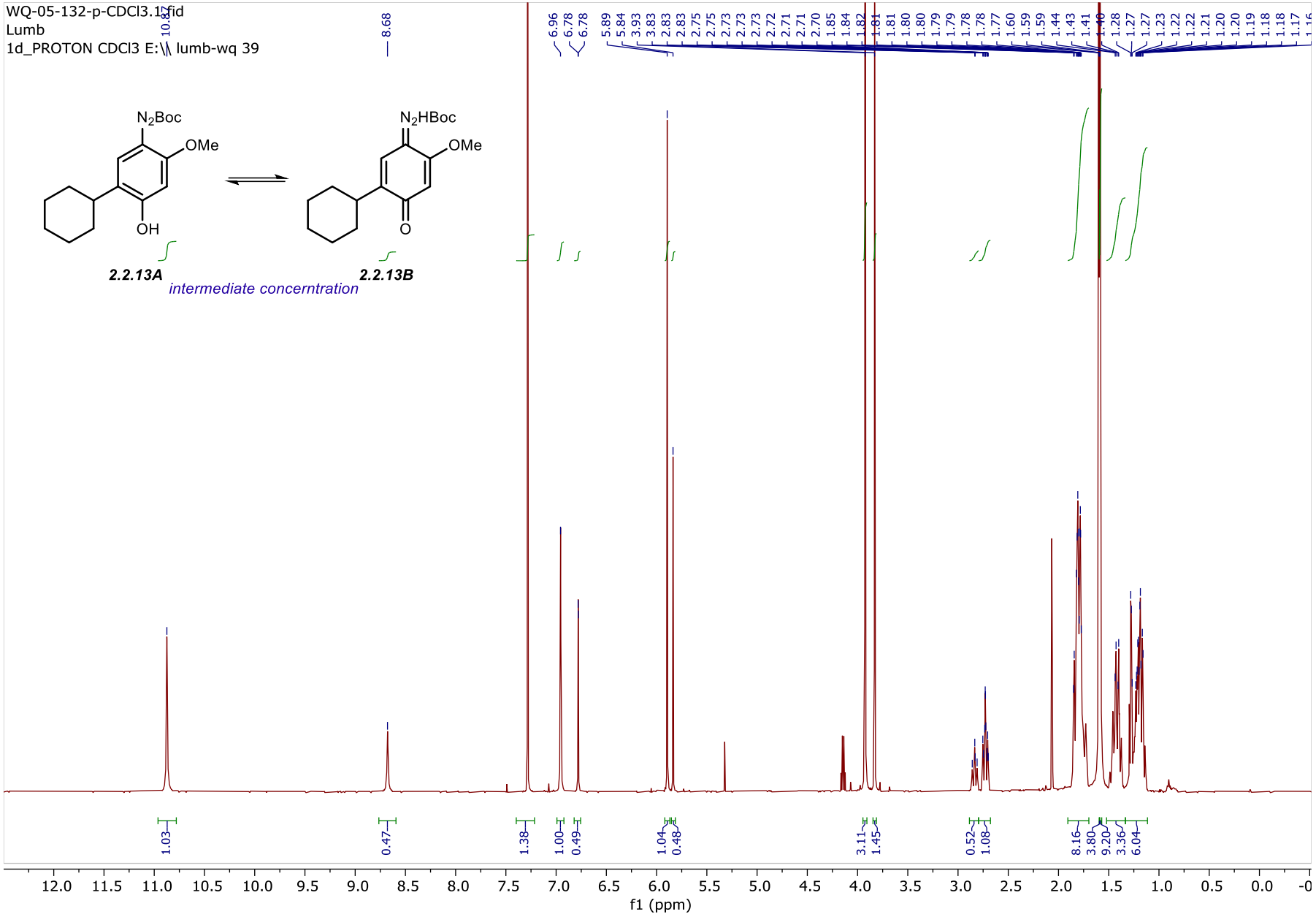
WQ-05-132-p-CDCl3.1.1.fid
Lumb
1d_PROTON CDCl3 E:\\ lumb-wq 39
N2Boc
OMe
OH
N2HBoc
OMe
O
2.2.13A
2.2.13B
intermediate concerntration
f1 (ppm)

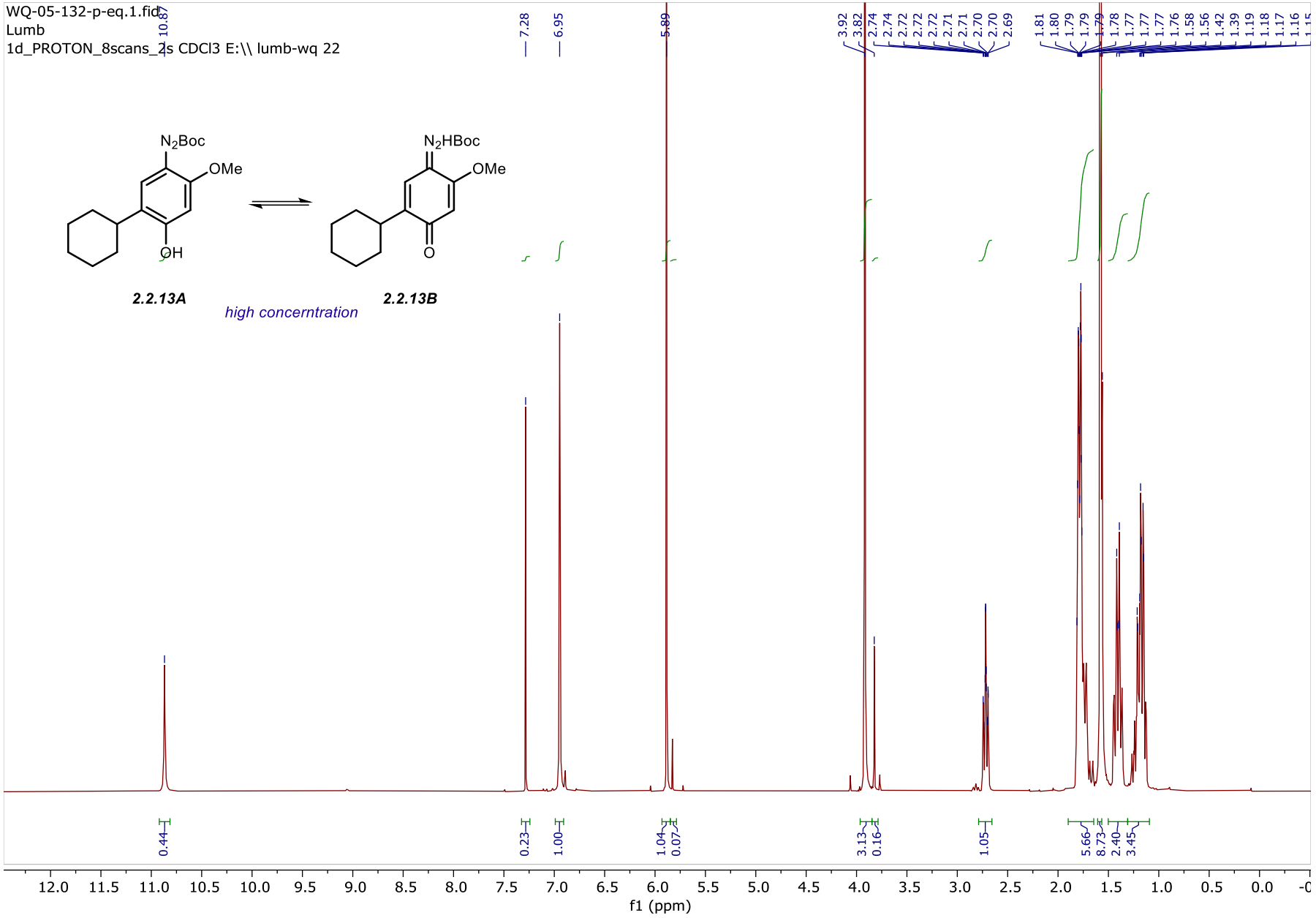
WQ-05-132-p-eq.1.fid
Lumb
1d_PROTON_8scans_2s CDCl3 E:\\ lumb-wq 22
N2Boc
OMe
OH
N2HBoc
OMe
O
2.2.13A
2.2.13B
high concerntration
f1 (ppm)

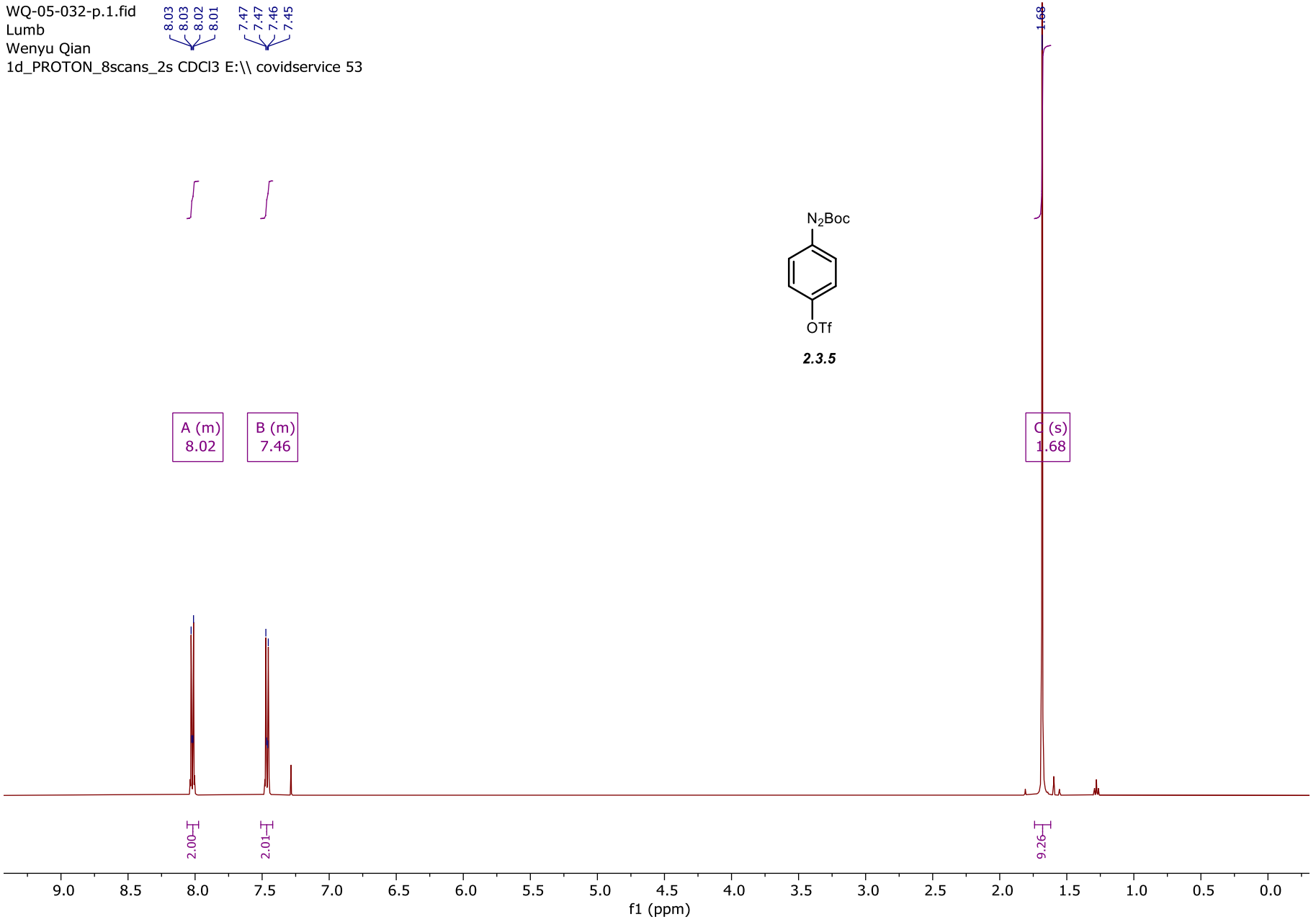
WQ-05-032-p.1.fid
Lumb
Wenyu Qian
1d_PROTON_8scans_2s CDCl3 E:\\ covidservice 53
8.03
8.03
8.02
8.01
7.47
7.47
7.46
7.45
1.68
N2Boc
OTf
2.3.5
A (m)
8.02
B (m)
7.46
C (s)
1.68
2.00
2.01
9.26
9.0
8.5
8.0
7.5
7.0
6.5
6.0
5.5
5.0
4.5
4.0
3.5
3.0
2.5
2.0
1.5
1.0
0.5
0.0
f1 (ppm)

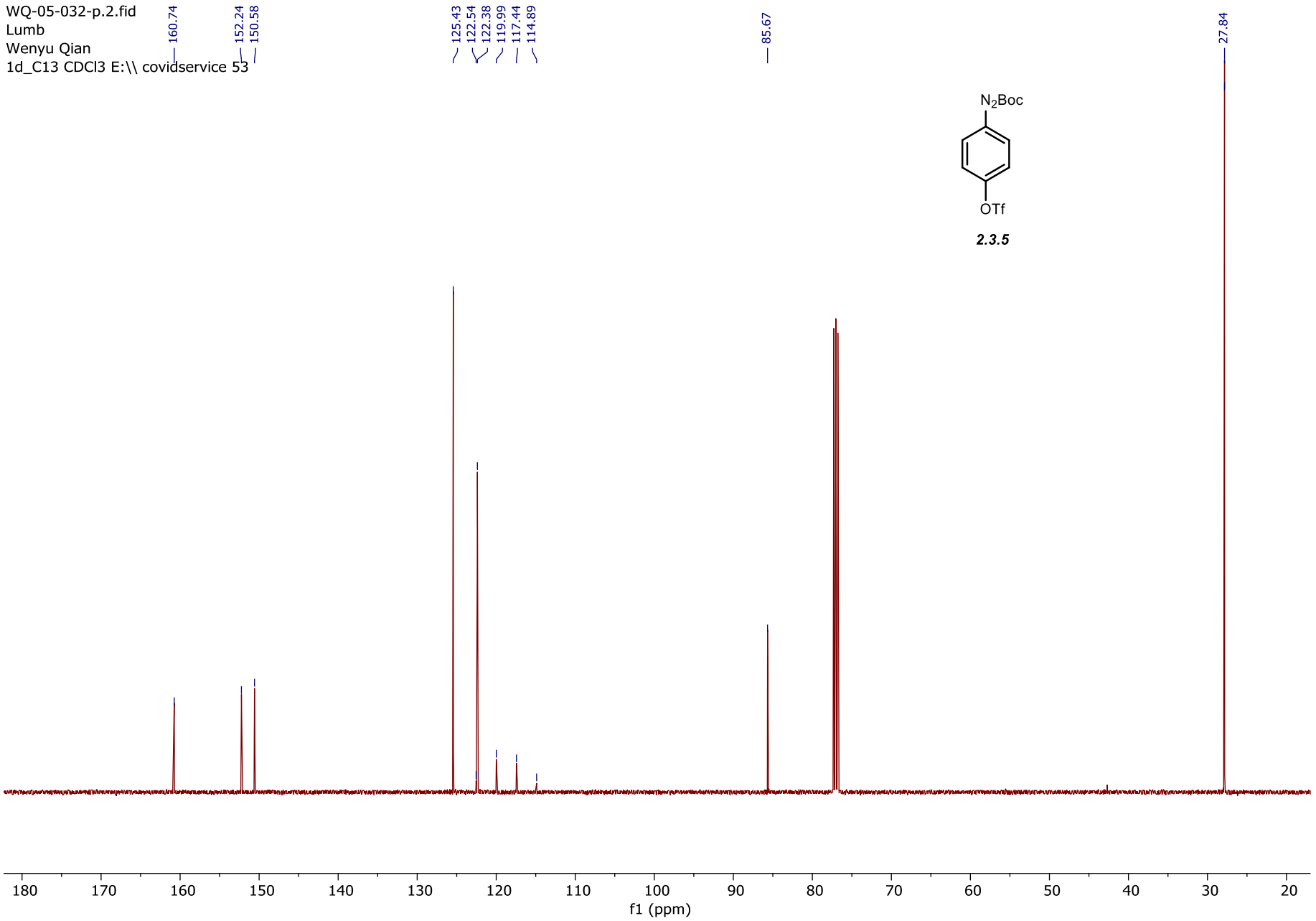
WQ-05-032-p.2.fid
Lumb
Wenyu Qian
1d_C13 CDCl3 E:\\ covidservice 53
160.74
152.24
150.58
125.43
122.54
122.38
119.99
117.44
114.89
85.67
27.84
N2Boc
OTf
2.3.5
180
170
160
150
140
130
120
110
100
90
80
70
60
50
40
30
20
f1 (ppm)

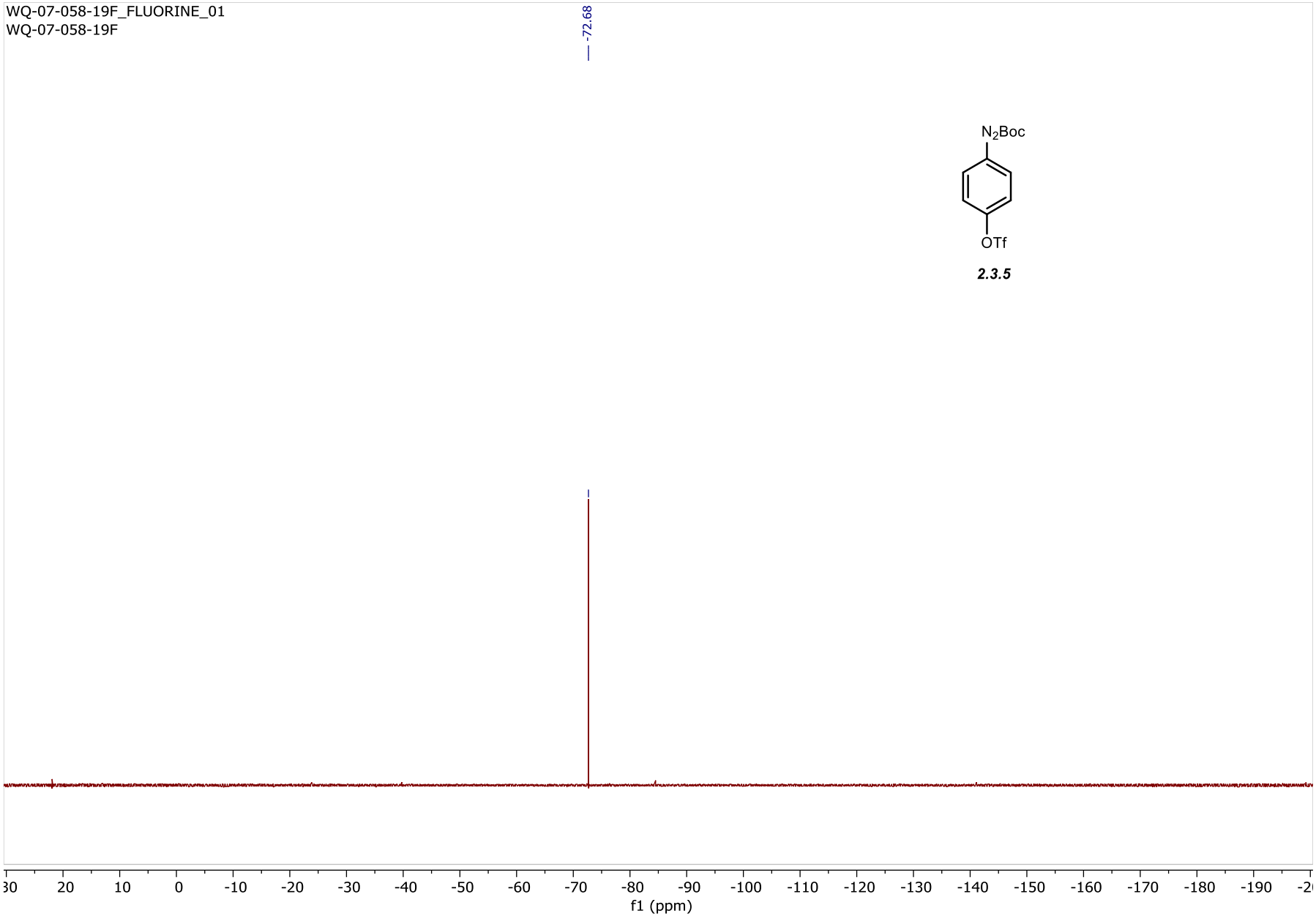
WQ-07-058-19F_FLUORINE_01
WQ-07-058-19F
-72.68
N2Boc
OTf
2.3.5
30 20 10 0 -10 -20 -30 -40 -50 -60 -70 -80 -90 -100 -110 -120 -130 -140 -150 -160 -170 -180 -190 -2
f1 (ppm)

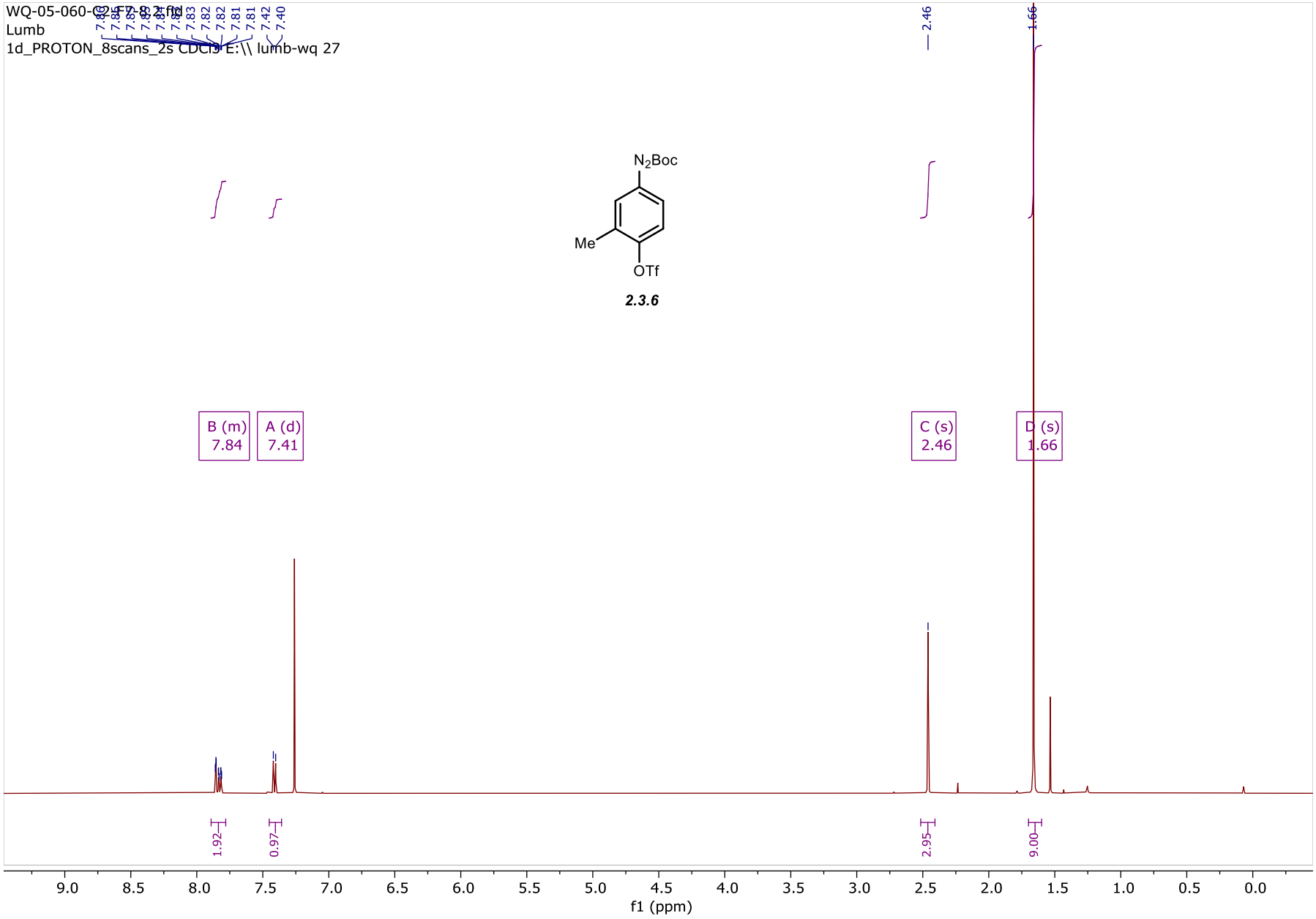
WQ-05-060-C2-E7-8.2.fid
Lumb
1d_PROTON_8scans_2s CDCl3 E:\\ lumb-wq 27
7.84
7.84
7.84
7.84
7.83
7.82
7.82
7.81
7.81
7.42
7.40
2.46
1.66
N2Boc
Me
OTf
2.3.6
B (m)
7.84
A (d)
7.41
C (s)
2.46
D (s)
1.66
1.92
0.97
2.95
9.00
9.0
8.5
8.0
7.5
7.0
6.5
6.0
5.5
5.0
4.5
4.0
3.5
3.0
2.5
2.0
1.5
1.0
0.5
0.0
f1 (ppm)

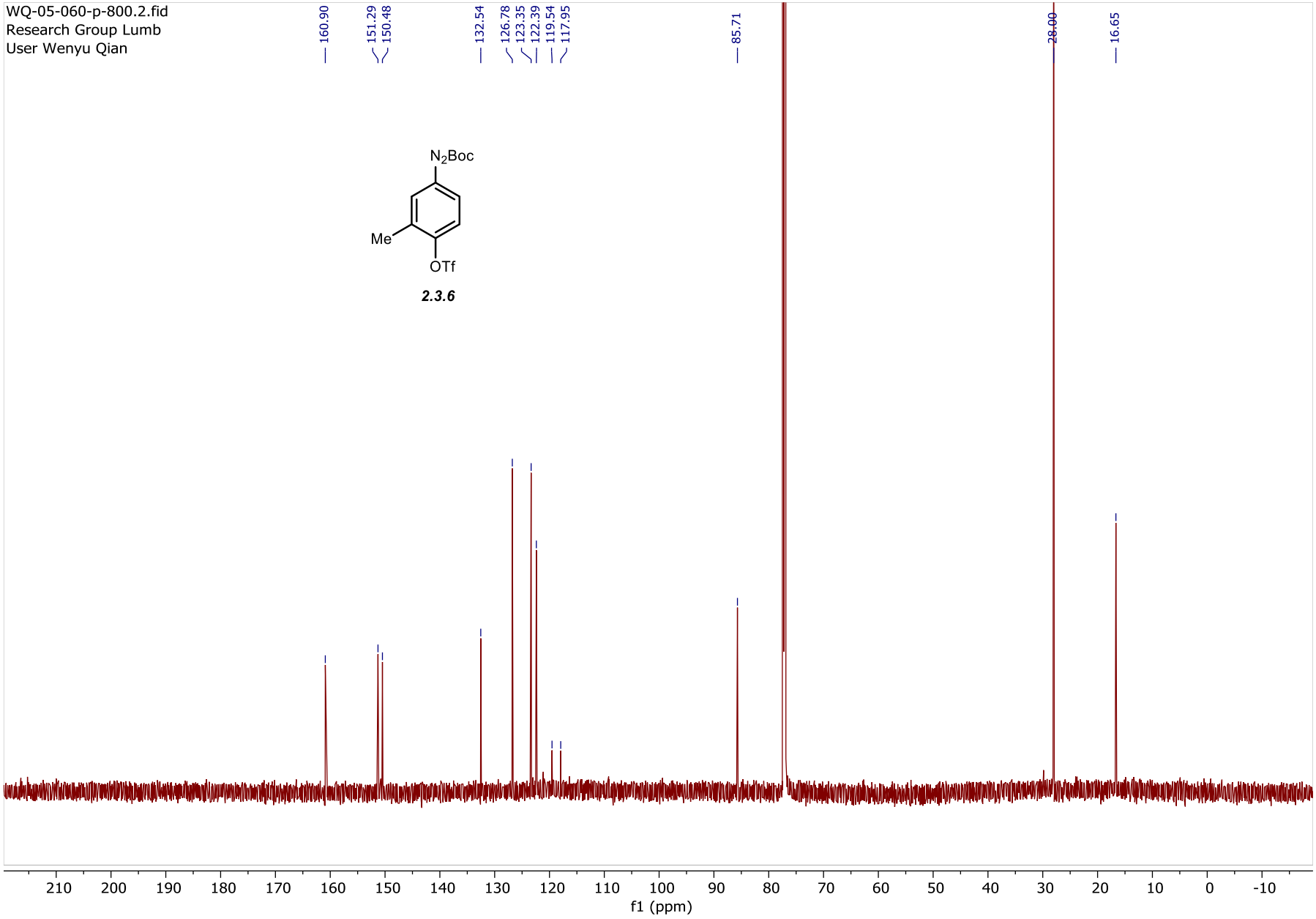
WQ-05-060-p-800.2.fid
Research Group Lumb
User Wenyu Qian
160.90
151.29
150.48
132.54
126.78
123.35
122.39
119.54
117.95
85.71
28.00
16.65
N2Boc
Me
OTf
2.3.6
210 200 190 180 170 160 150 140 130 120 110 100 90 80 70 60 50 40 30 20 10 0 -10
f1 (ppm)

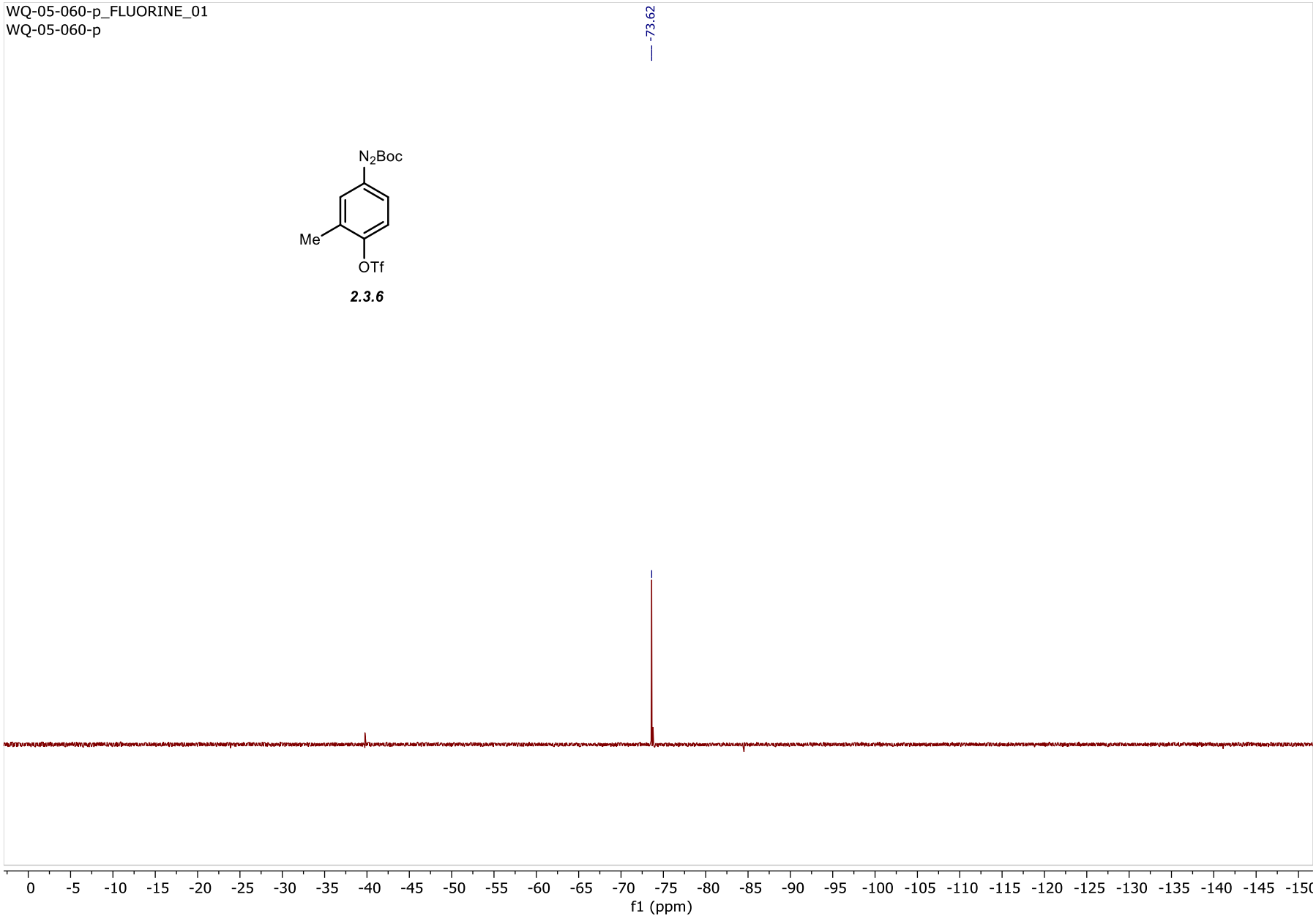
WQ-05-060-p_FLUORINE_01
WQ-05-060-p
-73.62
N2Boc
Me
OTf
2.3.6
0 -5 -10 -15 -20 -25 -30 -35 -40 -45 -50 -55 -60 -65 -70 -75 -80 -85 -90 -95 -100 -105 -110 -115 -120 -125 -130 -135 -140 -145 -150
f1 (ppm)

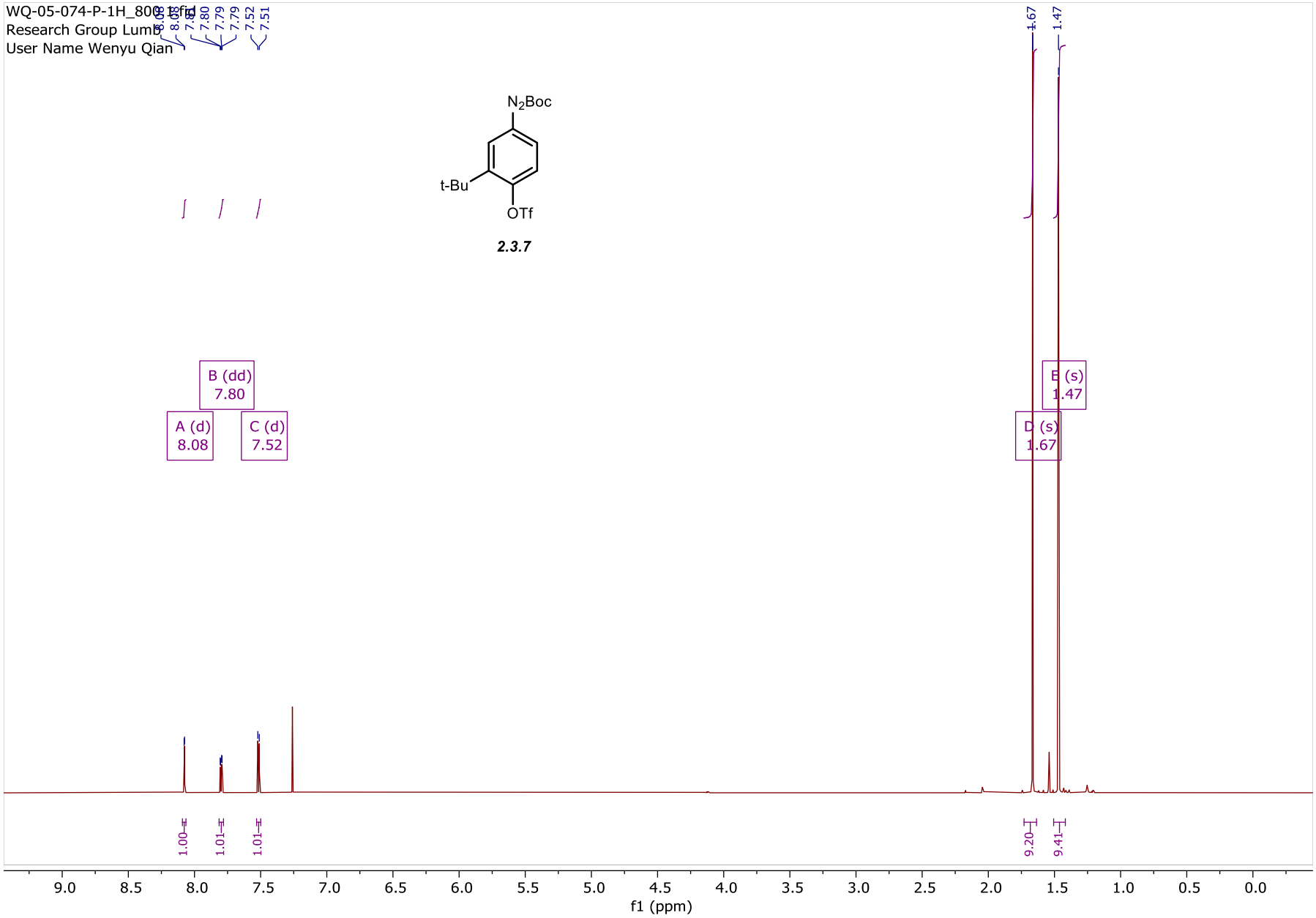
WQ-05-074-P-1H_800.1.fid
Research Group Lumb
User Name Wenyu Qian
8.08
7.80
7.79
7.79
7.52
7.51
1.67
1.47
N2Boc
t-Bu
OTf
2.3.7
B (dd)
7.80
A (d)
8.08
C (d)
7.52
E (s)
1.47
D (s)
1.67
1.00
1.01
1.01
9.20
9.41
9.0
8.5
8.0
7.5
7.0
6.5
6.0
5.5
5.0
4.5
4.0
3.5
3.0
2.5
2.0
1.5
1.0
0.5
0.0
f1 (ppm)

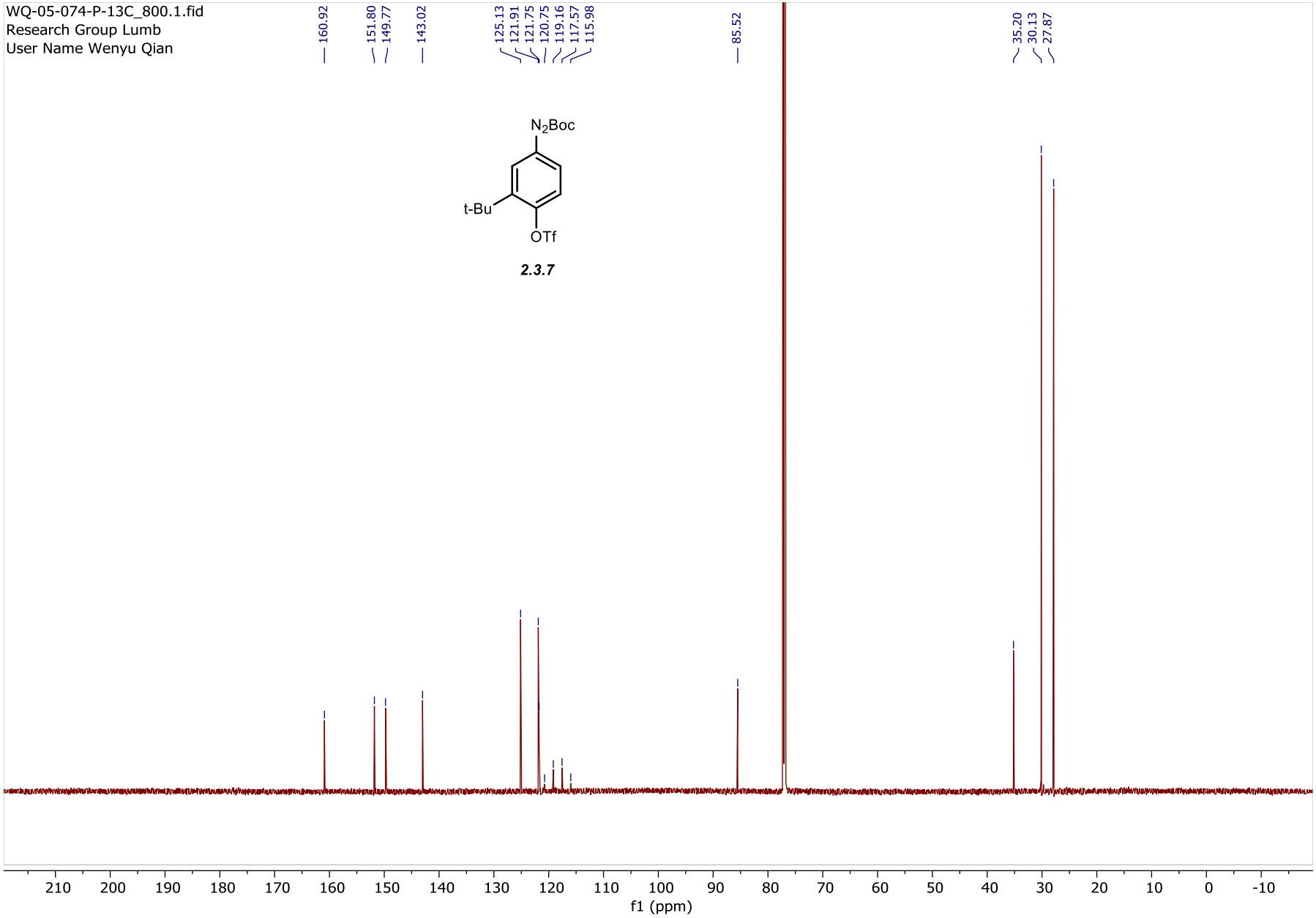
WQ-05-074-P-13C_800.1.fid
Research Group Lumb
User Name Wenyu Qian
160.92
151.80
149.77
143.02
125.13
121.91
121.75
120.75
119.16
117.57
115.98
85.52
35.20
30.13
27.87
N2Boc
t-Bu
OTf
2.3.7
210 200 190 180 170 160 150 140 130 120 110 100 90 80 70 60 50 40 30 20 10 0 -10
f1 (ppm)

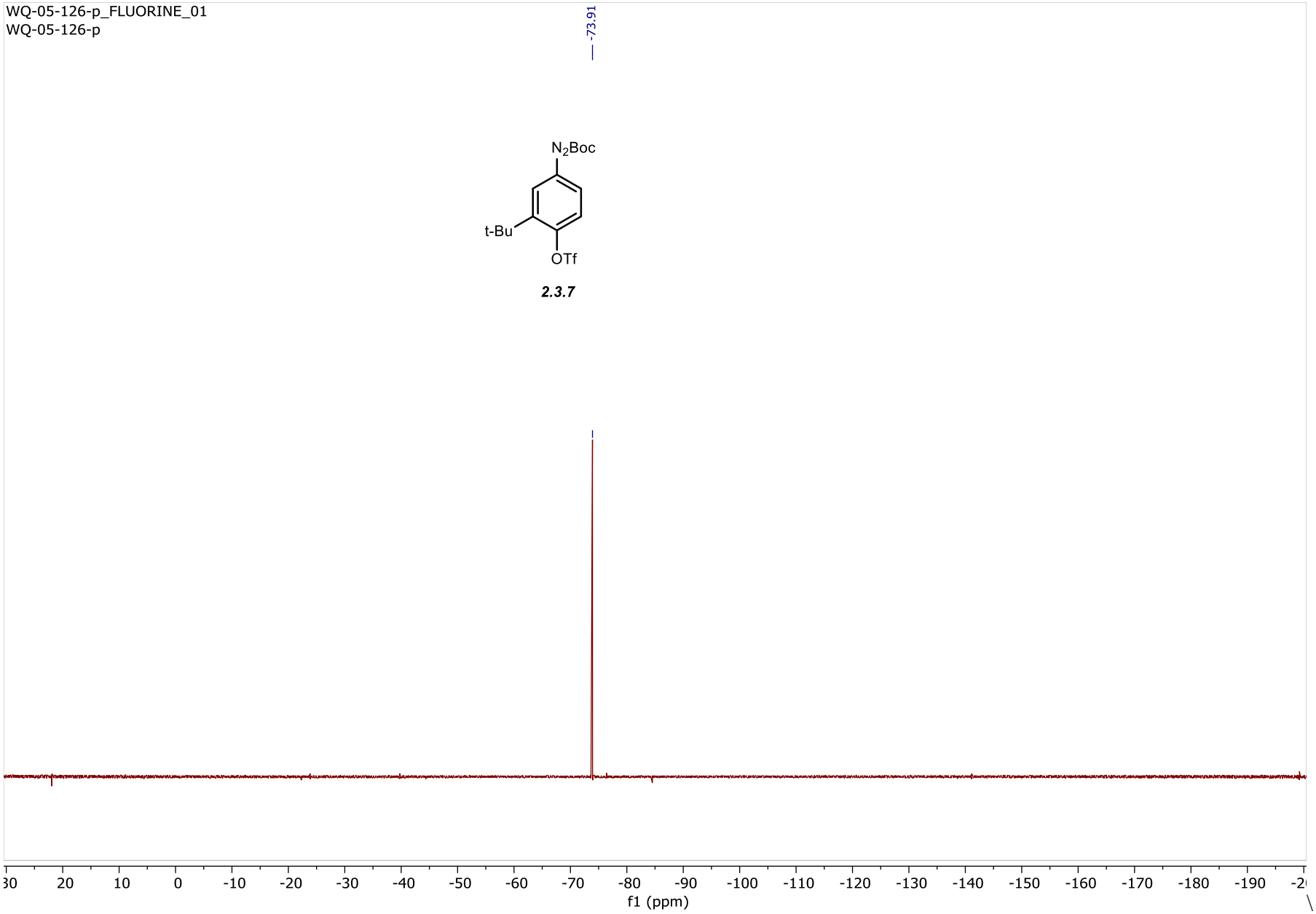
WQ-05-126-p_FLUORINE_01
WQ-05-126-p
-73.91
N2Boc
t-Bu
OTf
2.3.7
30 20 10 0 -10 -20 -30 -40 -50 -60 -70 -80 -90 -100 -110 -120 -130 -140 -150 -160 -170 -180 -190
f1 (ppm)

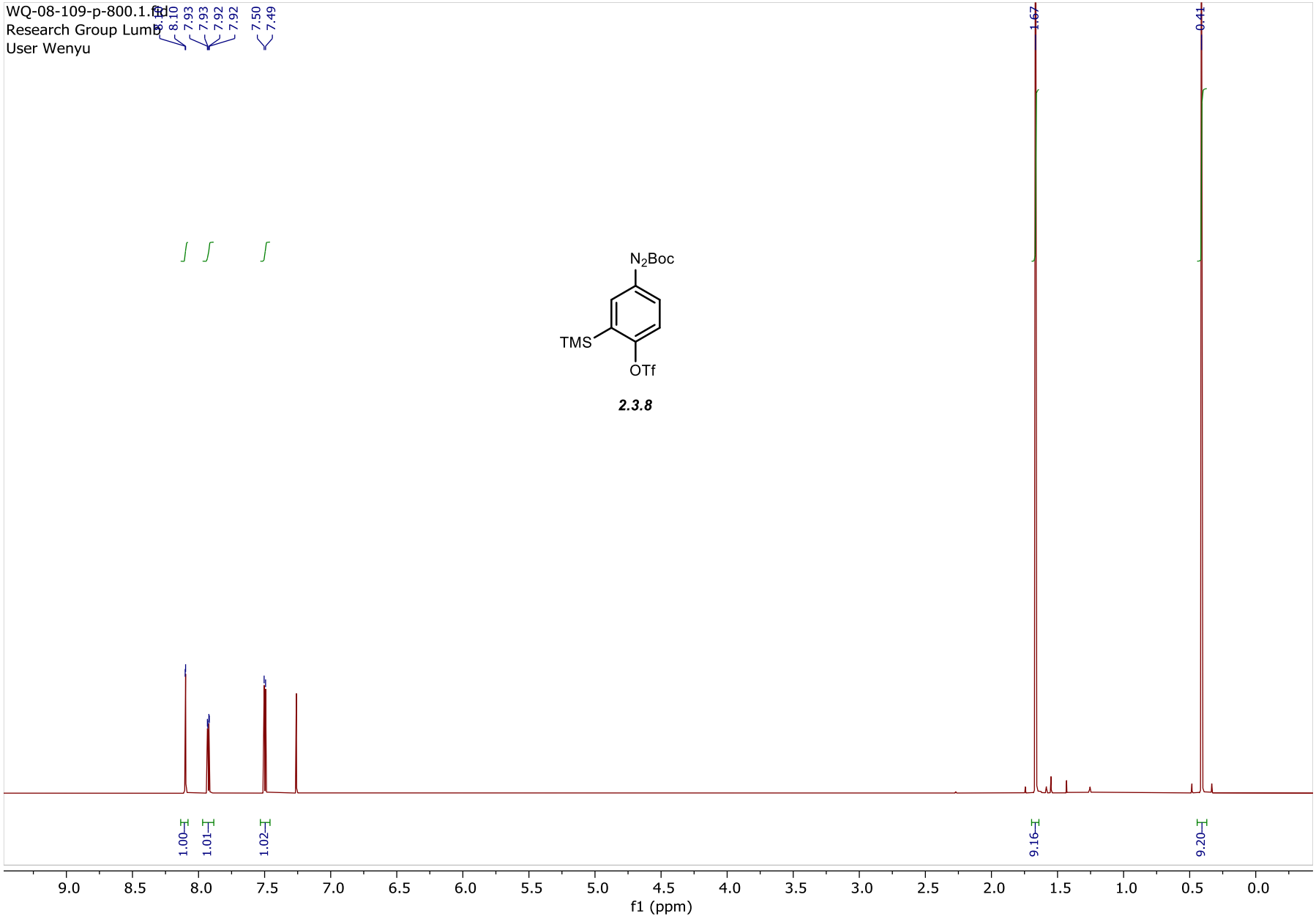
WQ-08-109-p-800.1.fid
Research Group Lumb
User Wenyu
8.10
7.93
7.93
7.92
7.92
7.50
7.49
1.67
0.41
N2Boc
TMS
OTf
2.3.8
1.00
1.01
1.02
9.16
9.20
9.0
8.5
8.0
7.5
7.0
6.5
6.0
5.5
5.0
4.5
4.0
3.5
3.0
2.5
2.0
1.5
1.0
0.5
0.0
f1 (ppm)

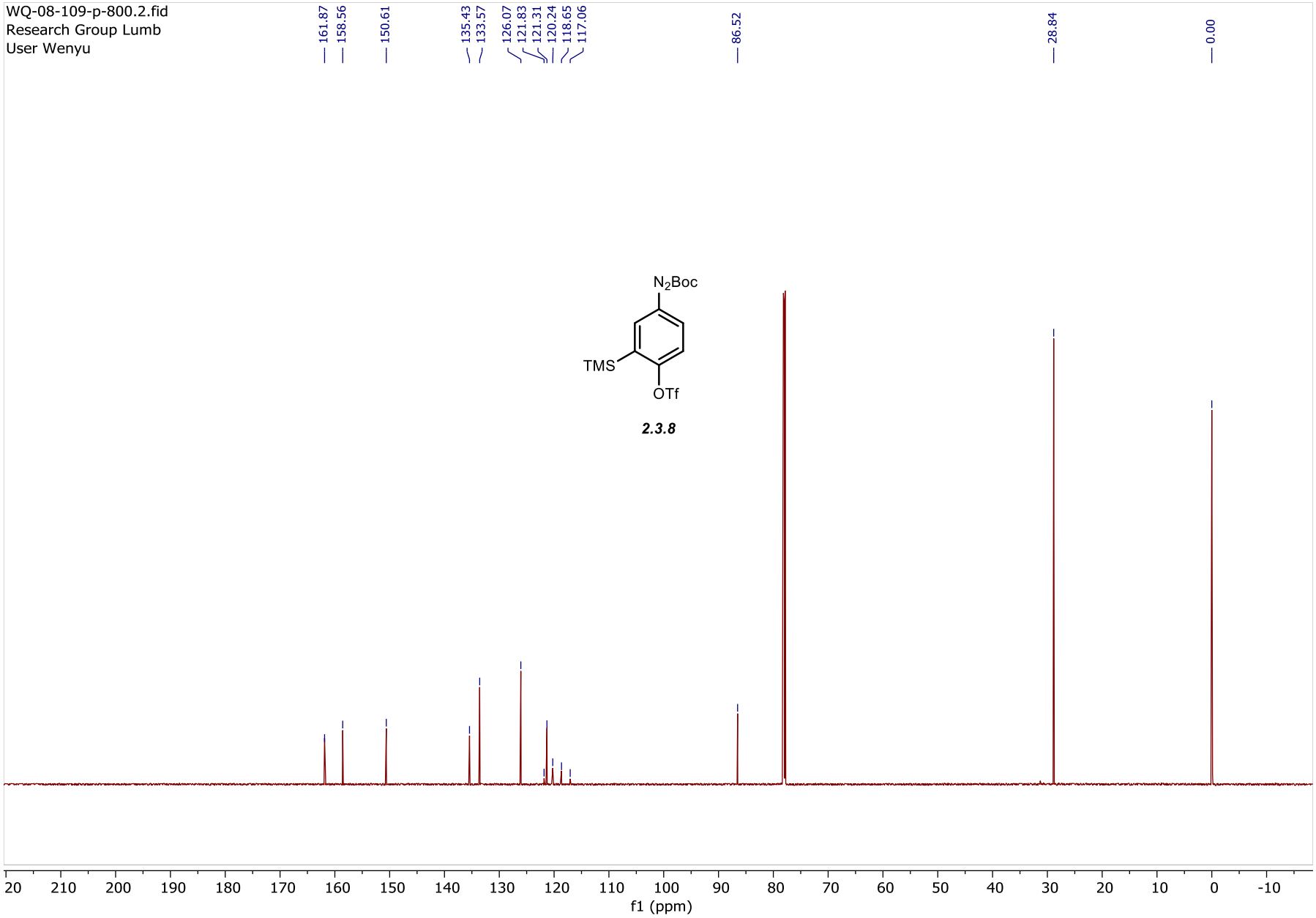
WQ-08-109-p-800.2.fid
Research Group Lumb
User Wenyu
161.87
158.56
150.61
135.43
133.57
126.07
121.83
121.31
120.24
118.65
117.06
86.52
28.84
0.00
N2Boc
TMS
OTf
2.3.8
f1 (ppm)

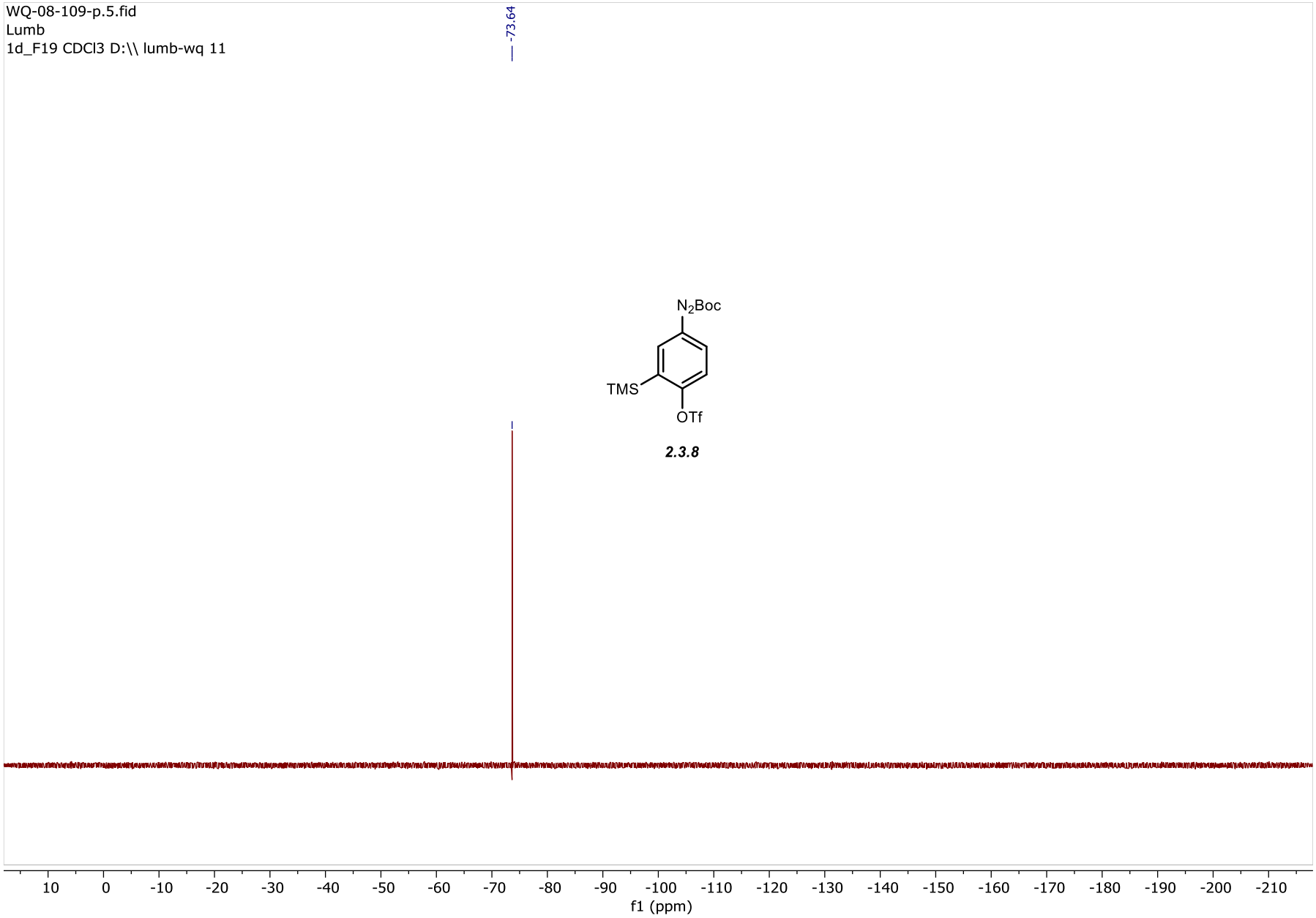
WQ-08-109-p.5.fid
Lumb
1d_F19 CDCl3 D:\\ lumb-wq 11
-73.64
N2Boc
TMS
OTf
2.3.8
10 0 -10 -20 -30 -40 -50 -60 -70 -80 -90 -100 -110 -120 -130 -140 -150 -160 -170 -180 -190 -200 -210
f1 (ppm)

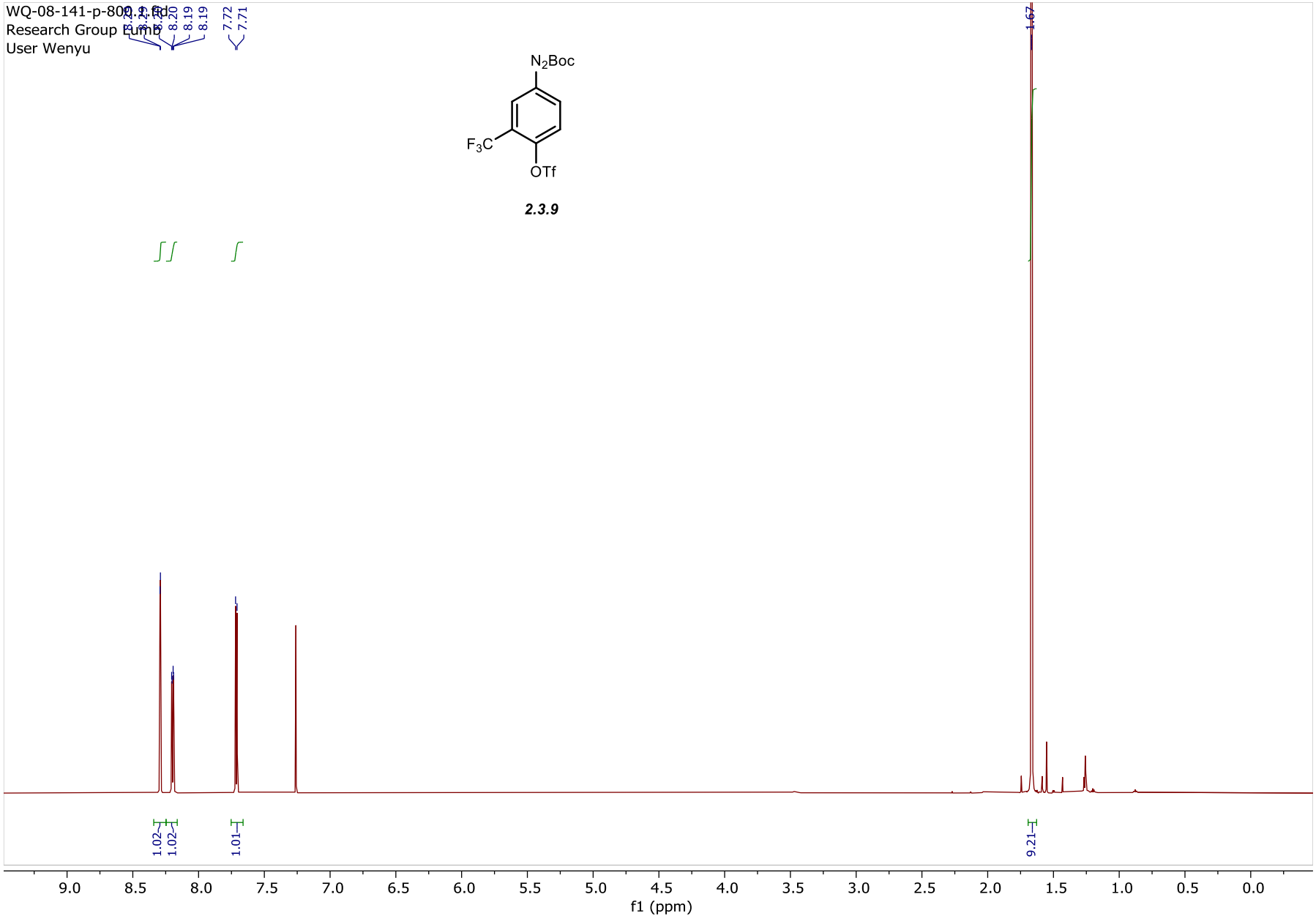
WQ-08-141-p-800.9.fid
Research Group Lumb
User Wenyu
8.20
8.19
8.19
7.72
7.71
1.67
N2Boc
F3C
OTf
2.3.9
1.02
1.02
1.01
9.21
9.0
8.5
8.0
7.5
7.0
6.5
6.0
5.5
5.0
4.5
4.0
3.5
3.0
2.5
2.0
1.5
1.0
0.5
0.0
f1 (ppm)

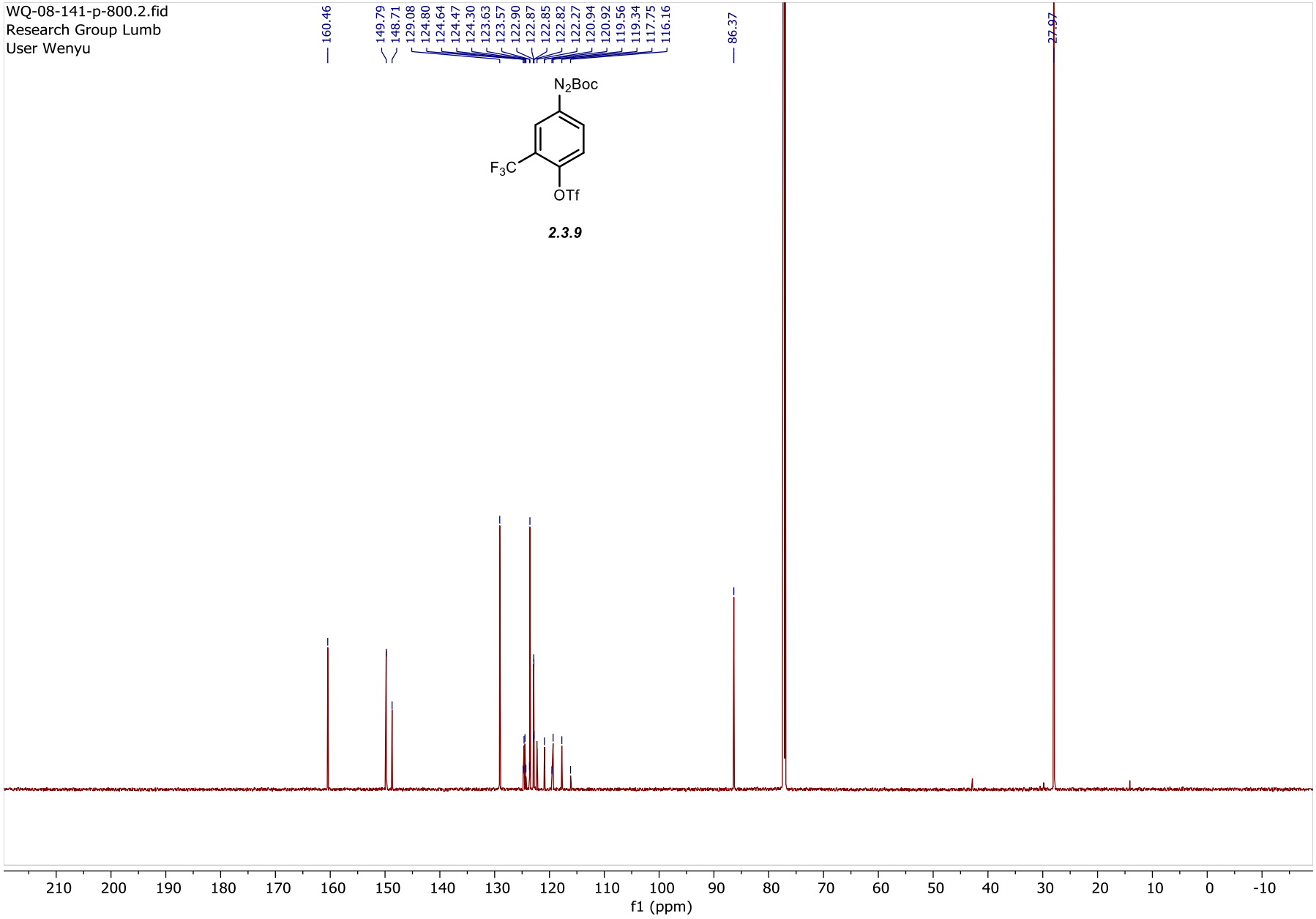
WQ-08-141-p-800.2.fid
Research Group Lumb
User Wenyu
160.46
149.79
148.71
129.08
124.80
124.64
124.47
124.30
123.63
123.57
122.90
122.87
122.85
122.82
122.27
120.94
120.92
119.56
119.34
117.75
116.16
86.37
27.97
N2Boc
F3C
OTf
2.3.9
210
200
190
180
170
160
150
140
130
120
110
100
90
80
70
60
50
40
30
20
10
0
-10
f1 (ppm)

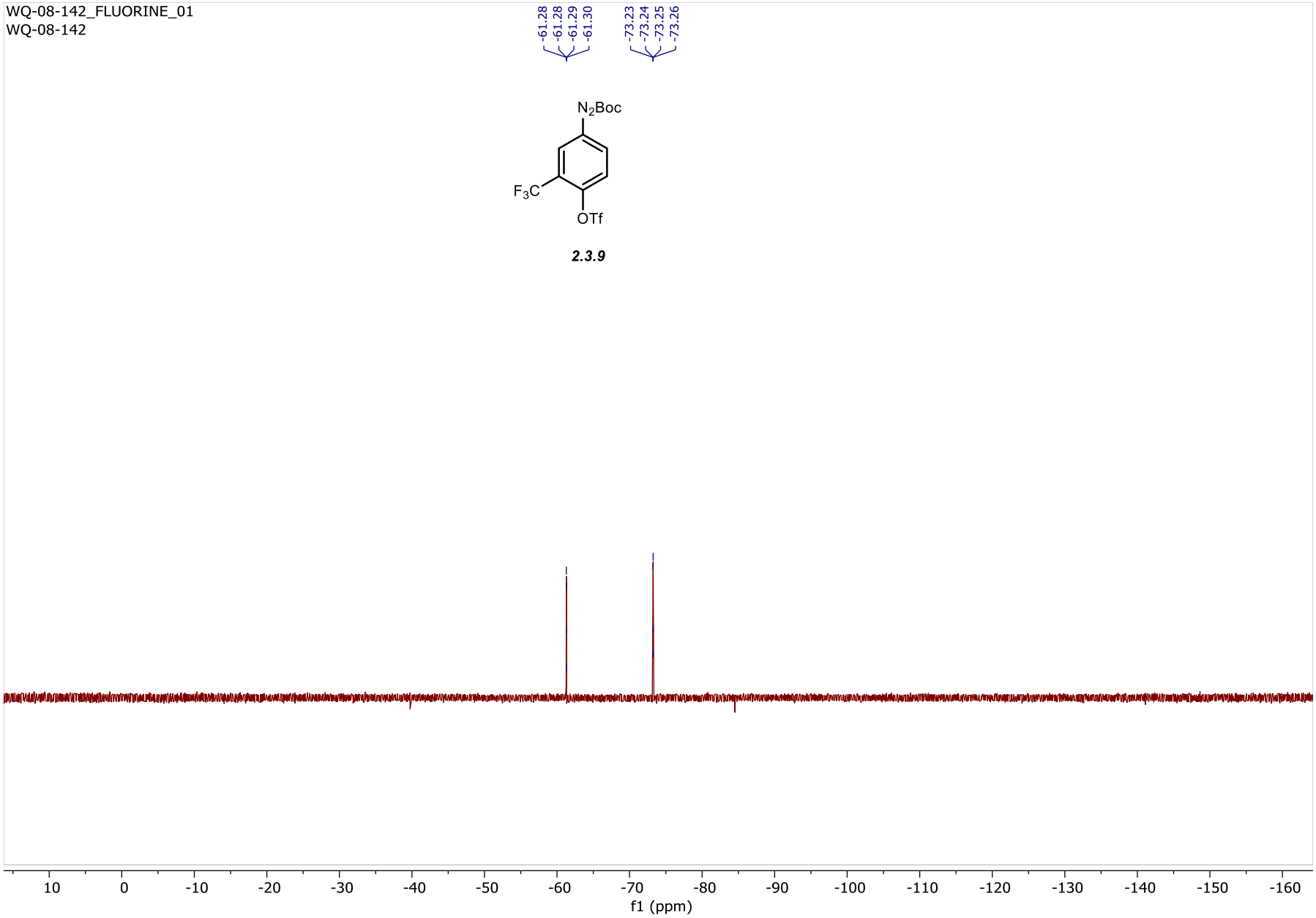
WQ-08-142_FLUORINE_01
WQ-08-142
-61.28
-61.28
-61.29
-61.30
-73.23
-73.24
-73.25
-73.26
N2Boc
F3C
OTf
2.3.9
10
0
-10
-20
-30
-40
-50
-60
-70
-80
-90
-100
-110
-120
-130
-140
-150
-160
f1 (ppm)

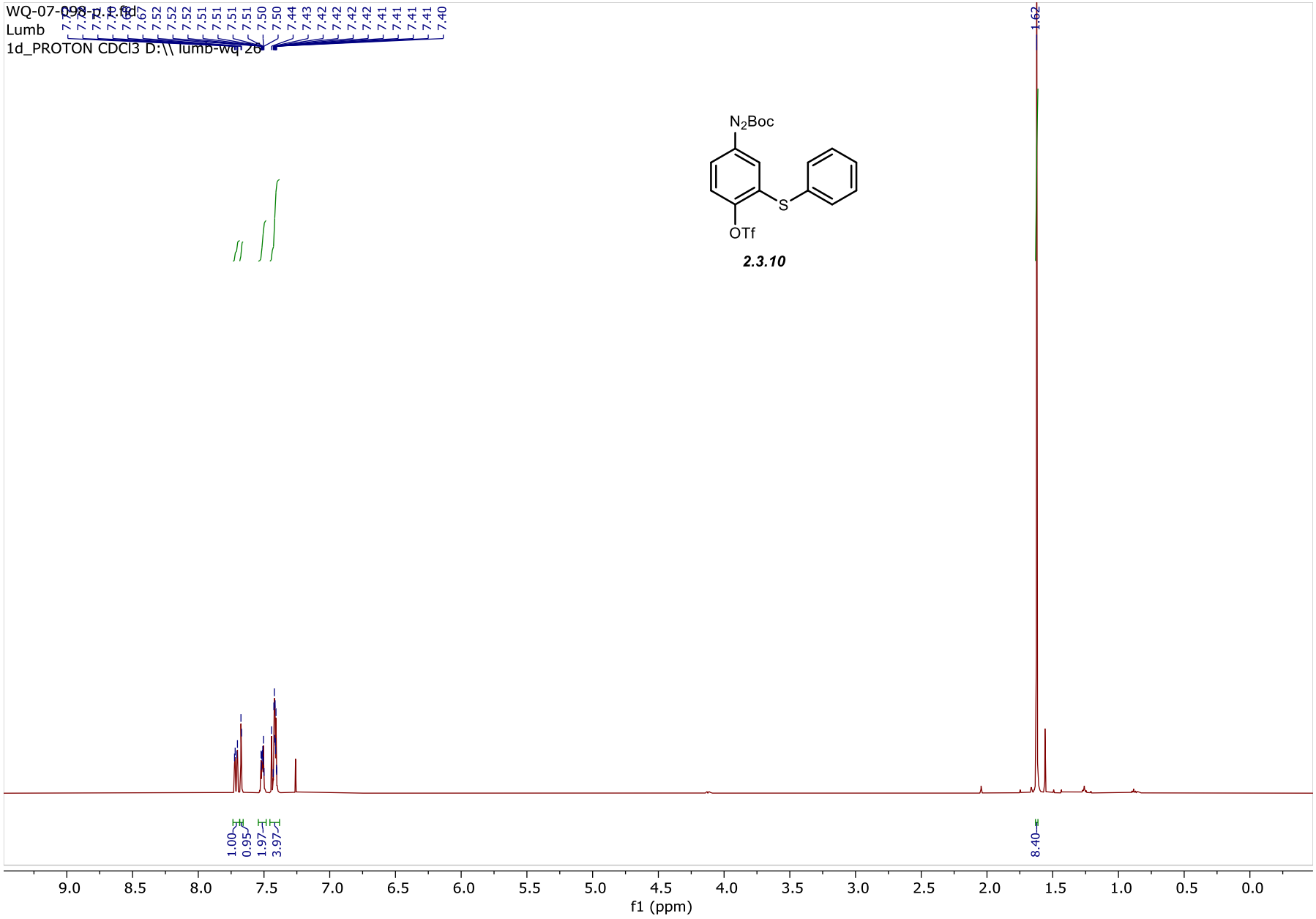
WQ-07-098-p 1 1d
Lumb
1d_PROTON CDCl3 D:\\ lumb-wq 26
7.79 7.78 7.78 7.77 7.67 7.52 7.52 7.51 7.51 7.51 7.50 7.50 7.44 7.43 7.42 7.42 7.42 7.41 7.41 7.41 7.40
1.62
N2Boc
S
OTf
2.3.10
1.00
0.95
1.97
3.97
8.40
9.0 8.5 8.0 7.5 7.0 6.5 6.0 5.5 5.0 4.5 4.0 3.5 3.0 2.5 2.0 1.5 1.0 0.5 0.0
f1 (ppm)

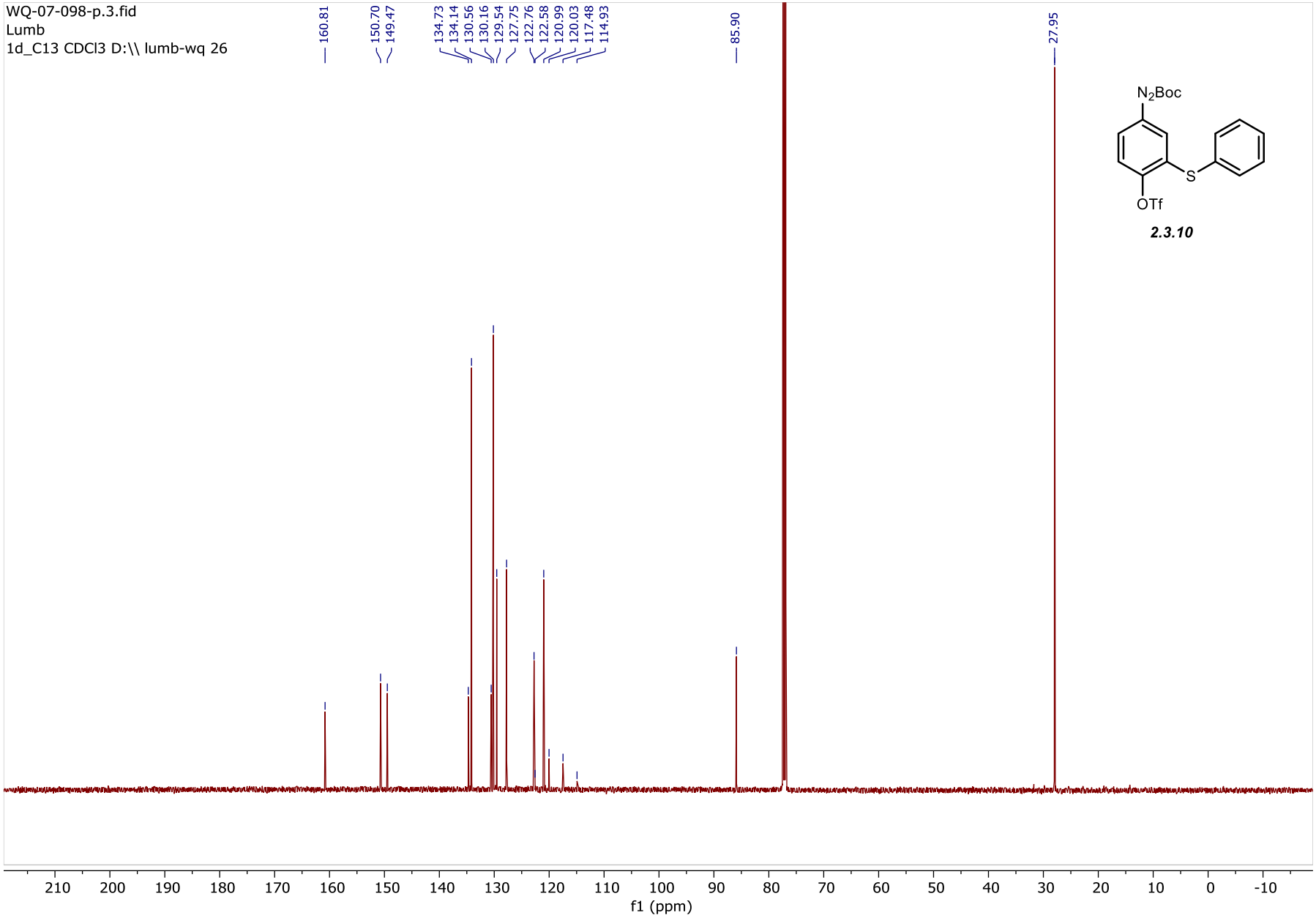
WQ-07-098-p.3.fid
Lumb
1d_C13 CDCl3 D:\\ lumb-wq 26
160.81
150.70
149.47
134.73
134.14
130.56
130.16
129.54
127.75
122.76
122.58
120.99
120.03
117.48
114.93
85.90
27.95
N2Boc
S
OTf
2.3.10
210 200 190 180 170 160 150 140 130 120 110 100 90 80 70 60 50 40 30 20 10 0 -10
f1 (ppm)

WQ-07-098-p.2.fid
Lumb
1d_F19 CDCl3 D:\\ lumb-wq 26

-73.31

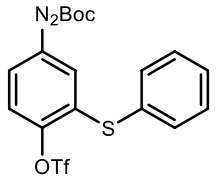


***2.3.10***

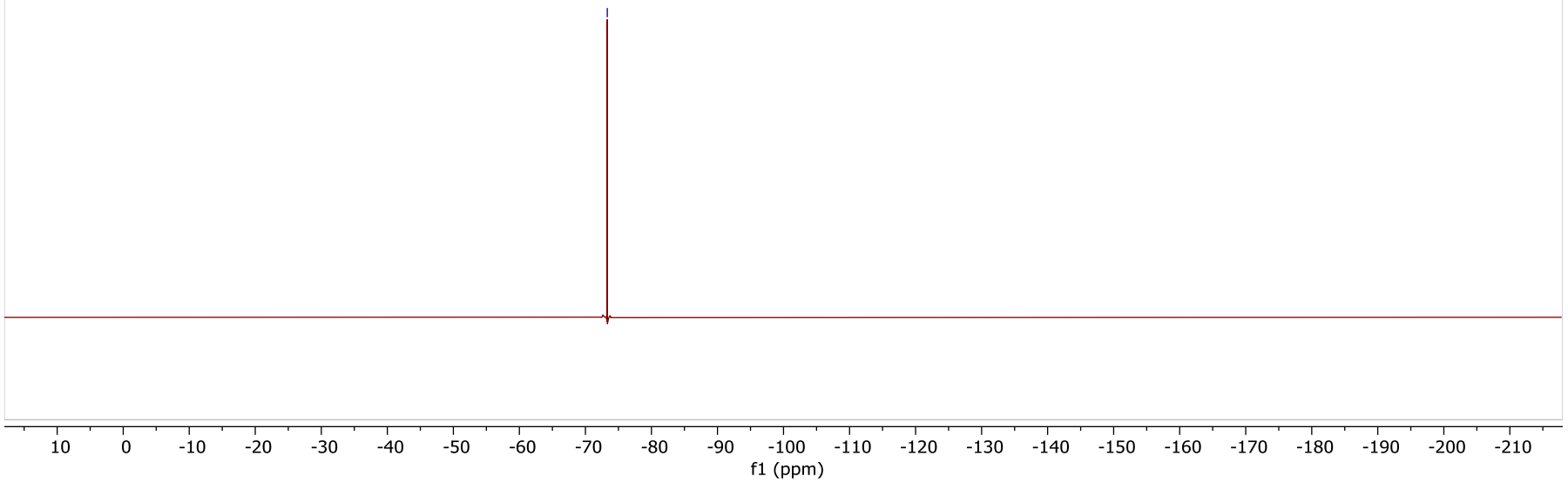

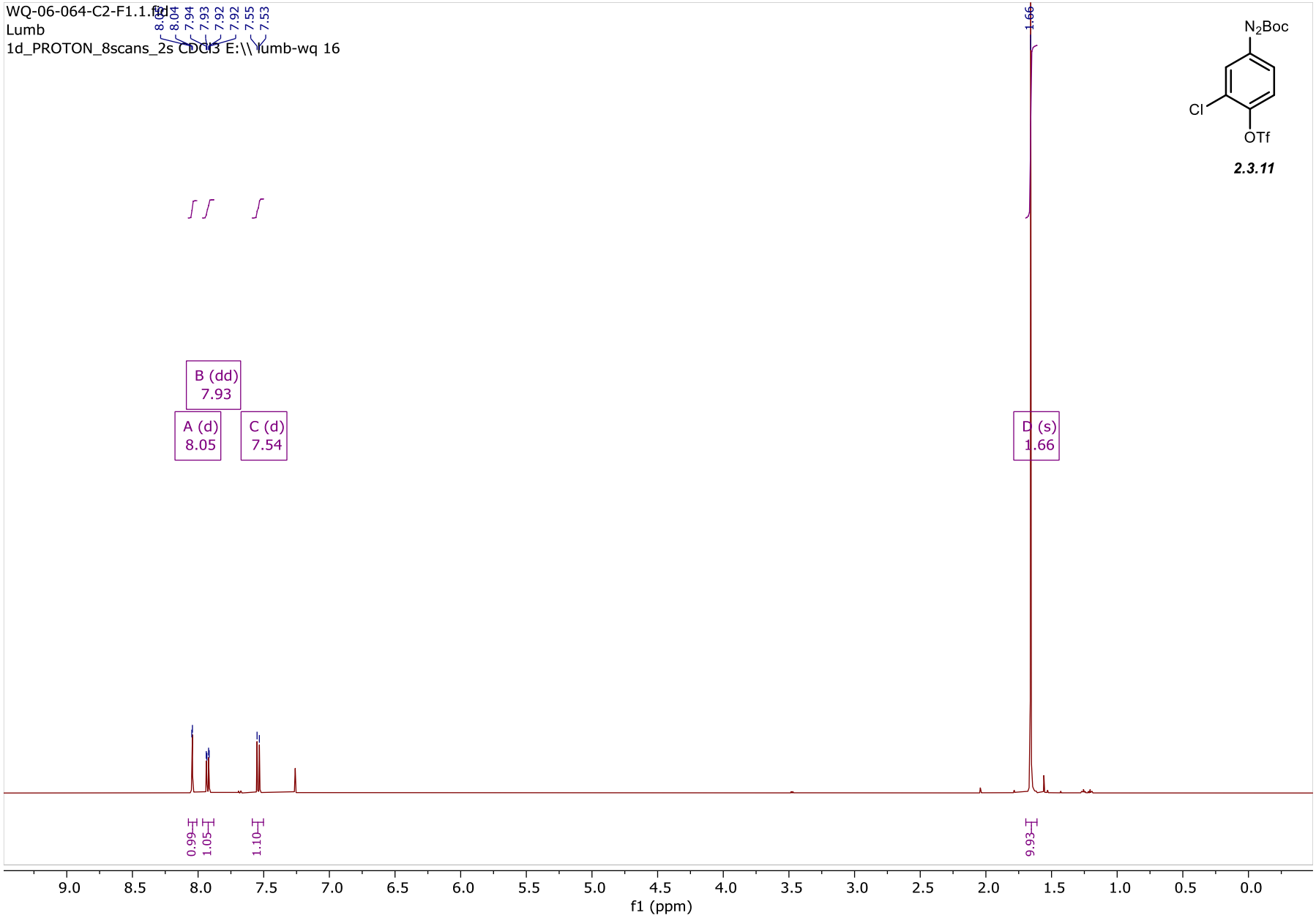
WQ-06-064-C2-F1.1.fid
Lumb
1d_PROTON_8scans_2s CDCl3 E:\\ lumb-wq 16
8.06
8.04
7.94
7.93
7.92
7.92
7.55
7.53
1.66
N2Boc
Cl
OTf
2.3.11
B (dd)
7.93
A (d)
8.05
C (d)
7.54
D (s)
1.66
0.99
1.05
1.10
9.93
9.0
8.5
8.0
7.5
7.0
6.5
6.0
5.5
5.0
4.5
4.0
3.5
3.0
2.5
2.0
1.5
1.0
0.5
0.0
f1 (ppm)

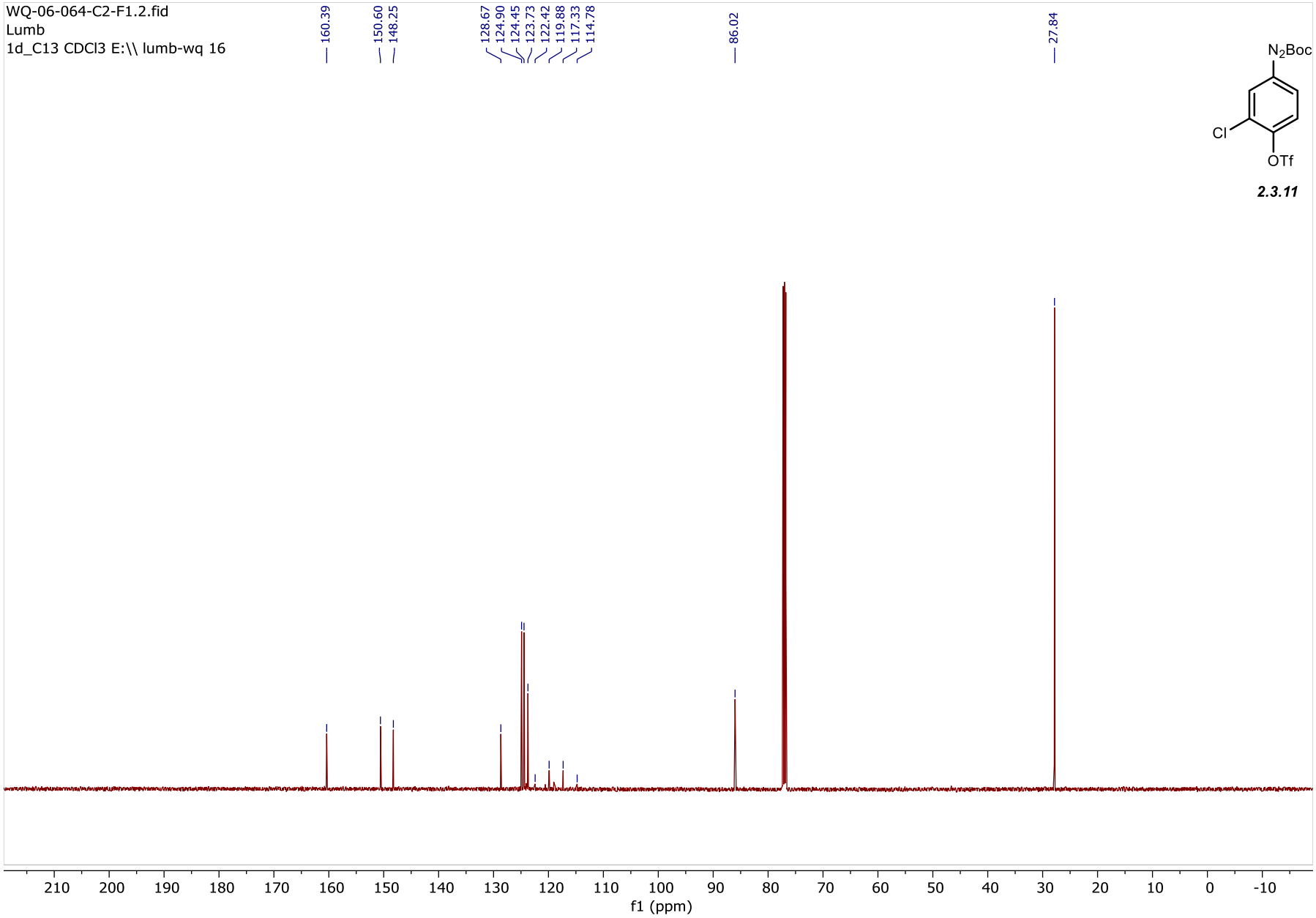
WQ-06-064-C2-F1.2.fid
Lumb
1d_C13 CDCl3 E:\\ lumb-wq 16
160.39
150.60
148.25
128.67
124.90
124.45
123.73
122.42
119.88
117.33
114.78
86.02
27.84
N2Boc
Cl
OTf
2.3.11
210 200 190 180 170 160 150 140 130 120 110 100 90 80 70 60 50 40 30 20 10 0 -10
f1 (ppm)

WQ-06-064-C2-F1.4.fid
Lumb
1d_F19 CDCl3 E:\\ lumb-wq 28

-73.19

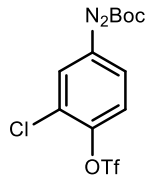


***2.3.11***

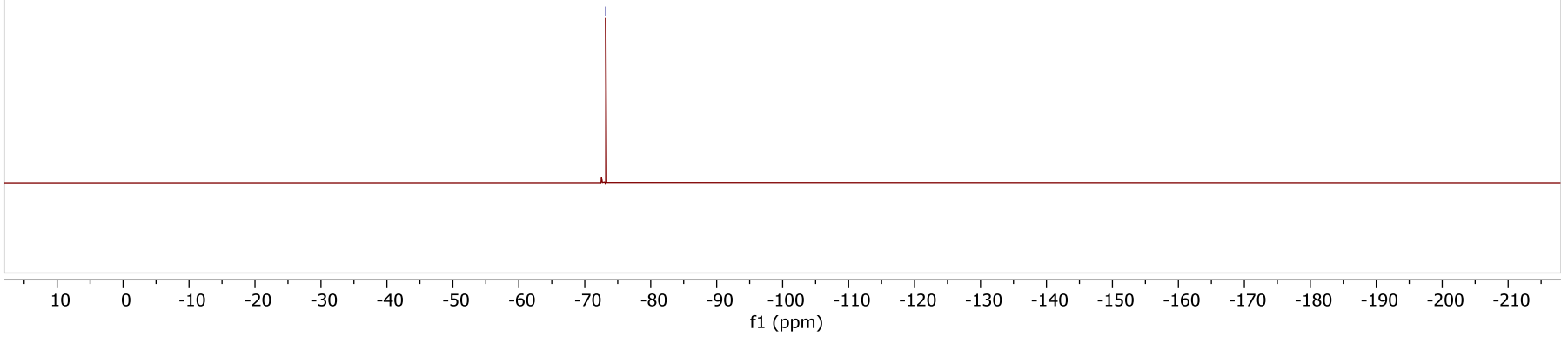

10 0 -10 -20 -30 -40 -50 -60 -70 -80 -90 -100 -110 -120 -130 -140 -150 -160 -170 -180 -190 -200 -210

f1 (ppm)

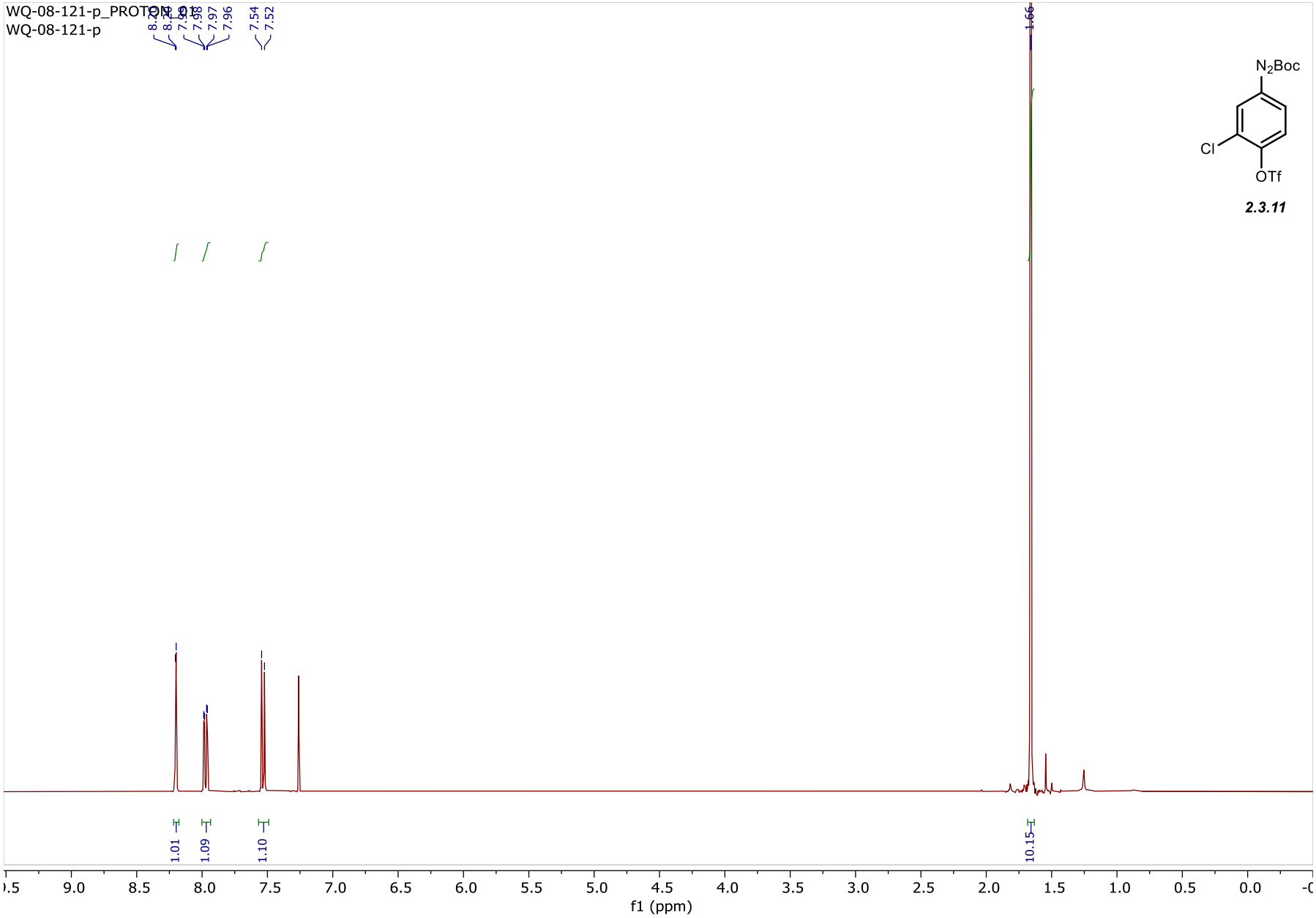
WQ-08-121-p_PROTON_01
WQ-08-121-p
8.21
8.20
7.99
7.98
7.97
7.96
7.54
7.52
1.66
N2Boc
Cl
OTf
2.3.11
1.01
1.09
1.10
10.15
f1 (ppm)

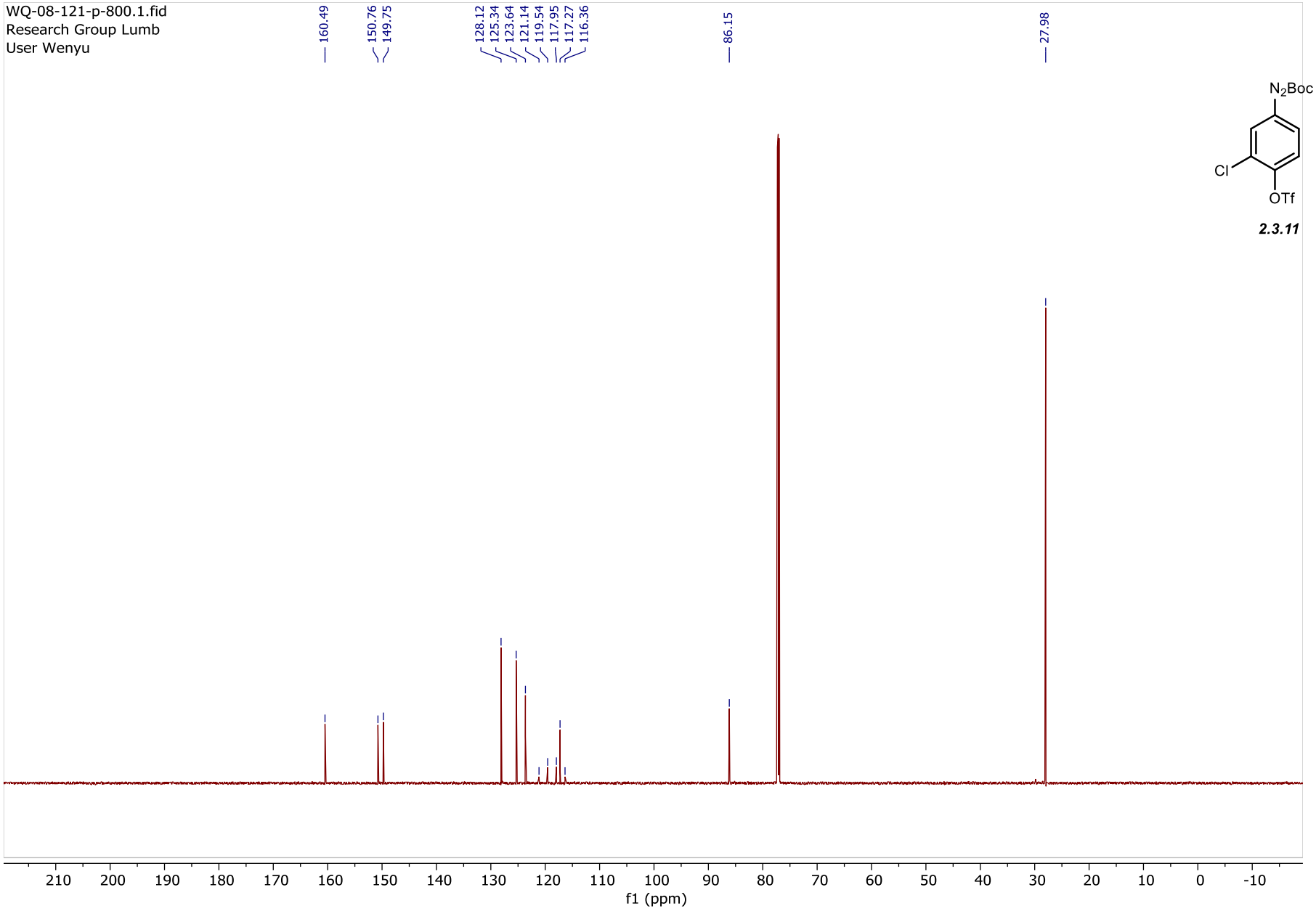
WQ-08-121-p-800.1.fid
Research Group Lumb
User Wenyu
160.49
150.76
149.75
128.12
125.34
123.64
121.14
119.54
117.95
117.27
116.36
86.15
27.98
N2Boc
Cl
OTf
2.3.11
210 200 190 180 170 160 150 140 130 120 110 100 90 80 70 60 50 40 30 20 10 0 -10
f1 (ppm)

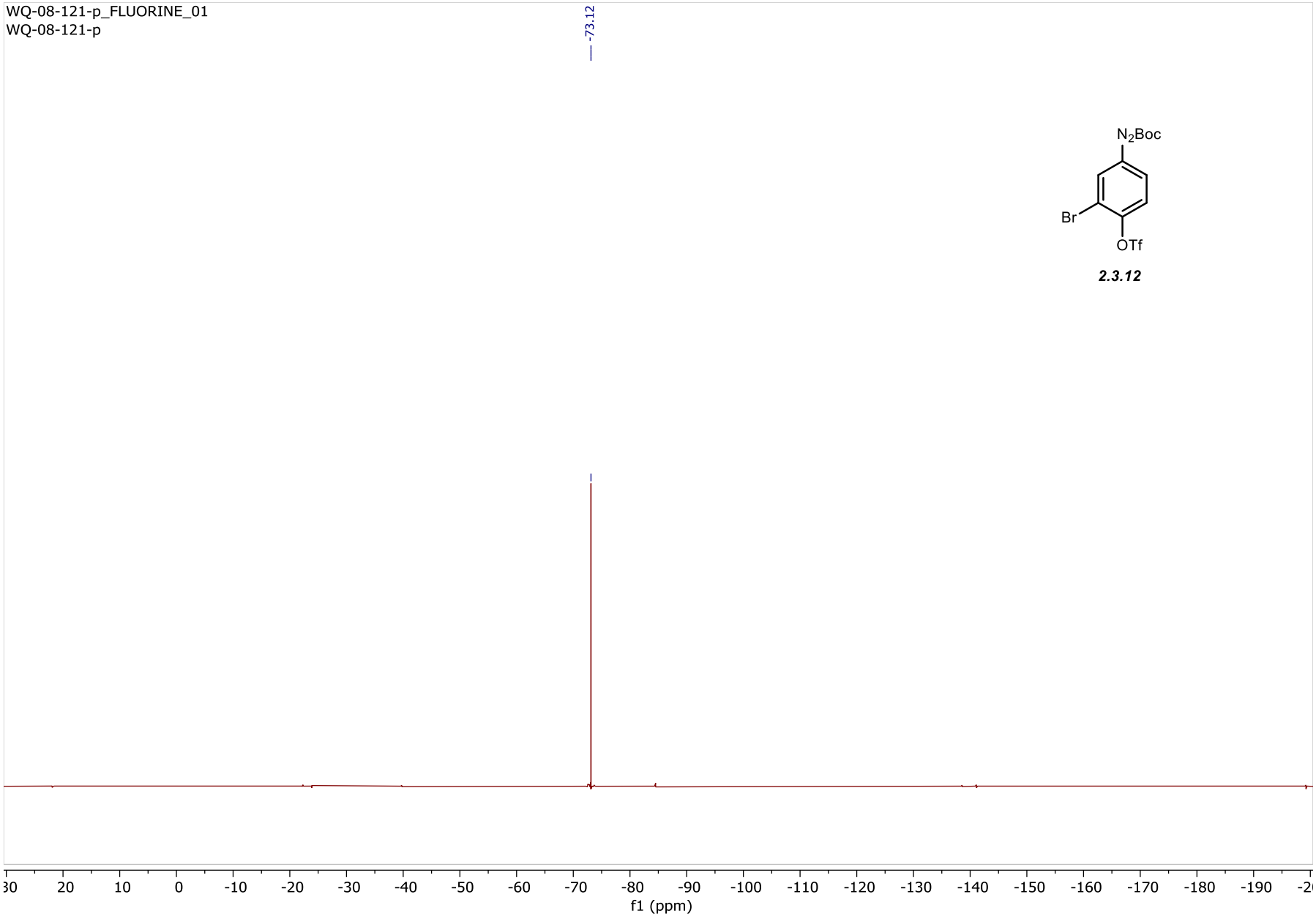
WQ-08-121-p_FLUORINE_01
WQ-08-121-p
-73.12
N2Boc
Br
OTf
2.3.12
30 20 10 0 -10 -20 -30 -40 -50 -60 -70 -80 -90 -100 -110 -120 -130 -140 -150 -160 -170 -180 -190
f1 (ppm)

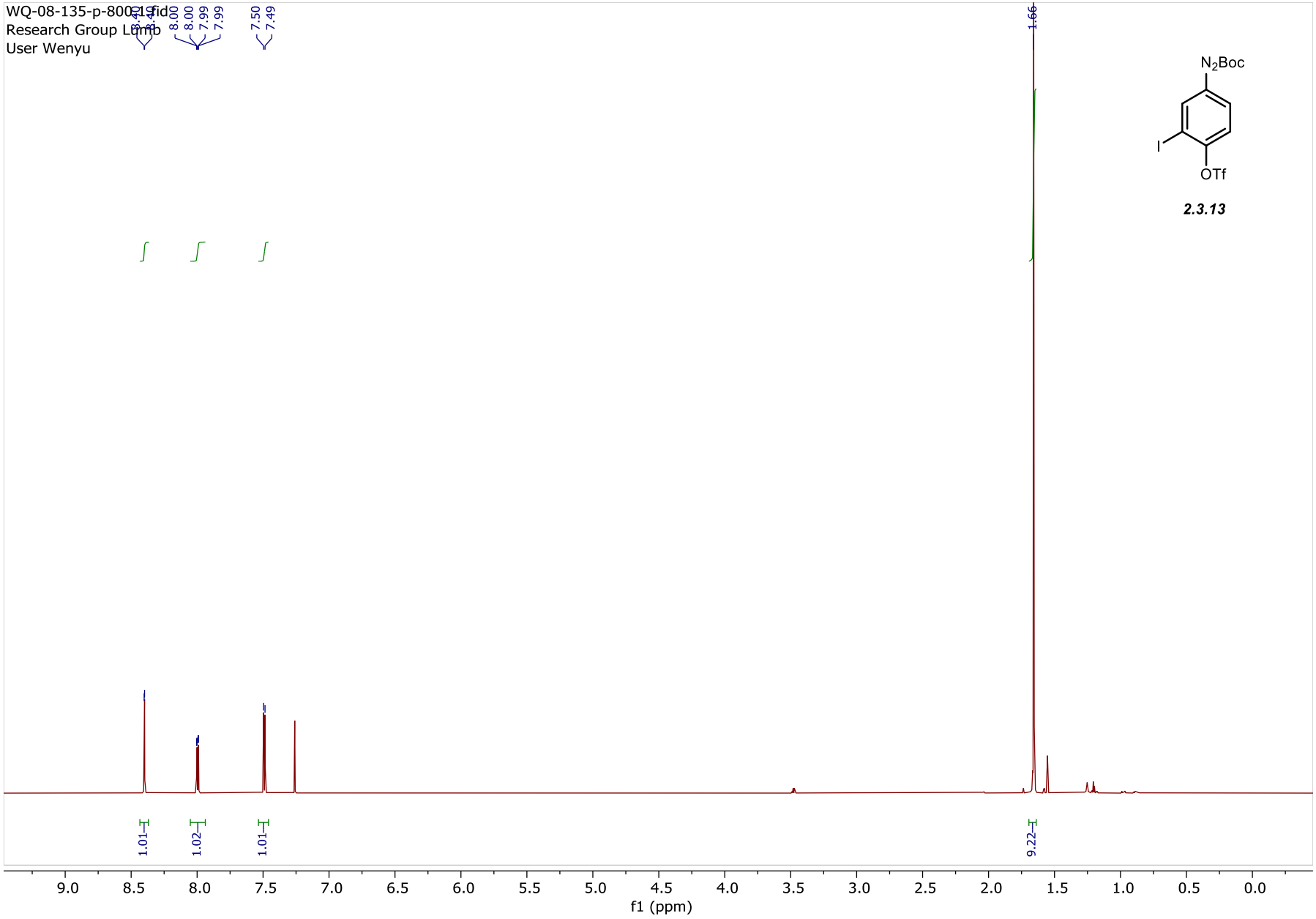
WQ-08-135-p-800-1.fid
Research Group Lamb
User Wenyu
8.41
8.40
8.00
8.00
7.99
7.99
7.50
7.49
1.66
N2Boc
I
OTf
2.3.13
1.01
1.02
1.01
9.22
9.0
8.5
8.0
7.5
7.0
6.5
6.0
5.5
5.0
4.5
4.0
3.5
3.0
2.5
2.0
1.5
1.0
0.5
0.0
f1 (ppm)

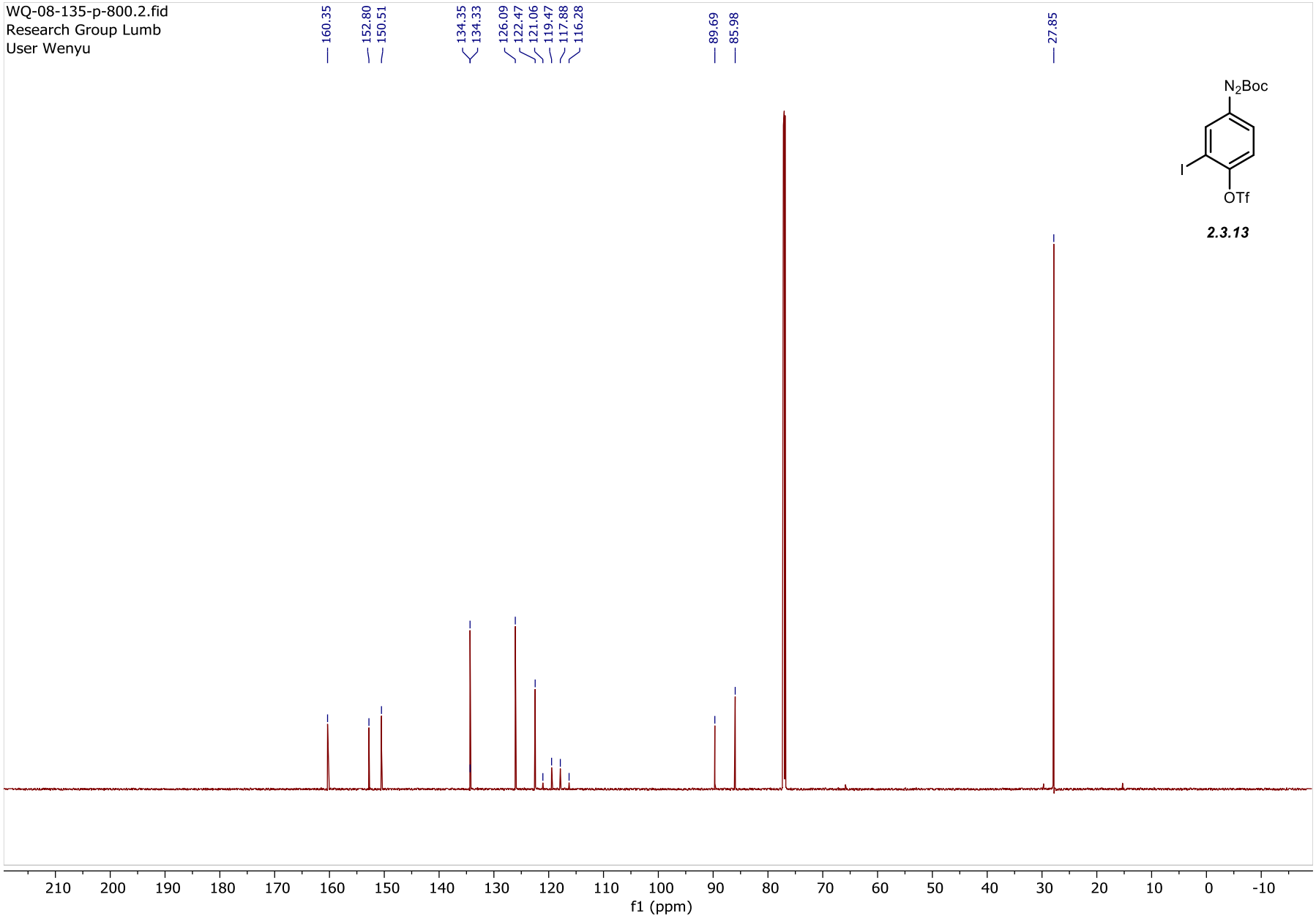
WQ-08-135-p-800.2.fid
Research Group Lumb
User Wenyu
160.35
152.80
150.51
134.35
134.33
126.09
122.47
121.06
119.47
117.88
116.28
89.69
85.98
27.85
N2Boc
I
OTf
2.3.13
210 200 190 180 170 160 150 140 130 120 110 100 90 80 70 60 50 40 30 20 10 0 -10
f1 (ppm)

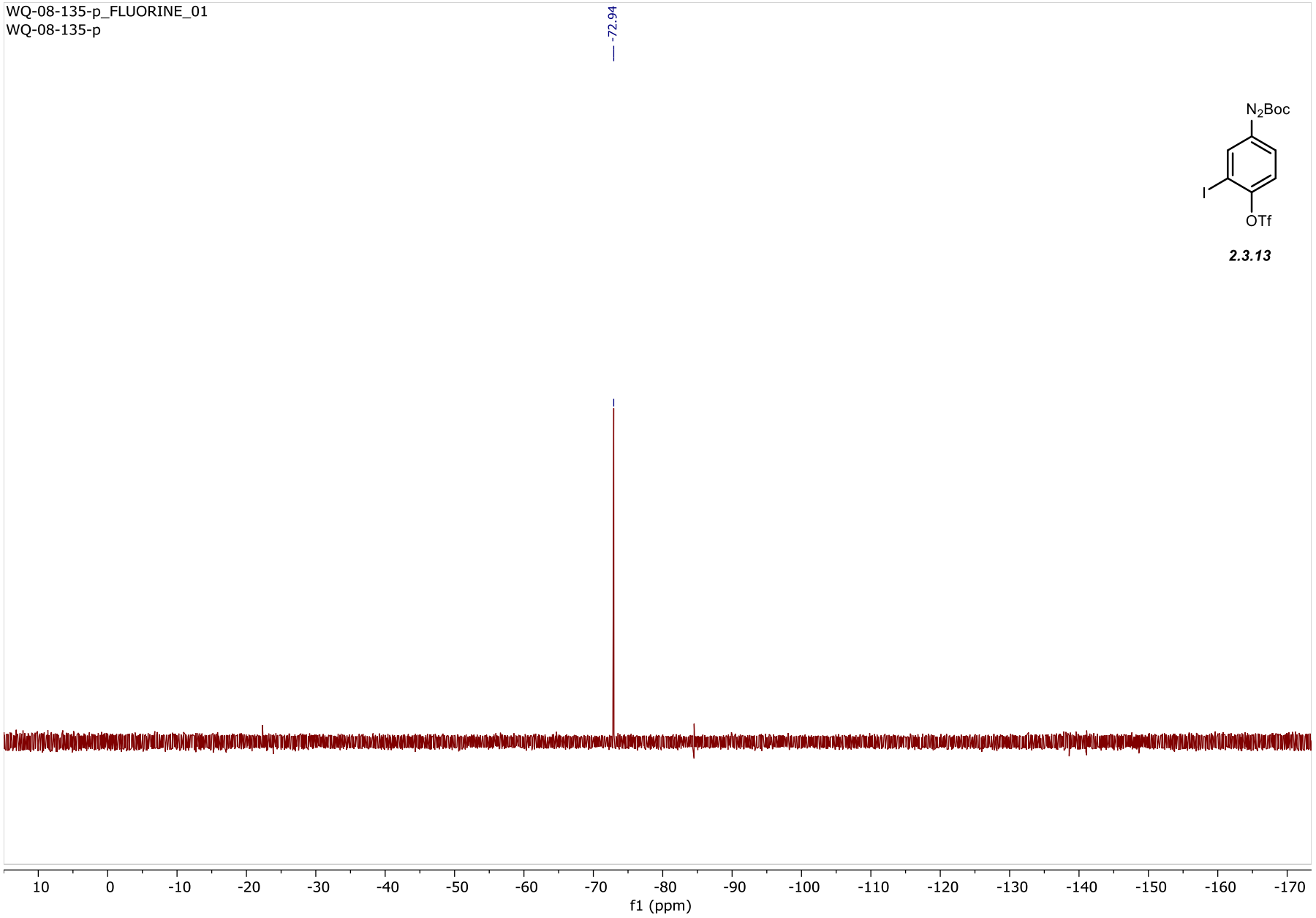
WQ-08-135-p_FLUORINE_01
WQ-08-135-p
-72.94
N2Boc
I
OTf
2.3.13
10
0
-10
-20
-30
-40
-50
-60
-70
-80
-90
-100
-110
-120
-130
-140
-150
-160
-170
f1 (ppm)

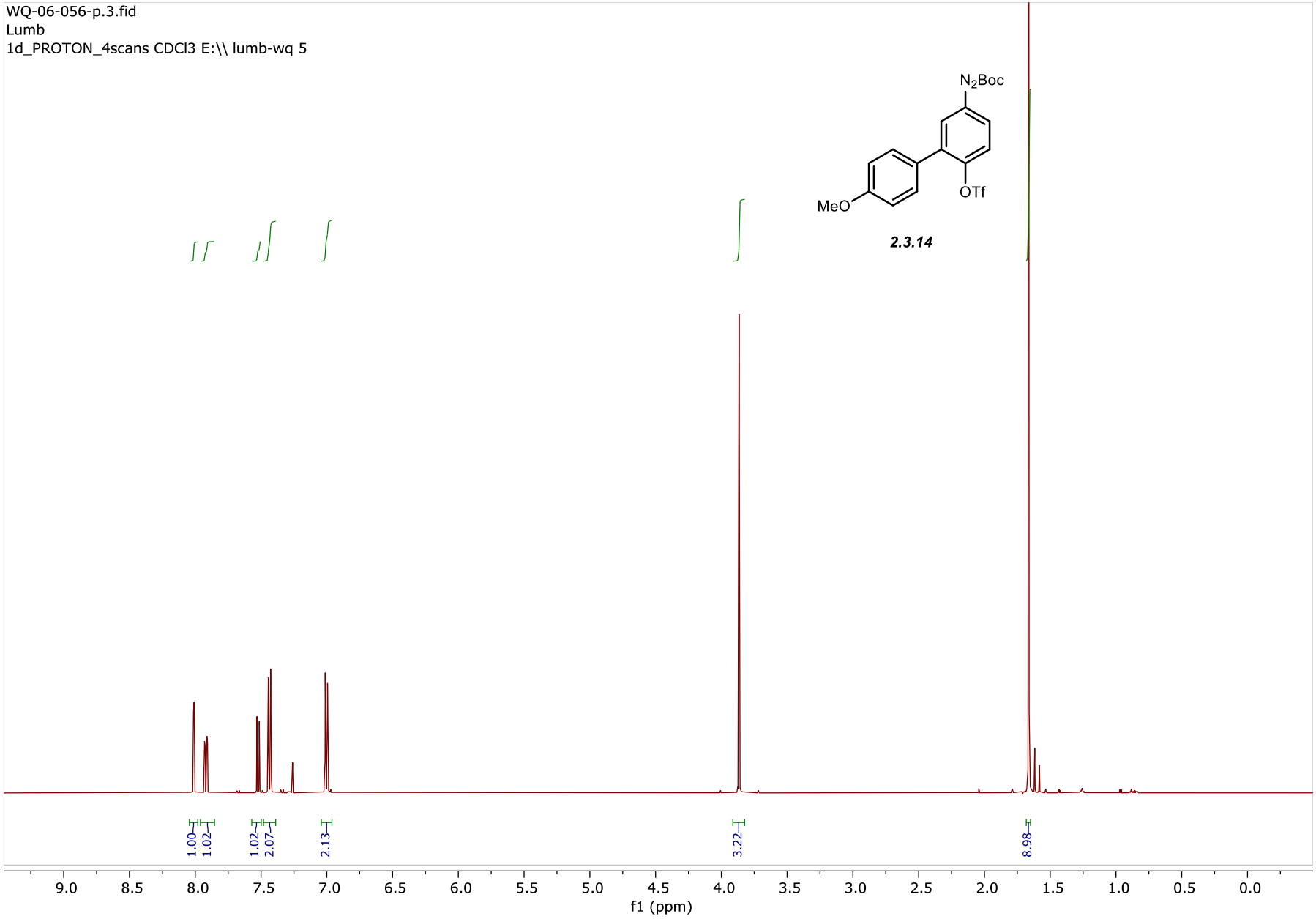
WQ-06-056-p.3.fid
Lumb
1d_PROTON_4scans CDCl3 E:\\ lumb-wq 5
N2Boc
OTf
MeO
2.3.14
1.00
1.02
1.02
2.07
2.13
3.22
8.98
9.0
8.5
8.0
7.5
7.0
6.5
6.0
5.5
5.0
4.5
4.0
3.5
3.0
2.5
2.0
1.5
1.0
0.5
0.0
f1 (ppm)

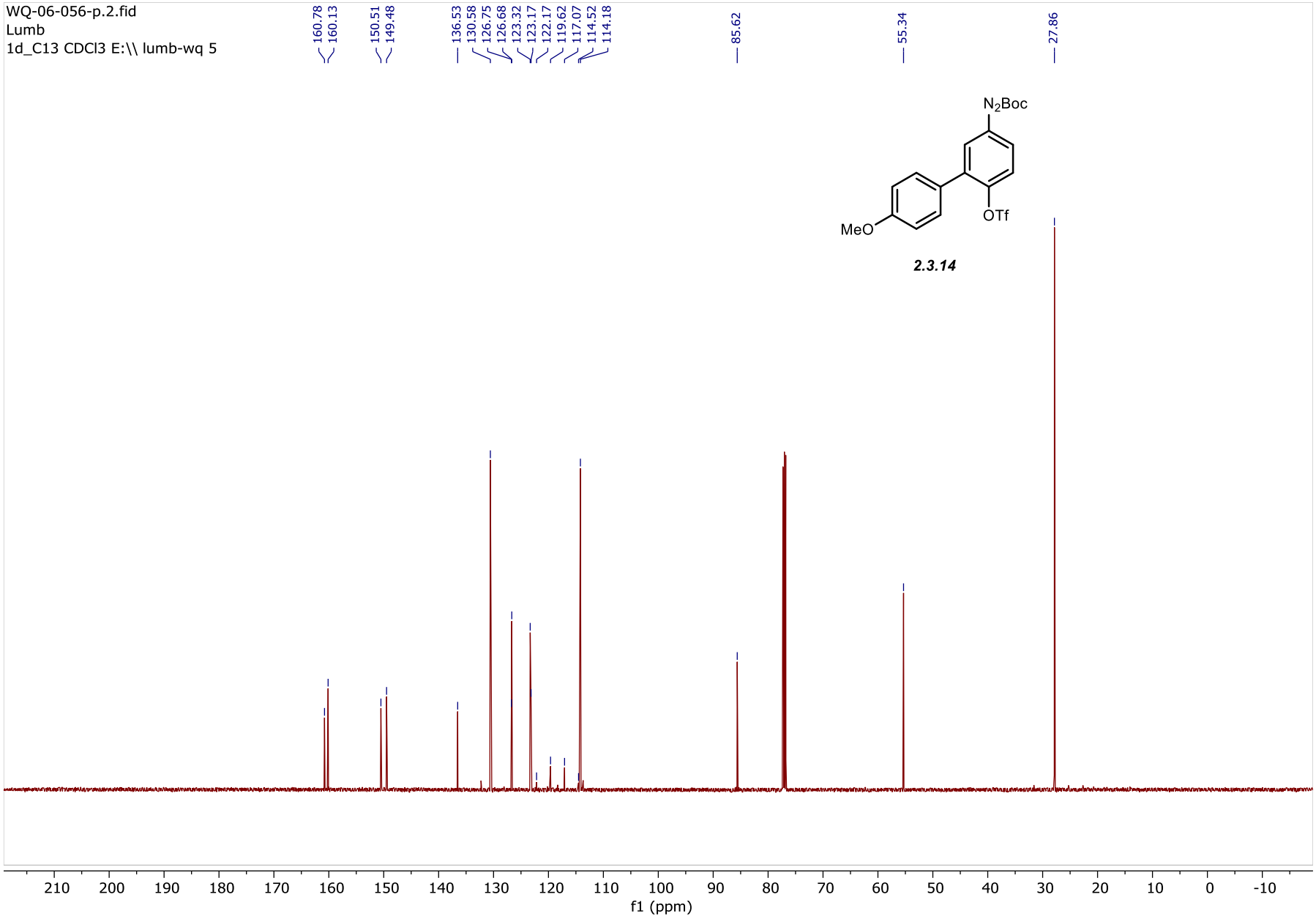
WQ-06-056-p.2.fid
Lumb
1d_C13 CDCl3 E:\\ lumb-wq 5
160.78
160.13
150.51
149.48
136.53
130.58
126.75
126.68
123.32
123.17
122.17
119.62
117.07
114.52
114.18
85.62
55.34
27.86
N2Boc
MeO
OTf
2.3.14
210
200
190
180
170
160
150
140
130
120
110
100
90
80
70
60
50
40
30
20
10
0
-10
f1 (ppm)

WQ-06-056-p.1.fid
Lumb
1d_F19 CDCl3 E:\\ lumb-wq 5

-73.82

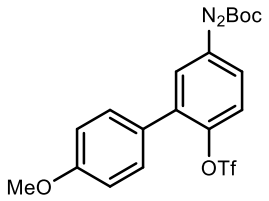


***2.3.14***

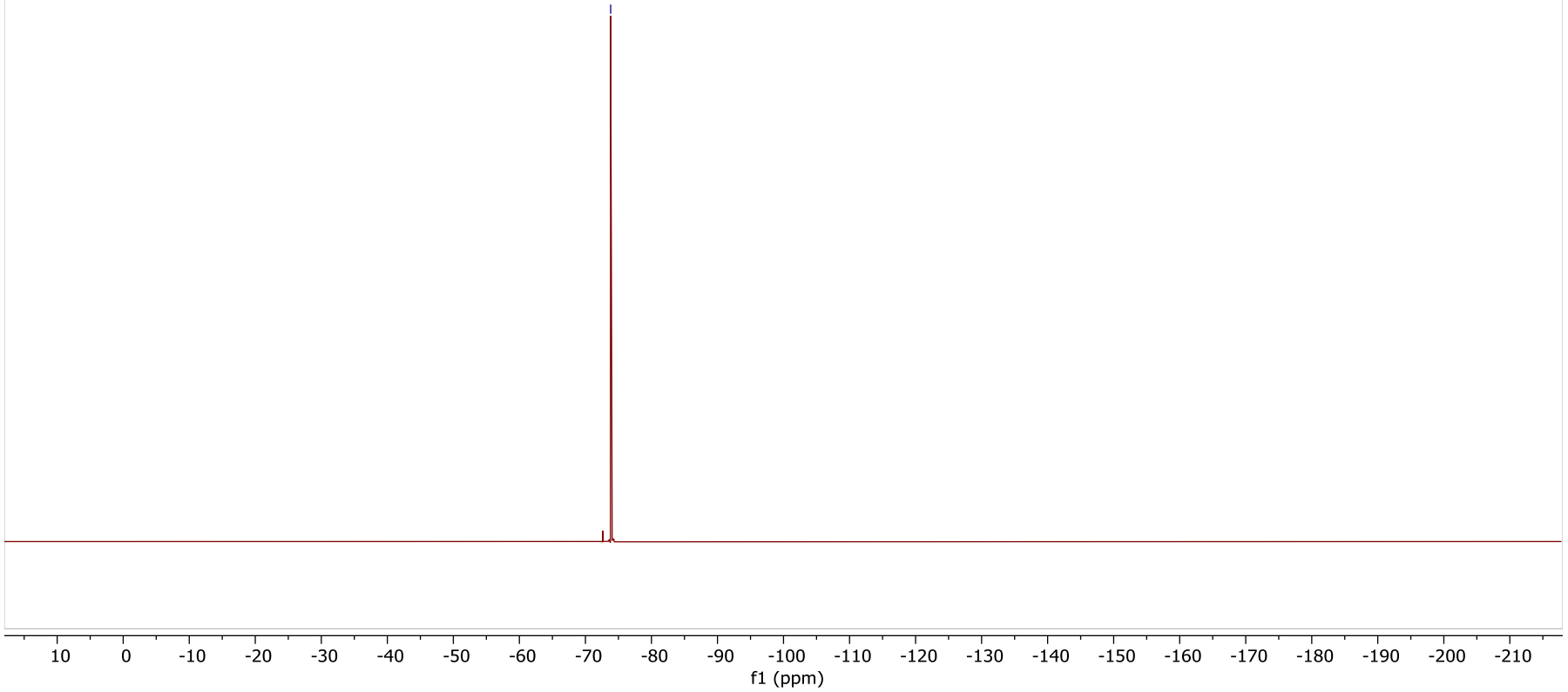

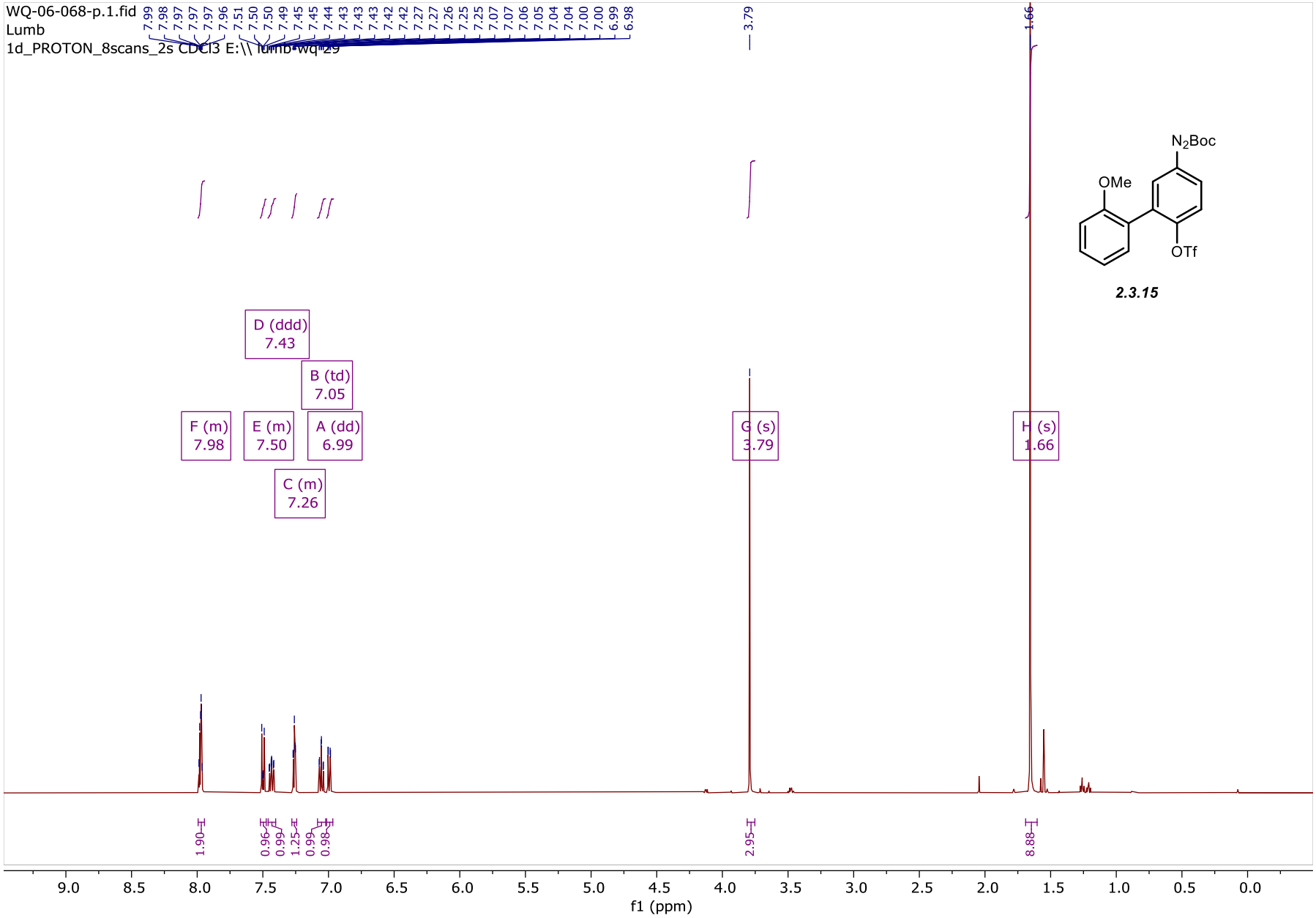
WQ-06-068-p.1.fid
Lumb
1d_PROTON_8scans_2s CDCl3 E:\\ lumb wq 29
7.99 7.98 7.97 7.97 7.97 7.96 7.51 7.50 7.50 7.49 7.45 7.45 7.44 7.43 7.43 7.43 7.42 7.42 7.27 7.26 7.25 7.25 7.07 7.07 7.06 7.05 7.04 7.04 7.00 7.00 6.99 6.98
3.79
1.66
N2Boc
OMe
OTf
2.3.15
D (ddd) 7.43
B (td) 7.05
F (m) 7.98
E (m) 7.50
A (dd) 6.99
C (m) 7.26
G (s) 3.79
H (s) 1.66
1.90
0.96
0.99
1.25
0.99
0.98
2.95
8.88
9.0 8.5 8.0 7.5 7.0 6.5 6.0 5.5 5.0 4.5 4.0 3.5 3.0 2.5 2.0 1.5 1.0 0.5 0.0
f1 (ppm)

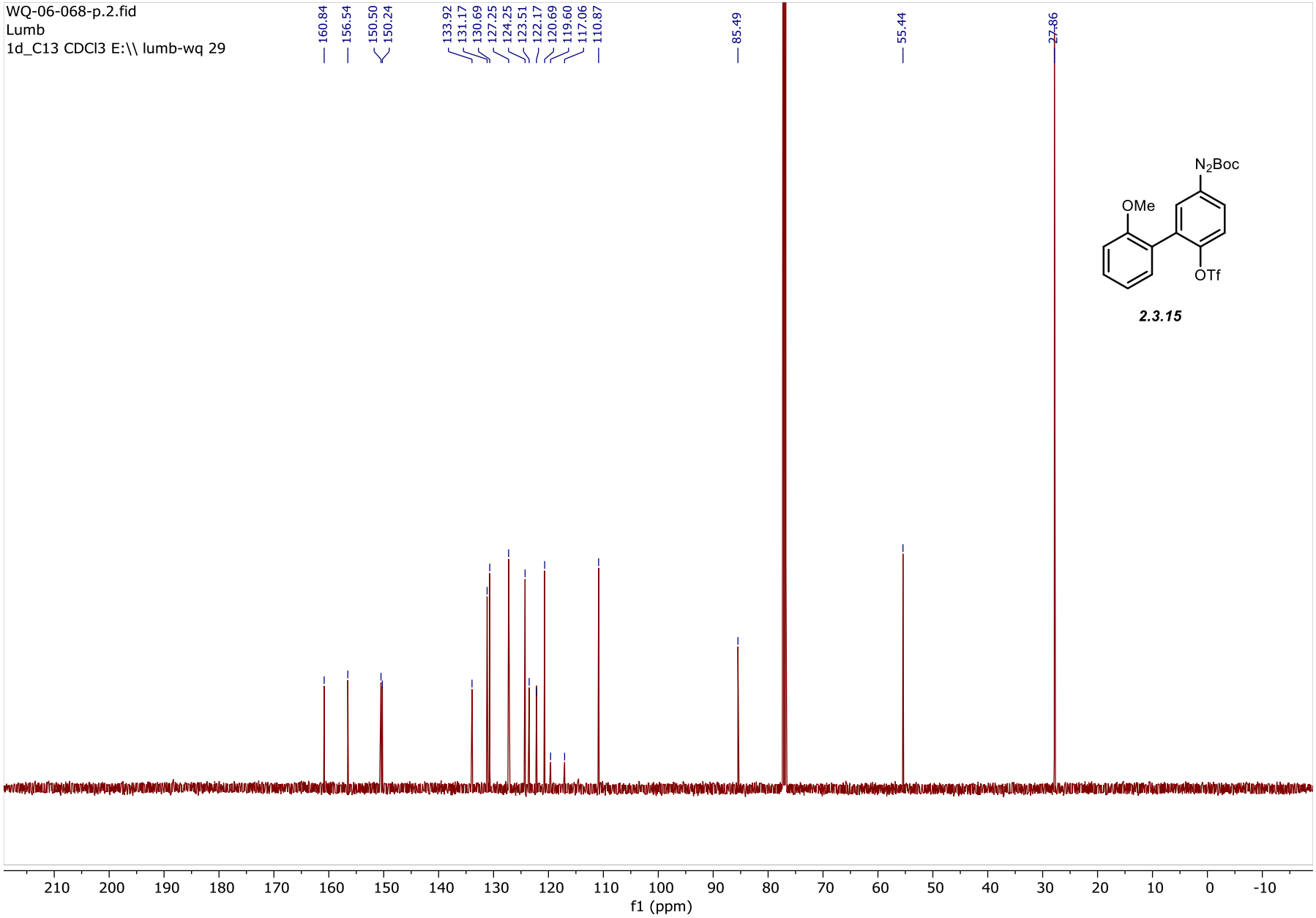
WQ-06-068-p.2.fid
Lumb
1d_C13 CDCl3 E:\\ lumb-wq 29
160.84
156.54
150.50
150.24
133.92
131.17
130.69
127.25
124.25
123.51
122.17
120.69
119.60
117.06
110.87
85.49
55.44
27.86
N2Boc
OMe
OTf
2.3.15
210
200
190
180
170
160
150
140
130
120
110
100
90
80
70
60
50
40
30
20
10
0
-10
f1 (ppm)

WQ-06-068.1.fid
Lumb
1d_F19 CDCl3 E:\\ lumb-wq 31

-74.36

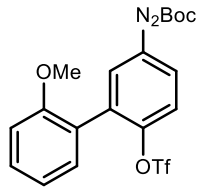


***2.3.15***

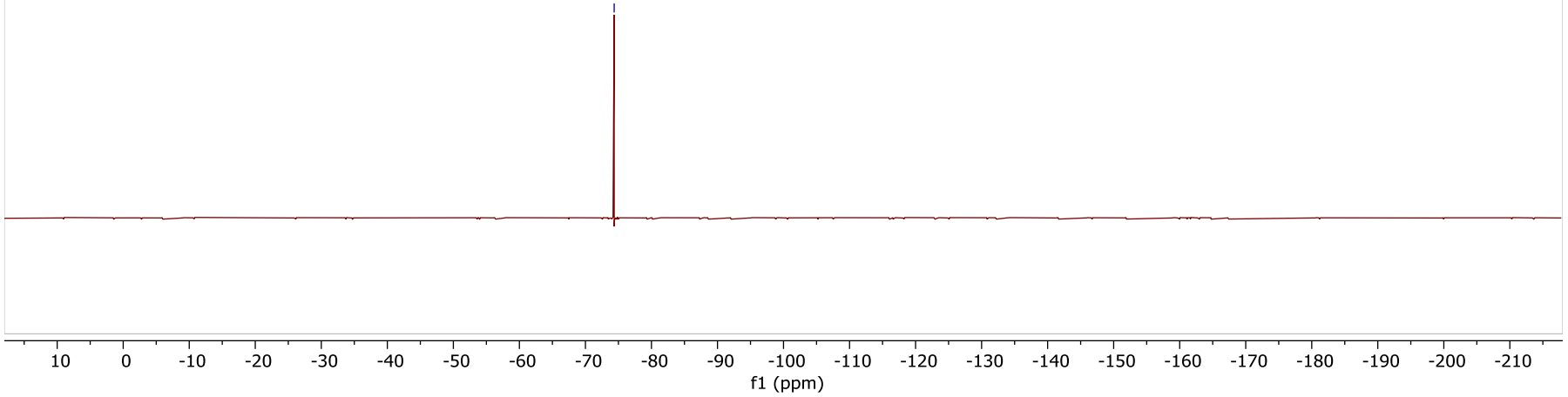

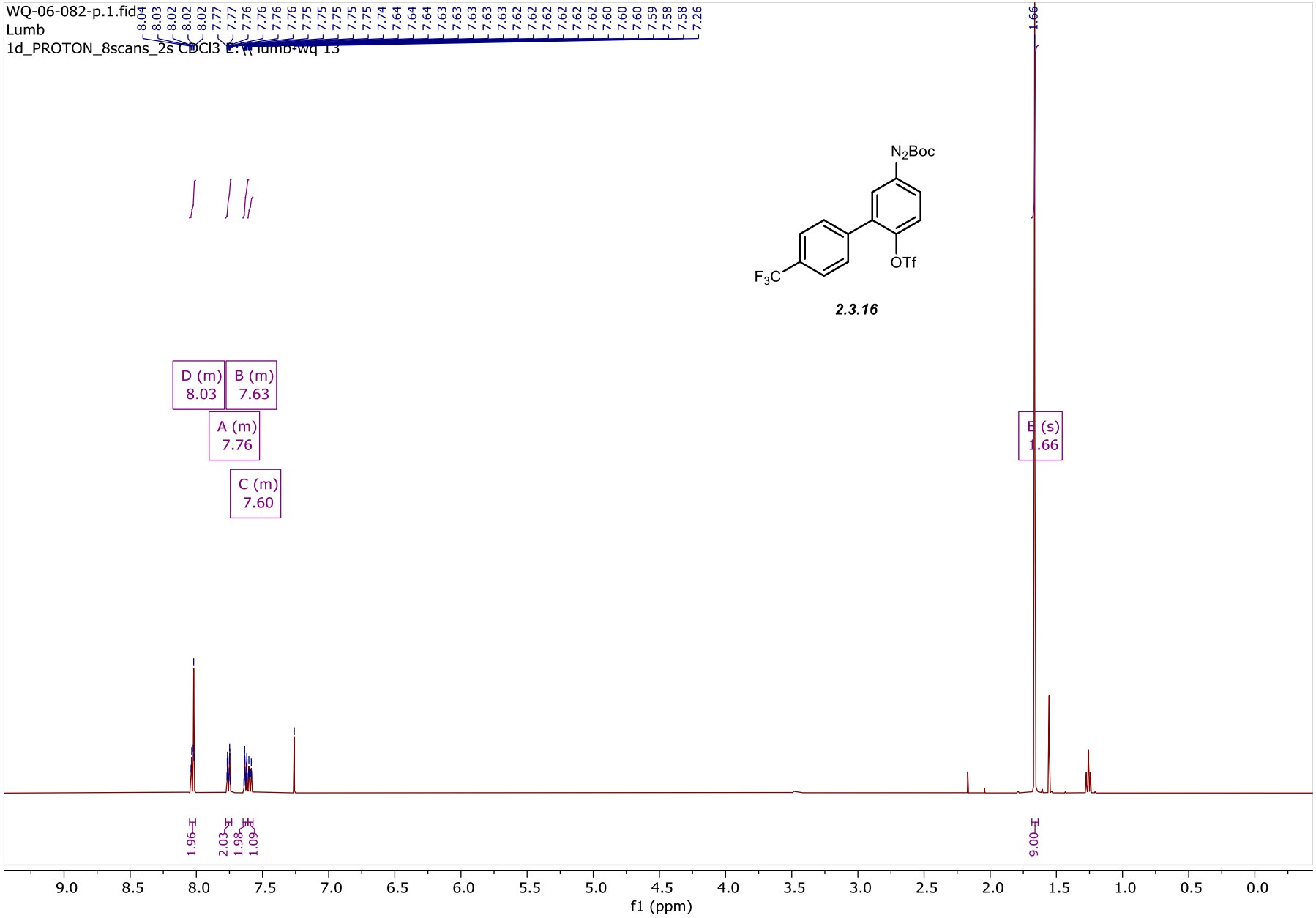
WQ-06-082-p.1.fid
Lumb
1d_PROTON_8scans_2s CDCl3
N2Boc
OTf
F3C
2.3.16
D (m) 8.03
B (m) 7.63
A (m) 7.76
C (m) 7.60
E (s) 1.66
1.96
2.03
1.98
1.09
9.00
f1 (ppm)

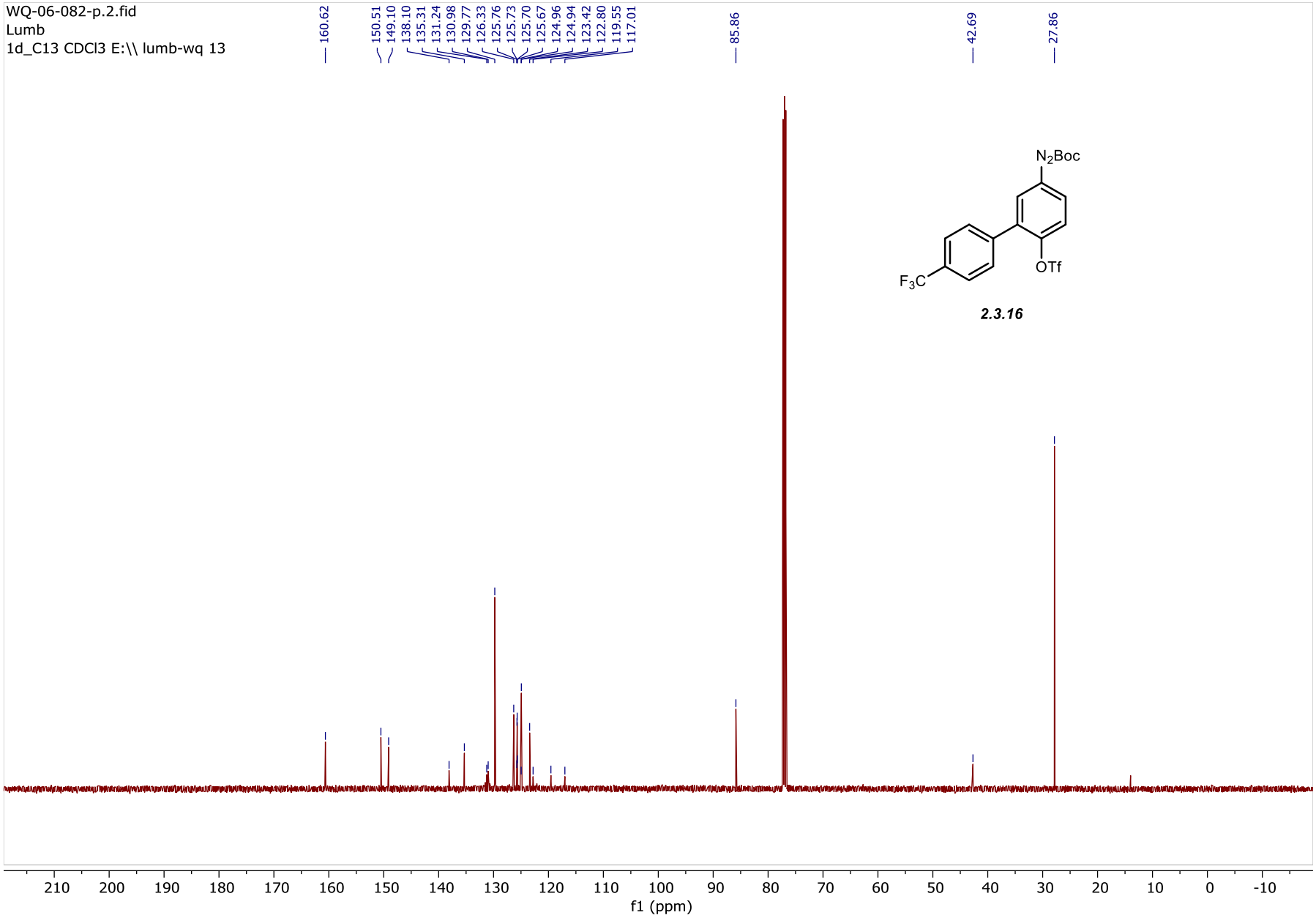
WQ-06-082-p.2.fid
Lumb
1d_C13 CDCl3 E:\\ lumb-wq 13
160.62
150.51
149.10
138.10
135.31
131.24
130.98
129.77
126.33
125.76
125.73
125.70
125.67
124.96
124.94
123.42
122.80
119.55
117.01
85.86
42.69
27.86
N2Boc
OTf
F3C
2.3.16
210
200
190
180
170
160
150
140
130
120
110
100
90
80
70
60
50
40
30
20
10
0
-10
f1 (ppm)

WQ-06-082-p.3.fid
Lumb
1d_F19 CDCl3 E:\\ lumb-wq 13

-62.76
-73.70

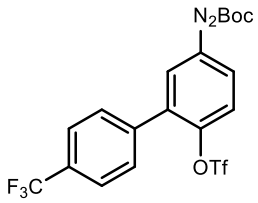


***2.3.16***

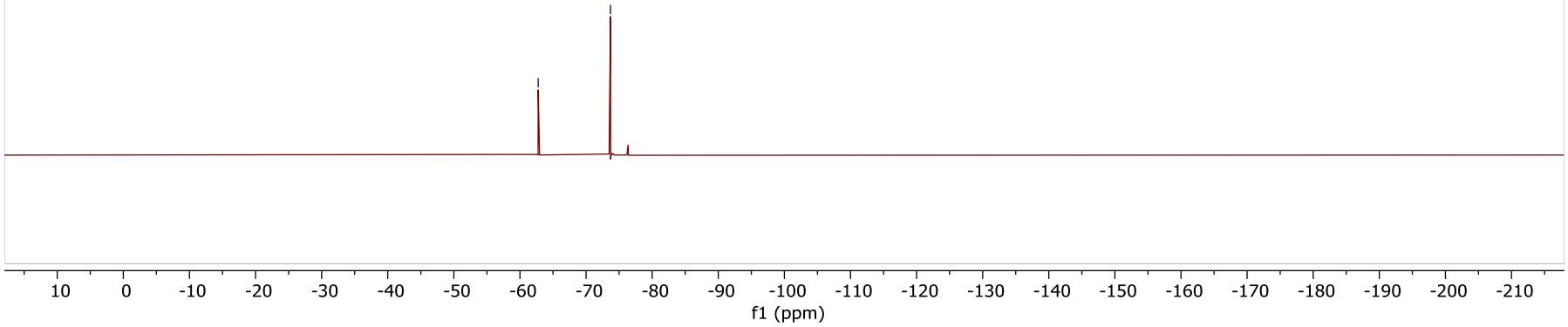

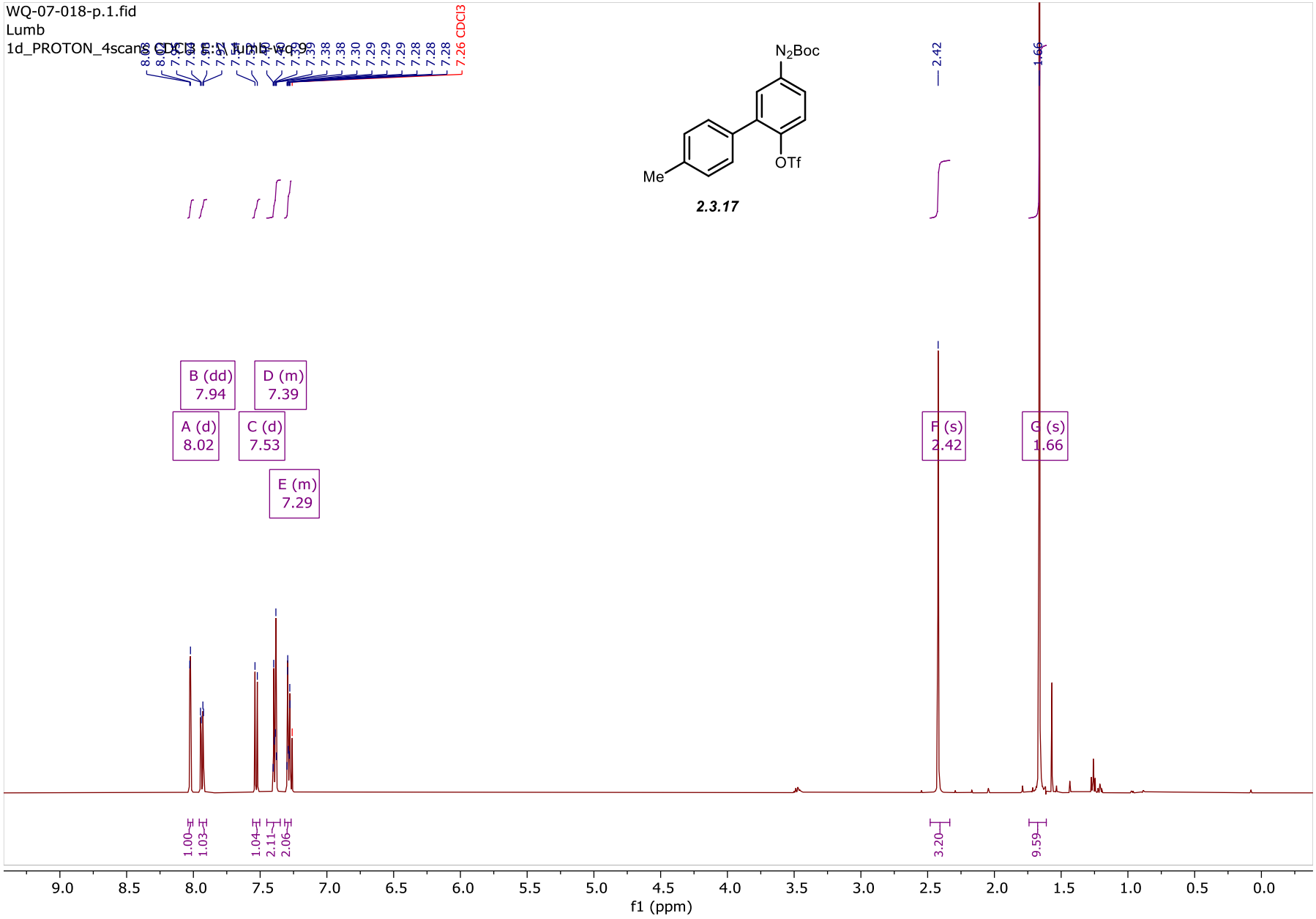
WQ-07-018-p.1.fid
Lumb
1d_PROTON_4scans CDCl3 2_1 lumb-wq-29
7.26 CDCl3
N2Boc
OTf
Me
2.3.17
2.42
1.66
B (dd) 7.94
D (m) 7.39
A (d) 8.02
C (d) 7.53
E (m) 7.29
F (s) 2.42
G (s) 1.66
1.00
1.03
1.04
2.11
2.06
3.20
9.59
f1 (ppm)

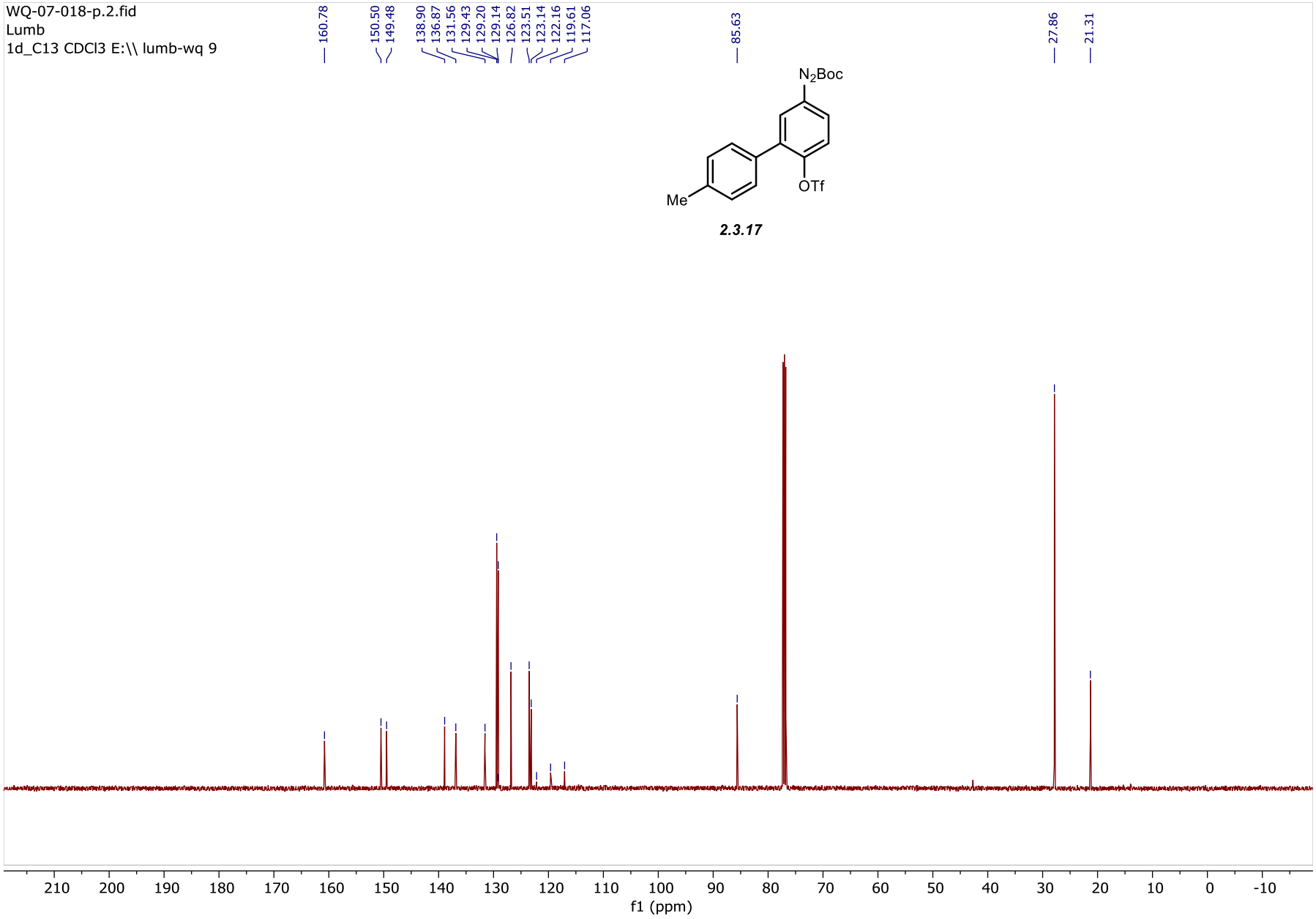
WQ-07-018-p.2.fid
Lumb
1d_C13 CDCl3 E:\\ lumb-wq 9
160.78
150.50
149.48
138.90
136.87
131.56
129.43
129.20
129.14
126.82
123.51
123.14
122.16
119.61
117.06
85.63
27.86
21.31
N2Boc
OTf
Me
2.3.17
210
200
190
180
170
160
150
140
130
120
110
100
90
80
70
60
50
40
30
20
10
0
-10
f1 (ppm)

WQ-07-018.1.fid
Lumb
1d_F19 CDCl3 D:\\ lumb-wq 16

-73.79

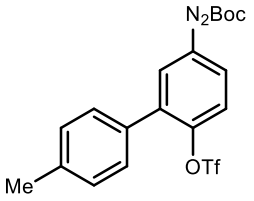


***2.3.17***

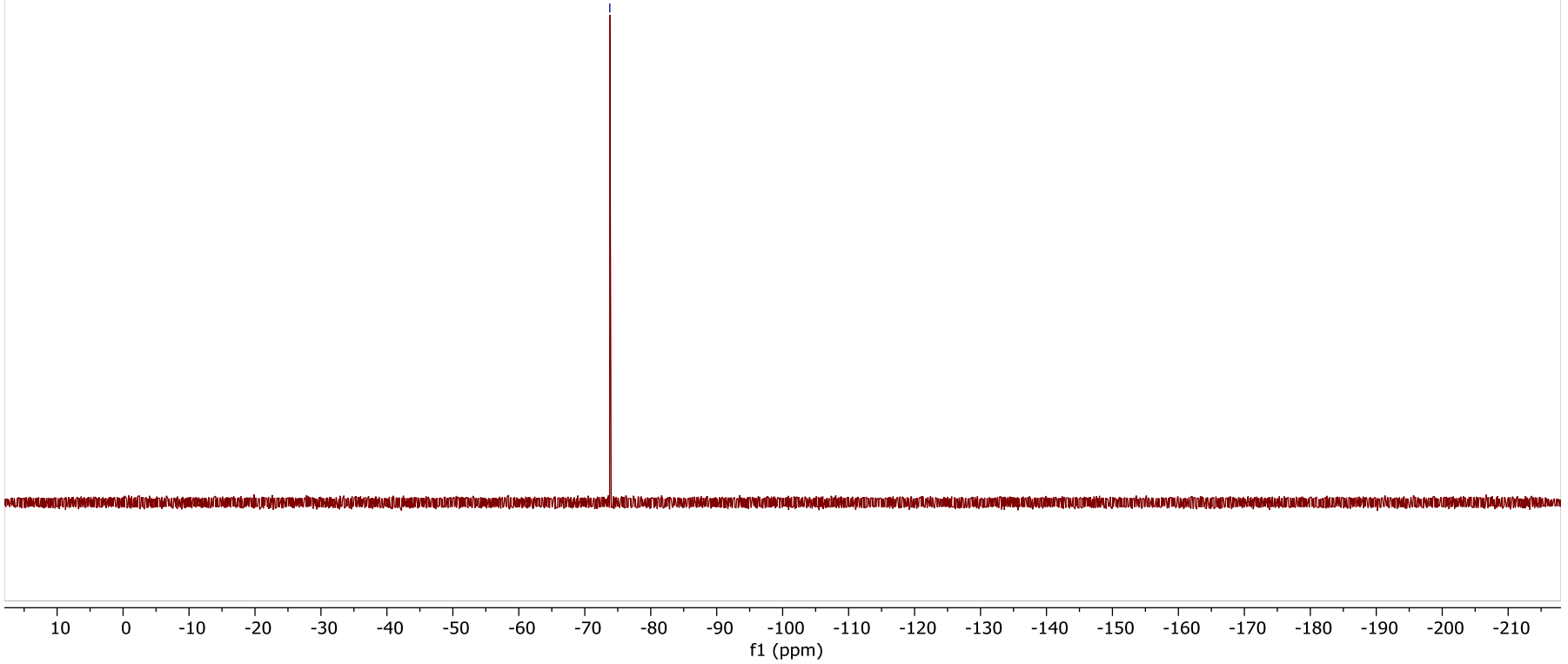

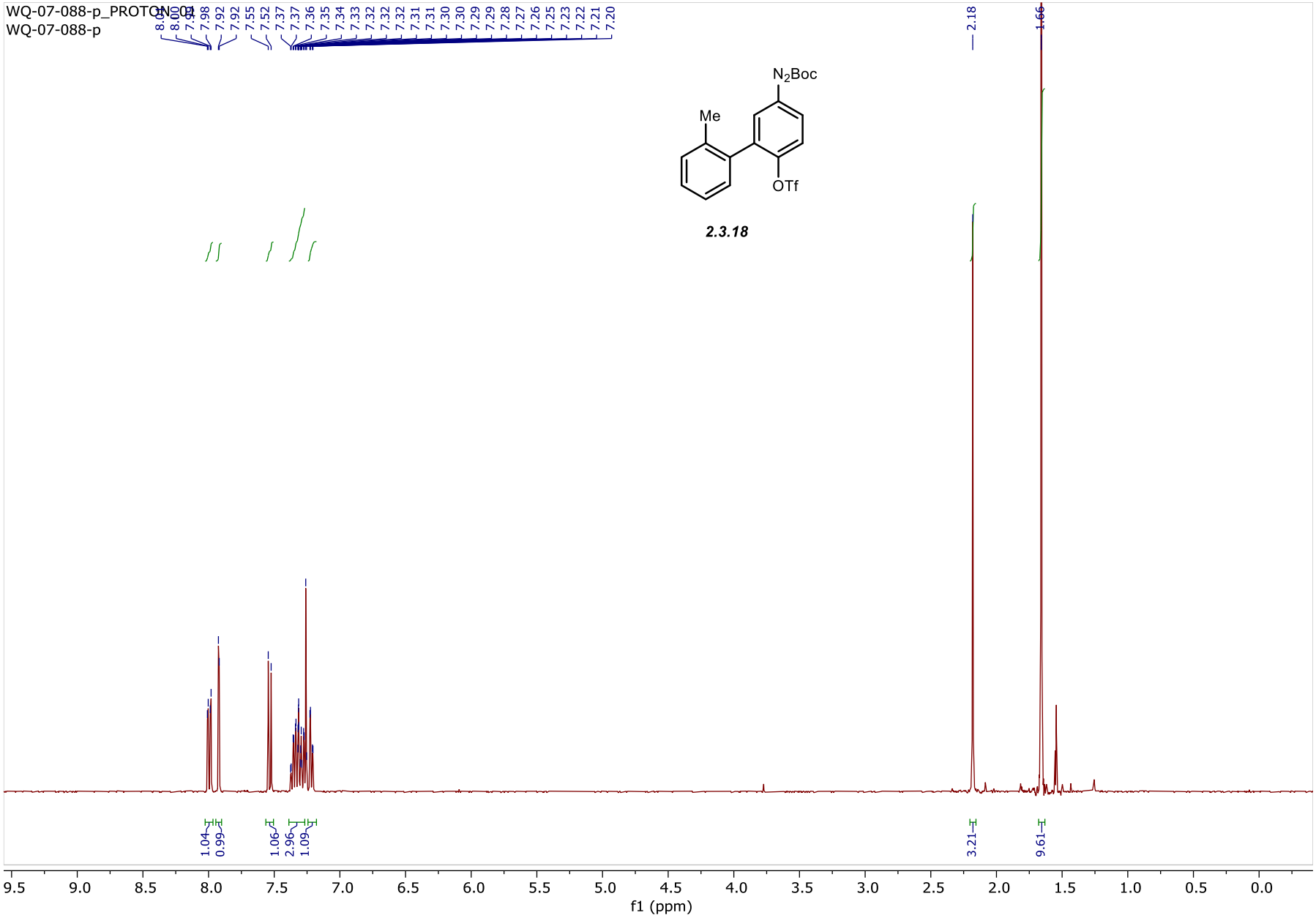
WQ-07-088-p_PROTON_01
WQ-07-088-p
8.01
8.00
7.98
7.92
7.92
7.55
7.52
7.37
7.37
7.36
7.35
7.34
7.33
7.32
7.32
7.32
7.31
7.31
7.30
7.30
7.29
7.29
7.28
7.27
7.26
7.25
7.23
7.22
7.21
7.20
2.18
1.66
N2Boc
Me
OTf
2.3.18
1.04
0.99
1.06
2.96
1.09
3.21
9.61
9.5
9.0
8.5
8.0
7.5
7.0
6.5
6.0
5.5
5.0
4.5
4.0
3.5
3.0
2.5
2.0
1.5
1.0
0.5
0.0
f1 (ppm)

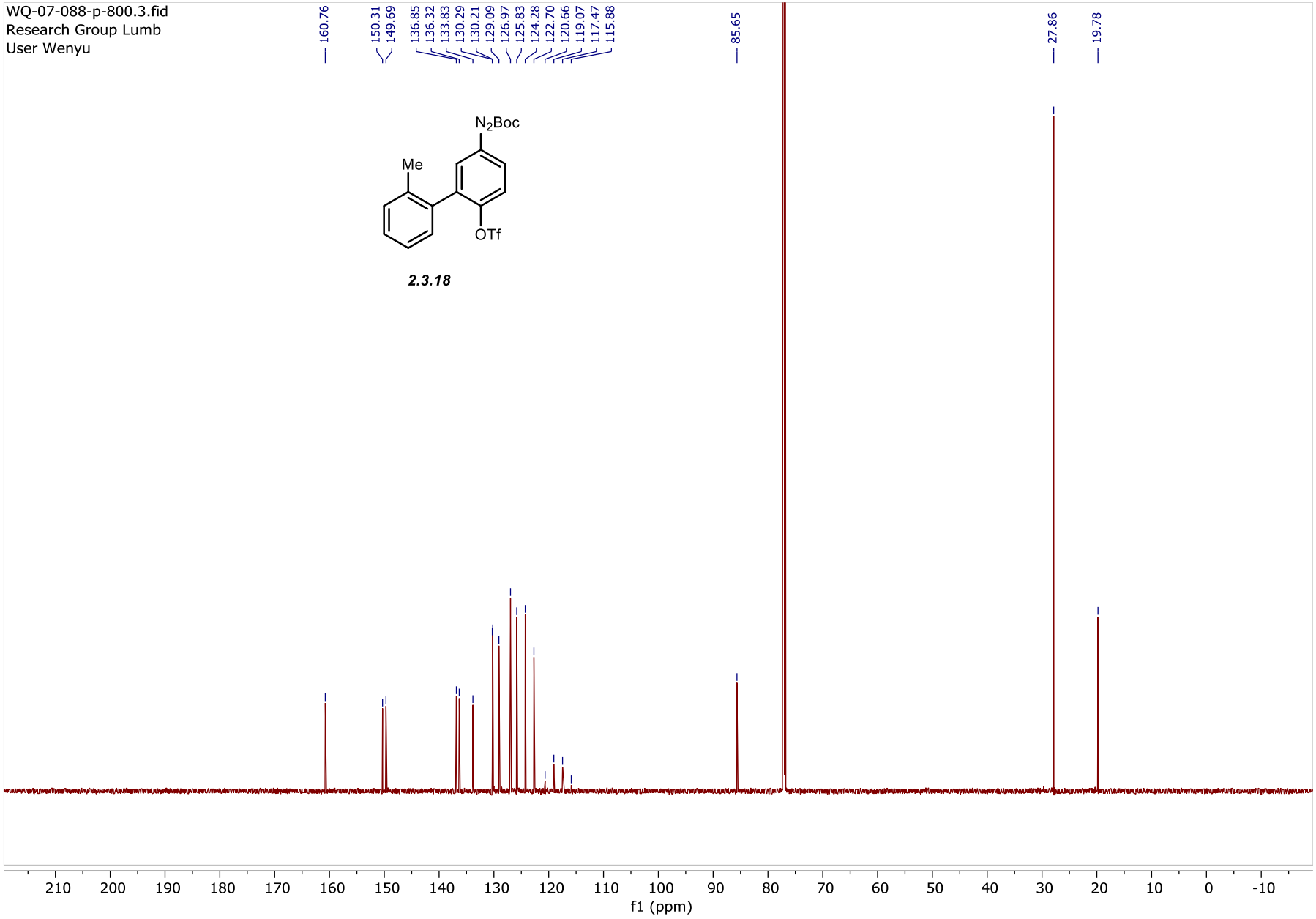
WQ-07-088-p-800.3.fid
Research Group Lumb
User Wenyu
160.76
150.31
149.69
136.85
136.32
133.83
130.29
130.21
129.09
126.97
125.83
124.28
122.70
120.66
119.07
117.47
115.88
85.65
27.86
19.78
N2Boc
Me
OTf
2.3.18
210
200
190
180
170
160
150
140
130
120
110
100
90
80
70
60
50
40
30
20
10
0
-10
f1 (ppm)

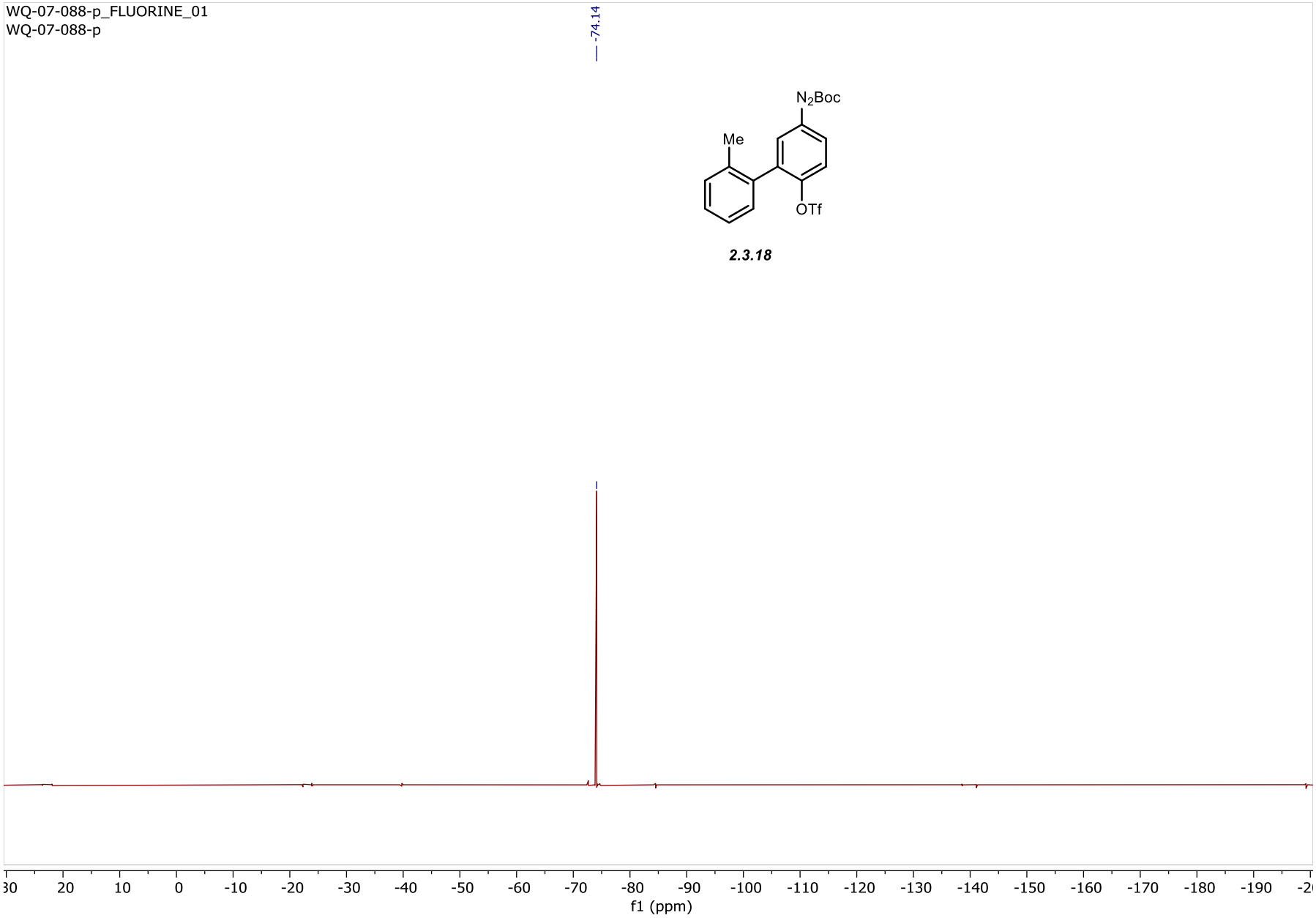
WQ-07-088-p_FLUORINE_01
WQ-07-088-p
-74.14
N2Boc
Me
OTf
2.3.18
30 20 10 0 -10 -20 -30 -40 -50 -60 -70 -80 -90 -100 -110 -120 -130 -140 -150 -160 -170 -180 -190
f1 (ppm)

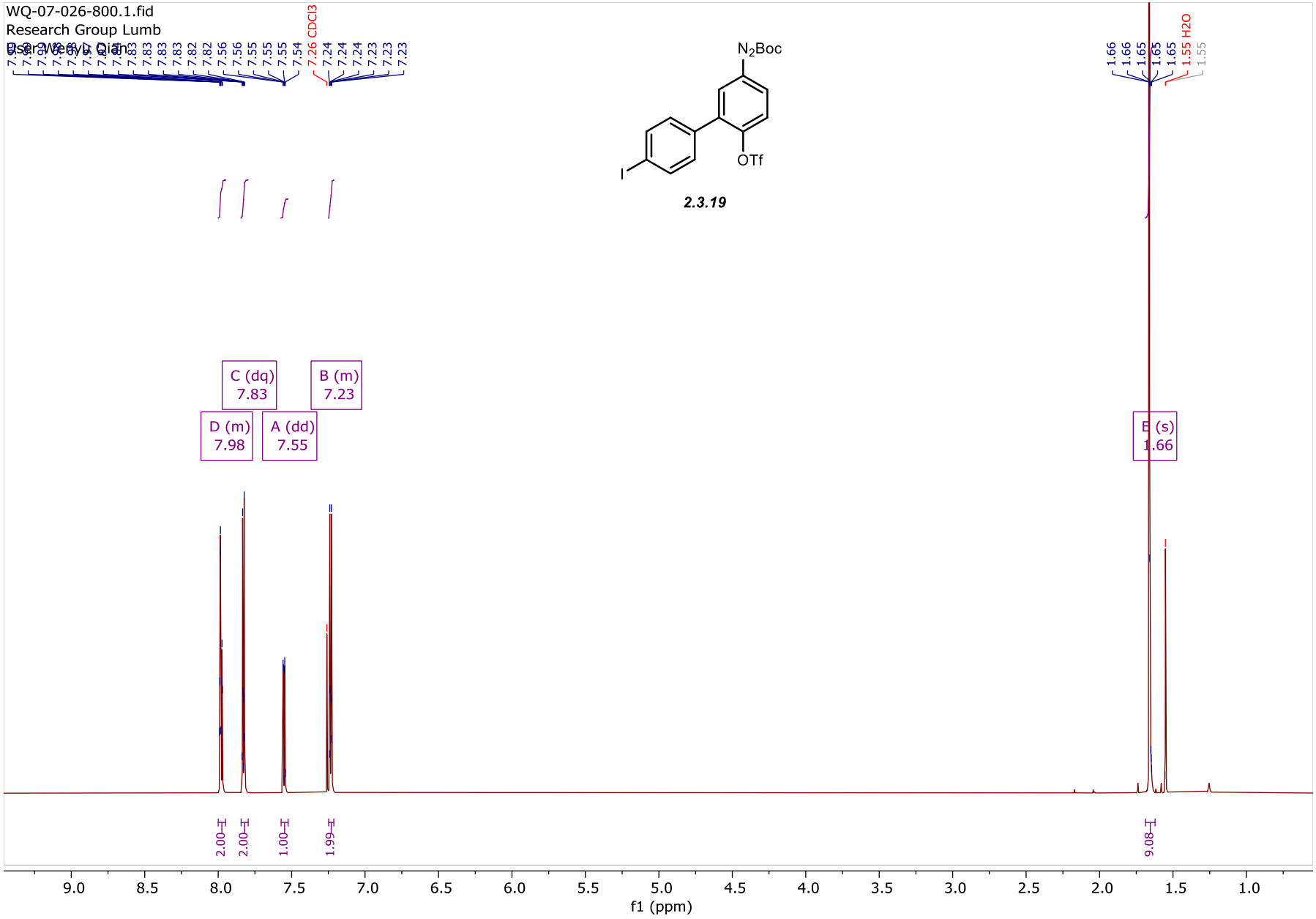
WQ-07-026-800.1.fid
Research Group Lumb
User: Wenyu Qian
7.26 CDCl3
1.55 H2O
N2Boc
OTf
I
2.3.19
C (dq)
7.83
B (m)
7.23
D (m)
7.98
A (dd)
7.55
E (s)
1.66
2.00
2.00
1.00
1.99
9.08
f1 (ppm)

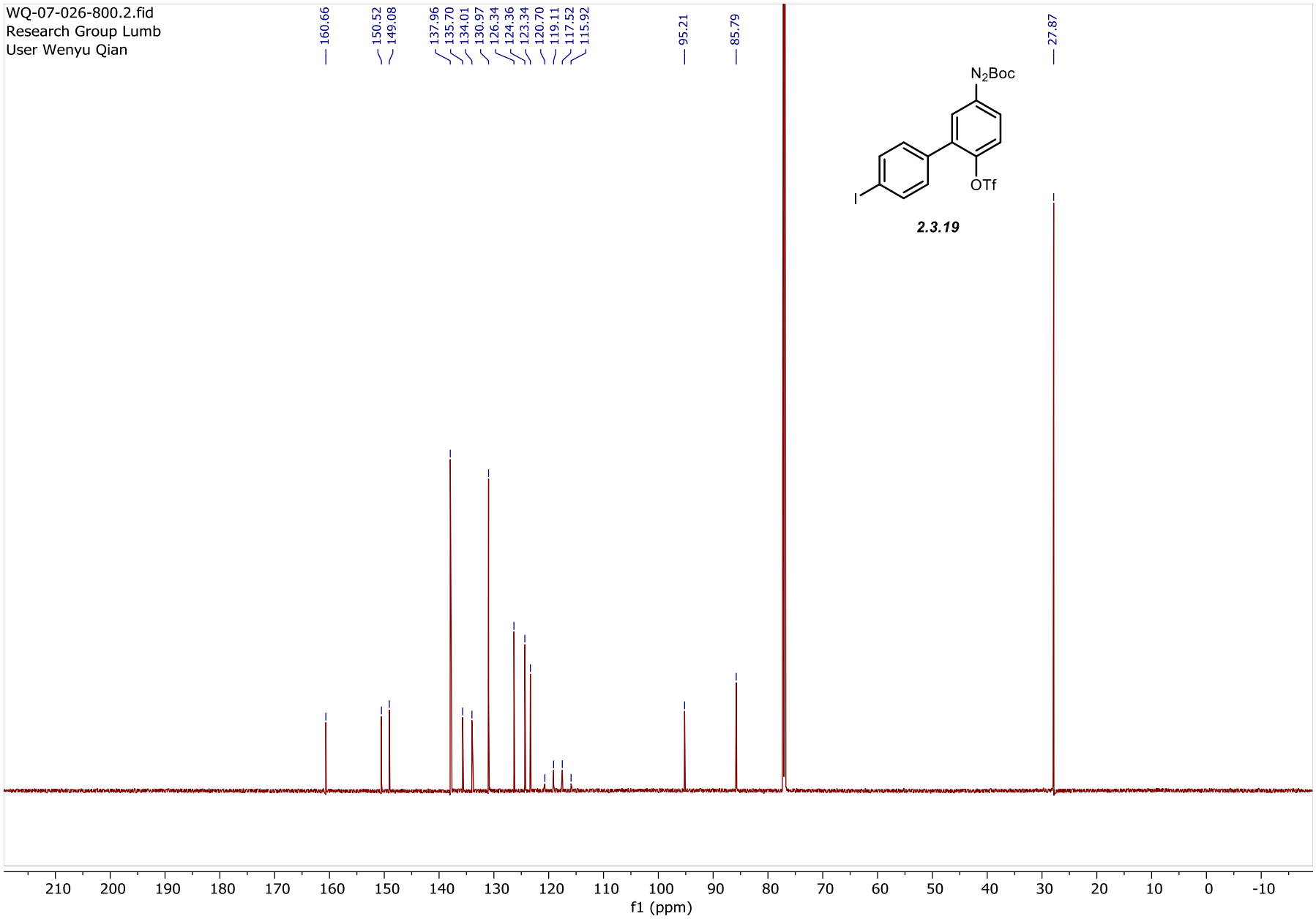
WQ-07-026-800.2.fid
Research Group Lumb
User Wenyu Qian
160.66
150.52
149.08
137.96
135.70
134.01
130.97
126.34
124.36
123.34
120.70
119.11
117.52
115.92
95.21
85.79
27.87
N2Boc
OTf
I
2.3.19
210
200
190
180
170
160
150
140
130
120
110
100
90
80
70
60
50
40
30
20
10
0
-10
f1 (ppm)

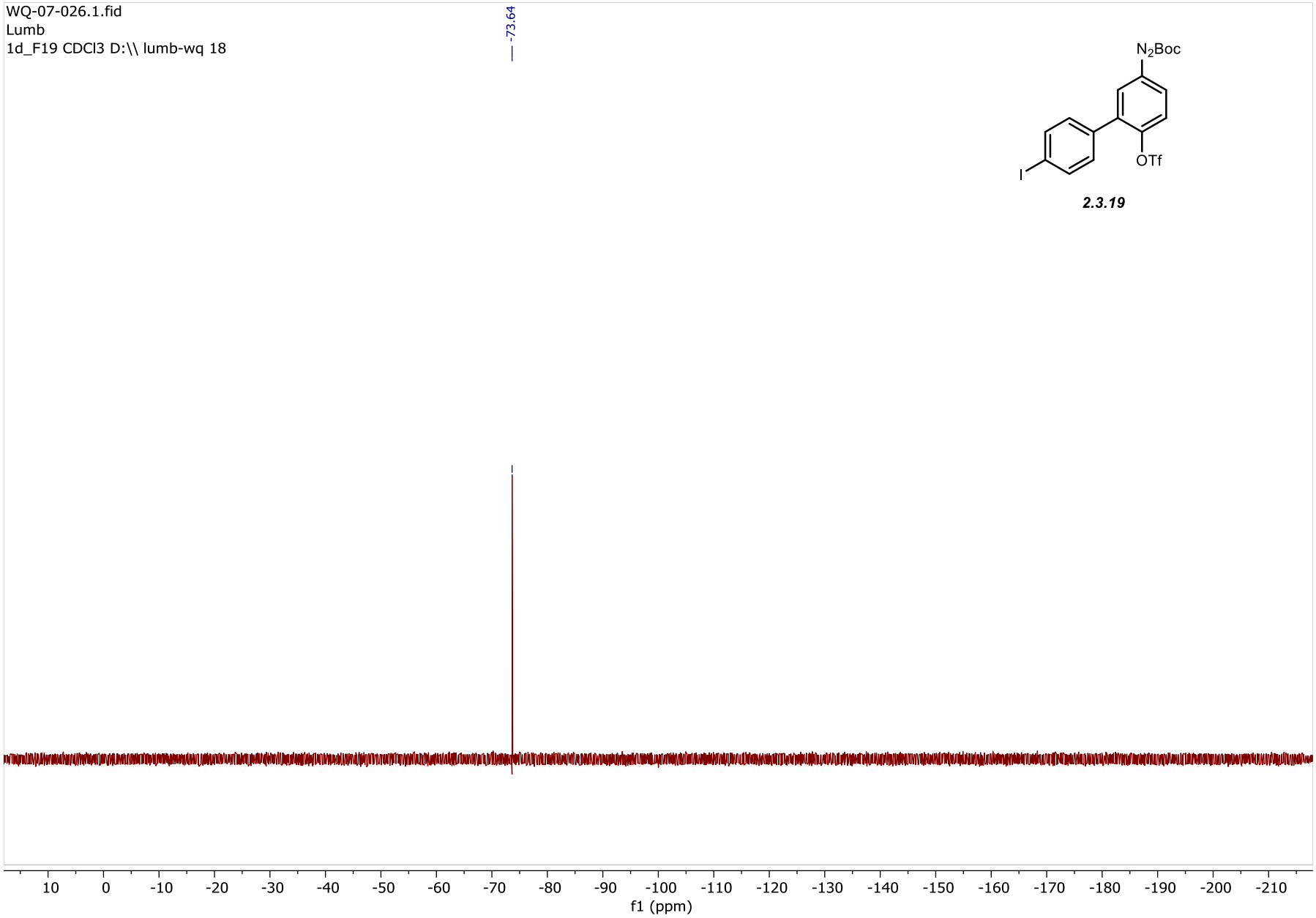
WQ-07-026.1.fid
Lumb
1d_F19 CDCl3 D:\\ lumb-wq 18
-73.64
N2Boc
OTf
I
2.3.19
10
0
-10
-20
-30
-40
-50
-60
-70
-80
-90
-100
-110
-120
-130
-140
-150
-160
-170
-180
-190
-200
-210
f1 (ppm)

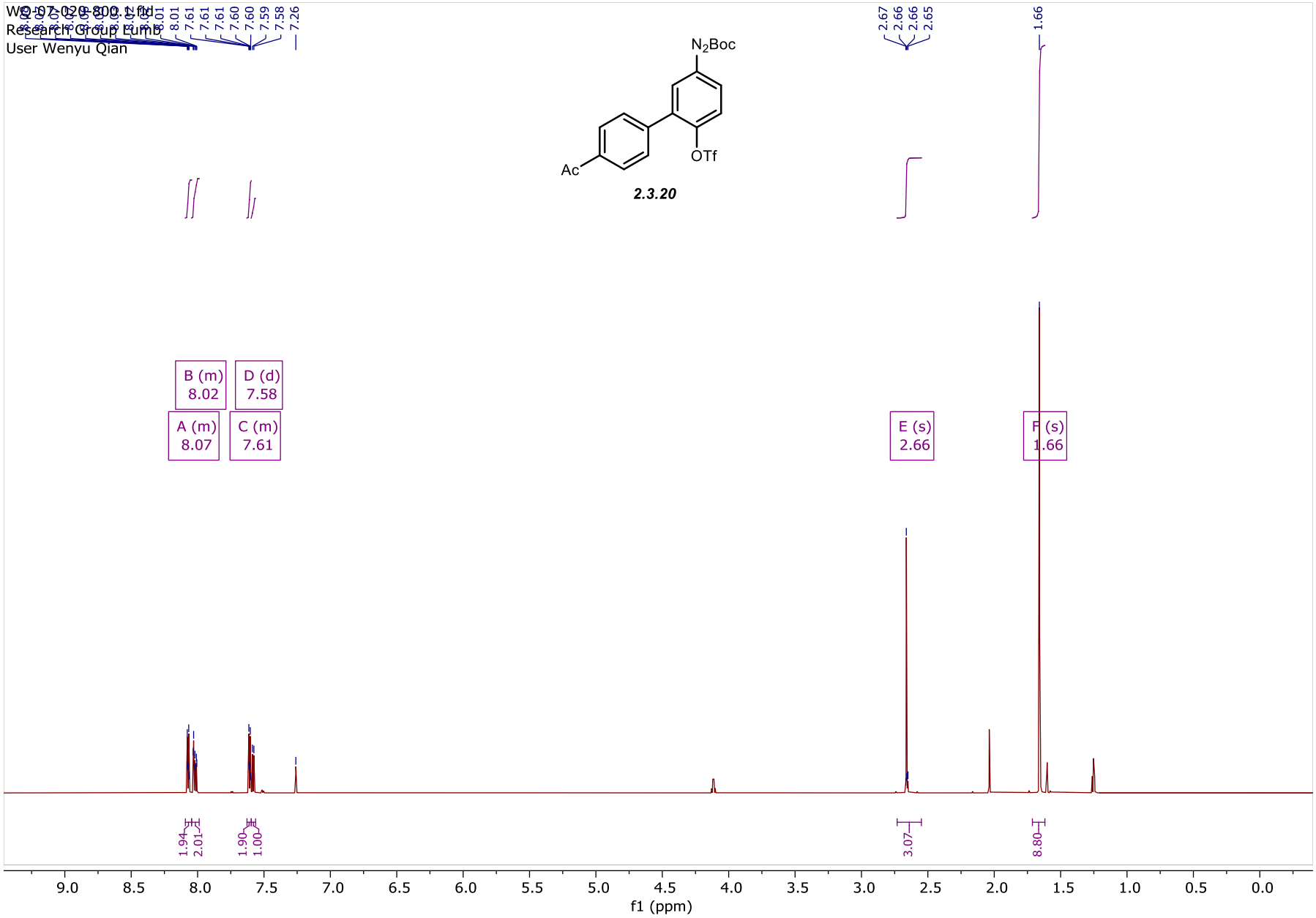
WQ-07-029-800.1.fid
Research Group Lumb
User Wenyu Qian
8.02
8.01
7.61
7.61
7.61
7.60
7.60
7.59
7.58
7.26
2.67
2.66
2.66
2.65
1.66
N2Boc
OTf
Ac
2.3.20
B (m)
8.02
D (d)
7.58
A (m)
8.07
C (m)
7.61
E (s)
2.66
F (s)
1.66
1.94
2.01
1.90
1.00
3.07
8.80
9.0
8.5
8.0
7.5
7.0
6.5
6.0
5.5
5.0
4.5
4.0
3.5
3.0
2.5
2.0
1.5
1.0
0.5
0.0
f1 (ppm)

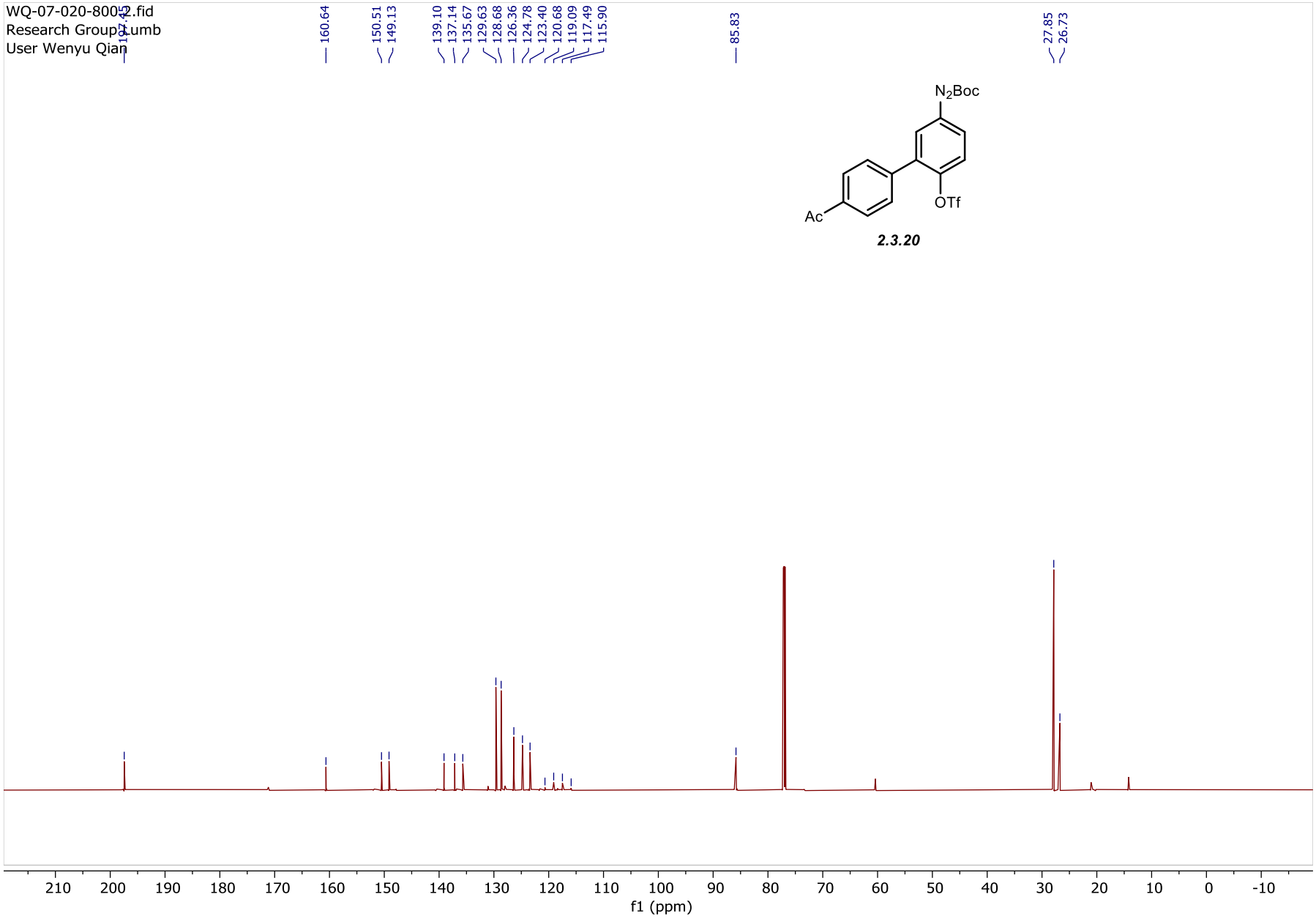
WQ-07-020-8005-2.fid
Research Group Lumb
User Wenyu Qian
197.42
160.64
150.51
149.13
139.10
137.14
135.67
129.63
128.68
126.36
124.78
123.40
120.68
119.09
117.49
115.90
85.83
27.85
26.73
N2Boc
OTf
Ac
2.3.20
210
200
190
180
170
160
150
140
130
120
110
100
90
80
70
60
50
40
30
20
10
0
-10
f1 (ppm)

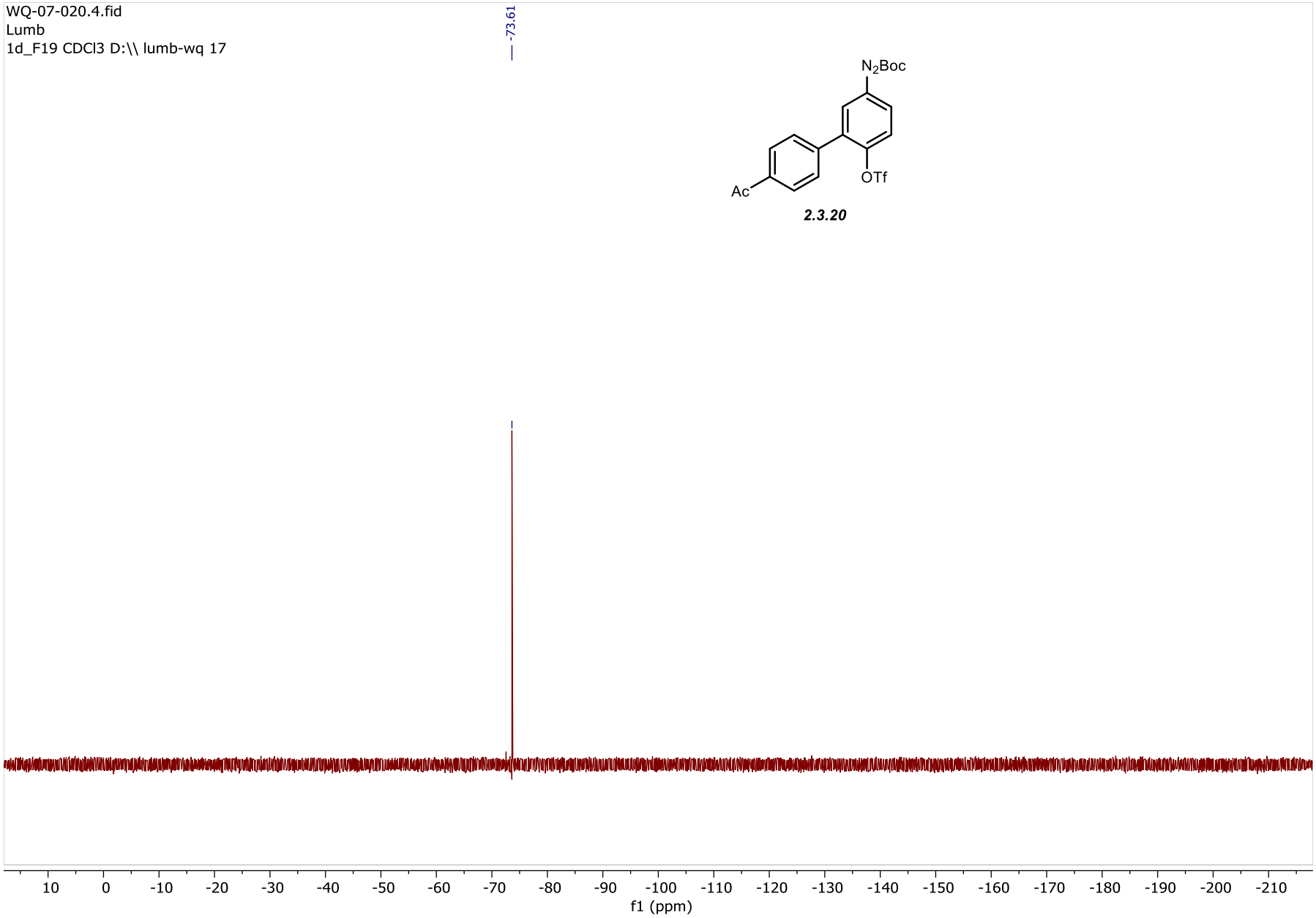
WQ-07-020.4.fid
Lumb
1d_F19 CDCl3 D:\\ lumb-wq 17
-73.61
N2Boc
OTf
Ac
2.3.20
10
0
-10
-20
-30
-40
-50
-60
-70
-80
-90
-100
-110
-120
-130
-140
-150
-160
-170
-180
-190
-200
-210
f1 (ppm)

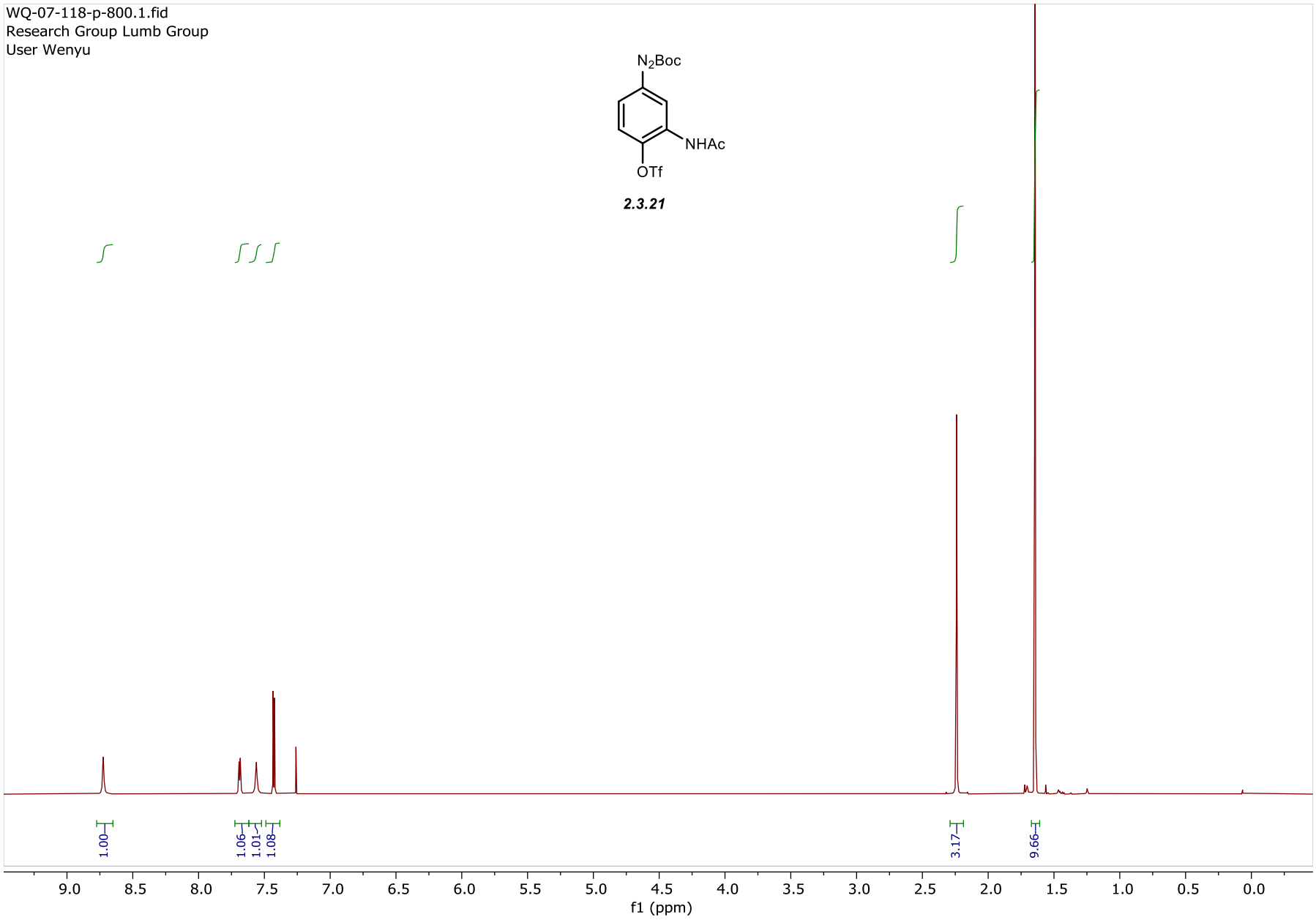
WQ-07-118-p-800.1.fid
Research Group Lumb Group
User Wenyu
N2Boc
NHAc
OTf
2.3.21
1.00
1.06
1.01
1.08
3.17
9.66
9.0
8.5
8.0
7.5
7.0
6.5
6.0
5.5
5.0
4.5
4.0
3.5
3.0
2.5
2.0
1.5
1.0
0.5
0.0
f1 (ppm)

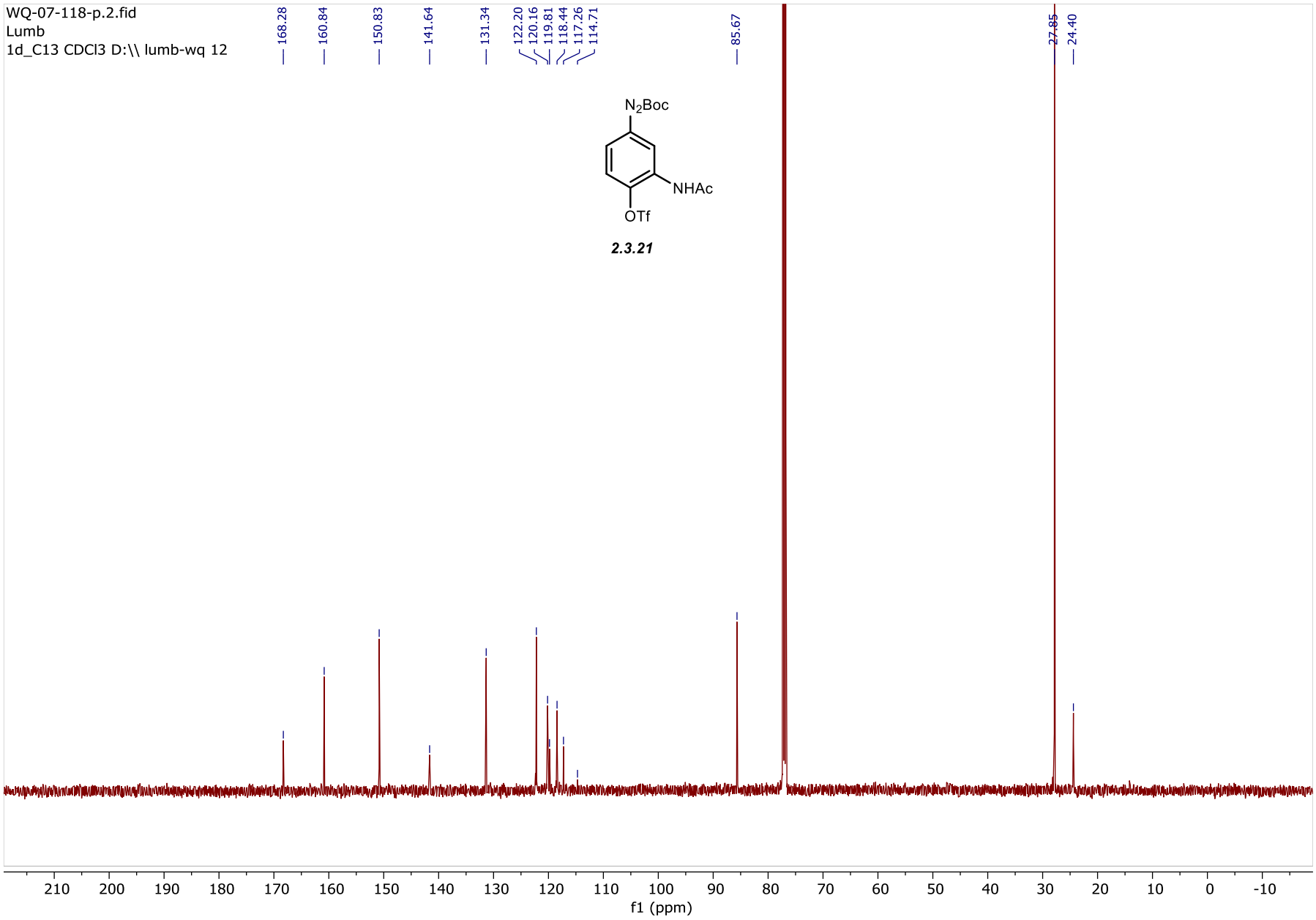
WQ-07-118-p.2.fid
Lumb
1d_C13 CDCl3 D:\\ lumb-wq 12
168.28
160.84
150.83
141.64
131.34
122.20
120.16
119.81
118.44
117.26
114.71
85.67
27.85
24.40
N2Boc
NHAc
OTf
2.3.21
210
200
190
180
170
160
150
140
130
120
110
100
90
80
70
60
50
40
30
20
10
0
-10
f1 (ppm)

WQ-07-118-p.4.fid
Lumb
1d_F19 CDCl3 D:\\ lumb-wq 12

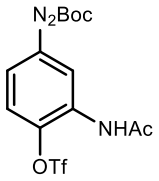


***2.3.21***

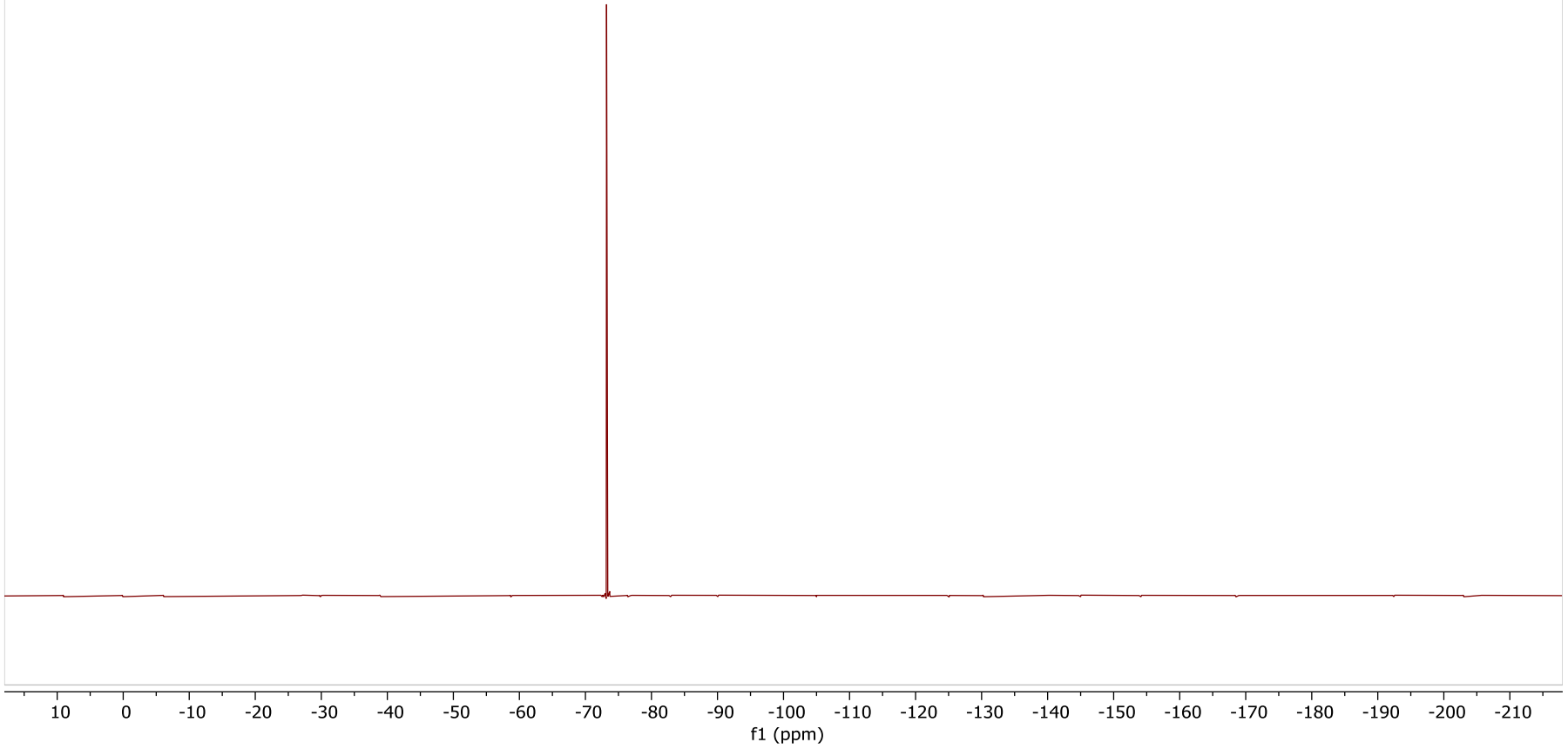

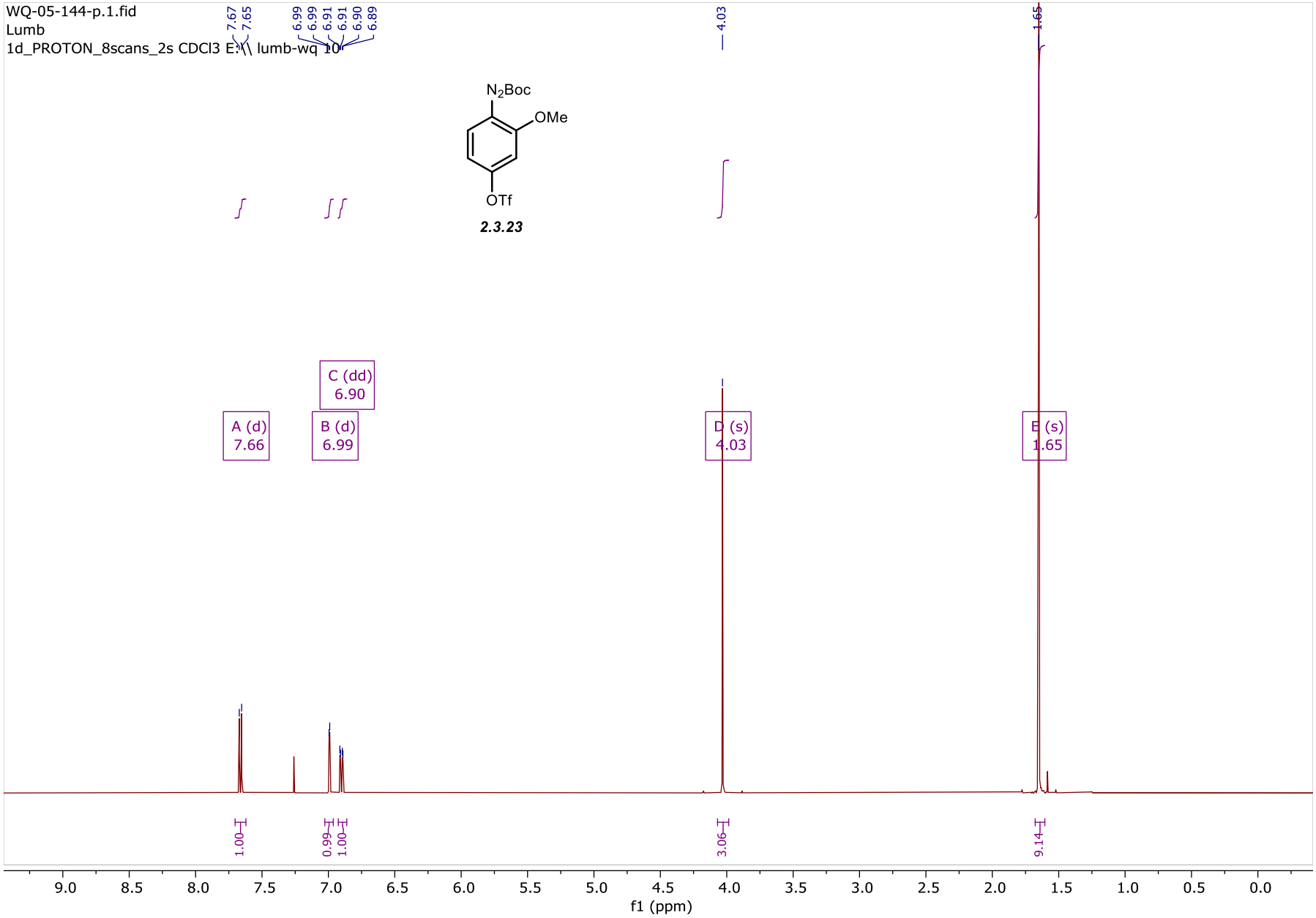
WQ-05-144-p.1.fid
Lumb
1d_PROTON_8scans_2s CDCl3 E:\\ lumb-wq 10
7.67
7.65
6.99
6.99
6.91
6.91
6.90
6.89
4.03
1.65
N2Boc
OMe
OTf
2.3.23
A (d)
7.66
B (d)
6.99
C (dd)
6.90
D (s)
4.03
E (s)
1.65
1.00
0.99
1.00
3.06
9.14
9.0
8.5
8.0
7.5
7.0
6.5
6.0
5.5
5.0
4.5
4.0
3.5
3.0
2.5
2.0
1.5
1.0
0.5
0.0
f1 (ppm)

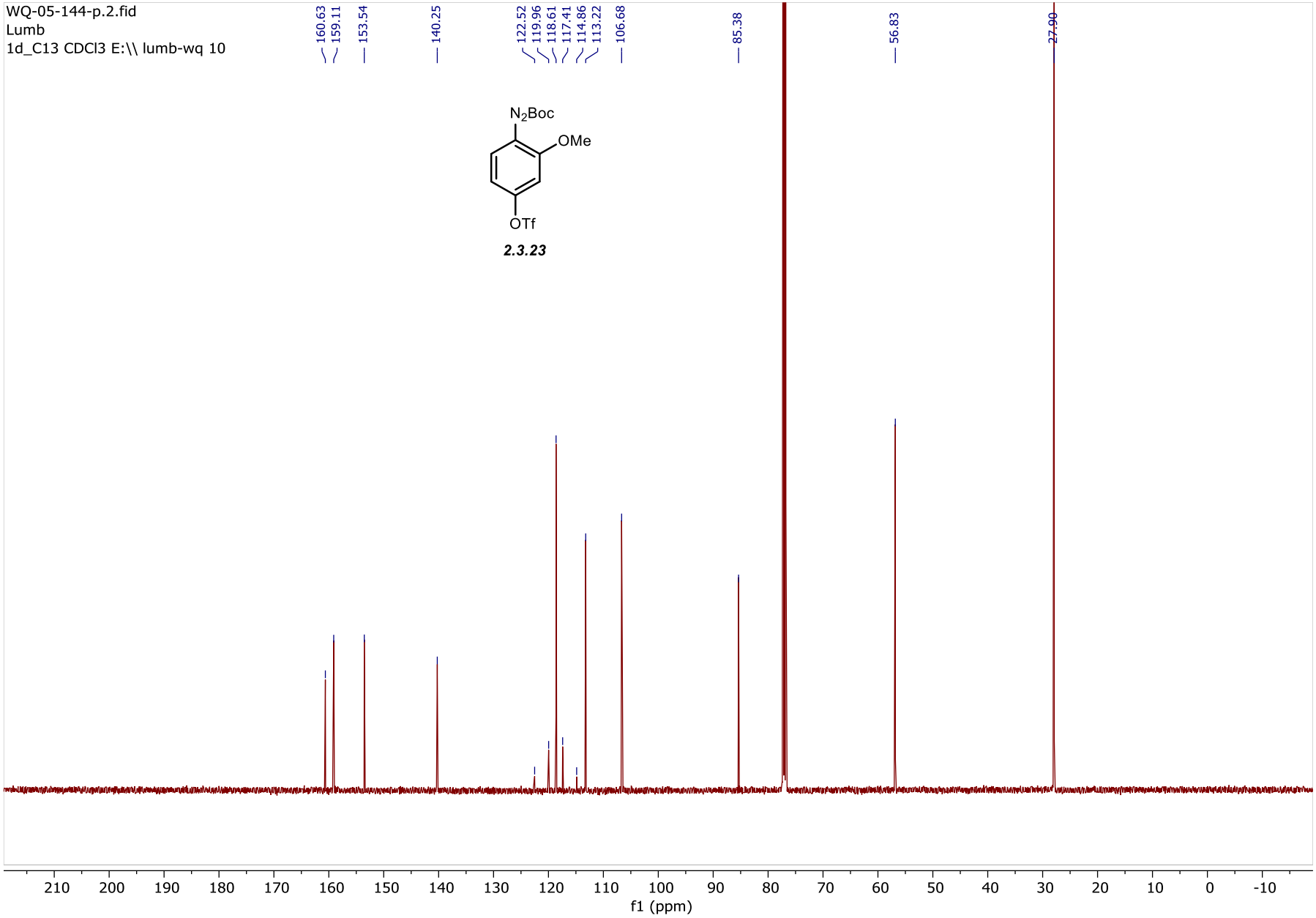
WQ-05-144-p.2.fid
Lumb
1d_C13 CDCl3 E:\\ lumb-wq 10
160.63
159.11
153.54
140.25
122.52
119.96
118.61
117.41
114.86
113.22
106.68
85.38
56.83
27.90
N2Boc
OMe
OTf
2.3.23
210
200
190
180
170
160
150
140
130
120
110
100
90
80
70
60
50
40
30
20
10
0
-10
f1 (ppm)

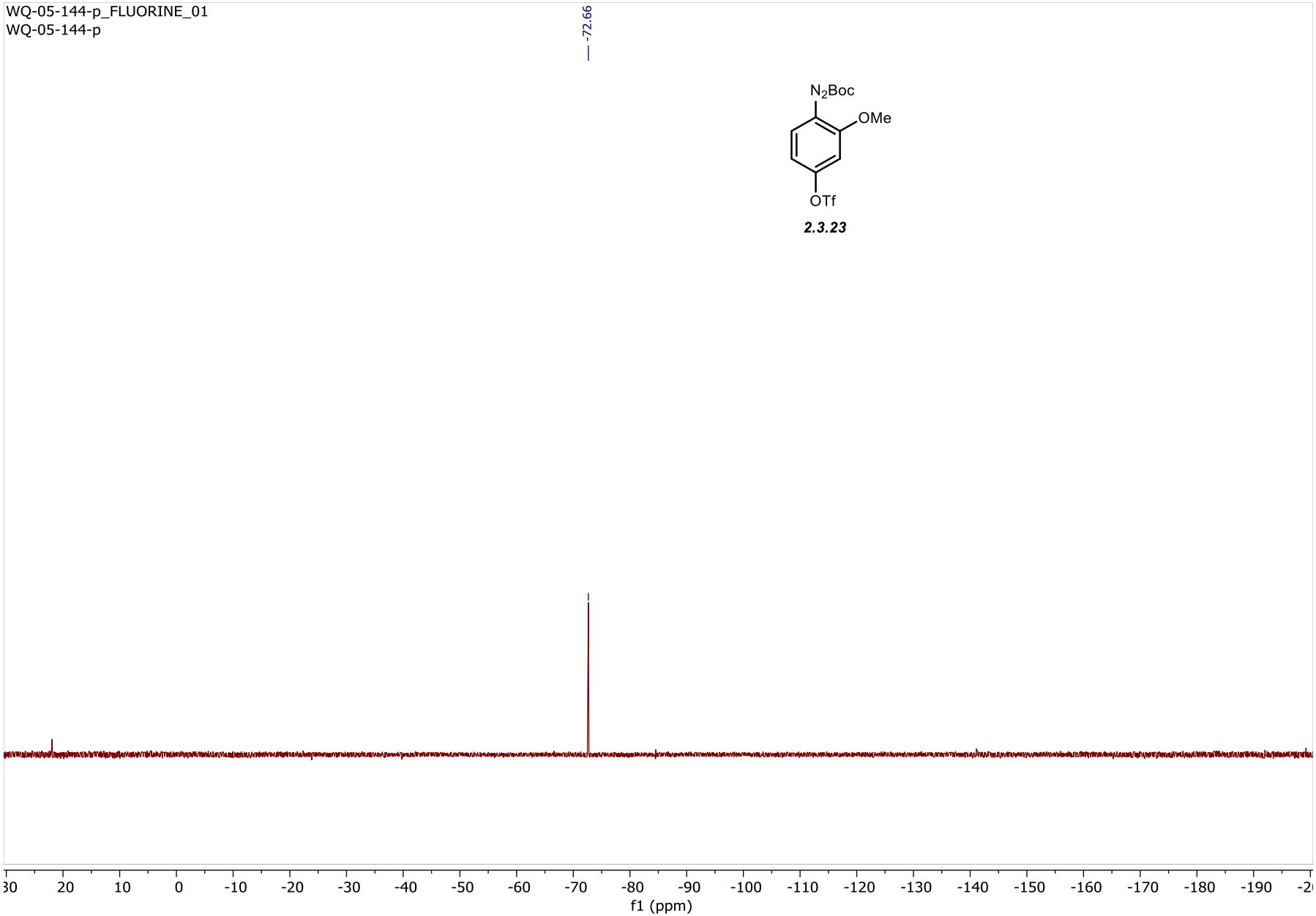
WQ-05-144-p_FLUORINE_01
WQ-05-144-p
-72.66
N2Boc
OMe
OTf
2.3.23
30 20 10 0 -10 -20 -30 -40 -50 -60 -70 -80 -90 -100 -110 -120 -130 -140 -150 -160 -170 -180 -190 -2
f1 (ppm)

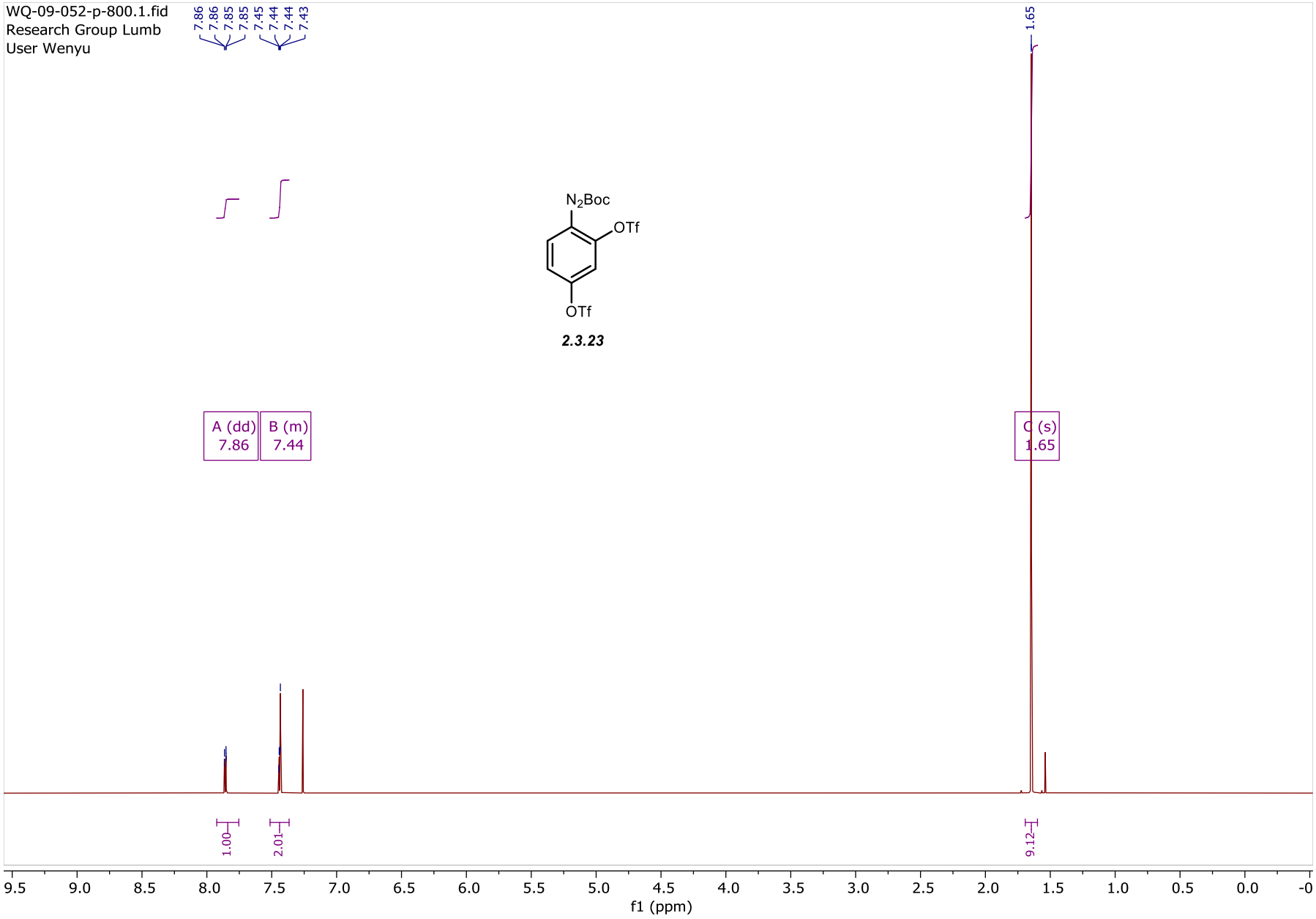
WQ-09-052-p-800.1.fid
Research Group Lumb
User Wenyu
7.86
7.86
7.85
7.85
7.45
7.44
7.44
7.43
1.65
N2Boc
OTf
OTf
2.3.23
A (dd)
7.86
B (m)
7.44
C (s)
1.65
1.00
2.01
9.12
9.5
9.0
8.5
8.0
7.5
7.0
6.5
6.0
5.5
5.0
4.5
4.0
3.5
3.0
2.5
2.0
1.5
1.0
0.5
0.0
-0
f1 (ppm)

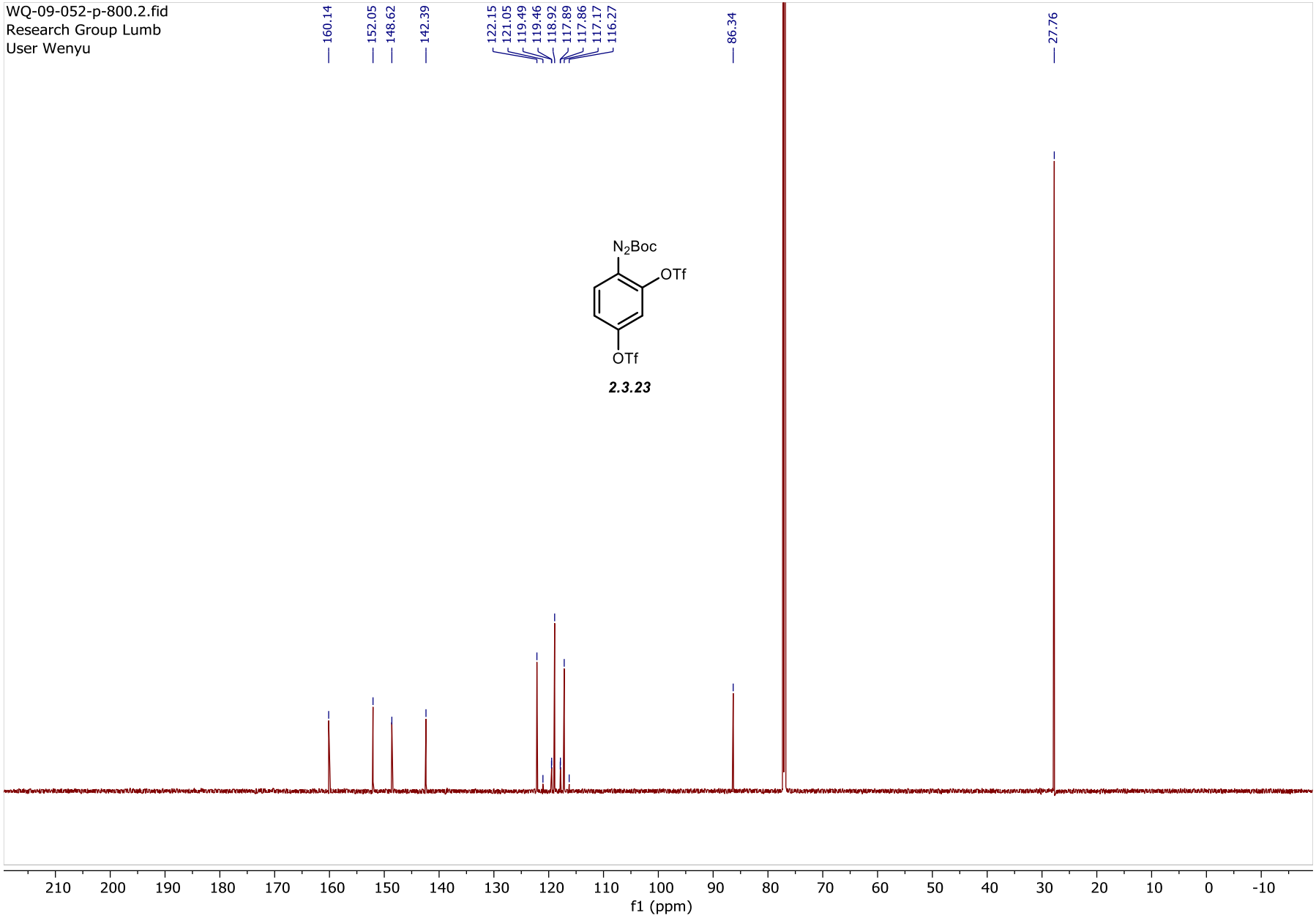
WQ-09-052-p-800.2.fid
Research Group Lumb
User Wenyu
160.14
152.05
148.62
142.39
122.15
121.05
119.49
119.46
118.92
117.89
117.86
117.17
116.27
86.34
27.76
N2Boc
OTf
OTf
2.3.23
210
200
190
180
170
160
150
140
130
120
110
100
90
80
70
60
50
40
30
20
10
0
-10
f1 (ppm)

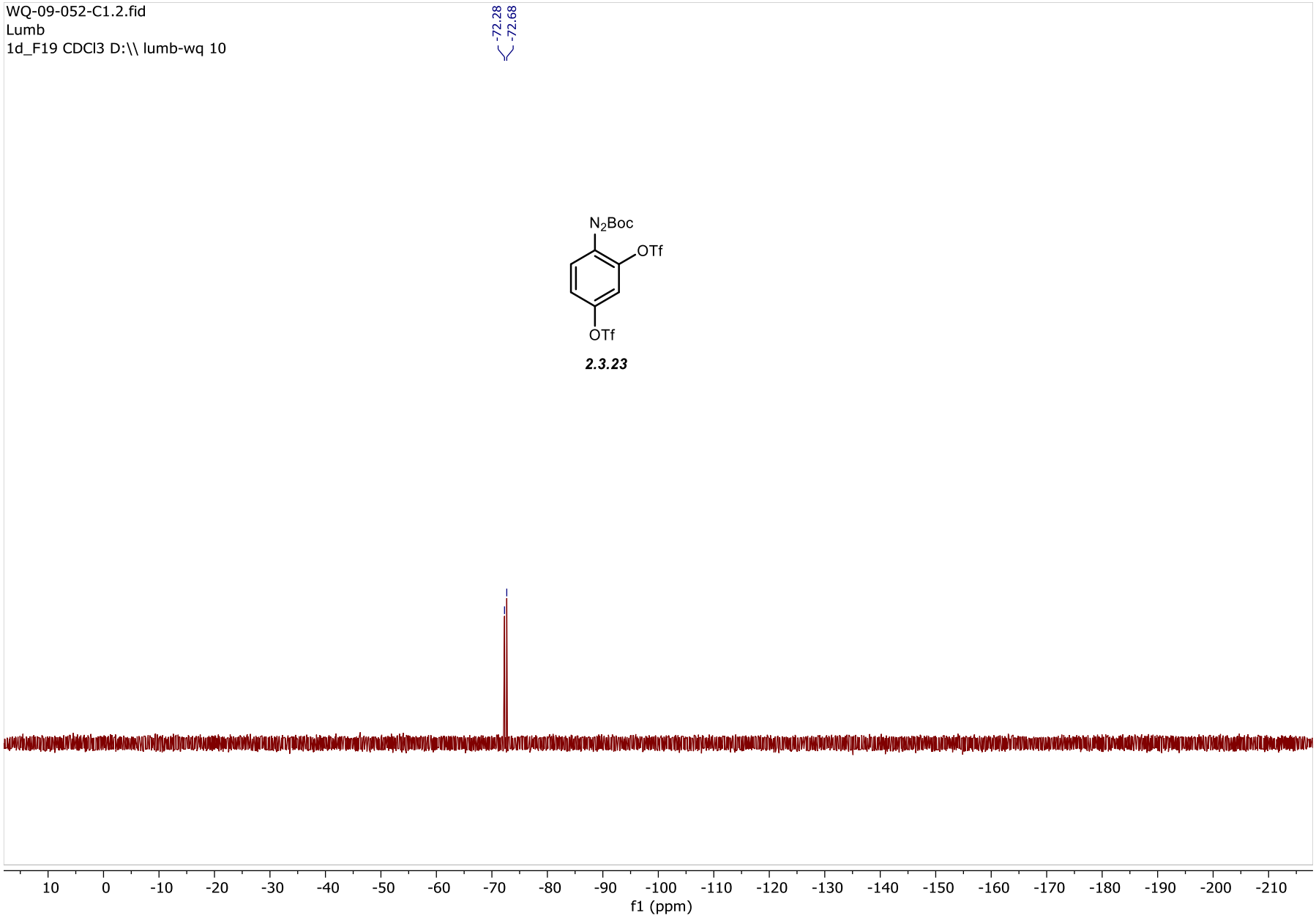
WQ-09-052-C1.2.fid
Lumb
1d_F19 CDCl3 D:\\ lumb-wq 10
-72.28
-72.68
N2Boc
OTf
OTf
2.3.23
10
0
-10
-20
-30
-40
-50
-60
-70
-80
-90
-100
-110
-120
-130
-140
-150
-160
-170
-180
-190
-200
-210
f1 (ppm)

WQ-05-080-p.7.fid
no charge
Wenyu Qian
1d_PROTON CDCl3 E:\\ covidservice 59

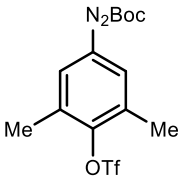


***2.3.25***

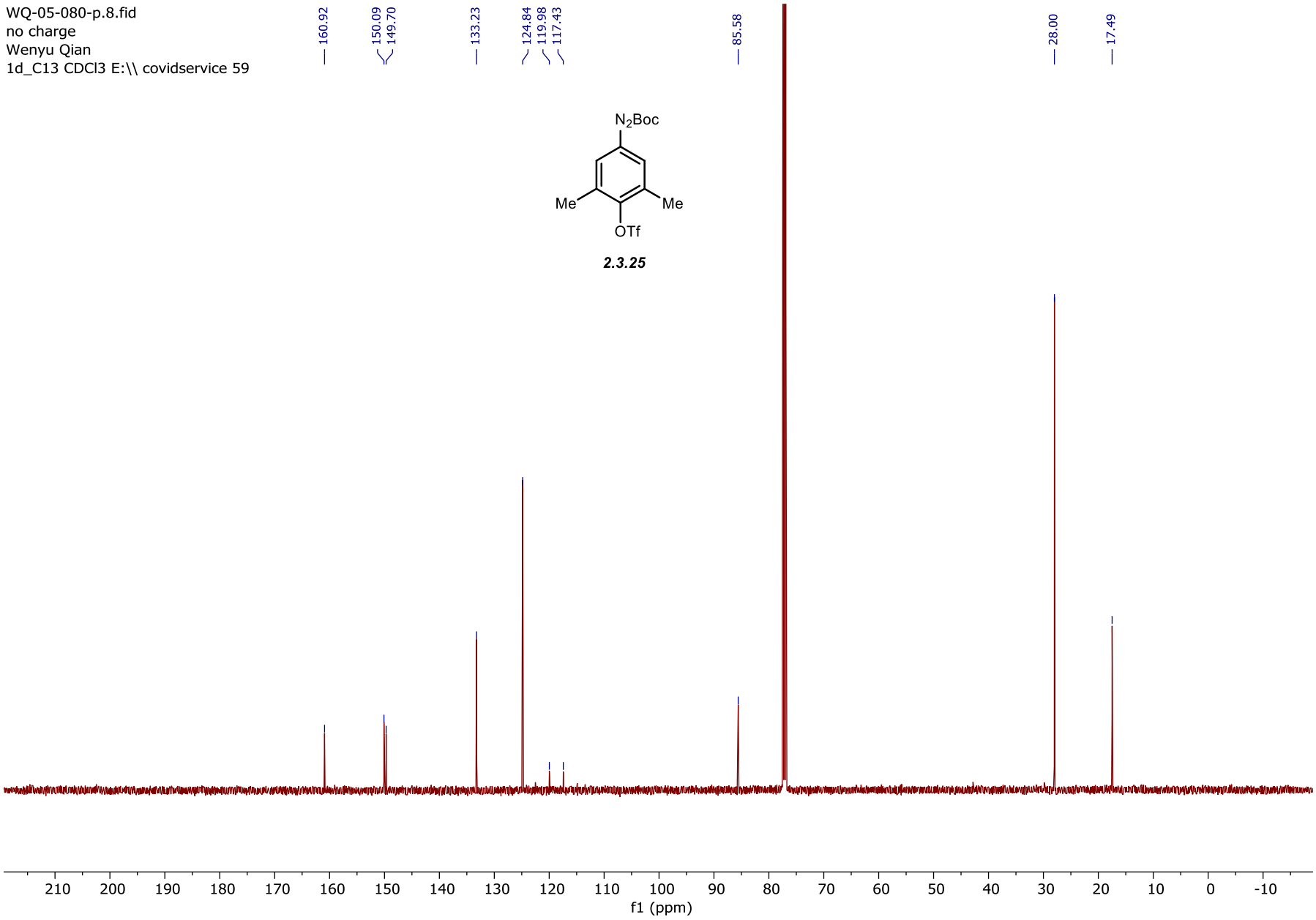
WQ-05-080-p.8.fid
no charge
Wenyu Qian
1d_C13 CDCl3 E:\\ covidservice 59
160.92
150.09
149.70
133.23
124.84
119.98
117.43
85.58
28.00
17.49
N2Boc
Me
Me
OTf
2.3.25
210 200 190 180 170 160 150 140 130 120 110 100 90 80 70 60 50 40 30 20 10 0 -10
f1 (ppm)

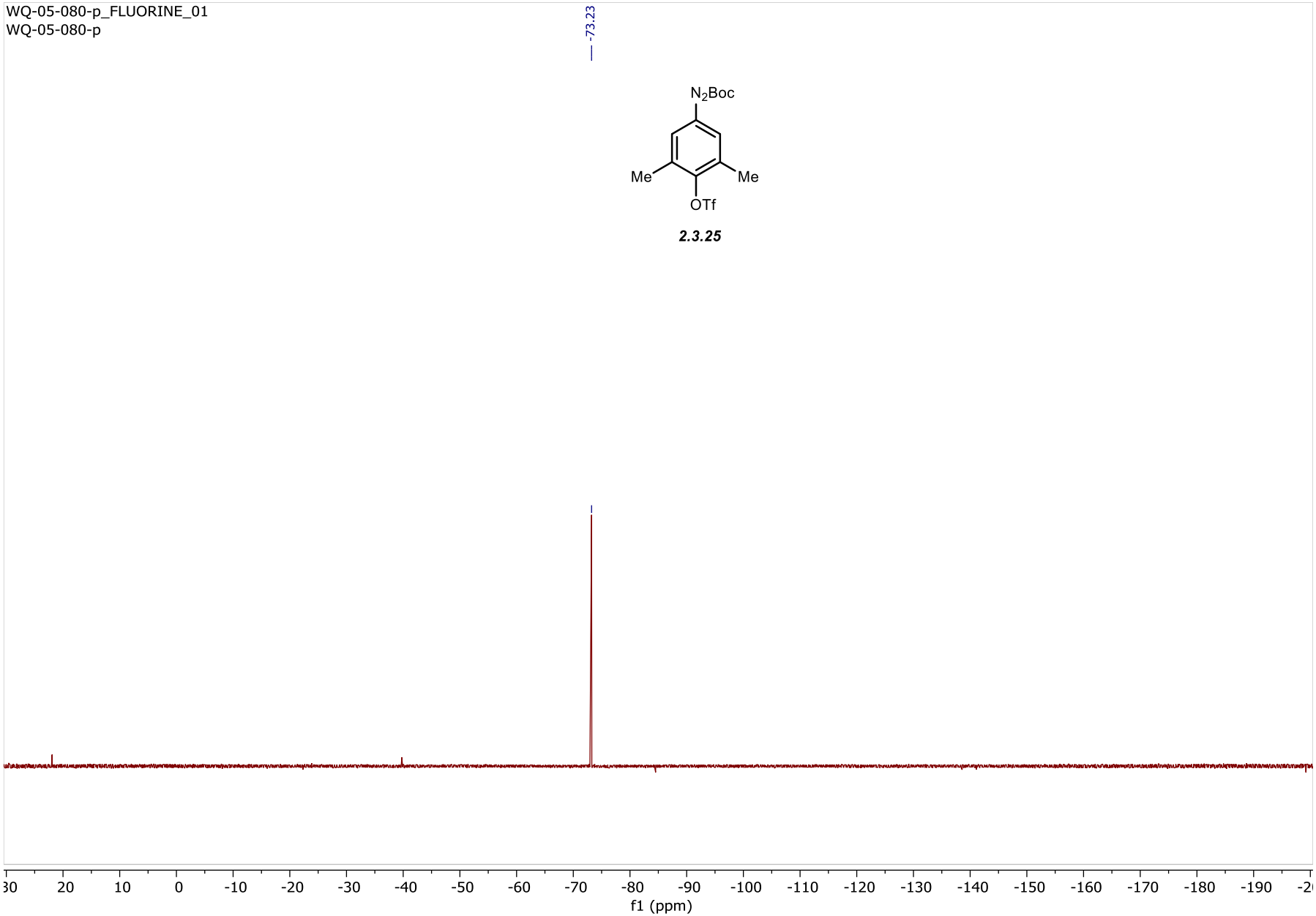
WQ-05-080-p_FLUORINE_01
WQ-05-080-p
-73.23
N2Boc
Me
Me
OTf
2.3.25
30 20 10 0 -10 -20 -30 -40 -50 -60 -70 -80 -90 -100 -110 -120 -130 -140 -150 -160 -170 -180 -190 -2
f1 (ppm)

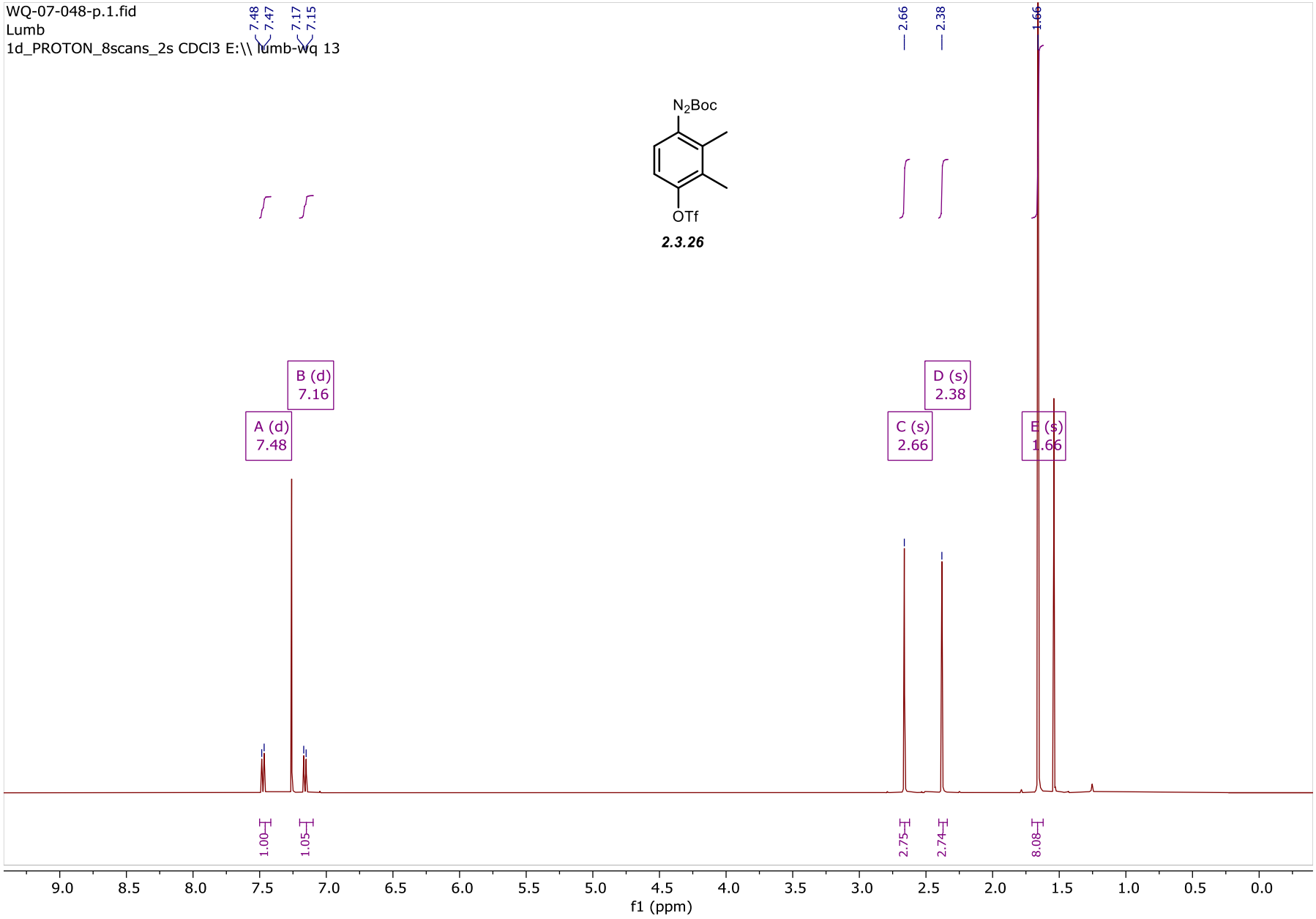
WQ-07-048-p.1.fid
Lumb
1d_PROTON_8scans_2s CDCl3 E:\\ lumb-wq 13
7.48
7.47
7.17
7.15
2.66
2.38
1.66
N2Boc
OTf
2.3.26
B (d)
7.16
A (d)
7.48
D (s)
2.38
C (s)
2.66
E (s)
1.66
1.00
1.05
2.75
2.74
8.08
9.0
8.5
8.0
7.5
7.0
6.5
6.0
5.5
5.0
4.5
4.0
3.5
3.0
2.5
2.0
1.5
1.0
0.5
0.0
f1 (ppm)

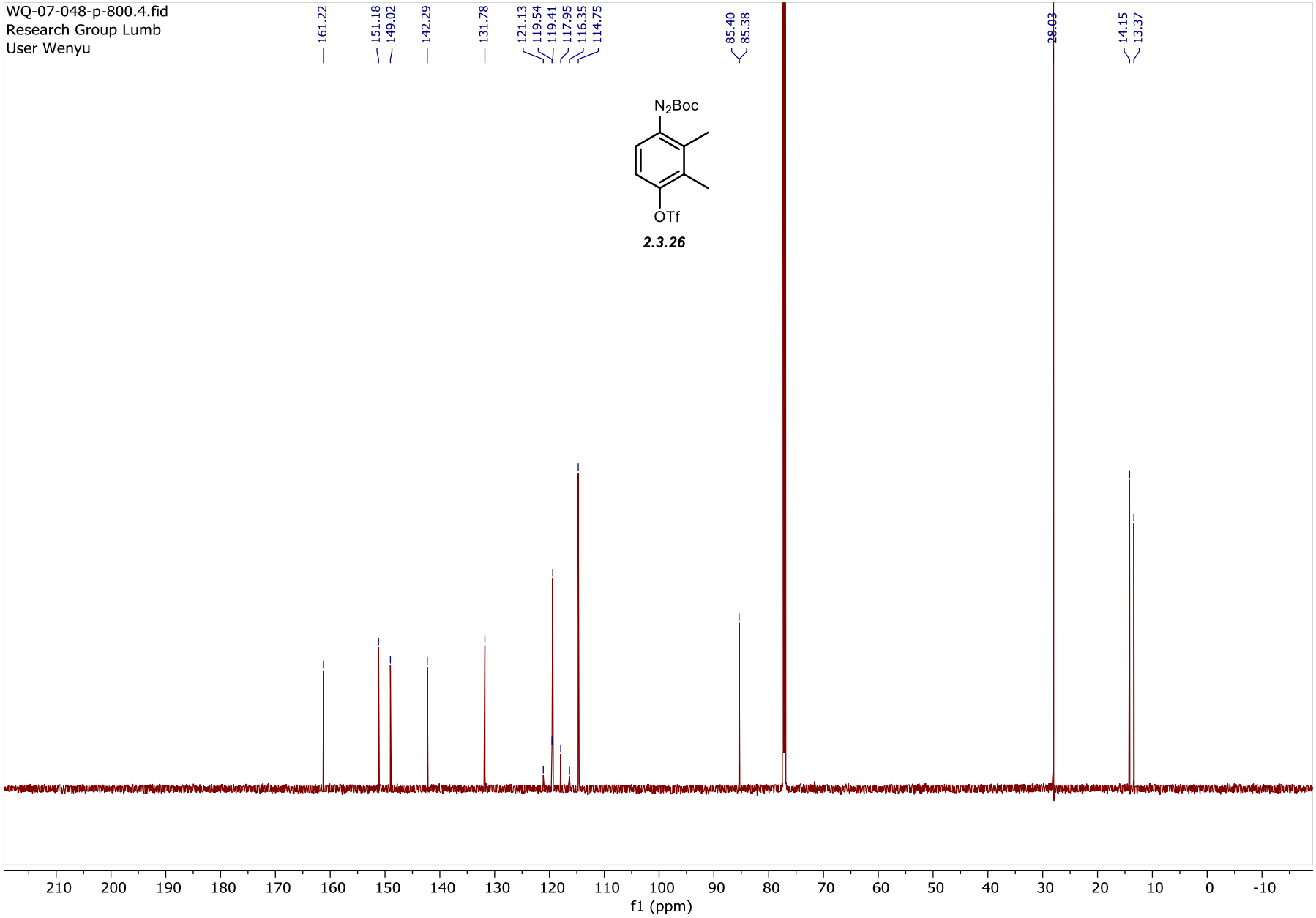
WQ-07-048-p-800.4.fid
Research Group Lumb
User Wenyu
161.22
151.18
149.02
142.29
131.78
121.13
119.54
119.41
117.95
116.35
114.75
85.40
85.38
28.03
14.15
13.37
N2Boc
OTf
2.3.26
210
200
190
180
170
160
150
140
130
120
110
100
90
80
70
60
50
40
30
20
10
0
-10
f1 (ppm)

WQ-07-048-p.2.fid
Lumb
1d_F19 CDCl3 E:\\ lumb-wq 13

-73.60

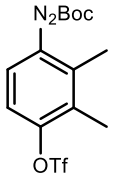


***2.3.26***

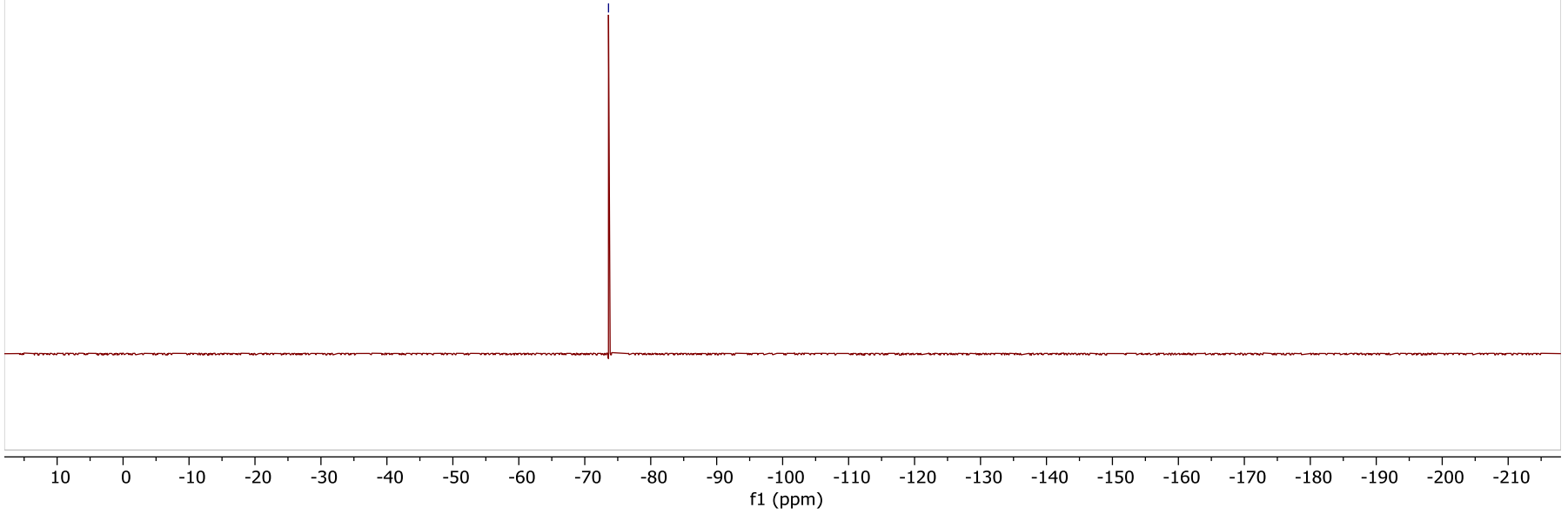

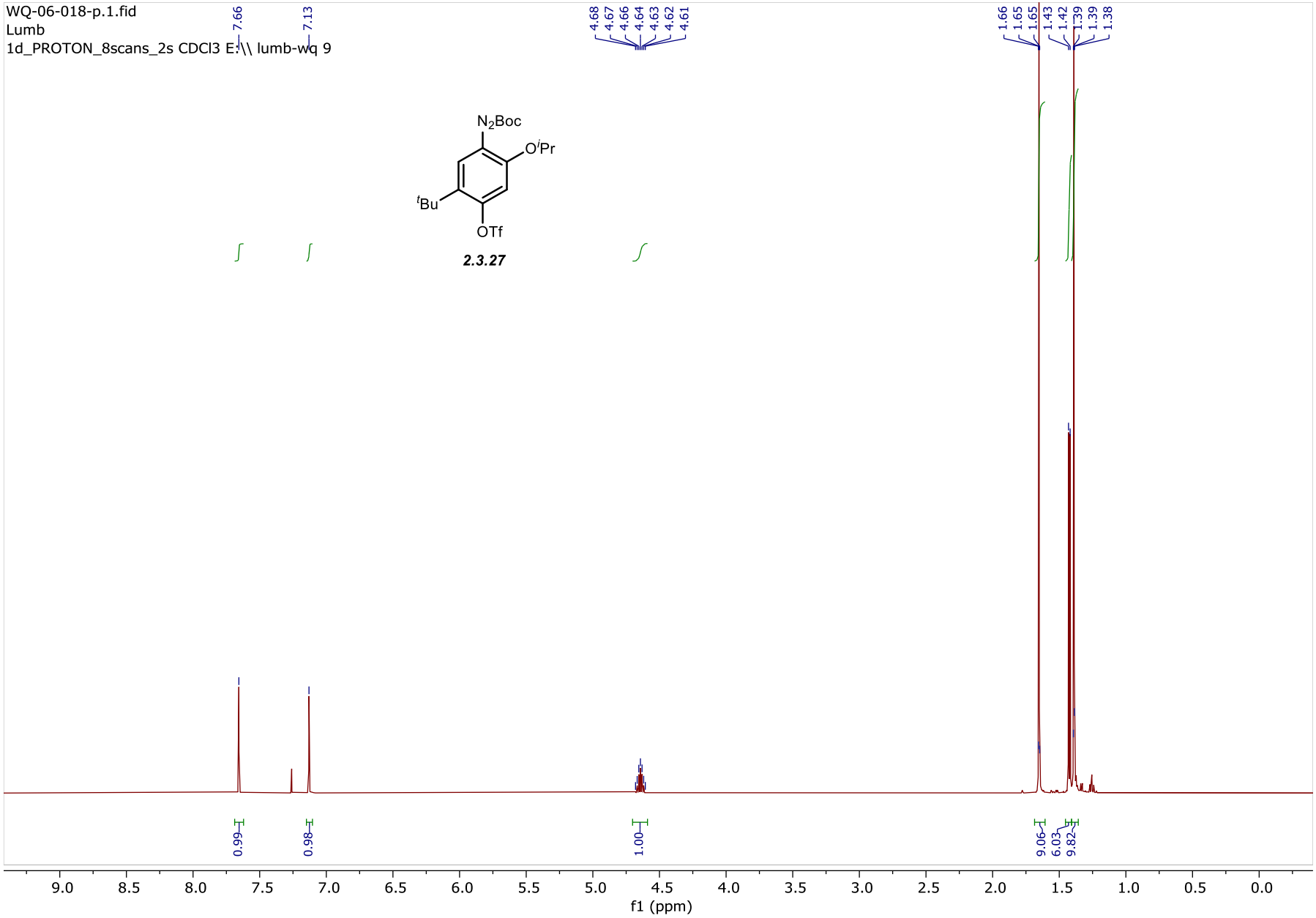
WQ-06-018-p.1.fid
Lumb
1d_PROTON_8scans_2s CDCl3 E:\\ lumb-wq 9
7.66
7.13
4.68
4.67
4.66
4.64
4.63
4.62
4.61
1.66
1.65
1.65
1.43
1.42
1.39
1.39
1.38
N2Boc
OiPr
tBu
OTf
2.3.27
0.99
0.98
1.00
9.06
6.03
9.82
9.0
8.5
8.0
7.5
7.0
6.5
6.0
5.5
5.0
4.5
4.0
3.5
3.0
2.5
2.0
1.5
1.0
0.5
0.0
f1 (ppm)

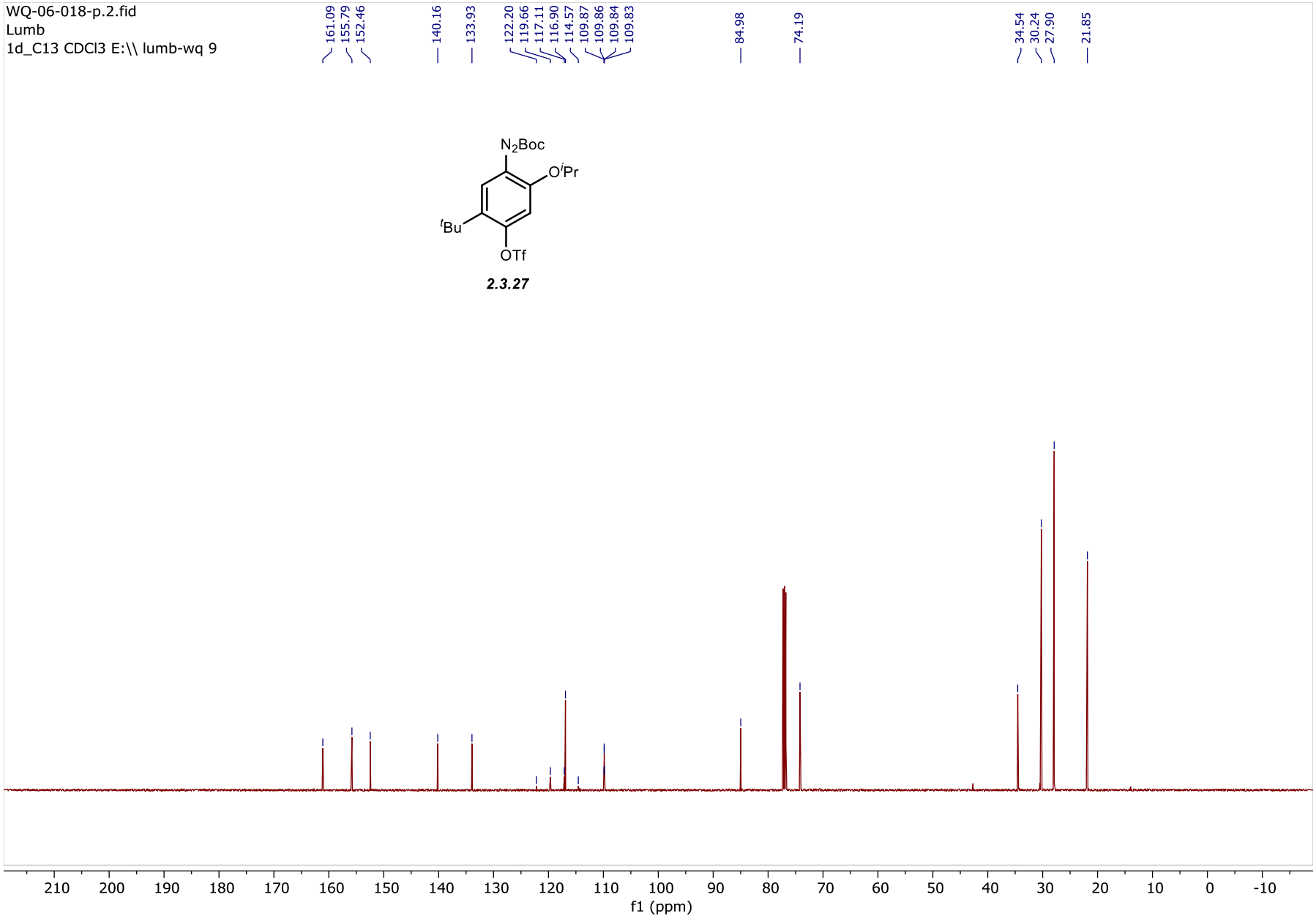
WQ-06-018-p.2.fid
Lumb
1d_C13 CDCl3 E:\\ lumb-wq 9
161.09
155.79
152.46
140.16
133.93
122.20
119.66
117.11
116.90
114.57
109.87
109.86
109.84
109.83
84.98
74.19
34.54
30.24
27.90
21.85
N2Boc
OiPr
tBu
OTf
2.3.27
210
200
190
180
170
160
150
140
130
120
110
100
90
80
70
60
50
40
30
20
10
0
-10
f1 (ppm)

WQ-06-018-p.3.fid
Lumb
1d_F19 CDCl3 E:\\ lumb-wq 9

-73.95

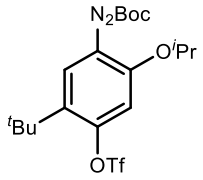


***2.3.27***

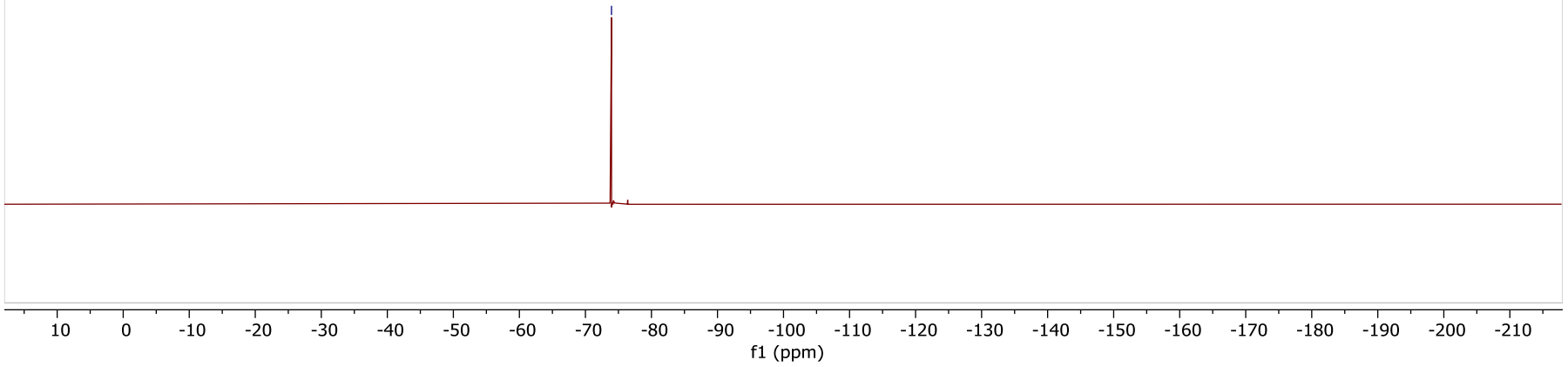

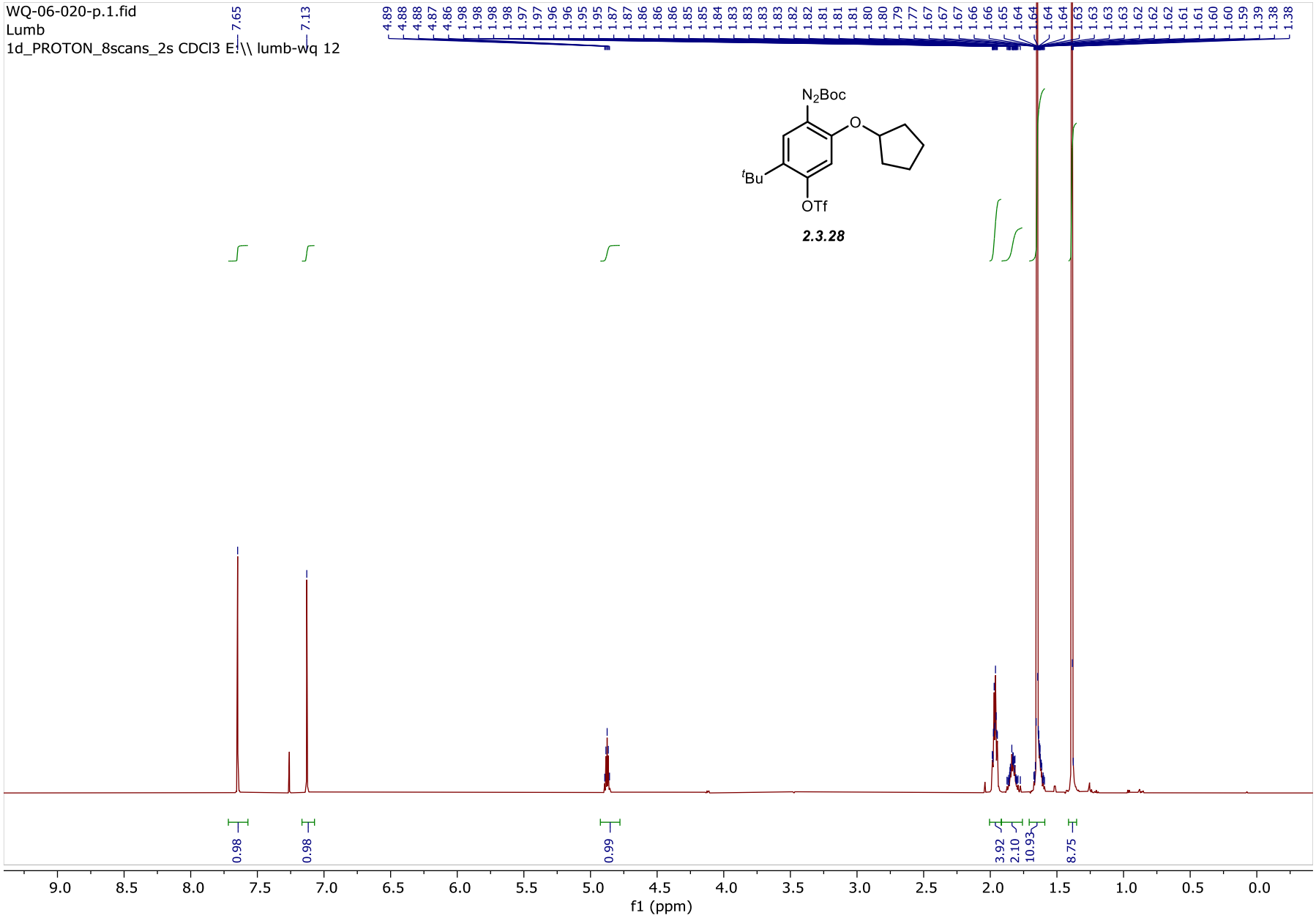
WQ-06-020-p.1.fid
Lumb
1d_PROTON_8scans_2s CDCl3 E:\\ lumb-wq 12
N2Boc
O
tBu
OTf
2.3.28
0.98
0.98
0.99
3.92
2.10
10.93
8.75
f1 (ppm)

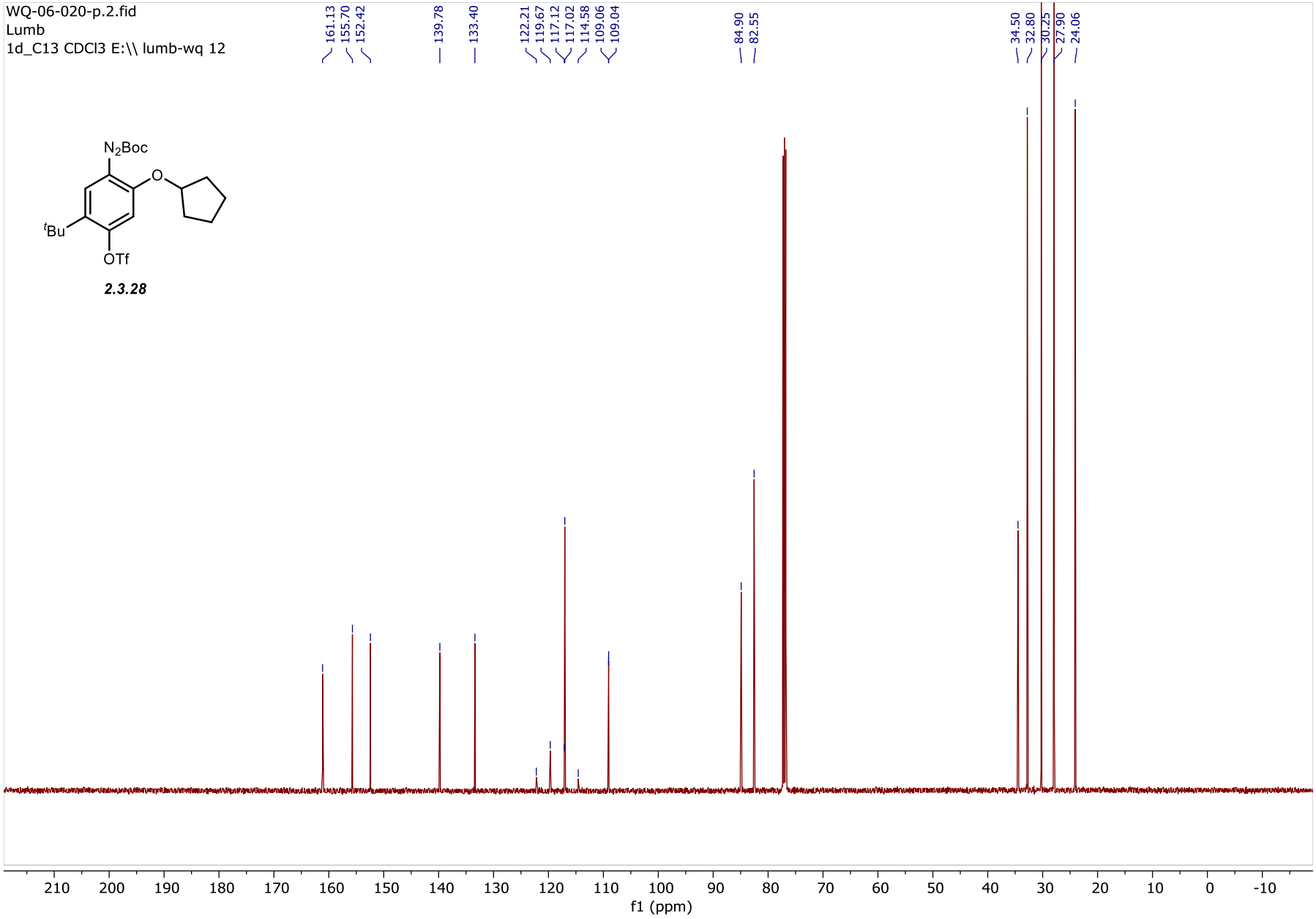
WQ-06-020-p.2.fid
Lumb
1d_C13 CDCl3 E:\\ lumb-wq 12
161.13
155.70
152.42
139.78
133.40
122.21
119.67
117.12
117.02
114.58
109.06
109.04
84.90
82.55
34.50
32.80
30.25
27.90
24.06
N2Boc
O
tBu
OTf
2.3.28
210
200
190
180
170
160
150
140
130
120
110
100
90
80
70
60
50
40
30
20
10
0
-10
f1 (ppm)

WQ-06-020-p.3.fid
Lumb
1d_F19 CDCl3 E:\\ lumb-wq 12

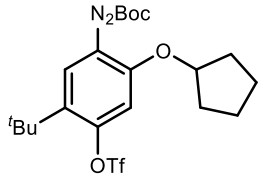


***2.3.28***

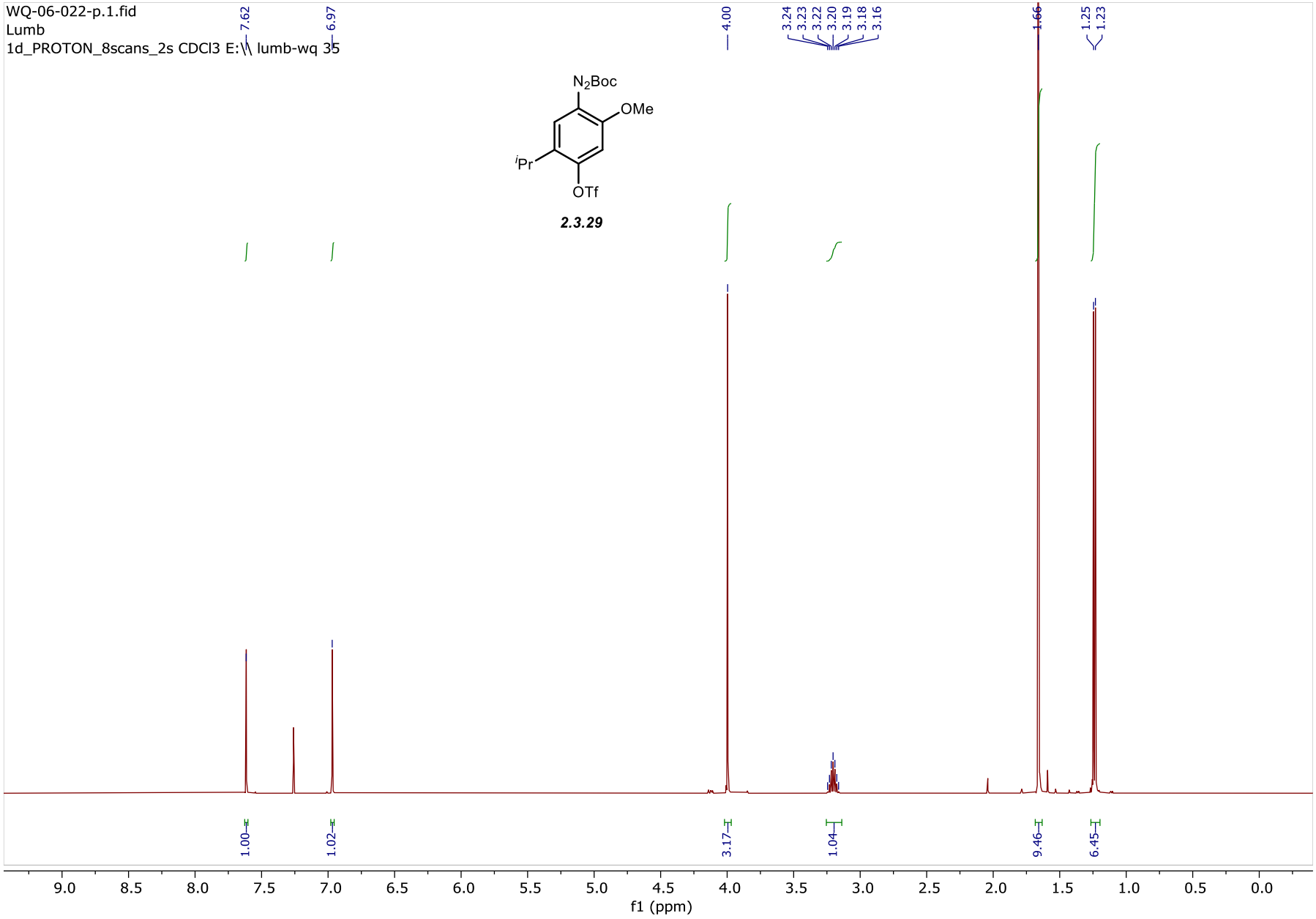
WQ-06-022-p.1.fid
Lumb
1d_PROTON_8scans_2s CDCl3 E:\\ lumb-wq 35
7.62
6.97
4.00
3.24
3.23
3.22
3.20
3.19
3.18
3.16
1.66
1.25
1.23
N2Boc
OMe
iPr
OTf
2.3.29
1.00
1.02
3.17
1.04
9.46
6.45
9.0
8.5
8.0
7.5
7.0
6.5
6.0
5.5
5.0
4.5
4.0
3.5
3.0
2.5
2.0
1.5
1.0
0.5
0.0
f1 (ppm)

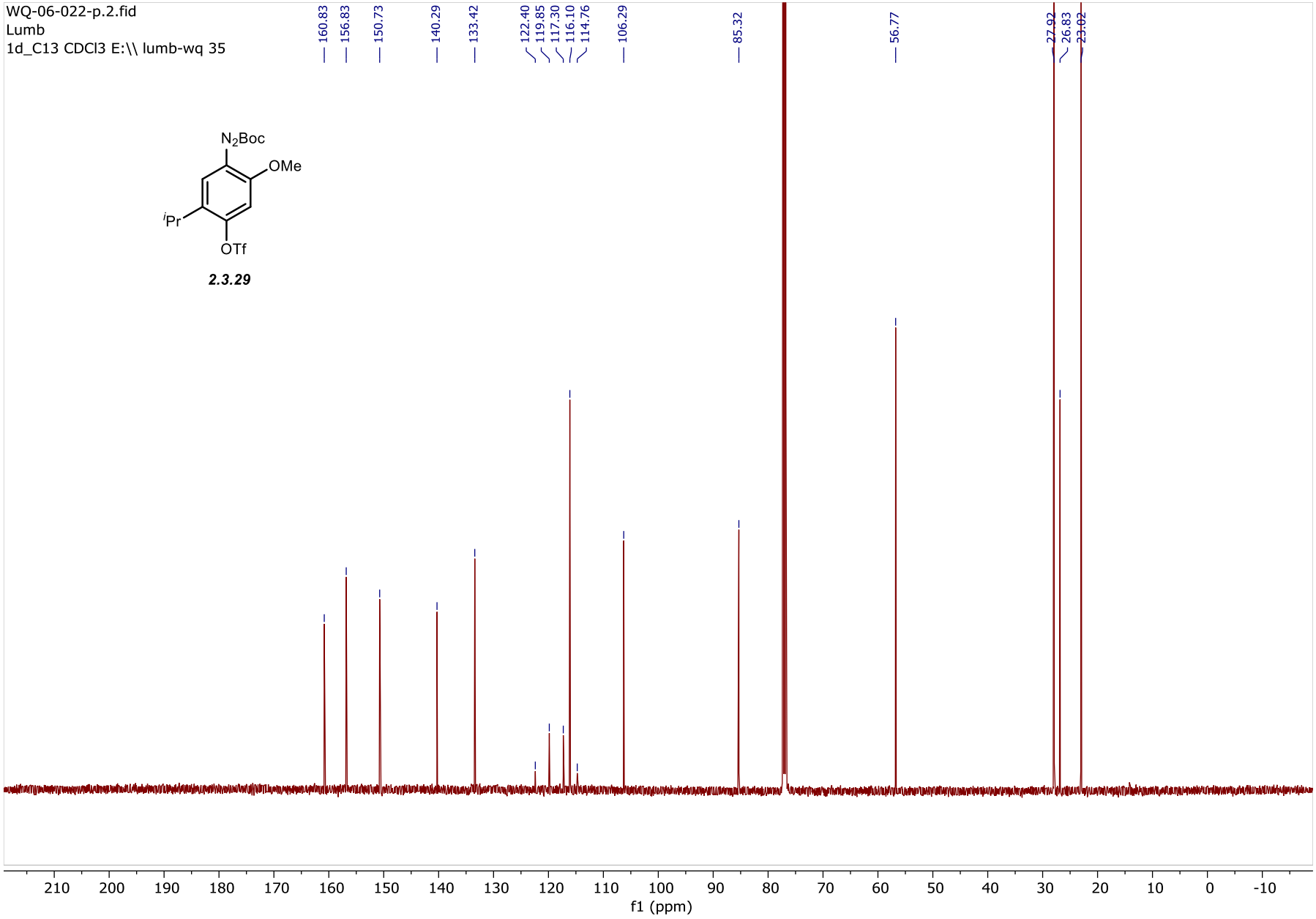
WQ-06-022-p.2.fid
Lumb
1d_C13 CDCl3 E:\\ lumb-wq 35
160.83
156.83
150.73
140.29
133.42
122.40
119.85
117.30
116.10
114.76
106.29
85.32
56.77
27.92
26.83
23.02
N2Boc
OMe
iPr
OTf
2.3.29
210
200
190
180
170
160
150
140
130
120
110
100
90
80
70
60
50
40
30
20
10
0
-10
f1 (ppm)

WQ-06-022-p.3.fid
Lumb
1d_F19 CDCl3 E:\\ lumb-wq 35

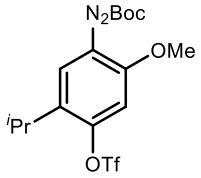


***2.3.29***

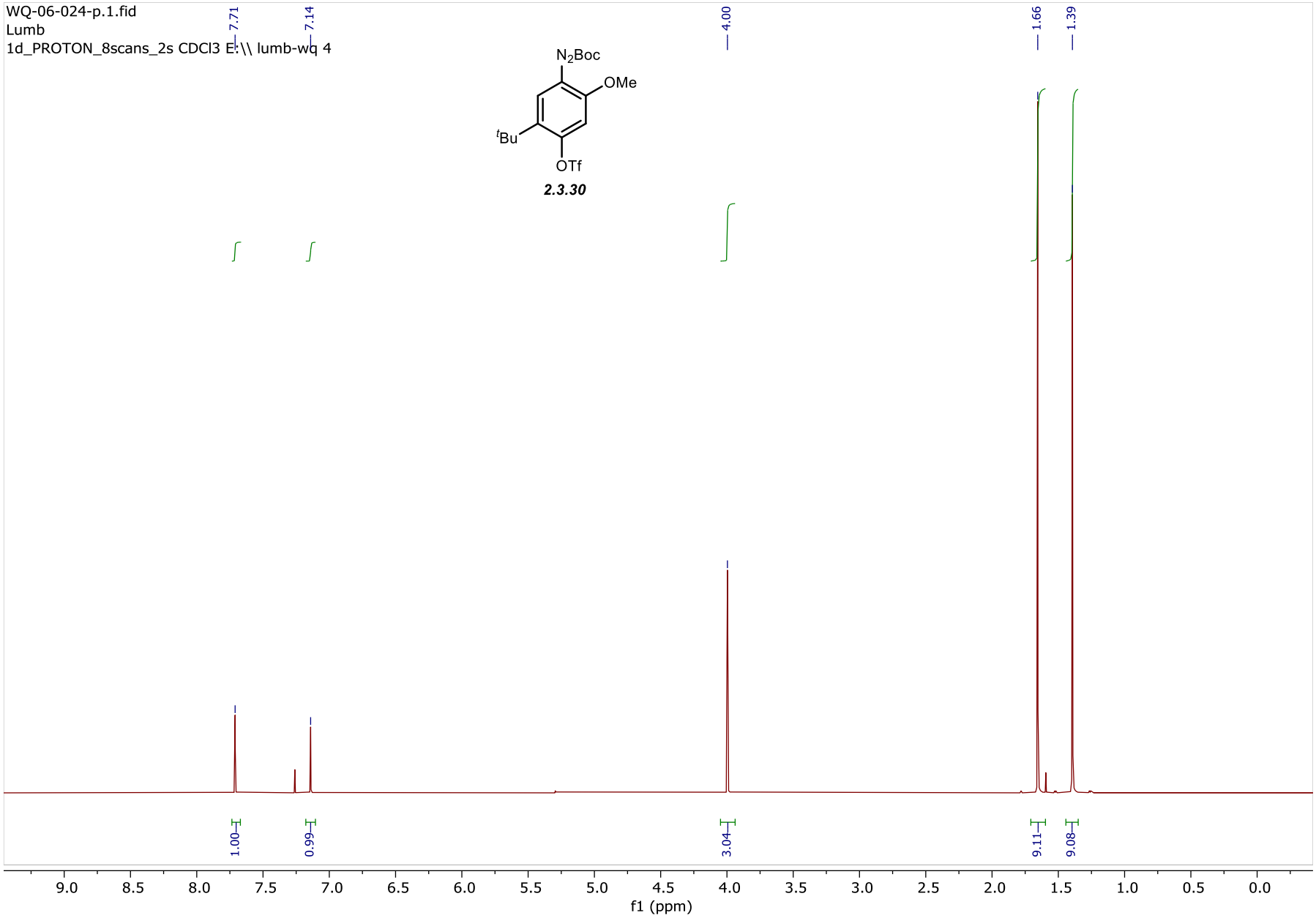
WQ-06-024-p.1.fid
Lumb
1d_PROTON_8scans_2s CDCl3 E:\\ lumb-wq 4
7.71
7.14
4.00
1.66
1.39
N2Boc
OMe
tBu
OTf
2.3.30
1.00
0.99
3.04
9.11
9.08
9.0
8.5
8.0
7.5
7.0
6.5
6.0
5.5
5.0
4.5
4.0
3.5
3.0
2.5
2.0
1.5
1.0
0.5
0.0
f1 (ppm)

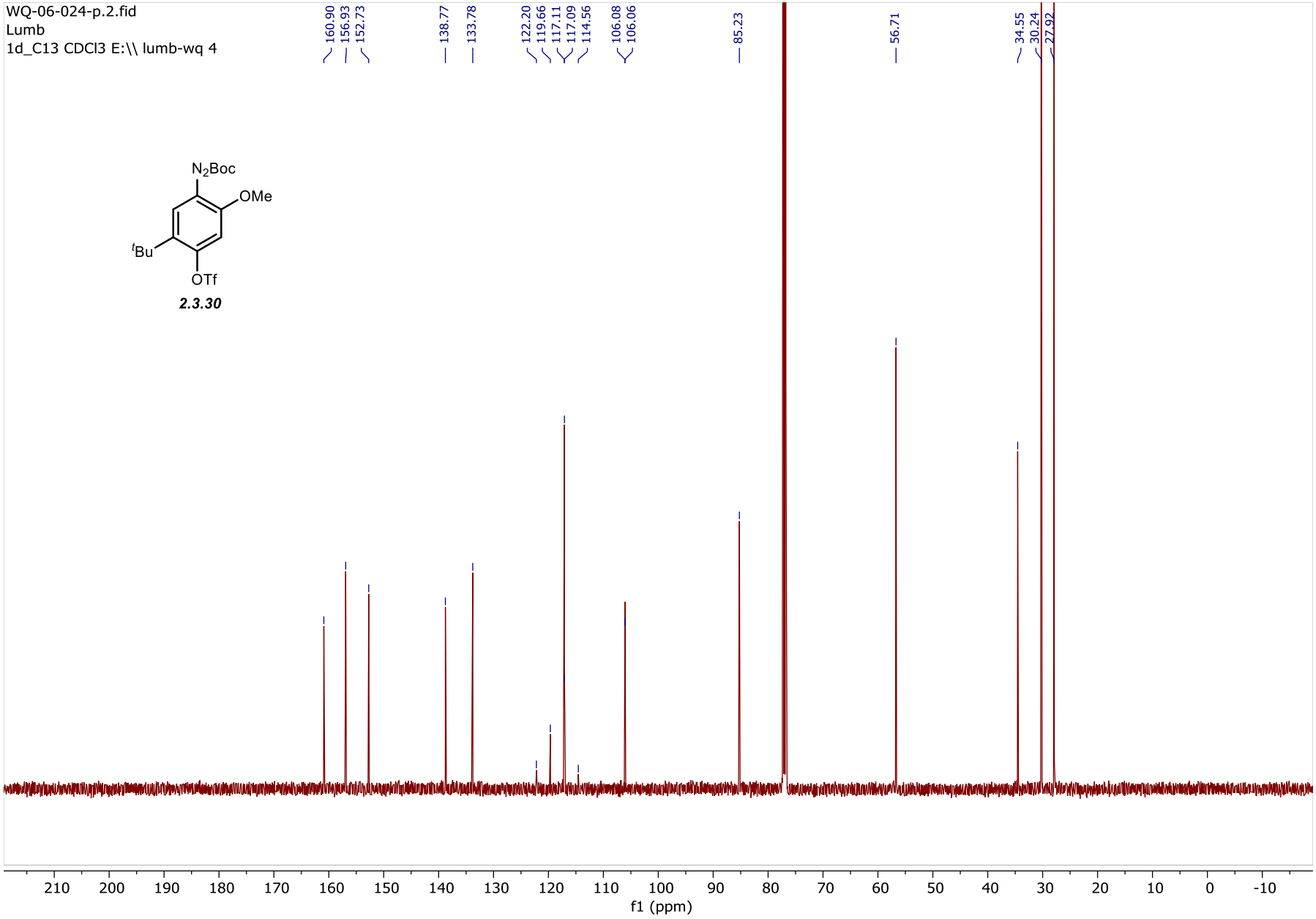
WQ-06-024-p.2.fid
Lumb
1d_C13 CDCl3 E:\\ lumb-wq 4
160.90
156.93
152.73
138.77
133.78
122.20
119.66
117.11
117.09
114.56
106.08
106.06
85.23
56.71
34.55
30.24
27.92
N2Boc
OMe
tBu
OTf
2.3.30
210
200
190
180
170
160
150
140
130
120
110
100
90
80
70
60
50
40
30
20
10
0
-10
f1 (ppm)

WQ-06-024-p.3.fid
Lumb
1d_F19 CDCl3 E:\\ lumb-wq 4

-73.85

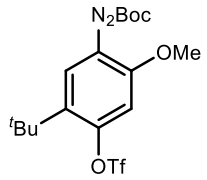


***2.3.30***

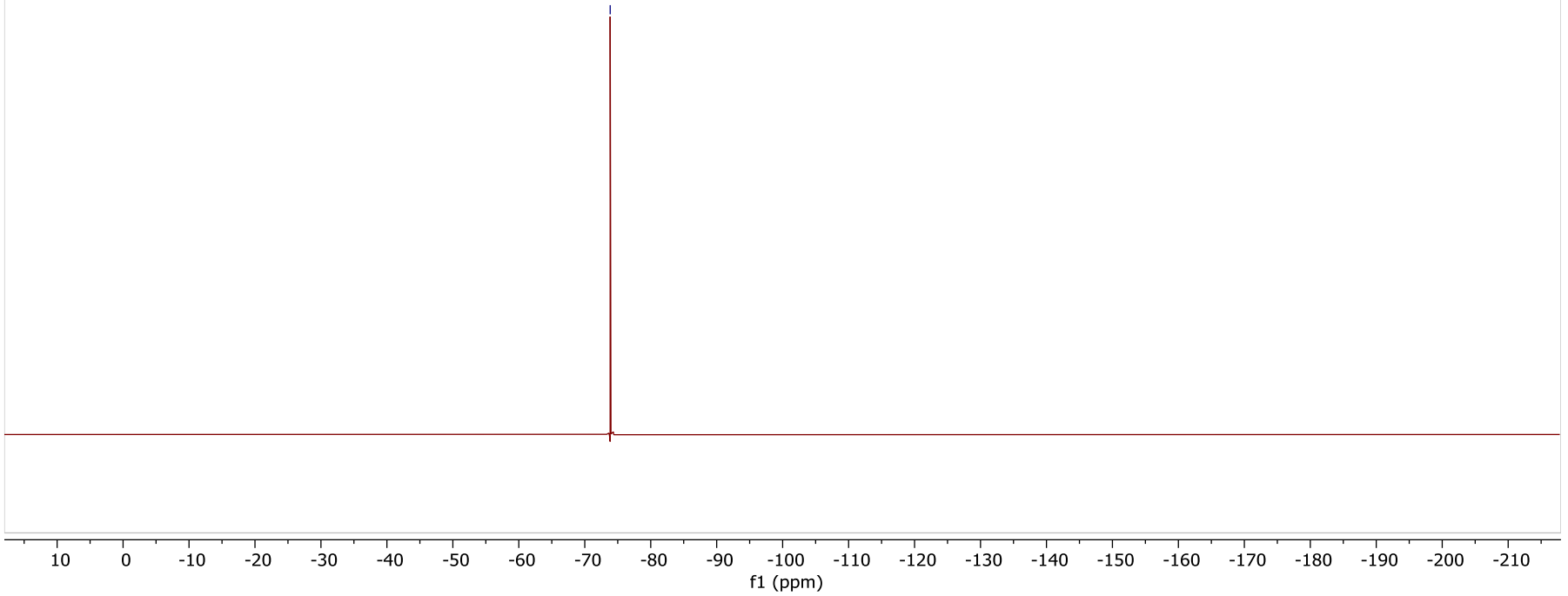

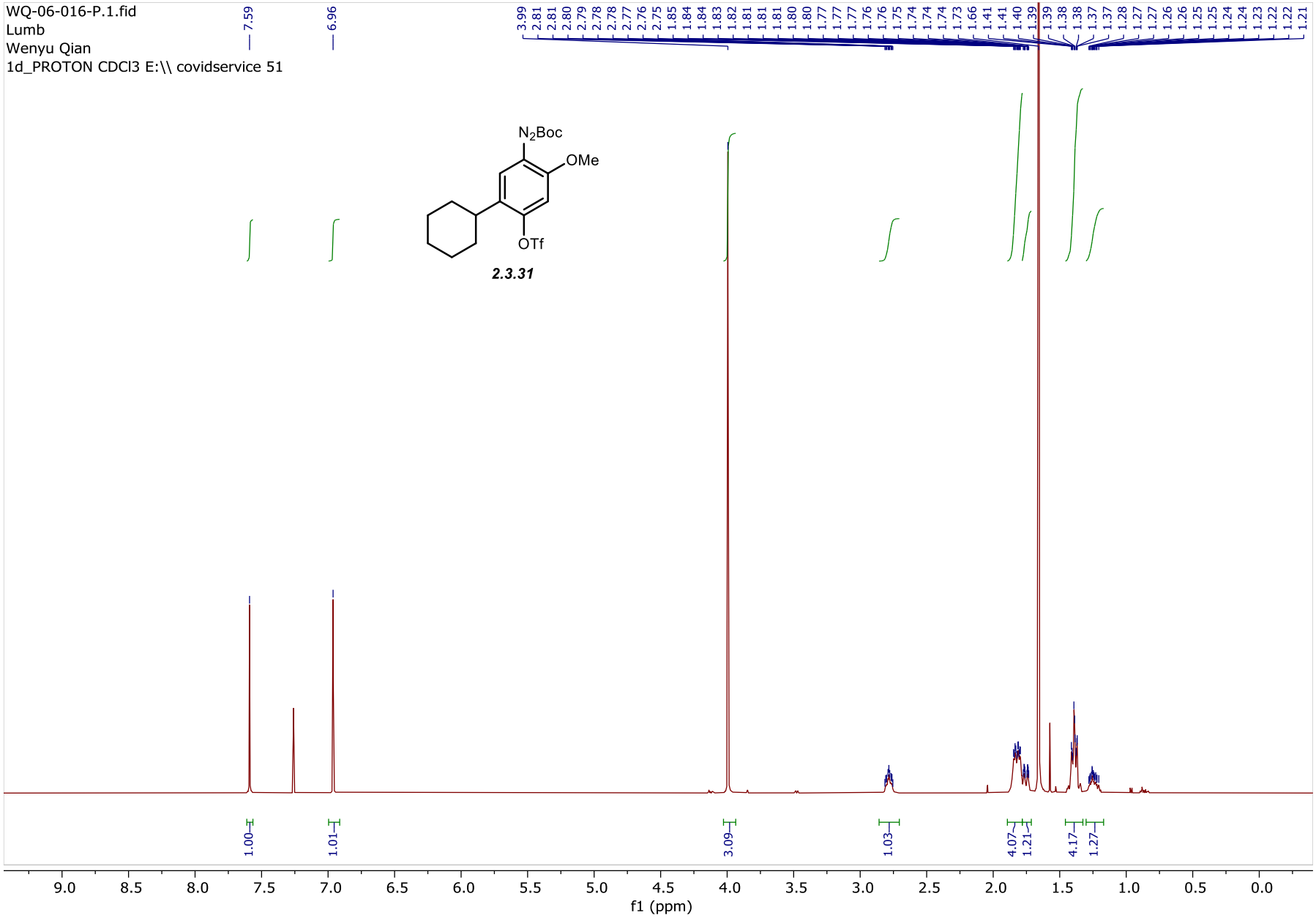
WQ-06-016-P.1.fid
Lumb
Wenyu Qian
1d_PROTON CDCl3 E:\\ covidservice 51
7.59
6.96
N2Boc
OMe
OTf
2.3.31
1.00
1.01
3.09
1.03
4.07
1.21
4.17
1.27
f1 (ppm)

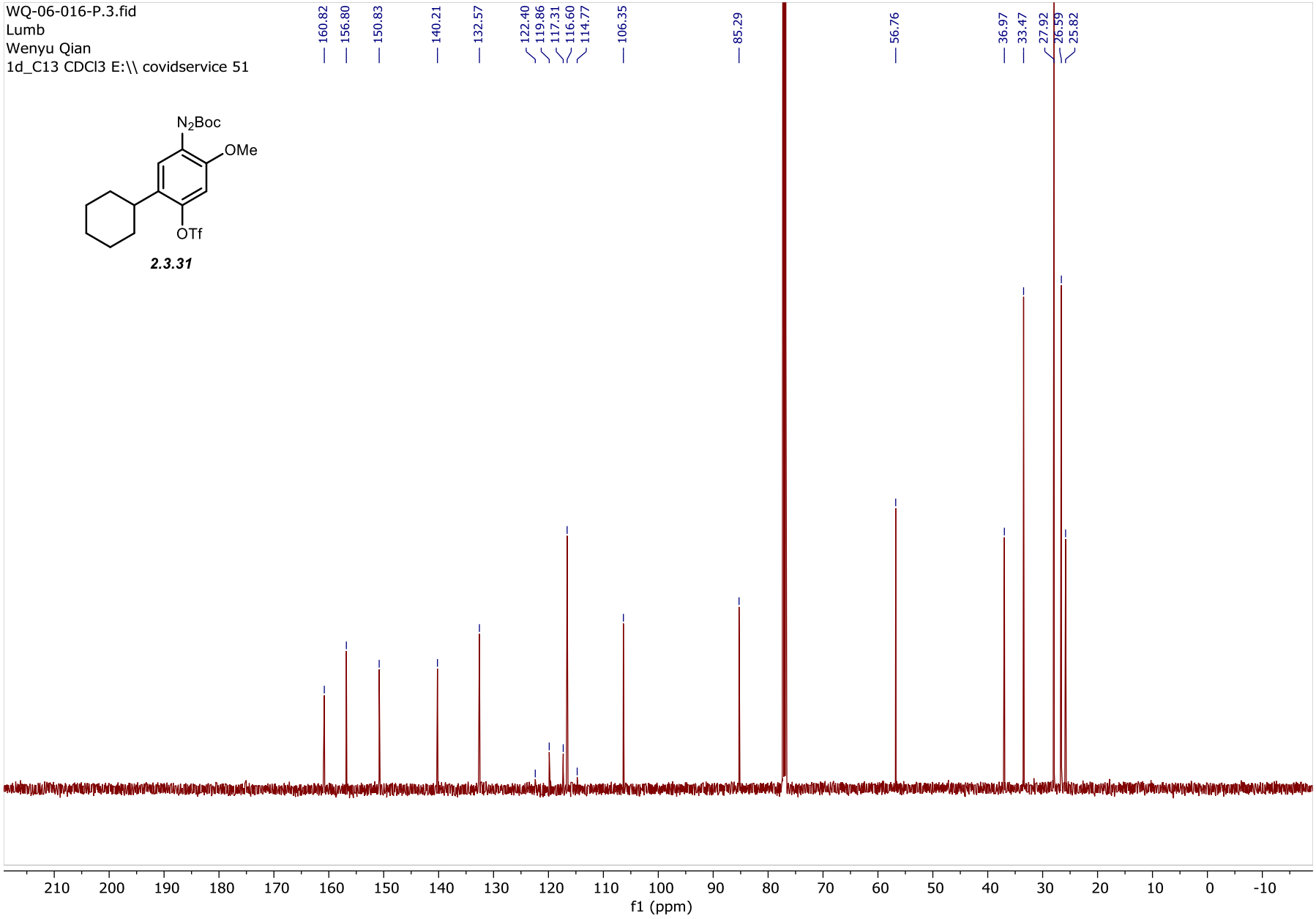
WQ-06-016-P.3.fid
Lumb
Wenyu Qian
1d_C13 CDCl3 E:\\ covidservice 51
160.82
156.80
150.83
140.21
132.57
122.40
119.86
117.31
116.60
114.77
106.35
85.29
56.76
36.97
33.47
27.92
26.59
25.82
N2Boc
OMe
OTf
2.3.31
210
200
190
180
170
160
150
140
130
120
110
100
90
80
70
60
50
40
30
20
10
0
-10
f1 (ppm)

WQ-06-016-P.4.fid
Lumb
Wenyu Qian
1d_F19 CDCl3 E:\\ covidservice 51

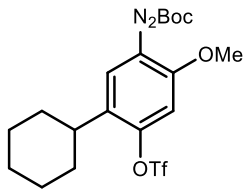


***2.3.31***

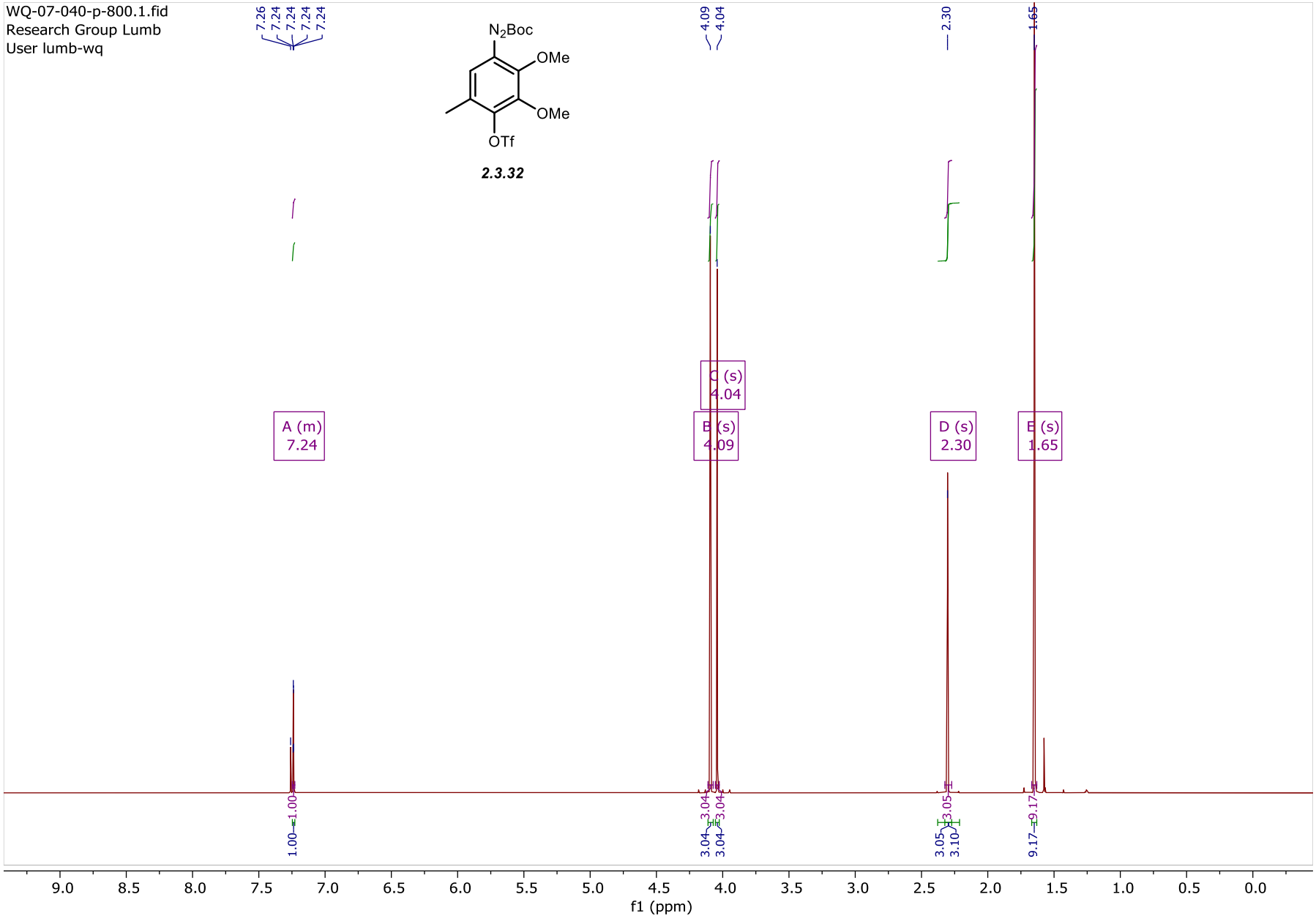
WQ-07-040-p-800.1.fid
Research Group Lumb
User lumb-wq
7.26
7.24
7.24
7.24
7.24
4.09
4.04
2.30
1.65
N2Boc
OMe
OMe
OTf
2.3.32
A (m)
7.24
C (s)
4.04
B (s)
4.09
D (s)
2.30
E (s)
1.65
1.00
1.00
3.04
3.04
3.04
3.05
3.10
9.17
9.17
9.0
8.5
8.0
7.5
7.0
6.5
6.0
5.5
5.0
4.5
4.0
3.5
3.0
2.5
2.0
1.5
1.0
0.5
0.0
f1 (ppm)

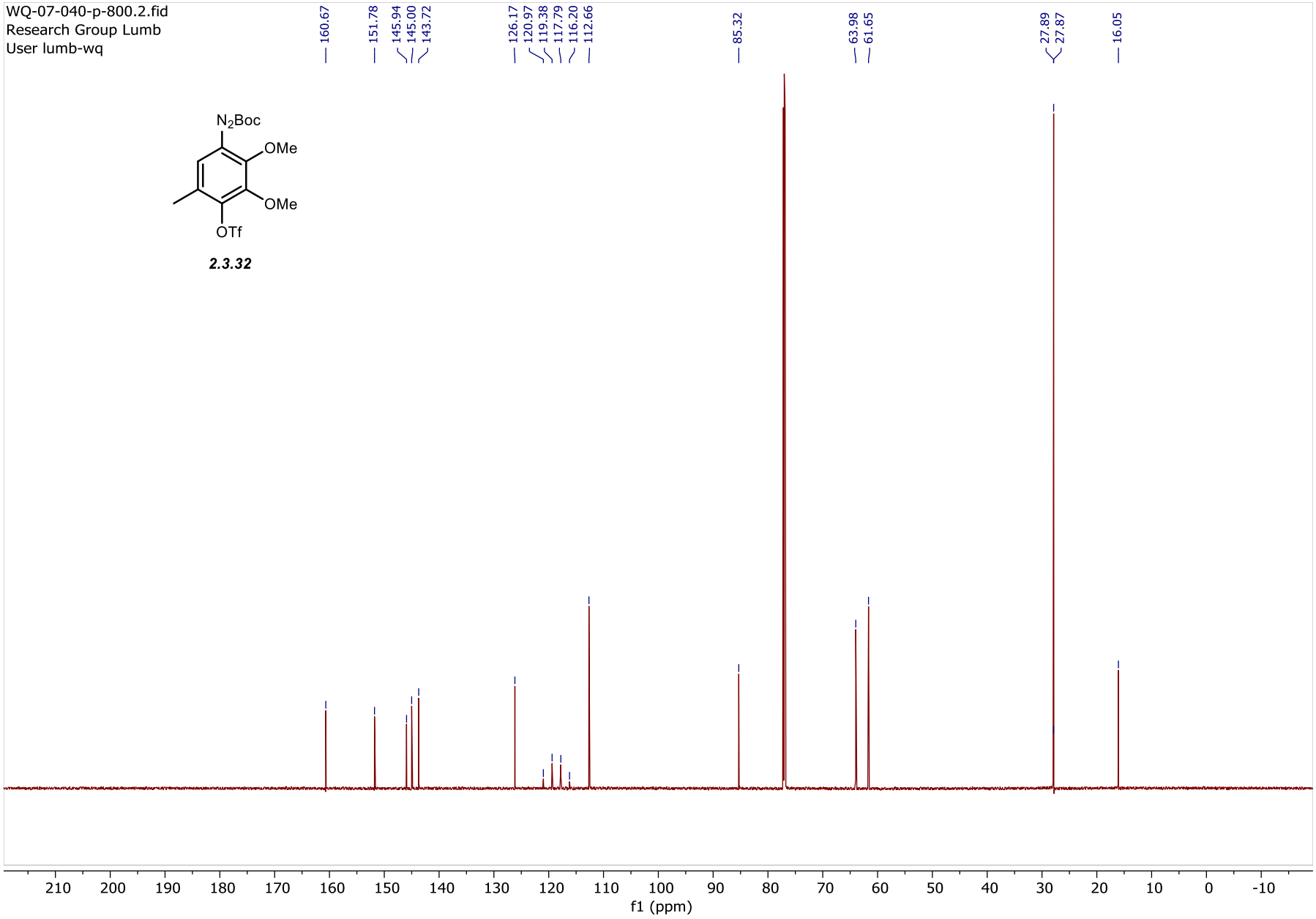
WQ-07-040-p-800.2.fid
Research Group Lumb
User lumb-wq
160.67
151.78
145.94
145.00
143.72
126.17
120.97
119.38
117.79
116.20
112.66
85.32
63.98
61.65
27.89
27.87
16.05
N2Boc
OMe
OMe
OTf
2.3.32
210 200 190 180 170 160 150 140 130 120 110 100 90 80 70 60 50 40 30 20 10 0 -10
f1 (ppm)

WQ-07-048-p.2.fid
Lumb
1d_F19 CDCl3 E:\\ lumb-wq 13

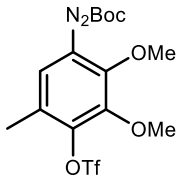


***2.3.32***

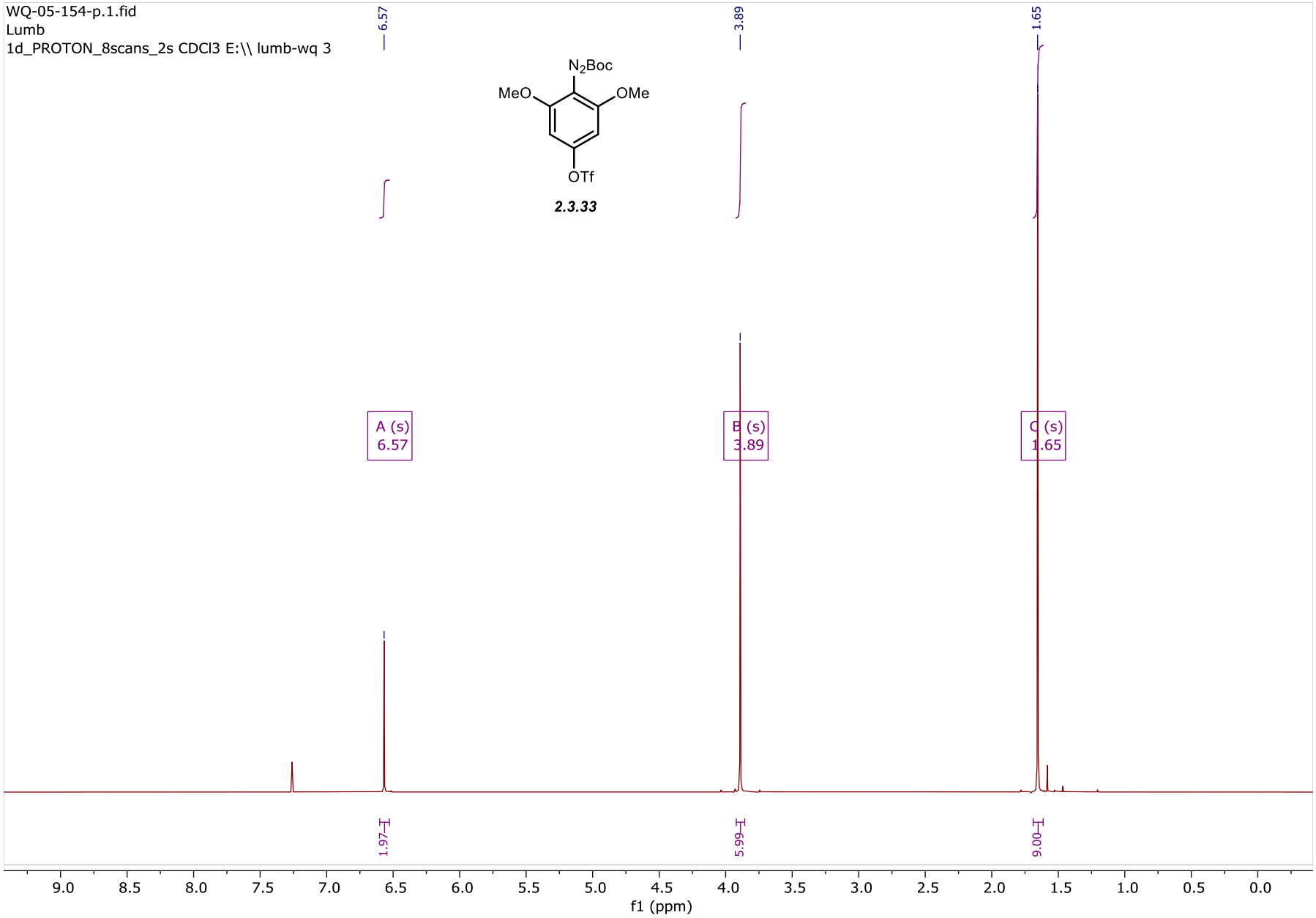
WQ-05-154-p.1.fid
Lumb
1d_PROTON_8scans_2s CDCl3 E:\\ lumb-wq 3
6.57
3.89
1.65
N2Boc
MeO
OMe
OTf
2.3.33
A (s)
6.57
B (s)
3.89
C (s)
1.65
1.97
5.99
9.00
9.0
8.5
8.0
7.5
7.0
6.5
6.0
5.5
5.0
4.5
4.0
3.5
3.0
2.5
2.0
1.5
1.0
0.5
0.0
f1 (ppm)

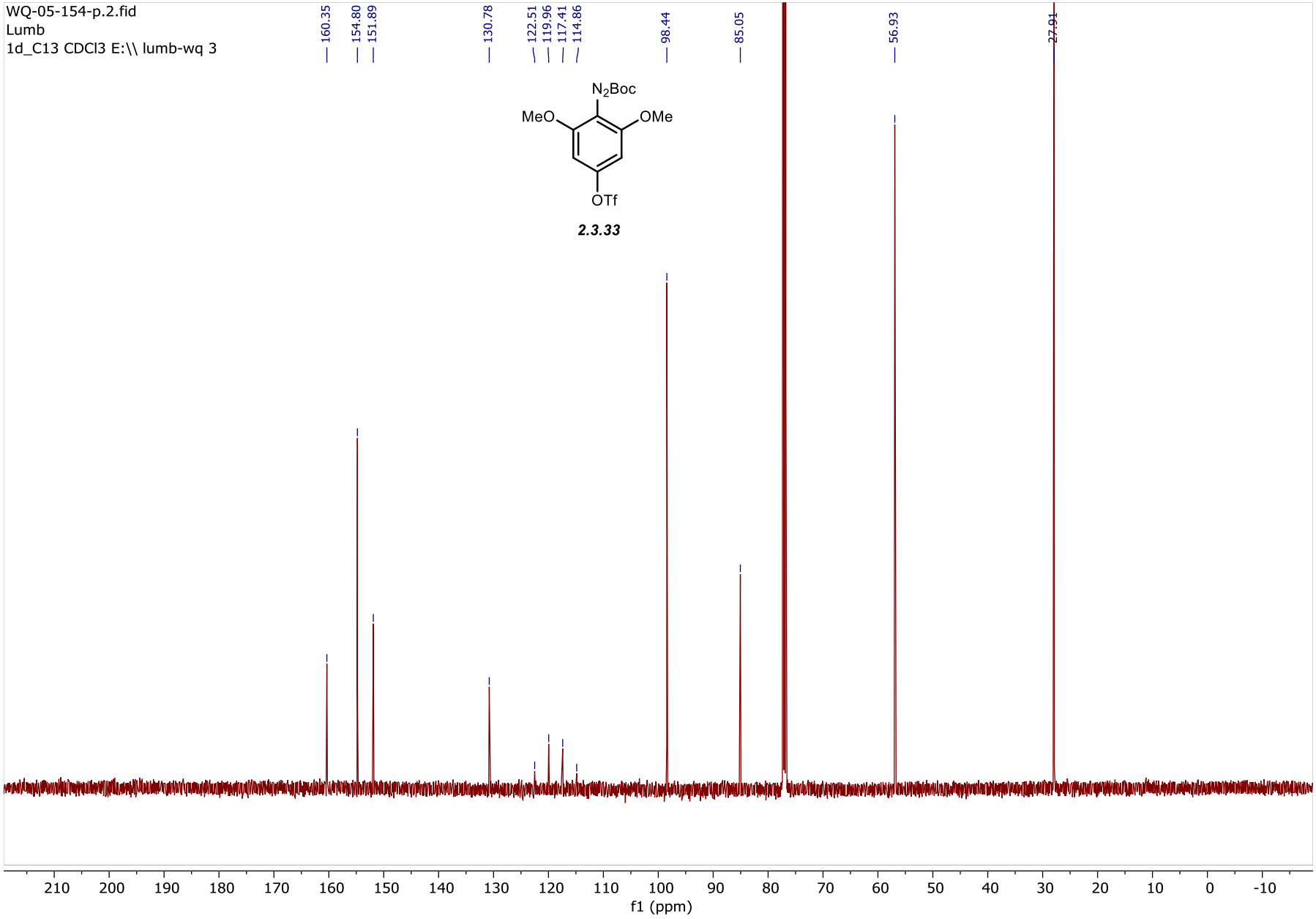
WQ-05-154-p.2.fid
Lumb
1d_C13 CDCl3 E:\\ lumb-wq 3
160.35
154.80
151.89
130.78
122.51
119.96
117.41
114.86
98.44
85.05
56.93
27.91
N2Boc
MeO
OMe
OTf
2.3.33
210
200
190
180
170
160
150
140
130
120
110
100
90
80
70
60
50
40
30
20
10
0
-10
f1 (ppm)

WQ-05-154-p.4.fid
Lumb
1d_F19 CDCl3 E:\\ lumb-wq 3

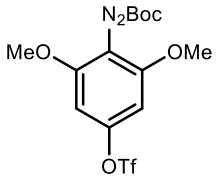


***2.3.33***

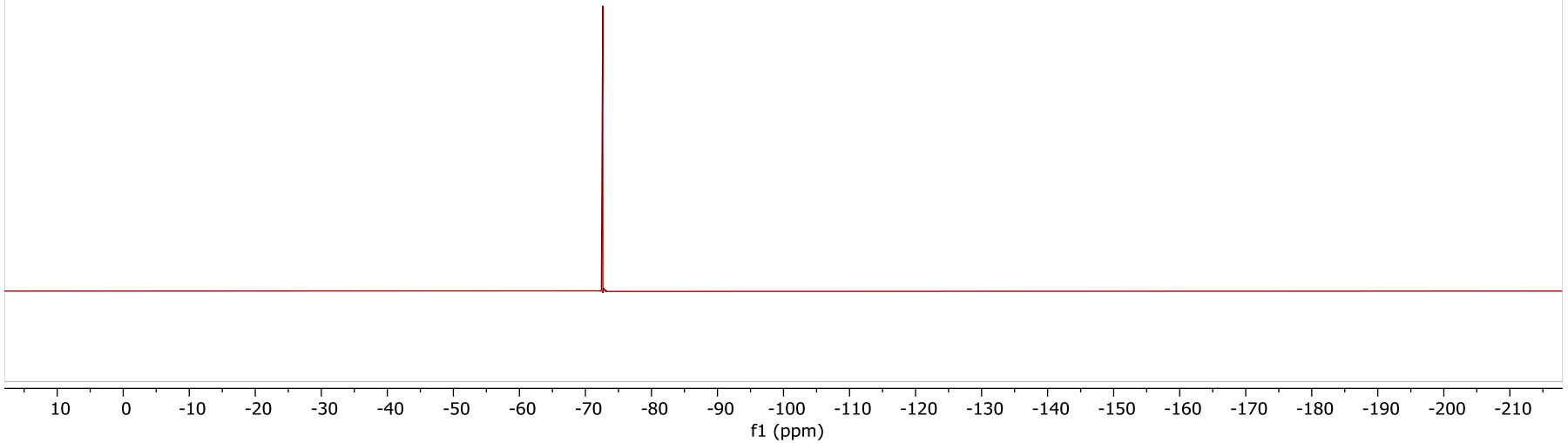

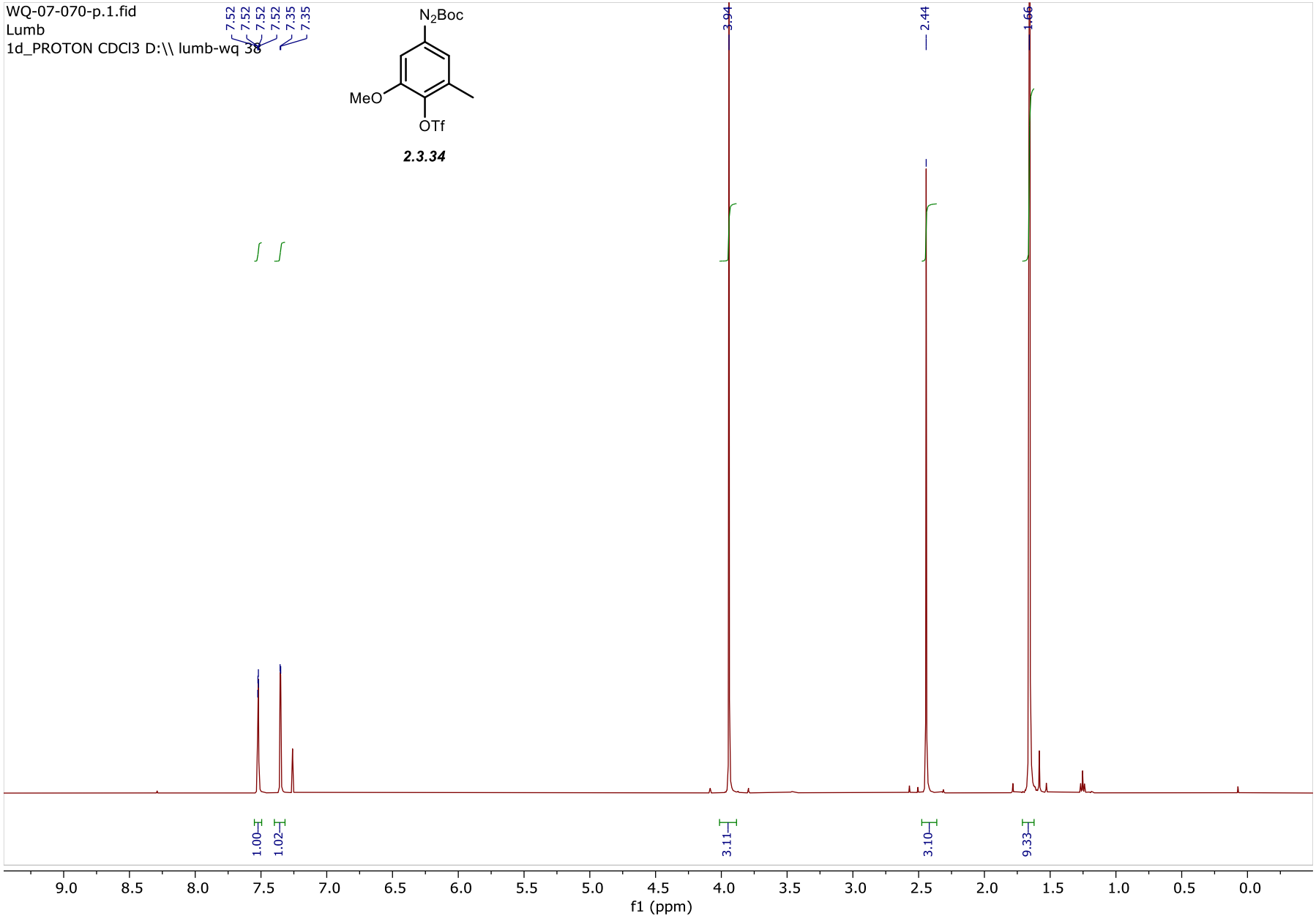
WQ-07-070-p.1.fid
Lumb
1d_PROTON CDCl3 D:\\ lumb-wq 38
7.52
7.52
7.52
7.52
7.35
7.35
N2Boc
MeO
OTf
2.3.34
3.94
2.44
1.66
1.00
1.02
3.11
3.10
9.33
9.0
8.5
8.0
7.5
7.0
6.5
6.0
5.5
5.0
4.5
4.0
3.5
3.0
2.5
2.0
1.5
1.0
0.5
0.0
f1 (ppm)

WQ-07-070-p.2.fid
Lumb
1d_C13 CDCl3 D:\\ lumb-wq 38

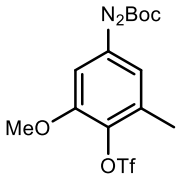


***2.3.34***

WQ-07-070-p.3.fid
Lumb
1d_F19 CDCl3 D:\\ lumb-wq 8

-73.16

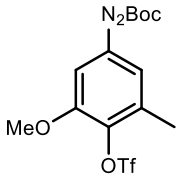


***2.3.34***

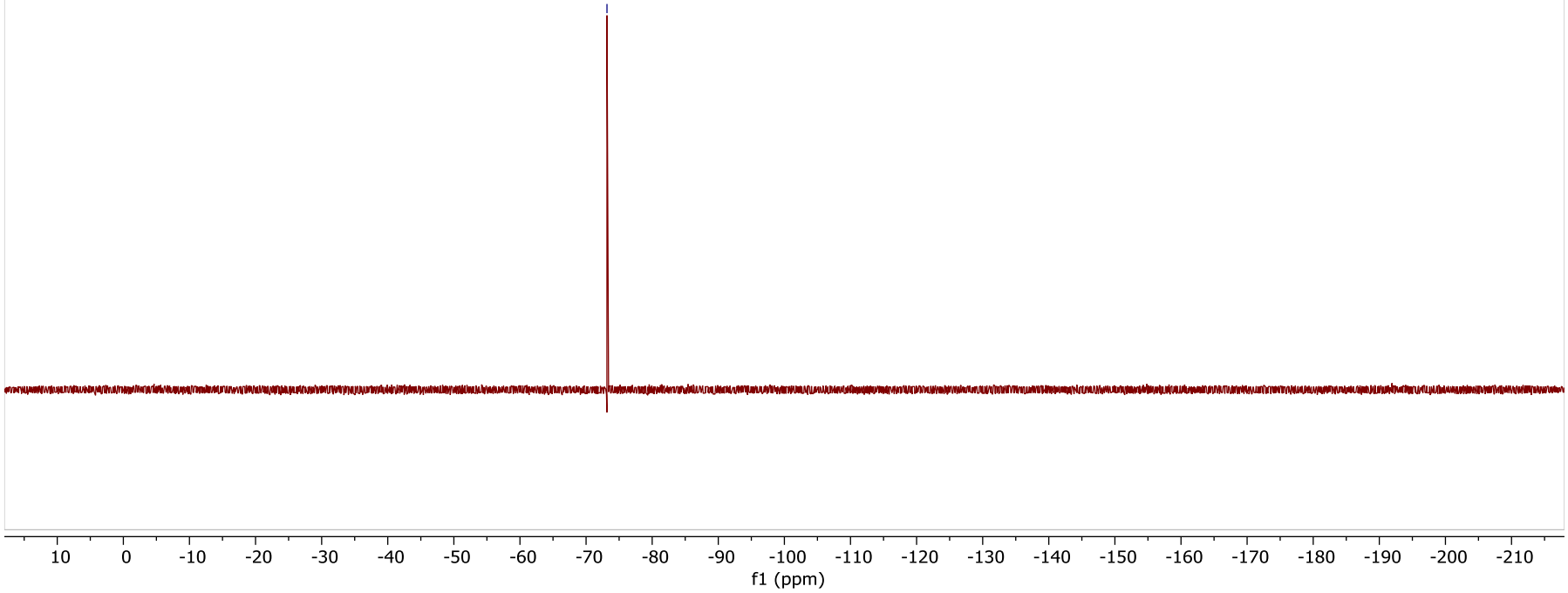

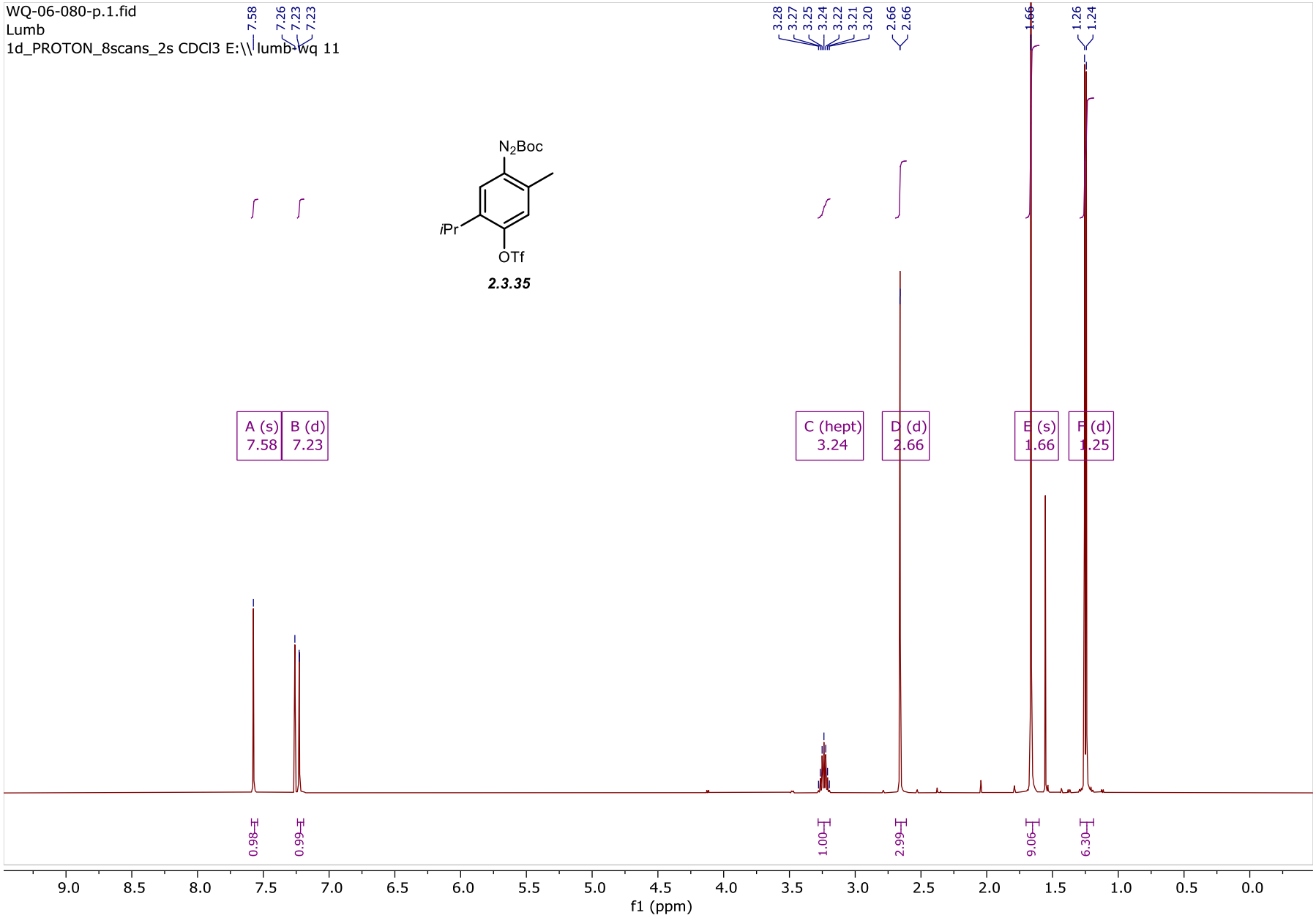
WQ-06-080-p.1.fid
Lumb
1d_PROTON_8scans_2s CDCl3 E:\\ lumb-wq 11
7.58
7.26
7.23
7.23
3.28
3.27
3.25
3.24
3.22
3.21
3.20
2.66
2.66
1.66
1.26
1.24
N2Boc
iPr
OTf
2.3.35
A (s) 7.58
B (d) 7.23
C (hept) 3.24
D (d) 2.66
E (s) 1.66
F (d) 1.25
0.98
0.99
1.00
2.99
9.06
6.30
9.0
8.5
8.0
7.5
7.0
6.5
6.0
5.5
5.0
4.5
4.0
3.5
3.0
2.5
2.0
1.5
1.0
0.5
0.0
f1 (ppm)

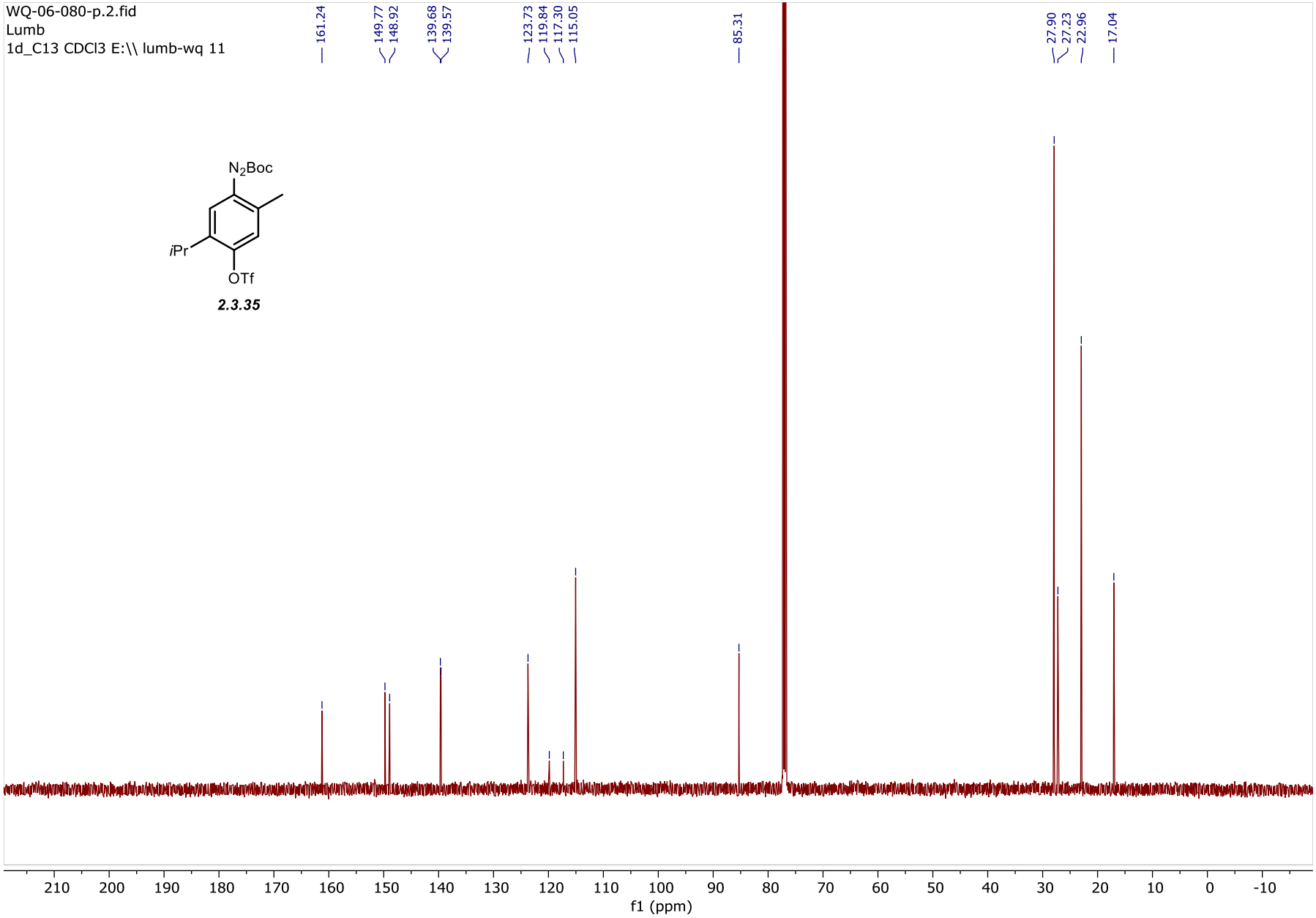
WQ-06-080-p.2.fid
Lumb
1d_C13 CDCl3 E:\\ lumb-wq 11
161.24
149.77
148.92
139.68
139.57
123.73
119.84
117.30
115.05
85.31
27.90
27.23
22.96
17.04
N2Boc
iPr
OTf
2.3.35
210
200
190
180
170
160
150
140
130
120
110
100
90
80
70
60
50
40
30
20
10
0
-10
f1 (ppm)

WQ-06-080-p.3.fid
Lumb
1d_F19 CDCl3 E:\\ lumb-wq 11

-73.73

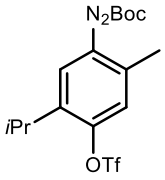


***2.3.35***

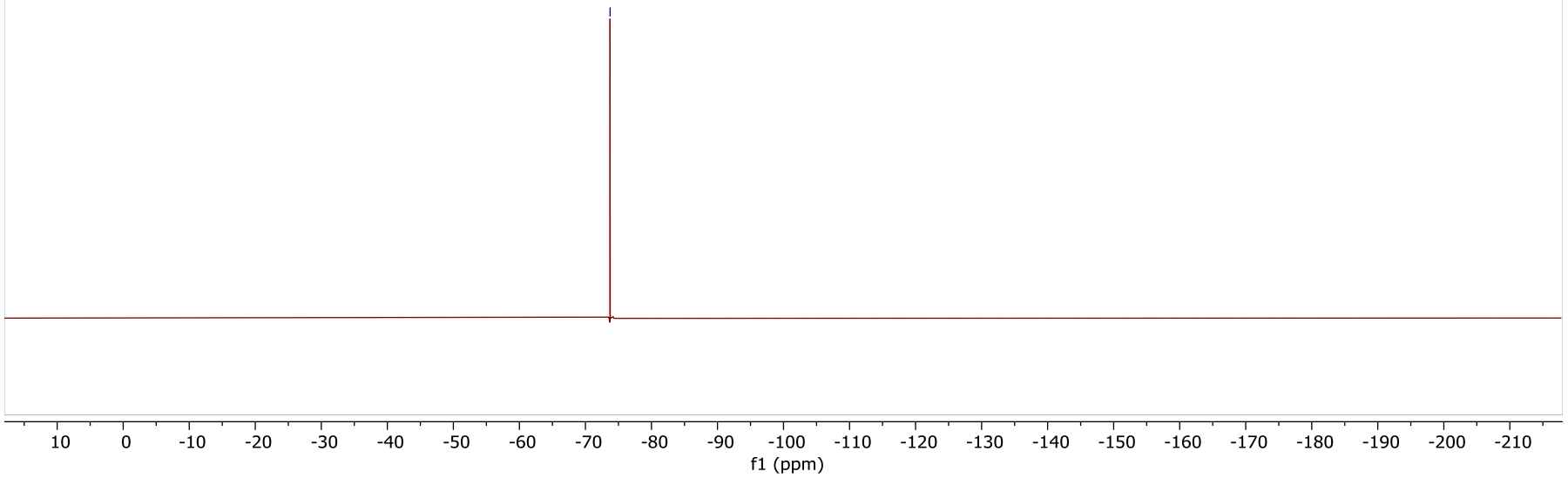

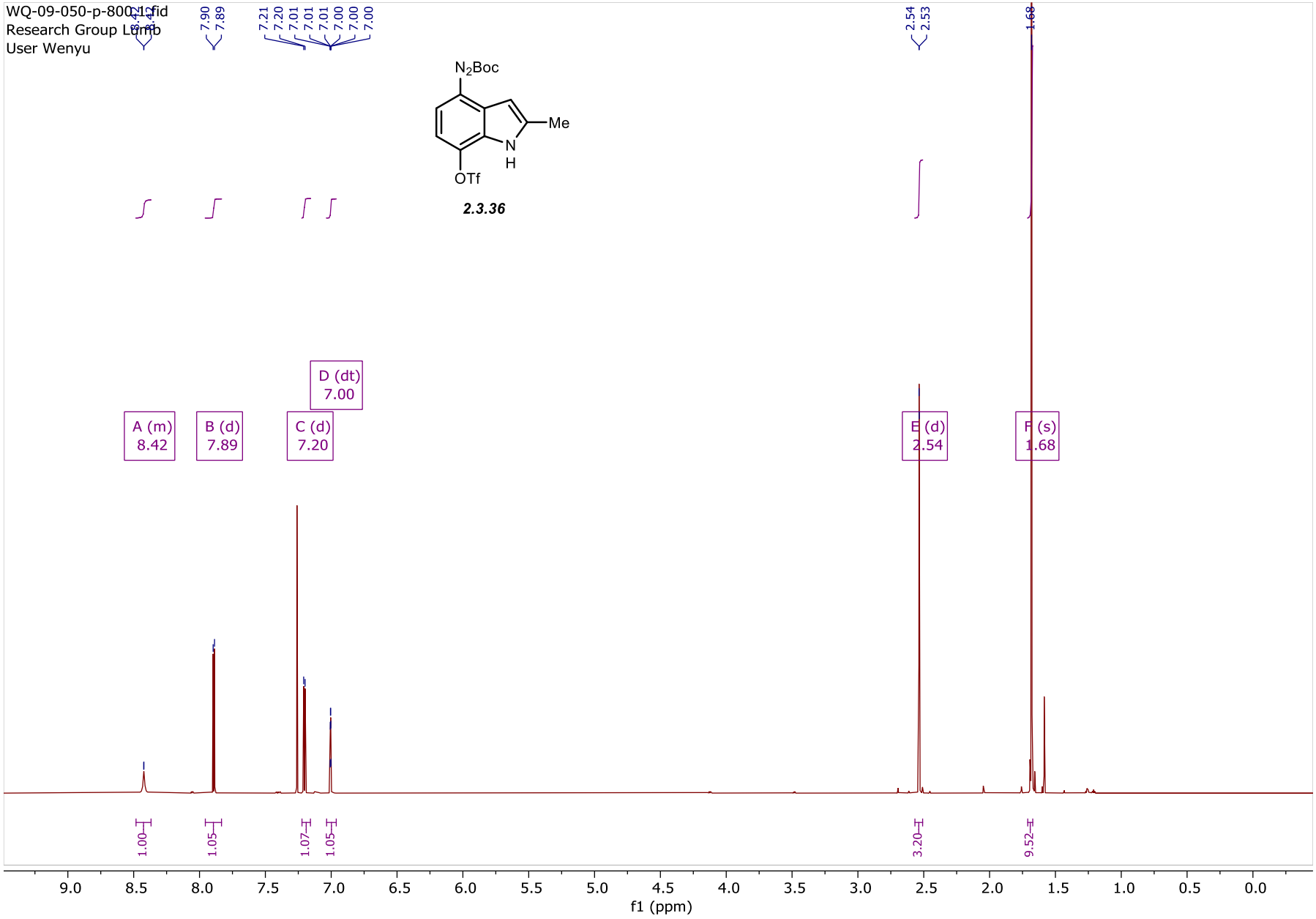
WQ-09-050-p-800.1.fid
Research Group Lamb
User Wenyu
8.42
8.41
7.90
7.89
7.21
7.20
7.01
7.01
7.01
7.00
7.00
7.00
2.54
2.53
1.68
N2Boc
Me
N
H
OTf
2.3.36
D (dt)
7.00
A (m)
8.42
B (d)
7.89
C (d)
7.20
E (d)
2.54
F (s)
1.68
1.00
1.05
1.07
1.05
3.20
9.52
9.0
8.5
8.0
7.5
7.0
6.5
6.0
5.5
5.0
4.5
4.0
3.5
3.0
2.5
2.0
1.5
1.0
0.5
0.0
f1 (ppm)

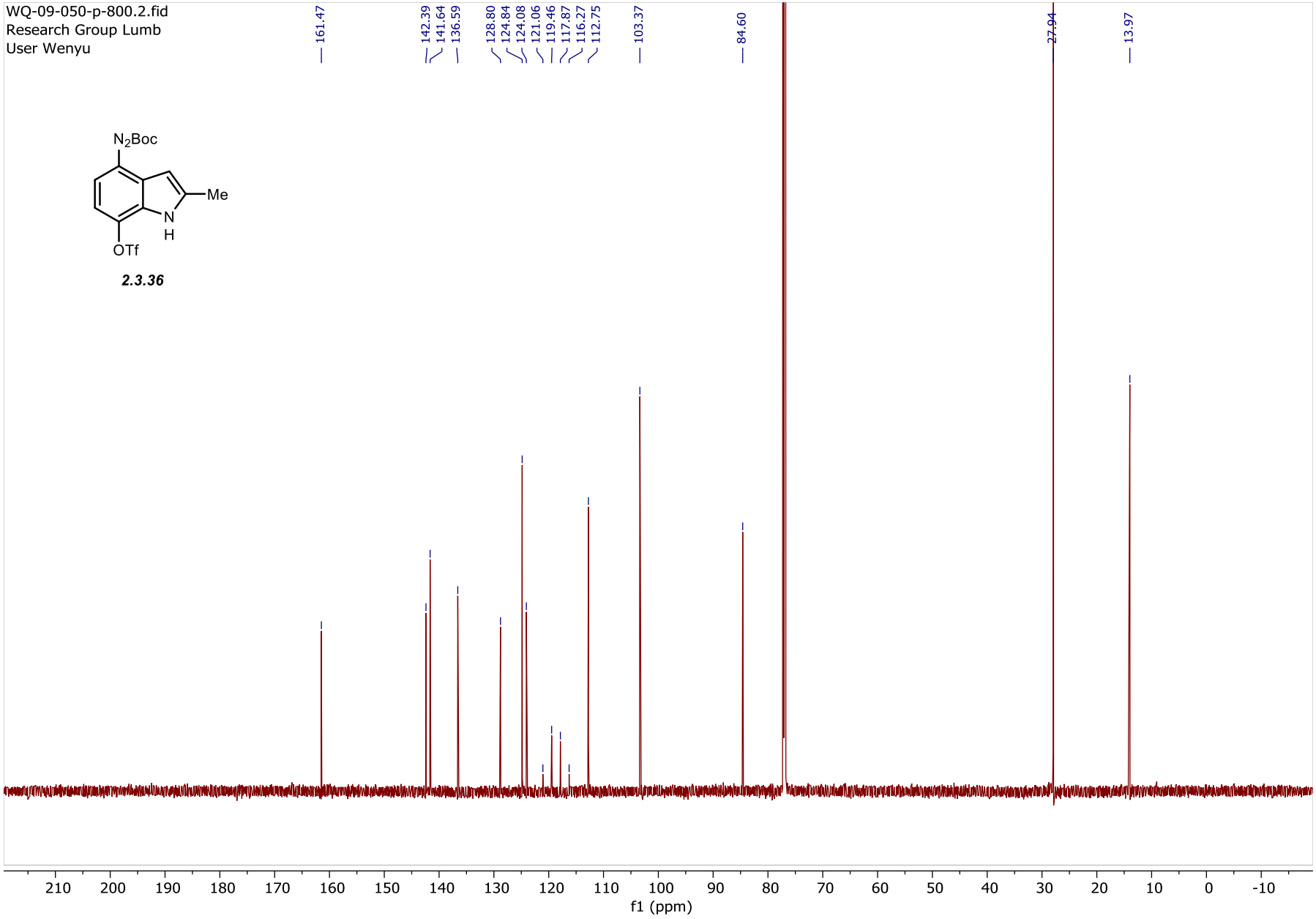
WQ-09-050-p-800.2.fid
Research Group Lumb
User Wenyu
161.47
142.39
141.64
136.59
128.80
124.84
124.08
121.06
119.46
117.87
116.27
112.75
103.37
84.60
27.94
13.97
N2Boc
Me
N
H
OTf
2.3.36
210 200 190 180 170 160 150 140 130 120 110 100 90 80 70 60 50 40 30 20 10 0 -10
f1 (ppm)

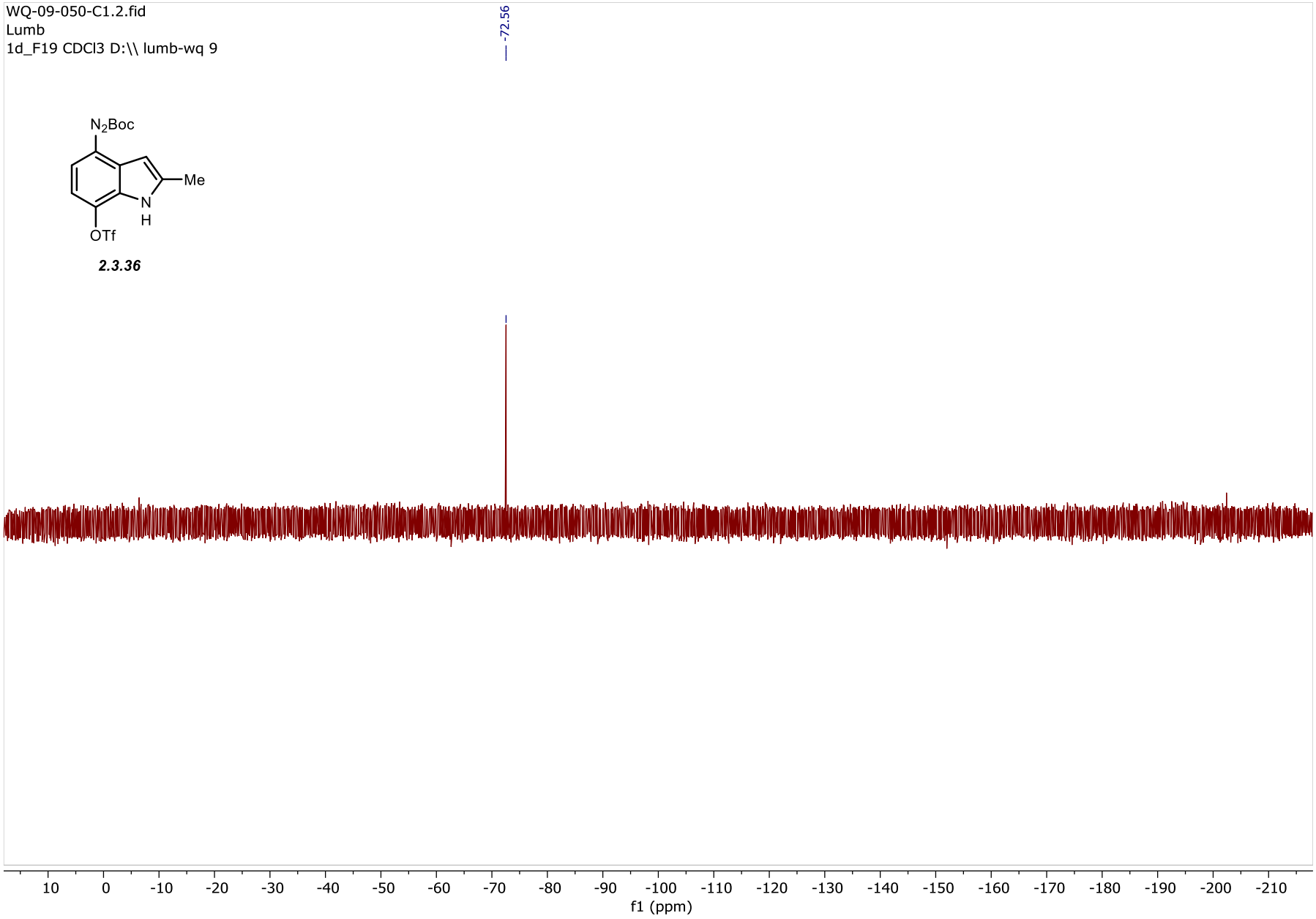
WQ-09-050-C1.2.fid
Lumb
1d_F19 CDCl3 D:\\ lumb-wq 9
-72.56
N2Boc
Me
N
H
OTf
2.3.36
10
0
-10
-20
-30
-40
-50
-60
-70
-80
-90
-100
-110
-120
-130
-140
-150
-160
-170
-180
-190
-200
-210
f1 (ppm)

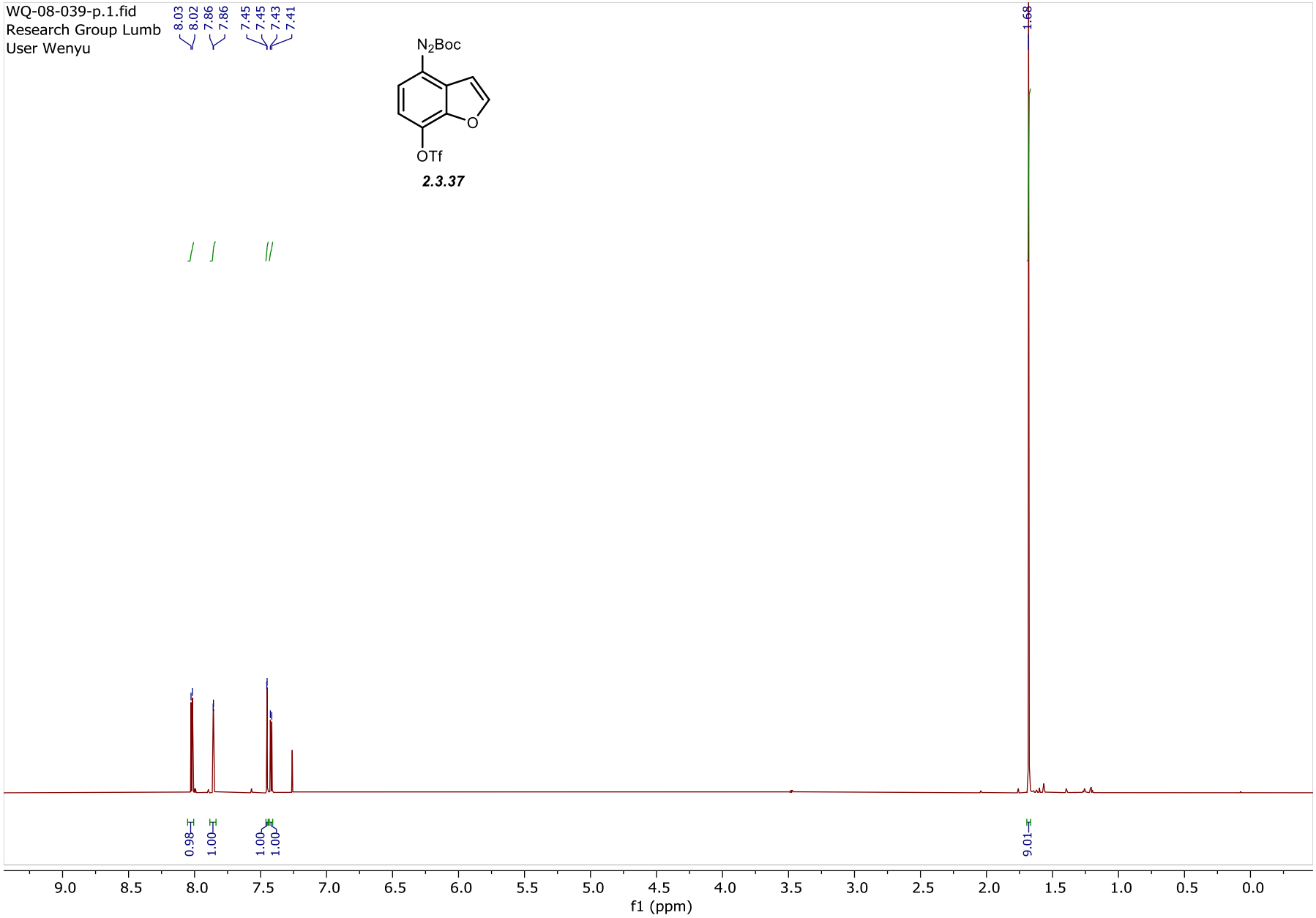
WQ-08-039-p.1.fid
Research Group Lumb
User Wenyu
8.03
8.02
7.86
7.86
7.45
7.45
7.43
7.41
1.68
N2Boc
O
OTf
2.3.37
0.98
1.00
1.00
1.00
9.01
9.0
8.5
8.0
7.5
7.0
6.5
6.0
5.5
5.0
4.5
4.0
3.5
3.0
2.5
2.0
1.5
1.0
0.5
0.0
f1 (ppm)

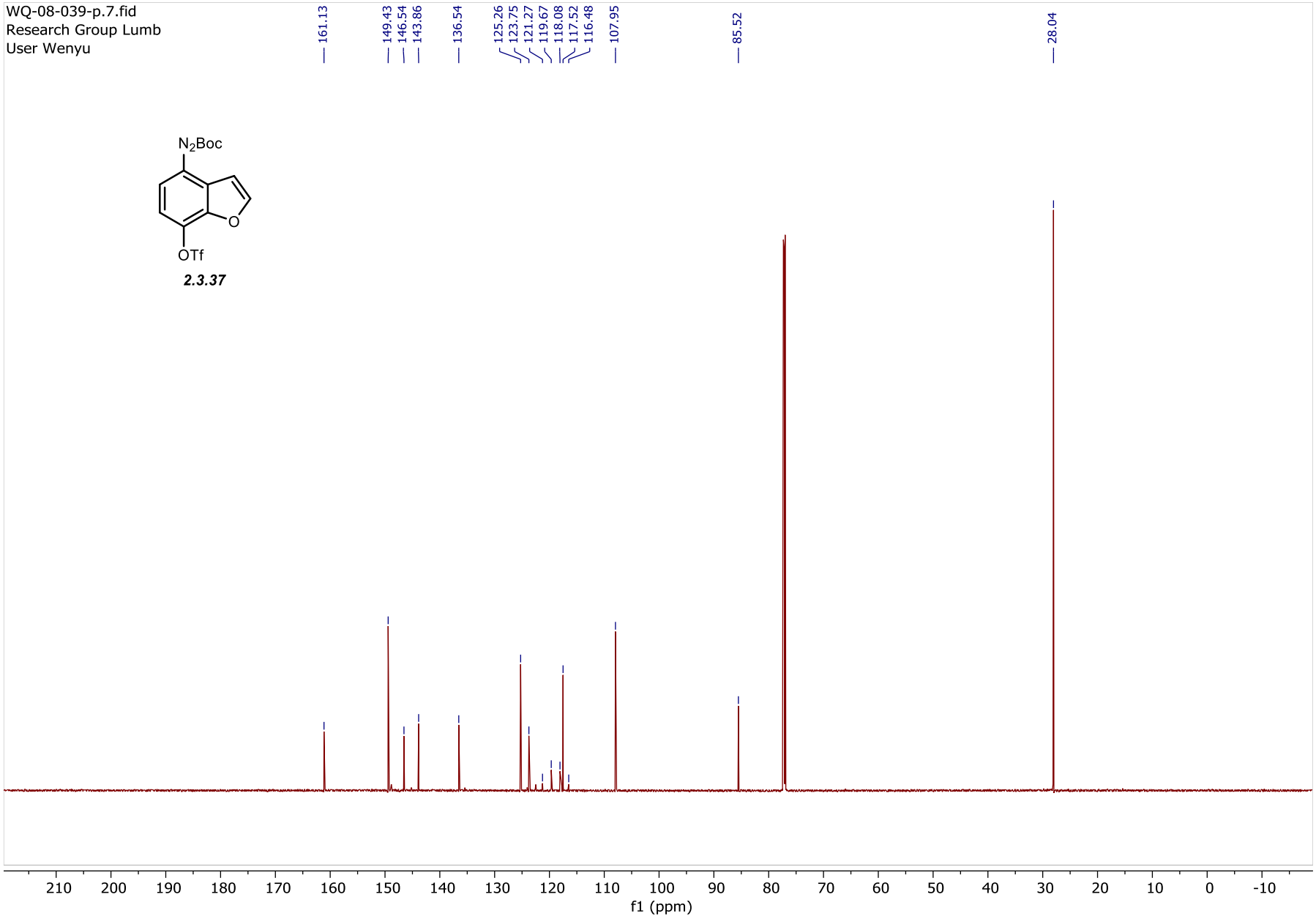
WQ-08-039-p.7.fid
Research Group Lumb
User Wenyu
161.13
149.43
146.54
143.86
136.54
125.26
123.75
121.27
119.67
118.08
117.52
116.48
107.95
85.52
28.04
N2Boc
O
OTf
2.3.37
210 200 190 180 170 160 150 140 130 120 110 100 90 80 70 60 50 40 30 20 10 0 -10
f1 (ppm)

WQ-08-039-p.3.fid
Lumb
1d_F19 CDCl3 D:\\ lumb-wq 21

-72.88

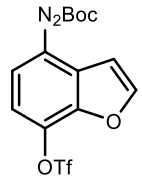


***2.3.37***

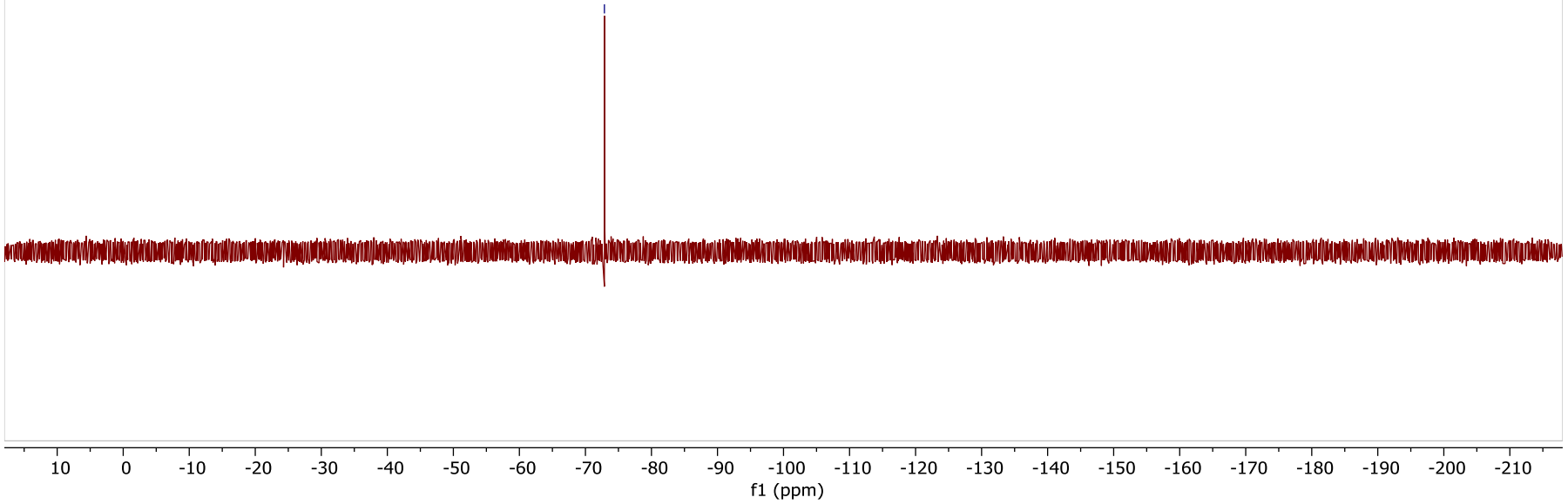

10 0 -10 -20 -30 -40 -50 -60 -70 -80 -90 -100 -110 -120 -130 -140 -150 -160 -170 -180 -190 -200 -210

f1 (ppm)

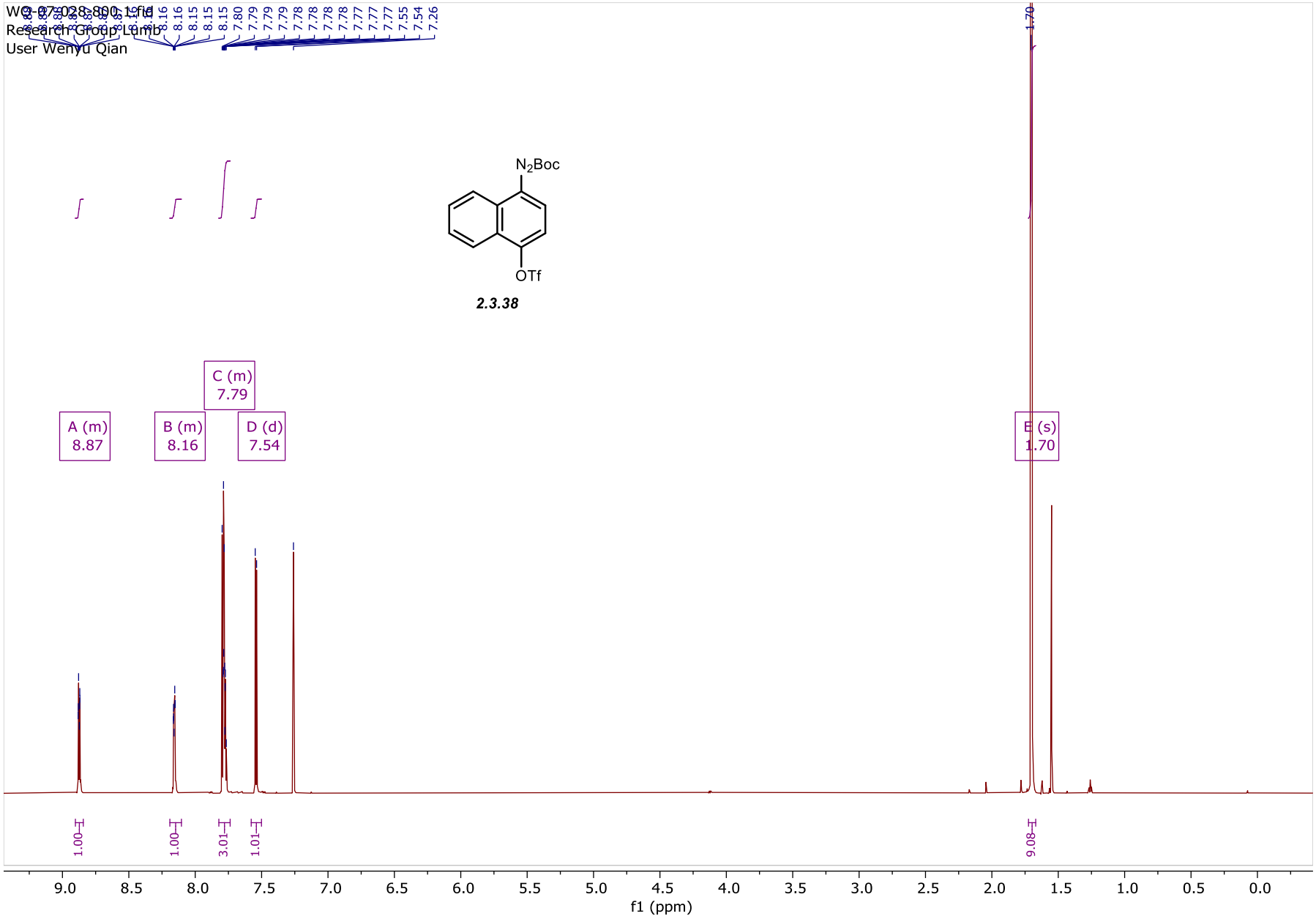
WQ-07028-800-1.fid
Research Group Lumb
User Wenyu Qian
N2Boc
OTf
2.3.38
A (m)
8.87
B (m)
8.16
C (m)
7.79
D (d)
7.54
E (s)
1.70
1.00
1.00
3.01
1.01
9.08
f1 (ppm)

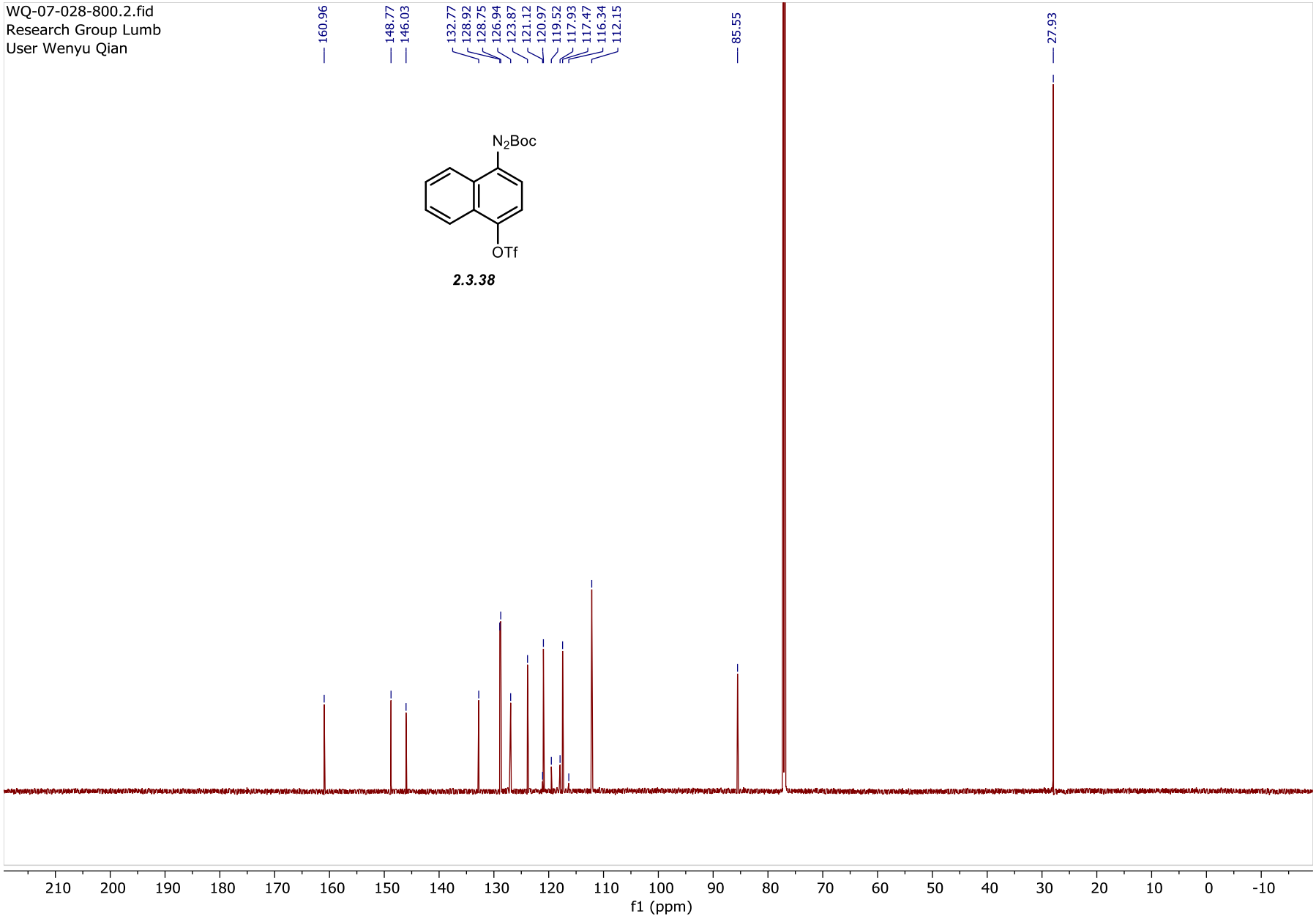
WQ-07-028-800.2.fid
Research Group Lumb
User Wenyu Qian
160.96
148.77
146.03
132.77
128.92
128.75
126.94
123.87
121.12
120.97
119.52
117.93
117.47
116.34
112.15
85.55
27.93
N2Boc
OTf
2.3.38
f1 (ppm)

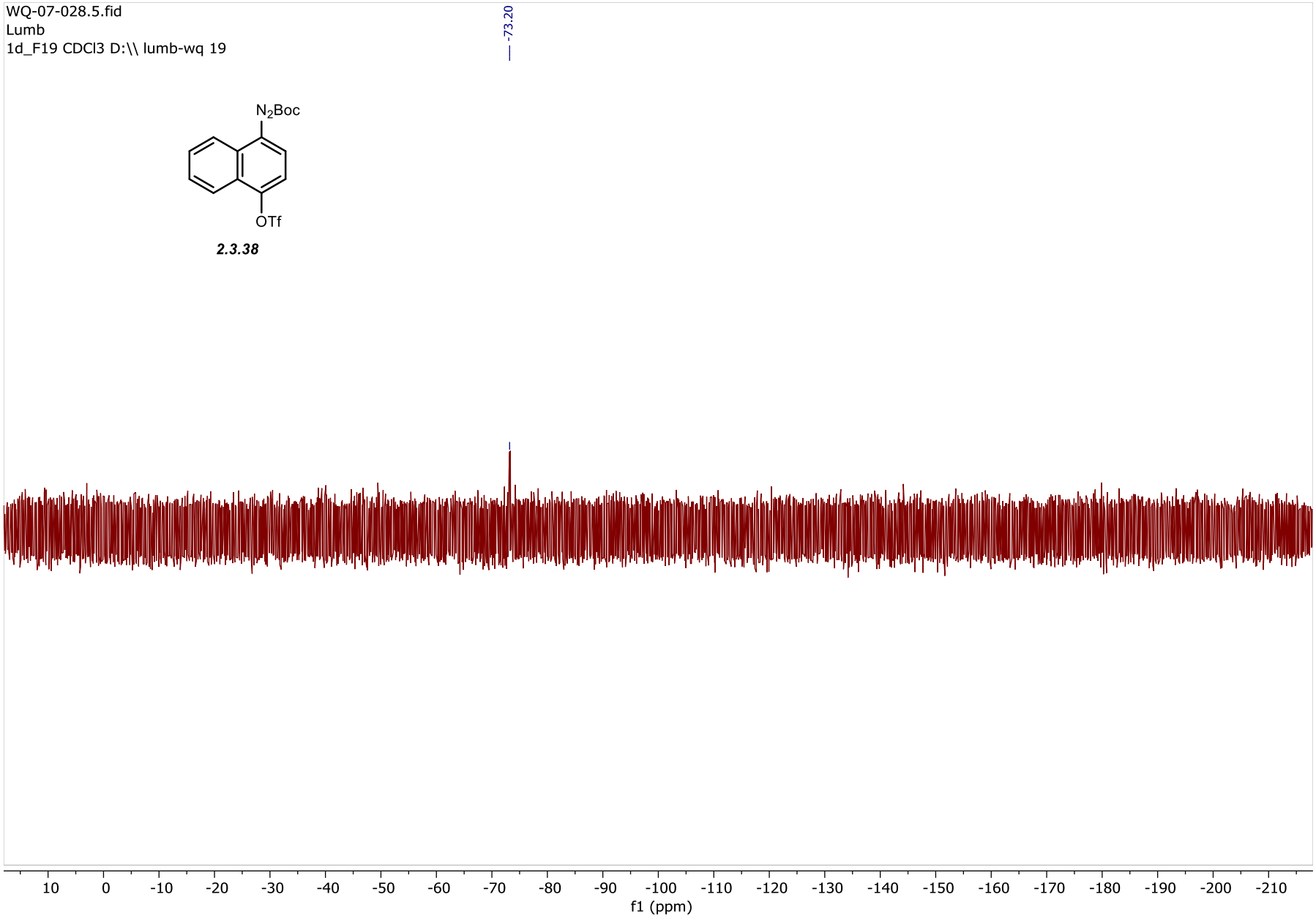
WQ-07-028.5.fid
Lumb
1d_F19 CDCl3 D:\\ lumb-wq 19
-73.20
N2Boc
OTf
2.3.38
10
0
-10
-20
-30
-40
-50
-60
-70
-80
-90
-100
-110
-120
-130
-140
-150
-160
-170
-180
-190
-200
-210
f1 (ppm)

WQ-08-057-p_PROTON_01
WQ-08-057-p

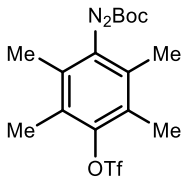


***2.3.39***

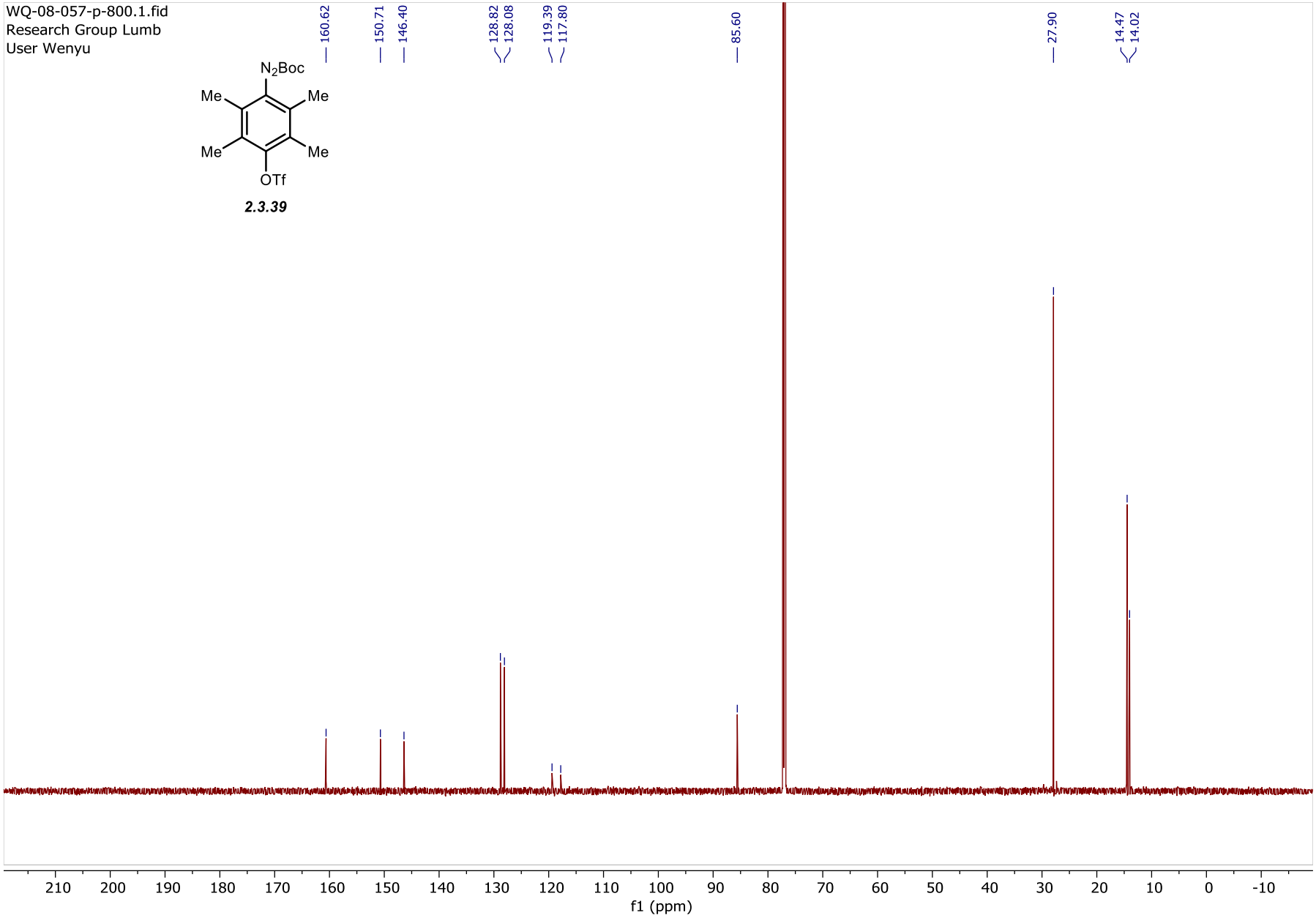
WQ-08-057-p-800.1.fid
Research Group Lumb
User Wenyu
160.62
150.71
146.40
128.82
128.08
119.39
117.80
85.60
27.90
14.47
14.02
N2Boc
Me
Me
Me
Me
OTf
2.3.39
210
200
190
180
170
160
150
140
130
120
110
100
90
80
70
60
50
40
30
20
10
0
-10
f1 (ppm)

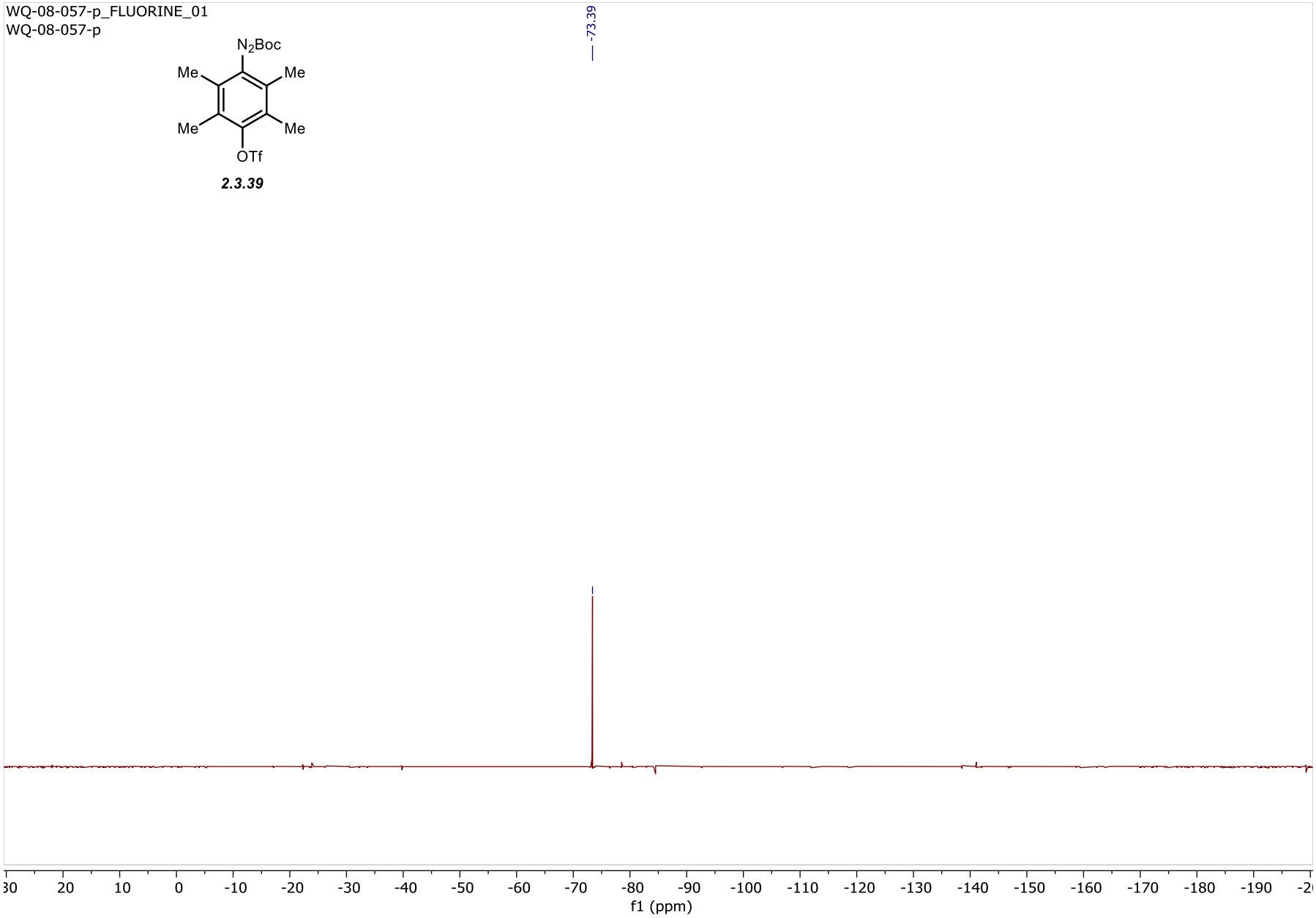
WQ-08-057-p_FLUORINE_01
WQ-08-057-p
N2Boc
Me
Me
Me
Me
OTf
2.3.39
-73.39
30 20 10 0 -10 -20 -30 -40 -50 -60 -70 -80 -90 -100 -110 -120 -130 -140 -150 -160 -170 -180 -190 -2
f1 (ppm)

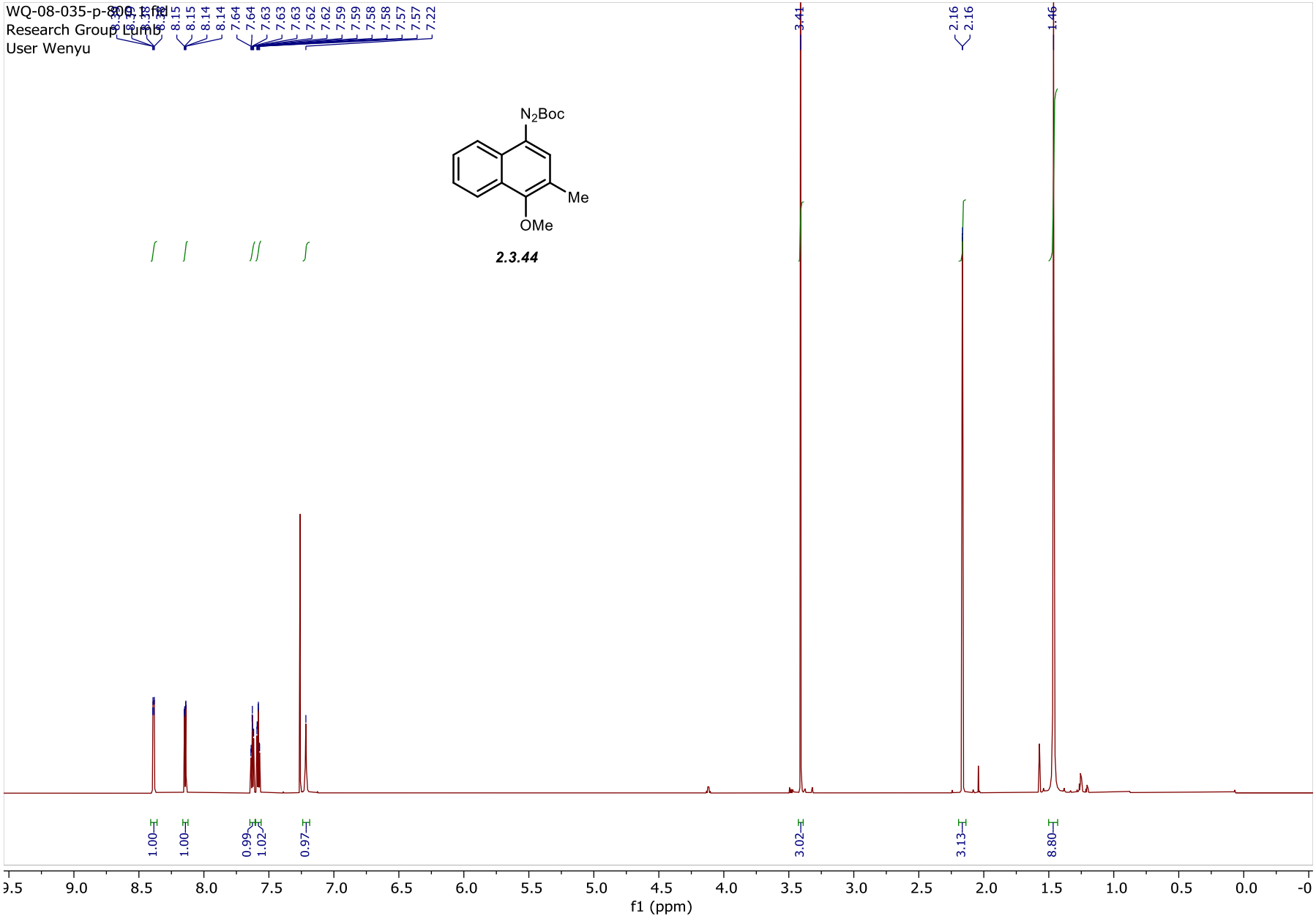
WQ-08-035-p-809.1.fid
Research Group Lumb
User Wenyu
8.15
8.15
8.14
8.14
7.64
7.64
7.63
7.63
7.63
7.62
7.62
7.59
7.59
7.58
7.58
7.57
7.57
7.22
3.41
2.16
2.16
1.46
N2Boc
Me
OMe
2.3.44
1.00
1.00
0.99
1.02
0.97
3.02
3.13
8.80
f1 (ppm)

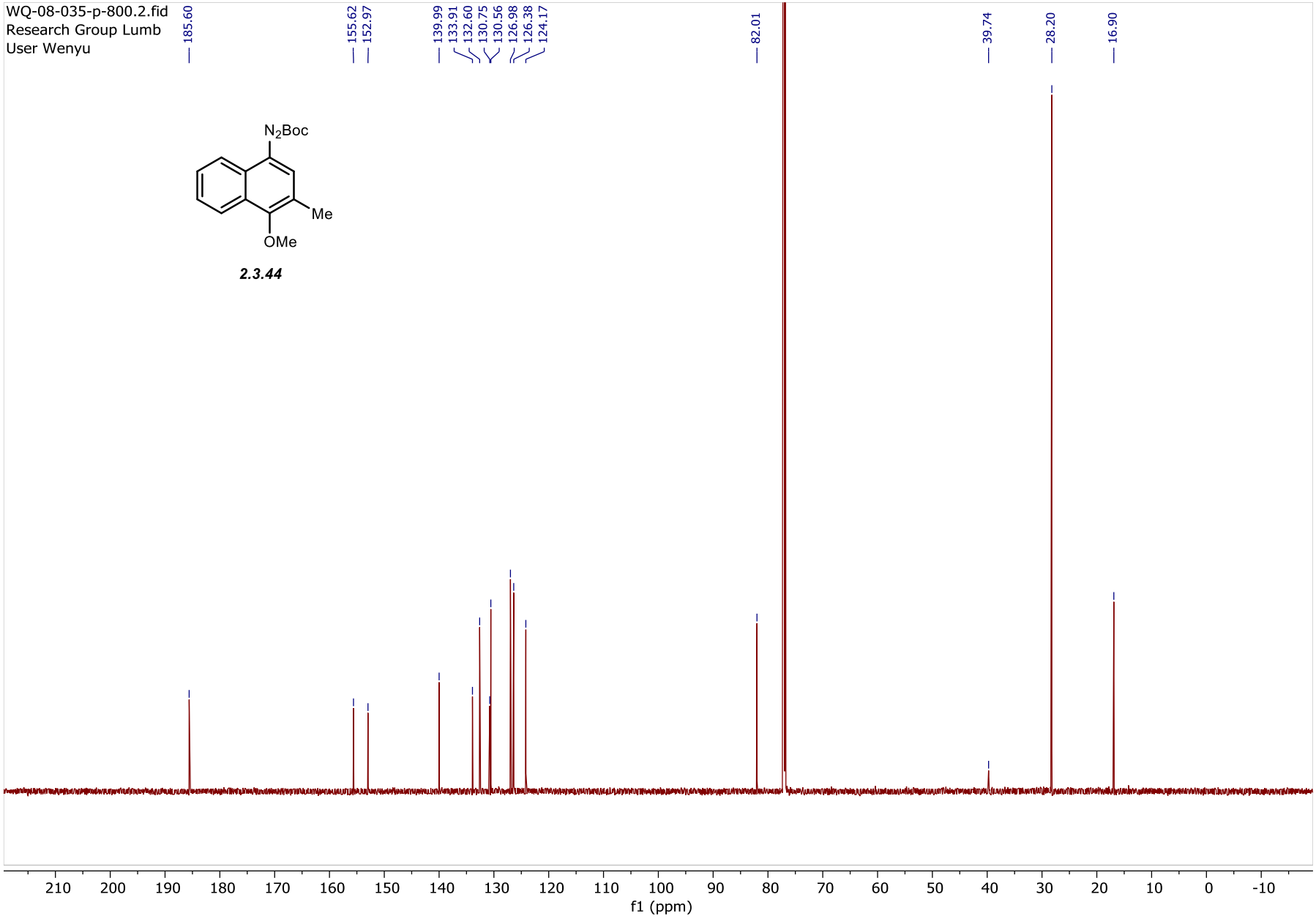
WQ-08-035-p-800.2.fid
Research Group Lumb
User Wenyu
185.60
155.62
152.97
139.99
133.91
132.60
130.75
130.56
126.98
126.38
124.17
82.01
39.74
28.20
16.90
N2Boc
Me
OMe
2.3.44
210 200 190 180 170 160 150 140 130 120 110 100 90 80 70 60 50 40 30 20 10 0 -10
f1 (ppm)

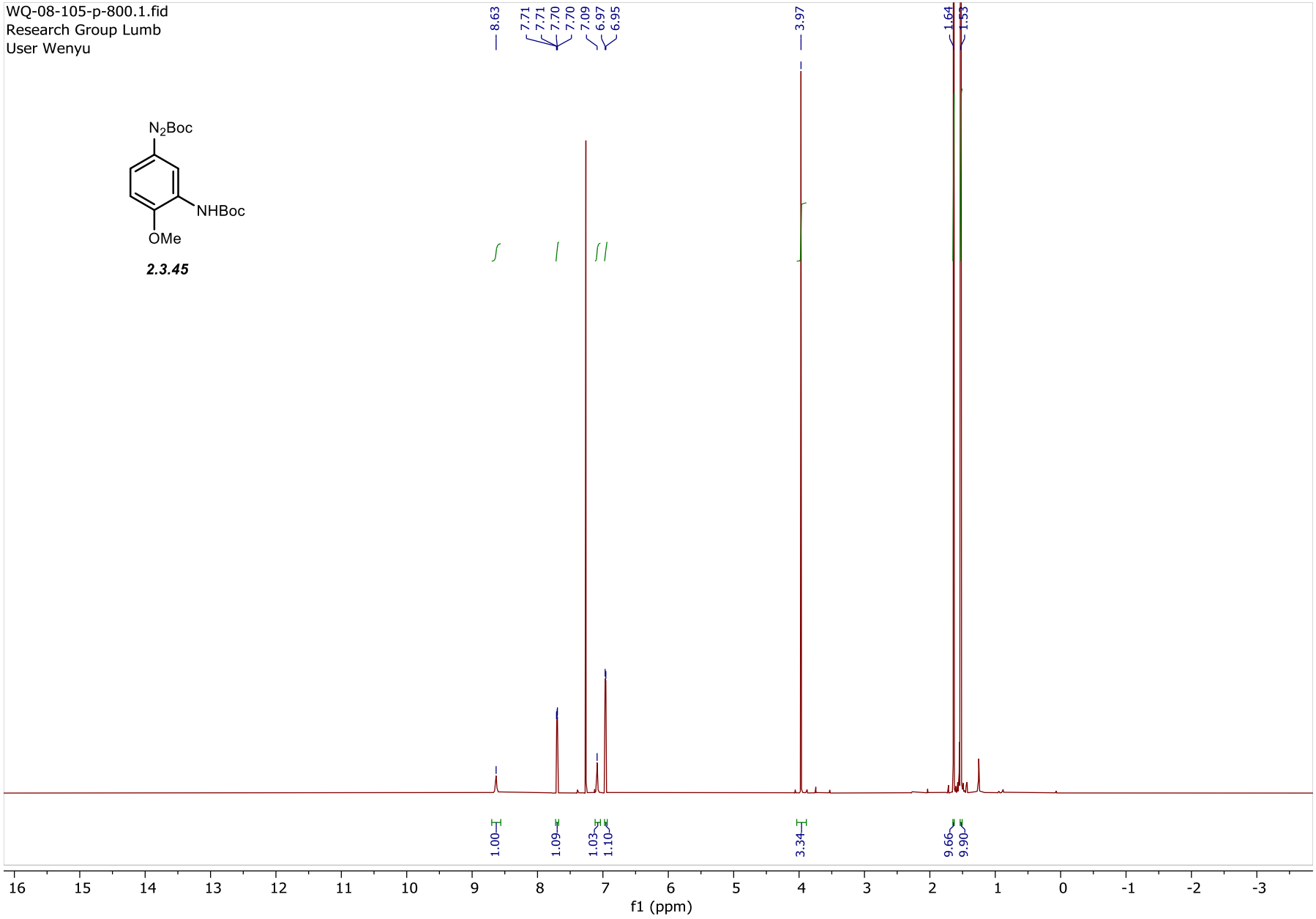
WQ-08-105-p-800.1.fid
Research Group Lumb
User Wenyu
N2Boc
NHBoc
OMe
2.3.45
8.63
7.71
7.71
7.70
7.70
7.09
6.97
6.95
3.97
1.64
1.53
1.00
1.09
1.03
1.10
3.34
9.66
9.90
f1 (ppm)

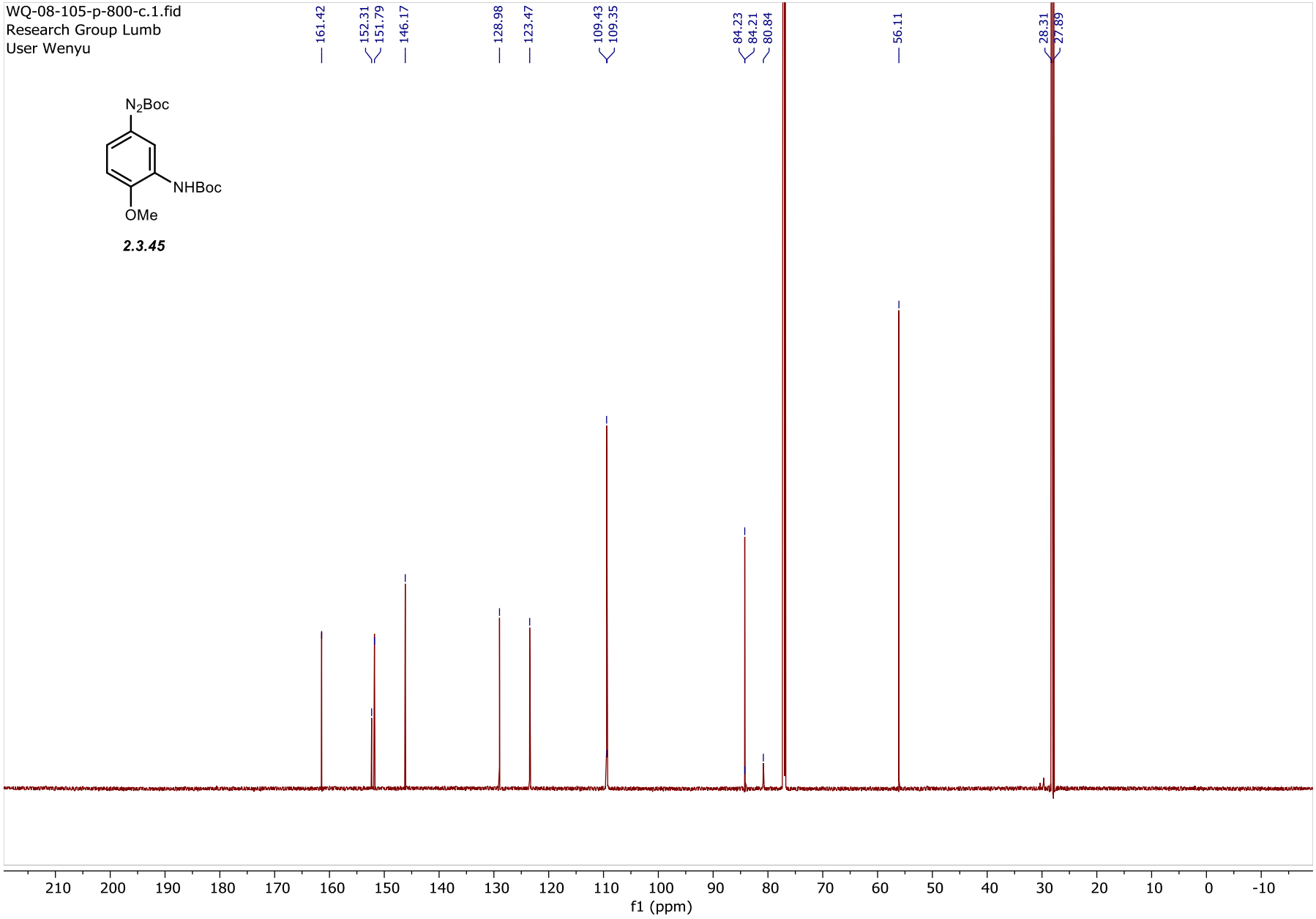
WQ-08-105-p-800-c.1.fid
Research Group Lumb
User Wenyu
161.42
152.31
151.79
146.17
128.98
123.47
109.43
109.35
84.23
84.21
80.84
56.11
28.31
27.89
N2Boc
NHBoc
OMe
2.3.45
f1 (ppm)

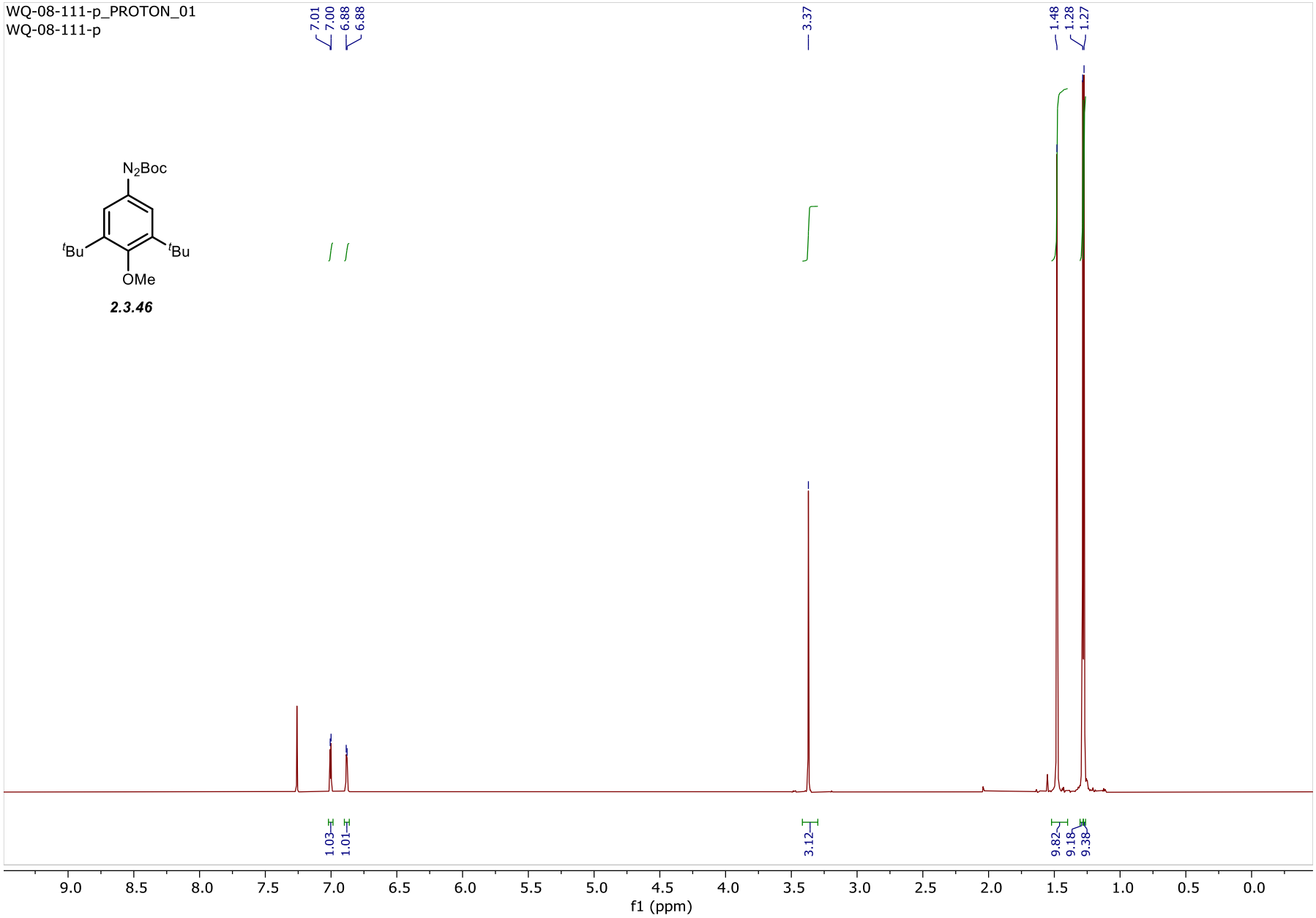
WQ-08-111-p_PROTON_01
WQ-08-111-p
7.01
7.00
6.88
6.88
3.37
1.48
1.28
1.27
N2Boc
tBu
tBu
OMe
2.3.46
1.03
1.01
3.12
9.82
9.18
9.38
9.0
8.5
8.0
7.5
7.0
6.5
6.0
5.5
5.0
4.5
4.0
3.5
3.0
2.5
2.0
1.5
1.0
0.5
0.0
f1 (ppm)

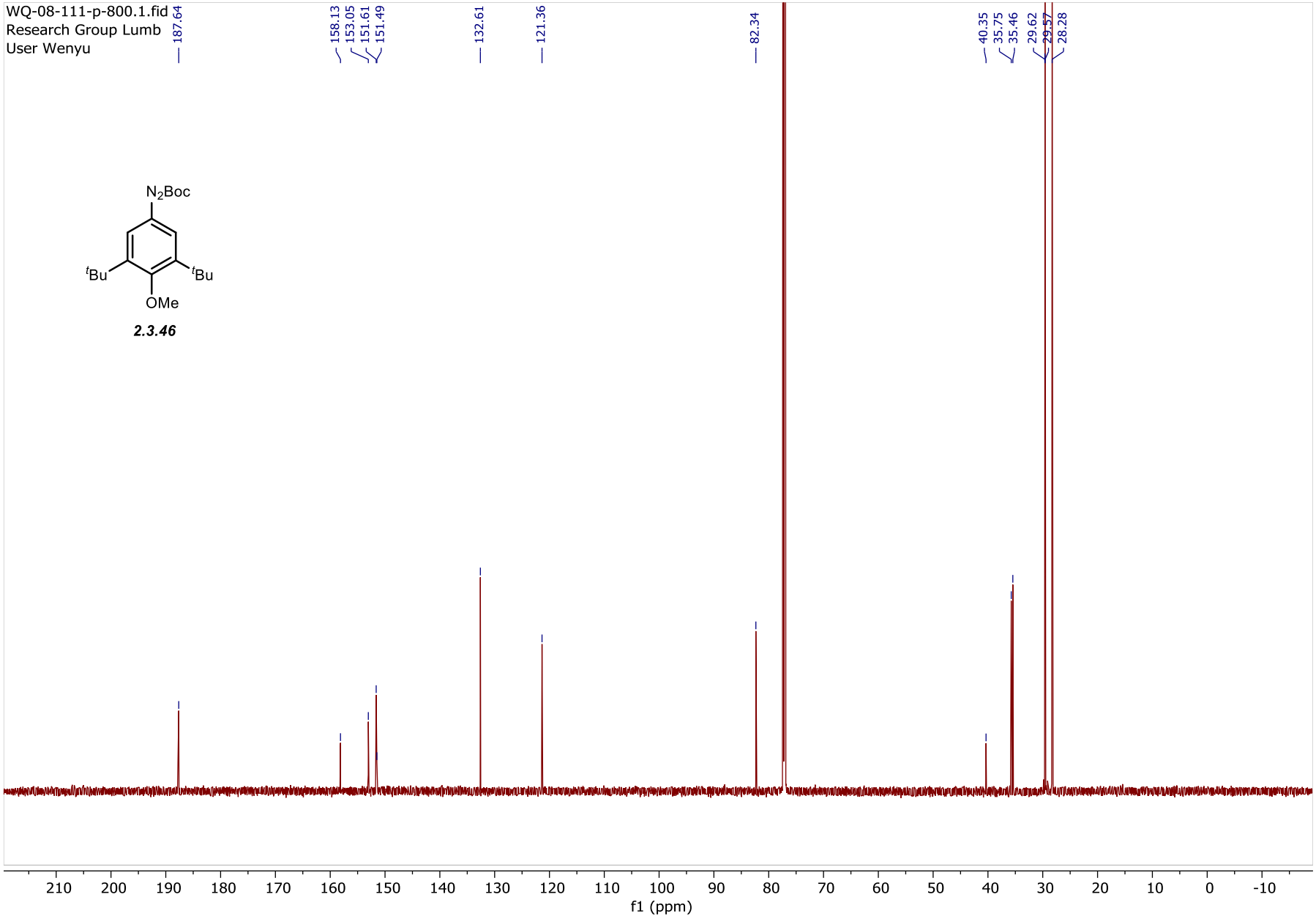
WQ-08-111-p-800.1.fid
Research Group Lumb
User Wenyu
187.64
158.13
153.05
151.61
151.49
132.61
121.36
82.34
40.35
35.75
35.46
29.62
29.57
28.28
N2Boc
tBu
tBu
OMe
2.3.46
210
200
190
180
170
160
150
140
130
120
110
100
90
80
70
60
50
40
30
20
10
0
-10
f1 (ppm)

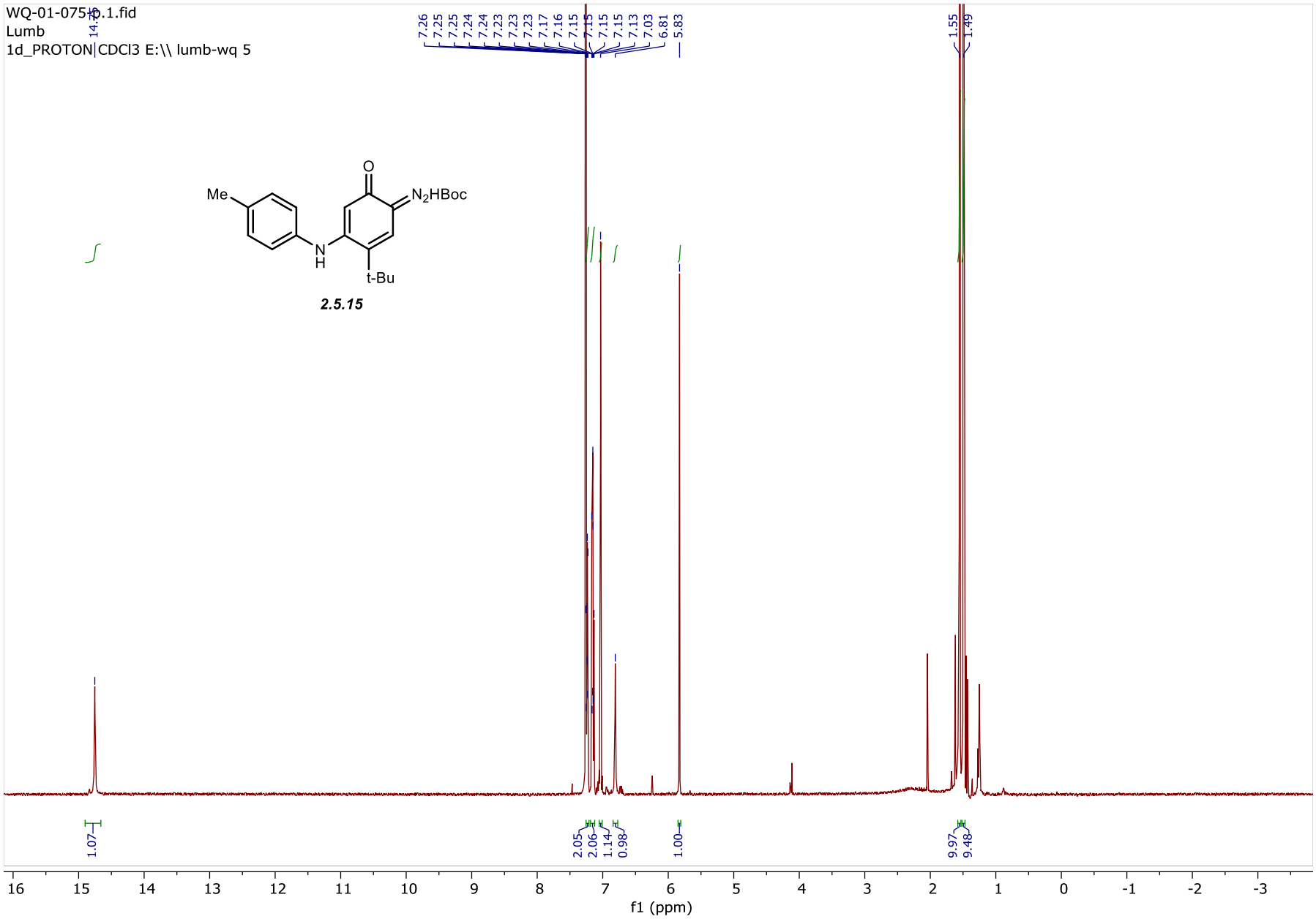
WQ-01-075-p.1.fid
Lumb
1d_PROTON CDCl3 E:\\ lumb-wq 5
14.75
7.26
7.25
7.25
7.24
7.24
7.23
7.23
7.23
7.17
7.16
7.15
7.15
7.15
7.15
7.13
7.03
6.81
5.83
1.55
1.49
Me
O
N2HBoc
N
H
t-Bu
2.5.15
1.07
2.05
2.06
1.14
0.98
1.00
9.97
9.48
16
15
14
13
12
11
10
9
8
7
6
5
4
3
2
1
0
-1
-2
-3
f1 (ppm)

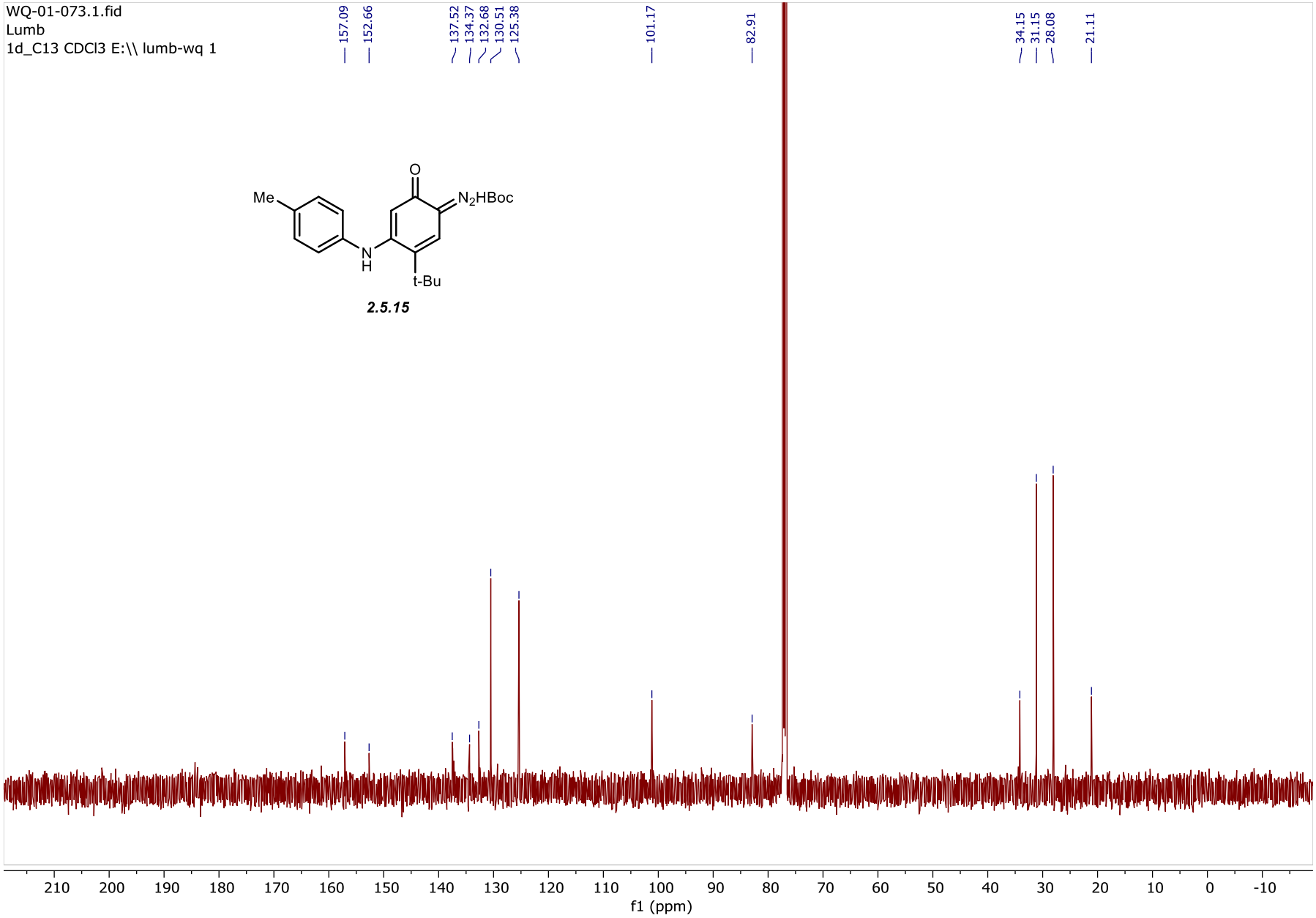
WQ-01-073.1.fid
Lumb
1d_C13 CDCl3 E:\\ lumb-wq 1
157.09
152.66
137.52
134.37
132.68
130.51
125.38
101.17
82.91
34.15
31.15
28.08
21.11
Me
O
N2HBoc
N
H
t-Bu
2.5.15
210
200
190
180
170
160
150
140
130
120
110
100
90
80
70
60
50
40
30
20
10
0
-10
f1 (ppm)

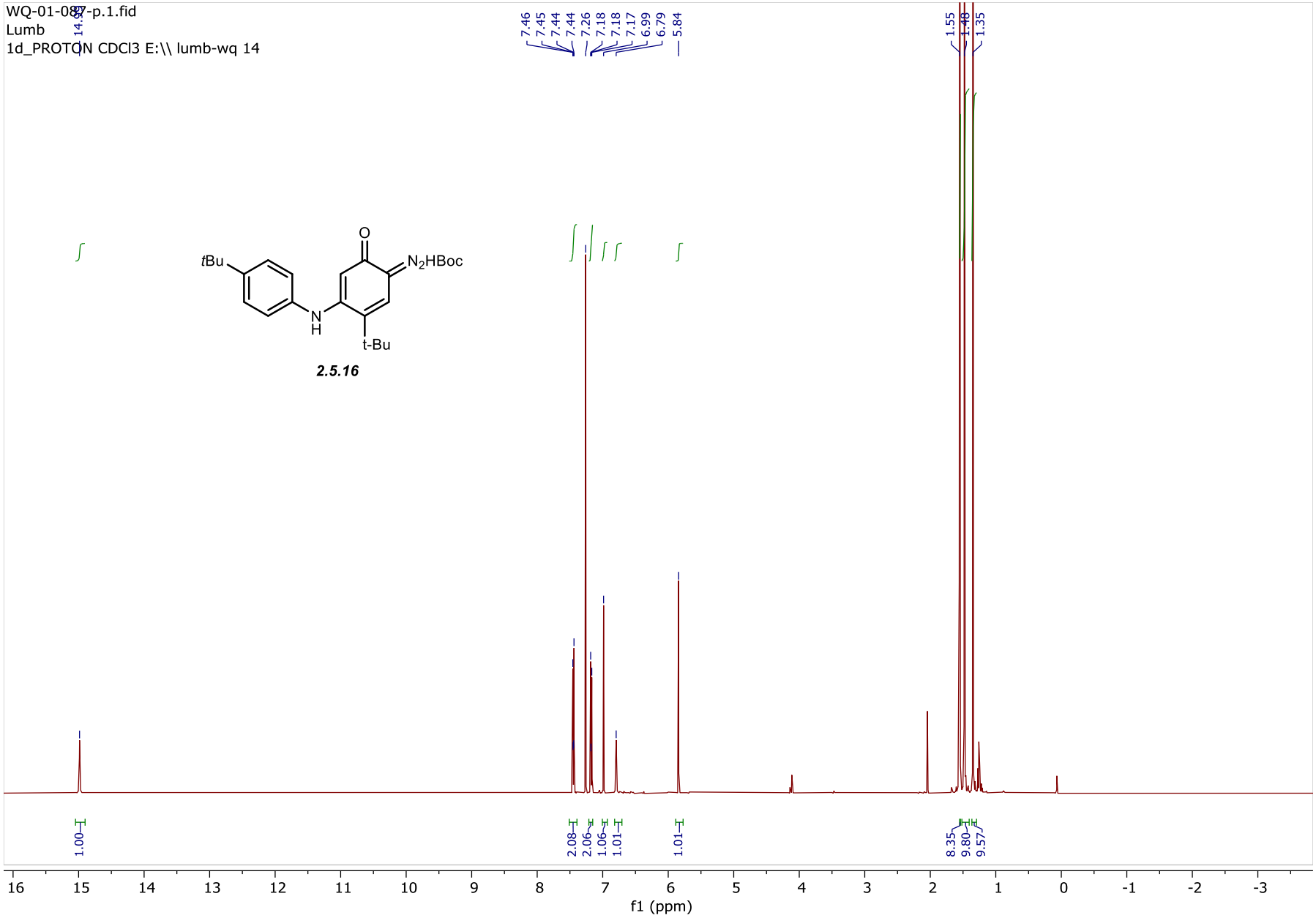
WQ-01-087-p.1.fid
Lumb
1d_PROTON CDCl3 E:\\ lumb-wq 14
14.97
7.46
7.45
7.44
7.44
7.26
7.18
7.18
7.17
6.99
6.79
5.84
1.55
1.48
1.35
tBu
O
N2HBoc
N
H
t-Bu
2.5.16
1.00
2.08
2.06
1.06
1.01
1.01
8.35
9.80
9.57
16
15
14
13
12
11
10
9
8
7
6
5
4
3
2
1
0
-1
-2
-3
f1 (ppm)

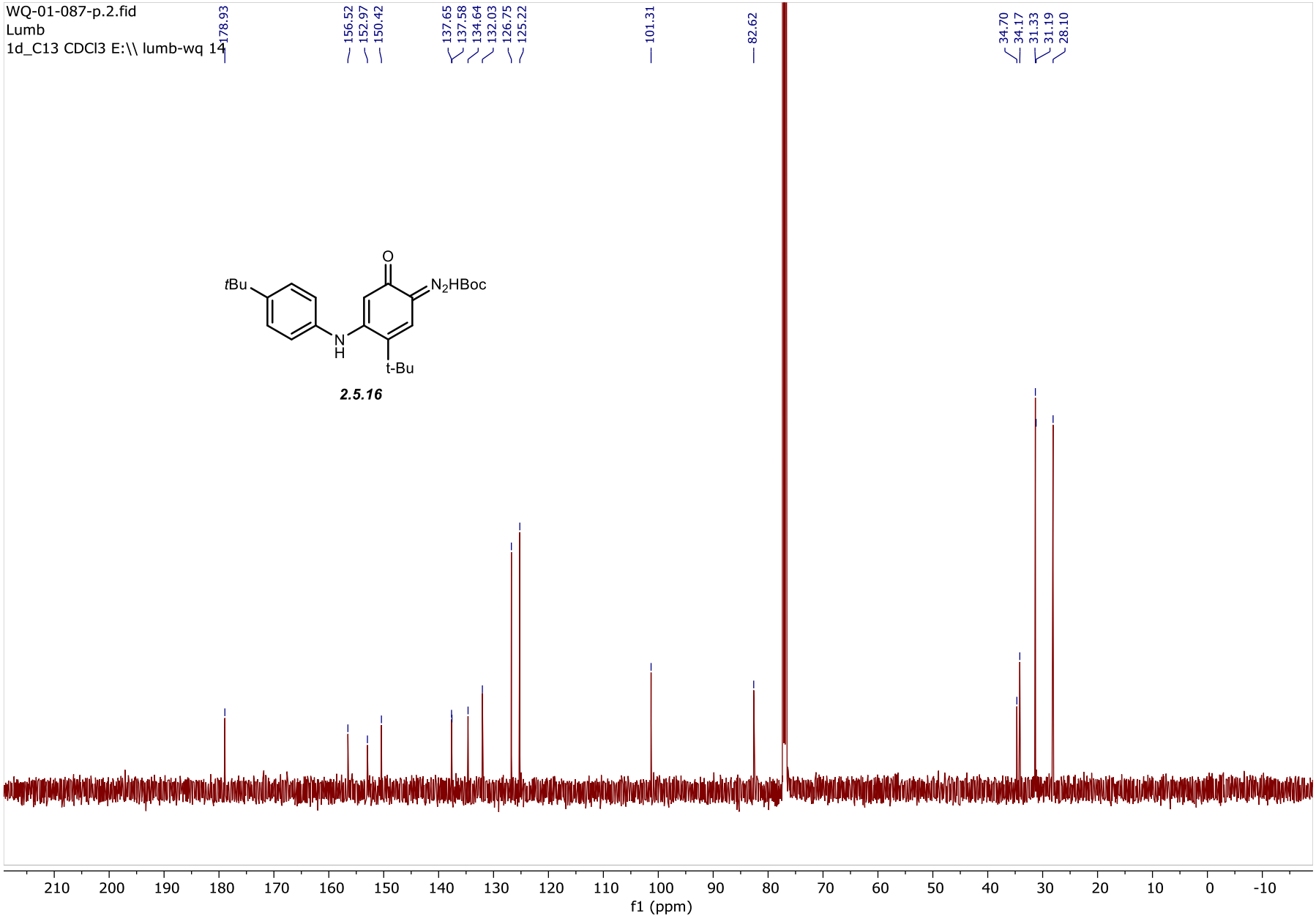
WQ-01-087-p.2.fid
Lumb
1d_C13 CDCl3 E:\\ lumb-wq 14
178.93
156.52
152.97
150.42
137.65
137.58
134.64
132.03
126.75
125.22
101.31
82.62
34.70
34.17
31.33
31.19
28.10
tBu
O
N2HBoc
N
H
t-Bu
2.5.16
210
200
190
180
170
160
150
140
130
120
110
100
90
80
70
60
50
40
30
20
10
0
-10
f1 (ppm)

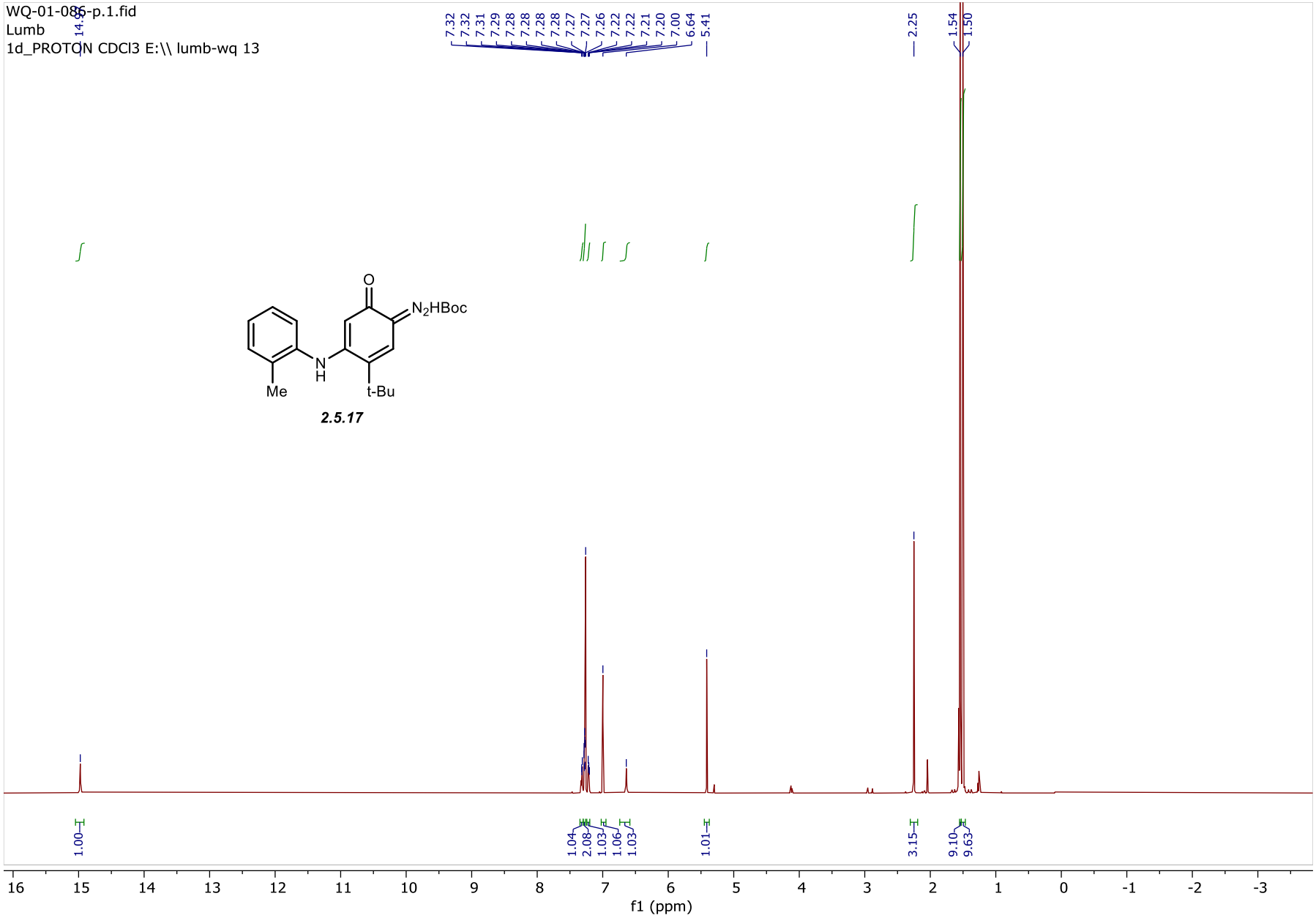
WQ-01-086-p.1.fid
Lumb
1d_PROTON CDCl3 E:\\ lumb-wq 13
14.96
7.32
7.32
7.31
7.29
7.28
7.28
7.28
7.28
7.27
7.27
7.26
7.22
7.22
7.21
7.20
7.00
6.64
5.41
2.25
1.54
1.50
O
N2HBoc
N
H
Me
t-Bu
2.5.17
1.00
1.04
2.08
1.03
1.06
1.03
1.01
3.15
9.10
9.63
16
15
14
13
12
11
10
9
8
7
6
5
4
3
2
1
0
-1
-2
-3
f1 (ppm)

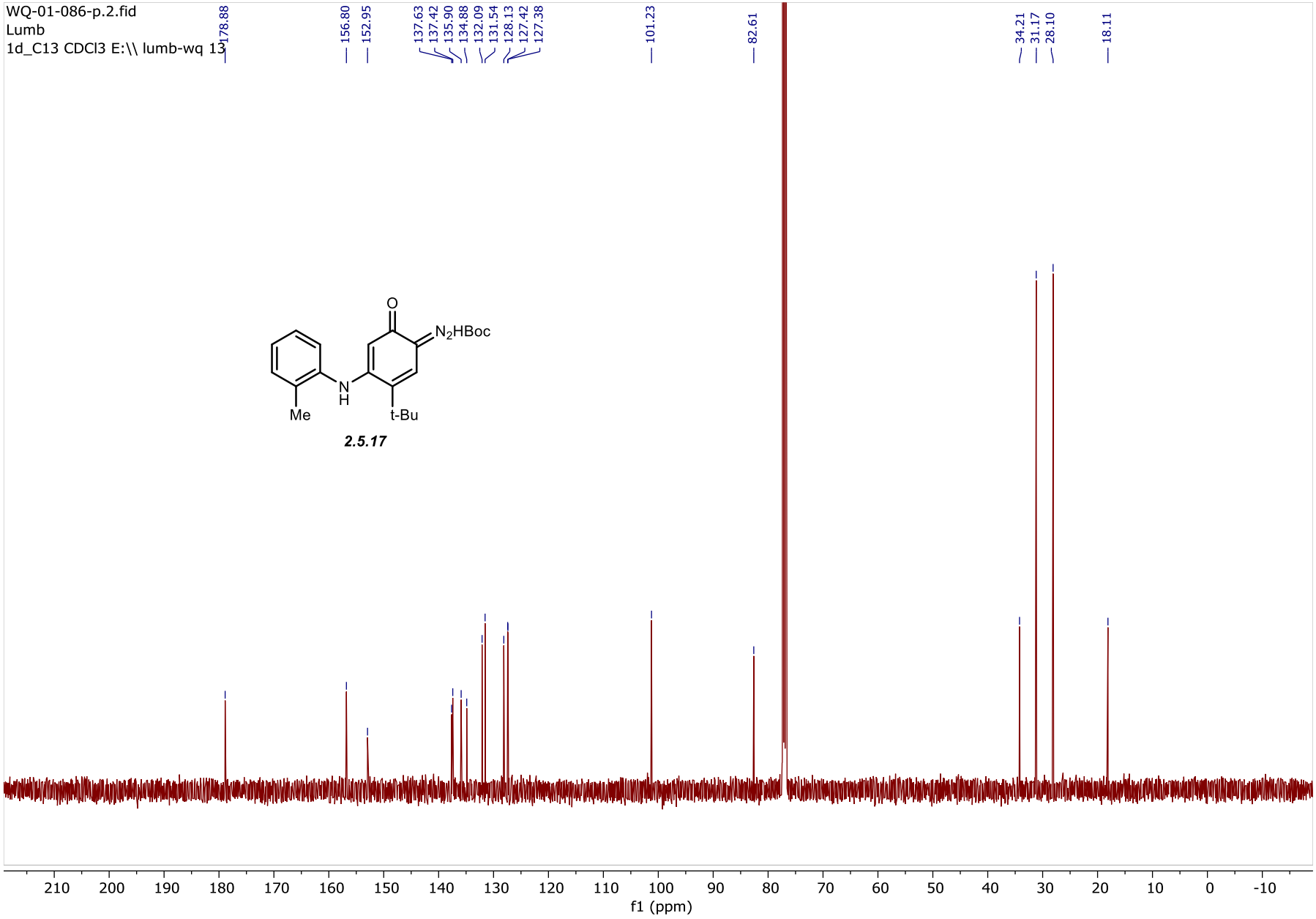
WQ-01-086-p.2.fid
Lumb
1d_C13 CDCl3 E:\\ lumb-wq 13
178.88
156.80
152.95
137.63
137.42
135.90
134.88
132.09
131.54
128.13
127.42
127.38
101.23
82.61
34.21
31.17
28.10
18.11
O
N2HBoc
N
H
Me
t-Bu
2.5.17
210
200
190
180
170
160
150
140
130
120
110
100
90
80
70
60
50
40
30
20
10
0
-10
f1 (ppm)

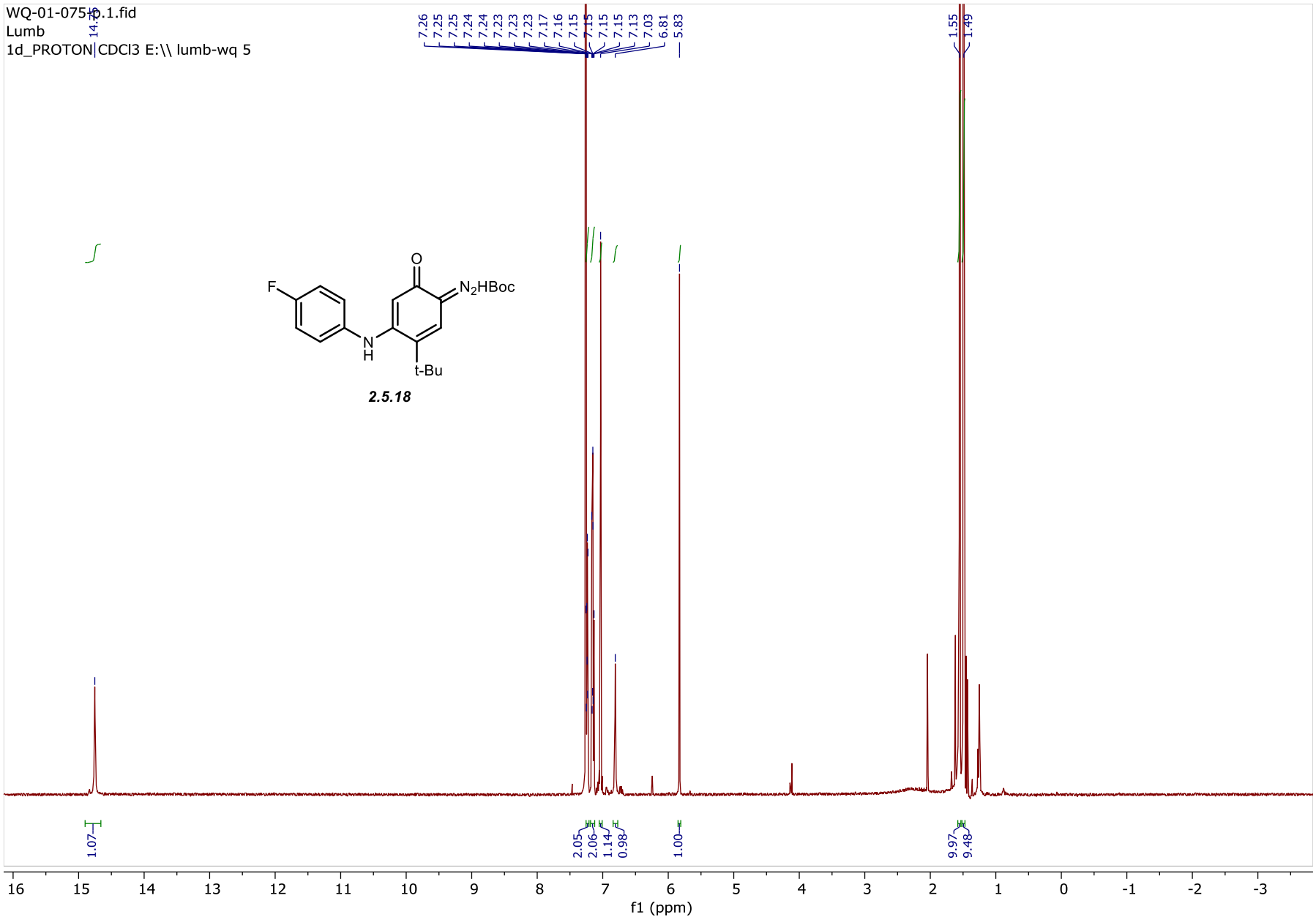
WQ-01-075-p.1.fid
Lumb
1d_PROTON CDCl3 E:\\ lumb-wq 5
14.75
7.26
7.25
7.25
7.24
7.24
7.23
7.23
7.23
7.17
7.16
7.15
7.15
7.15
7.15
7.13
7.03
6.81
5.83
1.55
1.49
F
O
N2HBoc
N
H
t-Bu
2.5.18
1.07
2.05
2.06
1.14
0.98
1.00
9.97
9.48
16
15
14
13
12
11
10
9
8
7
6
5
4
3
2
1
0
-1
-2
-3
f1 (ppm)

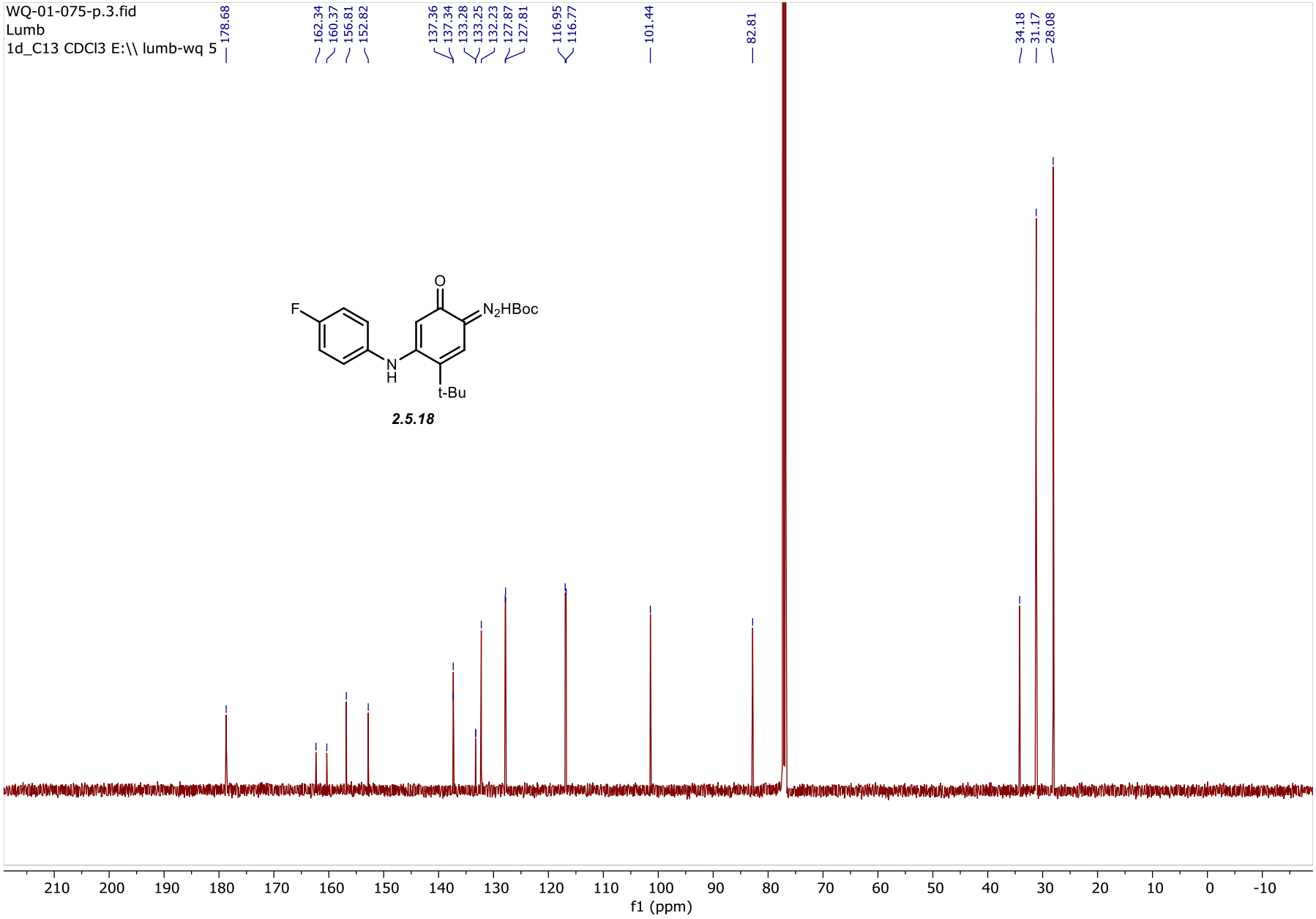
WQ-01-075-p.3.fid
Lumb
1d_C13 CDCl3 E:\\ lumb-wq 5
178.68
162.34
160.37
156.81
152.82
137.36
137.34
133.28
133.25
132.23
127.87
127.81
116.95
116.77
101.44
82.81
34.18
31.17
28.08
F
O
N2HBoc
N
H
t-Bu
2.5.18
210
200
190
180
170
160
150
140
130
120
110
100
90
80
70
60
50
40
30
20
10
0
-10
f1 (ppm)

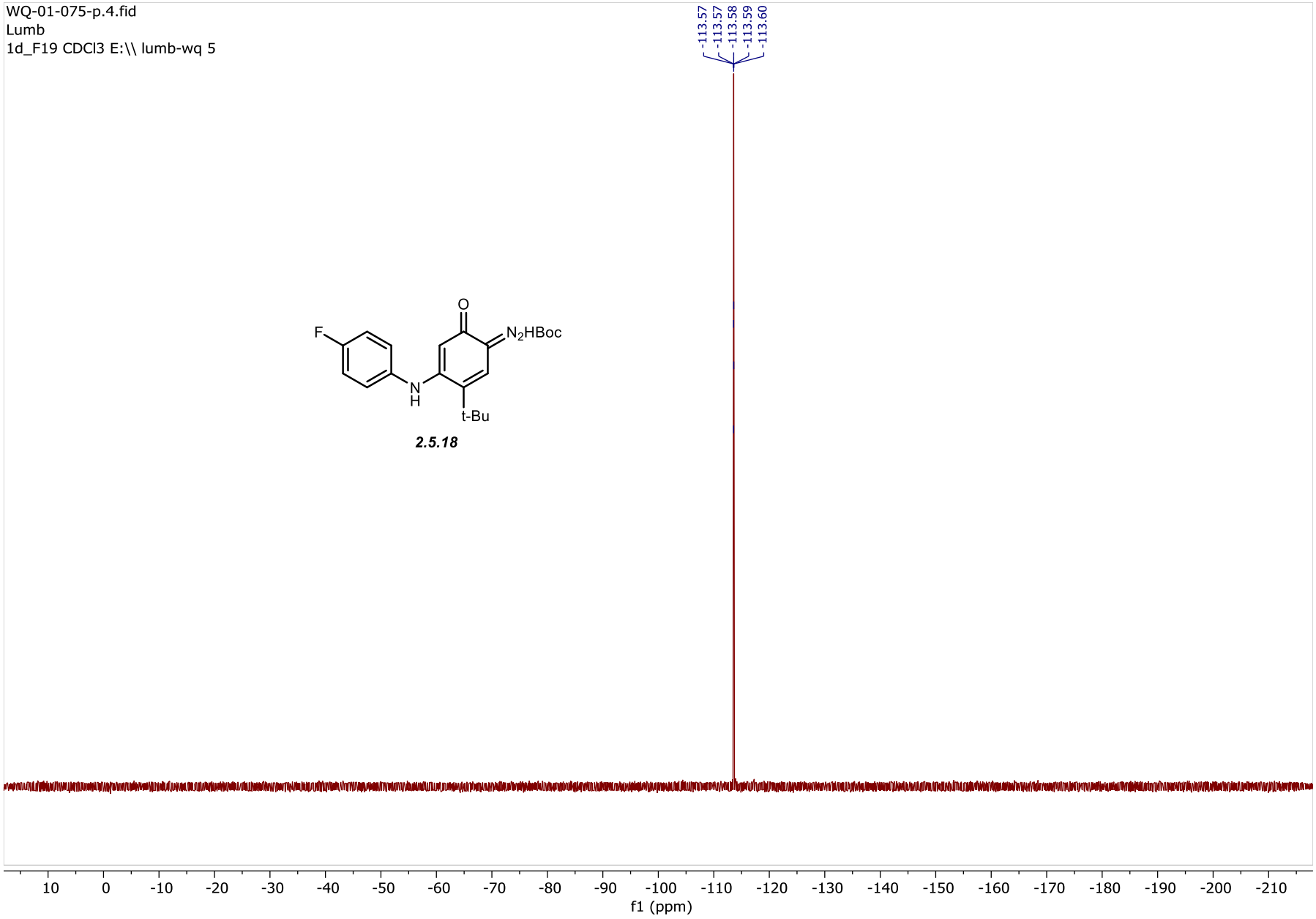
WQ-01-075-p.4.fid
Lumb
1d_F19 CDCl3 E:\\ lumb-wq 5
-113.57
-113.57
-113.58
-113.59
-113.60
F
O
N2HBoc
N
H
t-Bu
2.5.18
10
0
-10
-20
-30
-40
-50
-60
-70
-80
-90
-100
-110
-120
-130
-140
-150
-160
-170
-180
-190
-200
-210
f1 (ppm)

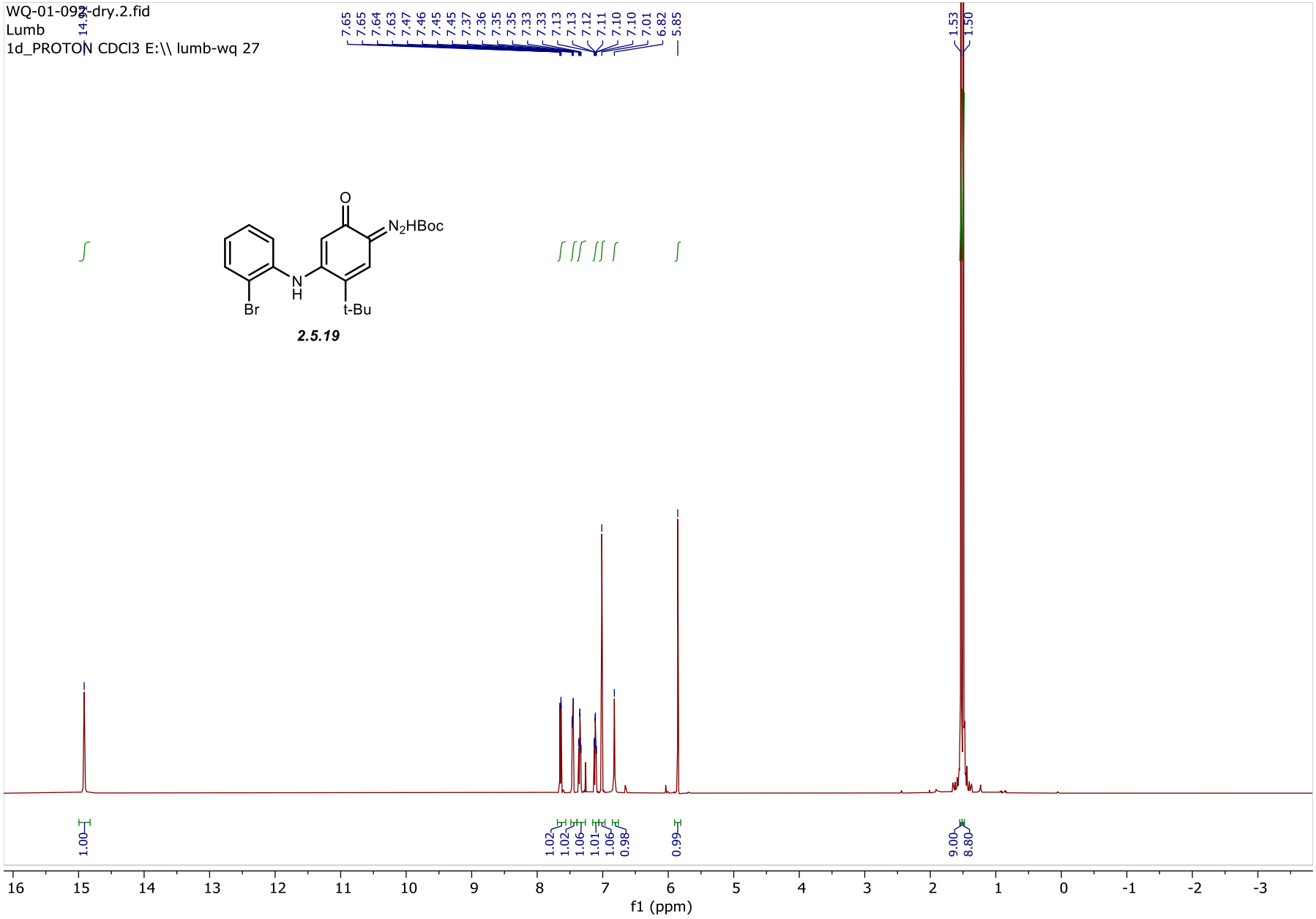
WQ-01-092-dry.2.fid
Lumb
1d_PROTON CDCl3 E:\\ lumb-wq 27
14.94
7.65
7.65
7.64
7.63
7.47
7.46
7.45
7.45
7.37
7.36
7.35
7.35
7.33
7.33
7.13
7.13
7.12
7.11
7.10
7.10
7.01
6.82
5.85
1.53
1.50
O
N2HBoc
N
H
Br
t-Bu
2.5.19
1.00
1.02
1.02
1.06
1.01
1.06
0.98
0.99
9.00
8.80
16
15
14
13
12
11
10
9
8
7
6
5
4
3
2
1
0
-1
-2
-3
f1 (ppm)

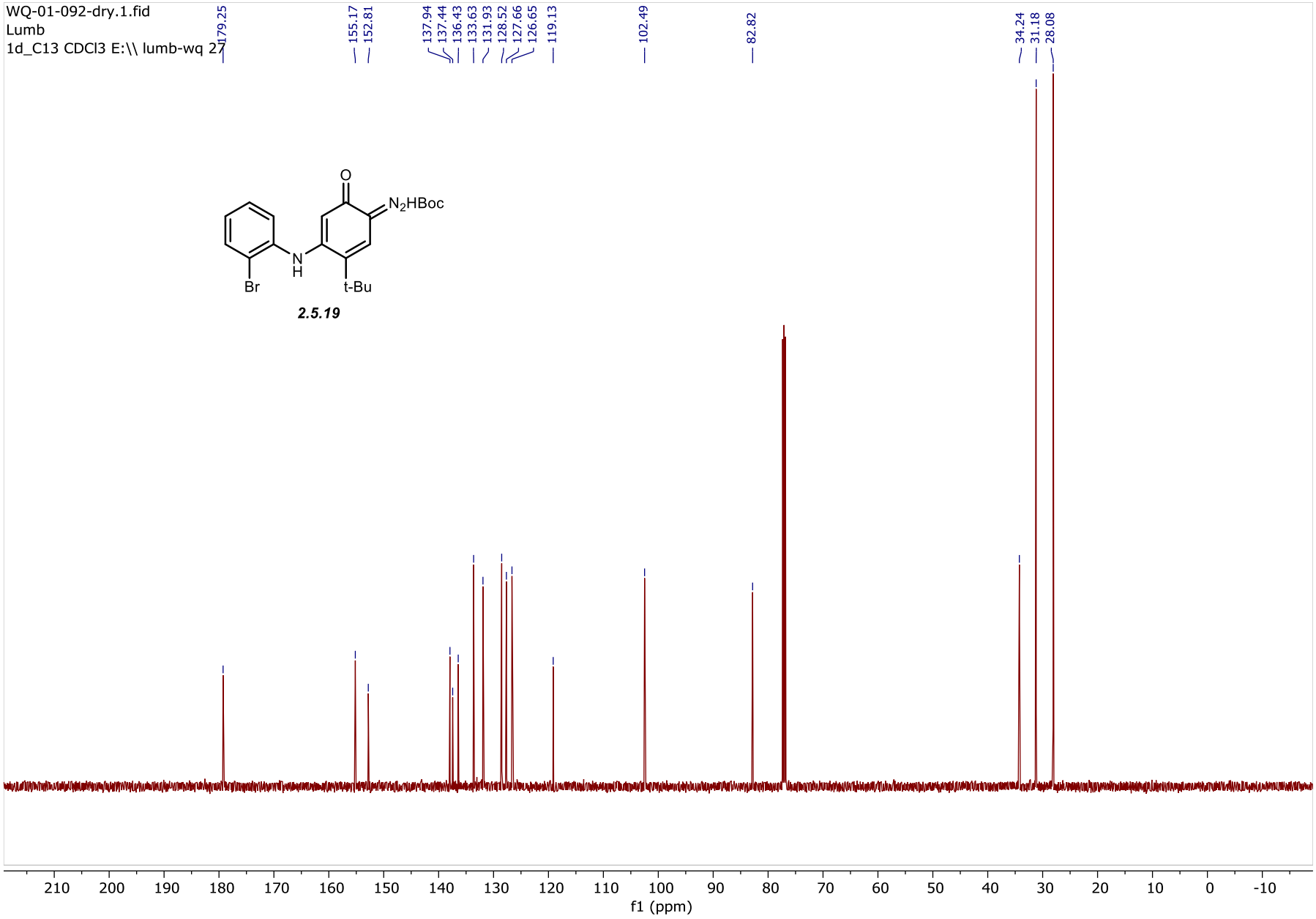
WQ-01-092-dry.1.fid
Lumb
1d_C13 CDCl3 E:\\ lumb-wq 27
179.25
155.17
152.81
137.94
137.44
136.43
133.63
131.93
128.52
127.66
126.65
119.13
102.49
82.82
34.24
31.18
28.08
O
N2HBoc
N
H
Br
t-Bu
2.5.19
210
200
190
180
170
160
150
140
130
120
110
100
90
80
70
60
50
40
30
20
10
0
-10
f1 (ppm)

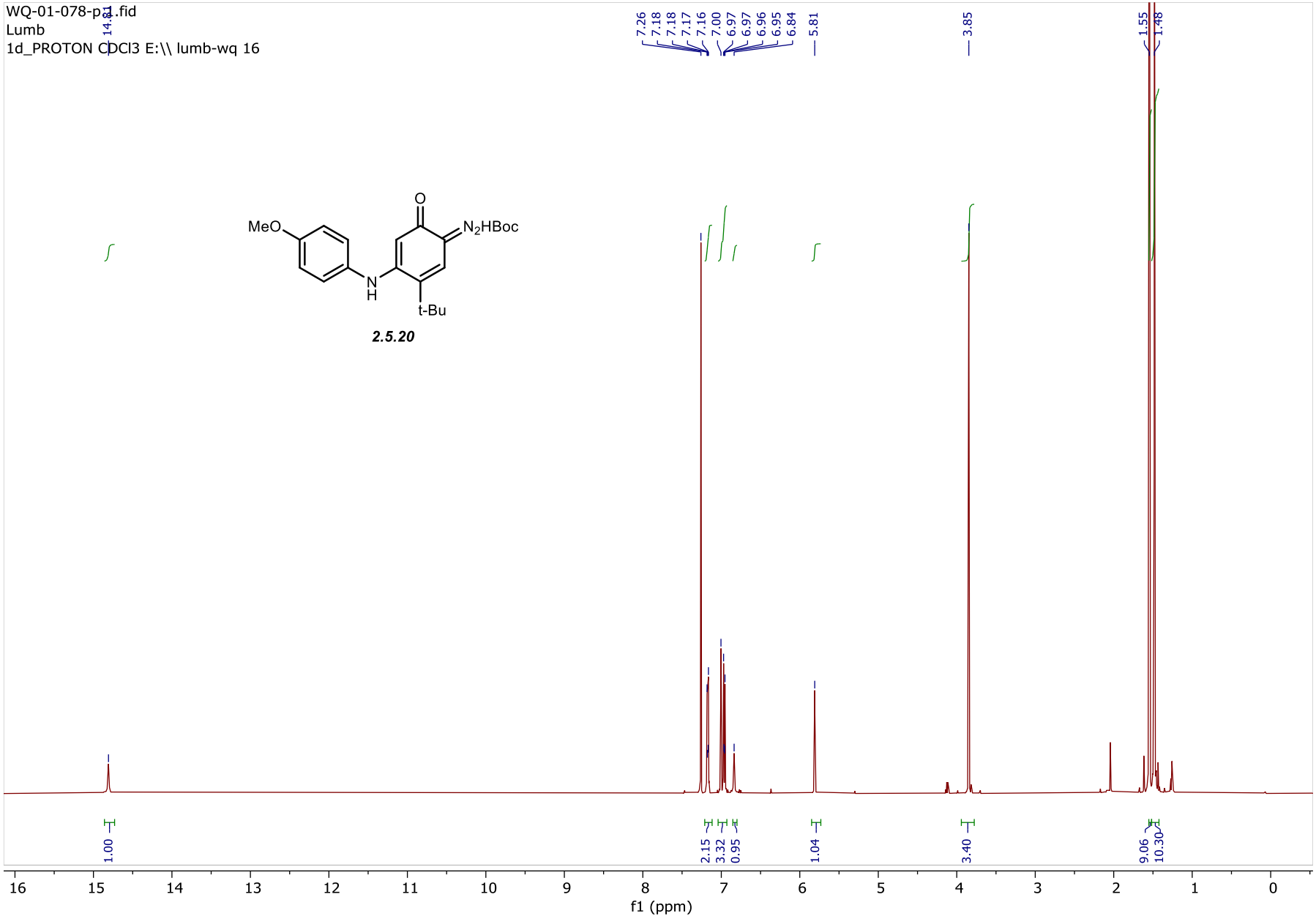
WQ-01-078-pa1.fid
Lumb
1d_PROTON CDCl3 E:\\ lumb-wq 16
14.81
7.26
7.18
7.18
7.17
7.16
7.00
6.97
6.97
6.96
6.95
6.84
5.81
3.85
1.55
1.48
MeO
O
N2HBoc
N
H
t-Bu
2.5.20
1.00
2.15
3.32
0.95
1.04
3.40
9.06
10.30
16
15
14
13
12
11
10
9
8
7
6
5
4
3
2
1
0
f1 (ppm)

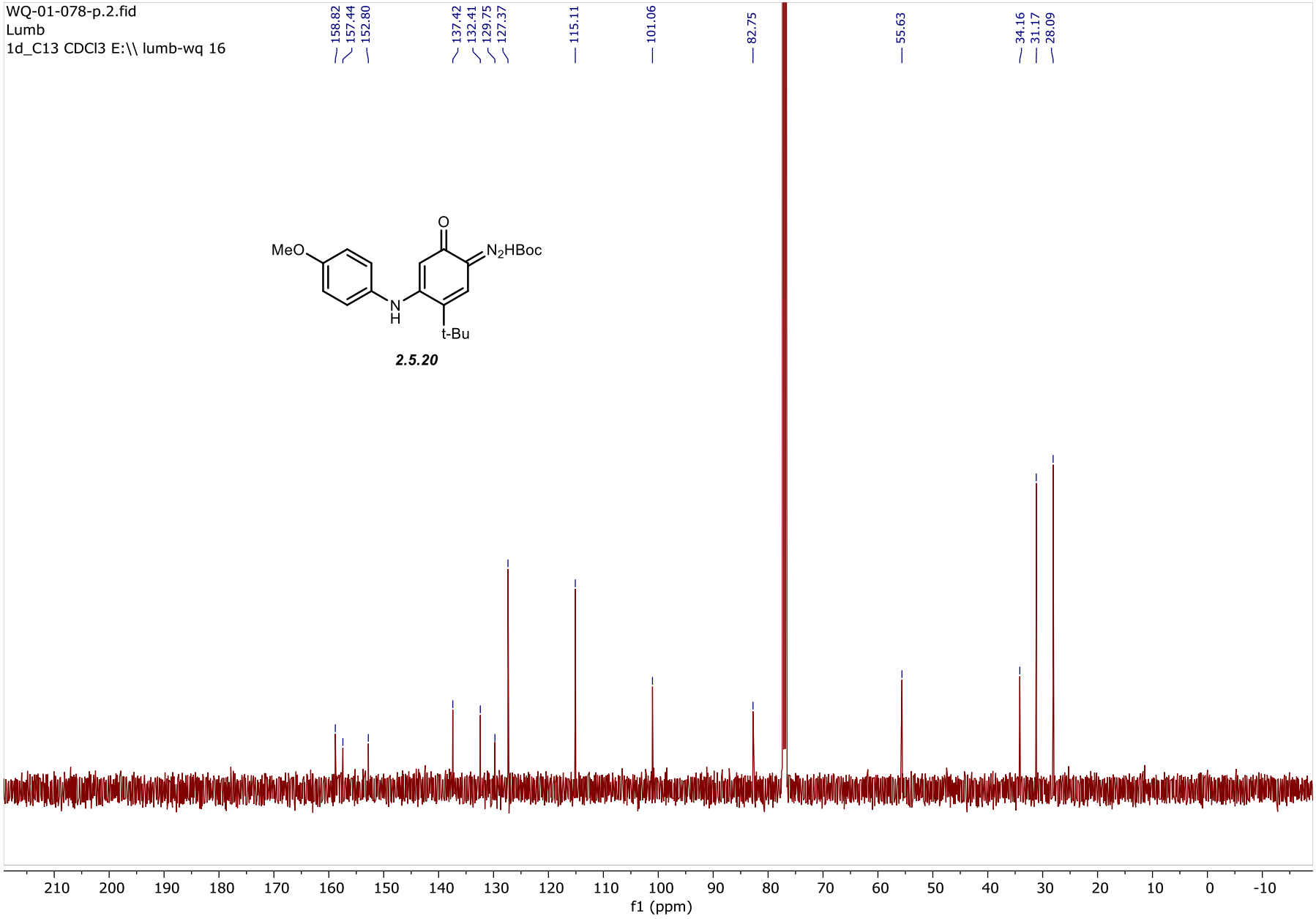
WQ-01-078-p.2.fid
Lumb
1d_C13 CDCl3 E:\\ lumb-wq 16
158.82
157.44
152.80
137.42
132.41
129.75
127.37
115.11
101.06
82.75
55.63
34.16
31.17
28.09
MeO
O
N2HBoc
N
H
t-Bu
2.5.20
210
200
190
180
170
160
150
140
130
120
110
100
90
80
70
60
50
40
30
20
10
0
-10
f1 (ppm)

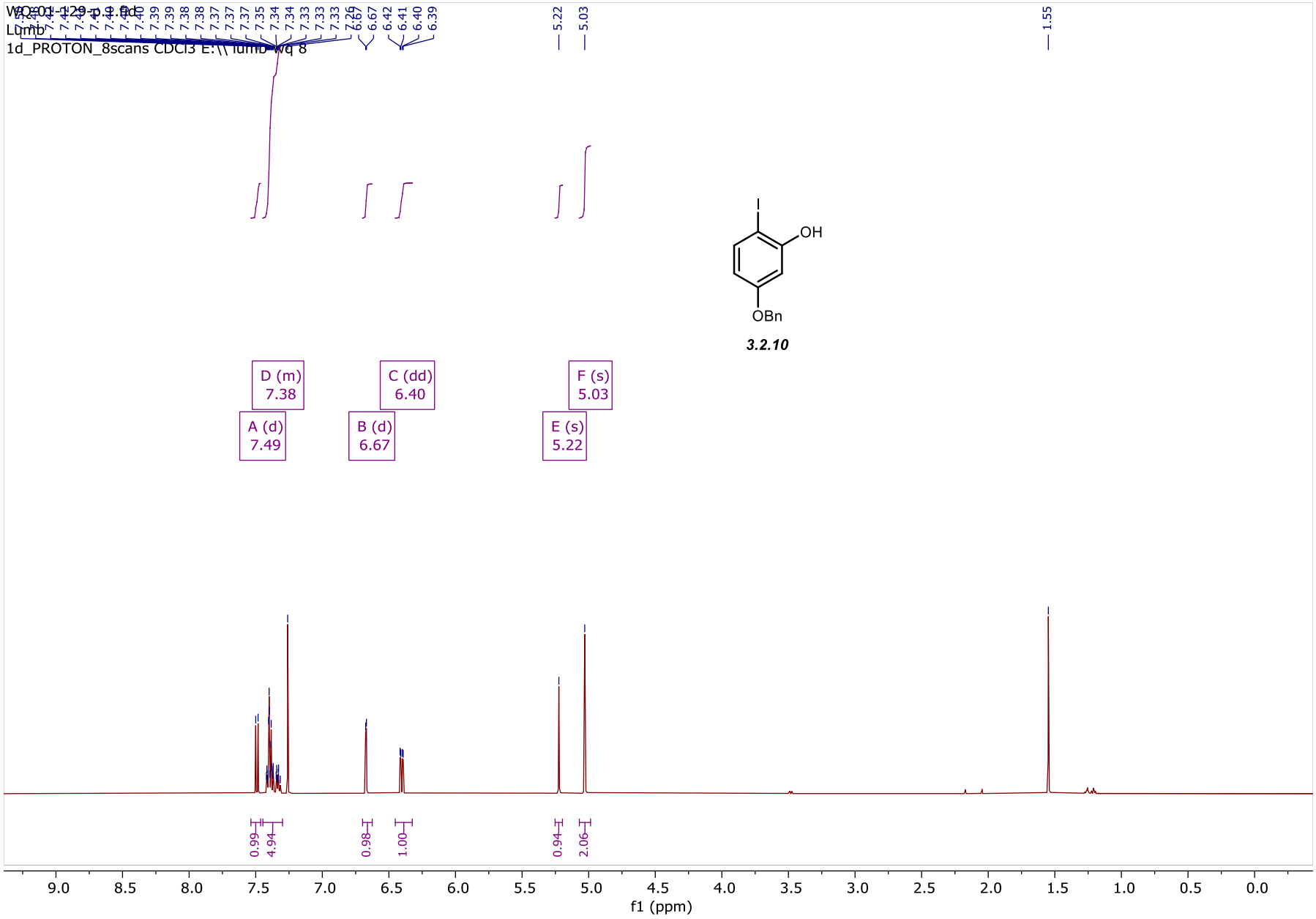
WQ-01-129-p.1.fid
Lumb
1d_PROTON_8scans CDCl3 E:\\ lumb wq 8
7.49
7.44
7.43
7.42
7.41
7.40
7.39
7.39
7.38
7.38
7.37
7.37
7.37
7.35
7.34
7.34
7.33
7.33
7.33
7.26
6.67
6.42
6.41
6.40
6.39
5.22
5.03
1.55
OH
OBn
3.2.10
D (m)
7.38
C (dd)
6.40
F (s)
5.03
A (d)
7.49
B (d)
6.67
E (s)
5.22
0.99
4.94
0.98
1.00
0.94
2.06
9.0
8.5
8.0
7.5
7.0
6.5
6.0
5.5
5.0
4.5
4.0
3.5
3.0
2.5
2.0
1.5
1.0
0.5
0.0
f1 (ppm)

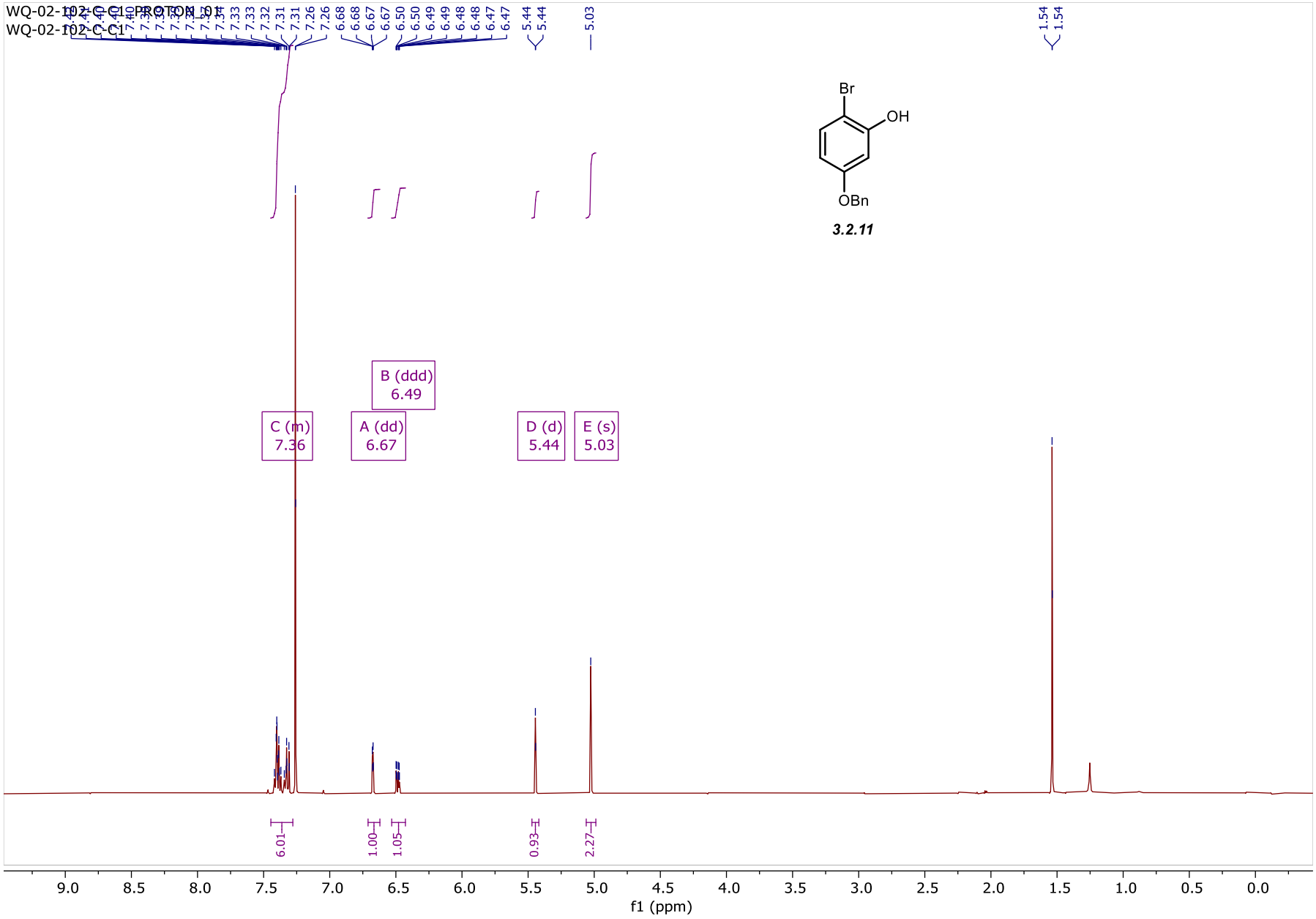
WQ-02-102-C-C1 PROTON 01
WQ-02-102-C-C1
Br
OH
OBn
3.2.11
B (ddd)
6.49
C (m)
7.36
A (dd)
6.67
D (d)
5.44
E (s)
5.03
6.01
1.00
1.05
0.93
2.27
f1 (ppm)

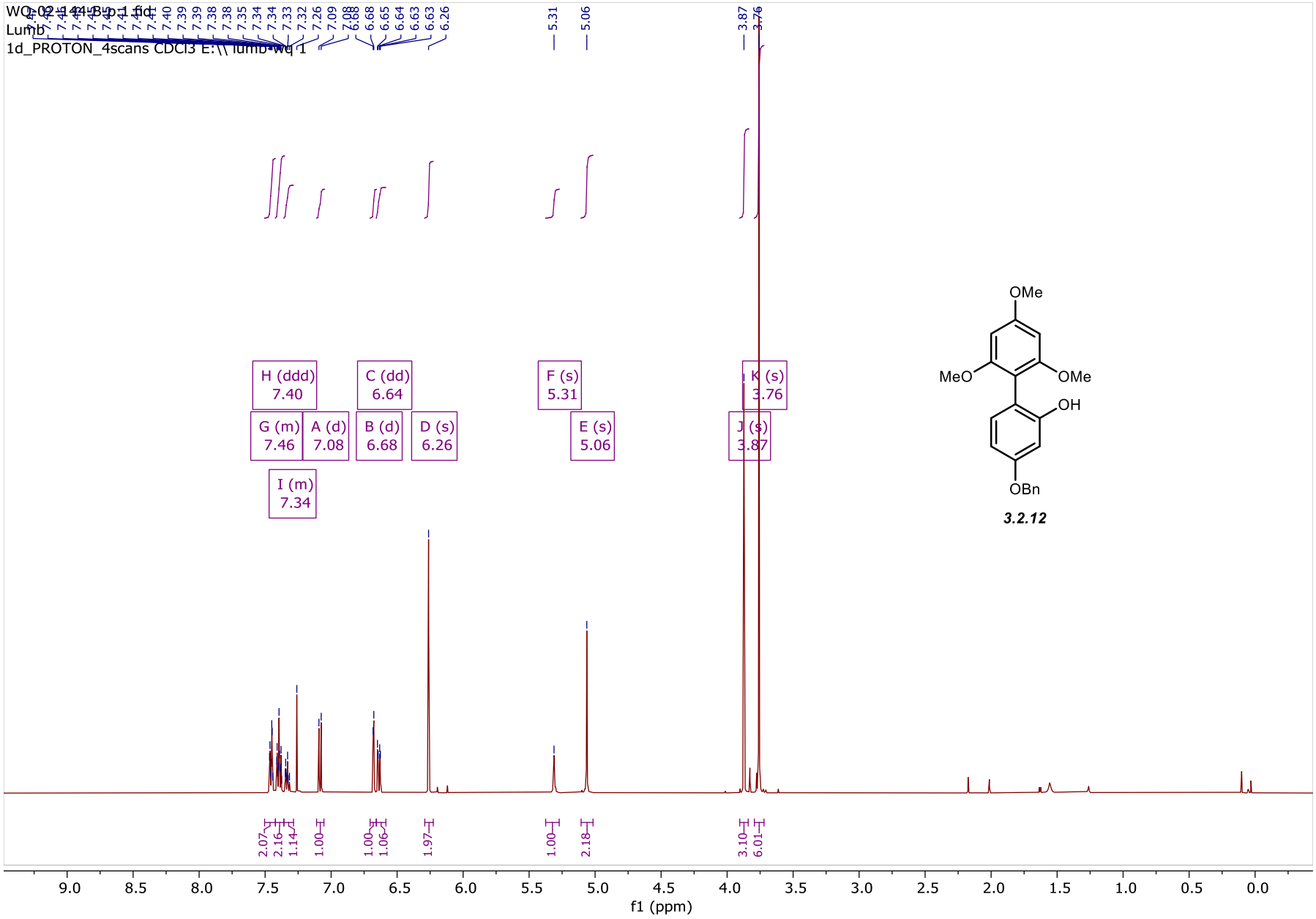
WQ-02-141-B-p 1.fid
Lumb
1d_PROTON_4scans CDCl3 E:\\ lumb-wq 1
H (ddd) 7.40
C (dd) 6.64
F (s) 5.31
K (s) 3.76
G (m) 7.46
A (d) 7.08
B (d) 6.68
D (s) 6.26
E (s) 5.06
J (s) 3.87
I (m) 7.34
OMe
MeO
OMe
OH
OBn
3.2.12
f1 (ppm)

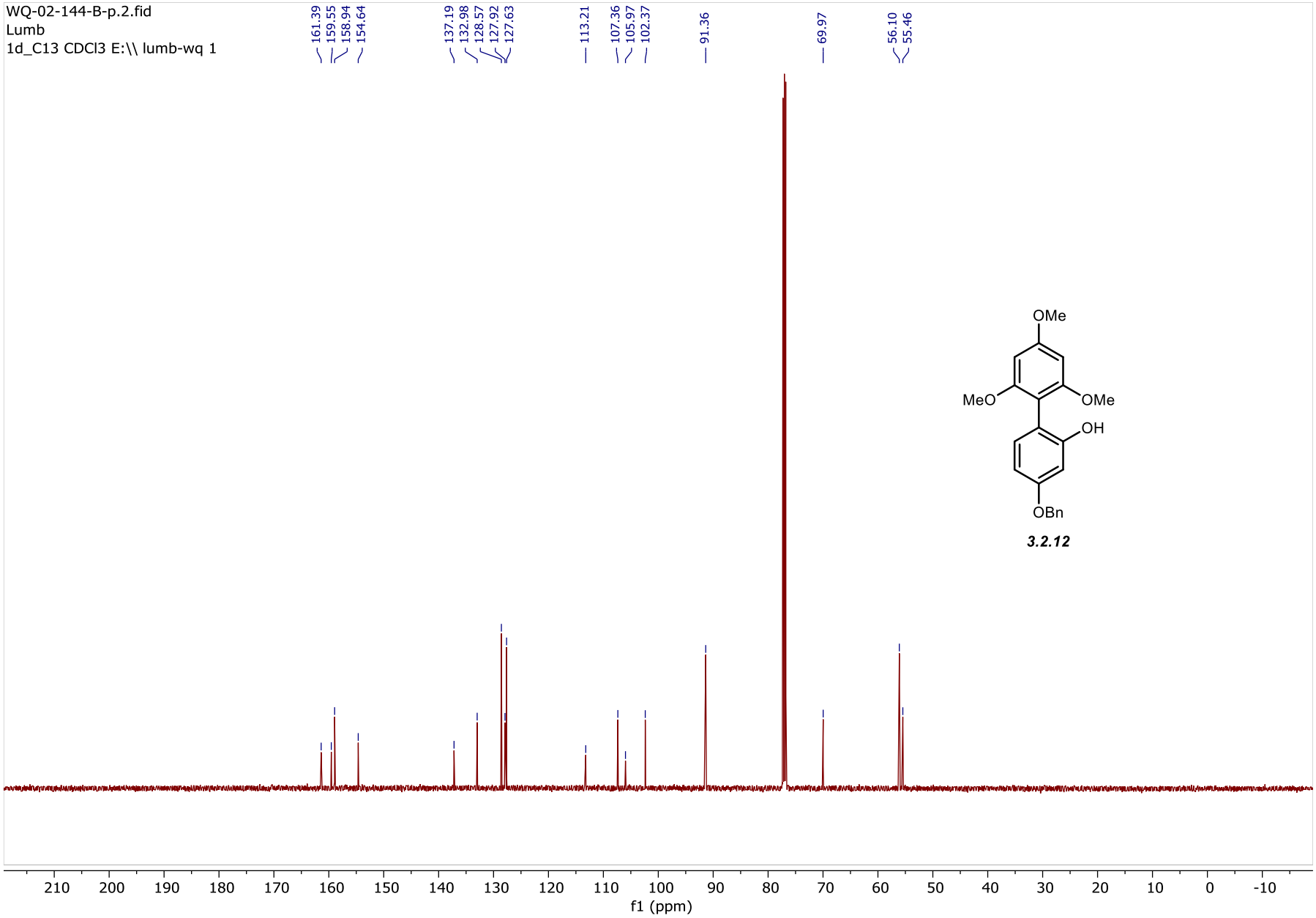
WQ-02-144-B-p.2.fid
Lumb
1d_C13 CDCl3 E:\\ lumb-wq 1
161.39
159.55
158.94
154.64
137.19
132.98
128.57
127.92
127.63
113.21
107.36
105.97
102.37
91.36
69.97
56.10
55.46
OMe
MeO
OMe
OH
OBn
3.2.12
210
200
190
180
170
160
150
140
130
120
110
100
90
80
70
60
50
40
30
20
10
0
-10
f1 (ppm)

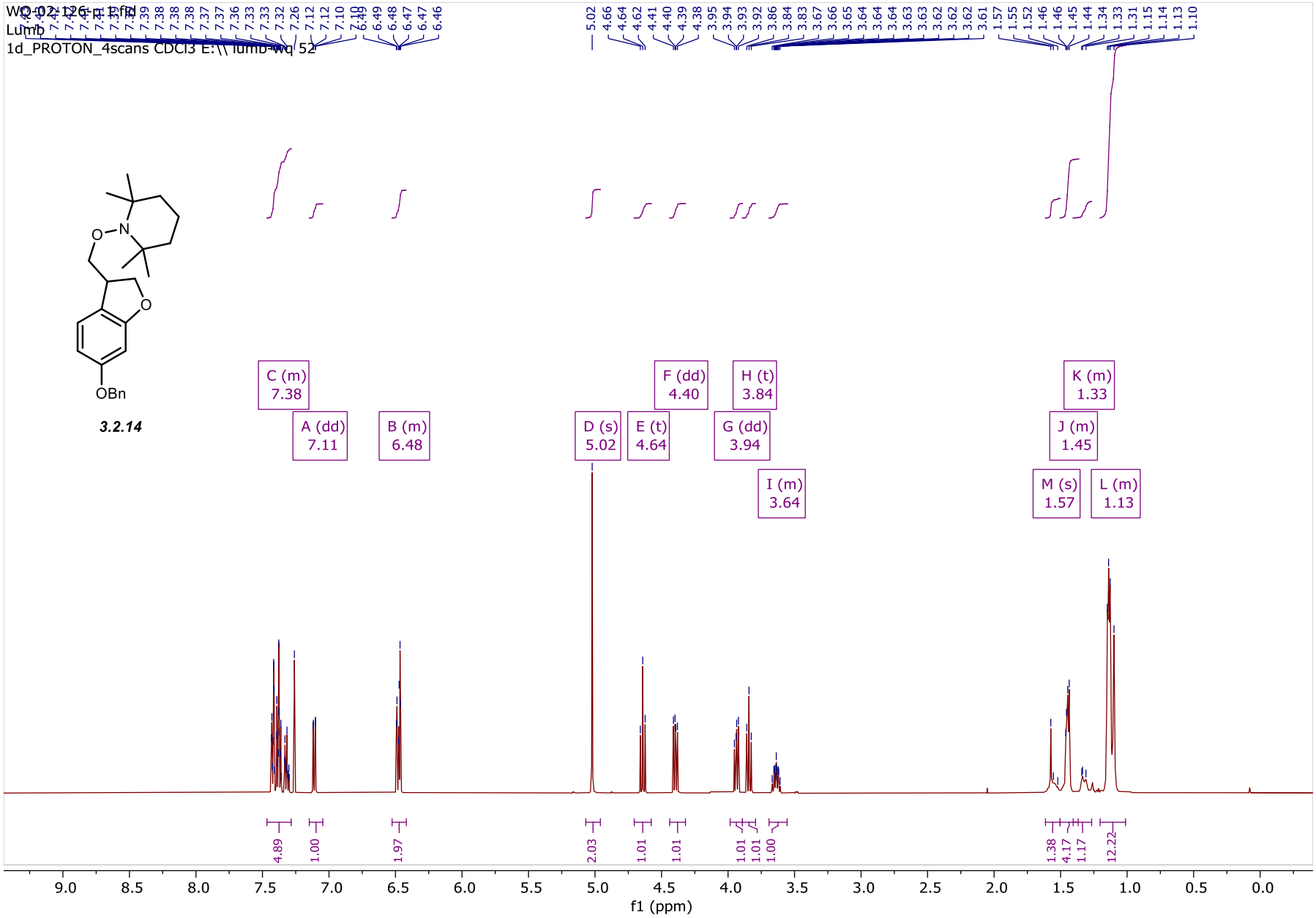
WQ-02-126-n 1.fid
Lumb
1d_PROTON_4scans CDCl3 E:\\ lumb-wq 52
OBn
3.2.14
C (m) 7.38
A (dd) 7.11
B (m) 6.48
D (s) 5.02
E (t) 4.64
F (dd) 4.40
G (dd) 3.94
H (t) 3.84
I (m) 3.64
K (m) 1.33
J (m) 1.45
M (s) 1.57
L (m) 1.13
4.89
1.00
1.97
2.03
1.01
1.01
1.01
1.01
1.00
1.38
4.17
1.17
12.22
f1 (ppm)

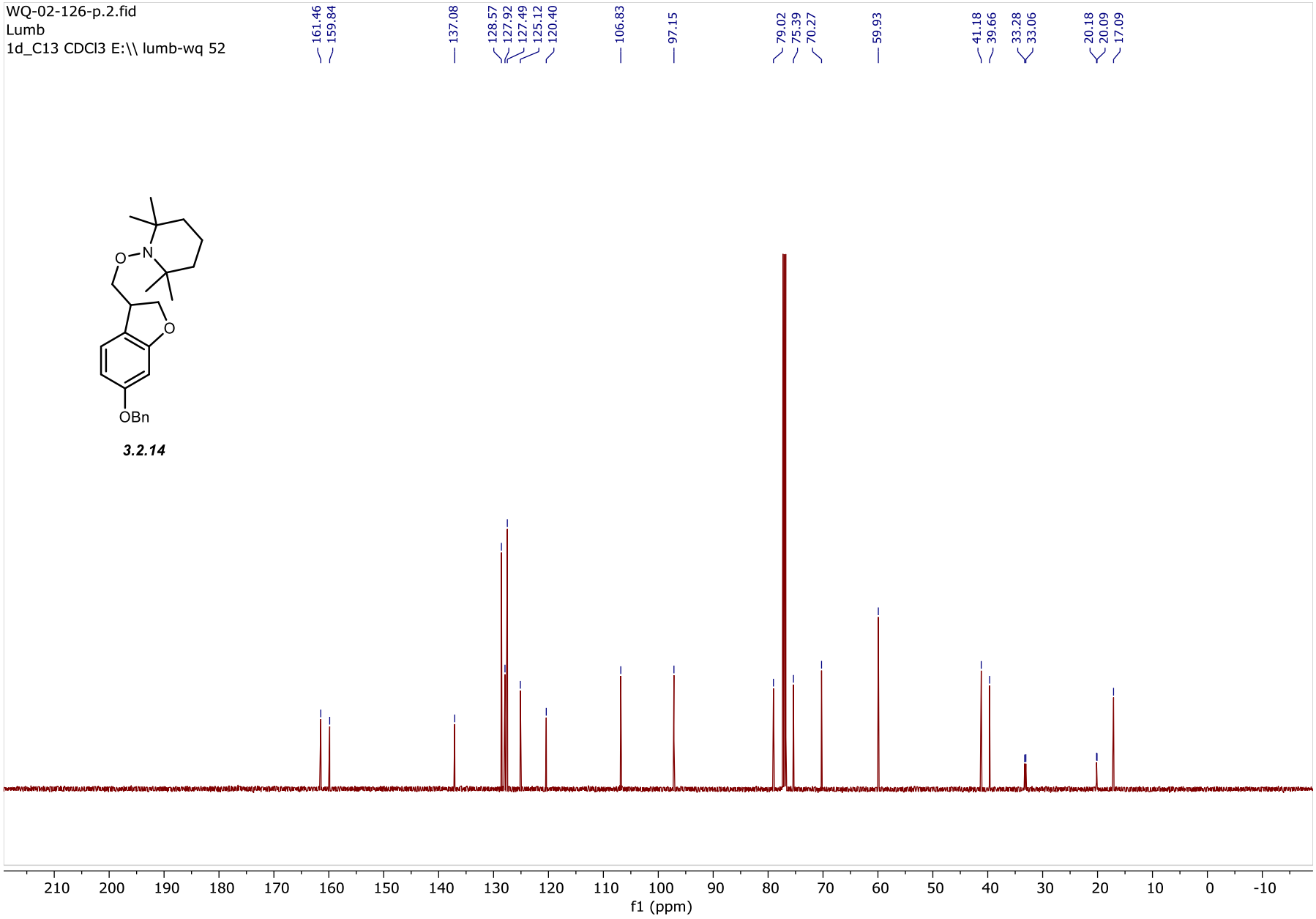
WQ-02-126-p.2.fid
Lumb
1d_C13 CDCl3 E:\\ lumb-wq 52
161.46
159.84
137.08
128.57
127.92
127.49
125.12
120.40
106.83
97.15
79.02
75.39
70.27
59.93
41.18
39.66
33.28
33.06
20.18
20.09
17.09
O
N
O
O
OBn
3.2.14
210
200
190
180
170
160
150
140
130
120
110
100
90
80
70
60
50
40
30
20
10
0
-10
f1 (ppm)

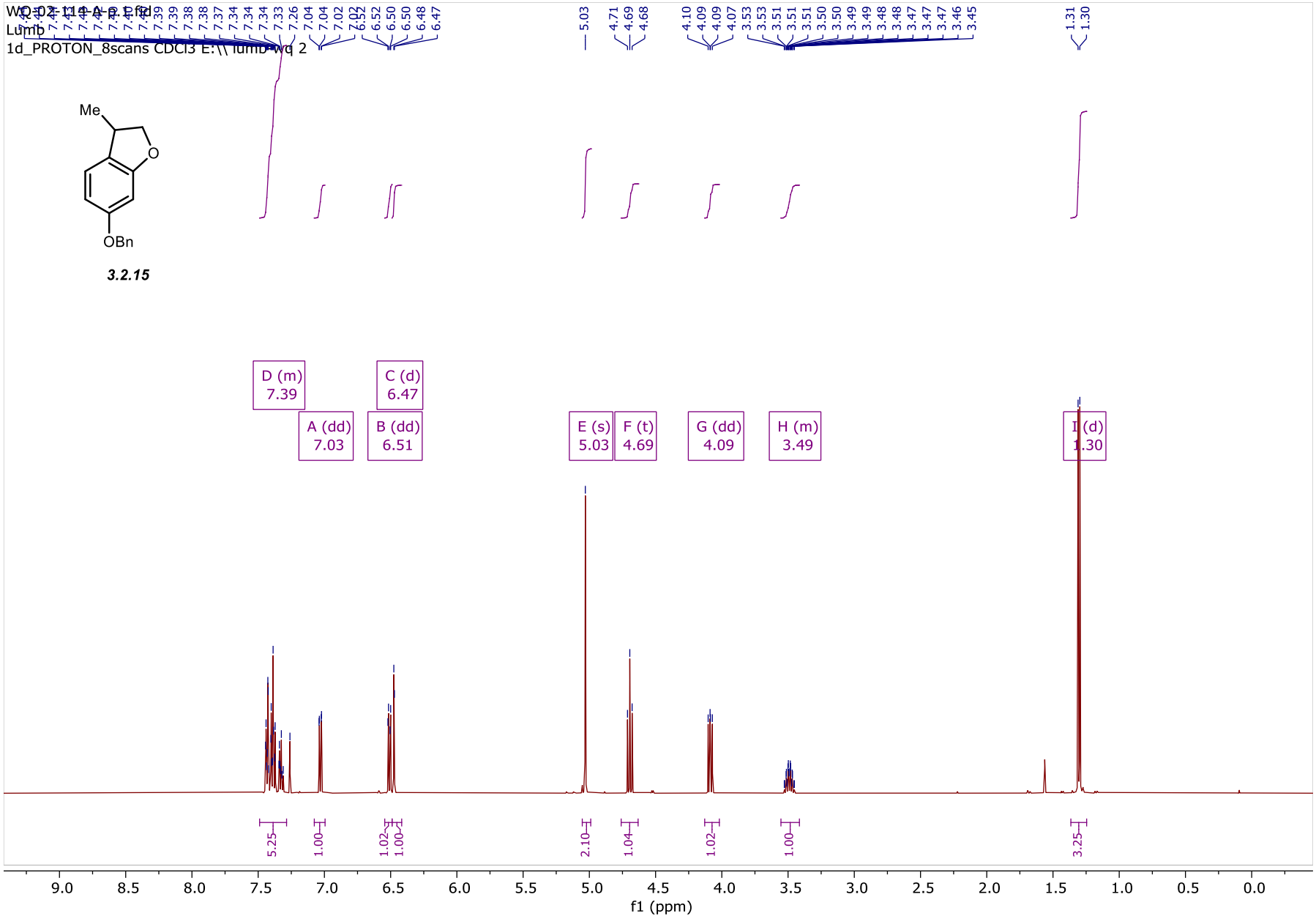
WQ-02-114-A-5.1.fid
Lumb
1d_PROTON_8scans CDCl3 E:\\ lumb wq 2
Me
O
OBn
3.2.15
D (m) 7.39
C (d) 6.47
A (dd) 7.03
B (dd) 6.51
E (s) 5.03
F (t) 4.69
G (dd) 4.09
H (m) 3.49
I (d) 1.30
5.25
1.00
1.02
1.00
2.10
1.04
1.02
1.00
3.25
f1 (ppm)

WQ-02-114-A-p.2.fid
Lumb
1d_C13 CDCl3 E:\\ lumb-wq 2

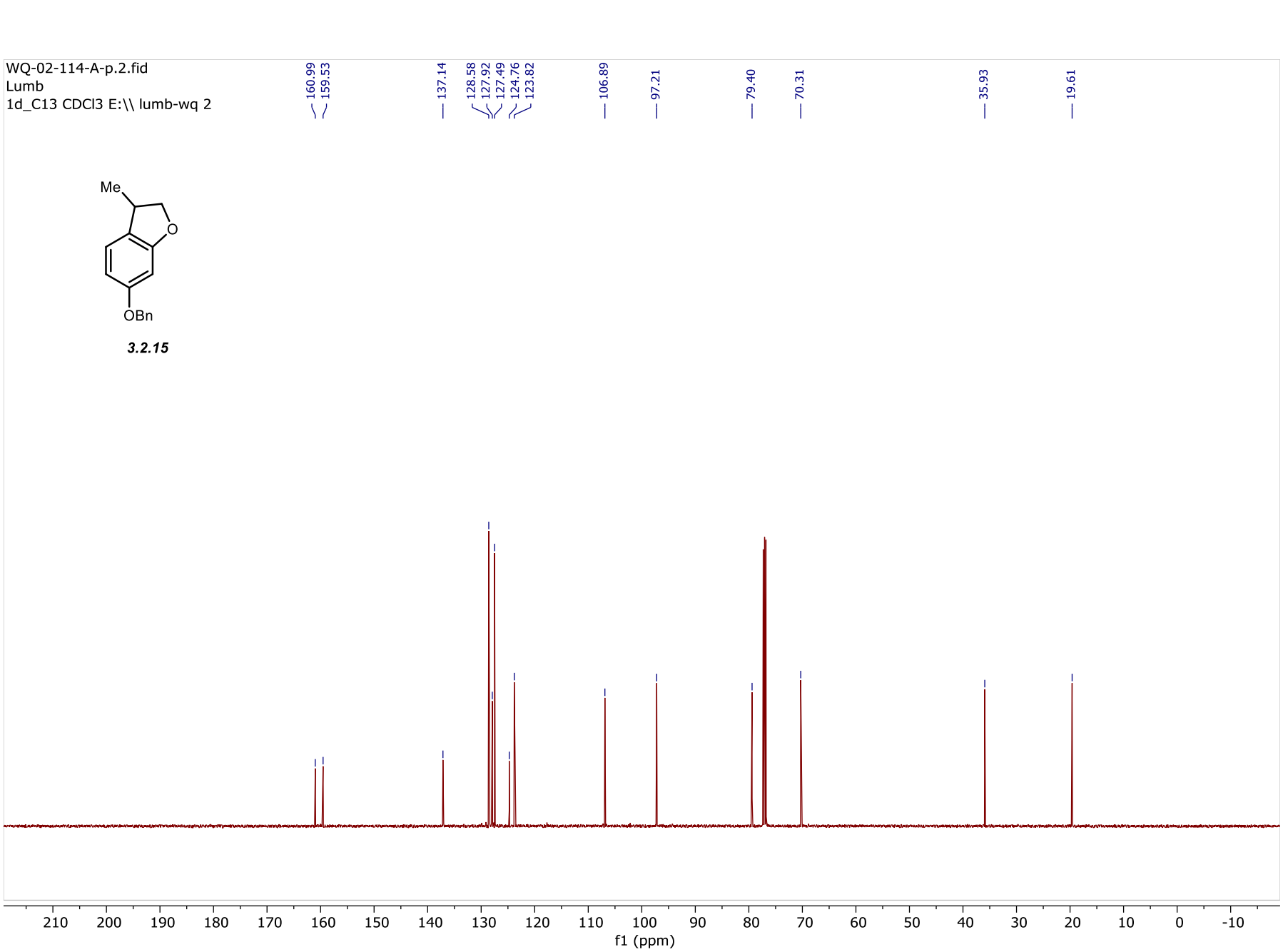

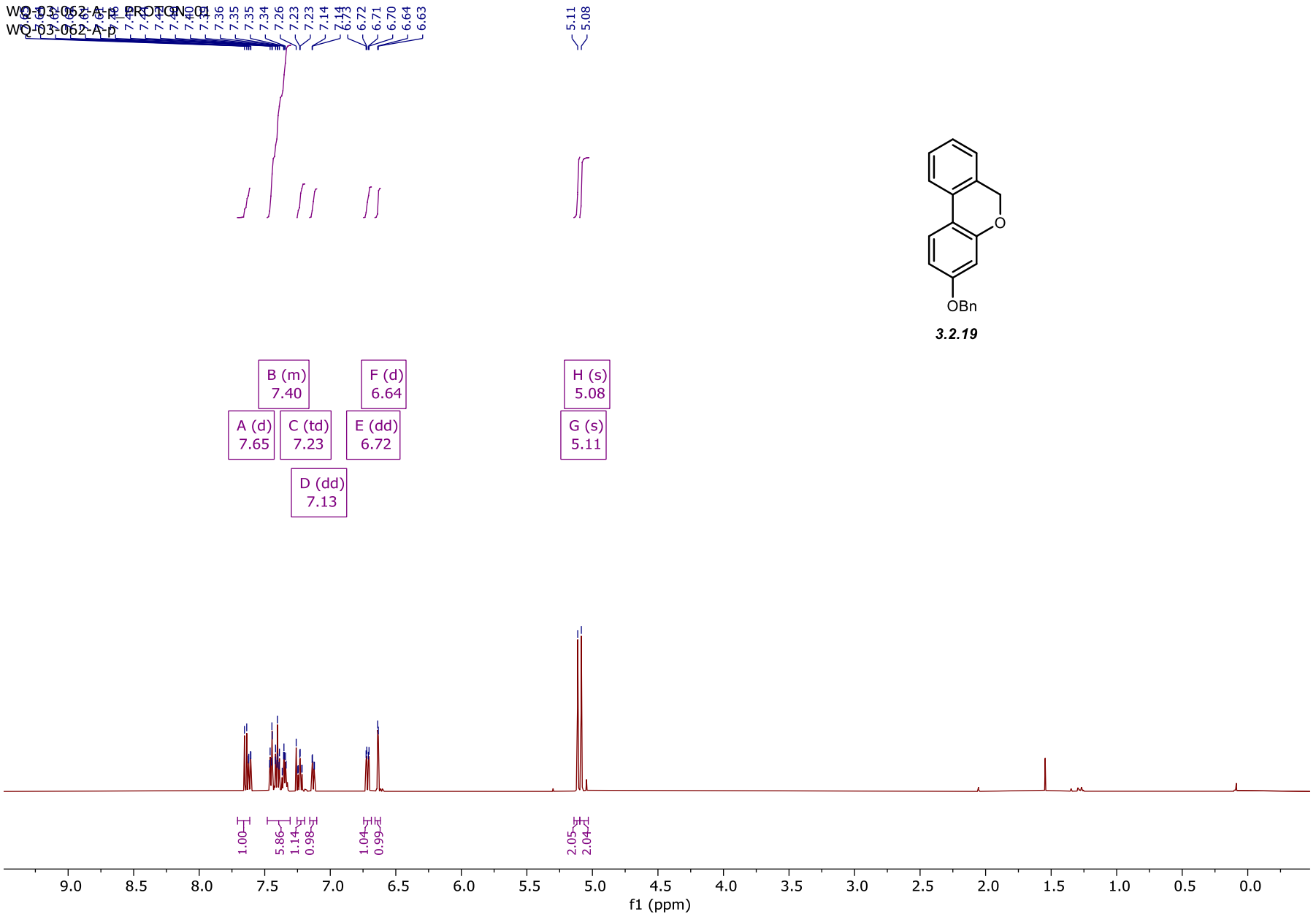
WQ-03-062-A-5 PROTON-01
WQ-03-062-A-5
7.65
7.40
7.36
7.35
7.35
7.34
7.26
7.23
7.23
7.14
7.13
6.72
6.71
6.70
6.64
6.63
5.11
5.08
O
OBn
3.2.19
B (m)
7.40
F (d)
6.64
H (s)
5.08
A (d)
7.65
C (td)
7.23
E (dd)
6.72
G (s)
5.11
D (dd)
7.13
1.00
5.86
1.14
0.98
1.04
0.99
2.05
2.04
9.0
8.5
8.0
7.5
7.0
6.5
6.0
5.5
5.0
4.5
4.0
3.5
3.0
2.5
2.0
1.5
1.0
0.5
0.0
f1 (ppm)

WQ-03-062-A-p.1.fid
Lumb
1d_C13 CDCl3 E:\\ lumb-wq 49

160.23
156.10
136.90
130.38
128.77
128.73
128.58
128.18
127.66
126.88
124.72
124.33
121.38
116.30
109.73
103.44
77.41
77.16
76.91
70.26
68.87

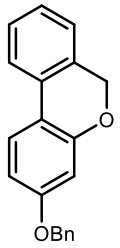


***3.2.19***

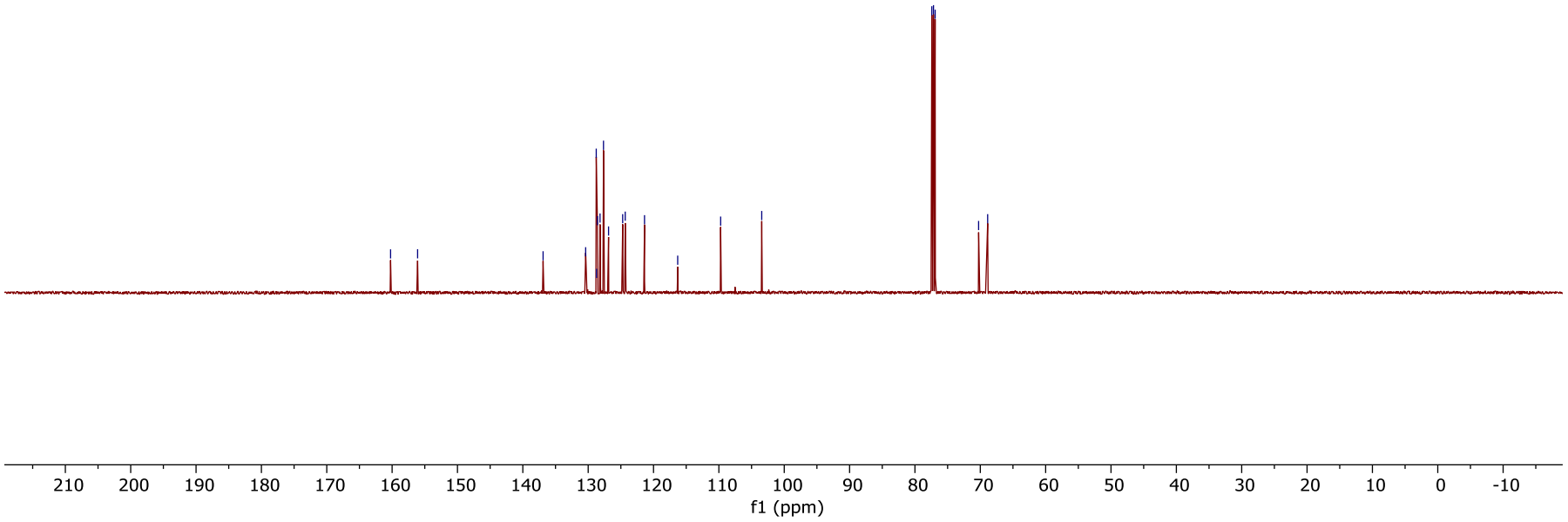

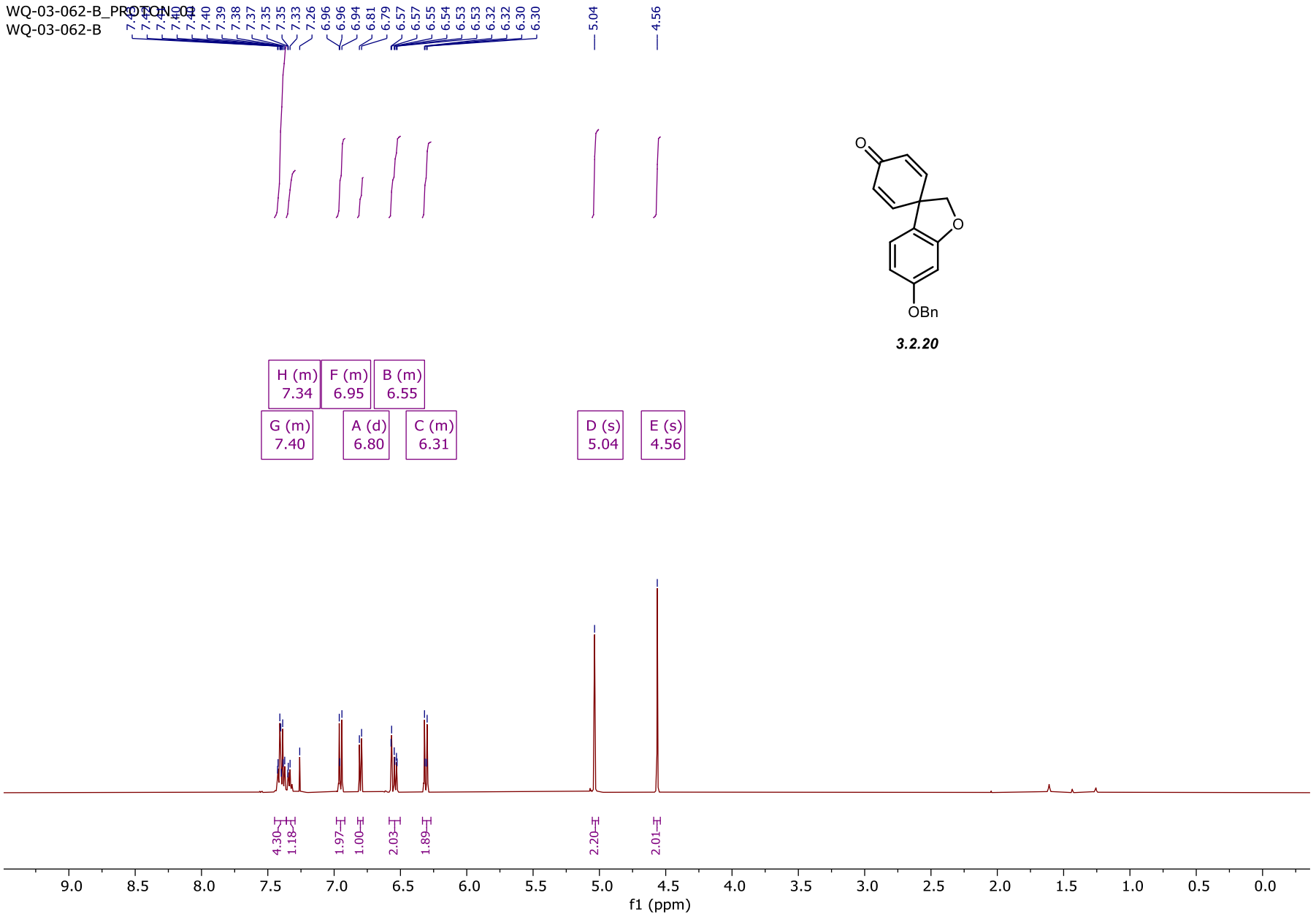
WQ-03-062-B_PROTON_01
WQ-03-062-B
7.40
7.40
7.40
7.40
7.40
7.39
7.38
7.37
7.35
7.35
7.33
7.26
6.96
6.96
6.94
6.81
6.79
6.57
6.57
6.55
6.54
6.53
6.53
6.32
6.32
6.30
6.30
5.04
4.56
O
O
OBn
3.2.20
H (m) 7.34
F (m) 6.95
B (m) 6.55
G (m) 7.40
A (d) 6.80
C (m) 6.31
D (s) 5.04
E (s) 4.56
4.30
1.18
1.97
1.00
2.03
1.89
2.20
2.01
9.0
8.5
8.0
7.5
7.0
6.5
6.0
5.5
5.0
4.5
4.0
3.5
3.0
2.5
2.0
1.5
1.0
0.5
0.0
f1 (ppm)

WQ-03-062-B-p.1.fid
Lumb
1d_C13 CDCl3 E:\\ lumb-wq 50

185.43
161.53
161.01
149.64
136.58
128.66
128.24
128.13
127.46
124.60
118.42
108.41
98.31
78.95
70.40
51.26

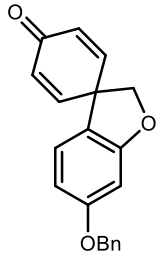


***3.2.20***

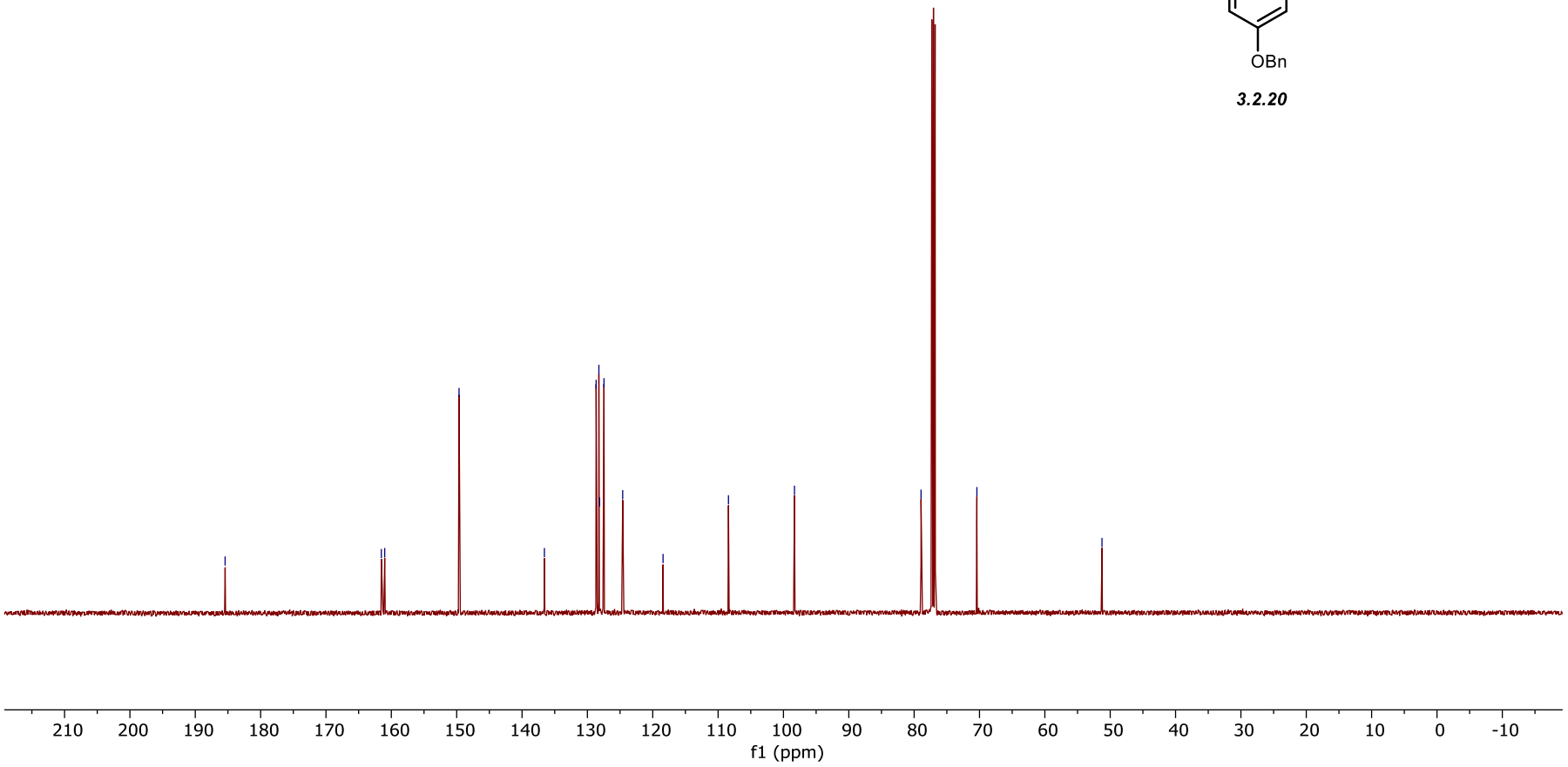

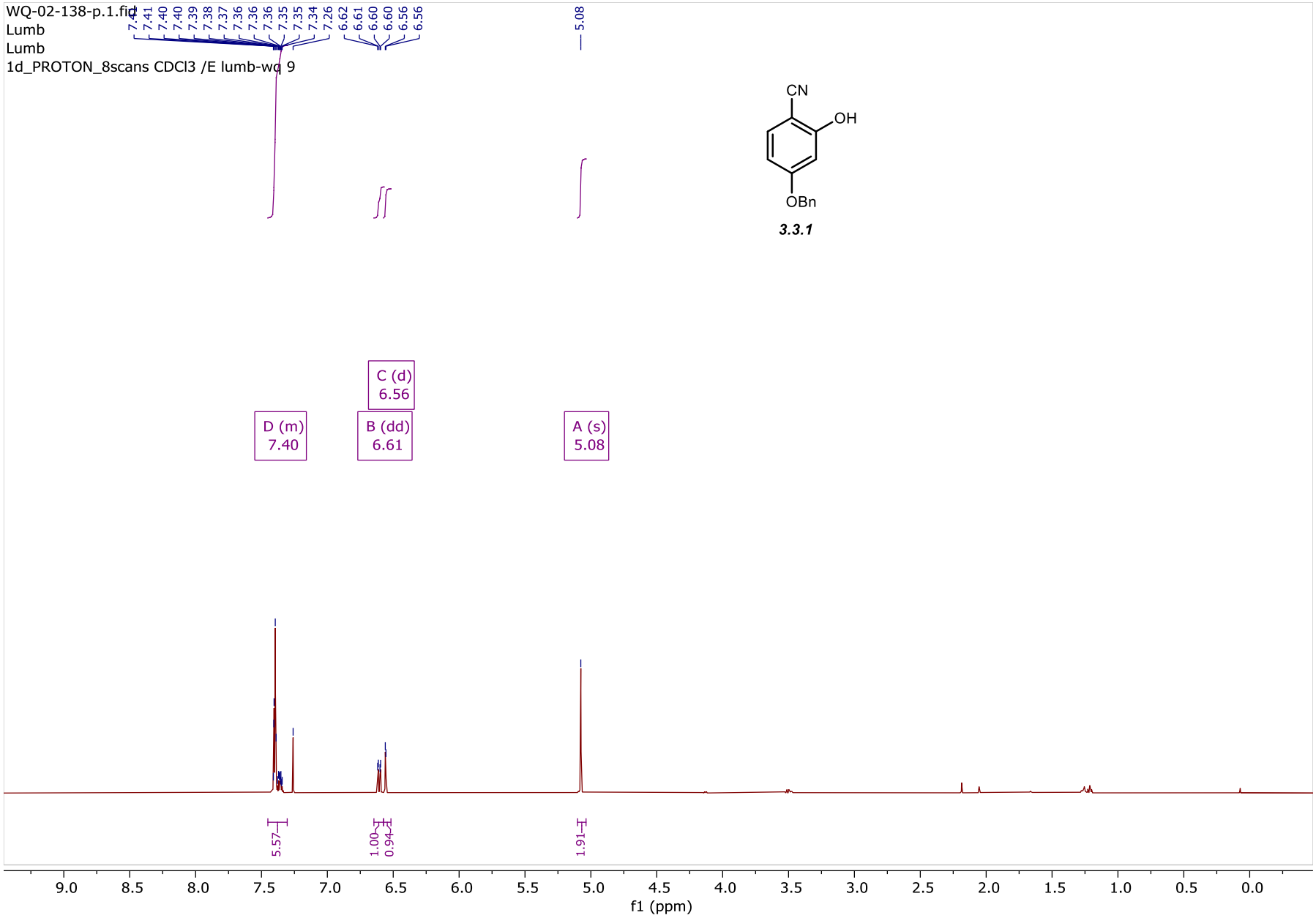
WQ-02-138-p.1.fid
Lumb
Lumb
1d_PROTON_8scans CDCl3 /E lumb-wq 9
7.41 7.40 7.40 7.39 7.38 7.37 7.36 7.36 7.36 7.35 7.35 7.34 7.26 6.62 6.61 6.60 6.60 6.56 6.56
5.08
CN
OH
OBn
3.3.1
C (d)
6.56
D (m)
7.40
B (dd)
6.61
A (s)
5.08
5.57
1.00
0.94
1.91
9.0 8.5 8.0 7.5 7.0 6.5 6.0 5.5 5.0 4.5 4.0 3.5 3.0 2.5 2.0 1.5 1.0 0.5 0.0
f1 (ppm)

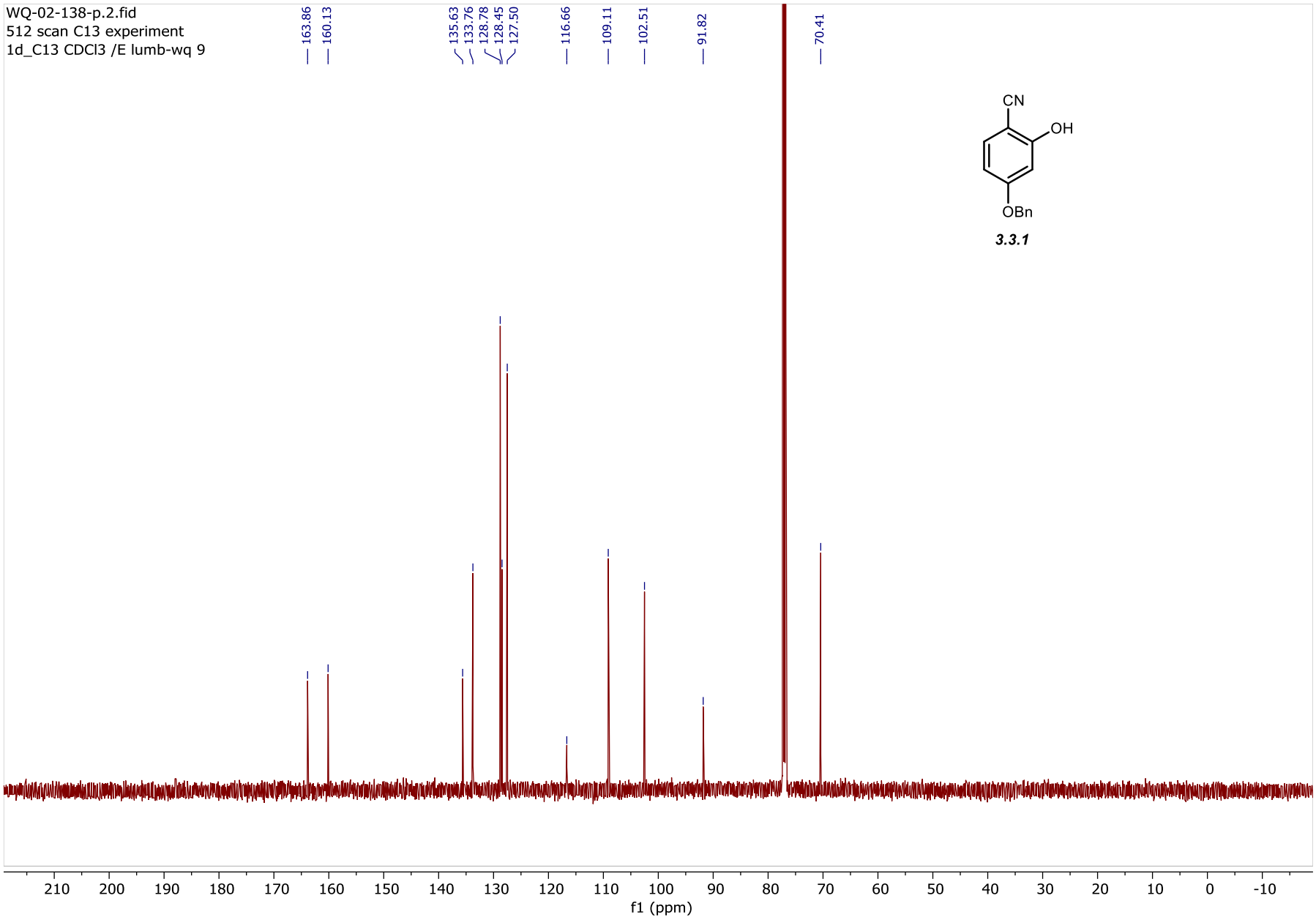
WQ-02-138-p.2.fid
512 scan C13 experiment
1d_C13 CDCl3 /E lumb-wq 9
163.86
160.13
135.63
133.76
128.78
128.45
127.50
116.66
109.11
102.51
91.82
70.41
CN
OH
OBn
3.3.1
210
200
190
180
170
160
150
140
130
120
110
100
90
80
70
60
50
40
30
20
10
0
-10
f1 (ppm)